Proceedings

11th Inter Guiana Geological Conference: Tectonics and Metallogenesis of NE South America

Paramaribo, Suriname
19th-20th February, 2019

Mededeling Geologisch Mijnbouwkundige Dienst Suriname 29

Conference Sponsors

Diamond Sponsor

IAMGOLD

Gold Sponsor

FILAB SURINAME

Silver Sponsor

Chisu

Bronze Sponsor

NANARESOURCES

STAATSOLIE

Conference Organisers

ANTON DE KOM UNIVERSITEIT VAN SURINAME

Theo Wong
Salomon Kroonenberg
Nicole Kioe-A-Sen
Clyde Griffith

THE UNIVERSITY OF WESTERN AUSTRALIA

Mark Jessell
Sandra Occhipinti
Corinne Debat

GEOLOGISCH MIJNBOUWKUNDIGE DIENST

Reenuska Mahabier

SAXI Partners

AMIRA INTERNATIONAL · ADIMB · AngloAmerican · AngloGold Ashanti · ANTON DE KOM UNIVERSITEIT VAN SURINAME · BARRICK · CPRM Serviço Geológico do Brasil

Centre for EXPLORATION TARGETING · CODELCO · GEOLOGISCH MIJNBOUWKUNDIGE DIENST · GOLDCORP · GRASSALCO We bring prosperity to the surface · Guyana Geology & Mines Commission

IRD Institut de Recherche pour le Développement FRANCE · NEWCREST MINING LIMITED · Universiteit Utrecht · OZ MINERALS · RANDGOLD RESOURCES · REUNION GOLD CORPORATION · Universidad de Chile

UFMG · Laurentian University Université Laurentienne · Université de Lorraine · USP · Université Toulouse III Paul Sabatier · The University of Western Australia

Front Cover: Pillow Lavas from the Paramaka Fm., Suriname. S. Kroonenberg

Inside Back Cover: Batea with gold specks. S. Kroonenberg

Back Cover: Voltzberg, Suriname. T. Wong

Table of Contents

History of the Inter Guiana Geological Conferences

The idea of an Inter Guiana Geological Conference was in 1949 first proposed by Hendricus (Henk) Schols, at that time head of the Geological and Mining Service of Suriname. He had graduated as a mining engineer from Delft University of Technology, and had passed the years of the Second World War in Suriname on secondment from a private organisation. After the war, he was asked by the governor of Suriname to set up the Geological and Mining Service.

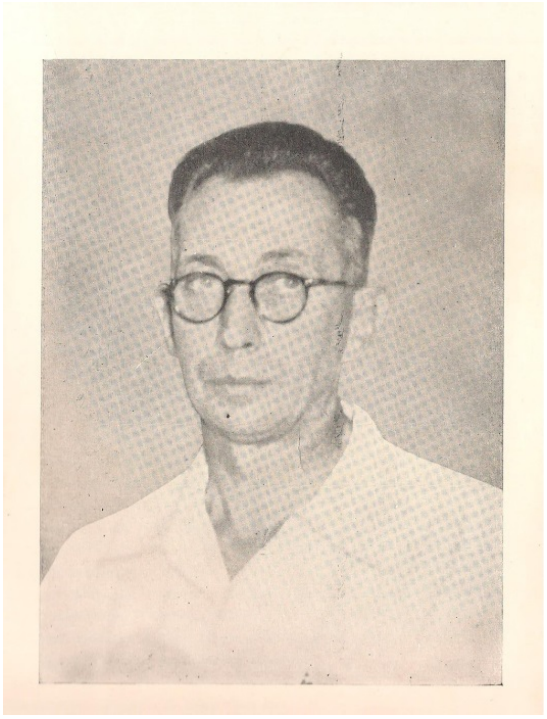

Left: Hendricus Schols at the age of 24, painting by Etie van Reest, now at Phophonyane Falls, Swaziland. Right: photograph at In Memoriam (1957), GMD Jaarboek 1956-1958.

He organised the first Inter Guiana Geological conference in Paramaribo from September 23 to October 3, 1950. It was attended from French Guiana by the famous Russian-born French geologist Boris Choubert, geologist of the Office Scientifique d'Outre-mer (now the IRD, l'Institut de Recherche pour le Développement), who already since the 1930s was a staunch supporter of Wegener's Continental Drift theory, against the mainstream consensus in those years. He had worked extensively in Gabon before, and wrote a number of important books and papers on the geology of French Guiana. British Guiana was represented by the Director of the British Guiana Geological Survey Smith Bracewell, also a prolific publisher on the geology of that country in the years before, and discoverer of a series of unusual chromium minerals in the Merume River of British Guiana, one of which was named after him (bracewellite).

In the following years the tradition of Inter Guiana Conferences was continued in the different Guianian capitals (see table). In the fourth one a Brazilian representative was present, and the fifth also one from Venezuela. Proceedings were published from the fourth conference onward, always by local government institutes and all in different formats. Participants came from all Guianian countries including Colombia and also from beyond, including Bolivia, United States, Canada, UK, Switzerland, France, Gabon and Tanzania.

The 10th Conference in Belém, Brazil in 1975 was a hugely impressive event, in which the complete geological inventory of the Amazonian Craton was shown on the basis of radar images, the RADAMBRASIL programme.

Also geomorphology, vegetation and soil maps were produced in the programme, and published in a great number of volumes with maps which even now are standard reference works.

Suriname committed itself during that conference to organise the 11th Interguiana conference in 1978. Somehow this did not materialise, but now, 40 years later, thanks to the upsurge of geological interest in the Guiana Shield, we are happy we can take up the initiative again, and we hope that in spite of the long break there will be forthcoming conferences as well in the other Guianian countries.

I thank Mrs Fiona Berrangé-Schols, daughter of Henk Schols, now in Phophonyane Falls, Swaziland, for information about her father and for permission to publish the nice painting of him as a young man.

Salomon Kroonenberg, Anton de Kom University of Suriname.

Interguiana geol conf		Year	Venue
1e	Sep 23-oct 3	1950	Paramaribo
2e	Mar 15-28	1951	Cayenne
3e	Sep 21-27	1953	Georgetown
4e	Sep	1957	Cayenne
5e	Oct 28-Nov 6	1959	Georgetown
6e	Oct 1-8	1963	Belem
7e	Nov 21-25	1966	Paramaribo
8e	Aug 11-15	1969	Georgetown
9e	May 7-14	1972	Ciudad Guayana
10e	Nov 9-16	1975	Belem

Proceedings

1e GMD Jaarboek 1950 p. 74-77;

2e GMD Jaarboek 1951, p. 43-46

3e GMD Jaarboek 1953, p. 20-23

4e Communications Quatrieme Conf Geol Guyanes, 1959, Paris, 139 pp.

5e Proc Fifth InterGuiana Geol. Conf,n 1961, Georgetown, 320 pp.

6e Anais da VI Conferencia Geologica das Guianas, 1966, Rio de Janeiro, 193 pp (scan)

7e Proc 7th Guiana Geol. Conf, Verh Kon Ned geol Mijnb Gen., 27, 1969, 175 pp.+encl.

8e Proceedings of the Eighth Guiana Geological Conference, Georgetown, Guyana, 1970, 21 loose papers

9e Memoria de la 9a Conf Geol Inter-Guayanas. Min Minas Hidrocarb, Bol Geol (Caracas) Publ esp. 6, 692 pp

10e Anais da Decima Conferencia Geologica Interguianas, 1975, Belem, 820 pp

SAXI: The South American Exploration Initiative

The AMIRA International Project P1061A South American Exploration Initiative aims to enhance the exploration potential of the Guiana Shield and neighbouring terranes in northeast South America through an integrated program of research and data gathering into its 'anatomy'. There is an equally strong commitment to training and training by research to produce the next generation of local industry-aware geoscientists. As part of this commitment, a two-day conference was planned to coincide with the final project sponsors' meeting for the one-year pilot project, to ensure that all stakeholders in the region had the opportunity to highlight their latest ideas research ideas and propose future research priorities. The idea for integrating this conference with the 11th Interguiana conference resulted from discussions between the SAXI team and Salomon Kroonenberg and Theo Wong.

The Stage 1 of the SAXI project has brought together 10 minerals exploration companies, 2 geological surveys and 7 Research origanisations to develop the basis for a long-term renewal of our scientific understanding of the tectonics and metallogenesis of the region.

The current SAXI Partners are:

AMIRA International, Anglo American, Anglogold Ashanti, Anton de Kom University of Suriname, Avanco, Barrick, Codelco, Federal University of Minas Gerais at Belo Horizonte, Geologisch Mijnbouwkundige Dienst, Goldcorp, Grassalco, Guyana Geology and Mines Commission, IRD, Laurentian University, Newcrest, Randgold, Reunion Gold, The University of Western Australia, Uni Lorraine, Universidad de Chile, Universidade de Sao Paulo and the University of Toulouse.

The SAXI project is a partner project to the West African Exploration Initiative (WAXI), which started in 2006. The WAXI project is a public-private partnership that has brought together seventy of the principal stakeholders in the domain of mineral exploration in West Africa:

- The government surveys and departments of mines of eleven West African states (Burkina Faso, Ghana, Guinea, Ivory Coast, Liberia, Mali, Mauritania, Niger, Sierra Leone, Senegal and Togo).
- Seven West and South African universities (from Burkina Faso, Côte d'Ivoire, Ghana, Mali, Senegal and South Africa).
- Thirty-four international mining companies.
- Researchers from twelve European and Australian research institutions.
- AMIRA International, an independent association of minerals companies that develops, brokers and facilitates collaborative research projects.
- NGOs based in Burkina Faso, Ghana and Luxembourg.
- A professional training centre based in Burkina Faso.
- National research and aid agencies in South Africa, France and Australia.

This initiative demonstrates the significant research and development achievements that can be made when the different stakeholders in the minerals sector (industry, academia, government and non-government organizations) work together to achieve their diverse goals.

The WAXI project in numbers:

- 12 countries.
- 73 partner organisations over 12 years.
- 92 Postdoc, PhD, Masters and Honours Projects, two-thirds of them African.
- 86 International Publications.
- 650 GB exploration geoscience databases.
- 5600 person-days of technical training in West Africa.

Petrogenesis, Hydrothermal Alteration and Metamorphism of the Poederberg Pillow Basalts in the Paleoproterozoic Greenstone Belt of Suriname

Stacey Amattaram

Anton de Kom Universiteit van Suriname

staceyamat@hotmail.com

Salomon Kroonenberg

Anton de Kom Universiteit van Suriname

Theo Wong

Anton de Kom Universiteit van Suriname

Paul Mason

Universiteit Utrecht

SUMMARY

This study of the morphology of the Poederberg pillows, petrography of the pillow core, rim and its interstitial material and the geochemistry give an insight on pre-metamorphic sea-water alteration, hydrothermal alteration, metamorphism and the depositional environment. According to the morphology and chemical analyses the pillows are formed at oceanic spreading centers at mid-oceanic ridges or back-arc basins with water depths of at least 2000 m. Pillow rims show alteration to palagonite, epidote, chlorite, opaques, actinolite and zoisite. During sea-water alteration palagonite is formed from the volcanic glass and elements such as Fe, Mg, Ca, N and K were likely mobilized by interaction with the heated seawater. Dissolution of Fe from the outer rims and their precipitation further inward indicates the magma flowed out in an anoxic environment. During the regional metamorphism basaltic minerals in the pillow core are metamorphosed where upon hydrothermal fluids provided cracks with quartz, calcite and epidote and hosted sulphide and gold(?).

Key words: Paleoproterozoic Greenstone Belt, pillow basalts, alteration

INTRODUCTION

The Paleoproterozoic Greenstone Belt of Suriname (Marowijne TTG Greenstone Belt) is part of a larger Greenstone Belt and metamorphosed to the Greenschist-facies. It is part of the Guiana Shield formed during the Trans Amazonian Orogeny 2.26 Ga years ago (Bosma et al., 1983; de Vletter, 1983; Delor et al., 2003a). The Marowijne Greenstone Belt is a NW-SE stretching belt in Suriname consists of three formations (Daoust et al., 2011; Kroonenberg et al., 2016).

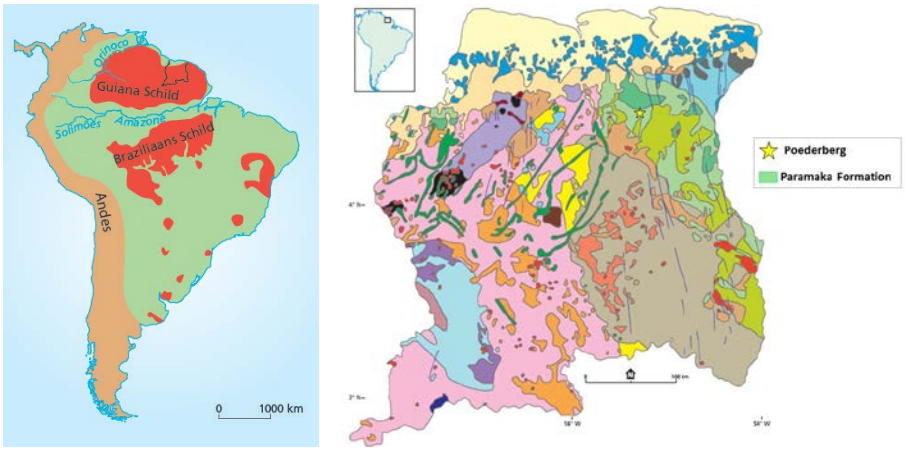

The Poederberg pillow basalts are part of the Paramaka Formation, the lowest formation. Rocks formed at this age have not yet been dated in Suriname, but it is probable that the tholeiitic basalts of the Paramaka Formation have been formed during the main phase of the Trans-Amazonian Orogeny (2.26 Ga) where new ocean crust is formed (Kroonenberg et al., 2016).

Figure 1: a) The Guiana Shield and the Brazilian Shield form together the Amazonian Craton (modified after Cordani & Sato, 1999). b) Simplified geological map of Suriname with Poederberg location (Kroonenberg et al., 2016).

The Poederberg is located in the Brokopondo District. When pillow basalts erupt under water the rim cools rapidly due to temperature differences and glass forms (Moore, 1975; Kennish & Lutz, 1997). Glass is very reactive and can be altered to the first stable minerals

called palagonite (Stroncik &Schmincke, 2002). The objective of this research was to elaborate the chemical impact of sea-water alteration, hydrothermal alteration and metamorphism on the geochemistry of the pillow lavas.

METHODS

Fieldwork to the Poederberg was conducted to describe the outcrop, collect samples and measure the width and height of the pillows. The samples were labeled by name (PB01, PB02, SA02, SA03, SA06, SA10, SA12, SA13, SA14-1 en SA30) and were send to the University of Utrecht for thin sections. Poederberg sample PB01 and samples collected by Veenstra (1983) from the Brokolonko area were analyzed using the XRF and the LA-ICP-MS. After studying the thin sections, micro XRF analysis was carried out in Utrecht to study the behavior of elements from the pillow core towards the rim.

RESULTS AND DISCUSSIONS

Morphology

The pillows have a dip of 38° with a flow direction of N320°W. An outcrop wall is divided into 4 sections (each 2x1 m) in which 51 pillows were measured. The height is parallel to the dip of the pillow and the width is perpendicular the height. The height varies from 0.2-1 m and the width varies from 0.2-1.2 m. Interstitial material is rarely present and radial cracks are absent. Chilled margins are narrow. No hyaloclastite nor vesicles are present suggesting deposition in a submarine environment at water depths of at least 2000 m (Lonsdale & Batiza, 1980). Amygdales are found in the cores. These results match with studied pillows formed at ancient BAB (Wells et al., 1979; Wilson & Versfeld, 1994; Farahat et al., 2010).

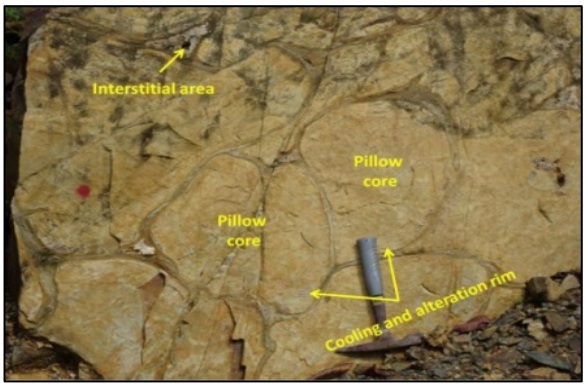

Figure 2: Sharp pointed pillow underside indicates the pillows are in normal, nearly horizontal.

Petrography

The *pillow core* is composed of radiating aggregates of actinolite, chlorite, epidote, plagioclase phenocrysts and albite. Skeletal plagioclase is altered to chlorite and epidote. Epidote is formed by pseudomorphism after pyroxene. In *pillow rim* PB02 six textural zones are observed, while in SA10 only 4 zones are present (Figure 3a,b). Zone 1 is the altered metabasalt. Zone 2-6 are formed by metamorphism of palagonite. Zone 2 is metabasalt as zone 1, but with remnants of palagonite (Figure 3c). Zone 3 consists of spherulites of tremolite, actinolite and epidote. Zone 4 is a foliated zone of chlorite, epidote spherulites, calcite and albite (Figure 3d). Zone 5 has micro-folds with epidote, titanite, quartz clusters, epidote-calcite-quartz veins (Figure 3e). Zone 6 is composed of chlorite, epidote, muscovite and has chlorite-epidote-quartz veins (Figure 3f). In SA10 a gel-like mass of epidote, quartz and actinolite is on top of zone 4 (Figure 3g). The gel show concentric bands in pillow rim SA12 and amygdale SA13 (Figure 3h,i). The *interstitial material* is composed of quartz and some amphibole.

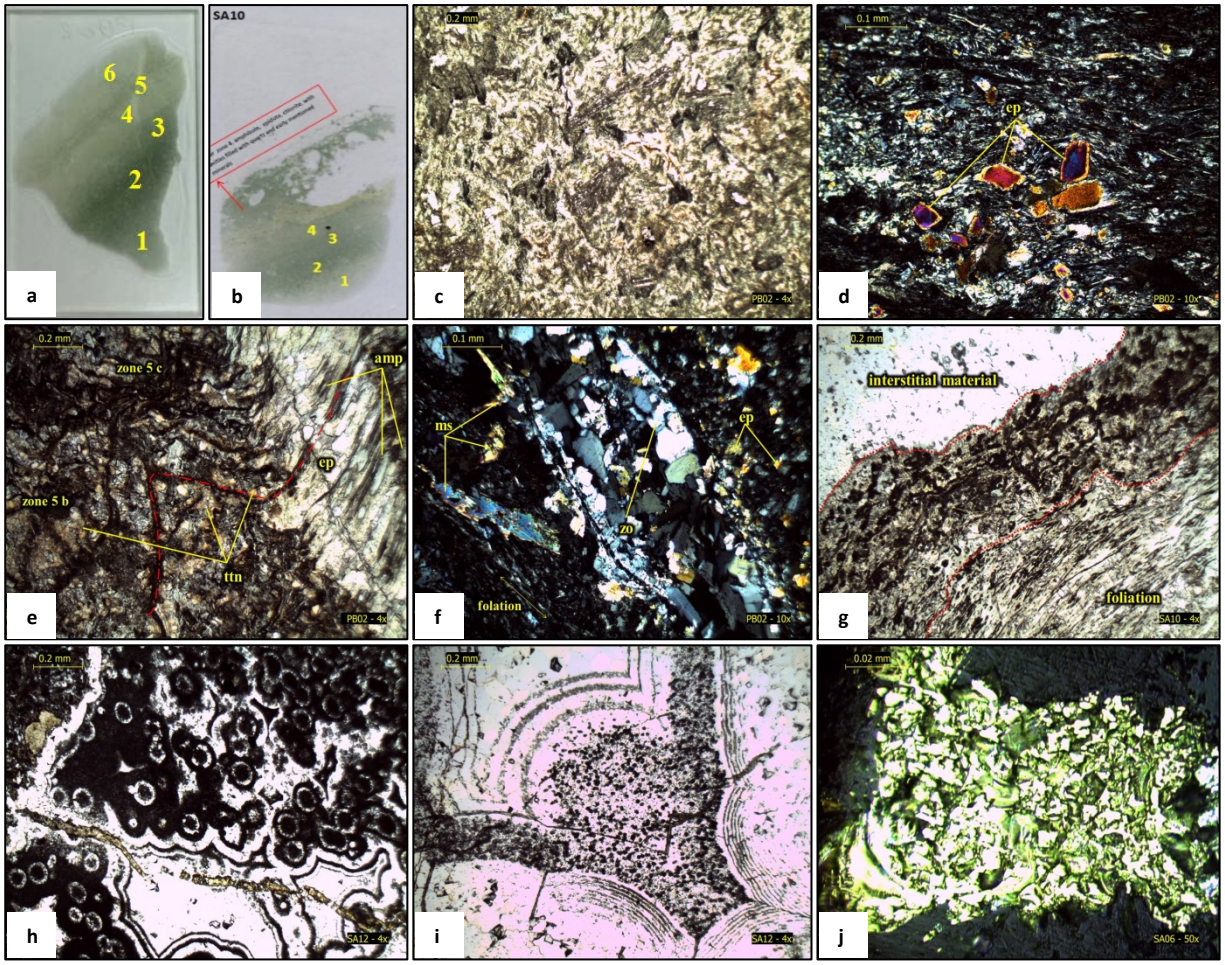

Figure 3: a) Pillow rim PB02. b) Pillow rim SA10. c) Zone 2 metabasalt and palagonite of PB02. d) Foliated zone 4 of PB02. e) Micro-folds and clustered titanite in zone 5 of PB02. f) Zone 6 of PB02. g) Gel-like mass between zone 4 and interstitial material in pillow rim SA10. h) Concentric bands in pillow rim SA12 with epidote and quartz on top of zone 1 i) Amygdale SA13 with concentric bands on top of zone 1. j) Gold inclusions in pyrite.

Geochemistry

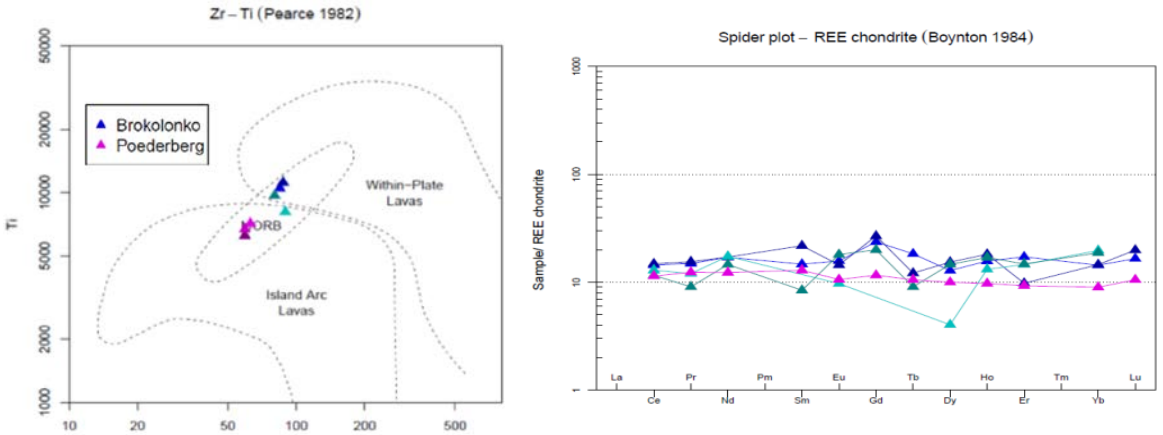

Figure 4: a) Poederberg pillows and Brokolonko basalts show MORB characteristics according to the Zr-Ti diagram by Pierce (1982). b) A flat chondrite-normalized REE diagram by Boynton (1984) indicating deposition at spreading zones.

The micro XRF given results are relative amounts in terms of counts or intensities, because the absolute quantities are hard to determine. One type of data consists of continuous counts of the zones altogether. Zone 1 which represents the metabasalt is used to determine the loss or gains in the other zones.

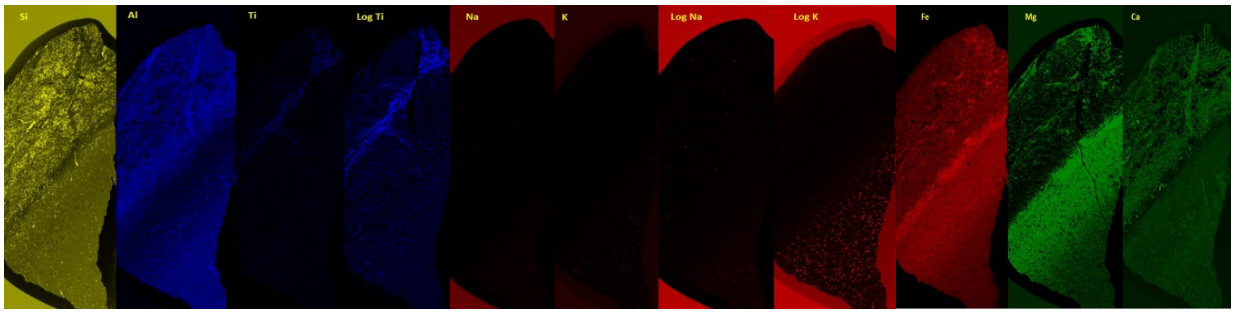

Figure 5: Spatial distribution map of PB02. Log data intensifies the color for visual purposes.

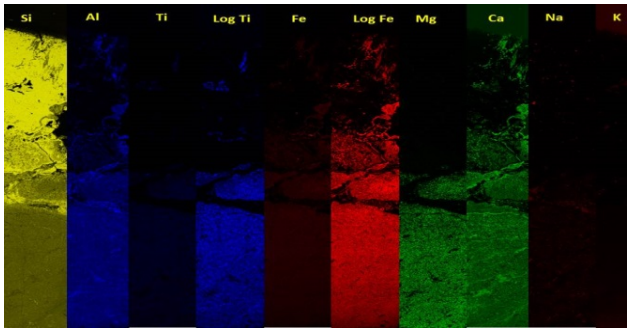

Figure 6: Spatial distribution map of SA12.

PB02: Si enriches in the outer zones, where palagonite is present. Al is in abundance in zone 4 and 5. Ti is present in de zone where titanite is in abundance. Fe is enriched in zone 1 and zone 2 along with Mg. Ca is concentrated in the outer zones due to the carbonate and calcite veins. Even though K is included in plagioclase in zone 1, there is still a low concentration in this zone. In other zones K and Na are depleted, thus there is no enrichment by seawater (Figure 5).

SA12: Si increases in the interstial material, because of quartz and quartz veins. Al, Ti, Mg and Fe are in abundance in zone 1 and the transition to interstitial material (Figure 6).

Correlation mineralogy and geochemistry

The pillow rims PB02 and SA12 are two different kind of pillow rims. Altered palagonite is present in PB02, but absent in SA12. On top of the metabasalt of SA12 a gel is precipitated with concentric bands from which epidote, quartz and less amphibole is altered. Na and K are depleted in the rims of PB02. These elements are likely dissolved in seawater during the deposition. In SA12 there is an enrichment in the rims, probably p due to the gel that is precipitated rather than enrichment by seawater.

In PB02, Mg and Fe are concentrated in the metabasalt zone 1 and zone 2 included in actinolite, chlorite and epidote. The spherulitic zone with actinolite and fine epidote (zone 3) and the foliated chlorite-rich zone with few actinolite (zone 4) are both enriched in Mg and Fe. Epidote preferentially concentrates Fe, while chlorite and actinolite can have varying proportions of Mg and Fe. Iron is depleted in SA12. But in PB02 iron Fe gets less in the rim oppose to zone 1 (metabasalt) to zone 4. However, it is still enriched (ratio is greater than 1) in the rims, because of the epidote crystals. There are two explanations for the behavior of Fe in the rims:

1. During the deposition of the metabasalt 2.26-2.0 Ga years ago, the Great Oxygenation Event just started and oxygen started to develop in the atmosphere (Holland, 2006; Session et al., 2009; Delor et al., 2003a). However, the deep ocean was still anoxic and iron was in its reduced state and therefore mobile (Holland, 2006). Iron probably dissolved in seawater and there is a chance that the iron enriched fluid migrated towards the inner palagonite zones, providing these zones with iron to form actinolite and chlorite.
2. Epidote concentrates Fe^{3+} en could be formed by epidotization. Epdiote kan be formed by pseudomorphism of actinolite and plagioclase where Fe^{3+} and Ca are enriched and Fe^{2+}, Mg, Si and H2O are depleted.

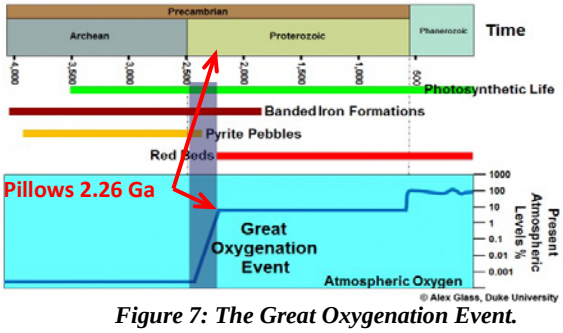

Figure 7: The Great Oxygenation Event.

Substance are being added during the epidotization (Condie et al., 1977). It is not ruled out that epidotization took place in the rims, but actinolite must have formed first after palagonite by metamorphism.

Mg is depleted in the rims of PB02, but enriched in the zone 6, because of the presence of chlorite crystals. Mg is depleted in the interstitial material of SA12.

CONCLUSIONS

The morphology shows that the Poederberg pillows have been deposited in a BAB with a water depth of at least 2000 m. According to the chemical analyses, the Poederberg pillows are deposited at spreading centers of either the MOR or BAB. The origin of the different alterations is as follow (Figure 8):

1. Sea-water (pre-metamorphic) alteration: palagonite is formed from the volcanic glass by interaction with sea-water. - Fe, Mg, Ti, Ca and (N+K) were likely mobilized by interaction with the heated seawater. - In the interstitial material a gel-like mass is deposited.
2. Regional metamorphism during Trans-Amazonian Orogeny: Basaltic minerals and palagonite are metamorphosed to actinolite, epidote, chlorite, albite. And the Gel is metamorphosed to quartz, epidote, garnet and chlorite.
3. Late-orogenic hydrothermal alteration: veins are filled with quartz-calcite and epidote, the sulfide and gold(?) mineralization are hosted by hydrothermal fluids.

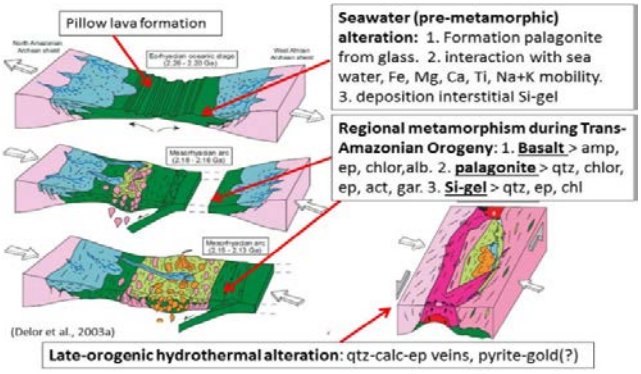

Figure 8: Schematic representation of timing of alterations (After Delor et al., 2003a).

REFERENCES

Bosma W., Kroonenberg S.B., Maas K., de Roever E.W.F., 1983. Igneous and metamorphic complexes of the Guiana Shield in Suriname, Geologie en Mijnbouw 62, p. 241-254.

Condie K.C., Viljoen M.J., Kable E.J.D., 1977. Effects of alteration on element distributions in Archean tholeiites from the Barberton Greenstone Belt, South Africa. Contributions to Mineralogy and Petrology, 64, p. 75-89.

Daoust C., Voicu G., Brisson H., Gauthier M., 2011. Geological setting of the Paleoporoterozoic Rosebel gold district, Guiana Shield, Suriname, Journal of South American Earth Sciences, p. 222-245.

de Vletter D.R., Pengel S.E., Kartoredjo H.W., 1984. Synthesis of the Precambrian of Suriname and review of some outstanding problems, Contributions to the geology of Suriname 8, Geologisch Mijnbouwkundige Dienst Suriname, Mededeling 27, p. 13-16.

Delor C., Lahondére, D., Egal, E., Lafon, J., Truffert, C., Théveniaut, H., et al., 2003a. Transamazonian crustal growth and reworking as revealed by the 1:500,000-scale geological map of French Guiana (second edition), Geologie de la France, issue 2-3-4, p. 5-57.

Farahat E.S., El Mahallwai M.M., Hoinkes G., Abdel Aal A.Y., Hauzenbeger C.A., 2010. Pillow form morphology of selected Neoproterozoic metavolcanics in the Egyptian Central Eastern Deasert and their implications. Journal of African Earth Sciences, p. 163-168.

Holland H.D., 2006. The oxygenation of the atmosphere and oceans. Dep. of Earth and Planetary Sciences, Harvard University, Cambridge, USA, p. 903-9015.

Kennish M.J., Lutz R.A., 1997. Morphology and distribution of lava flows on mid-oceanic ridges: a review. Institute of Marine and Coastal Sciences, Ruthers University, New Brunswick, NJ, USA, p.63-90.

Kroonenberg S.B., de Roever E.W.F., Fraga L.M., Reis N.J., Lafon J.M., Cordani U., Wong T.E., 2016. Paleoproterozoic evolution of the Guiana Shield in Suriname: A revised model, Netherlands Journal of Geosciences, Geologie en Mijnbouw, p. 491-522.

Lonsdale P., Batiza R., 1980. Hyaloclastite and lava flows on young seamounts examined with a submersible. Geol. Soc. America Bull., v. 91, p. 229-255.

Moor J.G., 1975. Mechanism of Formation of Pillow Lava: Pillow lava, produced as fluid lava cools underwater, is the most abundant volcanic rock on earth, but only recent have divers observed it forming. Sigma Xi, The Scientific Research Society, American Scientist, Vol. 63, p. 269-277.

Sessions A.L., Doughty D.M., Welander P.V., Summons R.E., Newman D.K., 2009. The Continuing Puzzle of the Great Oxidation Event. Review. Current Biology, v.19, p. 567-574.

Stroncik N.A., Schmincke H., 2002. Palagonite – a review. Int J Earth Sciences (Geol Rundsch), v. 91, p. 680-697.

Veenstra, E., 1983. Petrology and geochemistry of sheet Stonbroekoe, sheet 30, Suriname. Thesis Univ. Amsterdam. Also : Mededelingen Geologisch Mijnbouwkundige Dienst Suriname 26: 1-138.

Wells G., Bryan W.B., Peace T.H., 1979. Comparative morphology of ancient and modern pillow lavas. The Journal of Geology, Vol. 87, No. 4, p. 427-440.

Wilson A.H., Versfeld J.A., 1994. The early Archaean Nondweni greenstone belt, southern Kaapval Craton, South Africa, Part II. Charactersitics of the volcanic rocks and contrains on magma genesis. University of Natal, Dep. of Geology, Precambrian Research, p. 227-320.

http://www.luckysci.com/2014/09/easy-science-the-great-oxygenation-event/

The Caicara-Dalbana Belt, a Belt of Felsic and Intermediate Metavolcanics of 1.99 Ga in the Guiana Shield, and Probably Across, in the Guapore Shield

Reenuska Anandbahadoer- Mahabier
Ministry of Natural Resources of Suriname

reenuska.a.mahabier@gmail.com

Emond W.F. de Roever
Dept. of Earth Sciences, VU Amsterdam, Amsterdam, the Netherland

ederoever@ziggo.nl

SUMMARY

The felsic to intermediate metavolcanics of the Dalbana Formation in western Suriname are intermediate- to high-K calc-alkaline rocks with an age of 1.99 Ga. In the Pearce diagrams for the distinction of the tectonic setting of granites the less evolved metavolcanics plot in the volcanic arc granite (VAG) zone. Therefore, the metavolcanics are concluded to have a VAG setting. The metavolcanics of the Dalbana Formation can be correlated with the Caicara Formation in Venezuela, the Surumu Formation in Roraima, the Iwokrama volcanics in Guyana and the Igarapé Paboca Formation in Para, Brazil. The name Caicara-Dalbana belt is proposed for the 1400 km long belt of metavolcanics and associated subvolcanic granites, which stretches from Venezuela to Para, north of the Amazon. The belt probably continues south of the Amazon, in the Tapajos Gold province, where the Vila Riozinho Formation consists of similar metavolcanics, with the same age and chemistry.

Key words: Trans-Amazonian Orogeny, Guiana Shield, Metavolcanics, Dalbana Formation

INTRODUCTION

A large part of western Suriname, in the northern part of the Guiana shield, is occupied by felsic to intermediate metavolcanics of the Dalbana Formation, closely associated with subvolcanic granites and biotite granites (figure1). A zircon Pb/Pb analysis for a metavolcanic sample from the Sipaliwini River, near the border with Brazil gave an age of 1.99 Ga (de Roever et al., 2011). Geochemical results show that these rocks are intermediate- to high-K calc-alkaline, with I-type affinity. Metavolcanics with similar geochemistry and age can be found in the Caicara Formation in Venezuela, the Surumu formation in Roraima and the Iwokrama volcanics in Guyana.

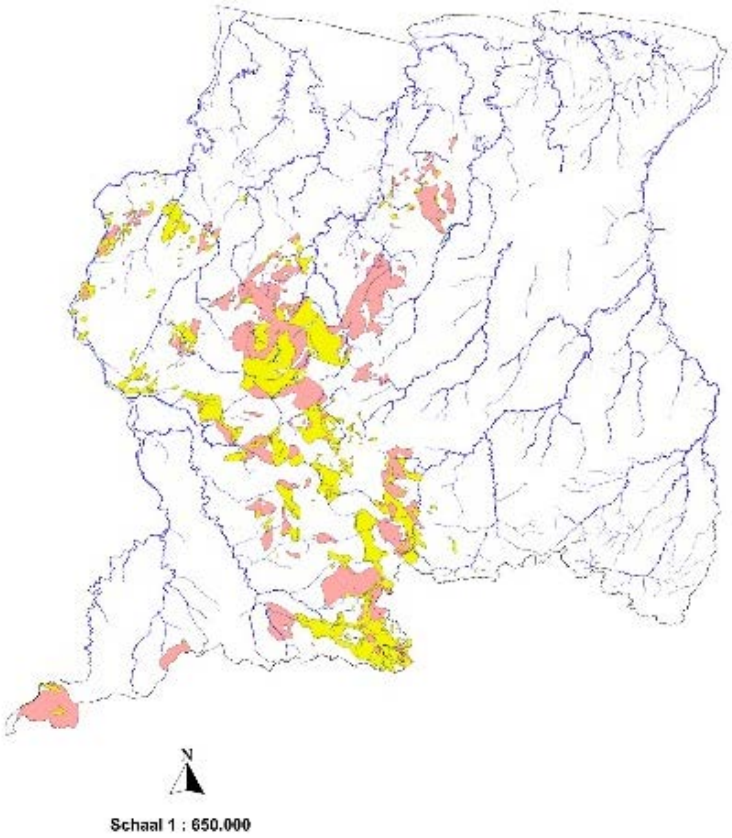

Figure 1: Felsic to intermediate metavolcanics (yellow) with associated subvolcanic granites (pink) in Suriname.

METHODS

A total of thirteen metavolcanics rocks, ranging from acid to intermediate, from the central part (Wilhelmina Mountains) and southern part (Sipaliwini River) were analyzed by XRF and ICP-MS in the Geological department at the Vrije Universiteit Amsterdam. The XRF data of the rocks from the Wilhelmina Mountains (Verhofstad, 1971) have been used, as well.

CHEMISTRY RESULTS

The metavolcanics of the analyzed rocks of Suriname range from basaltic andesite to rhyolite, with 3-8 % alkalies and a silica content between 52 to 78%, figure 3 and 4. The symbols used for the results are given in figure 2. The variation diagrams for the major elements show clear differentiation trends, with a positive correlation of SiO_2 with K_2O, a negative correlation with FeO, MgO, Al_2O_3 and CaO, and an initial positive correlation for Na_2O and Al_2O_3, followed by a negative correlation from around 65% SiO_2. These rocks are further intermediate- to high-K calc-alkaline rocks (figure 5), with an I-type affinity. The multi-element variation diagram shows a strong negative anomaly for Nb and Ta (characteristic of volcanic arcs) and Ti as well as a marked LILE enrichment compared to HFSE, figure 7. Trace element levels suggest an active continental margin as setting for the volcanics (see Schandl and Gorton, 2002), figure 8.

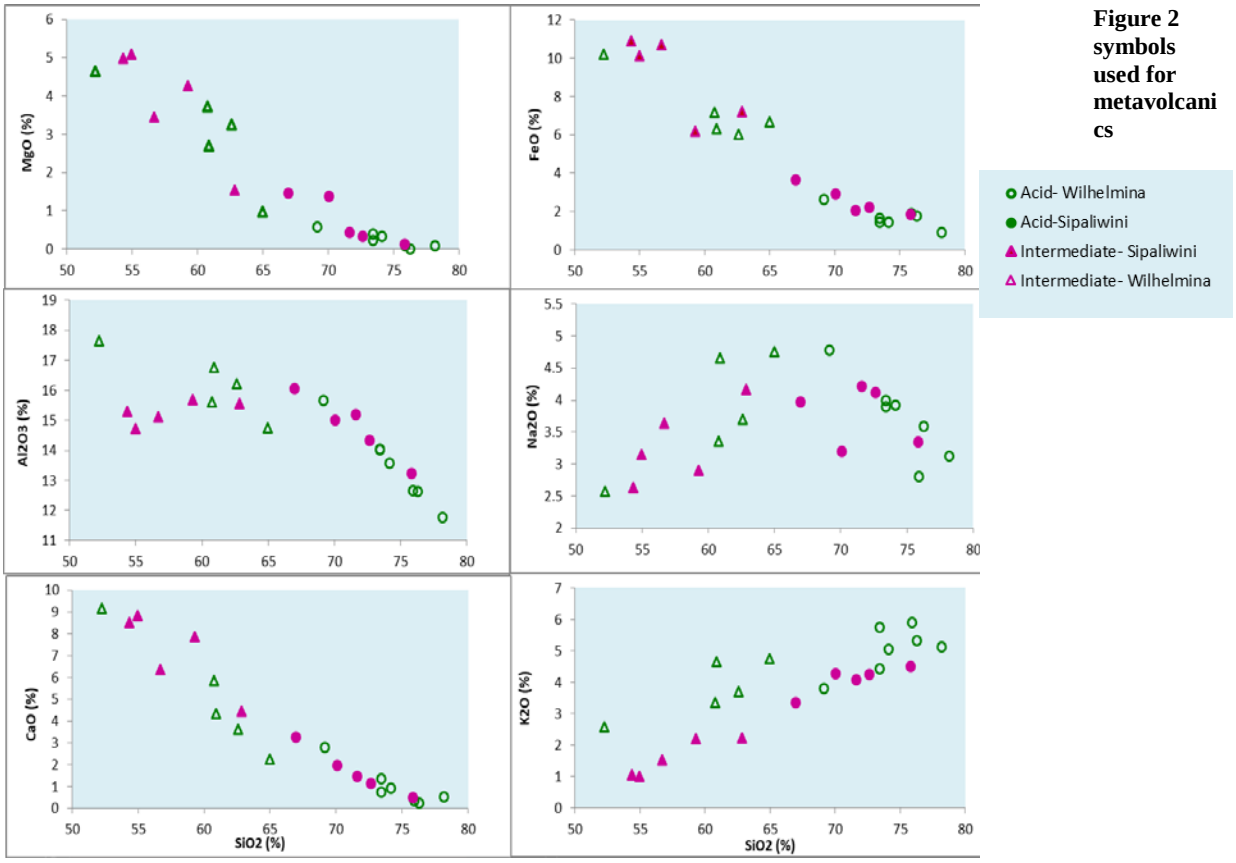

Figure 2 symbols used for metavolcanics

Figure 3 Silica vs major elements, variation diagrams

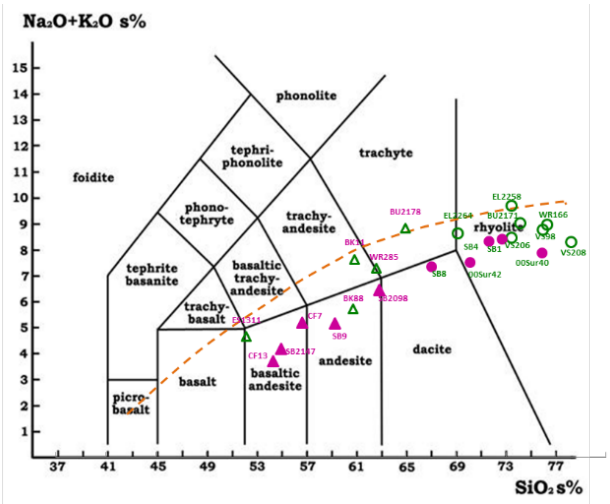

Figure 4: TAS diagram by Le Bas et al (1986) for volcanic rocks

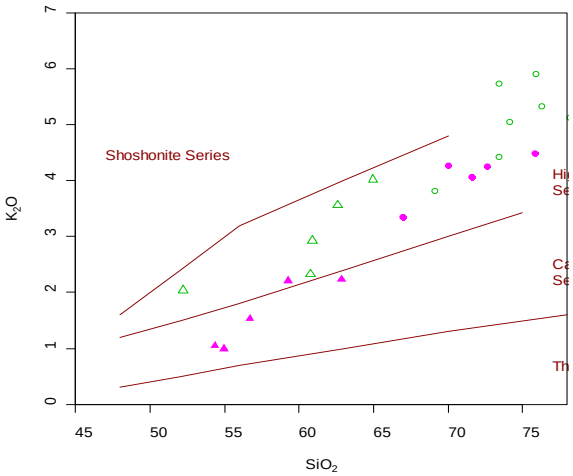

Figure 4: K2O versus silica plot by Taylor et al. (1976)

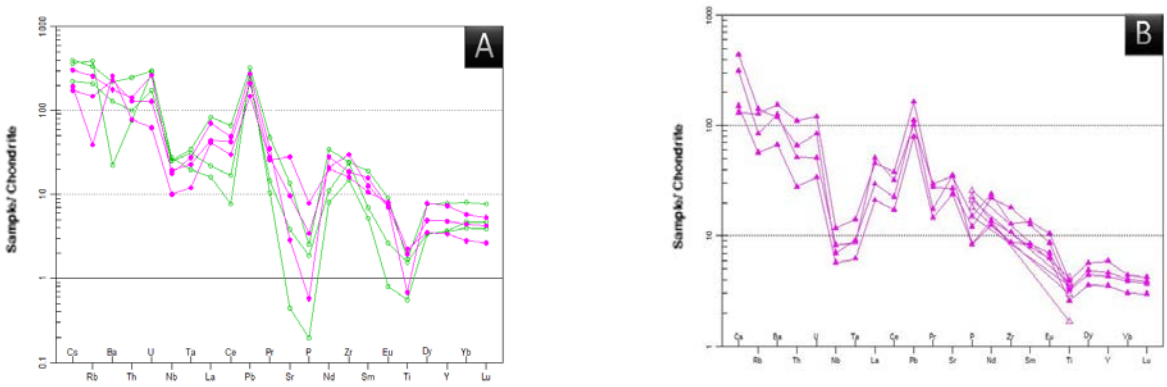

Figure 5: Multi-element variation diagram after Sun and Mc Donough (1989) a) for the felsic rocks and b) for the mafic ones.

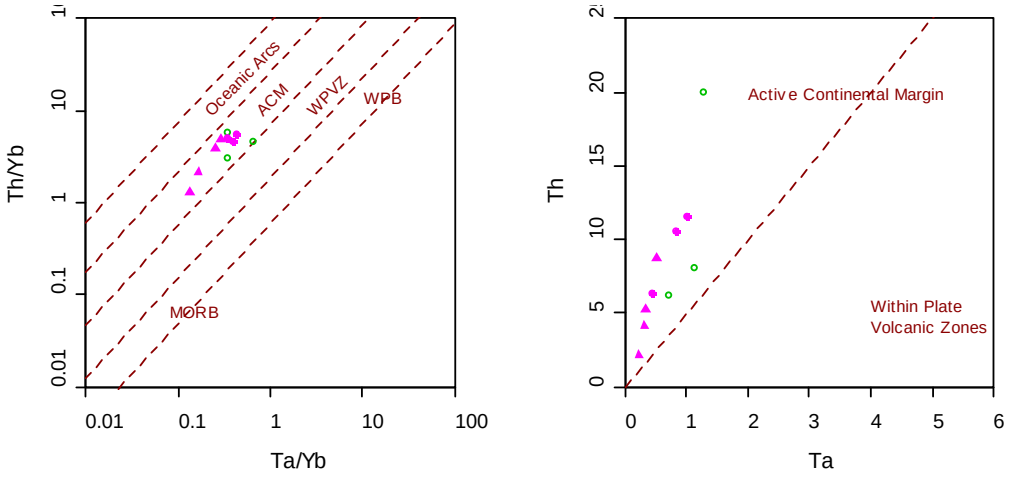

Figure 6: Granite tectonic diagrams by Schandl and Gorton (2002).

In the Pearce diagrams, figure 9, for the distinction of the tectonic setting of granites the analysed metavolcanics plot mainly in the field where the volcanic arc granite (VAG) zone overlaps with the post-collisional granite zone, but less evolved samples plot outside that field, in the VAG zone. Therefore, the metavolcanics are concluded to have a VAG setting. Verhofstad (1971) concluded that the metavolcanics indicate a subduction zone.

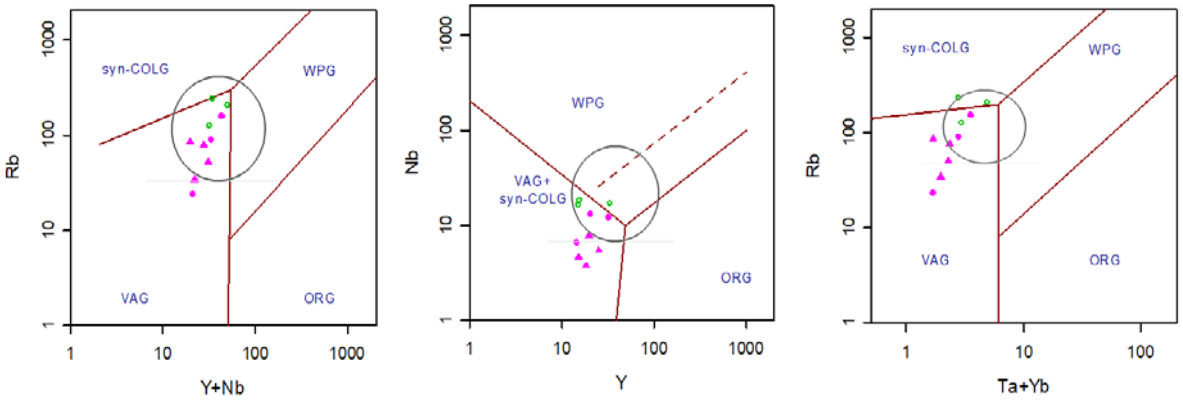

Figure 7 Trace element discrimination diagrams for granitic rocks by Pearce et al (1984), WPG= Within Plate Granites, VAG= Volcanic Arc Granites, COLG= Collisional Granites, ORG= Ocean Ridge Granites

DISTRIBUTION OVER THE GUIANA SHIELD

The metavolcanics of the Dalbana Formation can be correlated with the Caicara Formation in Venezuela, the Surumu Formation in Roraima State, Brazil and the Iwokrama Formation in Guyana, as they show close similarities in major and trace element composition (Brooks et al., 1995; Fraga et al., 2010; Berrange, 1977) and also have an age of around 1.99 Ga, figure 10 and table 1. The belt was

named the CSID belt by Klaver et al. (2015) after the first letters of the formations. However, the belt continues across the southern border of Suriname into Para State, Brazil. More to the south, near the Trombetas River north of the Amazon, the metavolcanic Igarapé Paboca Formation was recently mapped in several areas (Castro et al., 2014; Barreto et al., 2013) and was found to have a similar age. The name Caicara – Dalbana belt is proposed for the belt of metavolcanics, which runs for more than 1400 km through the center of the Guiana Shield. The 1.99 Ga age is a clear distinction from the 1.88-1.89 Ga age of volcanics of the Iricoumé volcanics, which occur in large areas in Para State.

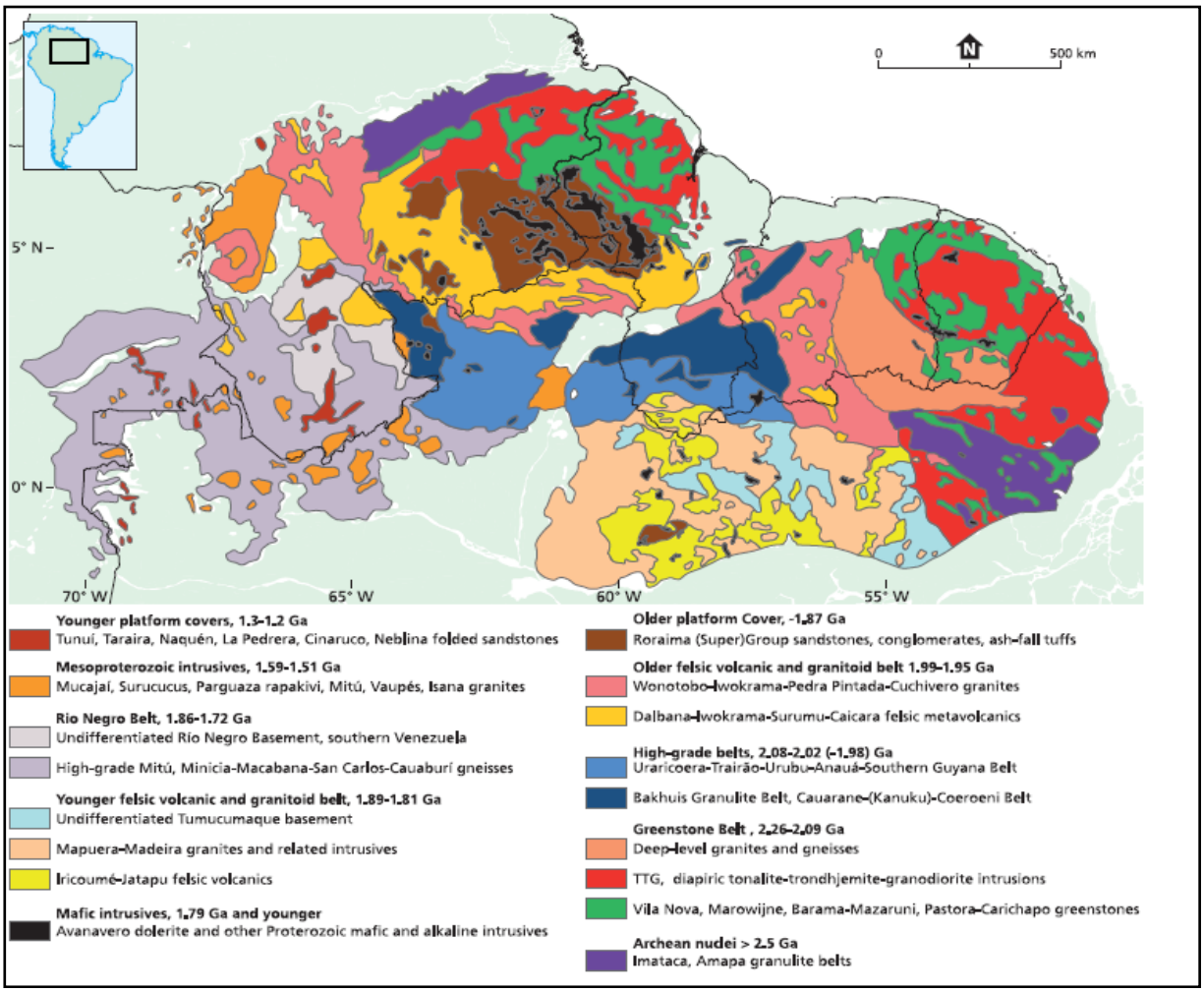

Figure 8 Simplified geological map of Guiana shield (Kroonenberg et al. 2016)

Dalbana (Suriname)	1987	±4	Pb-Pb evap.	de Roever et al., 2011, 16
Surumu (prov. Roraima)	1966	±9	U-Pb convent.	Schobbenhaus 1994
	1977	±8	U-Pb SHRIMP	Santos in Reis et al, 2000
	1984	±9	U-Pb SHRIMP	Santos et al., 2003
	2006	±4	Pb-Pb evap.	Costa et al., 2001
	1990	±3	Pb-Pb evap.	Fraga et al., 2010
Cachoeira de Ilhas (prov. Roraima)	1990	±5	Pb-Pb evap.	Fraga et al., 2010
Caicara (Venezuela)	1980			Brooks et al, 1995
Iwokrama volc + subvolc. (Guyana)	1980-91		U-Pb LA-ICP-MS	Nadeau et al., 2013
Igarapé Paboca (prov. Para)	1992	±3	Pb-Pb evap.	Barreto et al., 2013
	1992	±6	Pb-Pb evap.	Castro et al., 2014
	1948	±6	Pb-Pb evap.	Castro et al., 2014
Vila Riozinho (Tapajos prov.)	1998	±3	Pb-Pb evap.	Lamarao et al., 2002
	2000	±4	Pb-Pb evap.	Lamarao et al., 2002

Table 1 Age of the metavolcanics

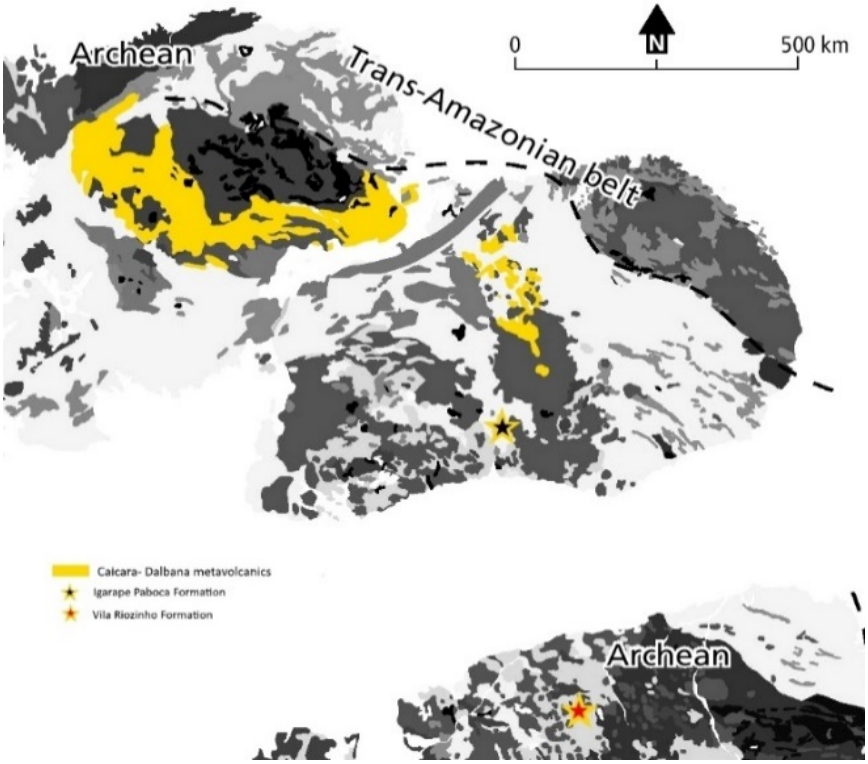

Figure 9 Location of Vila Riozinho Formation on map modified after Kroonenberg (2010)

The belt most probably continues south of the Amazon Basin, in the Tapajos Gold province, where the Vila Riozinho Formation, figure 11, consists of metavolcanics with the same age and chemistry (Lamarao et al., 2002). Leal et al. (2018) has found large similarity of the metavolcanics and associated granites from this area with those from the Trombetas River area north of the Amazon.

DISCUSSION

The Caicara-Dalbana belt is rather complex, because it consists of two branches. From Venezuela to Surinam the belt runs roughly W/NW to E/SE. In NW Surinam, near the Bakhuis Granulite Belt, the direction changes abruptly to NNW – SSE, and continues in that direction towards the Amazon. The Dalbana metavolcanics are concluded to indicate volcanic arc magmatism (Mahabier, 2017; see above). The same holds for the Igarapé Paboca Formation of Para State, where subduction probably was to the E-ENE, towards the continental mass in the East (Leal et al., 2018). However, in the western part of the belt northward subduction is assumed. The Surumu metavolcanics of Roraima State have been suggested to represent post-collisional magmatism, formed after the collision of the high-grade Cauarane-Coeroeni belt with the Rhyacian greenstone block north of it, at 2.00 – 1.99 Ga (Fraga et al., 2008), as a result of the northward subduction. The 1.99 Ga age of the metavolcanics of Suriname and Roraima and Para States is hardly different from the collision age. It is difficult to consider the metavolcanics as post-collisional volcanism, the more so since usually there is a considerable time gap between collision and post-collisional magmatism. In view of their age and VAG setting the Suriname metavolcanics are considered to represent a pulse of end-arc volcanism with which subduction ends in many cases. For the southern branch of the Caicara-Dalbana belt, in Para State, the picture is more simple, collision did not occur, a high-grade metamorphic belt is not present. At present an explanation for the complexity of the Caicara-Dalbana belt is lacking. With their age of 1.99 Ga, the metavolcanics clearly form part of the Trans-Amazonian Orogeny (2.3 – 1.95 Ga), but represent only a late stage, after the main stage during which the greenstone belt was formed and metamorphosed. The metavolcanics show open folding and low-grade regional metamorphism, which are absent in the post-Trans-Amazonian Roraima sandstone. Therefore, the folding and metamorphism are also concluded to be due to the Trans-Amazonian orogeny, but to an even later stage.

CONCLUSIONS

- The metavolcanics of the Dalbana Formation in western Suriname can be correlated with the Caicara Formation in Venezuela, the Surumu Formation in Roraima, the Iwokrama Formation in Guyana and the Igarapé Paboca Formation in northern Para, as they show similar major and trace element chemistry and have an age of around 1.99 Ga. The name Caicara – Dalbana belt is proposed for the belt, which runs for more than 1400 km through the center of the Guiana Shield.
- The Caicara-Dalbana belt, the greenstone-TTG belt along the Atlantic coast and the high-grade Cauarane-Coeroeni belt are the major belts of the Guiana Shield.
- The Caicara-Dalbana belt most probably continues south of the Amazon Basin, in the Tapajos Gold province, where the Vila Riozinho Formation consists of similar metavolcanics, with the same age and chemistry.
- The belt has a complex character, with two branches of different direction.
- The volcanic arc character considered for the Dalbana Formation agrees with that found for the Igarapé Paboca and Vila Riozinho Formations in Para State.

REFERENCES

Barreto, C., Lafon, J., Da Rosa-Costa, L., & de Lima, E. (2013). Vulcanismo félsico Paleoproterozoico do Grupo Iricoumé, Domínio Erepecuru-Trombetas, Província Amazônia Central: Dados de campo, caracterização petrográfica e geocronologia Pb-Pb em zircão. *Revista do Instituto de Geosciencias - USP 13*, 47-72.

Berrangé, J. (1977). The geology of southern Guyana, South America. *Overseas Memoir 4*, Institute of Geological Sciences, London.

Castro, J., Silva, R., Rosa-Costa, L., & Barbosa, J. (2014). Mapa geológico da folha Rio Trombetas – SA.21-X-A. Belém, CPRM-Serviço Geológico do Brasil, Programa Geologia do Brasil. Escala 1:250.000.

Fraga, L., Reis, N., Dall'Agnol, R., & Armstrong, R. (2008). Cauarane - Coeroene belt - the tectonic southern limit of the preserved Rhyacian crustal domain in the Guyana shield, northern Amazonian craton. 33th Internat. Geol. Congress Oslo, Abstract AMS-07.

Kroonenberg S.B., de Roever E.W.F., Fraga L.M., Reis N.J., Faraco T., Lafon J.-M., Cordani U. and Wong T.E. (2016). Paleoproterozoic evolution of the Guiana Shield in Suriname: A revised model, *Netherlands Journal of Geosciences*, pp 1 - 32.

Klaver, M., de Roever, E., Nanne, J., Mason, P., & Davies, G. (2015a). Charnockites and UHT metamorphism in the Bakhuis Granulite Belt, western Suriname: Evidence for two separate UHT events. *Precambrian Research 262*, 1–19.

Lamarao, C. N., Dall'Agnol, R., Lafon, J.-M., & Lima, E. F. (2002). Geology, Chemistry, and Pb- Pb zircon geochronology of the Paleoproterozoic magmatism of Vila Riozinho, Tapajos Gold Province, Amazonian craton, Brazil. *Precambrian Research 119*, 189-223.

Leal R. E. , Lafon J. M., Rosa- Costa L. T. & Dantas E. L. (2018). Orosirian magmatic episodes in the erepecuru-trombetas domain (southeastern Guyana shield): Implications for the crustal evolution of the Amazonian craton. *Journal of South American Earth Sciences 85*, 278–297

Mahabier R (2017). Geological history of the Dalbana Formation and its relation to the Trans-Amazonian Orogeny, Suriname, South America, Master thesis, Anton De Kom University of Suriname, pp. 1 - 95.

Verhofstad, J. (1971). The geology of the Wilhelmina Mountains in Suriname, with special referene to the occurrence of Precambrain ash-flow tuffs. Thesis Univ. Amsterdam.

A multi-scale roughness map of the Guiana shield

David Baratoux*

Geosciences Environnement Toulouse

14, Avenue Edouard Belin
31400, Toulouse, France

david.baratoux@ird.fr

SUMMARY

Roughness mapping is a common technique in geomorphology which have been widely applied for geological mapping of extra-terrestrial planets. Application of this technique is less common on the Earth, where field mapping is possible. Recent work at the West African Craton illustrates the value of this technique in the Sahelien or tropical contexts where outcrops are scare. Lithology, tectonic activity and climatic history control surface roughness. In order to separate the contribution of the different factors, roughness maps are generally calculated at different scales. We present here the first roughness maps of the Guiana shield at a resolution of ~100 m/pixel with baselines of respectively 990m, 2790 m and 8190 m. The maps are derived from denoised SRTM data that were released recently. Individual 5°*5° SRTM tiles in cylindrical projections were first converted to UTM projections. The roughness algorithm was then applied to each tile. Roughness tiles where then converted back to cylindrical projection and assembled to form a complete roughness map of the Guiana shield that is presented a RGB composite (R = roughness at 990m, blue = roughness at 2790m and blue = roughness at 8190 m). We will present the preliminary interpretations of the map focusing on the apparent large-scale correlations between geological units and roughness units. We will also present a few examples illustrating the potential value of this roughness map for high-resolution geological mapping and mineral exploration.

Key words: Topography, morphology**,** Roughness, Guiana shield.

INTRODUCTION

Roughness mapping is a standard technique in geomorphology which have been widely applied for geological mapping of extra-terrestrial planets (e.g., Shepard et al. 2001, Kreslavsky et al. 2000). Applications to morphological studies in the Earth are less frequent, with a focus on physical volcanology and fluvial landforms (Smith 2014). The roughness of a the Earth surface is controlled by surface processes and climate and by the lithology of the rocks underlying superficial materials (soils, regoliths). Recent work at the West African Craton illustrates the potential of this technique to support geological mapping and characterization of surface processes in the Sahelien or tropical contexts where outcrops are scare (Niang et al. 2018). The purpose of this study is to explore the value of roughness mapping over the Guiana shields in a similar fashion. We present at this stage the first roughness map of the Guiana shield at 100 m/pixel, calculated for three different scales (990m, 2790 m and 8190 m) from denoised SRTM data (Yamaziki et al. 2017). A shaded relief map of the Guiana shield has been also produced from these data. Denoised SRTM data, named MERIT DEM, calculated by Yamaziki et al. (2017), were downloaded from http://hydro.iis.u-tokyo.ac.jp/~yamadai/MERIT_DEM/index.html. These data have been first processed to generate a shaded relief map of the Guiana shields (Fig. 1), which highlight existing correlations between topography and certain geological units (Fig. 2). The Figure 1 and 2 illustrate existing and non-existing correlation between the shaded relief map and main geological units. For instance, the Older platform cover (brown unit) is easily delineated in the shaded relief map. Dykes and faults are also apparent. Preliminary examination of specific areas, such as younger mafic intrusive rocks suggest possible improvement of the contours of geological units. However, there are many lithological contacts which does not correspond to obvious topographic expressions. We therefore explore here the value of roughness maps calculated at different scales.

METHOD

These MERIT DEM are provided as 5°*5° tiles in cylindrical projection. The cylindrical projection stretches distances east-west and is not appropriate for roughness calculation. The appropriate projections for calculation for roughness maps are conformal projection, such as the widely used Universal Transverse Mercator projection. Given the large volume of data (540 millions of pixels), it is difficult to process the entire area of the Guiana shield globally on laptop computer. The roughness algorithm that is described below is applied on separate files containing 5000*5000 pixels. The following procedure is therefore applied : a) re-organization of the data as overlapping tiles, since the edges of each file have to be discarded after application of the reprojection steps and roughness calculation, b) reprojection of each tile in UTM projection at 90m/pixel, using the center of the tile to define the most appropriate UTM projection parameters, c) removal of edges of the file (the initially square tile is now slightly deformed, and blank edges need to be removed before application of the roughness algorithm), d) application of the roughness algorithm to the tile in UTM projection, e) reprojection

of the roughness tile in cylindrical coordinates at a resolution of 0.001 degre/pixel. The tiles in cylindrical coordinates are finally assembled to produce the roughness maps of the Guiana shield.

There are alternative options to calculate roughness parameters, since there is no universal definition of the intuitive notion (Kreslavsky et al. 2013). In this investigation, the roughness is quantified using the interquartile scale variation of topography in a sliding window (Aharonson et al. 1998) :

$$R = \frac{N}{0.673(2N-1)}(Q_3 - Q_1) \qquad (1)$$

where Q_i is the elevation of the i^{th} quartile point and N is the number of points. The term 0.673 is a normalization factor corresponding to a normal distribution (i.e., R = 1 for a normal distribution). The roughness is calculated for 990 m, 2970 m, 8910 m, corresponding to window widths of 11, 31 and 91 pixels, respectively (odd numbers are chosen, so the roughness may be easily calculated at the center of each window). The three roughness maps are represented as a RGB image, with small scale roughness (990 m) assigned to the red channel, intermediate-scale roughness (2970 m) assigned to the green channel, and larger-scale roughness (8910 m) assigned to the blue channel. An image with a different color stretch may be produced to focus on rough or smooth areas (it is generally difficult to represent the wealth of information contained as float values using the 256 levels of each channel).

The roughness map is then compared to the most recent geological map of the Guiana shield (Kroonenberg et al. 2016). For this purpose, the map provided by Kroonenberg et al. 2016 has been georeferenced using 50 ties points across the shield (based on the shape of the boundaries of the countries). The geological map has then been reprojected in cylindrical projection.

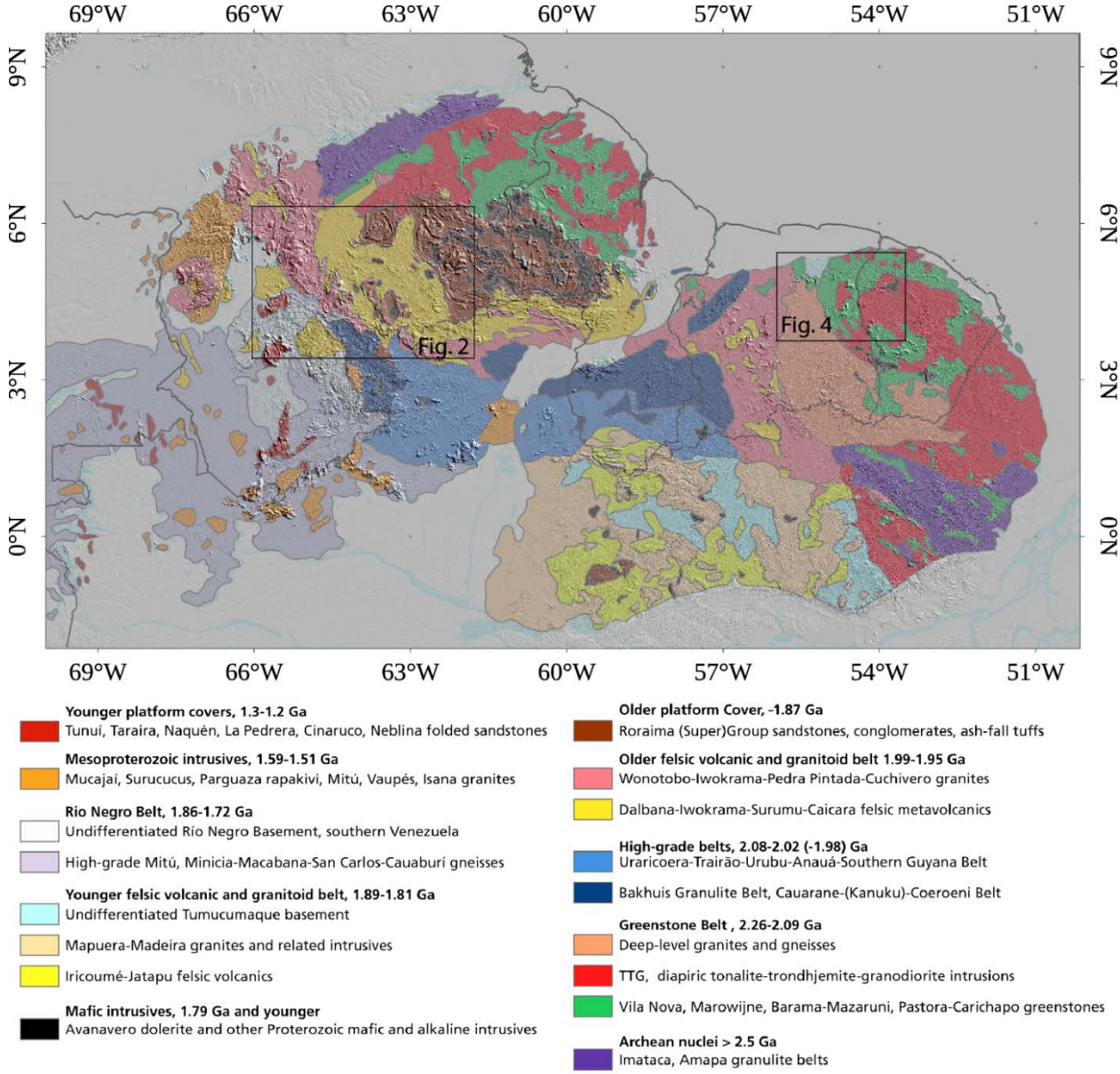

Figure 1 – Geological map of the Guiana shield from Kronenberg et al. (2016) overlaid on a shaded relief image derived from denoised SRTM data (Yamaziki et al. 2017).

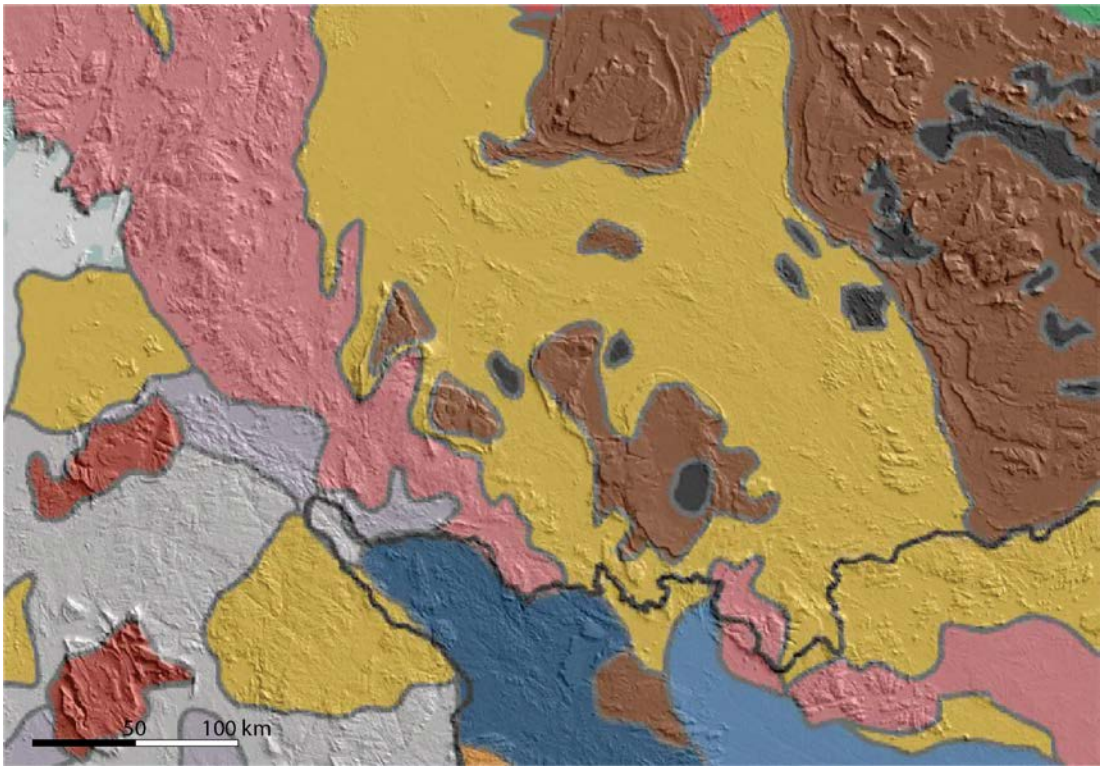

Figure 2 – Close-up view of relationships between the shaded relief map and the geological map provided by Kronenberg et al. (2016). Note for instance the association of sandstones with topographic highs.

RESULTS

At this stage, the roughness calculation has been achieved for the the northern part of the Guaina shield. The roughness map is presented in Figure 3. Figure 4 illustrates the correlation between roughness of lithological units.

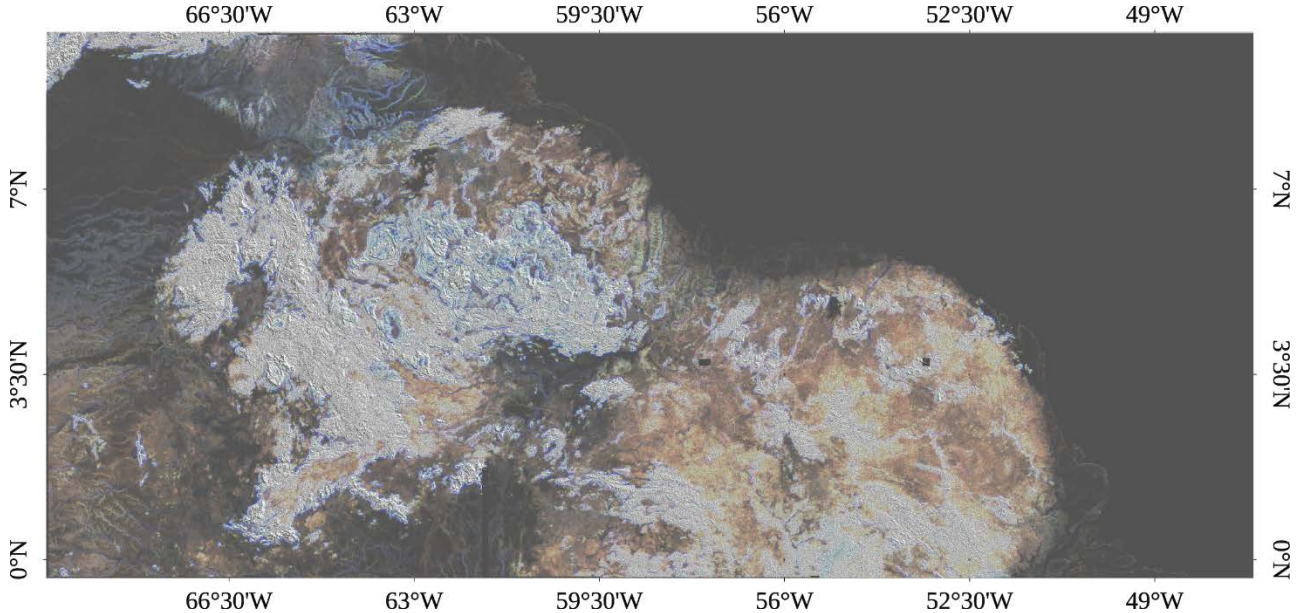

Figure 3 – Northern part of the roughness map of the Guiana shield (Red channel = rougness at 990m, Green channel = rougness at 2790 m and Blue channel = roughness at 8190 m).

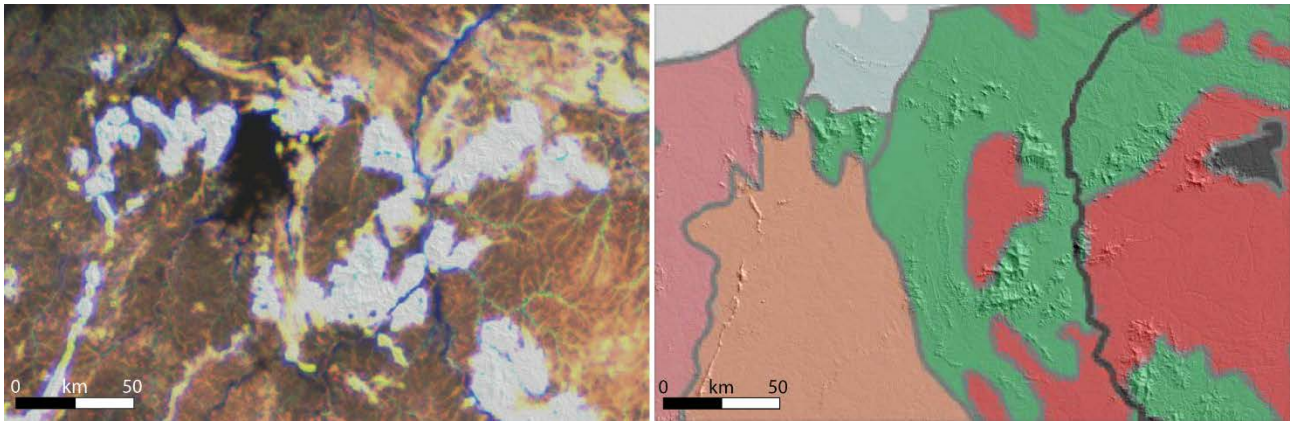

Figure 4 – Illustration of the association of roughness units (left) with geological units (right, see Fig. 1 for legend and location of the close-up view). For the roughness map, the R, G and B channels correspond to roughness values calculated with baselines of 990m, 2790m and 8190m, respectively.

Several first-order associations between lithology and geology are noted. Sandstones, high-grade belts, felsic and mafic rocks may be distinguished on the roughness map. The close-up view of the roughness map presented in Figure 4 illustrates for instance the association of high roughness values with greenstones and mafic intrusive rocks and lower roughness values association with TTG, granites and other felsic rocks. Such association may be used to refine the outlines of geological units. Active and ancient fluvial networks may be also recognized.

CONCLUSIONS

The following products have been derived in support to global-scale and high-resolution geological mapping of the Guiana shield: a) a shaded relief map of the Guiana shield at 0.001 degree/pixel (~100 m/pixel) available in geotif format (cylindrical projection) and kml format for visualisation with the Google Earth software, c) a roughness containing three bands for roughness values at 990m, 2790 m and 8190 m. The resolution of each band are respectively 90m, 270 m and 810 m. The map is available in geotif format and as a RGB composite image in geotif and kml format for visualization with Google Earth. The preliminary examination of shaded relief and roughness maps indicate their potential for geological mapping and characterization of surface processes, as in the context of the West African Craton. The value of roughness maps with shorter and longer baselines needs to be examined. In particular, we expect that roughness maps calculated from high precision and high-resolution Lidar would be of great value for characterization of surface processes. Roughness maps should also be used jointly with geophysical and satellite imagery, focusing for instance on the significance of the existence of similar geometric patterns in multiple data sets.

ACKNOWLEDGMENTS

Dr. Dai Yamaziki is acknowledged for providing access to the denoised SRTM data.

REFERENCES

Kreslavsky, M.A., Head, J.W., 2000. Kilometer-scale roughness of Mars: results from MOLA data analysis. Journal of Geophysical Research 105, 26695–26712.

Kroonenberg, S.B.,. de Roever, E.W.F , Fraga, L.M., Reis, N.J., Faraco, T. , Lafon, J.-M., Cordani, U., and Wongn T.E. (2016) Paleoproterozoic evolution of the Guiana Shield in Suriname: A revised model. Netherlands Journal of Geosciences, doi:10.1017/njg.2016.10.

Niang, I. (2018) The roughness map of the West African Craton: application to geological mapping and identification of superficial processes, master thesis, University Cheikh Anta Diop.

Shepard, M.K., Campbell, B.A., Bulmer, M.H., Farr, T.G., Gaddis, L.R., Plaut, J.J. (2001) The roughness of natural terrain: A planetary and remote sensing perspective. Journal of Geophysical Research, 106, E12, 32777-32795.

Mapping and correlation of West African and South American mafic dykes

Lenka Baratoux*
IRD GET
14 avenue E. Belin, Toulouse, France
lenka.baratoux@ird.fr

Mark W. Jessell
CET UWA
35 Stirling Highway, Crawley Australia
mark.jessell@uwa.edu.au

Richard E. Ernst
Carleton Uni
Ottawa, ON K1S 5B6, Canada &
Tomsk State U., Tomsk, 634050 Russia
Richard.Ernst@ernstgeosciences.com

SUMMARY

Mapping of dyke swarms of Large Igneous Provinces provides key constraints for the reconstruction of paleocontinents. In this paper, we propose an updated map of dyke swarms in the Guiana Shield based on regional airborne magnetic database combined with dykes and sills from existing literature. We compare this dyke distribution with the dykes mapped and dated in the West African Craton. We also discuss possible links between the swarms of the West African Craton and the Guiana Shield through time.

Key words: West African Craton, Guiana Shield, Large Igneous Provinces

INTRODUCTION

The history of the West African Craton (WAC) and the Guiana Shield of the Amazonian Craton spans over 3.5 Ga, with evidence of multiple mafic intrusive events, which may be classified as Large Igneous Provinces (Ernst 2014). Many of these have an undetermined age or an age determined by K-Ar methods, which is considered to be unreliable in the light of recent U-Pb baddeleyite ages (e.g. Ernst et al., 2013; Reis et al., 2013; Jessell et al. 2015; Baratoux et al., in press). Mapping of dyke swarms provides key constraints for the reconstruction of paleocontinents. The connection between the South America and West Africa since the Paleoproterozoic was suggested by several authors (e,g., Ledru et al., 1994; Nomade et al. 2003; Johansson 2014; Pisarevsky et al. 2014; Baratoux et al., in press). A link between the ~1790 Ma Libiri swarm (West Africa) and Avanavero swarm (South America) and ~1520-1528 Ma Essakane and Sambarabougou swarms (West Africa) and Käyser swarm (South America) was proposed by Baratoux et al. (in press) based on U-Pb baddeleyite ages.

The recent map of the dykes in the West African Craton comprises dykes found in the field and in an airborne magnetic database (Jessell et al., 2015). The most complete maps of the doleritic dykes in the Guiana Shield are those of Sial et al. (1987), Gibbs (1987) and Reis et al. (2013); however, none of these provide detailed maps based on airborne geophysical data. In this paper, we propose an updated map of the dyke swarms in the Guiana Shield based on the regional airborne magnetic database. We compare this dyke distribution with the dykes mapped and dated in the West African Craton (Jessell et al., 2015; Baratoux et al., in press) using a 200 Ma reconstruction of Matthews et al. (2016).

GEOLOGICAL SETTING

Both West African Craton and Guiana Shield are made of Archean nuclei of ages ranging in age between 3.3 and 2.6 Ga, which are tectonically juxtaposed to Paleoproterozoic granitoid-greenstone domains (2.25 – 1.95 Ga) (Delor et al. 2003; Kroonenberg et al. 2016; Montgomery 1979; Tassinari and Macambira, 1999; Avelar et al. 2003; Ledru et al. 1994, Kouamelan et al. 2015; Parra-Avila et al. 2017). In West Africa, this older basement is unconformably covered by Meso- and Neoproterozoic sedimentary basins (Taoudeni, Volta, Iullemeden (Teal and Kah 2005; Rooney et al. 2010; Kah et al. 2012). The southernmost part of the Guiana Shield is formed of felsic volcanics and granitic intrusions, dated at 1.89-1.81 Ga (Reis et al. 2003). The Río Negro belt in the southwest yields even younger ages of 1.86-1.72 Ga and is intruded by Mesoproterozoic granitoids (1.59-1.51 208 Ga) (Tassinari and Macambira 1999; Santos, et al. 2000). Scarce sediments of the younger platform cover (1.3-1.2 Ga) were found on the Río Negro belt (Kroonenberg et al. 2016).

In the West African Craton and the Guiana Shield, up to 26 and 19 distinct dyke swarms were identified by previous work, respectively (Reis et al., 2013; Jessell et al., 2015). These dyke swarms and associated sills span ages between 2688 Ma and 201 Ma and the youngest basalt intrusions in Senegal are as young as 500 000 Ma (for the review of published ages on dyke swarms see Ernst et al., 2013; Jessell et al., 2015; Baratoux et al., in press; Teixeira et al., in press).

RESULTS

We have mapped the dykes occurring in the Guiana Shield (Figs. 1, 2) by visual inspection of regional geological survey airborne magnetic data, which we have completed by previously published data (Gibbs and Barron, 1983; Gibbs, 1987; Sial et al., 1987; Reis et al., 2013). The method used is similar to the mapping done in the West African Craton (Jessell et al., 2015). Most of the dykes and sills are tholeiitic basalts composed of plagioclase + quartz + clinopyroxene ± orthopyroxene ± olivine ± K-feldspat. Sometimes, secondary amphibole, biotite and chlorite replace the primary minerals. The dykes usually contain accessory Ti-Fe oxides, and in

particular magnetite, which makes it possible to trace them in airborne magnetic data. Over 750 new dykes were traced in airborne magnetic data and they were added to 209 dykes and 129 sills digitized from the Figure 6 in Reis et al. (2013).

In Figure 1, we show the dykes from three different sources: Sial et al. (1987), Reis et al. (2013), and our new interpretation. The dykes in the Sial et al. (1987) paper are rather schematic and will not be used for further discussion, however, they give an idea of areas where dyke occurrences were documented and which may be studied by future work. All ages indicated for the dyke swarms in Sial et al. (1987) and most of ages in Reis et al. (2013) were all obtained by K-Ar or Rb-Sr method and therefore are considered as rather unreliable. Only few high-precision U-Pb ages exist up to date on the dykes in the Guiana Shield: the Avanavero swarm dated at ~1794 Ma and 1782 ± 3 Ma (Norcross et al., 2000; Reis et al., 2013; Santos et al. 2001, 2002, 2003) and the Käyser swarm dated at 1528 ± 2 Ma (Baratoux et al., in press). The newly mapped dykes are indicated in black. We suppose that dykes, which have the same orientation and the same geographic location as the known swarms are of the same age, such as the Apatoe swarm. However most of the newly mapped swarms are of unknown age as they cannot be correlated with any of the existing dyke and sill swarms.

Reis et al. (2013) distinguished 19 dyke and sill swarms and we use the names of these for the newly mapped swarms which are clearly parallel and at the same area as the known swarms. Besides these, we have traced 14 new dyke swarms (Fig. 2). Some of the swarms are nearly parallel to the existing swarms (e.g. Cassipore and 4); however we prefer to keep them separate and test their relationship in the future. For some originally short swarms (e.g. Taiano), we suggest the extension of more than 200 km. Several new and relatively long (over 200 km) dykes were identified in magnetic data (1, 5, 6, 12) while some dykes are very short (11, 13, 14). The short swarms might be connected to the existing swarms further apart (e.g. 14 and Avanavero or Taiano); however this hypothesis must be tested by further work.

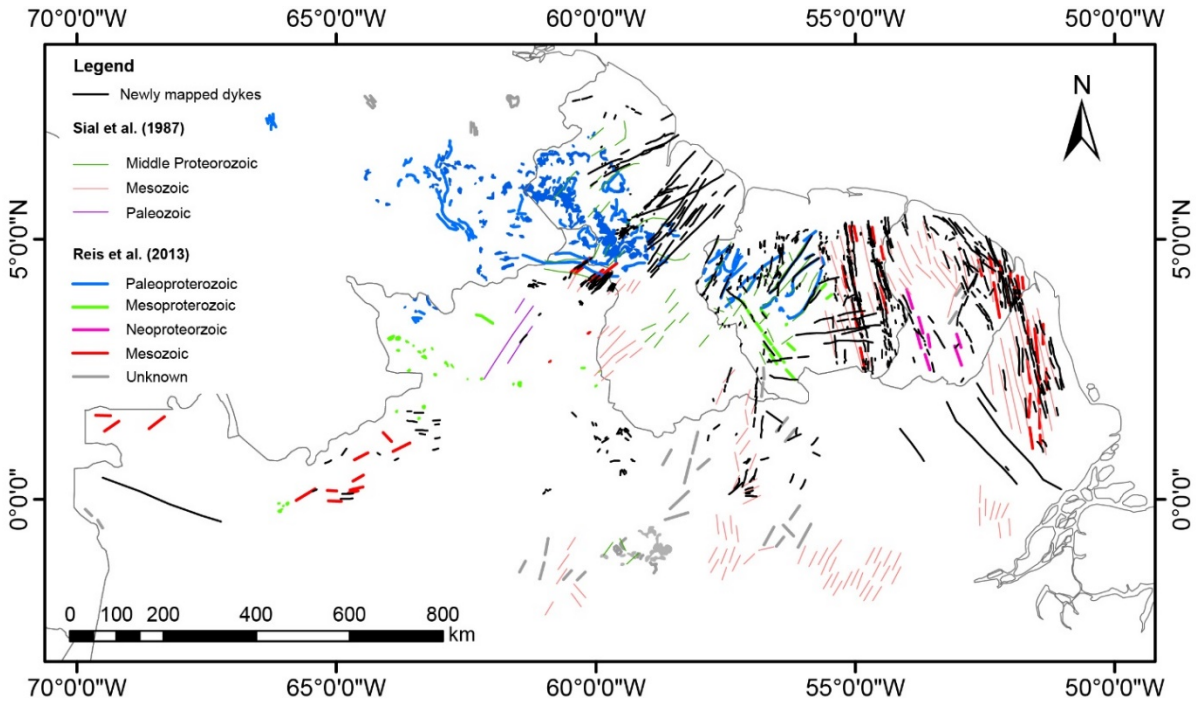

Figure 1: Map of the doleritic dykes and sills in the Guiana Shield color-coded based on their age as indicated in Sial et al. (1987) (fine lines) and Reis et al. (2013) (bold lines). Bold black lines are new dykes drawn using airborne magnetics.

The West Africa – South America reconstruction at 200 Ma (Matthews et al., 2016) shows, that there is a clear connection of the dyke swarms between the two continents (Figure 3). The dykes are color-coded based on their orientation and ages, where known. We can observe a continuation of several swarms in both continents. Knowing that the dyke swarm may change their orientation at long distances (Ernst, 2014), there may be even more swarm connections than those visible at the first sight. For example the ~1520-1528 Ma Essakane (Burkina Faso) and Käyser (Suriname) swarms have NW orientation, while the Sambarabougou swarm (Senegal) has an E-W orientation (Baratoux et al., in press). Detailed mapping of the orientation of the dyke swarms in conjunction with precise U-Pb dating and paleomagnetic data will thus help to better determine the paleogeography of the two continents through time, in particular for the period since the emplacement of the major Paleo- and Mesoproterozoic dyke swarms up to present day.

Based on our experience with mapping and dating of the West African dykes, we suggest that the following hypotheses are worth testing. i) Two swarms of different ages may have only slight different orientation at a craton scale (e.g. Korsimoro and Essakane swarms and Libiri and Manso swarms; Baratoux et al., in press). Therefore the Cassipore, Tampok, Apatoe, Seringa and swarm 4 should be sampled and dated carefully to decipher whether they form one, two or more swarms. ii) Usually, one swarm has only one dominant orientation at a local (10s of km) scale. Therefore, each of the dyke swarms Uarana, Seringa, Avanavero and Penatecaua as indicated in Reis et al. (2013) might be formed by two or more swarms. iii) Even dyke swarms which are not well expressed in magnetic data may be of crucial importance and size (e.g. Libiri swarm, Baratoux et al., in press). Attention should be therefore paid not only to

the well-visible swarms such as Cassipore, Taiano, Apatoe, etc. but also to the tiny bits of dykes here and there across the craton (Aro, Guaniamo, Uraricaá, 10, 11, 13, 14 and others).

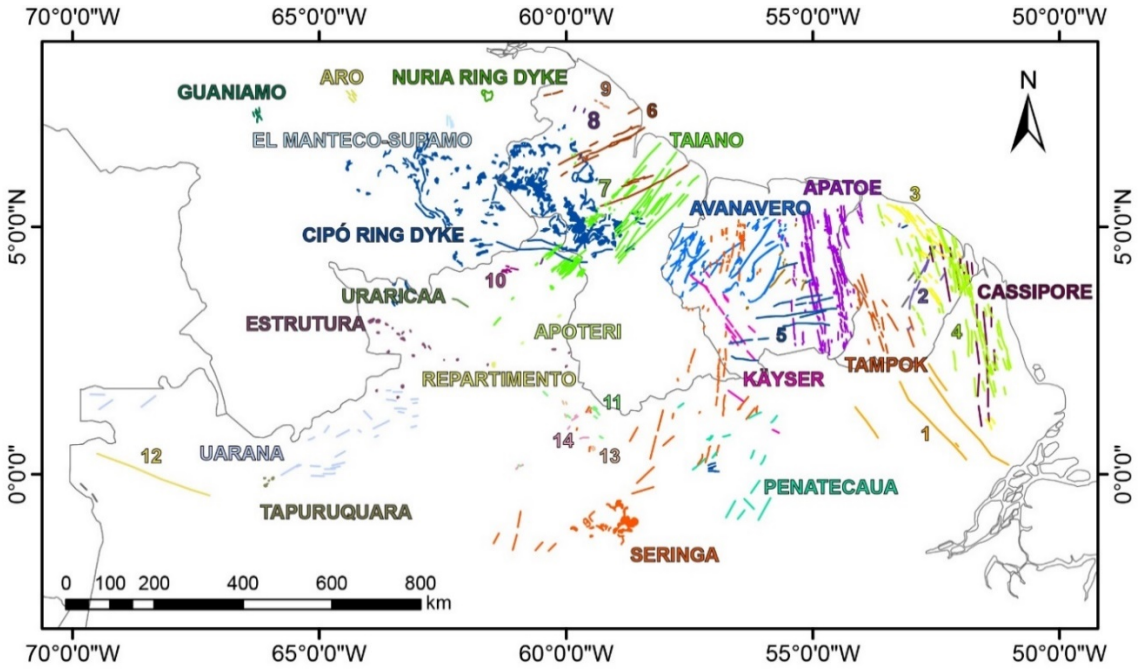

Figure 2: Map of the doleritic dykes and sills in the Guiana Shield color-coded based on their orientation and age as indicated in Reis et al. (2013). Only dykes and sills from Reis et al. (2013) and newly mapped dykes are shown. The names of the swarms are those indicated by Reis et al. (2013). The newly identified dyke swarms are numbered (1-14).

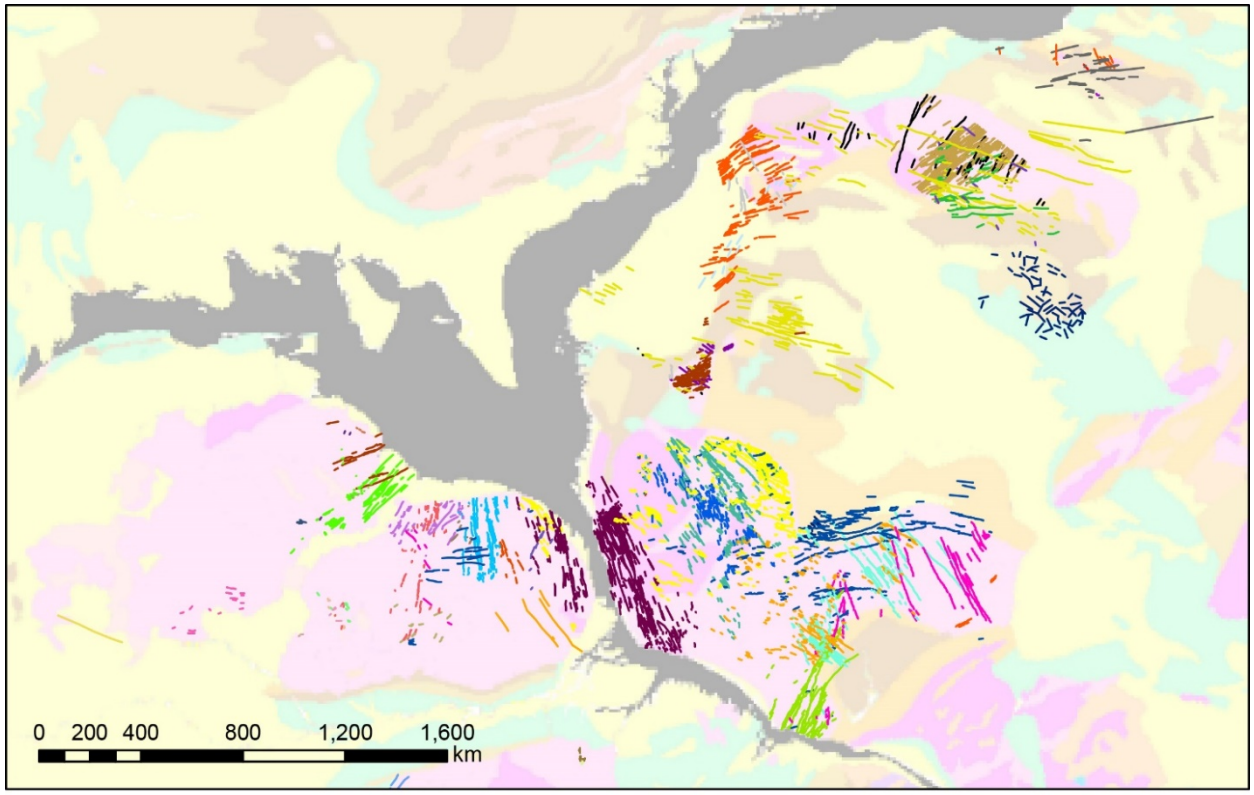

Figure 3: A reconstruction of the South America and West Africa at 200 Ma based on the model of Matthews et al. (2016) with the dykes shown on the geological map of the world (Geological Survey of Canada, 1995). The dykes are colour coded based on their orientation. Pink colour shows Precambrian shields.

CONCLUSIONS

We suggest an updated map of 750 dykes for the Guiana Shield based on the interpretation of airborne magnetic database completed by dykes and sills existing in the literature. We have identified several new swarms not described in the literature and also found extensions of existing swarms. Precise mapping of the dyke is a first step in the paleocontinent reconstruction, which needs to be completed by petrographic and geochemical analyses, U-Pb dating and paleomagnetic data in order to determine the paleogeography of South America and West Africa since Paleoproterozoic up to present time. Based on our experience from the West African Craton, we suggest several working hypotheses to be tested in order to obtain a more precise map of the dyke swarms in the Guiana Shield.

REFERENCES

Avelar, V.G., Lafon, J.M., Delor, C. Guerrot, C., and Lahondere, D., 2003, Archean crustal remnants in the easternmost part of the Guiana Shield: Pb-Pb and Sm-Nd geochronological evidence for Mesoarchean versus Neoarchean signatures: Géologie de la France, 2-3-4,83-99.

Baratoux, L., Soderlund, U., Ernst, R.E., de Roever, E., Jessell, M.W., Kamo, S., Naba, S., Perrouty, S., Metelka, V., Yatte, D., e, in press. New U-Pb baddeleyite ages of mafic dyke swarms of the West African and Amazonian Cratons: implication for their configuration in supercontinents through time: In: Srivastava, R.K., Ernst, R.E., Peng, P. (eds.) Dyke Swarms of the World – A Modern Perspective. Springer book volume.

Delor, C., de Roever, E.W.F., Lafon, J.M., Lahondere, D., Rossi, P., Cocherie, A., Potrel, A., 2003, The Bakhuis ultra-high-temperature granulite belt (Suriname) : II. Implications for the late Transamazonian crustal stretching in a revised Guiana Shield framework: Géologie de la France, 2-3-4, 207-230.

Ernst, R.E., 2014, Large Igneous Provinces: Cambridge University Press, pp 653.

Ernst, R.E., Bleeker, W., Söderlund, U., and Kerr, A.C., 2013, Large Igneous Provinces and supercontinents: toward completing the plate tectonic revolution: Lithos, 174, 1–14.

Geological Survey of Canada, 1995. Generalized Geology of the World and Linked Databases, Open File 2915d. https://mrdata.usgs.gov/geology/world/

Gibbs, A.K., 1987. Contrasting styles of continental mafic intrusions in the Guiana Shield: In: Halls, H.C., Fahrig, W.F. (Eds.), Mafic Dyke Swarms: Geological Association of Canada Special Paper, 34, 457–465.

Gibbs, A.K., and Barron, C.N. 1983. The Guiana Shield Reviewed: Episodes, 1983, 7-14.

Jessell, M.W., Santoul, J., Baratoux, L. Youbi, N., Ernst, R.E., Metelka, V., Miller, J., and Perrouty, S., 2015, An updated map of West African mafic dykes: Journal of African Earth Sciences, 112, 440-450. doi: 10.1016/j.jafrearsci.2015.01.007.

Johansson, Å. 2014, From Rodinia to Gondwana with the "SAMBA" model: a distant view from Baltica towards Amazonia and beyond: Precambrian Research, 244, 226–235.

Kah, L.C., Bartley, J.K., and Teal, D.A., 2012, Chemostratigraphy of the Late Mesoproterozoic Atar Group, Taoudeni Basin, Mauritania: Muted isotopic variability, facies correlation, and global isotopic trends: Precam Res, 200–203, 82–103.

Kouamelan, A.N., Djro, S.C., Allialy, M.E., Paquette, J-L., and Peucat, J-J., 2015, The oldest rock of Ivory Coast: Journal of African Earth Sciences, doi: 10.1016/j.jafrearsci.2014.12.004

Kroonenberg SB, de Roever EWF, Fraga LM, Reis, N.J., Faraco, T. Lafon, J-M., Cordani, U., and Wong, T.E., 2016, Paleoproterozoic evolution of the Guiana Shield in Suriname : a revised model: Netherlands Journal of Geosciences, 95(4), 491-522.

Ledru, P., Johan, V., Milési, J.P., and Tegyei, M., 1994, Markers of the last stages of the Paleoproterozoic collision: evidence for a 2 Ga continent involving Circum-South Atlantic provinces: Precambrian Research, 69, 169-191.

Matthews, K.J., Maloney, K.T., Zahirovic, S., Williams, S.E., Seton, M., Muller, R.D., 2016, Global plate boundary evolution and kinematics since the late Paleozoic: Global and Planetary Change. Doi: 10.1016/j.gloplacha.2016.10.002.

Montgomery, C.W., 1979, Uranium-lead geochronology of the Archean Imataca Series, Venezuelan Guyana shield: Contrib Min Petrol, 69, 167-176.

Nomade, S., Chen, Y., Pouclet, A., Feraud, G., Theveniaut, H., Daoud., B.Y., Vidal, M., and Rigollet, C., 2003, The Guiana and West-African Shield Paleoproterozoic grouping: new paleomagnetic data for French Guiana and Ivory Coast: Geophysical Journal International, 154, 677-694.

Parra-Avila, L.A., Kemp, A.I.S., Fiorentini, M.L., Belousova, E., Baratoux, L., Block, S., Jessell, M.W., Bruguier, O., Begg, G.C., Miller, J., Davis, J., and McCuaig, T.C., 2017, The geochronological evolution of the Paleoproterozoic Baoulé-Mossi domain of the Southern West African Craton, Precambrian Research. doi: 10.1016/j.precamres.2017.07.036.

Pisarevsky S.A., Elming, S.Å., Pesonen, L.J., and Li, Z.X., 2014, Mesoproterozoic paleogeography: Supercontinent and beyond: Precambrian Research, 244, 207-225.

Reis, N.J., Teixeira, W., Hamilton, M.A., Bispo-Santos, F., Almeida, M.E. and D'Agrella-Filho, M.S., 2013, Avanavero mafic magmatism, a late Paleoproterozoic LIP in the Guiana Shield, Amazonian Craton: U–Pb ID-TIMS baddeleyite, geochemical and paleomagnetic evidence: Lithos, 174, 175–195.

Rooney AD, Selby D, Houzay JP, and Renne, P.R., 2010, Re–Os geochronology of a Mesoproterozoic sedimentary succession, Taoudeni basin, Mauritania: Implications for basin-wide correlations and Re–Os organic-rich sediments systematics.: Earth and Planetary Science Letters, 289, 486–496.

Santos, J.O.S., Hartmann, L.A., Gaudette, H.E., Groves, D.I., McNaughton, N.J., and Fletcher, I.R., 2000, A new understanding of the provinces of the Amazon Craton based on integration of field mapping and U–Pb and Sm–Nd geochronology: Gond. Res, 3, 453–488.

Sial, A.N., Oliveira, E.P., and Choudhuri, A. 1987, Mafic Dyke Swarms of Brazil: In: Halls, H.C., and Fahrig, W.F. (Eds.), Mafic Dyke Swarms. Geological Association of Canada Special Paper, 34, 467-481.

Tassinari, C.C.G. and Macambira, M.J.B. 1999, Geochronological provinces of the Amazonian Craton: Episodes, 1999, 174-182.

Teixeira, W., Reis, N.J., Bettencourt, J.S., Klein, E.L., Oliveira, D.C., in press. Intraplate Proterozoic Magmatism in the Amazonian Craton Reviewed: Geochronology, Crustal Tectonics and Global Barcode Matches. In: Srivastava, R.K., Ernst, R.E., Peng, P. (eds.) Dyke Swarms of the World – A Modern Perspective. Springer book volume.

Basalt-hosted gold in the Paleoproterozoic Marowijne greenstone belt (Suriname): first insights into volcanic setting and alteration style of the Saramacca deposit

Sabrina K. Beek*

Suriname Exploration, Iamgold &
Anton de Kom University of Suriname
President Da Costalaan 2, Paramaribo, Suriname

sabrina_beek@iamgold.com

Manfred J. van Bergen

Universiteit Utrecht
Budapestlaan 4, Utrecht, Netherlands

M.J.vanBergen@uu.nl

SUMMARY

Geochemical signatures and alteration mineralogy of the newly developed Saramacca gold deposit in the Paleoproterozoic Marowijne greenstone belt of Suriname provide insight into the original emplacement setting of its basalt host rocks and guidelines for exploration in similar greenschist-metamorphosed mafic volcanics in Suriname. Trace-element geochemistry of the Saramacca basalts is consistent with an oceanic plateau setting, possibly plume-related, which has potential implications for the origin of the gold. Alteration associated with the gold mineralization is expressed as fault-bounded compositional zoning involving carbonate, mica and chlorite minerals, which can be used as vectors towards ore.

Key words: Gold, Suriname, Marowijne greenstone belt, Basalt, Alteration

INTRODUCTION

The Saramacca gold deposit (Figure 1), situated within Suriname's prospective Marowijne greenstone belt, presents notable differences in host-rock lithology and mineralization style compared to previously studied mineralization in the nearby gold-producing Rosebel district. Gold in the Rosebel district occurs in vein sets related to structural heterogeneities, principally along volcano-sedimentary contacts and fold hinges, and is hosted in meta-sediments as well as felsic to mafic meta-volcanic rocks (Daoust et al., 2011). In contrast, the Saramacca gold is accommodated in breccia fill along a major vertical fault and associated subsidiary shear zones, and is completely hosted in meta-basalt. Most Paleoproterozoic basalts within the Guiana Shield have a tholeiitic affinity, usually attributed to emplacement in back-arc to mid-ocean-ridge environments (Vanderhaeghe et al., 1998; Daoust et al., 2011). On the other hand, Velásquez et al. (2011) proposed that tholeiitic basalts of the gold-bearing El Callao Formation in Venezuela were emplaced in an oceanic plateau setting, sourced from a mantle plume. Here, we present the first lithogeochemical and petrographic insights into the affinity of the basaltic rocks and the nature of alteration that accompanied deposition of the Saramacca gold.

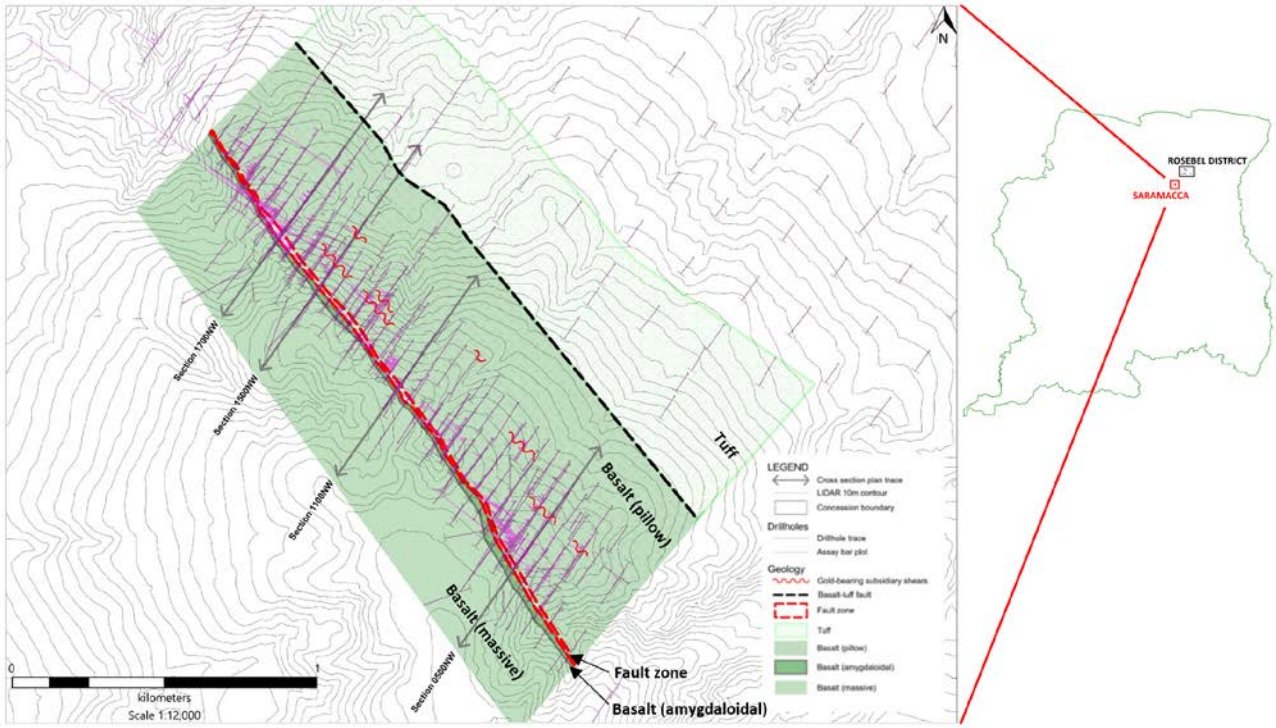

Figure 1. Location and simplified geology of the Saramacca gold deposit.

METHODS

Lithogeochemistry Representative samples of halved diamond drill core were selected along two cross-sections (1500NW and 1700NW) through a barren and a gold-bearing portion of the fault, respectively. All samples were analysed at ALS Peru following procedures comprising lithium borate fusion with ICP-AES finish for major rock-forming elements, and lithium borate fusion with ICP-MS finish for trace elements including REE.

Reflectance spectroscopy Spectral readings were collected from a selection of dry, halved diamond drill core along the cross sections 1500NW and 1700NW at 5 to 10m spacing in fresh rock and where notable changes in alteration mineralogy were observed. Quality control was performed by comparison with known mineral spectra. Results yielded 3-D spatial distributions of compositional varieties of carbonate, chlorite and mica minerals.

RESULTS

All mafic volcanic rocks macroscopically logged as basalt classify as basalt in the TAS diagram of Le Bas et al. (1986) and the Nb/Y-Zr/Ti diagram of Pearce (1996) (Figure 2). Major and trace-element discrimination diagrams (Figure 3) further demonstrate their tholeiitic affinity. They tend to rank as Fe-rich tholeiitic basalt according to the cationic plot after Jensen (1976) (Figure 4). Compositional differences between pillow, massif and amygdaloidal basalts are minor and can be ignored here. Despite the local presence of calc-alkaline tuffs, there is no gradual transition towards felsic volcanics, as is seen in andesite-dominated volcanic sequences elsewhere in the Marowijne greenstone belt.

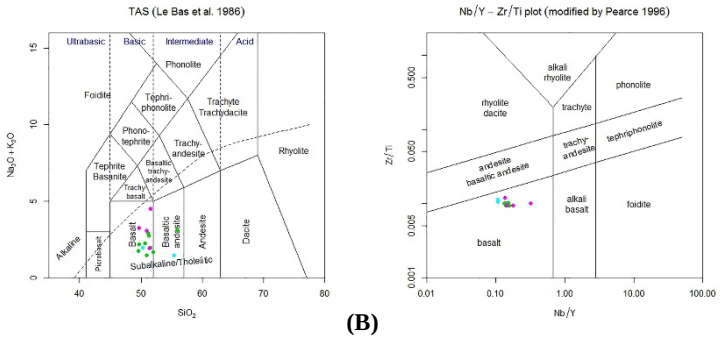

(A) **(B)**

Figure 10: Classification of Saramacca meta-volcanics according to (A) the TAS diagram of Le Bas et al. (1986), and (B) the Nb/Y vs Zr/Ti plot after Pearce (1996). See Figure 6 for color codes.

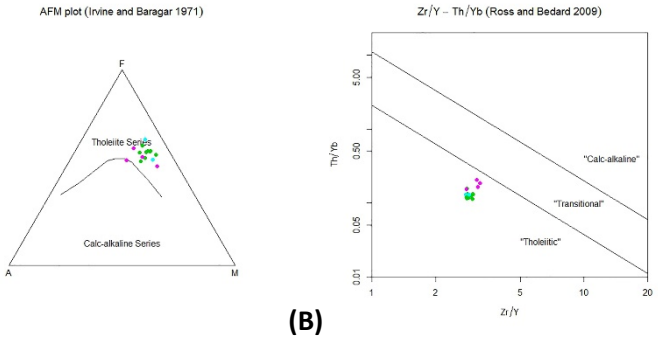

(A) **(B)**

Figure 3: (A) AFM plot after Irvine and Baragar (1971); (B) discrimination based on the Zr/Y vs Th/Yb diagram of Ross and Bedard (2009). See Figure 6 for color codes.

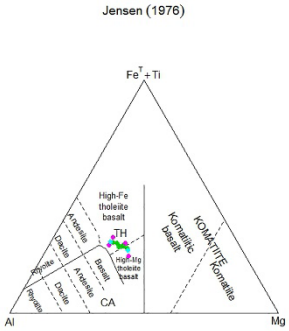

Figure 4: Classification of the Saramacca volcanic rocks in the cationic plot of Jensen (1976). See Figure 6 for color codes.

The Saramacca basalts exhibit flat chondrite-normalized REE patterns (Figure 5A) with $(La/Yb)_N$ ratios ranging between 0.82 and 1.66. There are no negative Eu anomalies. Multi-element spider plots, normalized to primitive mantle, show overall horizontal trends, except for elements that are relatively mobile under hydrothermal alteration or metamorphism (Figure 5B). These signatures point to an oceanic setting and absence of a relationship with converging plate boundaries. Ratio plots of Nb/Th vs Zr/Nb and Zr/Y vs Nb/Y after Condie et al. (2003) provide further clues as to the specific oceanic setting where the basalts originated. In Figure 6, their compositions are shown together with those of the El Callao basalts (Venezuela) and the Mana basalts (Burkina Faso), which have been characterized as basalts with an origin in an oceanic plateau setting (Velásquez et al., 2011; Augustin and Gaboury, 2016). The Saramacca basalts also plot in the field of ocean plateau basalt, showing close similarity with El Callao and Mana basalts as well as with basalts from Royal Hill in the nearby Rosebel district. Our results suggest that both Saramacca and Royal Hill basalts were emplaced in an oceanic plateau setting, possibly sourced by a mantle plume, similar to what has been proposed for the El Callao and Mana basalts. Such a setting may have significant implications for the origin of the gold, as plume-related oceanic plateau basalts tend to be more enriched in primary gold compared to MORB (Bierlein and Pisarevsky, 2008). If correct, this inferred oceanic signature of the Saramacca basalts would place their origin early in the Paleoproterozoic history of the Transamazonian evolution of the Guiana Shield (Eorhyacian), which is marked by the formation of juvenile oceanic crust (Delor et al., 2003).

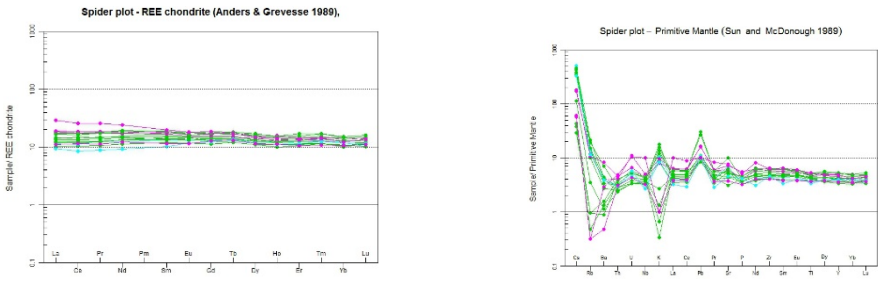

(A) **(B)**

Figure 5: (A) Chondrite-normalized REE patterns for Saramacca basalts. Normalization after Anders and Grevess (1989); (B) Multi-element spider diagram normalized to primitive mantle for Saramacca basalts. Normalization after Sun and McDonough (1989). See Figure 6 for color codes.

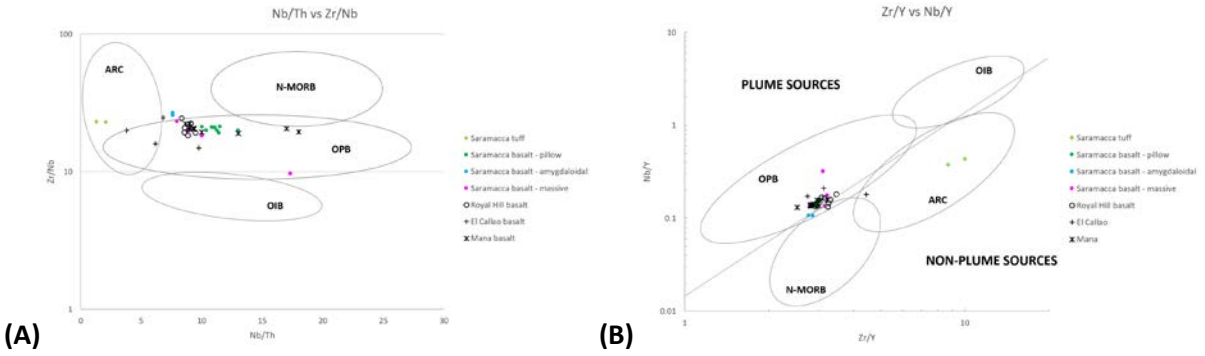

Figure 6: Geochemical affinity of basalts from Saramacca and Royal Hill (Suriname), El Callao (Venezuela) and Mana (Burkina Faso), based on (A) Zr/Nb vs Nb/Th ratios, (B) Zr/Y vs Nb/Y ratios. ARC: Arc-Related Basalt, OPB: Oceanic Plateau Basalt, N-MORB: Normal-Mid Ocean Ridge Basalt, OIB: Oceanic Island Basalt. Modified after Condie (2003).

Hydrothermal alteration related to gold mineralization is dominated by carbonate, mica and sulfide minerals with a proximal assemblage of dolomite-ankerite-siderite-paragonite-pyrite-gold and an intermediate calcite-dolomite-muscovite assemblage. A distal assemblage of chlorite-actinolite-epidote-plagioclase reflects the regional greenschist-grade metamorphism in the least altered rock (Figure 7). The mineralogical changes are consistent with an enrichment in K, Rb, Cs, Ba, C, volatiles as well as S and associated chalcophile elements in the direction towards the ore. The clear compositional zonation in carbonate, mica and chlorite perpendicular to the gold-bearing fault zone and subsidiary shears may be used to indicate proximity to mineralization.

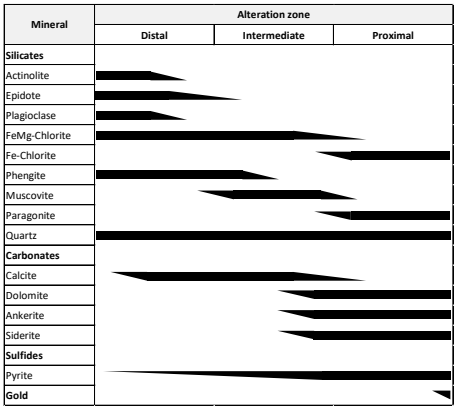

Figure 7: Alteration mineralogy of the Saramacca gold deposit hosted in greenschist-facies metamorphic basalt.

CONCLUSIONS

The sequence of events leading to the formation of the Saramacca gold deposit comprises the following elements: (1) Emplacement of basalt in a sub-aqueous oceanic plateau setting, possibly triggered by an upwelling mantle plume, (2) Basin closure, accretion of oceanic crust onto continental crust, convergence of continental blocks involving faulting and shearing (including formation of the main Saramacca gold-hosting fault structure) as well as regional metamorphism, (3) Mineralization from gold-bearing hydrothermal fluids percolating through the Saramacca fault and its subsidiary shear zones, and overprinting the greenschist-facies metamorphic assemblage.

REFERENCES

Anders, E. and Grevesse, N., 1989. Abundances of the elements: Meteoritic and solar. Geochimica et Cosmochimica Acta, Volume 53, Issue 1, January 1989, pp. 197-214.

Augustin, J., Gaboury, D., 2016. Paleaoproterozoic plume-related basaltic rocks in the Mana gold district in western Burkina Faso, West Africa: Implications for exploration and the source of gold in orogenic deposits. Journal of African Earth Sciences 129 (2017), pp. 17-30.

Bierlein, F. P., and Pisarevsky, S., 2008. Plume-related oceanic plateaus as a potential source of gold mineralization. Economic Geology v. 103, pp. 425-430.

Condie, K. C., 2003. Incompatible element ratios in oceanic basalts and komatiites: Tracking deep mantle sources and continental growth rates with time. Geochem. Geophys. Geosyst. 4 (1), 1005, doi:10.1029/2002GC000333, 2003.

Daoust, C., Voicu, G., Brisson, H., Gauthier, M., 2011. Geological setting of the Paleoproterozoic Rosebel gold district, Guiana Shield, Suriname. Journal of South American Earth Sciences 32 (2011), pp. 222-245.

Delor, C., Lahondére, D., Egal, E., Lafon, J-M., Cocherie, A., Guerrot, C., Rossi, P., Truffert, C., Théveniaut, H., Phillips, D., Avelar, V. G., 2003. Transamazonian crustal growth and reworking as revealed by the 1:500,000-scale geological map of French Guiana. Géologie de la France, 2003, n° 2-3-4, pp. 5-57.

Irvine, T. N. and Baragar, W. R. A., 1971. A guide to the chemical classification of the common volcanic rocks. Canadian Journal of Earth Sciences 8, pp. 523-548.

Jensen, L. S., 1976. A new Cation Plot for Classifying Subalkalic Volcanic Rocks. Ontario Geological Survey Miscellaneous Paper 66.

Le Bas, M. J., Le Maitre, R. W., Streckeisen, A., Zanettin, B., 1986. A chemical classification of volcanic rocks based on the total alkali-silica diagram. Journal of Petrology 27, pp 745-750.

Pearce, J. A., 1996. A user's guide to basalt discrimination diagrams. In: Wyman, D. A. (ed.) Trace Element Geochemistry of Volcanic Rocks: Applications for Massive Sulphide Exploration. Geological Association of Canada, Short Course Notes 12, pp 79-113.

Ross, P-S. and Bedard, J. H., 2009. Magmatic affinity of modern and ancient subalkaline volcanic rocks determined from trace-element discriminant diagrams. Canadian Journal of Earth Sciences, 2009, Vol. 46, No. 11, pp 823-839.

Sun, S. S. and McDonough, W. F., 1989. Chemical and isotopic systematics of oceanic basalts; implications for mantle composition and processes. In: Magmatism in the ocean basins. Saunders, A. D. and Norry, M. J. (Editors), Geological Society of London, London. 42: pp 313-345

Vanderhaeghe, O., Ledru, P., Thiéblemont, D., Egal, E., Cocherie, A., Tegyey, M., Milési, J-P., 1998. Contrasting mechanism of crustal growth: Geodynamic evolution of the Paleoproterozoic granite-greenstone belts of French Guiana. Precambrian Research 92 (1988), pp. 165-193.

Velásquez, G., Béziat, D., Salvi, S., Tosiani, T., Debat, P., 2011. First occurrence of Paleoproterozoic oceanic plateau in the Guiana Shield: The gold-bearing El Callao Formation, Venezuela. Precambrian Research 186 (2011), pp. 181-192.

Gold settings of the Guiana Shield

Marc Bardoux *

Barrick
6039 Boul. Lasalle
Montreal
Quebec Canada
H4H 1M8

mbardoux@barrick.com

Of the 1.2 million square kilometers defining the outline of the Guiana Shield, Rhyacian rocks are mainly occurring in its northern half. Primary gold of the Guiana Shield relates to Rhyacian supracrustals and small felsic plugs. The average grade of the deposits mined in the last four decades has been less than 1.6 gpt Au. The gold inventory of the Guiana Shield has grown by more than 30% in the last two decades and now exceeds 140Moz. The only two Tier 1 camps of the Guiana Shield occur in the very large Marowijne Basin and account for more than 20Moz. Exploration has been most successful following up on historical workings with creative soil sampling supported by careful regolith mapping. Many false soil anomalies have been drilled due to complex regolith. Surface gold is often nuggety and commonly supergene. Because of significant access restrictions and a lack of outcrop, detailed aeromagnetic surveys have greatly helped breaking down key elements of the stratigraphic and structural frameworks. Physical properties of rocks remain untested. Deformation styles usually consist of megascopic folds intersected by discrete shears along rheological boundaries. Large breaks are not common. Gold occurs commonly associated with pyrite or pyrrhotite in vein lodes or sulfide stringers. Vein geometries are often overlooked and oriented core drilling is not systematically utilized. Early stage RC drilling tends to kill targets. At least three ages of auriferous mineralization have been documented to date across the entire Rhyacian system. The youngest Rhyacian gold stage may be younger than 2Ga. Three principal gold settings have been defined to date. Two are related to mafic arc magmatism and felsic plutonism and the third ties up to large siliciclastic sequences with or without proximal felsic magmatism. Detrital gold has been found in shales and wackes. A thorough understanding of the tectonostratigraphic framework of the myriads of arcs, volcaniclastic basins and alluvial sedimentation in a logical and chronological order is greatly needed for a better understanding of the metallogenesis of the fertile parts of this complex framework. Knowledge needs to enter the modern era. SAXI will fill a major knowledge gap. Lessons learned from WAXI will most likely accelerate discovery rates. Some relationships between the regional geology and major gold deposits must be established.

Metallogeny of Gold, Copper and Iron in the Borborema Province

Gabriel V. Berni*

Universidade Federal do Ceará
Campus do Pici, Bloco 912
Fortaleza-CE-Brazil 60440-554
gvberni@ufc.br

Clóvis V. Parente

Universidade Federal do Ceará
Campus do Pici, Bloco 912
Fortaleza-CE-Brazil 60440-554
clovis@ufc.br

Lydia Maria Lobato

Universidade Federal do Minas Gerais
Campus Pampulha
Belo Horizonte, -MG-Brazil-31270-910
llobato.ufmg@gmail.com

Caio César F. T. de Sampaio

Universidade Federal do Ceará
Campus do Pici, Bloco 912
Fortaleza-CE-Brazil, 60440-554
caiocft92@gmail.com

Steffen Hagemann

Centre for Exploration Targeting
University of Western Australia
35 Stirling Highway, Perth, Australia, 6009
steffen.hagemann@uwa.edu.au

SUMMARY

The Borborema Province is defined as a structural province composed of several Proterozoic metavolcano-sedimentary and metasedimentary belts, which were amalgamated to Archean and Paleoproterozoic basement rocks. Gold mineralization formed during the Paleoproterozoic, associated with the metavolcano-sedimentary Algodões sequence (Pedra Branca) and during the Neoproterozoic, associated with shear zones and hosted by quartz veins. Copper is associated with mafic-ultramafic rocks (Serrote da Laje), stratabound Kupferschiefer-style (Pedra-Verde) and IOCG mineralization (Aurora, Rio do Pontal and Eopaleozoic rift basins). Iron deposits are BIF hosted as for example in the Bonito deposit (Rio Grande do Norte state) or related to Fe skarns in the Santa Quitéria magmatic arc. Gold, copper and iron mineralization is largely associated to the final periods of the Brasiliano event, suggesting that this represents a major period of metal transfer at the Borborema Province.
Key words: Borborema Province, Borborema Metallogeny

INTRODUCTION

The Borborema Province (BP) is defined as a structural province composed of several Proterozoic metavolcano-sedimentary and metasedimentary belts, which were amalgamated to Archean and Paleoproterozoic basement rocks (Oliveira & Medeiros, 2018 and references therein). These Archean and Paleoproterozoic terrains vary between high-to-low metamorphic grades, were formed at infracrustal levels, are affected by partial melting, are overlaid by Neoproterozoic supracrustal rocks, and intruded by Neoproterozoic granitoids. The terrain boundaries are defined by Neoproterozoic shear zones, subdividing the BP into five domains (Fig. 01). These shear zones were partially reactivated in the Eopaleozoic and Cretaceous periods (Trompette, 1997). The long and complex geological evolution of the BP terrains from the Archean to the Phanerozoic is also reflected in the wide variety of different ore deposits and tectonic settings within the Province.

This contribution intends to provide a review of the major gold, copper and iron ore deposits within the BP. Due to the extreme variety of terrains and long-lasting geological evolution, this review first defines the deposit based on the major commodity, followed by a division in different mineral systems.

GEOLOGICAL SETTING

The Borborema Province is a large mobile belt across the Gondwana supercontinent, which resulted from the convergence and collision of the West Africa, Amazonian, and São Francisco cratons during the Brasiliano-Pan African orogeny (Trompette, 1997). The BP borders the São Francisco-Congo craton in the south, and the Parnaíba basin in the east. The east and northern connections are with the Benin-Nigeria province in Africa (Trompette et al., 1997). The BP province is divided by most authors in five tectonic blocks separated by regional E-W- and NE-trending shear zones (e.g. Brito Neves et al., 2000; Arthaud et al., 2008). They are: (1) Médio Coreaú, (2) Ceará, (3) Rio Grande do Norte, (4) Central, and (5) Southern domains (Fig. 01).

The basement rocks are defined by orthogneisses with minor meta-ultramafics, meta-gabbro, meta-amphibolite and metasedimentary rocks. Three Archean terrains are located within the BP: (1) the 3.2-2.7-Ga Tróia Massif, which outcrops in the Ceará domain, and the other two outcropping at the Rio Grande do Norte domain; (2) the 3.4-2.5-Ga São José do Campestre, and (3) the 3.1-2.5-Ga Granjeiro Complex (Costa et al., 2015 and references therein).

Paleoproterozoic gneiss-migmatitic complexes are located within the five tectonic blocks of the BP (Fig. 1), with most geochronological U-Pb ages clustering at 2.0-2.2 Ga (Fetter et al., 2000 and references therein). Older Paleoproterozoic ages (2.27-2.35 Ga) are reported by Fetter et al. (2000) for the Médio Coreaú Domain. Near the margin of the Archean Cruzeta Complex (Tróia Massif), the Ceará Domain contains the important ~2.2-2.0-Ga Algodões metavolcano-sedimentary sequence. This sequence shares similar characteristics with the ~2.2-2.0-Ga granite-greenstone terranes in the South American and African cratons (Martins et al., 2009). The Transamazonian event was followed by intracrustal rifting and deposition of the 1.8-Ga metavolcano-sedimentary sequences of the Orós-Jaguaribe belt, in the Rio Grande do Norte domains (Sá et al., 1995). An important Meso- to early Neoproterozoic magmatic event (Cariris Velho) is recorded in the Central Domain (Brito Neves et al., 1995). This is represented by the Alto Pajeú and

Alto Moxotó complexes, with U-Pb zircon ages of metavolcanic rocks at 1.12–0.93 Ga (Van Schmus et al., 1995) and metagranitoids at 980–920 Ma (Van Schmus et al., 1995).

The Neoproterozoic supracrustal metasedimentary rocks are represented by the Ceará, Seridó and Cachoeirinha groups. The Ceará group is a thick sequence of terrigenous metasedimentary rocks dominated by metapelites and marbles (Arthaud et al., 2008), which outcrops in the Ceará domain. The Seridó group is a more diverse metasedimentary sequence including quartzites, conglomerates, BIF, marbles, and is exposed in the eastern part of the Rio Grande do Norte Domain (Caby et al. 1995). The Cachoeirinha group is a metasedimentary sequence with minor associated metavolcanic rocks in the Central Domain of the BP (Medeiros et al., 2004). Neoproterozoic magmatism is widespread in the BP (Arthaud et al, 2008). Ganade de Araújo et al. (2014) distinguished the different episodes of magmatism into: (1) pre-collisional (800-630 Ma); and (2) syn- (615-570 Ma); (3) late (ca. 530 Ma); and (4) anorogenic (500-460 Ma) granitic.

During the early Paleozoic, an extensional event was responsible for the formation of several Eopaleozoic rift basins which spread over all terrains in the BP. The basins contain generally two sedimentary units separated by an erosional unconformity (Arthaud, 2008). There is also extrusive bimodal magmatism within the basins, associated with or crosscutting the sedimentary rocks (Arthaud, 2008). Post-Brasiliano-age granites, such as the Mucambo and Meruoca granites, cross-cut the metasedimentary rocks of the basin.

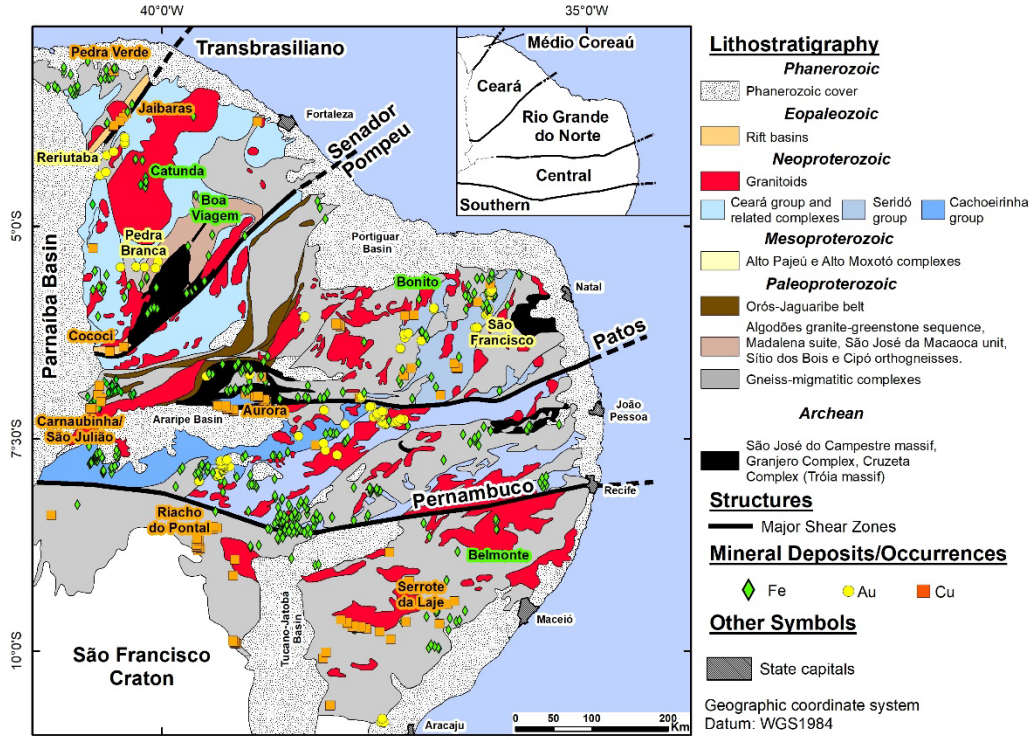

Figure 1 – Geological map of the Borborema Province displaying the major gold, copper and iron deposits/occurrences. Colored symbols show commodity and important deposits/occurrence in the BP. Major lineaments that define the Province´s domains are labelled. The distribution of the five main tectonic domains of the BP is shown in the insert.

GOLD, COPPER AND IRON AT THE BORBOREMA PROVINCE AND ITS COVER

GOLD

Gold occurrences within the BP are in the Ceará, Rio Grande do Norte and Central domains of the Borborema Province (Fig. 1). Gold mineralization is hosted by the (1) Paleoproterozoic metavolcano-sedimentary Algodões sequence (Pedra Branca) and basement (Reriutaba) in the Ceará Domain; (2) Neoproterozoic metasedimentary rocks of the Seridó group, in the Rio Grande do Norte Domain; (3) Neoproterozoic Cachoeirinha group, and Alto Pajeú complexes in the Central Domain.

With respect to mineral systems the gold occurrences are defined in the literature as orogenic with gold in quartz veins hosted by a variety of rock types within regional shear zones. There are two gold mineralization events in the Borborema Province: (1) a Paleoproterozoic 2.0-2.1 Ga orogenic gold mineralization (Costa et al., 2015) at Pedra Branca (in the state of Ceará), hosted by the Algodões metavolcano-sedimentary sequence. (2) syn-to-late Neoproterozoic gold deposits formed during the Brasiliano orogeny in quartz veins hosted in metasedimentary rocks and Paleoproterozoic basement (Reriutaba). The largest orogenic gold deposit is the São Francisco gold mine hosted in rocks of the Seridó group. There are similar, but smaller, orogenic gold deposits hosted in rocks of the Cachoeirinha group. In Reriutaba-Ceará gold mineralization is hosted in the Paleoproterozoic basement (CPRM, 1983), and is associated with pyrite-bearing quartz-hematite breccias.

COPPER

Different copper mineral systems are located within all five tectonic blocks of the Borborema Province (Fig 1). The most important deposits are Serrote da Laje (Alagoas), Pedra Verde (Ceará), Aurora (Ceará), the Riacho do Pontal prospect (in Pernambuco state), and the copper occurrences related to the Eopaleozoic basins of Jaibaras (Ceará), Cococi (Ceará), and Carnaubinha/São Julião (in Piauí state).

The copper-iron-gold mineralization at the Serrote deposit is associated with mafic-ultramafic rocks, with strong lithological control. Magnetitites and magnetite norites are the most common host rocks with chalcopyrite and bornite as the main ore minerals. The mineralization is mainly orthomagmatic with a hydrothermal overprint (Aura Minerals, 2012).

The Pedra Verde copper mine is hosted by metasedimentary rocks of the Martinópole group. Stratabound copper mineralization is spatially related to a redox boundary between phyllite and conglomerates (da Silva et al., 2017). The authors interpret this deposit as a syn-sedimentary stratiform copper (SSC) system formed by the movement of oxidized, copper-bearing fluids across reduced rocks (e.g. Kupferschiefer style). However, there is a significant difference in the timing of mineralization with syn-orogenic copper introduction related to the Gondwana agglutination (Brasiliano event).

The Aurora deposit and the Riacho do Pontal prospect are interpreted to belong to the IOCG mineral system. According to Huhn et al. (2011), these are Neoproterozoic to Paleozoic, shear-zone controlled mineralization with associated intense hydrothermal alteration. The ore zones consist of silica-hematite breccias with chalcopyrite, chalcocite and pyrite. The Riacho do Pontal prospect is also defined as an IOCG mineral system based on the association with potassic alteration and hematite. The copper occurrences are hosted by paragneiss and are spatially related to thrust zones. Ore minerals hosted by hematite breccias contain a chalcopyrite-pyrite-chalcocite assemblage (Huhn et al., 2014).

There are numerous prospects of copper mineralization hosted by metasedimentary rocks of the Eopaleozoic basins (Jaibaras, Cococi, Carnaubinha, São Julião and others) and their basement rocks (Fig.1). Copper mineralization is associated with hematite and siliceous breccias with chalcopyrite and chalcocite (Parente et al., 2011) as the main sulfide minerals. Widespread potassic alteration and hematite breccias are found in metasedimentary rocks of the basins and in the basement near basin-defining fault zones, suggesting that this mineralization is also of IOCG type. The mineralization age is uncertain, but likely Paleozoic, and clearly associated with extension.

IRON

There are essentially two types of iron mineralization in the BP (Fig.1): (1) BIF hosted, and (2) Fe-Skarns. Small BIF occurrences are widespread in the BP, with more than 60 occurrences (Beurlen, 1995). The largest occurrences are the Bonito deposit (Rio Grande do Norte state), and the São José do Belmonte deposit (in Pernambuco state). At the Bonito mine, the ore is essentially a massive magnetite orebody controlled by the hinge zone of a major fold within the BIFs of the Seridó group. The São José do Belmonte deposit contains hematite orebodies hosted in chlorite schists of the Cachoeirinha group (Beurlen, 1995 and references therein).

There Fe-Skarns within the BP are restricted to the Ceará Domain and are associated with the Santa Quitéria (e.g. Catunda) magmatic-arc. The skarns are associated with early to late-collisional, Neoproterozoic quartz monzonite crosscutting calc-silicate rocks and dolomitic and/or calcitic marbles in the Ceará Domain. Three types of iron-dominated skarn-related ores are distinguished: (1) banded magnetite; (2) disseminated magnetite; and (3) vein- hosted massive magnetite (Parente et al., 2015).

FINAL REMARKS

The metallogeny of the Borborema Province is yet to be comprehended. Although the last 10 years has seen an abundance of new geochronological data for the Province, with great advance in better definition of the different terrains, lithological units or metamorphic/thermal events, very few studies have focused on determining mineralization ages and relating those to the different tectonic events. For gold, a limited number of studies constrain alteration mineralogy and zoning, ore parageneses and timing of ore formation with respect to syn- to late-Brasiliano orogenic events. In contrast, Paleoproterozoic orogenic gold mineralization, associated with the Algodões greenstone belt, has been investigated and constrained in more detail. Ages for copper and iron mineralization are also scant. The Serrote da Laje deposit is a unique case for deposits related to mafic-ultramafic rocks, and in this case, mineralization is considered pre-Brasiliano orogeny. The Aurora Pedra Verde deposit is considered to be syn-Brasiliano, whereas the IOCG type occurrences are weakly associated with the late Neoproterozoic to Eopaleozoic time. Some authors (Huhn et al., 2011; 2014) associate local IOCG occurrences (e.g. Riacho do Pontal) with orebodies controlled by shear zones, i.e., with a ductile, compressive environment at the end of the Brasiliano orogeny. Other occurrences are clearly post-Brasiliano as they overprint Eopaleozoic sedimentary rocks. Iron mineralization is less well constrained for BIF-related mineralization, whereas the association of the Fe-Skarns at the end of the Brasiliano period is better established.

There are a great number of gold, copper and iron mineralization that are associated with the final periods of the Brasiliano orogenic event. This suggest that this period was a major event of metal transfer within the BP. More age determinations and more precise dating of the different mineral systems of different commodities is essential for a clearer definition whether mineralization has a time-overlap, or is part of the same mineral system.

REFERENCES

Aura Minerals, 2012, NI 43-101 Techinical Report on the Feasibility Study for the Serrote da Laje Project, Alagoas Brazil, Toronto, 286p.

Arthaud, M.H., Caby, R., Fuck, R.A., Dantas, E.L., Parente, C.V., 2008, Geology of the northern Borborema Province, NE Brazil and its correlation with Nigeria, NW Africa. In: Pankhurst, R.J., Trouw, R.A.J., Brito Neves, B.B., de Wit, M.J. (Eds.), West Gondwana: Pre-Cenozoic Correlations Across the South Atlantic Region, vol. 294. Geological Society of London, pp. 49e67. Special Publications.

Caby, R., M. H. Arthaud, and C. J. Archanjo, Lithostratigraphy and petrostructural characterization of supracrustal units in the Brasiliano belt of northeast Brazil: Geodynamic implications, J. South Am. Earth Sci., 8, 235 – 246, 1995

Brito Neves, B. B., E. J. Santos, and W. R. Van Schmus, Tectonic history of the Borborema province, northeastern Brazil, in Tectonic Evolution of South America, edited by U. G. Cordani et al., pp. 151 – 182, Int. Union of Geol. Sci., Ottawa, Ont., Canada, 2000.

Costa, F.G., Palheta, E.S.M, Rodrigues, G.B., Gomes, I.P., Vasconcelos, A.M., 2015, Geochemistry and U-Pb zircon ages of plutonic rocks from the Algodões granite-greenstone terrane, Tróia Massif, northern Borborema Province, Brazil: Implications for Paleoproterozoic subduction-accretion processes, Journal of South American Earth Sciences, 59, 45-68.

Companhia de Pesquisa de Recursos Minerais. Projeto Reriutaba: relatório preliminar de pesquisa, alvarás n. 2414/80; 2505/80; 2688/80; 2689/80; 2690/80; 2691/80; 2692/80; 2693/80; 2694/80. Fortaleza: CPRM, 1983.

da Silva J.N.M., dos Santos, T.J.S., Monteiro, L.V.S., 2017, The carbonaceous phyllite rock-hosted Pedra Verde copper mine, Borborema Province, Brazil: Stable isotope constraints, structural controls and metallogenic evolution, Journal of South American Earth Sciences, 80, 422-443.

Fetter, A.H., Van Schmus, W.R., Santos, T.J.S., Nogueira Neto, J.A., Arthaud, M.H., 2000. U-Pb and Sm-Nd geochronological constraints on the crustal evolution and basement architecture of Ceará State, NW Borborema Province, NE Brazil: implications for the existence of the Paleoproterozoic Supercontinent "Atlantica". Rev. Bras. Geociências, 30, 102-106.

Ganade de Araújo, C.E., Weinberg, R.F., Cordani, R.F., 2014, Extruding the Borborema Province (NE-Brazil): a two-stage Neoproterozoic collision process, Terra Nova, Terra Nova, 26, 157–168, 2014

Huhn S.R.B., Justo A.P., Souza Filho C.R., Monteiro L.V.S. 2011. Caracterização geológica do prospecto de óxido de ferro-cobre-ouro (IOCG) Aurora, Ceará, Brasil. Revista Brasileira de Geociências, 41(3):525-538.

Huhn S.R.B., Souza, M.J., Souza Filho., C.R, Monteiro, L.V.S., 2014, Geology of the Riacho do Pontal iron oxide copper-gold (IOCG) prospect, Bahia, Brazil: hydrothermal alteration approached via hierarchical cluster analysis. Brazilian Journal of Geology, 44(2): 309-324, June 2014

Martins, G., Oliveira, E.P., Lafon, J.M., 2009, The Algodões amphibolite-tonalite gneiss sequence, Borborema Province, NE Brazil: geochemical and geochronological evidence for Paleoproterozoic accretion of oceanic plateu/back-arc basalts and adakitic plutons, Gondwana Research. 15, 71-85.

Medeiros, V.C., 2004, Evolução geodinâmica e condicionamento estrutural dos terrenos Piancó-Alto Brígida e Alto Pajeú, domínio da zona transversal, NE do Brasil. 2004. 199 f. Tese (Doutorado em Geodinâmica; Geofísica) - Universidade Federal do Rio Grande do Norte, Natal, 2004.

Oliveira, R.G., Medeiros, W.E., 2018, Deep crustal framework of the Borborema Province, NE Brazil, derived from gravity and magnetic data, Precambrian Research, 315, 45-65.

Parente, C.V., Botelho, N.F., Santos, R.V., Garcia, M.G.M., Oliveira, C.G., Verissimo, C.U.V., 2011. Contexto Geológico, Tipológico e Geoquímico Isotópico das Brechas Hidrotermalizadas de Ferro e Cobre tipo IOCG, associadas _a Bacia Eo-Paleozóica Jaibaras, da Província Borborema, Brasil. In: Frantz, J.C., Marques, J., Jost, H. (Eds.), Contribuições _a Metalogenia do Brasil, vol. 1. Universidade do Rio Grande do Sul, 26p.

Parente, C.V., Veríssimo, C.U.V., Botelho, N.F., Santos, T.J.S, Oliveira, C.G., de Lira, J.A., Martins, D.T., 2015, Depósitos de escarnitos mineralizados em ferro e cobre do arco magmático de Santa Quitéria, Ceará, Provincia Borborema do nordeste do Brasil. Brazilian. Journal of. Geology, 45 (3), 359-382.

Sá, J. M., McReath, I., Leterrier, J. ,1995, Petrology, Geochemistry and Geodynamic Setting of Proterozoic Igneous Suites of the Orós fold Belt, Borborema Province, Northeast Brazil. Journal of South American Earth Sciences, 8(3), 299-314.

Trompette, R., 1997, Neoproterozoic (600 Ma) aggregation of western Gondwana: A tentative scenario, Precambrian Research, 82, 101-112.

Van Schmus, W. R., Brito Neves, B. B., Hackspacher, P. C., Babinski, M. (1995). U-Pb and Sm-Nd geochronological studies of the Eastern Borborema Province, Northeastern Brazil, initial conclusions. Journal of South American Earth Sciences, 8(3-4), 267-288.

The Nivré gold deposit, Dorlin Project, French Guiana

Carlos Bertoni* & the Dorlin Project team
Reunion Gold
cbertoni@reuniongold.com

SUMMARY

The Dorlin Project consists of an Exploitation Permit with an area of 84 km² in the Guiana Shield of French Guiana, approximately 180 km southwest of Cayenne. The Dorlin mining district has been one of the major artisanal gold producing areas in French Guiana since 1901, when alluvial gold was discovered along the Petit Inini River and the area became famous for producing large gold nuggets. From 1974 to 1998, the area was the object of gold and base metal exploration by the French geological survey (BRGM) and by private companies. Reunion Gold has followed-up with further exploration since 2017. The Project area is underlain by a sequence of Proterozoic ultramafic to felsic volcanic rocks with minor volcaniclastic intercalations belonging to the Paramaca Group, bordered to the west by granitoids of the Guyanais Granite event.

Regolith geochemistry identified an 11 km-long north-south trending gold anomaly, which is also coincident with potassium (radiometric) and magnetic anomalies. At the southern edge of this anomaly occurs the Nivré gold deposit, centered at a mountain with an eponymous name. The deposit has been tested by diamond drill cores spaced an average 50 m apart, several trenches and deep regolith auger sampling. The three zones forming the deposit (Nivré east, south and west) are hosted by intensely sheared and altered felsic to intermediate volcanic rocks forming up to 300 m-wide, north-south, sub-vertical mineralized deformation corridors characterized by tourmalinisation, silicification and pyritisation. At the core of each mineralized zone is a tourmalinite up to tens of meters wide. Gold grade is directly proportional to the proportion of tourmaline and pyrite in the host rock. All three zones of the deposit remain open on strike and at depth and there remains significant potential to increase gold resources. The Nivré gold mineralization is interpreted as the product of an orogenic shearing event overprinting a volcanogenic sequence that had anomalous gold and base metals content.

Regolith geology of the Saramacca project

Rayiez Bhoelan*
IAMGOLD -Suriname Exploration
Student Mineral Geosciences
Anton de Kom university of Suriname Paramaribo, Suriname

rayiez_bhoelan@hotmail.com rayiez_bhoelan@iamgold.com

Dennis Lapoint
Lecturer Mineral Geosciences
Anton de Kom university of Suriname Paramaribo, Suriname

dennis.lapoint@gmail.com

** corresponding author-poster is part of MSc thesis project*

SUMMARY

Exploration in a tropical environment as the rainforest in Suriname has many challenges. Deep weathering and a regolith ranging from two to two hundred meters is the norm in most of the Guiana shield. The Marowijne greenstone belt hosts some of the few gold deposits explored and exploited in the recent decades in Suriname. It is therefore of utmost importance to understand the landscape and the regolith developed onto this geological setting. The Saramacca gold project of the IAMGOLD provides the unique opportunity to "peek" into the regolith over the greenstones in Suriname. Field mapping was conducted first. And to complement the mapping approximately 450 surface samples were taken and assayed at Filab in Paramaribo for Au and a suite of 40 elements by FA, ICP-MS and ICP-AES. Correlations coefficients indicate As and Sb to be the best pathfinders for gold. Pulp analysed by a Terraspec High res SWIR mineral analyser indicate paragonite at surface within altered clays and may vector towards favourable structures.

Key words: Geochemistry, Regolith, Greenstone, Suriname, Gold, Laterite

INTRODUCTION

Saramacca gold project lies within the Saramacca concession of IAMGOLD in the district of Brokopondo, Suriname. Situated 27 km south west (straight line) of the Rosebel Gold Mines N.V. and 104 km south (straight line) of Paramaribo, the capital of Suriname. A laterite road heading west from" km 19" on the paved Browns road leads to the project area. The main mineralized zone is situated on the eastern flank of the hill name "Majoro dam". The Majorodam *gebergte (dutch for mountain)* is part of the NW-SE trending Brokolonko range, which's western flanks form the eastern part of the valleys and creeks that feed the Saramacca river. Geologically the project lies in the Paramacca formation which is dominated by pillow lavas, Andesites and tuffs (Kroonenberg, et al., 2016). The main objective of this study is to identify the behaviour of trace elements and alteration of surface materials to aid exploration efforts in these deeply weathered and dense vegetated areas as Saramacca within theMarowijne greenstone belt of Suriname.

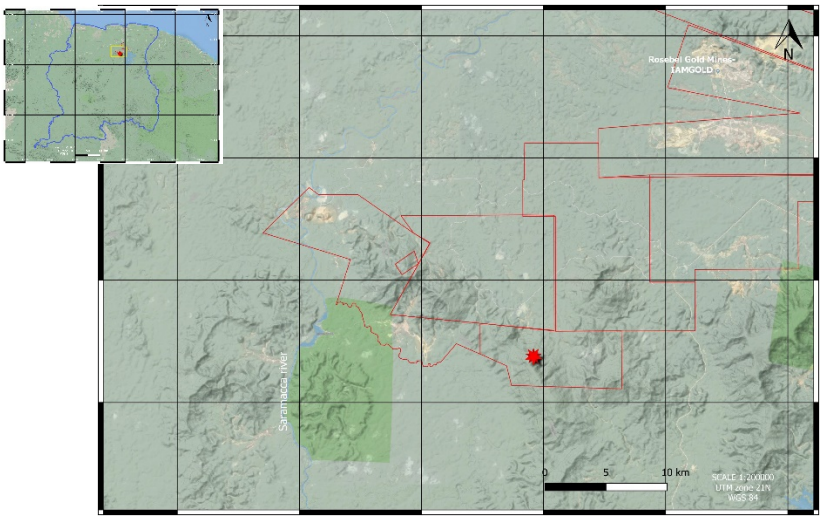

Figure 1: Location map of Saramacca project within IAMGOLD concessions and within Suriname. Saramacca project is located at the red star within the Saramacca concession (Background: Bing Areal overlain on DEM of SRTM data)

METHOD

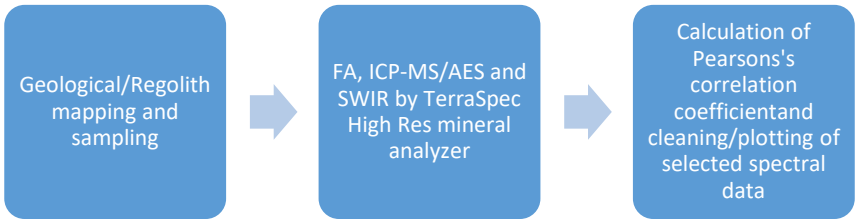

Figure 2: Generalized flowchart of methods used in this study

RESULTS

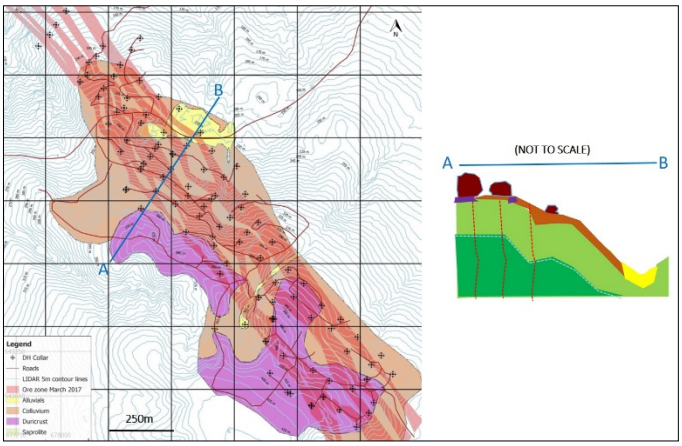

Figure 3: Plan map of the regolith cover over Saramacca project with a cartoon of the typical weathering profile in the area (note: section not to scale, and ferricrete blocks are not extensive enough to plot on plan map

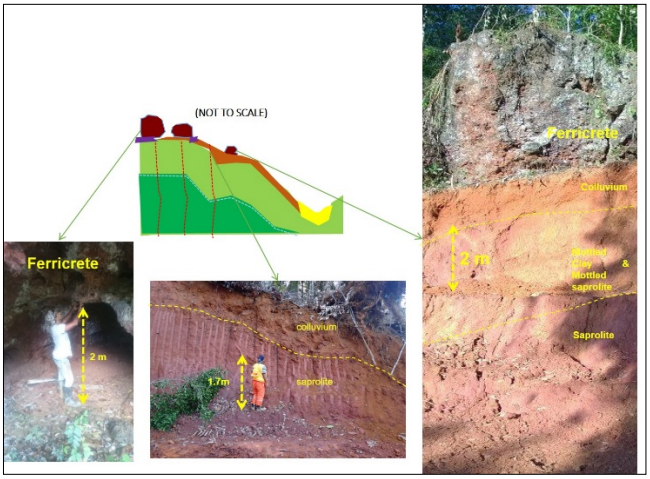

Figure 4: Collage of field images showing the mapped contacts of the different regolith units in Saramacca

Figure 5: Zoomed in photo of colluvium; which consists out of a poorly sorted matrix of clays, indurated fragments, Fe-and Mn-ox rich fragments of Duricrust and Ferricretes

It has been revealed from field mapping that the area is dominated by a 0.5m to 4.5m ranging cover of colluvium. This colluvium consists mostly of massive ferruginous clay with clasts of indurated saprolite, duricrusts and ferricrete fragments, ranging from 1 cm to 3m wide. Some of the clasts are in situ duricrust from the top of the profile, which have a gossanous texture (massive with beehive like texture as remnant of weathered sulfides). There are also clasts of porous duricrust which come from the un-mineralized portions of the relict landscape. On top of the duricrust sits are large (4m high) extremely weathered blocks of what I interpret to be ferricrete. Some boulders of this ferricrete have also been observed on top the colluvium.

Table 1: Pearsons correlation coefficient for the best five elements vs Au from ICP-MS data set

Element	As_ppm	Sb_ppm	Cd_ppm	W_ppm	Be_ppm
Au_ppm	0.68	0.63	0.41	0.30	0.25

Table 2: Pearsons correlation coefficient for the best five elements vs Au from ICP-AES data set

Element	As_ppm	Be_ppm	Bi_ppm	La_ppm	Mo_ppm

The difference in magnitude of detection limits between ICP-MS and ICP-AES explains why antimony is not correlating well with Au for ICP-AES data set. But there is a fair consistent correlation between gold and arsenic throughout the data sets.

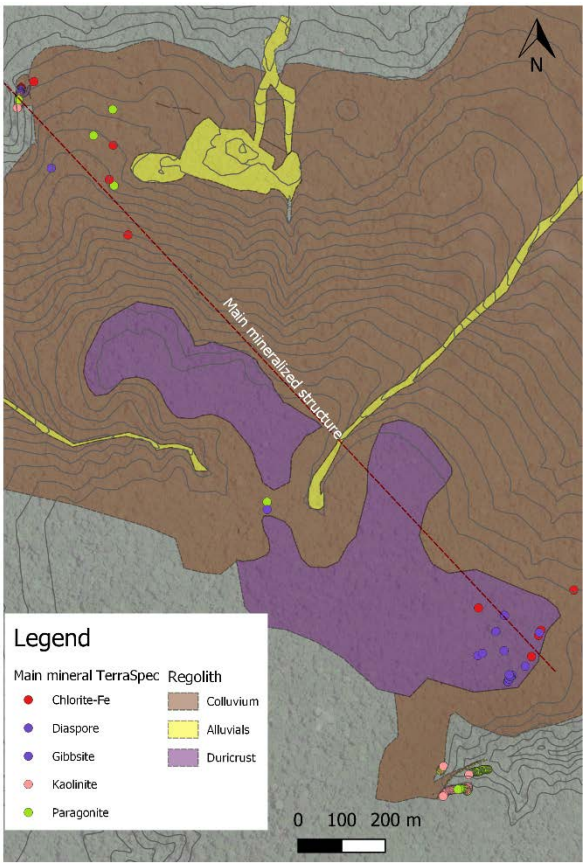

Figure 6: Selection of samples analysed by the Terraspec SWIR mineral analyser in the in situ domain (the duricrust) and in the transported domain (colluvium).

The plots clearly help map out the duricrust extents by plots of gibbsite and few diaspore occurences. In areas where altered clays were sampled and deeper parts of the weathering profile are visible and sampled, paragonite traces seems to make it to the surface.

CONCLUSIONS

The mapping shows a quite normal profile over the in situ part of the project where saprolite progresses into mottled clay and massive clays where the latter gets indurated into duricrust and a well-developed, but dissected, carapace exists over this south-eastern part of the project area. Given the location of the mineralized structure, which of course adds the facts that there will be preferential weathering the area, has had material move downslope, hence this extensive colluvium layer. For the sporadic but intriguing Ferricrete blocks I interpret that these are older gullies and streams. The nature of these at outcrop scale is that they are a mass of cemented boulders and cobbles, and not just because of extensive weathering adding circular or rounded features to these. But the macroscopic texture is that of creek bed conglomerate. When broken or sampled, all that is seen is massive hematite.

From the surface sampling over the Saramacca project it becomes clear that there is a strong correlation between gold and arsenic and bismuth. These are typical pathfinder elements in orogenic terrains (Goldfarb, et al., 2005). The implication of the plots in Figure 6 are that from the Saramacca deposit at first hand we can learn that from any surface mapping the duricrust cap can be distinguished by gibbsite content and that around structures paragonites survive within the weathering profile and may vector towards a favourable structure (Ojeda, 2017). These preliminary findings can be of significance for green field exploration strategies within the Marowijne greenstone belt.

REFERENCES

Goldfarb, R. J., Baker, T., Benoit, D., Groves, D. I., Hart, C. J., & Gosseline, P. (2005). Distribution, Character, and Genesis of Gold Deposits in Metamorphic Terranes. *Economic Geology 100th Anniversary Volume*, pp. 407-450.

Kroonenberg, S., De Roever, E., Fraga, L., Reis , N., Faraco, T., Lafon , J.-M., . . . Wong , T. (2016). Paleoproterozoic evolution of the Guiana Shield in Suriname: A revised model. *Netherlands Journal of Geosciences — Geologie en Mijnbouw*, 491–522.

Ojeda, F. R. (2017). *Report Spectrometry Saramacca.* Lima: UNPUBLISHED REPORT.

Polyphase gold mineralization at the Yaou deposit, French Guiana

Vincent Combes *
GeoRessources Université de Lorraine
Auplata SA Cayenne, Guyane
Nancy, France
vincentcombes25@gmail.com

Aurélien Eglinger
GeoRessources Université de Lorraine
Nancy, France
aurelien.eglinger@univ-lorraine.fr

Anne-Sylvie André Mayer
GeoRessources Université de Lorraine
Nancy, France
anne-sylvie.andre@univ-lorraine.fr

Christophe Scheffer
Université de Guyane, Cayenne France

Pierre Gibert
Auplata SA Cayenne, Guyane, France

Arnauld Heuret
Université de Guyane, Cayenne, France

**presenting author*

SUMMARY

This work, focusing on the study of the Yaou gold deposit in French Guiana, aims at characterizing the timing of lode gold in a polyphase deformation system. For that purpose, a precise study of deformation stages, microtectonics features, veining, pyritization (*in situ* LA-ICP-MS analyses on auriferous pyrite) and alteration style has been performed mainly from core logging, the area being covered by deep lateritization. First results define five deformation stages with at least two main gold events, with remobilizations and/or new gold inputs.

Key words: Orogenic gold, polyphased deposit, pyrite, deformation stages.

INTRODUCTION

The Yaou gold deposit, owned by the gold exploration and mining company Auplata, is located in French Guiana, South America, within in the Guiana Shield (figure 1).

The purposes of this present study are to define the single phase or polyphase character of the gold deposit, to understand the role of different units including intrusions and mylonite, to establish the link between deformation stages, quartz-carbonate vein generation, sulfide generations, alteration styles and gold mineralization. The ultimate goal is to establish a relative chronology of the deposit incorporating all of these studies.
Characteristics of orogenic gold deposits are discussed in publications of Dubé and Gosselin, (2007); Goldfarb et al. (2005); Groves et al. (2003); Goldfarb et al. (2001); Robert and Poulsen, (2001). Two models of Au mineralization deposition are discussed by Phillips and Powell, (2009). The continuum model (a single deposition event) originally proposed by Colvine et al. (1988) and reworked by Groves et al. (1990); and the Metamorphic model with several events, suggested as an alternative by Phillips and Powell, (2009). Various gold deposits have been identified as having polyphased release of gold as evidenced by Le Mignot et al. (2017) and references therein. *In situ* analyses of trace elements in pyrite using the LA-ICP-MS is a common technique to identified Au bearing pyrite generations associated to gold deposits (Velasquez et al., 2012; Sung et al., 2009; Large et al., 2007).

The Guiana shield located in South America hosts numerous gold mineralization in spatial and temporal relationship with the Transamazonian orogeny (2250-1950 Ma) as defined by Vanderhaeghe et al. (1998) and Delor et al. (2003a). The geological evolution of this Precambrian shield is defined by four phases, an Archean basement, a main Transamazonian orogeny (D1 and D2a), a late-Transamazonian orogeny (D2b), and minor late Proterozoic and Paleozoic events (Vanderhaeghe et al., 1998; Delor et al., 2003a). In terms of lithology units, French Guiana is composed of three TTG complexes and two greenstone belts. Yaou is located in the southern branch of the Proterozoic Paramaca Greenstone Belt (PGB) at the boundary with the southern TTG complex.

METHOD

Logging of deformation features, lithologies, veining and sulphides abundance together with sampling of more than 30 drillholes is carried out for this study. Petrographic and metallographic observations are made on 43 thin sections at GeoRessources, Nancy (France). Sulfide associated with deformations phases are studied and discriminated using, SEM-BSE images, trace elements mapping on EPMA (GeoRessources, Nancy, France) and *in situ* (70 ablations) trace elements analyses using LA-ICP-MS (GET, University of Toulouse, France).

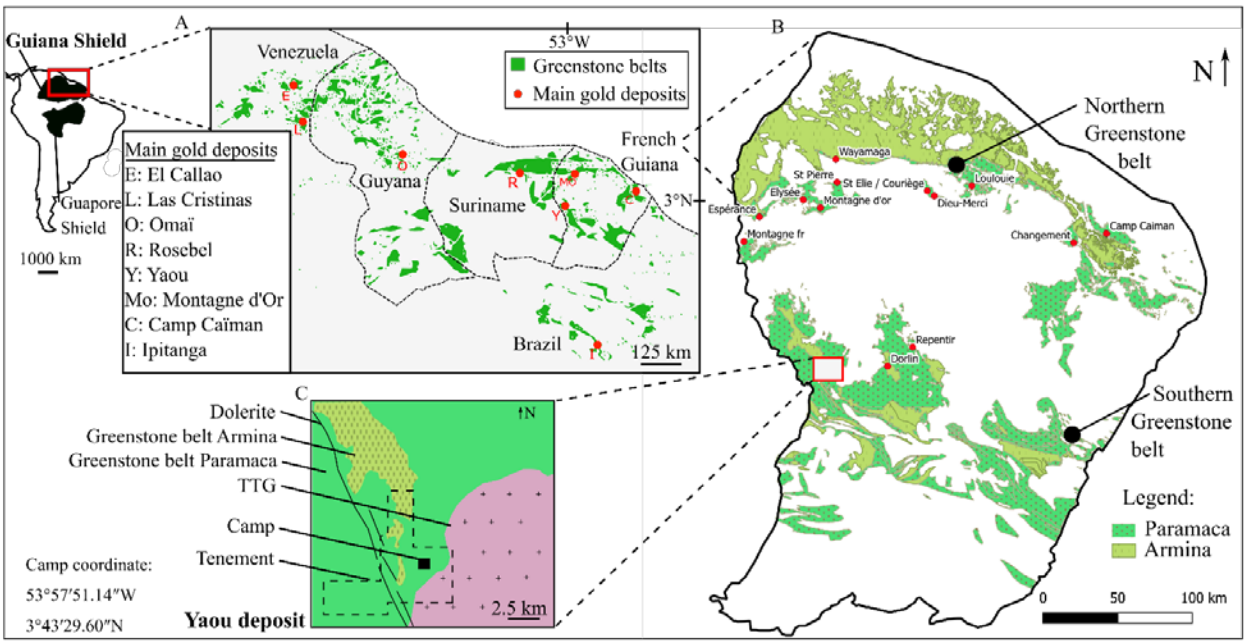

Figure 1: Simplified map of Guiana shield, French Guiana greenstone belts and main gold deposits with location of the Yaou deposit; Adapted from Delor et al. (2003a); Daoust et al. (2011) and Auplata internal reports (2016).

RESULTS

The Yaou deposit displays a rheologically controlled mineralized system associated with quartz-carbonate veins located mainly in intrusive bodies aligned in a 4.5 km structure striking N60° along a shear zone (figure 2). Gold is itself carried by pyrite. Two lithologies host the mineralized veins; a fine grained dioritic intrusive composed of hydrothermal albite, ankerite, minor quartz, sericite and pyrite, as well as a felsic mylonitized metasedimentary unit made of quartz, chlorite and sericite. The precise role of these two units is still debated, a chemical trap or a physical-rheological control. The surrounding area is characterized by mafic and ultramafic schist. The observed deformation stages show a progressive evolution from the ductile regime to the brittle one. Events are defined by crosscuttings relationships. Phases D_1 and D_2 are well marked in the host lithologies. The veins associated with D_1 and D_2 are boudinaged and folded. A post D_2 plutonic episode forms dykes and plutons of intermediate composition that are locally mylonitized by the D_3 deformation phase. The intrusion and the mylonitisation could be synchronous. This D_3 shear is mostly recorded in a felsic schist unit having a metasedimentary photolith. A S_3 foliation is observed together with a mylonitic gradient and millimeter scale pyrites with quartz-chlorite-calcite pressure fringes (porphyroclasts pre to syn D_3). A fragile deformation event gives D_4 quartz veins mostly in the intrusion, and more rarely cross-cutting the shear zone and the mafic schist. A late brecciation D_5 affects the intrusive unit. These monogenic cataclastites are cross-cutting the D_4 veins. By adding the observations of cores, petrographic data and trace elements analyses, it is possible to discriminate generations of vein and associated pyrite linked to deformation stages. Pyrite Py_0 are interpreted as diagenetic core within pyrite Py_3, these Py_3 being associated with the D_3 deformation. Two types of Py_4 are observed, a first population, disseminated along D_4 veins within the alteration halo. A second population is set only at the edges and within D_4 veins. The pyrite Py_5 are situated within the D_5 matrix in the cement of the breccia. Results of *in situ* analyses using LA-ICP-MS on pyrite show at least two gold events associated with D_3 and D_4 confirming the polyphased nature of the deposit (figure 3 and 4). Pyrite Py_3 exhibits an Au-As correlation with a cobalt and arsenic rhythmic zonation. The core is interpreted as detrital and diagenetic pyrite Py_0 that could be source for a primary gold release (the host rock being a metasediment). Gold in pyrite Py_4 is found as solid solution, as nanoparticles and as inclusions in association with elements such as Te (gold tellurium), Ag (electrum) and Bi.

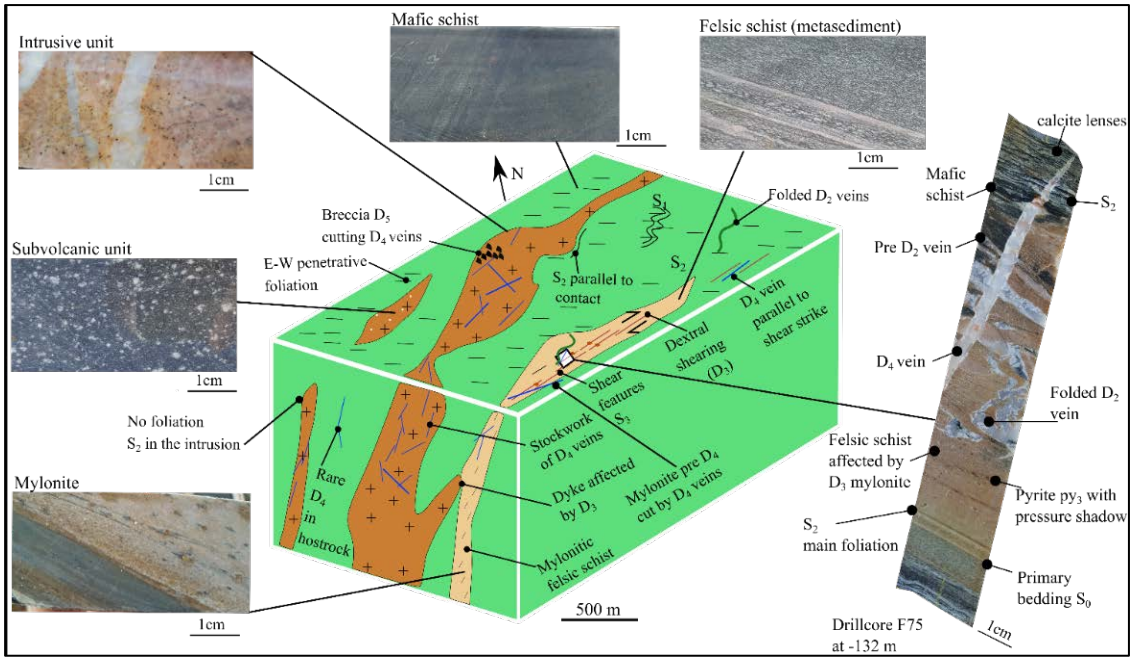

Figure 2: 3D block diagram showing the deposit geometry together with the main lithologies and deformation stages.

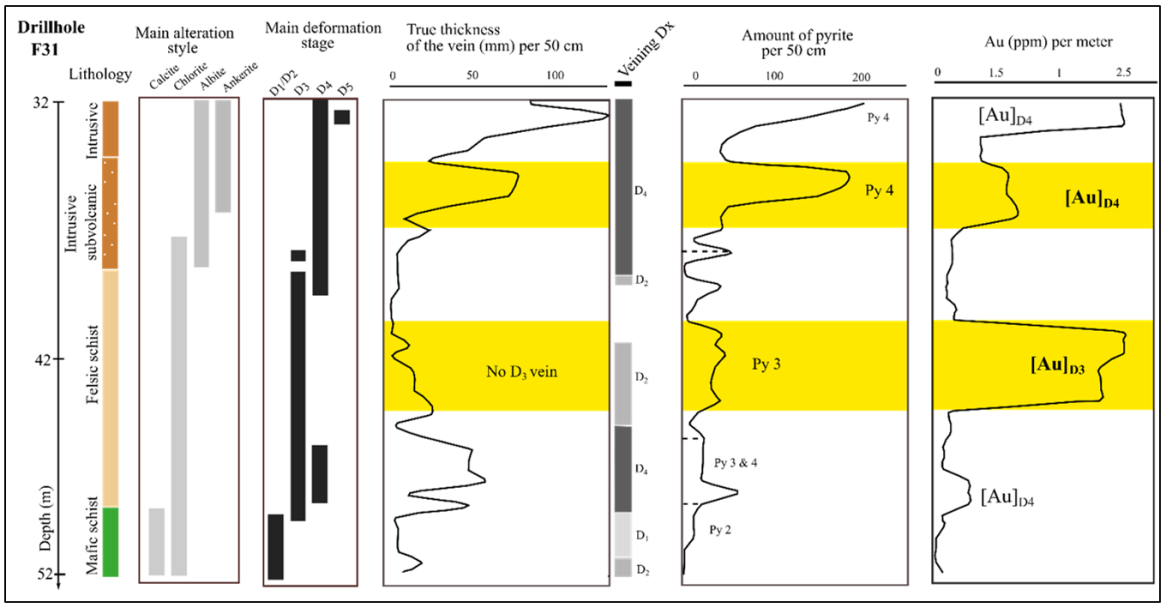

Figure 3: Relationships between lithology, vein abundance, amount of pyrite, alteration style, deformation stages and gold grades in a drillcore.

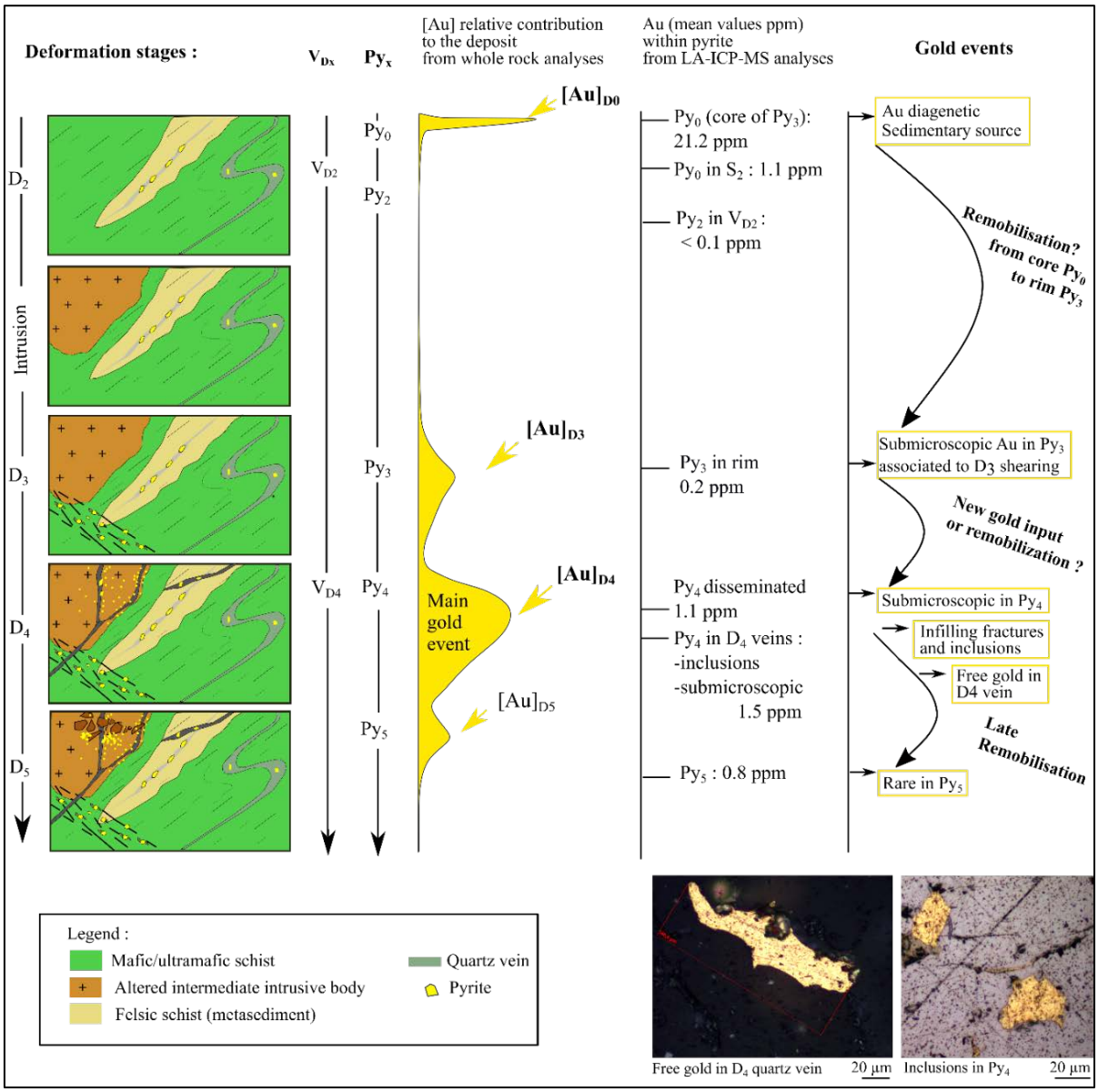

Figure 4: Paragenesis of gold and time showing the defined gold events.

CONCLUSIONS

Following this study, five deformation events are defined. A clear association lithology-veining is highlighted. Phases D_3 and D_4 are responsible for the bulk of the Au mineralization with D_3 being the shearing event and D_4 the main gold event marked by the D_4 auriferous pyritization. A high-grade source of gold is seen in diagenetic arsenian pyrite cores Py_0. D_5 contributed little to the total Au budget. Rare free gold is observed in quartz vein near Py_4 within D_4 veins. At a submicroscopic scale, gold is present in lattice as solid solution in Py_4 disseminated and as inclusion, nanoparticles and solid solution in Py_4 within D_4 veins using the solubility limit for gold from Reich et al. (2005). Gold in Py_0 is in association with As. The precise role of both the intrusive body and the D_3 mylonite is still unclear.

ACKNOWLEDGMENTS

This study is part of Vincent Combes's Ph.D. research at GeoRessources, Université de Nancy. This study was funded by Auplata SA Cayenne (France) and the CREGU-GeoRessources, Nancy (France). Didier. Tamagno, CEO of Auplata SA is acknowledged for allowing this work and for financial support. This present study greatly benefited from discussions and friendly support from Frédéric Tona.

REFERENCES

Daoust C, Voicu G, Brisson H, Gauthier M (2011) Geological setting of the Paleoproterozoic Rosebel gold district, Guiana Shield, Suriname. J. of S. Am. Earth Sciences 32:222-245.

Delor C, Lahondère D, Egal E, Lafon J-M, Cocherie A, Guerrot C, Rossi P, Truffert C, Théveniaut H, Phillips D, Avelar VGd (2003a) Transamazonian crustal growth and reworking as revealed by the 1:500000 scale geological map of French Guiana. Géologie de la Fr. 2-3-4:5-57.

Dubé, B. et Gosselin, P., 2007, Greenstone-hosted quartz-carbonate vein deposits, in Goodfellow, W.D., ed., Mineral Deposits of Canada: A Synthesis of Major Deposit Types, District Metallogeny, the Evolution of Geological Provinces, and Exploration Methods: Geological Association of Canada, Mineral Deposits Division, Special Publication No. 5, p. 49-73.

Goldfarb, R. J., Baker, T., Dubé, B., Groves, D. I., Hart, C. R. J., and Gosselin, P., 2005, Distribution, Character, and Genesis of Gold Deposits in Metamorphic Terranes, p. 407-450.

Goldfarb, R. J., Groves, D. I., and Gardoll, S., 2001, Orogenic gold and geological time: a global synthesis: Ore Geology Reviews, v. 18, p. 1-75

Groves, D.I., Goldfarb, R.J., Robert, F., and Hart, C.J.R., 2003, Gold deposits in metamorphic belts: Overview of current understanding, outstanding problems, future research, and exploration significance: Economic Geology, v. 98, p. 1-29.

Le Mignot, E., Reisberg, L., André-Mayer, A.-S., Bourassa, Y., and Miller, J., 2016, Re-Os geochronological evidence for multiple Paleoproterozoic gold events at the scale of the West African craton: Economic Geology, v. 112, p. 145–168.

Large, R.R., Maslennikov, V.V., Robert, V., Danyushevsky, L.V., and Chang, Z.S., 2007, Multistage sedimentary and metamorphic origin of pyrite and gold in the giant Sukhoi Log deposit, Lena gold province, Russia: Economic Geology, v. 102, p. 1233–1267.

Reich M., Kesler S. E., Utsunomiya S., Palenik C. S., Chryssoulis S. L. and Ewing R. C. (2005) Solubility of gold in arsenian pyrite. Geochim. Cosmochim. Acta 69, 2781–2796.

Phillips, G.N., Powell, R., 2009. Formation of gold deposits-review and evaluation of the continuum model. Earth-Science Reviews 94, 1–21

Robert, F. &. Poulsen, K. H. 2001. Vein formation and deformation in Greenstone Gold Deposits. Reviews in Economic Geology Volume 14, 111-155

Vanderhaeghe O, Ledru P, Thiéblemont D, Egal E, Cocherie A, Tegyey M, Milési J-P (1998) Contrasting mechanism of crustal growth: Geodynamic evolution of the Paleoproterozoic granite–greenstone belts of French Guiana. Precambrian Res. 92:165-193.

Velasquez G., Beziat D., Salvi S., Siebenaller L., Borisova A. Y., Pokrovski G. B. and de Parseval P. (2014) Formation and deformation of pyrite and implications for gold mineralization in the El Callao District, Venezuela. Econ. Geol. 109, 457–486.

The La Trampa wedge (SE Colombia) revisited

Hugo de Boorder
Faculty of Geosciences, Utrecht University
P.O. 80.115
3508 TC Utrecht
The Netherlands

H.deBoorder@uu.nl

SUMMARY

The La Trampa structure was conceived during geological interpretation of side-looking airborne radar (SLAR) imagery and field reconnaissance during the Proyecto Radargramétrico del Amazonas (PRORADAM). The objective of the project resided in the planning and orientation of the social-economic development of the Amazonas region of Colombia (1972-1982). The La Trampa structure is based on lineaments inferred from the imagery between the Putomayo and Atabapo Rivers with a length of ca. 1000 km. Additional research suggests its reality and relevance in a tectonic framework. Current satellite imagery provides an additional data base to place the structures in a continent-scale context.

Key words: Colombia, Amazonas, basement, structure.

INTRODUCTION

The knowledge of the lithological complexes of the western Guiana Shield has gradually increased. Their structural coherence, however, is still limited to a framework of steep faults largely inferred at different scales. In this context, the SLAR study from which the La Trampa wedge emerged (Figure 1; De Boorder, 1978, 1981) is, according to Kroonenberg (2018), still the only structural information in national maps. It was very tentatively conceived in the upper reaches of the Amazone Basin on the basis of apparent alignment in the imagery of stream courses and remnants of clastic formations and on reconnaisance along the Piráparaná, Vaupés and Apaporis Rivers (see PRORADAM, 1979). Earthquakes have been known in far-eastern Colombia (locally remembered as'Cuando se mueva La Tierra …'). A search of the seismological archive (Ramirez, 1975) in 1978 delivered a group of epicenters in southeastern Colombia and adjacent Peru (Figure 1) that scatter along the lineaments making up the La Trampa SLAR-derived inferences, some located about the intersections with long, NW-striking lineaments largely based on erosion scarps, stretches of the NW-SE running principal river courses (Vaupés, Apaporis, Caquetá and Putumayo Rivers) and isolated outcrops. The 200-600 km deep hypocentres are possibly attributable to remnants of a subducted lithosphere slab (M.J.R. Wortel, personal communication, 1982). Although these tend to lend support to the reality of the inferred structures, a relation in timing is unclear.

Since 1978, geological observations and insight have increased but the La Trampa structure is still enigmatic, although diverse observations appear converging:

• Confirmation of the some lineaments as faults in the course of later field work (C. Cáceres and F. Cediel, personal communication, 1992; Kroonenberg, 2018).

• The addition of dextral displacement along a NE-striking lineament (Geotec, 2000).

• The north-south trending stretch of depth to basement contours below Tertiary and Quaternary sediments, northwest of Mitú (Kroonenberg, 2018), in line with the very notable, exceptional north-south course of the Piráparaná River within the La Trampa domain,

• The concentration of small plutons within and along the inferred La Trampa domain northeast of Mitú (Kroonenberg, 2018).

• The potential extent of the linears defining the La Trampa structure in Colombia into Venezuela (Wynn et al., 1993; Hackley et al., 2005).

METHODS AND RESULTS

At the time I conceived the La Trampa structure (De Boorder, 1978, 1981), spectral remote sensing imagery was costly and its resolution still insufficient for geological interpretation purposes. Airborne magnetics flown for hydrocarbon exploration (Anonymous, 1987) appeared of reduced significance in the present study of the crystalline basement structure (Kroonenberg and Reeves, 2012). The current free and efficient availability of satellite spectral imagery, together with updated geological maps and national and continent-wide geoinformation systems supports further interpretation even in some regions of tropical rainforest. In the interpretation of SLAR imagery most linear features are suggested to represent faults and joint systems. In satellite spectral imagery, foliations become visible where lithological banding is apparent. Here, the GoogleEarth imagery is now an important supplementary tool as is demonstrated for instance in the area south of Ciudad Bolivar when compared with the geologic shaded relief map of Venezuela (Hackley et al., 2005). Important factors in the reconaissance of the crystalline basement are topographic relief, thickness of sedimentary cover and vegetation density. In the case of the La Trampa structure, GoogleEarth imagery now suggests its defining lineaments extend into western Venezuela.

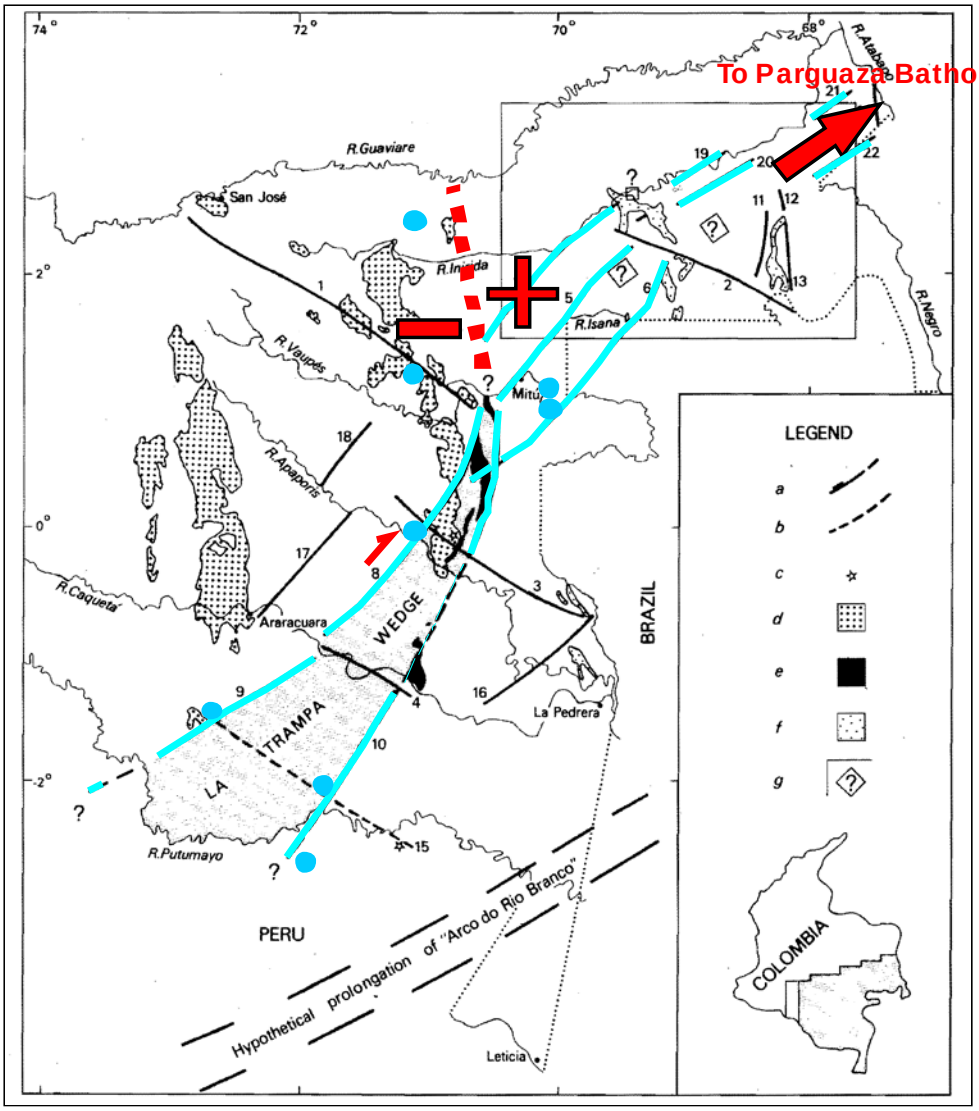

Figure 1. Overview of the La Trampa stucture, modified after De Boorder (1981). Blue - Originall lineaments and earthquake epicentres (closed circles). Red – New data: dotted line - trend of basement gradient (after Kroonenberg, 2018); + and – corresponding shallow and deep sectors; NE striking arrow – extent of La Trampa faults towards the Parguaza Batholith in Venezuela; half arrow – dextral displacement (after Geotec, 2000).

Here, immediately across the border between Colombia and Venezuela, NE-striking morphological linears link on to the southern tip of the ovoid Parguaza batholith and a trend of strongly elongated ridges which wraps around the entire eastern margin of the batholith along an approximately 200 km northerly trend as far as the town of Puerto Carreño on the Orinoco River. The positive relief of the ridges indicates relative resistance to weathering and erosion and suggests a foliation in the country rock made up by the Early Proterozoic Cuchivero Group consisting of silicic intrusive rocks (Hackley et al., 2005). Hackley and co-workers interpret the ridges in terms of faults and report a strongly faulted eastern margin of the c. 1500 Ma Parguaza Batholith. U.S. Geological Survey and Corporación Venezolano de Guayana, Técnica Minera, C.A. (1993) reported some potential of tin, tantalum, niobium and titanium mineralization. Speculating from the above map and GoogleEarth imagery, the Parguaza Bathlith appears located in the junction of the NE-striking sinistral Bolívar Fault System (Short and Steenken, 1962), defined by the El Pao, Guri and Ciudad Piar shear zones and their possible southwesterly extent, and the La Trampa structure. This junction, in part speculative, would place the La Trampa structure in an overall tectonic framework of (sub)continental proportions.

CONCLUSIONS

Since 1978, the La Trampa structure has gained in geological significance from the results of regional and local studies. Its nature is, however, still enigmatic. Efficiently available GoogleEarth imagery is a supplementary tool which suggests that the c. 1100 km long La Trampa structure is only a segment of a much wider and longer tectonic framework of subcontinental proportions. The emplacement of the Parguaza Batholith in a node of this framework further suggests its reality and, in view of the mineral potential of the Parguaza granites, a potential target for continuing regional investigation.

REFERENCES

Anonymous, 1987. Amoco explores big Colombian region: First Break, 1987, 5(3), 81.

De Boorder, H., 1978, Contribución a la geología de las cuencas de los ríos Vaupés, Piráparaná yTaraira: Unpublished report PRORADAM, Bogotá, 50 pp.

De Boorder, H., 1980, Contribución preliminar al estudio de la estructura geológica de la Amazonia colombiana: Revista CIAF, 5(1), 49–96.

De Boorder, H., 1981, Structural-geological interpretation of SLAR imagery of the Colombian Amazones: Transactions Institution of Mining and Metallallurgy 90:B145–B152.

Geotec Ltd 2000 Sistema de Información Geográfica de la Geología de Colombia, Bogota.

Hackley, P. C., Urbani, F, Karlsen, A. W., and Garrity CP, 2005, Geologic shaded relief map of Venezuela, 1:750.000: USGS Open File Rep, 2005–1038.

Kroonenberg, S.B., 2018, The Proterozoic Basement of the Western Guiana Shield and the Northern Andes, In: Cediel, F. and. Shaw R.P. (eds.), Geology and Tectonics of Northwestern South America, Frontiers in Earth Sciences, https://doi.org/10.1007/978-3-319-76132-9_3

Kroonenberg, S. B., and Reeves, C.V., 2012, Geology and petroleum potential, Vaupés-Amazonas Basins, Colombia, In: Cediel, F. (Ed.) Petroleum Geology of Colombia, Universidad EAFIT, Medellín, 92 p.

PRORADAM, 1979, La Amazonía colombiana y sus recursos: Instituto Geográfico ‘Agustin Codazzi’, Proyecto Radargramétrico del Amazonas, Bogota, 590 p.

Ramirez, J. E., 1975, Historia de los Terremotos de Colombia: Instituto Geográfico 'Agustin Codazzi', Bogota, 250 p.

Short, K.C., and Steenken, W. F., 1962, A reconnaisance of the Guayana Shield from Guasipati to the Rio Aro, Venezuela: Boletin Informativo, Asociación Venezolano de Geología, Minería y Petróleo, 5(7), 189-221.

U.S. Geological Survey and Corporación Venezolano de Guayana, Técnica Minera, C.A., 1993, Geology and Mineral Resource Assesment of the Venezuelan Guayana Shield: U.S.Geological Survey Bulletin 2062.

Wynn, J.C., Cox, D.P., Gray, F., and Schruben, P.G. (Compilers), 1993, Geologic and Tectonic Map of the Venezuelan Guayana Shield, 1:1,000,000: U.S. Geological Survey, Bulletin 2062.

Complex 3D Integration for Mineral Exploration

Eric A. de Kemp *

Geological Survey of Canada
601 Booth Street, Ottawa,
Ontario, Canada, K1A 0E9

Eric.dekemp@canada.ca

SUMMARY

The future success of frontier mineral exploration exercises are in no small part dependant on development of a common practice that efficiently deals with big and complex mineral exploration data. Dealing with the diversity and size of geospatial data required to support an exploration cycle for a specific commodity and target type can be overwhelming. This problem needs to be overcome through investment in development of expertise and tools, so emergent technologies for multi-scaler 3D modelling can be reasonably applied. Simple data analysis techniques can reduce data size and complexity, supporting the establishment of links from mine to green-fields targets.

Key words: Regional, Greenfields, Targeting, Complex Geological Data, Integration

The Bakhuis Granulite Belt in W Suriname, its development and exhumation

E.W.F. de Roever*
Dept. of Earth Sciences
VU Amsterdam,
De Boelelaan 1085,
1081 HV Amsterdam,
the Netherlands
ederoever@ziggo.nl

F.F. Beunk
Dept. of Earth Sciences
VU Amsterdam,
De Boelelaan 1085,
1081 HV Amsterdam,
the Netherlands

K. Yi
KBSI
YangCheong 804-1,
Ochang, Cheongwon
Chungbuk 363-883,
Korea
kyi@kbsi.re.kr

K. de Groot
Dept. of Earth Sciences
VU Amsterdam,
De Boelelaan 1085,
1081 HV Amsterdam,
the Netherlands

M. Klaver
Dept. of Earth Sciences
VU Amsterdam,
De Boelelaan 1085,
1081 HV Amsterdam,
the Netherlands

J.A.M. Nanne
Dept. of Earth Sciences
VU Amsterdam,
De Boelelaan 1085,
1081 HV Amsterdam,
the Netherlands

W. van de Steeg
Dept. of Earth Sciences
VU Amsterdam,
De Boelelaan 1085,
1081 HV Amsterdam,
the Netherlands

A.C.D. Thijssen
Dept. of Earth Sciences
VU Amsterdam,
De Boelelaan 1085,
1081 HV Amsterdam,
the Netherlands

B. Uunk
Dept. of Earth Sciences
VU Amsterdam,
De Boelelaan 1085,
1081 HV Amsterdam,
the Netherlands

H. Vos
Dept. of Earth Sciences
VU Amsterdam,
De Boelelaan 1085,
1081 HV Amsterdam,
the Netherlands

G.R. Davies
Dept. of Earth Sciences
VU Amsterdam,
De Boelelaan 1085,
1081 HV Amsterdam,
the Netherlands

F.M. Brouwer
Dept. of Earth Sciences
VU Amsterdam,
De Boelelaan 1085,
1081 HV Amsterdam,
the Netherlands

SUMMARY

The Bakhuis Granulite Belt (BGB) was a deep part of the crust during the Trans-Amazonian orogeny, before ~ 2.0 Ga. The precursor rocks of the granulites are Paleoproterozoic sediments and volcanics, probably deposited near the West-African Craton. They underwent ultrahigh-temperature metamorphism (UHTM) at 2.09 – 2.03 Ga, after the main metamorphism in the greenstone belt. Charnockites in the SW are not related to the UHTM. Exhumation of the BGB started during the final stages of the Trans-Amazonian orogeny, after ~ 1.98 Ga, and lasted until the present. The Bakhuis Horst may be a pop-up structure instead of a horst, at least during the Nickerie Metamorphic Episode at ~ 1.2 Ga.

Key words: Bakhuis Granulite Belt, UHT metamorphism, charnockite, Bakhuis Horst, bauxite

INTRODUCTION

The Bakhuis Granulite Belt (BGB) lies in the northern-central part of the Guiana Shield and divides the Trans-Amazonian Greenstone belt along the Atlantic coast in two parts (Figure 1a). The BGB consists mainly of intermediate and mafic granulites, with metapelitic intercalations. Younger mafic and felsic intrusions are numerous in the SW part of the belt, but occur throughout (Figure 1b).

The metamorphism and magmatism documented in the BGB were initially studied by the first author together with geologists of the BRGM and the UFPA, Brazil. Then the study was, and is, continued with staff and students of the VU Amsterdam, and a student from the Anton de Kom University in Paramaribo, for their MSc thesis. Many results have not yet been published, but it is important to show here how the development of the BGB and the Guiana Shield influenced each other.

METHODS

Geochronological analysis was carried out by LA-ICP-MS at Utrecht University and at the Westfälische Wilhelms-Universität Münster and with the SHRIMP IIe at the Korea Basic Science Institute (KBSI) operated by Dr. Keewook Yi.

PRECURSOR ROCKS OF THE GRANULITES

The granulites are characterised by banding on a dm-m scale (Figure 2b) and represent supracrustal rocks of Paleoproterozoic age (de Roever et al., 2003). Bands of quartzite and Ca-silicate granulite and intercalations of Al-silicate-rich metapelite have a sedimentary origin. Trace element analysis of the mafic granulites indicates a volcanic origin (Klaver et al., 2015; Vos, 2016). Intermediate granulites are in part of volcanic origin and in part metasediments. Zircon analysis of an intermediate granulite indicated a volcanic origin, a basaltic andesite. The – euhedral -- zircons have pre-UHTM ages of 2146 – 2168 Ma, on average 2156 ± 6 Ma (Vos, 2016). The age agrees with the age of volcanism in the eastern arm of the greenstone belt in French Guiana, 2135 – 2160 Ma (Delor et al., 2003a). Zircons from another intermediate granulite gave pre-UHTM ages of 2167 – 2263 Ma. The large spread in ages and the irregular shape of most zircons suggest this rock is a former sediment (Vos, 2016). In the SW of the belt younger detrital zircons were found in a metapelite, LA-ICP-MS dating gave an average age of 2131 ± 11 Ma (Nanne, 2013). The precursor rocks may in part be older than the greenstone belt rocks (see below).

ULTRAHIGH-TEMPERATURE METAMORPHISM

A rather small metapelite area in the NE of the BGB, near the upper Fallawatra (UF), shows the assemblage aluminous orthopyroxene + sillimanite + quartz, diagnostic of UHTM. The orthopyroxene contains 8-10% Al_2O_3. Sapphirine occurs in some of the rocks, locally in contact with quartz (de Roever et al., 2003). Feldspar thermometry showed peak temperatures of 1000 – 1030°C (de Groot, 2009) Metapelites elsewhere in the BGB show CO_2-bearing cordierite + sillimanite ± aluminous orthopyroxene and have feldspar thermometry temperatures of 900 – 1050°C, indicating that the assemblage with primary cordierite is an UHTM assemblage, as well (Nanne, 2013; de Roever et al., 2016). These results suggest that nearly the entire BGB was subjected to UHTM. The pressure was estimated from e.g., a garnet – opx pair in the UF area, as ~ 9 – 10 kbar.

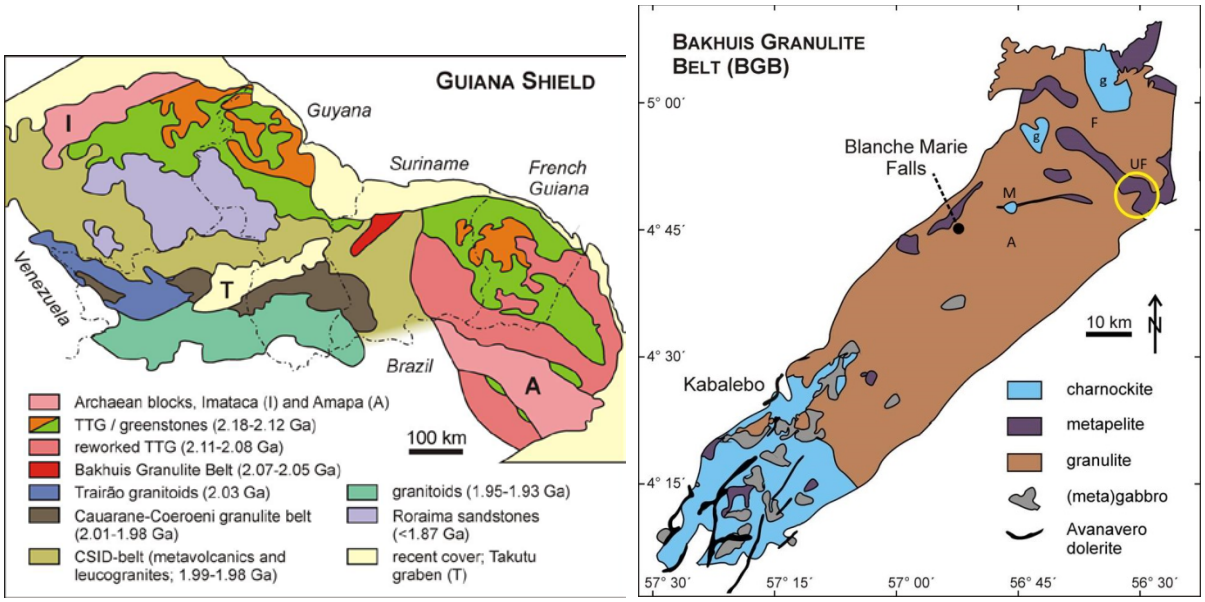

Figure 1a : simplified geology of the northern part of the Guiana Shield (Klaver et al., 2015); 1b : geology of the BGB. M : Mozes creek; F : Fallawatra creek; A : anorthosite; UF Upper Fallawatra area (yellow circle); g biotite granite

The UHTM was followed by extensive retrograde metamorphism. Orthopyroxene grains with an Al_2O_3-rich core (up to 10%) have rims with 6% Al_2O_3 and are surrounded by zones of fine, less aluminous opx and fine sillimanite. Cordierite has been replaced by fine-grained biotite-sillimanite-orthopyroxene intergrowths, usually with some kyanite. The retrograde path was anti-clockwise. Secondary CO_2 fluid inclusions in UHT quartz have a higher density than primary CO_2 inclusions, indicating a near-isobaric cooling path down to 700-750°C (de Roever et al., 2016).

Zircons from a 1-2 m wide quartz-feldspar vein at Blanche Marie Falls (Figure 1b) have an age of 2088 ± 4 Ma (van de Steeg, 2016). The vein probably formed at an early stage of UHT metamorphism, which is also indicated by the rather high Th/U ratio, 0.15 – 0.5, of the zircon. Monazite formed later in the vein, at 2056 ± 15 Ma. LA-ICP-MS dating of zircons in a Kabalebo metapelite gave an age of 2073 ± 7 Ma for the large cores, but the rims were too narrow for the laser spot (Nanne, 2013). SHRIMP dating of the rims gave an age of 2031 ± 4 Ma. Based on these ages the UHT metamorphism of the Bakhuis belt may have lasted ~50 to 65 Ma, which is rather long compared to many other UHTM occurrences, but shorter than the 100 Ma found for the Eastern Ghats, India, and the Musgrave Range, Australia (Kelsey and Hand, 2015). With its age of 2.09 – 2.03 Ga UHT metamorphism occurred after the two stages of metamorphism in the eastern arm of the greenstone belt (D1 and D2a; see Delor et al, 2003a), probably during or just after the collision of the two cratons.

A common problem in the study of UHTM is the source of the heat required to reach the extremely high temperatures at crustal depth. In several UHTM terranes the heat required was derived from contemporaneous mafic magmatism, but this is more commonly lacking (Kelsey and Hand, 2015). For the BGB asthenosphere advection or "mafic underplating" has been considered as the most likely cause of UHT metamorphism (Delor et al, 2003b). However, no clear evidence has been found for synmetamorphic mafic magmatism.

Narrow metadolerite dykes might be an indication, but show only slight folding (Figure 2d) and therefore postdate the UHTM. Earlier dating of zircons in the dykes at ~ 2060 Ma (de Roever et al., 2003) is considered to be erroneous, the zircons are heavily corroded and probably have been derived from the surrounding granulites (Uunk, 2015). The dykes are too narrow for geochronological analysis.

According to Delor et al (2003b), UHTM occurred specifically in the weak zone between the western and eastern arms of the greenstone belt, which acted as continental-scale boudins. A rather different hypothesis is provided here, which also accounts for the deep burial. The BGB is mainly surrounded by metavolcanics and granites with an age of 1.99-1.98 Ga, which replaced older rocks of which remnants are locally present, such as a small area with low-grade metabasalts and Mn-quartzites, a remnant of the greenstone belt against the SE side of the BGB. Disregarding the younger rocks, the BGB appears to divide the long greenstone belt in two parts, a western arm and an eastern one. Differences between the two arms appear to confirm this picture, e.g., only the eastern belt has an upper detrital unit, deposited in pull-apart basins (de Roever et al., 2015). However, the BGB represents only the deep crust below the greenstone belt, which may have been continuous at the time of UHTM. The greenstone belt consists of juvenile material, but that does not hold for the BGB. Four out of 12 zircon cores from a metapelite have an age of 2130 - 2230 Ma, the oldest having an age of 2233 ± 18 Ma (van de Steeg, 2016). Four out of 10 zircon cores from an intermediate granulite have an age of 2200 Ma or older, but only the oldest core, 2263 ± 72 Ma, is significantly older than 2.19 Ga (Vos, 2016). Detrital zircon from the eastern greenstone arm is derived from TTG intrusions with an age of 2.13 – 2.17 Ga and metavolcanics with an age of 2.13-2.16 Ga (Delor et al, 2003a). The BGB detrital zircons might have come from far away, but several zircon grains gave such older ages. The best explanation for these old ages is an origin outside the greenstone belt, near a craton with older material. In the model of Delor et al (2003a) the greenstone belt was formed above a south-dipping subduction zone. The Bakhuis metapelites and other sediments probably were positioned on the West African passive margin, north of the greenstone belt. They may have been subducted from the north below the greenstone belt, to a depth of ~ 30 km. If UHTM of the Bakhuis belt indeed occurred in or near the subduction zone below the greenstone belt, UHTM may have taken place below the length of the greenstone belt. However, granulites of comparable metamorphic age in the far west, the Imataca complex (Figure 1a) lack UHTM (T 750-800°C), and UHTM has not been found in granulites in the far east, in Amapa (NE Brazil). Only the BGB shows UHTM, at 1000°C. A position near a subduction zone at only 30 km depth is not a probable place for UHTM, so an external source is needed for the heat required. A modification of the hypothesis of Delor et al (2003) for the striking position of the BGB between the two arms of the greenstone belt is that "UHT metamorphism ….. is the result of mantle upwelling in a slab tear in the subducted West African slab that formed as the result of crustal scale shearing and boudinage" (Klaver et al., 2015).

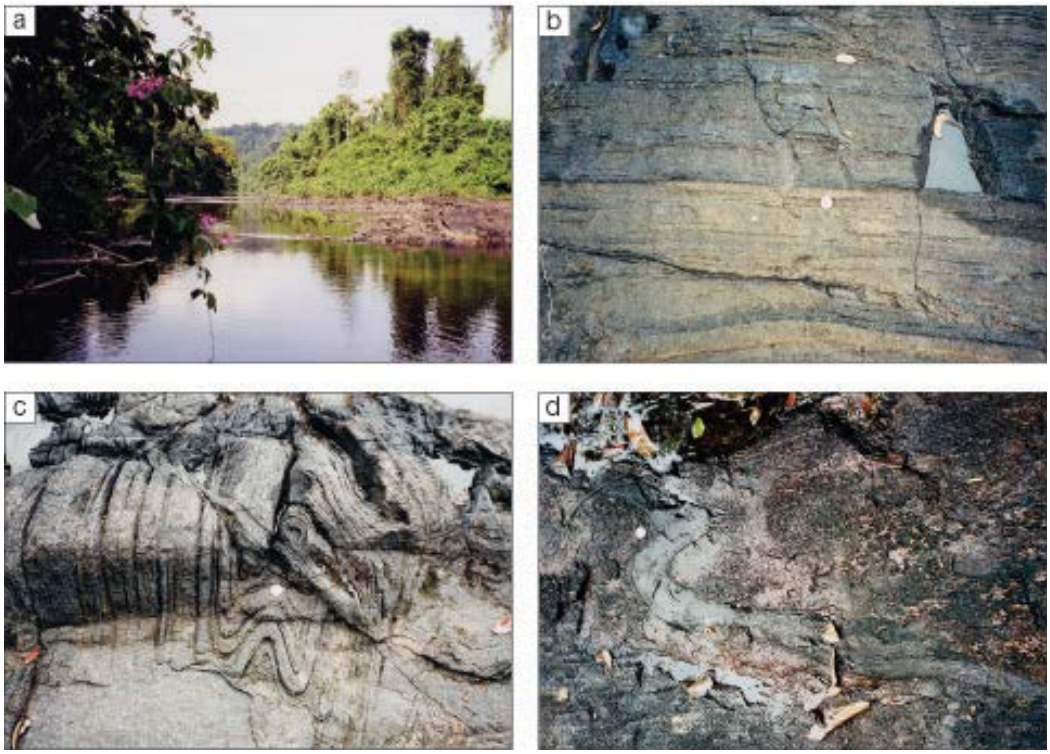

Figure 2. a) typical outcrop, b) granulite banding, c) upright folding, d) partly folded metadolerite dyke.

YOUNGER MAGMATISM IN THE BGB

Charnockites dominate the SW corner of the belt, near Kabalebo. They intruded at 1993 – 1984 Ma, at 960-990°C (Klaver et al, 2015), representing a second period of extreme temperature, > 900°C. Their intrusion is ~ 60 Ma after the UHT metamorphism of the granulites and their subsequent cooling. The charnockites are associated with many mafic to ultramafic bodies, characterized by coarse primary hornblende and medium- to high-grade metamorphism, the Moi-Moi Metagabbro, dated at 1984 ± 4 Ma and 1984 ± 5 Ma (Thijssen, 2015) . The charnockites and associated mafic intrusions are not related to the earlier UHTM. The BGB is bordered at both sides by metavolcanics and granites (1.99-1.98 Ga) belonging to the 1400 km long Caicara-Dalbana belt (CSID belt in figure 1a), which formed as a result of northward subduction after approx. 2.03 Ga (Mahabier and de Roever, 2018). This belt should be reflected in the deeper

crust, that is, in the Bakhuis belt. “Northward subduction at 1.99-1.98 Ga caused the emplacement of voluminous hot, mafic magma in the lower crust…., resulting in partial melting of the Bakhuis granulite suite to form the Kabalebo charnockites” (Klaver et al., 2015, 2016).

The Moi-Moi Metagabbro bodies contain magmatic hornblende, indicative of a hydrous magma generated in a volcanic arc, and show a LILE-enriched volcanic arc signature, with Nb-Ta trough (Thijssen, 2015). They probably represent Alaskan-type complexes, which nowadays usually are considered as roots of volcanic arc complexes. A striking aspect is that the mafic-ultramafic bodies are NOT limited to the BGB, but occur scattered throughout western Surinam, in the metavolcanic-granitic areas and the Coeroeni Gneiss. A well exposed body at the border of the Coeroeni Gneiss and granite is the Lucie Gabbro body, with an age of 1985 ± 2 Ma (Pb-Pb age), with the same characteristics as the Moi-Moi Metagabbro bodies. The latter bodies thus form a link between the Caicara-Dalbana belt and the BGB, whereas charnockites were formed only in the BGB.

In the centre of the BGB a rather small, layered, anorthosite body has been found, with an age of 1980 ± 5 Ma (de Roever et al., 2003). Its granular microstructure points to high-grade metamorphism. The BGB has major bauxite reserves of varying quality. The best bauxite of the BGB has been found on top of the anorthosite, as this is a perfect parent rock for bauxite..

In the NE corner of the belt lies a rather large intrusion of hornblende-biotite granite, with some clinopyroxene and rare orthopyroxene, quite different from the charnockites but rather similar to biotite granite outside the BGB. Samples were dated at 1980 ± 9 Ma and 1978 ±11 Ma (van de Steeg, 2016). These ages are not significantly lower than the age of the Kabalebo charnockite in the SW, 1984-1993 Ma, but correspond better with granite ages from outside the BGB, from SW Surinam, 1980 ± 6, 1983 ± 9 and 1980 ± 4 Ma (de Roever et al, 2015; Kroonenberg et al., 2016).

Still younger magmatism has been found locally in the SW and NE of the BGB. A small charnockite body along the Mozes creek in the NE has an age of 1969 ± 3 Ma (van de Steeg, 2016). The Charlie Gabbro body near Kabalebo in the SW has an U-Pb age of 1970 ± 17 Ma (Thijssen, 2015). The body does not show a (high-grade) metamorphic overprint and contains hardly any hornblende, contrary to the Moi-Moi Metagabbro bodies of 1984 - 1985 Ma.

EXHUMATION

The BGB shows a dome-like structure at its NE side, shown by the subvertical orientation and bending around of the metapelite intercalations (Figure 1b). The doming at the NE side is considered to indicate the end of the belt. Indications for doming have also been found at the SW side, where, in addition, major mylonite zones in biotite granite form the end of the BGB. The dome is cut off along its SE side by a long fault (see below). The banding and foliation of the granulites is largely subvertical throughout the BGB. In a layered anorthosite body in the BGB core, dated at 1980 ± 5 Ma, the originally horizontal igneous layering is also subvertical, just as the granulite banding and foliation. The steep orientation and doming was acquired after ~1980 Ma (de Roever et al., 2003) but before the end of the Trans-Amazonian orogeny (~1.95 Ga). This would imply that until 1980 Ma the high-grade rocks were still at a deep crustal level. The absence of metamorphism in the Charlie Gabbro body (1970 ± 17 Ma) might constrain the onset of steepening and exhumation. The regional steepening cannot easily be explained by ‘upright’ folds (Figure 2c), as these have been rarely observed. Most of the BGB exhumation is assumed to have occurred during the late stage of the Trans-Amazonian orogeny (see below).

Further exhumation occurred during the Nickerie Metamorphic Episode at approx. 1200 Ma, which caused mylonitization along the BGB and was accompanied by widespread Rb-Sr and K-Ar resetting of biotite in the high-grade rocks and granites and by local low-grade metamorphism. In view of the low metamorphic grade of the mylonites the earlier, Trans-Amazonian, exhumation was probably more substantial than the Nickerie exhumation. The BGB is bordered by long and km-wide NE-SW striking mylonitic zones, commonly with abundant pseudotachylite veins. The NW mylonite zone probably developed along pre-existing Transamazonian discontinuities, such as the dome-like structure, whereas the SE mylonite zone transects the dome structure. Together the two mylonite zones form the ”Bakhuis horst”, the term used in most publications on the geology of Surinam (e.g., Bosma and de Roever, 1975), which separates the granulites from surrounding granites and metavolcanics. However, a horst is a raised fault block bound by steep normal faults, formed during extension. Instead, the kinematics of the mylonitization suggest the BGB to be a compressive ‘pop-up’, genetically related to intraplate stresses from Grenvillian compression under the Andes. The north-western mylonites dip steeply to the SE, towards the BGB, and show a ‘Bakhuis-up’ reverse dip-slip sense of shear. Low-temperature deformation fabrics similar to those of the mylonites abound within the BGB itself, such as small-scale shear bands indicating E-W horizontal compression. Ar-Ar dating on an augen gneiss with pseudotachylite veins from an old quarry in the NW mylonite zone showed that coarse biotite from undeformed fragments gave ages of 2020 and 2027 Ma, whilst fine biotite from a deformed part had an age of 1214 ± 5 Ma (Enjolvy et al., 2007). Glass chips from pseudotachylite gave concordant ages of approx. 950 Ma, indicating that the pseudotachylite veins represent a phenomenon younger than the mylonite zones.

Exhumation continued after the Nickerie Event, as indicated by the Ar-Ar age of the pseudotachylite, and by the presence of different bauxite-laterite levels in the BGB formed during the Tertiary. Relatively late uplift is clearly recognised from the relief of the BGB, rising up to 300-500 m, but also from the raised Precambrian basement and parts of the Cretaceous-Holocene sedimentary sequence below the coastal plain of Suriname (Fig. 5 of Bosma and De Roever, 1975).

Table 1. Geochronological data from the Bakhuis Granulite Belt

Sample	Mineral	Location	Method	Age (Ma)	Reference
Intermediate granulite	zircon (core)	Blanche Marie	SHRIMP	2156 ± 6	Vos, 2016
Intermediate granulite	zircon (core)	Mozes creek	SHRIMP	2167-2263	Vos, 2016
Metapelite	zircon (core)	Fallawatra creek	SHRIMP	2130-2230	v d Steeg, 2016
Metapelite	zircon (core)	Kabalebo river	LA-ICP-MS	2131 ± 11	Nanne, 2013
Quartz-feldspar vein	zircon	Blanche Marie	SHRIMP	2088 ± 4	v d Steeg, 2016
Quartz-feldspar vein	monazite	Blanche Marie	SHRIMP	2056 ± 15	v d Steeg, 2016
Metapelite	zircon core	Kabalebo river	LA-ICP-MS	2073 ± 7	Nanne, 2013
Metapelite	zircon rim	Kabalebo river	SHRIMP	2031 ± 4	v d Steeg, 2016
(Kabalebo) Charnockite	zircon core	SW end of belt	LA-ICP-MS	1993-1984	Klaver et al., 2015
(Moi-Moi) Metagabbro	zircon core	Moi-Moi, Kabalebo river	SIMS	1984 ± 4	Klaver et al., 2016
(Moi-Moi) Metagabbro	zircon	East of Kabalebo river	LA-ICP-MS	1984 ± 5	Thijssen, 2015
Anorthosite	zircon	Mozes creek upstream	Pb-Pb evap.	1980 ± 5	de Roever et al., 2003
Hbl-bi granite	zircon	Fallawatra downstream	LA-ICP-MS	1980 ± 9	v d Steeg, 2016
Hbl-bi granite	zircon	Fallawatra downstream	SHRIMP	1978 ±11	v d Steeg, 2016
(Charlie) Gabbro (Mozescreek)	baddeleyite	creek near Kabalebo river	TIMS	1970 ± 17	Thijssen, 2015
Charnockite	zircon	Mozes creek	SHRIMP	1969 ± 3	v d Steeg, 2016
Mylonite, undeformed pt.	coarse biotite	old quarry Apoera road	Ar-Ar	2020 ± 11	Enjolvy et al., 2007
Mylonite, undeformed pt.	coarse biotite	old quarry Apoera road	Ar-Ar	2027 ± 7	Enjolvy et al., 2007
Mylonite, deformed part	fine biotite	old quarry Apoera road	Ar-Ar	1214 ± 5	Enjolvy et al., 2007
Pseudotachylite vein	glass	old quarry Apoera road	Ar-Ar	~950	Enjolvy et al., 2007

ACKNOWLEDGMENTS

The Dr. Schürmann Foundation is thanked for financing expeditions and fieldwork (since 2005) and SHRIMP, LA-ICP-MS and EMP analyses. The Molengraaff Foundation and the Faculty of Science of VU Amsterdam financed the travel and lodging costs of the students. The Geological and Mining Service (GMD) is thanked for its support and use of its facilities.

REFERENCES

Bosma, W. and de Roever, E., 1975, Results of recent geological studies in Suriname : Geol. Mijnb. Dienst Sur., Med., 23, 9-25. Also Paper 2nd Latin-American Geological Congress, Caracas, Venezuela, 1973

Delor, C., Lahondère, D., Egal, E., Lafon, J.-M., Cocherie, A., Guerrot, C., Rossi, P., Trufert, C., Theveniaut, H., Phillips, D., Avelar, V., 2003a, Transamazonian crustal growth and reworking as revealed by the 1:500,000-scale geological map of French Guiana (2nd edition). Géologie de la France, 2003, 2–3–4 : 5–57

Delor, C., de Roever, E., Lafon, J.-M., Lahondère, D., Rossi, P., Cocherie, A., Guerrot, C. and Potrel, A. 2003b. The Bakhuis ultrahigh-temperature granulite belt (Suriname): II. Implications for late Transamazonian crustal stretching in a revised Guiana Shield framework. Géologie de la France, 2003, 2–3–4 : 207–230

Enjolvy, R., Monié, P., Arnaud, N., Chauvet, A. and Vauchez, A., 2007, A comparative study of the variability of argon isotopic behaviour in pseudotachylites : Geophysical Research abstracts vol. 9, 07896, 2007, EGU2007-A-07896

de Groot, K., 2009, Geothermo(baro)metry of UHT metamorphism in the Bakhuis Mountains, Surinam. MSc thesis VU Amsterdam

Kelsey, D. and Hand, M., 2015, On ultrahigh temperature crustal metamorphism : Geoscience Frontiers 6, 311 – 356

Klaver, M., 2011, The relationship between dry granitoid magmatism and UHT metamorphism, Bakhuis Granulite Belt, western Surinam. MSc thesis VU Amsterdam

Klaver, M., de Roever, E., Nanne, J., Mason, P. and Davies, G., 2015, Charnockites and UHT metamorphism in the Bakhuis Granulite Belt, western Suriname: Evidence for two separate UHT events : Precambrian Research 262, 1–19

Klaver, M., de Roever, E., Thijssen, A., Bleeker, W., Söderlund, U., Chamberlain, K., Ernst, R., Berndt, J., and Zeh, A., 2016, Mafic magmatism in the Bakhuis Granulite Belt (western Suriname): relationship with charnockite magmatism and UHT metamorphism : GFF, 138:1, 203-218

Kroonenberg, S., de Roever, E., Fraga, L., Reis, N., Faraco, T., Lafon, J.-M., Cordani, U., and T.E. Wong, 2016, Paleo-proterozoic evolution of Guiana Shield in Suriname: A revised model : Netherlands Journal of Geosciences 95, 491-522

Mahabier, R. and de Roever, E., 2018, The Caicara-Dalbana belt in the Guiana Shield, a belt of 1.99 Ga felsic and intermediate metavolcanics from Venezuela to the Amazon and probably across, in the Guaporé Shield : 49° Congresso Brasileiro de Geologia, Rio de Janeiro, Abstract

Nanne, J.A.M., 2013, The regional extent of UHT metamorphism in the Bakhuis Granulite Belt, W Surinam. MSc thesis VU Amsterdam

de Roever, E., Lafon, J.-M., Delor, C., Cocherie, A., Rossi, P., Guerrot, C., Potrel, A., 2003, The Bakhuis ultrahigh-temperature granulite belt (Suriname): I. petrological and geochronological evidence for a counterclockwise P–T path at 2.07–2.05 Ga. Géologie de la France, 2003, 2–3–4 : 175–206

de Roever, E., Lafon, J.-M., Delor, C., Cocherie, A., and Guerrot, C., 2015, Orosirian magmatism and metamorphism in Surinam: new geochronological constraints : In Contribuiçoes á Geologia da Amazônia, vol. 9, 359-372

de Roever, E., Hooijschuur, J., Harley, S., Huizenga, J., Nanne, J. and van Ryt, M., 2016, Widespread CO_2-rich cordierite in the UHT Bakhuis Granulite Belt, Suriname **:** 35th International Geological Congress, Capetown, S Africa, Abstract 1843

van de Steeg, W., 2016, The geochemistry and geochronology of the northeastern opx-bearing granitoids in relation to UHT metamorphism in the Bakhuis Granulite Belt, Suriname. MSc thesis VU Amsterdam

Thijssen, A.C.D., 2015, The age and geochemistry of the mafic-ultramafic intrusions and their relation to UHT metamorphism in the Bakhuis Granulite Belt, western Suriname. MSc thesis VU Amsterdam

Uunk, B., 2015, Geochemistry of mafic magmatism in the Bakhuis Granulite Belt, western Surinam; implications for UHT metamorphism. MSc thesis VU Amsterdam

Vos, H., 2016, The origin of the mafic and intermediate granulites in the Bakhuis Granulite Belt, West Suriname. MSc thesis VU Amsterdam

Early Orosirian tectonic evolution of the Central Guiana Shield: insights from new U-Pb SHRIMP data

***Lêda Maria Fraga**
Geological Survey of Brazil – CPRM
leda.fraga@cprm.gov.br

Umberto Cordani
Universidade de São Paulo - USP
ucordani@usp.br

SUMMARY

U-Pb SHRIMP analyses of detrital zircon from paragneisses of the Cauarane-Coeroeni Belt (CCB) indicate major provenance from Rhyacian (2210-2050 Ma) and Early Orosirian (2050-2010 Ma) sources, and subordinate contribution from Archaean and Siderian sources. The deposition of the CCB basin post-dates the evolution of the Bakhuis Belt. The closing of the basins and syn-kinematic high-grade metamorphism are tentatively admitted at 2020 Ma, associated to the amalgamation of Early Orosirian 2.04-2.03 Ga magmatic arcs. Ages within the 1990-1960 Ma and 1940-1920 Ma intervals, obtained in zircon crystals rims, exhibiting low Th/U ratios (<0.1), are interpreted as reflecting thermal perturbation, fluid input and migmatization caused by the emplacement of nearby huge igneous belts. The Early Orosirian Orogeny is named here Akawai Orogeny.

INTRODUCTION

The Guiana Shied, in the northern part of the Amazonian Craton, remains barely studied mainly due to the great difficulties of access and the wide coverage of rainforest.
In Brazil, *airborne geophysical magnetic and gamma-ray spectrometry* data are available and geological mapping programs have been carried out in many parts of the shield during the last decades, including studies along the Brazil-Suriname and Brazil-Guyana borders. The interpretation and integration of the available information and the revaluation of the geological maps and reports of the sixties and seventies allowed the characterization of the Cauarane-Coeroeni Belt (CCB) (Fraga *et al.*, 2009a, b) and led to the proposition of a new tectonic configuration for the central part of the shield.
This short paper presents U-Pb SHRIMP zircon ages for rocks of the CCB and discusses the contribution of the new data for the understanding of the geodynamic evolution of the Guiana Shield. Four key samples were analyzed at the Geochronology Research Center of the Universidade de São Paulo (USP) as part of a broad geochronological program carried out by the second author.

GEOLOGICAL SETTING

A vast Early to Meso-Rhyacian granite-greenstone terrain extends along the northeast border of the Guiana Shield, between two Achaean domains: the NE-SW-trending Imataca Complex (IC), at the northwest; and the NW-SE-trending Amapá Block (AB) at the southeast (Fig.1). The Archaean protoliths along the AB and IC were intensely reworked during two Paleoproterozoic tectono-thermal episodes of continental *collision that occurred in the Late Rhyacian for the AB and in the Early Orosirian for the IC.*
The assembly of the granite-greenstone terrain with the AB, associated with crustal thickening and c*lockwise P-T-t path* high-grade metamorphism, took place around 2.10-2.08 Ga, and was followed by post-collisional magmatism and migmatization at about 2.06-2.04 Ga (Rosa-Costa *et al*., 2008, and references therein). Far north of the AB, the amalgamation of island arcs occurred without significant crustal thickening. Along that part of the Guiana shield, prolonged oblique convergence associated with sinistral shear zones led to the opening and closing of pull-apart-basins (Delor *et al.*, 2003 and references therein) and to the development of anticlockwise ultra-high temperature metamorphism in the NE-SW-trending Bakhuis Belt at 2.07-2.05 Ga (Klaver *et al.*, 2015 and references therein). In a different scenario, within the IC, the peak conditions of the c*lockwise P-T-t path* high-grade metamorphism occurred around 2.02 Ga (Tassinari *et al.*, 2004). After that, the Imataca complex was submitted to exhumation and cooling until 1.96 Ga, when the rocks passed below 600-550 °C (Tassinari *et al.*, 2004). The main elements of the Early Orosirian tectonic evolution of the shield are preserved along its central part, and will be discussed below.
Early Orosirian 2.04-2.03 Ga granitoids and gneisses of the Anauá Complex and the Trairão Suite were identified in the Roraima State of Brazil (Fig. 1) and interpreted as recording magmatism along island or continental arc settings (Faria *et al*., 2002; Santos, 2003; Almeida *et al.*, 2007; Fraga *et al.*, 2009a, b). U-Pb zircon ages reported for these granitoids and gneisses correspond to 2028±9 Ma for the Anauá Complex (SHRIMP, Faria *et al.* 2002) and to 2026±5 Ma and 2044±17 Ma for the Trairão Suite (LA-ICPMA, Fraga *et al.*, 2009 a, b). The Anauá and Trairão units exhibit medium to /high-K calc-alkaline affinities and record juvenile contribution for their magma genesis, as indicated by Sm-Nd data (Fraga *et al.*, 2009 a).
The Early Orosirian 2.04-2.03 Ga crustal fragments occur in the vicinities of the CCB (Fraga *et al.*, 2009 a), which corresponds to a sinuous structure joining the high-grade supracrustal rocks of the Cauarane Group (Brazil), Kanuku Complex (Guyana) and Coeroeni Group (Suriname) (Fig. 1). The NW-SE-ENE-WSW-NE-SW disposition of the CCB largely fits to the structural and aeromagnetic lineaments on the central part of the Guiana Shield. The supracrustal rocks, within the entire belt correspond to migmatitic aluminous paragneisses with subordinate calc-silicate rocks, amphibolites, meta-cherts, quartzites, gondites and mafic schists recording syn-kinematic metamorphism at amphibolite to granulite facies, with a superimposed static amphibolite facies metamorphism (Kroonenberg, 1976; Berrangé, 1977; Dreher *et al.*, 2009).

Concerning the provenance of the CCB supracrustals, detrital zircon crystals of 2074 Ma and 2038 Ma have been reported by Santos (2003). Values of 1969±4 Ma (U-Pb-SHRIMP zircon, Santos, 2003) and 1995±4 Ma (U-Pb SHRIMP on monazite for an S-type granite, Fraga *et al.*, 2009a) have been interpreted as reflecting the main high-grade syn-kinematic metamorphism on the supracrustal rocks. Concerning the static metamorphism, Berrangé, (1976), Kroonenberg (1977) and Fraga *et al.* (2009) interpreted it as the effect of extensive granitic plutonism bordering the CCB. Fraga *et al*. (2009a), proposed for the CCB an evolution from a series of coeval sedimentary basins, associated with the Trairão and Anauá arcs, which were closed during the amalgamation of these Early Orosirian magmatic arcs with older Rhyacian crustal blocks.

With a different point of view, Kroonenberg *et al.* (2016) proposed a common evolution for the CCB and the Bakhuis Belt (Fig. 1) with an initial prograde metamorphic path between 2.07 and 2.05 Ga, and a retrograde path around 1.98 Ga. In our view, this interpretation cannot be supported taking into account the geochronological data presented in this abstract and commented below. Moreover, the evidence reported by Klaver *et al*. (2015) for the Bakhuis Belt does not support the assumption that a metamorphism around 1.98 Ga could corresponds to the retrograde phase of a metamorphic event that had its first phase around 2.07-2.05 Ga.

Bordering the CCB to the north, the extensive volcanic-plutonic felsic magmatism linked to the Orocaima Igneous Belt (OIB), named after Reis et al. (2003) extends for almost 1000 km from Suriname to Venezuela (Fig 1) (Fraga *et al.*, 2017). The belt consists of 1.99-1.96 Ga A-type, shoshonitic and high-K calc-alkaline high crustal level granitoids and volcanic rocks. U-Pb SHRIMP/LA-ICP-MS and Pb-Pb evaporation zircon ages for this belt (Santos, 2003; De Roever *et al*., 2015; Nadeau, 2014; Fraga *et al*., 2017, and references therein) vary from 1989±20 Ma to 1956±5 Ma. Santos (2003) and Kroonenberg *et al.* (2016) proposed a magmatic arc setting for this magmatism. However, the presence of coeval shoshonitic, high-K calc-alkaline and A-type granitoids, including riebeckite granite bodies (Fraga *et al.* 2017), without any zoning across the OIB, makes it very difficult to conciliate with syn-subduction setting magmatism. Otherwise, this is a common scenario for post-collisional magmatism, as proposed by Fraga *et al.* (2009a), after the suturing of the CCB. Granitoids of 1.99-1.96 Ga have also been identified in the southern part of the shield (Almeida *et al.*, 2007; Castro *et al*., 2014). Immediately to the south of the CCB, 1.95-1.93 Ga granitoids and gneisses predominate along the Rio Urubu Igneous Belt (RUIB) (Fraga *et al.*, 2017). These granitoids and gneisses exhibit A-type and high-K calc-alkaline affinities and in addition charnockites and granulite lens crop out, recording emplacement and crystallization/ recrystallization / metamorphism occurring during post-collisional transpression at deeper crustal levels (Fraga *et al.*, 2009b). Xenoliths of high-grade supracrustal rocks very similar to those making part of the CCB occur inside the granitoid rocks of the OIB and RUIB. In this context, we infer that the age of these granitoids constrains the maximum age for the syn-kinematic high-grade metamorphism that affected the CCB.

U-Pb SHRIMP AGES - RESULTS AND DISCUSSION

We present new U-Pb SHRIMP analytical results for four samples of poli-folded (biotite)-cordierite-(garnet)-sillimanite migmatitic gneisses of the CCB: UC-30, LM-13, SK-811 and SK-826 (Fig.1). The information on the three former samples have been preliminary reported by Fraga *et al*. (2017). Figure 2 shows the $^{207}Pb/^{206}Pb$ ages (<10% discordance) in a probability diagram with green and red colors indicating respectively analyzed spots with Th/U<0.1 and with Th/U>1. CL images of a few selected zircons are also shown and illustrate the typical structures observed in the analyzed crystals, with detrital nuclei and metamorphic/metasomatic overgrowths. Some of the nuclei exhibit original igneous oscillatory zoning and othersshow a complex internal structure.

An integration of all ages obtained from the detrital zircon crystals of the 4 samples shown in figure 2 record the contribution of Archaean (20 crystals) and Siderian (10 crystals) sources, but the major contribution was due to Rhyacian (47 crystals with ages between 2210 and 2050 Ma) and Early Orosirian (17 crystals with ages between 2050 and 2010 Ma) sources. One probable source area for the Archaean zircon population could correspond to the AB ancient landmass which records important additions to the crust by 3.26-2.83 Ga and a widespread reworking at 2.65-2.60 Ga (Rosa-Costa *et al*., 2008). However, concerning the Siderian zircon nuclei, rocks with ages in this time interval are not yet known within the Guiana Shield. Moreover, the possible source areas for the inherited Early to Meso-Rhyacian zircon populations could be found in the granite-greenstone-belt terrains, as well as in the collisional terrains at the northern and western parts of the shield. Finally, the detrital zircon crystals, which form the highest peaks in all four probability diagrams, within the 2070-2050 Ma interval, may correspond to the post-collisional magmatism that followed the Late Rhyacian collisional event. It is worth noting that this is the time interval of the ultra-high temperature metamorphism in the Bakhuis Belt (De Roever *et al.*, 2003; Klaver *et al.*, 2015). Otherwise, the internal structures of the nuclei of the zircon crystals within the 2070-2050 Ma interval suggest that most of them are of igneous origin, but some shows complex structure, and are possibly derived from the Bhakhuis Belt.

As reported by Fraga *et al*. (2017), some rims of the zircon crystals, or patches crossing through them were also analyzed in order to investigate the age of the metamorphic events described for the CCB. The analytical results (forming the younger peaks with green color in Fig. 2) are related to rims with very low Th/U ratios < 0.1, falling into two main intervals, 1990-1960 Ma (13 crystals) and 1945-1915 Ma (5 crystals). Although not diagnostic, these low Th/U ratios <0.1 are common in metamorphic and hydrothermal environments and reflect element availability and partitioning between zircon and co-existing minerals, fluids and melts (Harley et al., 2007). This evidence is in concordance with earlier propositions (Berrangé, 1977; Kroonenberg, 1976; Fraga *et al*., 2009a) arguing in favor of a static thermal metamorphism affecting the CCB, probably related to the emplacement of granitic plutons. On this subject, Fraga *et al.* (2017) suggested that the zircon populations with ages of 1990-1960 Ma and 1940-1920 Ma are related to the emplacement of the Orocaima and Rio Urubu igneous belts, respectively. Allied to the thermal perturbation, the emplacement of these two continental scale igneous belts providedan important fluid/melt input inside the previously metamorphosed supracrustal rocks of the CCB, resulting in local migmatization and static metamorphism. Concerning the syn-kinematic metamorphic phase, the data is yet very limited. Only two zircon rims with very low Th/U ratios were dated at *ca*.2020 Ma and could be related to this metamorphic phase.

Considering the geological data available for the central part of the shield and the U-Pb data for the supracrustal rocks of the CCB, we propose that after the final episodes of the Rhyacian orogeny, the continuity of the oblique approximation of the paleoplates and possibly the docking of some unknown terrane led to a shift in the stress field in *inner* regions of the "Amazonia" *plate. This may have produced extensional stresses with the consequent* development of narrow oceans and the formation of 2.04-2.02 Ga magmatic arcs, installed at the margins of the recently built continental masses. The assembly of Archaean and Rhyacian crustal fragments with the 2.04-2.02 Ga magmatic arcs occurred during the Early Orosirian collisional event at 2.02-2.00 Ga and is recorded on the IC and on the CCB. The

final tectonic event, over the stabilized continental mass, was the post collisional magmatism that took place earlier in the northern part of the CCB, forming the OIB, and later in the southern part, forming the RUIB.
Considering the importance of the Early Orosirian orogeny to the evolution of the Guyana Shield, we propose to name it as Akawai Orogeny, in a reference to the word for-the Amerindian populations in the language of the Wapixana people, that occupy large areas on the central part of the shield, where the main tectonic elements of the orogeny are exposed.

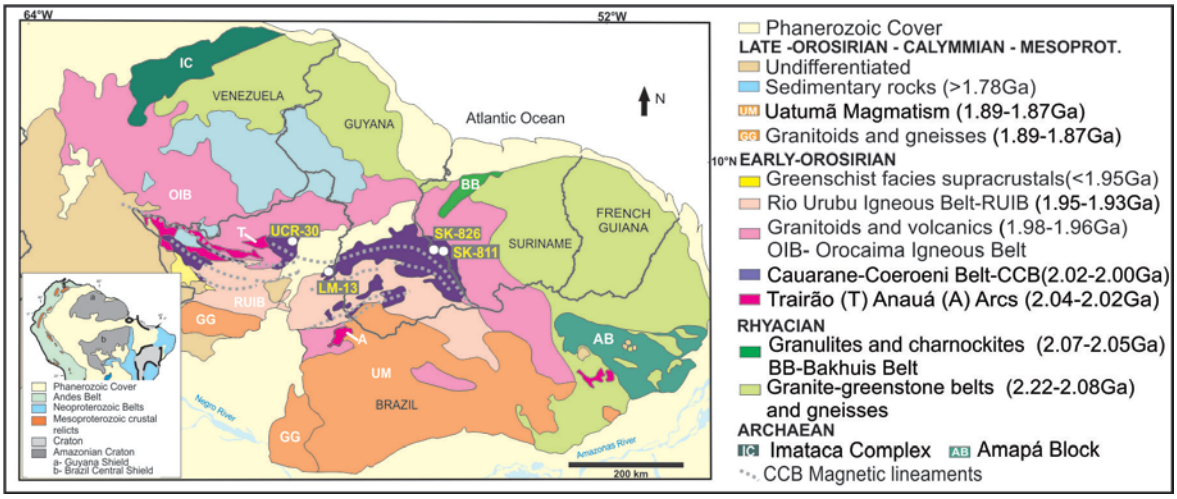

Figure 1- Simplified Geological Map of the Guiana Shield.

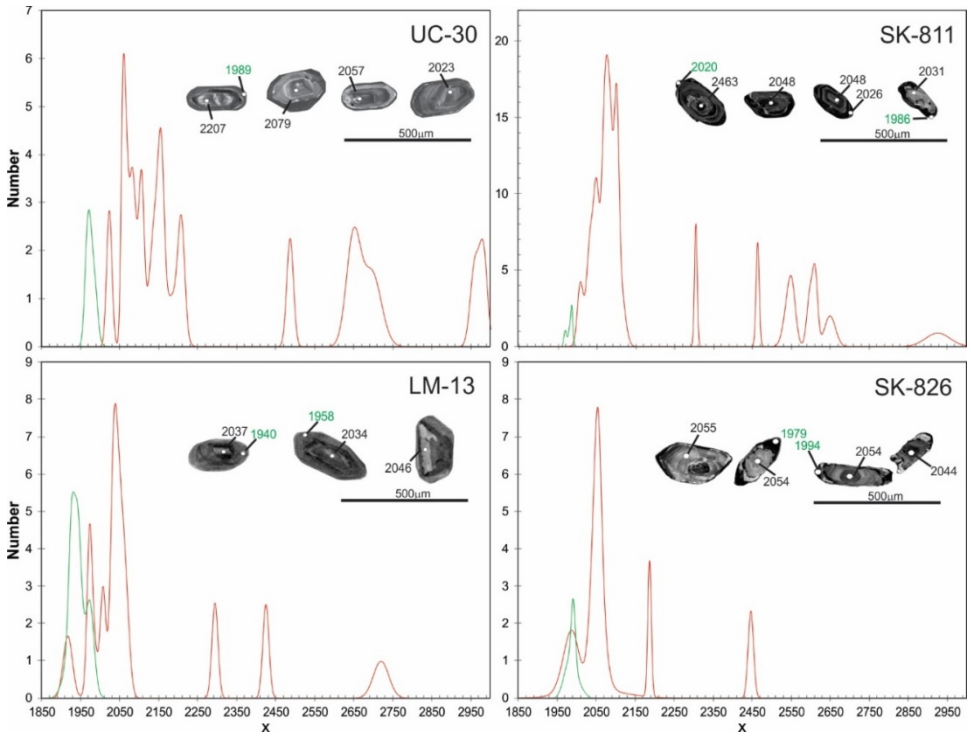

Figure 2 – Probability diagram for $^{207}Pb/^{206}Pb$ ages (<10% discordance) and CL images of selected zircon crystals of samples UCR-30, LM-13, SK-811 and SK-826.

CONCLUSIONS

The interpretation of the U-Pb SHRIMP data for four samples of paragneisses of the Cauarane-Coeroeni Belt within the context of the geology of the Guiana Shield indicates that:

- Archaean (2980-2540 Ma) and Siderian sources (2500-2300 Ma) contributed to the CCB basins. However, the data suggests major contributions of Rhyacian sources (2210-2050 Ma) and Early Orosirian sources with younger ages to 2010 Ma;
- The deposition of The CCB basins post-date the evolution of the Bakhuis belt;
- The syn-kinematic high grade metamorphism and the closing of the CCB basins is tentatively admitted at*ca.*2020 Ma, coeval to the high grade metamorphism on the IC;

- The emplacement of the Orocaima and Rio Urubu igneous belts caused important thermal perturbations, associated to fluid input and migmatization, as recorded by zircon borders with Th/U ratios (<0.1) which yielded ages falling into the 1990-1960 and 1940-1920 Ma intervals;
- The main elements of the Early Orosirian Orogeny, to which the name Akawai Orogeny is proposed in this work, are represented along the central part of the Guyana Shield.

REFERENCES

Almeida M.E., Macambira M.J.B., Elma, C.O., 2007, Geochemistry and zircon geochronology of the I-type high-K calc-alkaline and S-type granitoid rocks from southeastern Roraima, Brazil: Orosirian collisional magmatism evidence (1.97–1.96 Ga) in central portion of Guyana Shield: Precambrian Research**,** 155, 69–97.

Berrangé, J.P., 1977, The geology of southern Guyana, South America: Overseas Memoir 4, Institute of Geological Sciences, London.

Castro J.M.R., Silva R.C.S., Rosa-Costa L.T., Barbosa J.P.O., 2014, Mapa geológico da folha Rio Trombetas – SA.21-X-*A.* Escala 1:250.000. CPRM - Companhia de Pesquisa de Recursos Minerais, Programa Geologia do Brasil - PLGB.

Delor, C., Lahondère, D., Egal, E., Lafon, J.-M., Cocherie, A., Guerrot, C., Rossi, P., Truffert, C., Théveniaut, H., Phillips, D., De Avelar, V.G., 2003, Transamazonian crustal growth and reworking as revealed by the 1:500,000-scale geological map of French Guiana (2nd edition): Géologie de La France 2-3-4, 5–57.

De Roever E.W.F., Lafon J.M., Delor C., Rossi P., Cocherie A., Guerrot C., Potrel A. 2003ª, The Bakhuis Ultra-high temperature granulite belt: I Petrological and geochronological evidence for a counterclockwise P-T path at 2.07-2.05 Ga: Geologie de la France, 2,3,4, 175-205.

De Roever, E.W.F., Lafon, J.-M., Delor, C., Cocherie, A. & Guerrot, C., 2015, Orosirian magmatism and metamorphism in Suriname: new geochronological constraints: Contribuicões a Geologia da Amazônia 9, 359–372.

Dreher A.M., Fraga L.M., Ragatky D., Grazziotin H., Reis N.J. 2009, O Grupo Cauarane na Folha Vila De Tepequém, Roraima: 11° Simpósio de Geologiada Amazônia. Manaus, Extended Abstract, 3 p.

Faria, M.S.G. de, Santos, J.O.S. dos, Luzardo, R., Hartmann, L.A., McNaughton, N.J.,2002, The oldest island arc of Roraima State, Brazil – 2.03 Ga: zircon SHRIMP UPb geochronology of Anauá Complex: 41° Congresso Brasileiro de Geologia, João Pessoa, 1, 306.

Fraga, L.M., Reis, N.J., Dall'Agnol, R. 2009ª, Cauarane–Coeroeni Belt - the main tectonic feature of the Central Guyana Shield, northern Amazonian Craton: 11° Simpósio de Geologia da Amazônia. Manaus, Expanded Abstract, 4p.

Fraga, L.M., Macambira, M.J.B., Dall'Agnol, R., Costa, J.B.S. 2009 b, 1.94-1.93.Ga charnockitic magmatism from the central part of the Guiana Shield, Roraima, Brazil: single zircon evaporation data and tectonic implications: Journal of South American Earth Sciences 27, 247–257.

Fraga, L.M., Cordani, U.,Kroonenberg, S., Reis, N.J., Dreher, A., DeRoever, E., Nadeau, S. Maurer, V.C..2017, U-Pb SHRIMP new data on the high-grade supracrustal rocks of the Cauarane-Coeroeni belt - insights on the tectonic Eo-Orosirian evolution of the Guiana: 15° Simpósio de Geologia da Amazônia. Belém, Expanded Abstract, 4p.

Harley, S.L., Kelly, N.M., Möller, A. 2007. Zircon Behaviour and the Thermal Histories of Mountain Chains: Elements,1, 3, 25-30.

Klaver M., De Roever E.W.F., Nanne J.A.M., Mason P.R.D., Davies G.R. 2015, Charnockites and UHT metamorphism in the Bakhuis Granulite Belt, western Suriname: Evidence of two separate UHT events: Precambrian Research, 262, 1-19.

Kroonemberg, S.B., 1976, Amphibolite-facies and granulite-facies metamorphism in the Coeroeni-Lucie area, southwestern Surinam. PhD Thesis, Univertity of Amsterdam.

Kroonenberg, S. B., Roever, E.W.F. de, Fraga, L.F., Reis, N.J., Faraco, T.M., Lafon, LM, Cordani, U., Wong, T.E. 2016, Paleoproterozoic Evolution of the Guyana Shield in Suriname: A revised model: Netherland Journal of Geosience- Geologieen Mijnbouw, 95, 491–522.

Nadeau S. 2014. *Guyana Geological time escale.*Guyana geological and Mining Commission, 1 p.

Reis, N.J., Fraga, L.M., Faria, M.S.G., Almeida, M.E. 2003, Geologia do Estado de Roraima, Brasil. Géologie de La France 2-3-4, 121-134.

Rosa-Costa L., Lafon J., Cocherie A., Delor C. 2008, Electron microprobe U–Th–Pb monazite dating of the Transamazonian high-grade metamorphic overprint on Archaean rocks from Amapa block, southeastern Guiana Shield, Northern Brazil. : Journal of South American Earth Sciences, 26, 445–462.

Santos, J.O.S. 2003, Geotectônica dos Escudos das Guianas e Brasil-Central: L. A. Bizzi, C. Schobbenhaus, R. M. Vidotti e J. H. Gonçalves (eds.) Geologia, Tectônica e Recursos Minerais do Brasil, CPRM, Brasília, 167-195.

Tassinari, C.G., Munhá, J.M.U., Teixeira, W., Palácios, T., Nutman, A.P., Sosa, C., Santos, A.P., Calado, B.O., 2004, The Imataca Complex, NW Amazonian craton, Venezuela: Crustal evolution and integration of geochronological and petrological cooling histories: Episodes, 27, 3-12.

The influence of climate and long term sea level change on terrace formation and preservation at the downstream part of the Suriname River, Suriname.

Kathleen Gersie
Anton de Kom Universiteit
Leysweg # 86

Kathleen.gersie@uvs.edu

Ronald T. van Balen
Vrije Universiteit of Amsterdam
De Boelelaan

R.T.van.balen@vu.nl

SUMMARY

Along the Suriname River only three terrace levels can be distinguished at approximately 5, 15, and 20 meters above the present-day river level. The purpose of this study is to determine the influence of climate alternation and sea level fluctuation on the downstream terraces of the Suriname River. Methods consisted of fieldwork, desktop study, and a laboratory part. The height difference between the oldest and youngest levels is in agreement with the drop in eustatic sea level since the late Miocene. Each of the three levels encompasses many climate cycles, which likely have resulted in terrace sub-levels.

Key words: terraces, Quaternary, Pleistocene, Pluvial, Interpluvial

INTRODUCTION

Fluvial landscapes over the world are an important part of the general geomorphological system at all latitudes (Vandenberghe, 2002). River terraces represent paleo-fluvial floodplains, formed by floodplain abandonment as a result of vertical incision (Stange et al., 2012). The origin of river terraces can be explained by tectonic movements in the earth's crust and by climate changes. The cyclical alternation of glacials (interpluvials) and interglacials (pluvials) in the Quaternary Period, for instance, has induced sedimentological and morphological phenomena such as river deposits and terraces (Vandenberghe, 2002).
The terraces in Suriname are supposed to be closely related to climatic changes during the Quaternary Period (De Boer, 1972). Alluvial sediments were deposited in the river valleys, and valley slopes retreated during interpluvials. As the river incised in its bedding during the subsequent pluvial distinct surfaces in the form of terraces can be left behind. If this model is correct, many terrace levels should be present along the river systems.
This study focuses on the spatial and temporal correlation with climate alternation and possible sea level fluctuation of terraces along the Suriname River. The purpose is to determine the influence of climate alternation and sea level fluctuation on the terraces along the downstream part of the Suriname River. The research method consisted of a fieldwork part, a desktop part, and a laboratory part. The main purpose of the fieldwork was to locate and characterize the various terraces. In the laboratory sieve analyses of subsoil samples were executed for supportive data on the lithology of the terraces. The desktop part was to process and interpret the fieldwork and laboratory data.
Location and level of the terraces has been determined using a GPS (Global Positioning System).

METHOD AND PRELIMINARY RESULTS

The research method consisted of a fieldwork part, a desktop part, and a laboratory part. The main purpose of the fieldwork was to locate and characterize the various terraces. In the laboratory sieve analyses of subsoil samples were executed for supportive data on the lithology of the terraces. The desktop part was to process and interpret the fieldwork and laboratory data.

Location and level of the terraces has been determined using a GPS (Global Positioning System). On selected levels a drill hole was made with an Auger drill or a Gouge, depending respectively on the type of material encountered. In case medium to very stiff clays were present the Auger drill was used, while the Gouge was used in slack clays.

Collected fieldwork data was processed with the help of GIS, logging and mapping software programs. A digital map was created with GIS. Sediment logs were created with the logging program. Mapping software was used for longitudinal and cross-sectional correlation of all related terrace levels at the different locations along the river.

Five boreholes were selected for analysing the particle size distribution. During laboratory analyses a HELOS laser diffraction was used for particle size analysis. The resulting plots from one coring but at different depths were placed one below the other to see the change in texture with depth.

Fieldwork was done at Victoria, Baboenhol, and Cassipora whereby four units were morphologically distinguished, namely the floodplain and three terrace levels at approximately 5m, 15m, and 20 m. At both Victoria and Baboenhol, the floodplain corings revealed silty clays of variable colors, locally presence of quartz gravels, and incidental presence of organic material.

The 5 m terraces at both Victoria and Baboenhol consist of clays with rust spots and gravels with a diameter of approximately 5 mm. The highest terraces at a level of circa 20m at Victoria and Cassipora consist respectively of sandy loams in the first meter followed by loamy sands with incidental gravel occurrence, and a gravel-sand mixture layer with a thick gravel layer in between.

Topographic sections were made for the Victoria, Baboenhol, and the Cassipora terraces. The Victoria terraces are characterized by a wide landscape of terraces with a very undulating landscape and show a gradual increase in level of approximately 6 à 7 km from the river. The Baboenhol terraces show very different characteristics from the Victoria ones, and its terrains rapidly increase in height. There is a sharp transition from one terrace to another, which is also the same for the Cassipora terraces whose height also quickly increases from about 7 to 30 m over a distance of approximately 50 m.

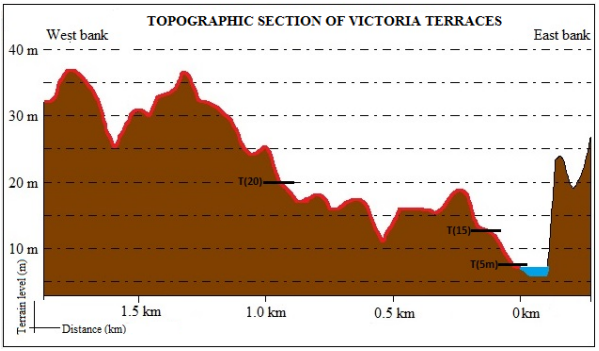

Figure 1: Topographic section of the Victoria terraces

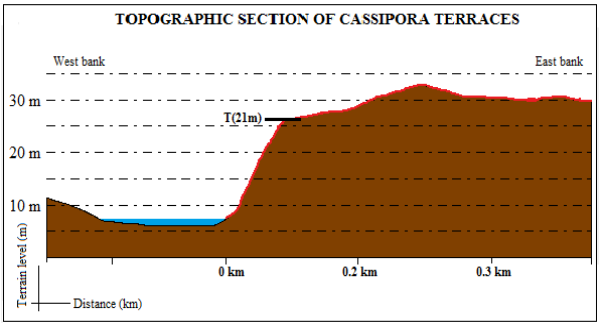

Figure 2: Topographic sections of the Cassipora terraces

CONCLUSIONS

Earlier research suggested that the development of terraces along the mid- to downstream part of the Suriname River are the result of climate alternation, and in particular the pluvials and interpluvials. However, the number of distinguishable terrace levels in our preliminary work is too low for such a correlation; only three levels were found The terraces and their levels studied at Victoria, Baboenhol and Cassipora on both sides of the river can be more or less correlated with each other. The difference in width and transitions of subsequent terraces can be related to their position along the river. The Victoria terraces are located in the inner bend and show a large width and gradual transitions, in contrast to the Cassipora terraces which show small widths and sharp transitions. This has to be the result of the flow velocity of the river water during formation of the terraces, which in turn can be pointed to the type of climate or climate period during formation. The three levels encompasses many climate cycles which is not visible in both the morphology and the corings. The work will continue by mapping terraces in the Middle reach of the river, and by studying the mechanism behind terrace staircase formation: long term eustatic sea level drop, flexural upwarping or slow tectonic uplift.

ACKNOWLEDGMENTS

We would like to thank Professor Salomon Kroonenberg, Em.Professor Pieter Augustinus, Dewany Monsels, Melvin Pigot and my students from the Anton de Kom University for their help during fieldwork.

.

REFERENCES

Stange, K.M., Van Balen, R., Vandenberghe, J., Peña, J.L., Sancho, C., 2012 – External controls on Quaternary fluvial incision and terrace formation at the Segre River, Southern Pyrenees. Tectonophysics 602, p. 316-331.

Van Balen, R.T., Van der Beek, P.A., and Cloetingh, S.A.P.L., 1995. - The effect of rift shoulder erosion on stratal patterns at passive margins: implications for sequence stratigraphy, Earth Planetary Science Letters, 134:527-544.

Vandenberghe, J., 1995 – Timescales, climate and river development. Quaternary Sciences Reviews, Vol.14, p. 631-638.

Timing of the origin and uplift of the Bakhuis-Tambaredjo Horst, Suriname

Rohini Girjasing
Anton de Kom Universiteit van Suriname

RohiniGirjasing@hotmail.com

Salomon Kroonenberg
Anton de Kom Universiteit van Suriname

Rakesh Ramdajal
StaatsolieMaatschappij Suriname N.V.

Theo Wong
Anton de Kom Universiteit van Suriname

SUMMARY

In order to elucidate the alleged structural continuity of the NE-SW stretching Bakhuis Horst in the Paleoproterozoic basement of the Guiana Shield, and the prominent Mesozoic-Tertiary Tambaredjo Uplift in the coastal plain of Suriname, a key feature in trapping oil from downdip, the nature of the rocks in well-bore cuttings and side-wall cores from Petrel-selected wells in the coastal plain that penetrated the Precambrian basement was investigated. Aeromagnetic data showing the Bakhuis Horst was cut off by the greenstone belt of NE Suriname had cast doubt on this continuity. The petrography showed that the Tambaredjo Uplift was indeed underlain by rocks from the greenstone belt. However, the shear zone that put the Bakhuis Horst in contact with the greenstone belt was demonstrated to be an entirely Paleoproterozoic feature that did not invalidate the continuity of the joint Mesozoic Bakhuis-Tambaredjo Horst.

Key words: Precambrian basement under oil field, aeromagnetics, Mesozoic uplift,

INTRODUCTION

The Bakhuis Mountains in western Suriname form a prominent NE-SW stretching horst structure, occupied mainly by Paleoproterozoic granulite-facies metamorphic rocks and charnockitic intrusives originated between 2.07-2.05 Ga within the Trans-Amazonian Orogeny (De Roever et al., 2003; Klaver et al., 2015). Extensive mylonitization along the border faults of this Bakhuis Granulite Belt has been attributed to the Nickerie Metamorphic around 1.2 Ga (Priem et al., 1971; Bosma et al., 1983), as a result of the collision of Laurentia and Amazonia during the Grenvillian orogeny (Kroonenberg, 1982, Kroonenberg et al., 2016). The morphological freshness of the eastern fault scarp suggests that the Bakhuis Horst has been active relatively recently, probably as a result of the Mesozoic break-up of Gondwana and the formation of the nearby Takutu graben, a failed triple junction arm.

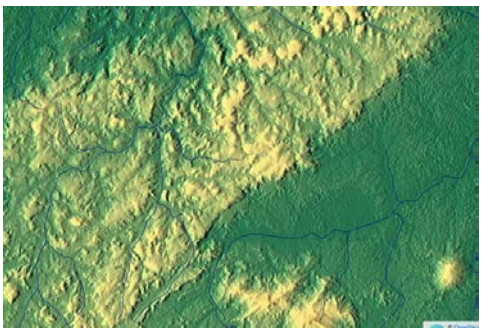

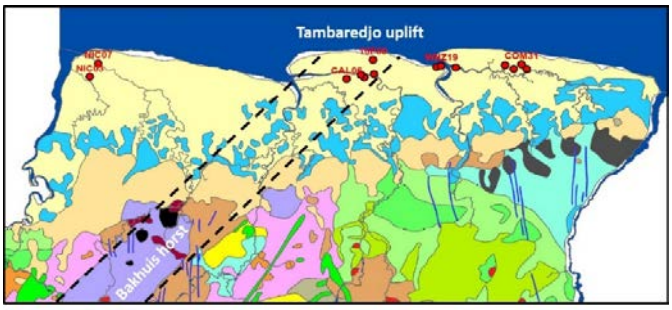

Fig. 1. The Bakhuis Horst and its eastern border fault. Fig. 2. Conjectural continuation of the Bakhuis horst into the Tambaredjo uplift, on a simplified geological map of northern Suriname. Red dots represent studied wells.

Seismic studies in the coastal plain carried out by Staatsolie in the framework of oil exploration and production around the Tambaredjo field revealed the presence of an uplifted structure below the main producing fields which is in line with the Bakhuis structure, and was therefore considered to form the continuation of the Bakhuis horst (Fig. 3, 4), implying the horst structure was also still active in the Cretaceous and Paleogene (Bosma et al., 1983, Nelson, 2016). Oil, generated down-dip in the Guiana Basin, migrated towards this prominent high structure and was locally trapped by small local faults and pinch-outs. This explains why all major oil occurrences in the coastal plain are confined to this area (Wong, 1998).

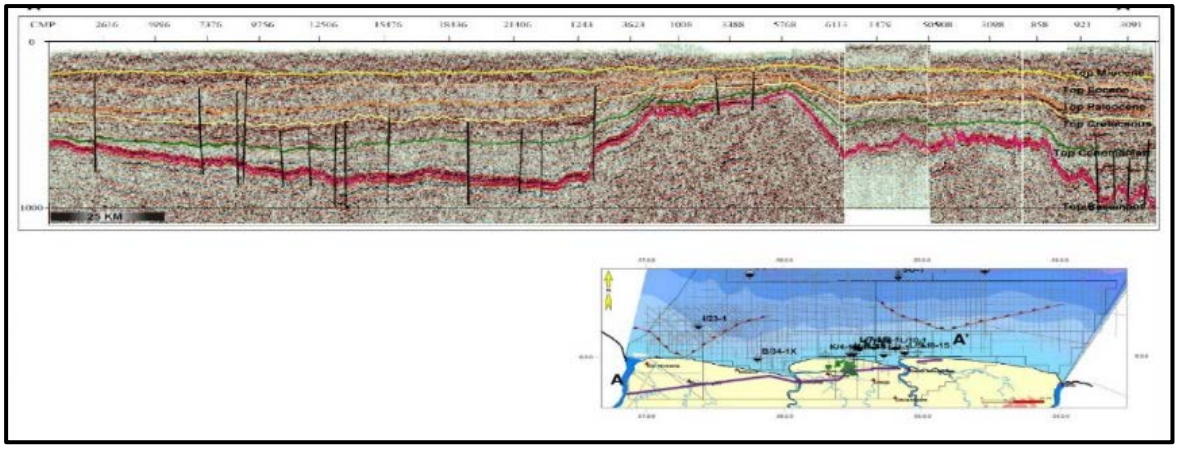

Fig. 3. The Tambaredjo uplift in a W-E seismic profile of the coastal plain. Nelson, 2016

However, perusal of recently remastered reduced-to-pole aeromagnetic data cast doubt on the continuation of the Bakhuis horst into the Tambaredjo uplift, as it seems that the Bakhuis structure is cut off by the 2.18-2.09 Ga Marowijne Greenstone Belt, in spite of its older age (Fig. 5). The aeromagnetically prominent border faults of the Bakhuis belt do not seem to continue into the greenstone belt, which is also strange as the Nickerie age mylonitization is younger than both the greenstone belt and the Bakhuis belt. . To solve these problems we first investigated the nature of Precambrian rocks from oil wells in the coastal plain, and especially whether they showed more similarity to the Bakhuis granulites or the Marowijne greenstones.

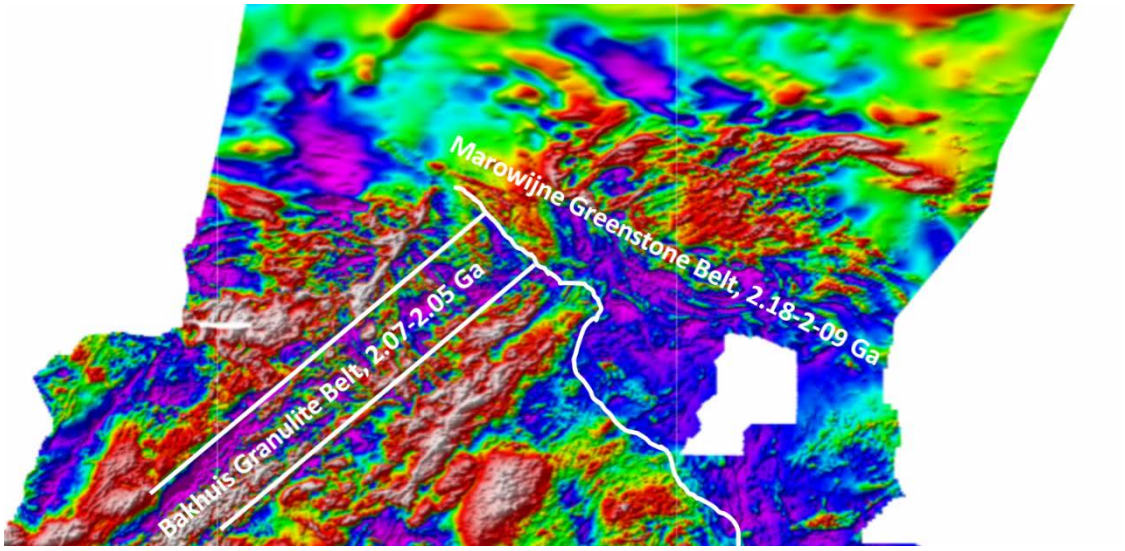

Fig 4. Aeromagnetics suggest that the Bakhuis Granulite Belt is cut off by the Marowijne Greenstone Belt.

METHODS

Using Petrel, out of 154 oil wells drilled by Staatsolie in the coastal plain, 15 were selected which penetrated the Precambrian basement. Well-bore cuttings and SWC (Side Wall Cores) from the basement were investigated in the stereomicroscope and in thin sections of impregnated material to establish the rock type below the oil fields.

RESULTS

The wells from the Calcutta, Tambaredjo and Weg naar Zee areas are mainly underlain by biotite-muscovite granite of the Patamacca type, and the Commewijne wells gave biotite-garnet-(sillimanite) gneiss of the Sara's Lust type, both characteristic for the greenstone belt. The Nickerie wells were inconclusive.

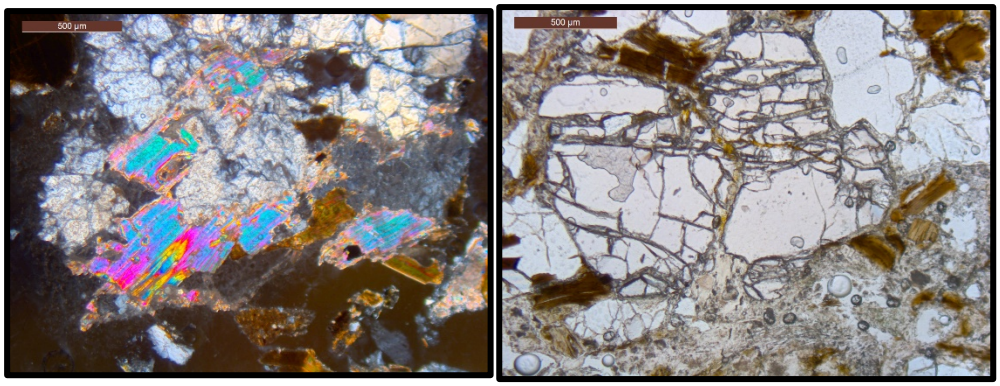

Fig. 5a: Patamacca bimica granite, Tambaredjo; 5b: Sara's Lust biotite-garnet gneiss, Commewijne

DISCUSSION

The results confirm that the Tambaredjo uplift is underlain by Patamacca type granites with greenstone belt affinity, not by Bakhuis-type granulites, corroborating the interpretation of the aeromagnetics. This asks for a revision of the timing of events. In the first place, the cutoff should have taken place after the formation of both units, so after 2.05 Ga. Furthermore, as also the border faults of the Bakhuis belt are cut off, it should be younger than the 1.2 Ga Nickerie Metamorphic Episode. However, no tectonic activity is known in this interval apart from the Mesozoic break-up of Gondwana; as this an extensional period, it is not likely to have generated the offset between the Bakhuis belt and the greenstone belt.

Another alternative is that the cutoff has been caused by a prominent shear zone in this area, the North Suriname Shear Zone postulated by Voicu et al. (2001). This shear zone is thought to continue into French Guiana, and would be roughly coeval with gold mineralisation in the area around 2.0 Ga (Voicu et al., 2001). This is indeed younger than both the Bakhuis and the greenstone belt, but in that case the 1.2 Ga Nickerie mylonitization faults should have also affected the greenstone belt north of the shear zone, which is contradicted by the aeromagnetics.,

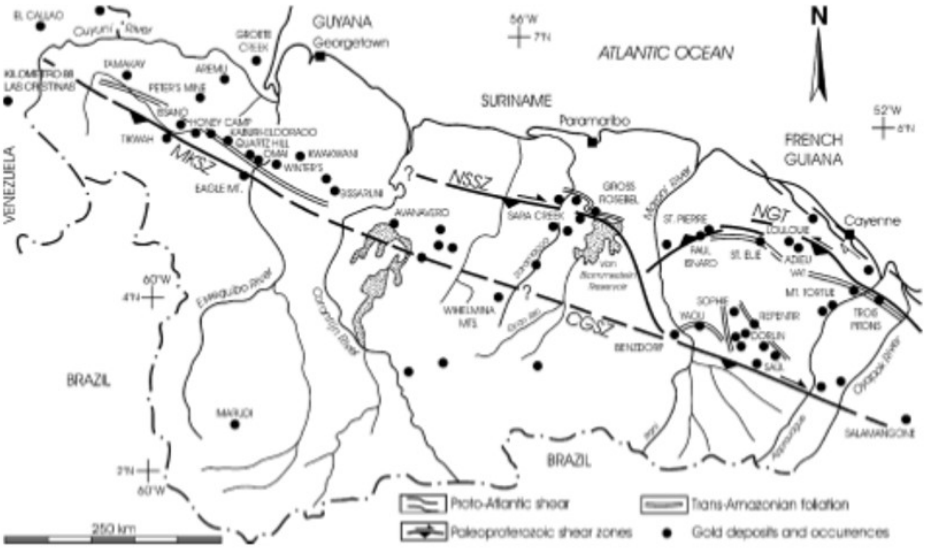

Fig. 5. Shear zones in the Guiana Shield according to Voicu et al., 2001

A solution can be formulated if we reconsider the Nickerie age of the Bakhuis mylonitic border faults. The Nickerie Metamorphic Episode (Priem et al., 1968, 1971, Bosma et al., 1983) is characterised as a tectonothermal event that overprinted biotite K-Ar and Rb-Sr ages and muscovite K-Ar ages in western Suriname down to about 1.2 Ga. Barron (1966, 1969) and Priem et al (1971) considered that the prominent mylonite zones in Guyana and Suriname are caused by this tectonic event, a conclusion based among others on mica rejuvenation in two mylonites of the Bakhuis belt.

However, mica rejuvenation also is widespread in undeformed Trans-Amazonian granitoid rocks in western Suriname, and elsewhere in the western Guiana Shield, far removed from the Bakhuis mylonites. The Nickerie-ages obtained for micas in the mylonite zones therefore do not prove conclusively that the mylonitization is caused by the Nickerie episode: they could equally represent Trans-Amazonian micas overprinted by the tectonothermal Nickerie event, just as all the other micas outside Bakhuis. It is therefore possible that the mylonites are not formed during the Nickerie Metamorphic Episode, but already earlier during the Trans-Amazonian Orogeny.

This hypothesis is supported by the fact that the Rb-Sr ages of the muscovites give still Trans-Amazonian ages (Priem et al., 1971). If the mylonites are Trans-Amazonian instead of Nickerie, their cutoff by the NSSZ becomes understandable.

This hypothesis then comes down to the following sequence of events

(1) Formation of the greenstone belt (2.18-2.09 Ga)
(2) Rifting, sedimentation and high-grade metamorphism in the Bakhuis Granulite Belt (2.07-2.05 Ga)
(3) (Late?) Trans-Amazonian mylonitization of the Bakhuis border faults.
(4) A sinistral shear zone (NSSZ) cuts off the Bakhuis belt and its mylonitized border faults (~2Ga)
(5) Nickerie Metamorphic Episode thermal rejuvenation of micas in the Bakhuis mylonites (~1.2 Ga) but not accompanied by mylonitization
(6) Mesozoic reactivation of border faults, affecting both the Bakhuis horst and the Tambaredjo uplift; this reactivation leaves no visible impact in the aeromagnetic imagery.

The fact that the eastern borderfault of the Bakhuis belt is morphologically well expressed and hardly affected by posterior erosion suggests recent uplift activity, just as the seismic profiles across the Tambaredjo uplift. This indicates that they indeed form together a single Bakhuis-Tambaredjo Horst, which however is not expressed in the aeromagnetic imagery. Uplift probably coincided with the Mesozoic break up of Gondwana and subsidence in the Takutu graben further west.

CONCLUSION

The Bakhuis-Tambaredjo horst is indeed a single uplift structure, originating during the Mesozoic breakup of Gondwana and the subsidence of the Takutu Graben. The uplift affected a slice of Precambrian basement which included both a part of the Bakhuis Granulite Belt, a part of the greenstone belt and the shear zone that separated them, as well as a part of the cover with coastal sediments. The aeromagnetically prominent border faults along the Bakhuis part of the horst are Trans-Amazonian in age, not Nickerie, as previously thought, and probably were reactivated during Mesozoic uplift. The Mesozoic border faults along the Bakhuis-Tambaredjo horst are not expressed in the aeromagnetics, as they are extensional faults and therefore not likely to have magnetic effects.

REFERENCES

Bosma, W., S.B. Kroonenberg, K. Maas & E.W.F. De Roever 1983 Igneous and metamorphic complexes of the Guiana Shield in Suriname. Geologie & Mijnbouw, 62:241

De Roever, E.W.F., Lafon, J.-M., Delor, C., Rossi, P., Cocherie, A., Guerrot, C. & Potrel, A., 2003a. The Bakhuis ultra-high temperature granulite belt : I Petrological and geochronological evidence for a counterclockwise P-T path at 2.07-–2.05 Ga. Géologie de la France 2003, 2-,3,-4: 175–205.

Klaver, M., De Roever, E. W.F., Nanne, J.A.M., Mason, P.R.D. & Davies G.R., 2015. Charnockites and UHT metamorphism in the Bakhuis Granulite Belt, western Suriname: Evidence for two separate UHT events. Precambrian Research 262: 1–19.

Kroonenberg, S.B., 1982. A Grenvillian granulite belt in the Colombian Andes and its relation to the Guiana Shield. Geologie en Mijnbouw 61: 325–333.

Kroonenberg, S.B., De Roever, E.W.F., Fraga, L.M., Reis, N.J., Faraco, M.T., Cordani, U.G., Lafon, J.-M & Wong, Th. E. (2016) Paleoproterozoic evolution of the Guiana Shield in Suriname – a revised model. Netherlands Journal of Geosciences-Geologie en Mijnbouw 95:491-522 143-254.

Nelson, A., 2016. Staatsolie's VISION 2030: the contributions of petroleum geology to Surinamese society. Netherlands Journal of Geosciences — Geologie en Mijnbouw, 95: 375-392.

Priem, H.N.A., Boelrijk, N.A.I.M., Hebeda, E.H., Verdurmen, E.A.Th. & Verschure, R.H., 1971. Isotopic ages of the Trans-Amazonian felsic magmatism and the Nickerie Episode in the Precambrian basement of Surinam, South America. Geological Society of America Bulletin 82: 1667-–1680.

Voicu, G., Bardoux, M. & Stevenson, R., 2001. Lithostratigraphy, geochronology and gold metallogeny in the northern Guiana Shield, South America: a review. Ore Geology Reviews 18: 211–236.

Wong, Th.E., 1998. Hydrocarbon exploration and exploitation in Suriname – In: Th.E. Wong, D.R. De Vletter, L. Krook, J.I.S Zonneveld & A.J. van Loon (eds): The history of earth sciences in Suriname- Kon. Ned. Akad. Wet. & Ned. Inst.Toegep. Geowet. TNO. P.377-393.

Stratigraphy of Guyana Greenstone Belts.

Linda Heesterman

Independent Geologist
Heesterman_Kemp@Hotmail.com

SUMMARY

A brief update is given of the stratigraphy of Guyana, especially that of the greenstone belts. An updated stratigraphical table and geological map are presented, including the geochronology. The Kwitaro Group is believed to be older, and can not be correlated with the Barama-Mazaruni Supergroup. The Barama and Mazaruni groups both appear to have similar stratigraphy, though the Mazaruni Group has a much greater thickness of mafic metavolcanics at the base. Felsic rocks from the central part of the sequence in both groups are of a similar age. Both groups have sediments such as phyllites high in the sequence. Only the Barama Group has manganiferous zones and regionally anomalous arsenic drainage geochemistry. Both areas have possibly unconformable greywackes and conglomerates as the youngest rocks, which have been deformed and metamorphosed with the rest of the sequence. I believe that folding and thrusting has juxtaposed a distal area with less sedimentation against a sediment rich area.

The Haimaraka Formation greywackes was originally considered to be the upper part of the Mazaruni Group. On the basis of it's much lower level of metamorphism, characteristic two phases of open folding, as well as field relationships to the Muruwa Formation I consider this to be part of the younger Burro Burro Group, which explains the lack of primary gold occurrences.

Key words: Guyana, Stratigraphy, Geochronology, Greenstone Belts, Kwitaro, Barama, Mazaruni, Haimaraka.

INTRODUCTION

Little has been published on the geology of on-shore Guyana during the last 25 years since the compilation on the Guiana Shield by Gibbs & Barron (1993), though fieldwork has been done by MSc or PhD researchers, the Guyana Geology and Mines Commission (GGMC) and by mineral exploration companies. Data from these sources, and especially new geochronology has been used to update the stratigraphic column shown in Table 1 for southern Guyana, and Table 2 for northern Guyana. In each case the most recent author who dated each unit is shown. Some dates are from adjacent countries. An update to the geological map is shown in Figure 1, which includes detail on the location and divisions of the greenstone areas. In southern Guyana the Kwitaro Group is briefly discussed. In northern Guyana an attempt is made to sub-divide the Barama from the Mazaruni Group, though it is likely that they represent the same sequence, one from an area with more sedimentation, which locally have been juxtaposed as a result of thrusting. The relationship of the Mazaruni Group with the younger Muruwa and Haimaraka Formations remains a significant problem.

SOUTHERN GUYANA; THE KWITARO GROUP.

A re-activated continent scale shear controls the margins of the Jurassic / Cretaceous Takutu Graben, and divides southern from northern Guyana (Szatmari, 1983). The two halves of the country have very different older geology, though they were probably adjacent since ~2 Ga since the Muruwa / Ston Formation and Roraima Group can be recognised in both Guyana and Suriname. Starting from the north, the geology of southern Guyana can be summarised as a gneissose zone (Kanuku Complex) immediately south of the Takutu Graben with associated granites including charnockites (1.96 Ga). To the south the Southern Guyana Granite Complex consists of an over 100km zone of assorted granites (1.93-1.98 Ga) with several major and many smaller enclaves of Kwitaro Group metasediments, before a zone with uncorrelated gneisses and the Kuyuwini Group. The Kuyuwini Group includes felsic volcanics, and is intruded by a variety of granitoids and sub-volcanic granophyres. Several larger charnockitic granites occur around the northern limit of the Kuyuwini Group. Historically the Kuyuwini rocks have been correlated with the Iwokrama rocks in northern Guyana, though they tend to be slightly metamorphosed. Recent age dating from adjacent Brazil suggests this belt is younger (1.89-1.81 Ga), while recent dates from Guyana show the Iwokrama Formation volcanics and granites to be 1.99-1,96 Ga (Tables 1 & 2). Mineralisation is not known associated with these units.

Strictly the Kwitaro Group are not greenstones, though minor volumes of andesitic rocks have been recognised in almost all areas. More importantly gold mineralisation occurs in some areas. Only limited mapping has been done in this remote region, with Berrange (1977) being the main authority. Lithologies consist of pelitic rocks including phyllites and psammitic rocks such as chert, meta-siltstones and quartzites, as well as amphibolites and minor meta-volcanics. Some of the amphibolitic zones appear to be conformable, after mafic meta-volcanics or basalts, while others represent basic dykes and gabbroic intrusions. Most information is derived from Marudi Mountain (59.16ºW / 2.22ºN), where a lower phyllitic unit, metachert ("quartzite"), and meta-andesite with subordinate tuff and ironstone are overlain by massive ortho-amphibolite / metabasalt (Guyana Goldstrike Inc., 2019).

In some areas banded iron formation / BIF-like rocks have been recognised. In the Mazoa Hill prospect at Marudi a magnetite-silicate iron band occurs, and quartzitic rocks with over 10% Fe were recognised ~800m to the SE by Zaleski (2005). Berrange (1977) describes

grey, fine grained quartzite with bedding defined by variation in magnetite abundance. BIF-like rocks are described from the Wakadanawa area 50km to the WSW by Gibbs & Barron (1993). The Wakadanawa area was flown by Macmillan Gold Corp / Exall Resources in 1997, and the Marudi area in 2018 by Guyana Goldstrike, but no public domain aeromagnetic data exists.

Rocks have been subjected to upper greenschist to amphibolite grade regional metamorphism, and at least 2 phases of folding. With increasing metamorphism, especially closer to granite contacts, rocks grade into schists with quartzo-feldspathic pinch-and-swell secretions, and locally into gneisses. Generally phyllitic rocks show a penetrative cleavage, while other rocks types do not. Within the Marudi area Lunceford (2009) reports post metamorphism felsic porphyry dikes with chilled contacts in some of the drill holes at Mazoa. The sub-vertical dykes strike easterly across the quartzite. The age is unknown. The Marudi Granite intrudes these rocks (2.22 Ga, Nadeau, 2014), partly via a migmatitic contact. The Southern Guyana Granite Complex surrounds almost all the enclaves of Kwitaro Group rocks, and has been dated at 1.93-1.98 Ga by Nadeau *et. al.* (2013).

Regional drainage geochemistry done by the Guyana Geology and Mines Commission (GGMC) covers only the Marudi and eastern part of the Wakadanawa / Takatu Head regions. (Heesterman *et. al.*, 2013a & b), Presence of amphibolitic zones can be recognised by elevated Cr, Ni, and Cu levels in drainage samples, while gold occurrences have a partial correlation with elevated arsenic levels. Soil samples with up to 240ppm As at Marudi Mountain are reported by Hawkes (1955).

NORTHERN GUYANA; THE BARAMA-MAZARUNI SUPERGROUP.

The name Barama-Mazaruni supergroup is a “bag” term that refers to the greenstone basement of Guyana north of the Takutu Graben. Several belts and smaller areas of greenstones occur, separated by areas of Bartica Assemblage gneisses and Younger Granites. Good detail is available on stratigraphy in some areas, with specific formation names that relate to sequences separated by local unconformities. However correlation between areas is not always easy. In general the Barama Group is sediment dominated, and the Mazaruni Group volcanic dominated, though a similar stratigraphic sequence occurs in both, suggesting they may be lateral equivalents. I have used the term Barama Group for those areas where manganiferous zones are known, and distinctive geochemistry occurs. A further problem is understanding of what is part of the greenstone basement, and what is part of the unconformably overlying supracrustal sediments such as the Muruwa, Haimaraka and Western Cuyuni Formations, which in turn are overlain by the Iwokrama Formation and Roraima Group, and occur immediately north of the Takutu Graben.

NORTHERN GUYANA; THE BARAMA GROUP.

The Barama Group was initially defined in the Barama River (7.3°N / 59.95°W), and the Matthews Ridge area (7.50°N / 60.17°W), and can be traced westwards into the El Callo Formation (Pastora Supergroup) in Venezuela. In some ways this group is the easiest to correlate across wide areas due to the presence of carbonaceous, ferruginous and especially manganiferous facies, including gondites. Drainage geochemistry is also distinctive, with -80 mesh stream sediment arsenic concentrations frequently over 10ppm As, with up to 1000 ppm arsenic in the core Matthews Ridge-Arakaka Region. Examples of this geochemistry can be found in Arjune *et. al.* (2006) & Kantharaja *et. al.* (2012). Antimony drainage geochemistry is also anomalous, with 1-2ppm Sb in most Barama Group areas, and up to 25ppm near Matthews Ridge. The main Barama Group area occurs as an east-west belt in north Guyana (Figure 1). Near the border with Venezuela a diverging belt, possibly a fold continuation, has similar geology (including some Mn zones), and anomalous arsenic and antimony geochemistry. This trends to the SE across to the Cuyuni and Puruni Rivers, and then swings E-W before trending NE at its eastern end. Much of this was historically called the Cuyuni Group.

In the Barama Group the oldest rocks are believed to be the Tenapu Formation (Williams et. al. 1967), consisting of mafic rocks such as amphibolites, chlorite schists and pillow basalts, with subordinate lenses of psammitic rocks and rare phyllites. Locally ultramafic zones such as serpentinites and talcose rocks occur, possibly representing komatiitic flows or sills (Gibbs & Barron 1993). In some areas these are overlain by more differentiated volcanics. In the central and lower Barama River Gibbs (1978) describes overlying calc-alkaline flows, tuffs and sub-volcanic porphyry stocks (Arawanta Formation), while in the western part of the main Barama Group belt calc-alkaline rocks, including stratiform shoshonitic hornblende-porphyries occur (Gibbs & Barron, 1993). In the central part of the main Barama Group Belt mafic rocks are covered by sediments of the Matthews Ridge / Pipiani Formations. Webber (1952), describes this as a sequence of dark coloured Lower Quartzites (~200m), red to brown to purple Lower Phyllites (~300m), pale to greenish sericite schist (~200m), and then the Upper Quartzite lens swarms in phyllites, including manganiferous zones (~300m), before the Upper Phyllite (~600m). At least some of the material that now looks like quartzite may originally have been chert. The Arakaka Formation, which may be the lateral equivalent of Webber’s Upper Phyllite zone, consists of phyllites and mudstones, with subordinate quartzites and chlorite schists. At the eastern end of the main Barama Group outcrop in the Tassawini area tuffaceous zones as well as quartzites occur in the upper parts of the sequence. The overlying 2-3km thick Kokerit Formation (Gibbs, 1978) is exposed extensively in the lower Barama and is dominated by clastic meta-sediments / greywackes, including volcaniclastic conglomerates and some fine-grained igneous rocks.

Very similar geology is described from several locations in the more southerly belt of Barama Group rocks, which was originally termed the Cuyuni Group. Geochemistry is similar, though more muted, with few drainage stream sediment samples with over 20ppm As, though still with a consistent background of 2-6ppm As. Geochemical data is presented in the GGMC Upper Puruni, Morabisi North, Kartuni and, Pashanamu project reports (Heesterman et. al. 2001, 2002, 2004 & 2005). Significant manganiferous zones are only known from the eastern part of this belt. Folding (some isoclinals) and belt-parallel shearing is more common, although some units can be traced along strike on the basis of geophysics and imagery. Guyana Goldfields (2018) describe the stratigraphy of the Aurora-Sulphur Rose district as tholeiitic basalts, then lecoxene-bearing mafic meta-volcanics overlain by clastic sediments including carbonaceous rocks, and then greywackes and conglomerates. The upper sediments are the Cuyuni Formation described by Williams et. al. (1967), which like the Kokrit Formation locally contains fine grained porphyritic igneous layers.

In the zone between the two Barama Group belts there are large areas of meta-volcanics, some meta-sediments and granites, charnockites and diorites, as well as gneises but no systematic arsenic or antimony anomaly. This area requires further work.

The regional structure in the northern E-W belt consists of a large scale re-folded syncline. The fold pattern is undoubtedly complicated by thrusts. Further west in the El Callao region Hildebrand *et. al.* (2014) provides good evidence that the mafic meta-volcanics and sediments of the Pastora supergroup are thrust over the younger Supamo Complex, as well as a pre-Roraima quartzite. The Supamo Complex is the equivalent of the Barima-Wahanamaparu / Bartica Gneiss, which occurs to the north and south of the northern Barama Group belt. In Guyana a thrust contact where greenstones overly gneissose rocks have not yet been identified. However a 20km mineralised low angle contact between granite and overlying Cuyuni Formation is known from Quartzstone (WDB Gold Inc, 2018), and a meta-conglomerate may be thrust over meta-volcanics and a small granitic intrusion at Million Mountain (59.32ºW / 6.3ºN). To the south of the southern Barama Group belt there are gneissose Bartica Assemblage zones and small areas of kyanitic rocks, and then the Mazaruni Group belt.

NORTHERN GUYANA; THE MAZARUNI GROUP.

The Mazaruni Group extends to the SE from the Venezuelan border to Suriname, swinging E-W at it's eastern end (Figure 1). Unlike the Barama Group, stream sediment arsenic geochemistry is muted. Isolated stream sediment arsenic concentrations over 2ppm are only seen in areas with known gold mineralisation. No manganiferous zones are known. Folding, shearing and normal faulting, large areas of granitic intrusions, as well as extensive White Sand cover adds uncertainty to correlation between areas.

Renner & Gibbs (1987) consider the Issineru / Haimaraka area in the west (60.4ºW / 6.4ºN), to be the type area on the basis that it is less deformed. A semi-continuous 5-7km sequence of mainly greenschist facies meta-volcanic rocks occur, some folded, but generally dipping ~60º to the SW. They describe a lower sequence of approximately 3km of tholeitic basalts, some pillowed, and minor tuff and chert. This is followed by intermediate and felsic meta-volcanic dominated zone, though mafic rocks still occur. Like Aurora, iron rich tholeitic basalts, as well as more calc-alkaline leucoxene-bearing basalts are recognised. Near the top of the volcanic Issineru Formation meta-greywackes and pelites are interbedded, and become more common. This is then covered by the wholly sedimentary Haimaraka Formation, which is dominated by greywackes and is clearly not overturned.

Having discussed what is supposed to be the type area, considerable problems exist with the relationships of the sedimentary Haimaraka Formation to the underlying meta-volcanic Issineru Formation. Barron (1975) describes the geology in the Cuyuni River along the border with Venezuela ~60km further west. A clear unconformity occurs between the underlying strongly folded Makapa Formation (Barama Group) and the quartz rich Western Cuyuni / Los Caribes Formation. Gibbs & Barron (1993) regard this as equivalent to the Muruwa Formation, and so part of the younger Burro Burro Group that overly the greenstones. This formation consists of reddish arkose / greywackes, minor felsic tuff bands and polymict conglomerates. Some 1-2m boulder beds occur, with clasts of quartz-porphyry, volcanics, quartzites or phyllites. The boulder beds appear to underly areas of Haimaraka Formation. The Haimaraka was originally defined as purple to brown shales with interbedded greywackes, often affected by 2 phases of gentle folding. The description by the USGS & CVG (1993) of the "pre-Roraima Group" sedimentary rocks further west in Venezuela is almost identical to the Haimaraka. If the Haimaraka overlies the equivalent of the Muruwa Formation, then it may be the time equivalent of the Iwokrama Formation, which itself underlies the Roraima Group. Of interest is the presence of 45 cm bands of felsic accretionary lapilli up to 7mm in diameter in the Merume area (59.97ºW / 5.79ºN) described by Bateson (1965). Very similar, though much larger beds of "rhyolite balls" up to 15cm in diameter are known from the Berbice River from the Iwokrama Formation (Gibbs & Barron 1993 & Heesterman *et. al.* 2014). Beyer *et. al.* 2015 describe Muruwa Formation rocks under Roraima Group rocks in a deep drill hole 19km to the west of Bateson's lapilli occurrence. Alluvial diamond and gold occurrences are known in Haimaraka Formation areas, but no primary gold mineralisation. Should the Haimaraka not be part of the greenstone basement, but much younger, this explains the zeolite facies metamorphism described by Renner and Gibbs (1987). For this reason I have been controversial and have included the known Haimaraka Formation areas with the Muruwa in Figure 1.

Though I believe the upper sedimentary sequence in the Issineru area is not part of the Mazaruni Group, further east in the Potaro, Kaburi and Omai areas there is no doubt that a sedimentary sequence overlies the volcanic part of the Mazaruni Group. Gibbs and Barron 1993 suggest that a 2-3km thickness of mafic metavolcanics is covered by 1-2km of intermediate to felsic volcanics and then 1-2km of meta-sediments. A recent description from the Karouni Mine (59.07ºW / 5.62ºN) in the Kaburi district is given by Tedeschi (2017), who describes a lower meta-volcanic unit consisting of ultramafic to high MgO basalts and tholeiitic basalts, and high Ti dolerite. These are followed by volcaniclastic conglomerates and coarse sandstones, which I believe to be very similar to those near Omai. An upper sequence of laminated, carbonaceous siltstone and fine sandstone occurs.

A good description of the stratigraphy in the immediate Omai area (58.76o W / 5.45o N) can be found in Voicu (1999). The sequence is partially dismembered at Omai, in that a phyllitic zone to the south is separated by a significant mineralised shear through the Wenot pit from pillowed basalts and andesitic to felsic rocks. Felsic dykes in the shear have been dated to 2.13 Ga by Norcross (1997), as has the dioritic stock (2.094 Ga) that hosts the mineralisation in the Fennell Pit. Volcaniclastic conglomerates which may represent the equivalent to the Kokrit Formation in the Barama Group occur several km further north. All the rocks dip steeply.

CONCLUSIONS

There is no correlation between the Kwitaro Formation of southern Guyana and the Barama-Mazaruni Supergroup in northern Guyana. The Kwitaro may be older as it is intruded by a 2,220 Ma granite, while felsic rocks in the middle part of the Barama and Mazaruni Groups range from 2,138 to 2,123 Ma., though this is based on a very limited number of modern age dates. Gold mineralisation occurs, but may be associated with BIF-like rocks. In northern Guyana manganiferous zones and anomalous arsenic geochemistry occur in the northern E-W sediment dominated Barama Group. The lower part of the sequence consists of mafic metavolcanics. Large scale regional

folding and later cross folding results in domal structures. A NW-SE trending zone of very similar rocks which also has manganiferous zones and anomalous arsenic geochemistry diverges near the Venezuelan border. This used to be called the Cuyuni Group, but is undoubtedly part of the Barama Group, though more affected by folding and belt parallel shearing. The Mazaruni Group has a very similar sequence starting with much greater thicknesses of tholeitic mafic meta-volcanics, and then calc-alkaline rocks and sediments such as phyllites. However there are no manganiferous zones and no anomalous arsenic drainage geochemistry. Again folding and shearing have dismembered the sequence. In both the Mazaruni and Barama Groups felsic volcanics appear to be about the same age (2,138-2,123 Ma). Volcaniclastic conglomerates and greywackes appear to be the youngest rocks in both greenstone groups, and may be unconformable. Primary gold mineralisation occurs throughout the Barama-Mazaruni Supergroup.

The Muruwa Formation sediments are unconformable on the greenstones in northern Guyana, yet older than the Iwokrama Formation felsic rocks (> 1.99 Ga), and older than the Roraima Group. The Haimaraka Formation was originally thought to be the upper part of the Mazaruni Group, but good evidence suggests this is part of the "pre-Roraima sequence". Both the Muruwa and Haimaraka show two phases of open folding. No primary gold mineralisation occurs, though palaeo alluvial occurrences may do. Further work is needed to understand whether there are more unconformable post gold-mineralisation formations.

Episode / Formation	Geology / Comments	Age date / Reference
Cover	River valley alluvium, lateritic peneplains. Sand dunes in the Takutu Graben area.	Berrangé (1977)
K'Mudku / Nickerie,	Muri Mountain. Nephaline syenite with a lateritic cap. Locally fenitised with rare earths (Gibbs & Barron 1993). A-Type magmatism	1,110 Ma Nadeau (2014)
	Shearing, mylonites & pseudo tachylites. Cataclasites. Mostly NE-SW, approximately parallel to the Takutu Graben	1,490-1,147 Ma da Silva Souza (2015)
Käyser Dykes?	Larger (50m) olivine dolerite dykes NW-SE recognized in SW Suriname. Not yet recognized in Guyana. Tensional features related to the K'Mudku Episode?	~1,500Ma De Roever *et. al.* (2003)
Kuyuwini Formation	Similar to the Iwokrama Formation volcanics & granites. Locally more metamorphosed. Some charnockitic granites near the northern edge of the area.	1.89-1.81 Ga Almeida (2006)
Appinitic / Baddidiku Suite	Ultramafic to anorthositic intrusions and gabbro-norites. Intrudes granite. Rare serpenitinite e.g in the New River; unknown affinity. One dubious date from a hornblende pyroxinite (Achiwuib Mountain) in southern Guyana.	1.9 Ga, Berrange (1977) No modern age dates
Granite Complex	Southern Guyana Granite Complex: Large granite areas, locally with enclaves of Kwitaro Group. Zircon xenocrysts 2,086 - 2,297 Ma.	1.925-1.984 Ga Nadeau *et. al.* (2013)
Kanuku Complex	Paragneisses , migmatites and granulites with charnockitic S-type granites (1,956 Ma). Inherited detrital zircons in paragneiss clustering at ~ 2.2- 2.7Ga. 1.94-1.92 Ga Thermal perturbation.	2,020 Ga Nadeau *et. al.* (2013) Fraga *et. al.* (2017)
Marudi Granite / migmatite	Granite appears to be intrusive into the Kwitaro Group rocks near the Marudi Mountain gold deposit.	2.22 Ga Nadeau (2014)
Kwitaro Group.	Gneissose meta-quartzites & amphibolite bands.	> 2.22 Ga
Uncorrelated Gneisses – several areas, *e.g.* Rewa & Kuyuwini		

Table 1: Southern Guyana Stratigraphic Summary, and references to the most recent geochronology.

Episode / Formation	Unit	Geology / Comments		Age date / Reference
"Cover" Corentyne Group	"White Sand" / Berbice Formation	Transgressive river sands, dunes and beaches, tectonically uplifted coastlines. Extensive river capture. Water feeds into coastal aquifers. Archaeological artifacts & giant sloth bones under sand in mining pits.	Holocene to Quaternary	>~10,000 years? Plew (2004)
	Montgommery Formation	Sands, lignites & clays. Under White Sand, and over the bauxite.	Miocene	<30Ma
	Laterite and bauxite.	Extreme weathering in a brackish to freshwater environment results bauxite on kaolinitic sediments and ferruginous laterite on higher ground. "Bauxite hiatus"	Oligocene	30-45Ma Van der Hammen & Wijmstra (1964)

Episode / Formation	Unit	Geology / Comments		Age date / Reference
	Mombaka Formation	Sand and clay on an irregular palaeosurface. Extensive Paleocene to Mesozoic sediments including 2 deeper sand aquifers near the coast. 66Ma K–T extinction; Chicxulub crater. Seawards lateral change into Guyana Basin Sediments	Eocene	
Takutu Group	Manari , Pirara, Takutu & Tucano	Sedimentary graben fill, including some evaporates. One bird / dinosaur? footprint known near Lethem.	Jurassic-Early Cretaceous	150-140Ma Crawford (1985)
	Apoteri Volcanics	Tholeitic basaltic (Takutu Graben). Structure related to opening of the Atlantic. Reactivation of an older continental scale shear partially controlled the position of transform faults.	Late Jurassic	153.5-149.5 Ma Reis *et. al.* (2006)
Younger Basic Dykes	Taino / Apatoe & PAPA	NE-SW tholeitic dykes. Central Atlantic Magmatic Province (CAMP). Extinction event. Dinosaurs flourish after this. Problematic dates on "PAPA" (post-Avanavero-pre-Apatoe) dykes.	Jurassic	191-202Ma : Reis *et. al.* (2006) Berrange (1977)
Avanavero Suite	Large gabbro-norite sills, especially in the Roraima Sediments, elsewhere mainly inclined sheets (*e.g.* Omai Sill) and dykes. Some are layered, with low level platinoid concentrations.			1.799-1.779 Ga Norcross (1997) Beyer *et. al.* (2015)
Roraima Group	Conglomerates and sandstones derived from the NE. Some tuffaceous bands (1,873, 1,901 & 1,903 Ma). Semi-conformable contacts on the Iwokrama in the east, unconformable to the south west. Rests on the Iwokrama & Muruwa Formations. Tepui landscape.			1,873-1,903 Frimmel *et. al.* (2005) Beyer *et. al.* (2015)
Burro-Burro Group	Iwokrama Granites	Leuco & biotite granites. Zircon xenocrysts of Hadean and Archean ages (2,519 to 4,219 Ma). The Makarapan Riebeckite Granite (1.97 Ga) gives a similar age, confirming problems with historical dates.		1.99-1,96 Ga Nadeau *et. al.* (2013) Nadea014) Reis *et. al.* (2017)
	Iwokrama Formation	< 2000m felsic volcanics & sub-volcanic intrusions folded in the SW, minor folding in NE, where it is semi-conformable on the Muruwa. 4,219 Ga Hadean xencrsyst.		
	Uranium Mineralisation?	Alteration age at Aricheng in "Younger Granite" Possible hydrothermal fluids associated with the Iwokrama Formation?		1,995 Ma Alexandre *et. al.* (2010)
	Haimaraka Formation	Brown-red shales & turbidites. *Cf.* the 'pre-Roraima Group' in Venezuela (Sidder *et. al.* 1993) / El Miamo Formation seen under on gneiss under thrusted greenstones.		Hildebrand *et. al.* (2014)
	Muruwa Formation	~1200m sandstones, minor cong. 2-phases of minor folding in central and eastern Guyana, unconformable contact with greenstones.		Xenoliths in Iwokrama Granites.
Appinitic Suite / (Older Basics)	Ultramafic to anorthositic intrusions and gabbro-norites with deuteric alteration. Intrudes greenstone basement. Not recognised intruding Roraima or Burro-Burro Groups.			No dates, 1.9 Ga, same as S Guyana?
Gold Mineralisation?	Omai, thermal/hydrothermal event that reset or recrystallized rutile and reset or grew titanite.			1,999 Ma Norcross (1997)
Lamprophyre dikes	Aricheng; foliated.			2,011 Ma Renaud (2014)
Bartica Gneiss / Devil's Hole / Barima-Wahanamaparu	Paragneiss, migmatite, amphibolite & quartzite. Associated syn-kinematic muscovite (biotite) granites *e.g.* Kartabu (2,080 Ma). Similar age to the "Younger Granites". Supamo Complex in Venezuela same as the Barima-Wahanamaparu gneiss in northern Guyana. Date on foliated granite gneiss (protolith age), thrust over greenstones and a pre-Roraima quartzite.			2,080 Ma Nadeau (2014); 2,132-2,108 Ma Hildebrand (2014)
Younger Granites, Trans-Amazonian	Omai Tonalite (2,094 Ma). Undeformed quartz diorite in Venezuela (2,092), Strong possibility that some Iwokrama Granites have been misidentified as part of this group.			2,094 -2,092 Ma, Norcross (1997)
	Kurupung Batholith / Aricheng foliated high Mg granodiorite.			2,103 Ma Renaud (2014)

Episode / Formation	Unit	Geology / Comments	Age date / Reference
Tectonothermal Event.		Nine-Mile granodiorite. Shrimp U-Pb analysis of 10 zoned zircons. 8 samples in this range, one 2,112 Ma zircon core, 1 sample probable Pb loss 1,988 Ma.	2,145 Ma Basoo & Murphy (2018)
Barama-Mazaruni Super Group: Greenstones; Sediment and volcanic dominated respectively. Mafic metavolcanics, including some ultramafic, possibly komatiitic layers, then intermediate-felsic metavolcanics (some shoshonitic), then clastic sediments such as quartzites and phyllites and subsequently minor tuffs and greywackes. Mostly greenschist facies, some amphibolitic, especially near granite contacts.			
Barama Group: Date on meta-dacitic tuffs from El Callao rocks in Venezuela directly equivalent to the Barama Group.			2,138-2,123 Ma Hildebrand *et. al.* (2014)
Mazaruni Group: Date on en-echelon felsic dykes in shear zone between mafic meta volcanics and sediments at Omai.			>2,130 Ma Norcross (1997)

Table 2: Northern Guyana stratigraphic summary, and references to the most recent geochronology.

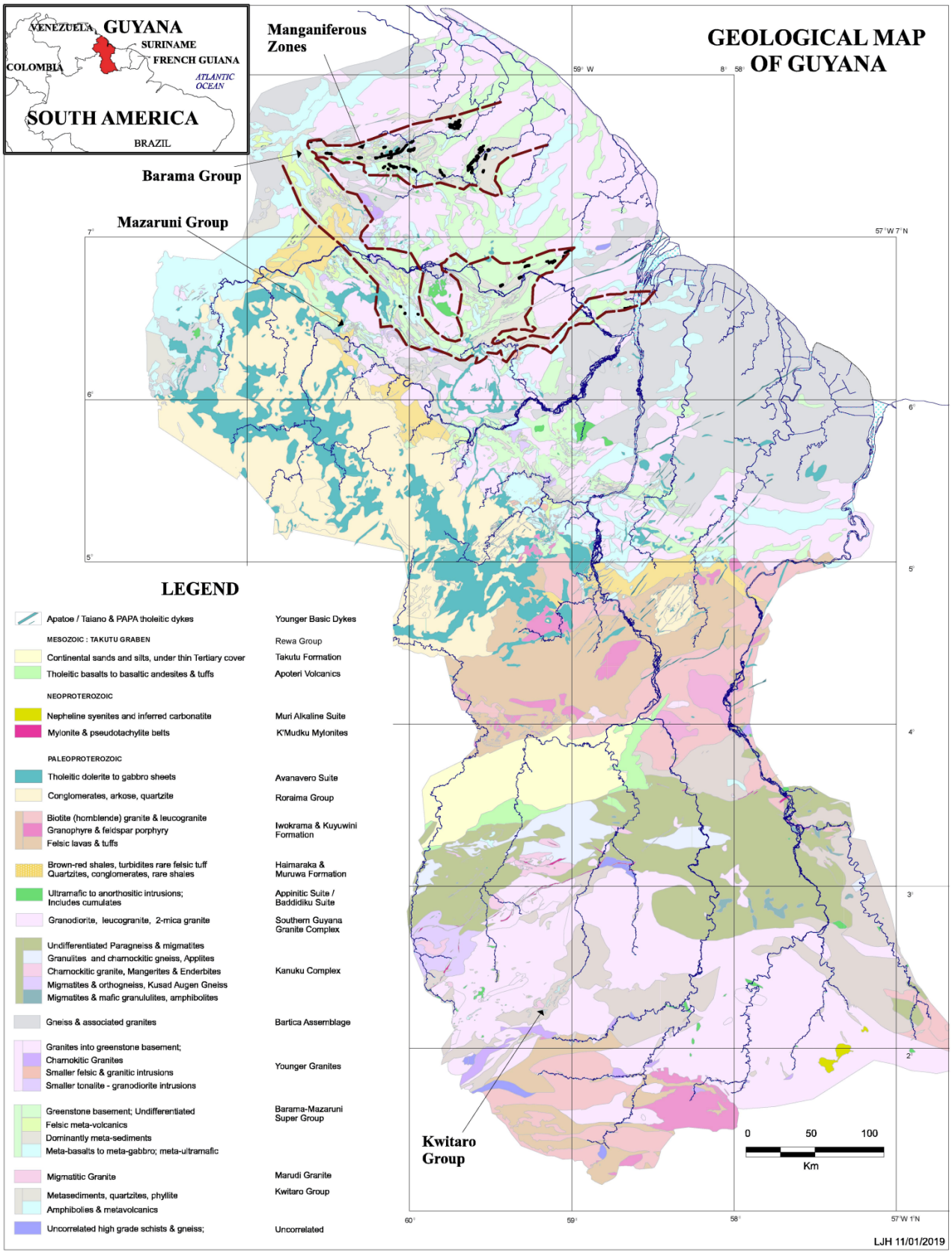

Figure 1. Geological Map of Guyana showing the main greenstone belts

REFERENCES

Alexandre, P., 2010, Mineralogy and geochemistry of the sodium metasomatism-related uranium occurrence of Aricheng South, Guyana: Miner Deposita (2010) 45, 351–367.

Almeida, M.E., 2006, Evolução Geológica Da Porção Centro-Sul Do Escudo Das Guianas Com Base No Estudo Geoquímico Geocronológico E Isotópico Dos Granitóides Paleoproterozóicos Do Sudeste De Roraima, Brasil: PhD Thesis, University of Para.

Arjune, B.K.A., Persaud, L., Reece, J. & Heesterman, L.J.L. 2006, Barama Roads Project Report: Guyana Geology and Mines Commission, Geoservices Division: Draft / Unfinished report.

Barron, C.N., 1975, Notes on the Geology of Guyana along the frontier with Venezuela: Anais Décima Conferência Geológica Interguianas, Belém, 1975, p 219-240.

Bassoo, R., Murphy, J.B., 2018, The 9 Mile Deposit of the Barama-Mazaruni Greenstone Belt of the Guiana Shield: geochemistry, geochronology and regional significance: Brazilian Journal of Geology, 48(4): 671-683.

Bateson, J.H., 1965, Accretionary Lapilli in a Geosynclinal Enviroment: Geological MagazineVolume102, no.1.

Berrangé, J.P., 1977, The Geology of Southern Guyana, South America: Institute of Geological Sciences, National Research Council, London, Overseas Memoir 4.

Beyer, S.R., Hiatt, E.E., Kyser, K., Drever, K.L., Marlatt, J., 2015, Stratigraphy, diagenesis and geological evolution of the Paleoproterozoic Roraima Basin, Guyana: Links to tectonic events on the Amazon Craton and assessment for uranium mineralization potential: Precambrian Research 267 (2015) 227–249.

Crawford, F.D., Szelewski, C. E. and Alvey, G.C., 1985, Exploration in the Takutu Graben of Guyana and Brazil: Journal of Petroleum Geology, 8, 5-36.

Fraga, L.M., Cordani, U., Kroonenberg, S., Reis, N., Dreher, M. De Roever, E., Nadeau, S. and Maurer, V.C., 2017, U-Pb Shrimp New Data On The High-Grade Supracrustal Rocks Of The Cauarane-Coeroeni Belt - Insights On The Tectonic Eo-Orosirian Evolution Of The Guiana Shield: Anais do XV Simpósio de Geologia da Amazônia, Belém, 2017.

Frimmel, H.E., Groves, D.I., Kirk, J. Ruis, J., Chesley, J. & Minter, W.E.L., 2005, The Formation and Preservation of the Witwatersrand Goldfields, the World's Largest Gold Province: Economic Geology 100th Anniversary Volume pp. 769–797.

Kantharaja, D.C., Pickett, K., Nestor, G., Persaud, L., Hicks, T. & Wilson, R., 2012, Barama Headwaters Project, (Barama Headwaters – I and Barama Head Gap Areas). A Summary of Geochemistry, Geology and Structure.

de Roever, E.W.F., Kroonenberg, S.B., Delor, C. & Phillips, D.m 2003, The Käyser dolerite, a Mesoproterozoic alkaline dyke suite from Suriname: Géologie de la France, 2003, n° 2-3-4, 161-174.

da Silva Souza, V. & de Souza, A.G.H., 2015, K´Mudku A-type magmatism in the southernmost Guyana Shield, central-north Amazon Craton (Brazil): the case of Pedra do Gavião syenogranite: Brazilian Journal of Geology, 45(2): 293-306, June 2015.

Gibbs, A.K., 1978, Field Report on the Barama River Section: Geological Survey of Guyana. Unpublished Report AKG 1/78, 58p.

Gibbs, A.K., and Barron, C.N., 1993, The Geology of the Guiana Shield: Oxford Monographs on Geology and Geophysics No.22.

Guyana Goldfields, 2018, Analyst & Investors Site Tour: Exploration Overview, November 13, 2018: Company Presentation.

Guyana Goldstrike Inc, 2019, https://www.guyanagoldstrike.com/projects/marudi-gold-project/geology accessed 13/01/2019.

Hawkes, D.D., 1955, A note on the geochemical dispersion of Arsenic in relation to gold mineralisation at Marudi Mountain: Geological Survey of British Guiana: Records Volume 3.

Heesterman, L.J.L, Kemp, A.W. & Nestor, G. 2001, Upper Puruni Project. A summary of Geochemistry, Geology & Structure in the Headwaters of the Puruni River: Guyana Geology and Mines Commission, Geoservices Division, Report No. GS 2/2001.

Heesterman, L.J.L, Kemp, A.W., Arjune, B.K. & Crawford, A., 2002, Morabisi North - Kamawari Project- A Summary of Geochemistry, Geology and Structure: Guyana Geology and Mines Commission, Geoservices Division, Report No. GS 1/2002.

Heesterman, L.J.L, Arjune, B.K., Cole, E, and Kemp, A.W., 2004, Kartuni Project: Geology Geochemistry and Structure. Guyana Geology and Mines Commission, Geoservices Division, Report No. GS 1/2004: Geology and Mines Commission, Geoservices Division, Report No. GS 1/2012.

Heesterman, L.J.L, Kemp, A.W., Arjune, B.K & Cole, E.W., 2005, Pashanamu Project. Geology, Structure and Geochemistry: Guyana Geology and Mines Commission, Geoservices Division: Report No. GS 1/2005.

Heesterman, L.J.L, Kemp, A.W, Zaleski, E, Chuck-A-Sang, N. Cole, E. & Crawford, A., 2013. Kuyuwini Project Geology & Geochemistry Re-visited: Geology and Mines Commission, Geoservices Division, Report No. GS 1/2013.

Heesterman, L.J.L., Pickett, K.M., & Kemp, A.W., 2013, Marudi North Project Geology and Geochemistry; Geology and Mines Commission, Geoservices Division, Report No. GS 2/2013.

Heesterman, L.J.L, Chuck-a-Sang, N., Clementson, N., Cole, E.W. & Kemp, A.W., 2014, Demerara Headwaters Project, Geochemistry & Geology: Guyana Geology and Mines Commission, Geoservices Division, Report No. GS 2/2015.

Hildebrand, R.S., Buchwaldt, R. & Bowring, S.A., 2014, On the allochthonous nature of auriferous greenstones, Guayana shield, Venezuela: Gondwana Research 26 1129–1140.

Lunceford, R.A., 2009, Geological Report And Summary Of Field Examination, Marudi Property, Region Nine (Upper Takutu-Upper Essequibo), Guyana: Prepared For Shoreham Resources Ltd. In Compliance With Ni 43-101 And Form 43-101f1.

Nadeau, S., Chen, W., Reece, J., Lachman, D., Ault, R., Faracao, T., Fraga, L., Reis, N. and Betiollo, L., 2013, Guyana: The Lost Hadean Crust Of South America?: Brazilian Journal of Geology, 43(4): 601-606.

Nadeau, S., 2014, Guyana Geological Time Scale: Poster for the Guyana Geology and Mines Commission Mining Week 2014. http://ggmc.gov.gy/main/sites/default/files/GeoServicesFeatureDownloads/6-GUYANA%20GEOLOGICAL%20TIMESCALE.pdf

Norcross, C., 1997, U-Pb Geochemistry of the Omai intrusion - hosted Au-Quartz vein deposit and host rocks. Guiana Shield, South America: M.Sc. Thesis, University of Toronto.

Plew, M., 2004, The archaeology of Iwokrama and the North Rupununi: Proceedings of the Academy of Natural Sciences of Philadelphia 154, p7-28.

Reis, N.J., Szatmari, J., Wanderley Filho, J.R., York, D., Evensen, N.M. and Smith, P.E., 2006, Dois eventos de magmatismo máfico mesozóico na fronteira Brasil-Guiana, escudo das Guianas: enfoque à região do rifte Tacutu-North Savannas: SBG, Cong. Bras. Geol., 43, Aracaju, 2006.

Reis, N.J., Nadeau, N., Fraga, L.M., Betiolo, L.N., Faraco, N.T.L, Reece, J., Lachman, D. & Ault, R., 2017, Stratigraphy of the Roraima Supergroup along the Brazil-Guyana border in the Guiana shield, Northern Amazonian Craton – results of the Brazil-Guyana Geology and Geodiversity Mapping Project: Brazilian Journal of Geology, 47(1): 43-57.

Renaud, J. A., 2014, The Aricheng Basement-Hosted Albitite-Type Uranium Deposit, Roraima Basin, Co-Operative Republic Of Guyana, South America: PhD Thesis. University of Western Ontario.

Renner, R. & Gibbs, A.K., 1987, Geochemistry and Petrology of Metavolcanic Rocks of the Early Proterozoic Mazaruni Greenstone Belt, Northern Guyana: Pharaoh, T. C., Beckinsale, R. D. & Rickard, D. (eds), Geochemistry and Mineralization of Proterozoic Volcanic Suites, Geological Society, London, Special Publications 1987, v.33; p289-309.

Szatmari, P., 1983 Amazon rift and Pisco-Jurua fault: Their relation to the separation of North America from Gondwana: Geology, v.11, 300-304.

Tedeschi, M., Hagemann, S. & Davis, J., 2017, Lithostratigraphic, structural and hydrothermal evolution of the Rhyacian Karouni orogenic Au deposit, Guyana South America: Conference Paper: SGA Quebec City, August 2017.

U.S. Geological Survey and Corporacion Venezolana de Guayana, Tecnica Minera, C.A., 1993, Geology and mineral resource assessment of the Venezuelan Guayana Shield: U.S.Geological Survey Bulletin 2062, 121 p.

Van Der Hammen, T. and Wymstra, T.A., 1964, A palynological study on the Tertiary and Upper Cretaceous of British Guiana: Leidse Geologische Mededelingen, Dl. 30, 183-241.

Voicu, G., 1999, Geology, Geochemistry and Metallogeny of the Omai Gold Deposit, Guiana Shield: Ph.D. Thesis, Université du Québec à Montréal.

WBD Gold Inc, 2018, Investor Presentation: Accessed 31/07/2018, http://wbdgold.com/wp-content/uploads/2018/07/WBDG-Investor-presentation_May2018.pdf

Webber, B.N., 1952, Manganese Deposits in the Northwest District, British Guiana: Geological Survey of British Guiana, Bull. 23.

Williams, E., Cannon, R.T. & McConnell, R.B., 1967, The Folded Precambrian of Northern Guyana Related to the Geology of the Guiana Shield: Geological Survey of British Guiana; Records Volume 5., 60 p.

Zaleski, E., 2005, Reconnaissance of the Marudi Mountain Area. Preliminary Structural Interpretation and Regional Implications: Guyana Geology & Mines Commission, Geoservices Division. Report No. GS 2/2005.

Guyana; unresolved geological questions.

Linda Heesterman

Independent Geologist
Heesterman_Kemp@Hotmail.com

SUMMARY

In the 15 years I worked in Guyana some aspects of the geology become better recognised (such as the Muruwa Formation), but in some areas further work is needed. A few of these are listed, in the hope this will act as a spur for discussion and future research.

Understanding of the different groups of magmatic intrusions is directly relevant to mineral exploration, while other relationships are more abstract. The origin of the Bartica Assemblage is revisited, and it's relationship to areas of higher grade, higher pressure metamorphic rocks in northern Guyana.

Key words: Guyana, Stratigraphy, Mineralisation, Metamorphism. Muruwa and Iwokrama Formation, Bartica Assemblage, Allanite.

INTRODUCTION

During the last 25 years since publication of "the bible" (Gibbs & Barron, 1993) some aspects of the geology of Guyana have become better understood, such as the Muruwa Formation and Iwokrama Granites. However there are also problematic areas, a few of which are briefly mentioned. Locations discussed below have been shown on Figure 1, modified after Fraga *et. al*. (2017b).

1. THE MURUWA FORMATION

The Muruwa Formation outcrops to the north of the Roraima Group in the Pakaraima Mountains and the Parish's Peak area (Locality 1a, Figure 1). It consists of quartzites, with some conglomerates, with a very similar appearance to those of the Roraima Group. Presence of Muruwa xenoliths in granites (Locality 2a & b) originally suggested this was a less metamorphosed part of the Mazaruni group. It is now clear that the host granites are Iwokrama Granites (see below). In the Muruwa and nearby Essequibo River west of Parish's Peak the Muruwa is unconformable on greenstone basement, and has two phases of slight folding. On the east side of Parish's Peak the overlying Iwokrama Formation volcanics and almost flat lying Roraima Group rocks appear to be semi-conformable (Heesterman et. al., 2015). Further west in Venezuela (1b) it appears that the Muruwa / Los Caribes Formation is more deformed, locally steeply dipping and folded, yet still overlain by semi-flat lying Roraima Group sediments. According to Gibbs & Barron (1993) the equivalent rocks to the east in Suriname is the Ston Formation (1c), which also shows open folding.

In conclusion in eastern Guyana and Suriname it appears that the Muruwa represents an early phase of sedimentation, which was slightly folded, before being covered by felsic volcanics of the Iwokrama Formation and intruded by sub-volcanic granites. Further west deformation appears to have been more extensive. Sedimentation resumed, and the main bulk of the Roraima Group was deposited. Larger granites intruded both the Muruwa and Iwokrama Formations, and in rare cases felsites intruded into the Roraima.

2. IWOKRAMA GRANITES

In Guyana larger granites were historically all considered to be ~2.1 Ga "Younger Granites". However in Suriname the Dalbana Formation (Iwokrama equivalent) has well described associated biotite and leuco-granites (Kroonenberg et. al. 2016). Dating of Iwokrama volcanics and granites near the Brazilian Border by Nadeau et. al. (2013), as well as the Makarapan Riebeckite Granite (Fraga et. al. 2017) has proved that these are of similar age (~1.98 Ga). The large areas of granite locally containing Muruwa xenoliths shown as 2a and 2b in Figure 1 are now also considered to be the same age, essentially shifting the known zone northwards.

Alexandre (2010) reports a granite host rock emplacement age of ~2.1 Ga and a uranium mineralisation age of 1.995 + 15 Ma at Aricheng (2c), on the north side of the Roraima Group area. The mineralisation age is similar to the age of the Iwokrama Formation, suggesting fluids could be related to this magmatic event. Barron (1968) reports small felsic intrusions into the Roraima in the Amatuk area (2d), also on the north side. Some tuffaceous bands are known within the Roraima Group. It appears that felsic rock emplacement continued after the Roraima Group was deposited, and such rocks occur further north than usually accepted.

An important question is how many granites have been wrongly grouped. This is particularly significant in that molybdenite and tungsten occur in the same area as the granite hosted gold mineralisation at Eagle Mountain (2e), as well as minor Sn drainage geochemistry. Such chemistry is more likely to be associated with the Iwokrama / Saracura Suite Granites.

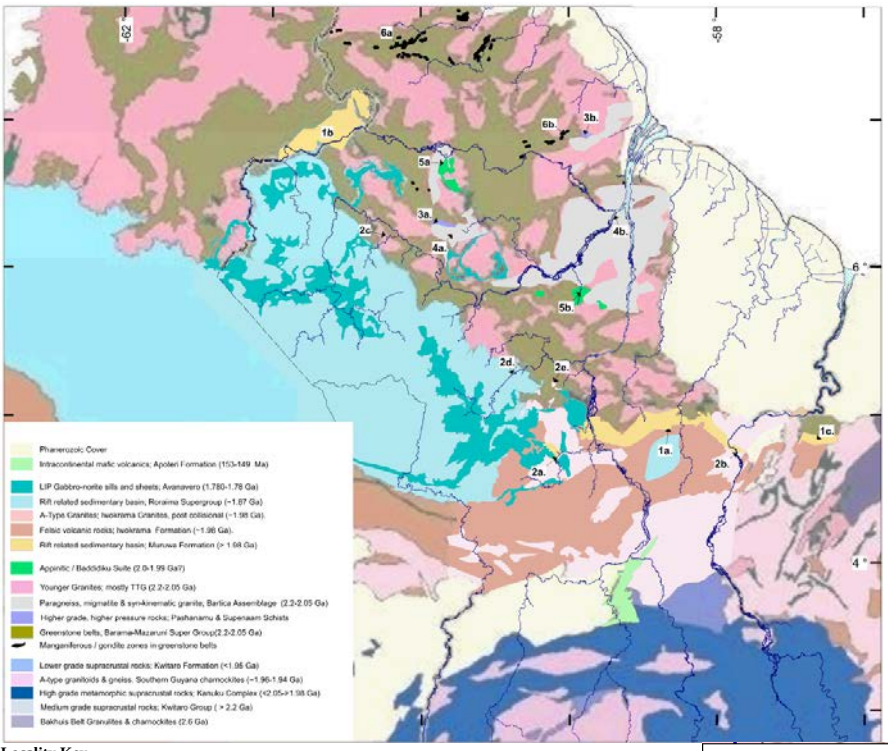

Locality Key
1a Muruwa Formation eastern Guyana.
1b Los Caribes Formarion Venezuela
1c Ston Formation Suriname.
2a & 2b, Iwokrama Granite with Muruwa xenoliths.
2c Aricheng; U mineralisation age ~1.99 Ga.
2d Felsic intrusions into the Roraima Group.
2e.Eagle Mountain area.
3a & 3b; Higher grade metamorphic grade rocks including kyanite schists in the Pashanamu and Supenaam areas
4a & 4b; Bartica Assemblage and syn-tectonic granites.
5a. Gabbro with deuteric alteration.
5b. Kaburi Anorthosite and other layered intrusions.
6a Manganiferous zones Arakaka District.
6b Pomeroon Head Mn & gondite zones.
Note: Mn areas have been exaggerated.

Figure 1: Geological map of northern Guyana modified after Fraga *et. al.* 2017

3. UNCORRELATED HIGHER GRADE ROCKS WITHIN THE GREENSTONE BELTS

Large areas of the greenstone belt are lower greenschist facies. However an area on the south side of the Puruni River (3a, Figure 1), has outcrops of muscovite-biotite-cordierite and chloritoid schist (Heesterman *et. al.*, 2005). A kyanite-sillimanite-muscovite schist outcrop occurs close to boulders of an unusual coarse iron rich cummingtonite / grunerite rock (Photomicrograph Figure 2a). Massive grunerite is more commonly found in amphibolitic banded iron formation rocks. Greenschist facies meta-siltstone and andesite occur within 1.5km on the other side of the Puruni River. Clearly this represents a fault contact. Bartica assemblage rocks which may include high pressure granites occur not far to the south, suggesting the possibility that these odd higher grade rocks are part of an uplifted (thrust?) block. A second location (3b) with folded kyanite-staurolite rocks believed to have formed after meta-pelites also occur in the Supenaam area (Barron 1965), again in proximity to rocks mapped as Bartica Assemblage. Further work is needed!

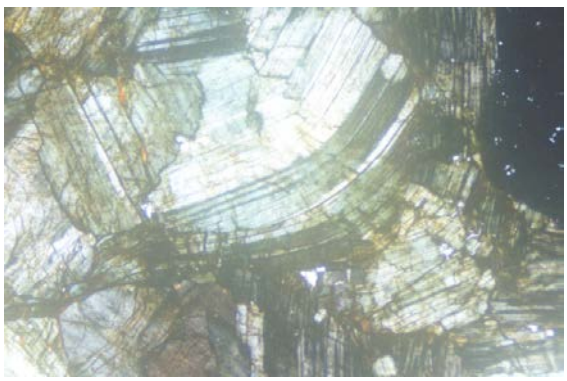

Figure 2a. Bent and fractured Fe-rich cummingtonite. Width of field 1.32mm. xpl. 176589E / 697217N, UTM PSAD56

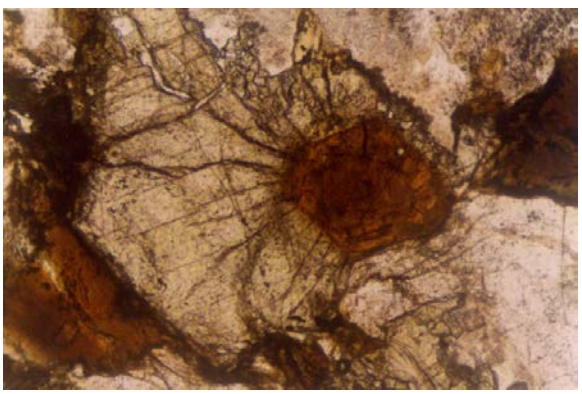

Figure 2b. Syn-tectonic adamellite. Zoned euhedral allanite in epidote. Width of field 1.3mm, ppl. 195203E / 715140N

4. THE BARTICA ASSEMBLAGE

Paragneiss, migmatite, amphibolite & quartzite with associated syn-kinematic muscovite (biotite) granite were considered to have been formed as a result of granitisation from the greenstone basement (Cannon, 1965). Cannon describes two phases of folding, and suggests that locally metamorphism reaches granulite facies. Some authors map the large coherent areas of amphibolite and quartzite as higher grade greenstones, and only gneissose and migmatitic rocks as Bartica Assemblage. Hildebrand *et. al.* (2014) shows that the greenstone belts in the El Callao district are thrust over quartzites (Muruwa Formation ?) that cover the Supamo Complex (Bartica Assemblage equivalent) in the El Callao District of Venezuela, and then folded. This means that the Bartica Assemblage relationship to the greenstone belts in Guyana also needs re-examination.

Petrology done on samples from several GGMC field projects showed that some of the gneissose looking granites, as well as undeformed associated granites contain euhedral allanite (some zoned) overgrown by euhedral magmatic epidote (Heesterman *et. al.* 2004 & 2005), which can not have formed as a result of metamorphism. An photomicrograph of an example is shown in Figure 2b. Allanite is a high pressure form of epidote with a high radioactive / Light Rare Earth element content, which is unstable at lower pressures. Similar mineralogy and textures have been used to infer a depth of formation of ~30km (Chang & Andronicos 2009). This suggests the possibility that at least some of these rocks are high pressure syn-tectonic granites with streaked out amphibolitic xenoliths. Interestingly a date on the Kartabu / Itabaru Granite which is described in detail by Cannon gives the same age as the Younger Granites (Nadeau, 2014). The association of Bartica Assemblage rocks with ambiguous areas of kyanite rich rocks (see above) suggests this issue is worth another look.

5. APPINITIC SUITE / BADDIDIKU SUITE (OLDER BASICS)

Not all large coarse grained gabbroic intrusions are part of the Avanavero Suite. Two other types of larger un-metamorphosed gabbroic intrusions can be recognised. These are appinitic gabbro / dolerite, frequently with deuteric alteration (5a, Figure1), and layered mafic intrusions, also often with hornblende as the dominant mafic mineral such as the Kaburi Anorthosite (5b).

Some of these areas have been investigated for their platinoid potential. Such rocks are never found intruded into the Muruwa, Iwokrama or Roraima Group, and so are probably older. One dubious age date (1.9Ga) is known from a layered intrusion at Achiwuib in southern Guyana (Berrange 1977). I suspect these rocks are similar to the Lucie Gabbro in Suriname (1,985 Ma) described by Kroonenberg *et. al.* (2016). Quite a bit of multi-element rock chemistry and petrology is available from GGMC projects, and along with age dating may help understand these rocks.

6. THE BARAMA AND THE MAZARUNI GROUPS – WHERE ARE THE BOUNDARIES? MANGANIFROUS / ARSENIC RICH ZONES AS MARKER HORIZONS?

The greenstones of Guyana are usually lumped as the “Barama-Mazaruni Super Group”. No one has clearly defined where one starts and the other ends, or where the contact is between groups, or whether the contact is structural, or whether the differences in dominant lithology are due to lateral variation. There are very few units that can be correlated over more than 10’s of kilometres.

The manganiferous zones (including gondites) in the sediment dominated Barama Group of northern Guyana are one of few possible marker horizons. Historical mapping shows that such manganiferous zones can be traced as a refolded belt of over 250km (6a, Figure 1). Other smaller areas of manganiferous rocks and gondites suggest Barama Group rocks can be recognised in other areas. One example is a zone between the Mazaruni River and the Pomeroon area (Locality 6b). A further step would be to examine the possibility of using such marker horizons to compare the greenstones in Guyana with those in adjacent countries. Examination of drainage geochemistry such as that done by GGMC may indicate that these manganiferous belts can also be traced over larger distances by the presence of associated elements such as arsenic or antimony.

REFERENCES

Alexandre, P., 2010, Mineralogy and geochemistry of the sodium metasomatism-related uranium occurrence of Aricheng South, Guyana: Miner Deposita (2010) 45, 351–367.

Barron, C.N., 1965, The geology and kyanite deposits of the Upper Supenaam River: Geological Survey of British Guiana, Records Vol 2. 11-17.

Barron, C.N., 1968, Notes on the stratigraphy of the Lower Roraima Formation in the Potaro-Ewang area of British Guiana, and on the discovery of acid intrusives within it: Geological Survey of British Guiana, Records Vol 4. 58-60.

Berrangé, J.P., 1977, The Geology of Southern Guyana, South America: Institute of Geological Sciences, National Research Council, London, Overseas Memoir 4.

Cannon, R.T., 1965, Anatexis in the Bartica Assemblage, British Guiana: Comptes Rendus de la Societe geologique de Finlande No XXXVII (1965), 177-192.

Chang, J.M, Andronicos, C.L., 2009, Constraints on the depth of generation and emplacement of a magmatic epidote-bearing quartz diorite pluton in the Coast Plutonic Complex, British Columbia: Terra Nova, Vol 21, No. 6, 480–488.

Fraga, L.M., Cordani, U., Reis, N., Nadeau, S. and Maurer, V.C., 2017a, U-Pb Shrimp And La-Icpms New Data For Different A-Type Granites Of The Orocaima Igneous Belt, Central Guyana Shield, Northern Amazonian Craton: Anais do XV Simpósio de Geologia da Amazônia, Belém, 2017.

Fraga, L.M., Dreher, A., Kroonenberg, S., de Roever, E.W.F., Faraco, T. Wong, T. Reis, N. and Lago, A., 2017b, Geological and Geodiversity Mapping Project on the Brazil – Suriname border: Explanatory note for the geological and mineral resources and geodiversity maps: Brazilian Geological Survey / Companhia de Pesquisa de Recursos Minerais.

Kroonenberg, S.B., de Roever, E.W.F., Fraga, L.M., Reis, N.J., Faraco, T., Lafon, J.N. Cordani, U. & Wong, T.E, 2016 Paleoproterozoic evolution of the Guiana Shield in Suriname: A Revised Model: Geologie en Mijnbouw, 95 (4) 491–522.

Gibbs, A.K., and Barron, C.N., 1993, The Geology of the Guiana Shield: Oxford Monographs on Geology and Geophysics No.22.

Heesterman, L.J.L, Arjune, B.K., Cole, E, and Kemp, A.W., 2004, Kartuni Project: Geology Geochemistry and Structure. Guyana Geology and Mines Commission, Geoservices Division, Report No. GS 1/2004.

Heesterman, L.J.L, Kemp, A.W., Arjune, B.K & Cole, E.W., 2005, Pashanamu Project. Geology, Structure and Geochemistry: Guyana Geology and Mines Commission, Geoservices Division, Report No. GS 1/2005.

Heesterman, L.J.L, Kemp, A.W., Arjune, B.K & Cole, E.W., 2015, Kurupukari Project, A Summary of Geochemistry and Geology: Guyana Geology and Mines Commission, Geoservices Division, Report No. GS 2/2015.

Hildebrand, R.S., Buchwaldt, R. & Bowring, S.A., 2014, On the allochthonous nature of auriferous greenstones, Guayana shield, Venezuela: Gondwana Research 26 1129–1140.

Nadeau, S., Chen, W., Reece, J., Lachman, D., Ault, R., Faracao, T., Fraga, L., Reis, N. and Betiollo, L., 2013, Guyana: The Lost Hadean Crust Of South America?: Brazilian Journal of Geology, 43(4): 601-606.

Nadeau, S., 2014, Guyana Geological Time Scale: Poster for the Guyana Geology and Mines Commission Mining Week 2014.

Structure, evolution and magmatic origin of the Demerara marginal plateau (French Guyana – Surinam) as revealed by multidisciplinary oceanographic exploration

Arnauld Heuret*
Université de Guyane
Campus de Troubiran
97300 Cayenne – France
arnauld.heuret@univ-guyane.fr

Lies Loncke
CEFREM – Université de Perpignan
52 avenue Paul Alduy
66860 Perpignan - France
lies.loncke@univ-perp.fr

Walter Roest
IFREMER
1625 route de Sainte-Anne
29280 Plouzané - France
walter.roest@ifremer.fr

Christophe Basile
ISTerre
1381 rue de la Piscine
38610 Gières

christophe.basile@univ-grenoble-alpes.fr

David Graindorge
Université de Bretagne Occidentale
3 rue des Archives
29238 Brest

david.graindorge@univ-brest.fr

Ewald Poetisi
Anton de Kom University of Suriname Leysweg 86, Tammenga Paramaribo Suriname
ewald.poetisi@uvs.edu

SUMMARY

The Demerara plateau is a 400 km wide submarine relief, located offshore Surinam and French Guyana, at the junction between the central and equatorial Atlantic. Since 2003, a scientific program sustained by 4 different oceanographic cruises has been dedicated to this seaward continental-like salient.

Dredging results together with seismic imaging confirm the magmatic nature of the basement of the Demarara plateau. Geochemical analysis unambigously point out an Ocean Island Basalt (OIB) signature and dated at 173.4±1.6 Ma. We propose to link this thick volcanic margin to the hotspot responsible to the Central Atlantic Magmatic Province (CAMP).

Key words: Dredging, seismic imaging, hotspot, CAMP.

INTRODUCTION

An updated inventory of transform passive continental margins in the world was published by Mercier de Lépinay et al. in 2016. This inventory shows that these margins represent 30% of passive continental margins and a cumulative length of 16% of non-convergent margins. The inventory also highlights the fact that many submarine plateaus prolong transform continental margins, systematically at the junction of oceanic domains of different ages. Globally, we identified twenty of these marginal submarine plateaus (Falklands, Voring, Demerara, Tasman, etc). They systematically experience two phases of deformation: a first extensional phase and a second transform phase that allows the individualization of those submarine reliefs appearing on bathymetry as seaward continental-like salients. Understanding of the origin, nature and evolution of those marginal plateaus has many scientific and economic implications.

METHOD AND RESULTS

The Demerara marginal plateau located off French Guyana and Surinam belongs to this category of marginal submarine plateaus. The French part of this plateau has been the locus of a first academic investigation in 2003 during the GUYAPLAC cruise dedicated to support the French delineation of the limits of the continental shelf beyond 200 nautical miles. This cruise was the starting point of a scientific program dedicated to geological investigations of the Demerara plateau, sustained by different cruises and collaborations: (1) IGUANES (2013) completed the mapping of this plateau including off Surinam, allowed to better understand the segmentation of the Northern edge of the plateau, and to demonstrate the combined importance of contourite and mass-wasting processes in the recent sedimentary evolution of this domain; (2) Collaboration with TOTAL (PhD thesis of Mercier de Lépinay) to better qualify the two main phases of structural evolution of the plateau, respectively during Jurassic times for its Western border and Cretaceous times for its Northern and Eastern borders; (3) DRADEM (2016) mapped the continental slope domain of the transform margin north of the Demerara plateau and was dedicated to the dredging of rocks outcropping on the continental slope, suspected to be Cretaceous in age and older; (4) MARGATS (2016) dedicated to the better understanding of the internal structure of the plateau and its different margins using multi-channel reflection and refraction seismic methods.

The combination of all those experiments allows us to provide key improvments in the knowledge of the structure, the origine and the evolution of the Demerara marginal plateau. In particular, data from the dredging cruise DRADEM and from the seismic cruise MARGATS confirm the magmatic nature of the basement of the Demarara plateau. Geochemical analysis of the few recovered samples unambigously point out an Ocean Island Basalt (OIB) signature, and U/Pb dating of magmatic zircons indicates cristallisation at 173.4±1.6 Ma.

Based on these new petrological and geophysical data, we propose a kinematic model where a single hot spot can both be the source of the CAMP and take into account the magmatic occurrences in the area of Demerara plateau and conjugated Guinea plateau since 200 Ma. This kinematic reconstruction has huge implications on the nature of the basement, and the evolution of both heat flow and vertical displacement (uplift and subsidence) during the Cretaceous history of the Demerara area.

CONCLUSIONS

The results of GUYAPLAC, IGUANES, DRADEM and MARGATS oceanographic exploration cruises allow us to paint an integrated portrait of the Demerara marginal plateau that may be very useful in understanding the processes involved (1) in the individualization of such plateaus (volcanism, heritages, kinematics, …) (2) in their evolution (subsidence, mass-wasting processes, domains of deep-sea current acceleration).

The next steps of our research program include a better understanding of kinematic conditions in this domain (based on new observations including magnetic data) and a better knowledge of the geology of the slope domain by in situ observations with either a ROV or a manned submersible.

ACKNOWLEDGMENTS

We thank all the participants of the GUYAPLAC, IGUANE, DRADEM and MARGATS oceanographic cruises.

REFERENCES

Basile, C., Maillard, A., Patriat, M., Gaullier, V., Loncke, L., Roest, W., Mercier de Lépinay, M., and Pattier, F., 2013, Structure and evolution of the Demerara Plateau, offshore French Guiana: Rifting, te 180 ctonic inversion and post-rift tilting at transform-divergent margins intersection: Tectonophysics, v. 591, p. 16-29, doi: 10.1016/j.tecto.2012.01.010.

Greenroyd, C.J., Peirce, C., Rodger, M.,Watts, A.B., Hobbs, R.W., 2008a. Demerara Plateau — the structure and evolution of a transform passive margin. Geophys. J. Int. 172, 549–564.

Loncke, L., Maillard, A., Basile, C., Roest,W.R., Bayon, G., Pattier, F.,Mercier de Lépinay, M.,Grall, C., Droz, L., Marsset, T., Giresse, P., Caprais, J.C., Cathalot, C., Graindorge, D., Heuret, A., Lebrun, J.F., Bermell, S., Marcaillou, B., Bassetti, M.-A., Tallobre, C., Buscail, R., Durrieu de Madron, X., Bourrin, F., 2015. Structure of the Demerara passive transform margin and associated sedimentary processes. Preliminary results from the IGUANES cruise. Geol. Soc. London.

Mercier de Lépinay, M., Loncke, L., Basile, C., Roest, W.R., Patriat, M., Maillard, A., and De Clarens, P., 2016, Transform continental margins – Part 2: A worldwide review: Tectonophysics, v. 693, p. 96-115, doi: 10.1016/j.tecto.2016.05.038.

Mercier de Lépinay, M., 2016, Inventaire mondial des marges transformantes et évolution tectono-sédimentaire des plateaux de Demerara et de Guinée. Ph.D thesis, University of Perpignan, 335 p.

Pattier F., L. Loncke, P. Imbert, V. Gaullier, C. Basile, A. Maillard, W.R. Roest, M. Patriat, B.C. Vendeville, T. Marsset, G. Bayon, C. Cathalot, J.C. Caprais, S. Bermell, C. Sotin, B. Hebert, M. Mercier de Lépinay, J.F. Lebrun, B. Marcaillou, A. Heuret, L. Droz, D. Graindorge, E. Poetisi, H. Berrenstein, Genavir team. Origin of deep fossil giant depressions on the Demerara plateau?, Marine Geology, http://dx.doi.org/10.1016/j.margeo.2015.04.001.

Reuber, K.R., Pindell, J., and Horn, B.W., 2016, Demerara Rise, offshore Surinam: magma-rich segment of the Central Atlantic Ocean, and conjugate to the Bahamas hot spot: Interpretation, v. 4, T141-T155, doi: 10.1190/INT-2014-0246.1.

The West African Exploration Initiative as a model for cooperative research and training in NE South America

Mark Jessell[*] **and the WAXI Team**[#]
Centre for Exploration Targeting
School of Earth Sciences
The University of Western Australia
35 Stirling Hwy, Crawley, WA, 6009, Australia
Institut de Recherche pour le Développement
Toulouse, France

mark.jessell@uwa.edu.au

SUMMARY

The twelve-year AMIRA International Project P934 'West African Exploration Initiative' (WAXI), having now completed its third phase, has the dual aims of scientific research focused on increasing our understanding the tectonic and regolith settings of ore deposits, and the development of the research and training capacity of West African geological surveys and universities. We describe the drivers for the WAXI initiative, as well as key research and capacity building outcomes. The WAXI project is a public-private partnership that has brought together seventy of the principal stakeholders in the domain of minerals exploration in West Africa. We discuss how this approach is being applied to the NE of South America.

Key words: West Africa, tectonics, metallogenesis, capacity building.

INTRODUCTION

The WAXI program has brought together the important stakeholders interested in the developing large-scale mining industry of West Africa:
• The government surveys and departments of mines of eleven West African states (Burkina Faso, Ghana, Guinea, Ivory Coast, Liberia, Mali, Mauritania, Niger, Sierra Leone, Senegal and Togo)
• Seven West and South African universities (from Burkina Faso, Côte d'Ivoire, Ghana, Mali, Senegal and South Africa)
• Thirty-four international mining companies
• Researchers from twelve European and Australian research institutions
• AMIRA International, an independent association of minerals companies that develops, brokers and facilitates collaborative research projects
• NGOs based in Burkina Faso, Ghana and Luxembourg
• A professional training centre based in Burkina Faso.
• National research and aid agencies in South Africa, France and Australia

This initiative demonstrates the significant research and development achievements that can be made when the different stakeholders in the minerals sector (industry, academia, government and non-government organisations) work together to achieve their diverse goals.

The WAXI project in numbers:
•12 countries
•73 partners over 11 years
•95 Postdoc, PhD, Masters and Honours Projects, 60% of them African
•85 International Publications
•650 GB exploration geoscience database
•5600 person-days of technical training in West Africa as part of 36 short courses
•650,000 km2 of geophysically constrained geological mapping

METHOD AND RESULTS

The West African Craton (WAC) consists of two Archean nuclei in the north-western and south-western parts of the craton juxtaposed against an array of Paleoproterozoic domains made up of greenstone belts, sedimentary basins, domains of extensive granitoid-TTG plutons and large shear zones, which are overlain by Meso- and Neoproterozoic and younger sedimentary basins (Bessoles, 1977; Feybesse et al., 1989; Feybesse and Milési, 1994; Kouamelan et al., 1997; Caby et al., 2000; Hirdes et al., 1992). The region has a thousand-year history of gold mining, and numerous gold deposits are shown in the 1934 Gold Coast Geological Survey map of what is now southern Ghana (Junner, 1934). The WAC is typically referred to as a gold province, although it also hosts contains world class iron ore and bauxite deposits (Milési et al., 1992; Markwitz et al., 2016). As early as 1916, systematic regional geological mapping

was being carried out by Henry Hubert, a French Government official working in what was then French West Africa. A period of data acquisition by colonial and post-colonial geological surveys ensued, followed by collaborations funded by transnational agencies (principally the UN, the World Bank, and the European Union) which enabled regional maps and geophysical surveys to be compiled for much of the craton. Building on this information, the WAC has seen a major increase in exploration and mining activity over the last 10 years, which in turn has incited renewed research interest in the tectonics and metallogenesis of the highly prospective Paleoproterozoic Birimian Terrane.

The AMIRA International P934 West African Exploration Initiative (WAXI) is a collaboration between the principal actors in the large-scale minerals sector of West Africa (Figure 1). The first (pilot) phase of the project ran from September 2006 to March 2008 (with 13 industry sponsors), the second phase ran from March 2010 until July 2013 (with 20 industry and government sponsors) and the third phase started in September 2014 and will run until August 2018 (with 13 industry sponsors to date). The overall aim of WAXI is to enhance the exploration potential of the West African Craton (WAC) through an integrated program of research and data gathering into its 'anatomy', and to augment the capacity of local institutions to undertake this form of work.

In the following sections we summarise the principal research and capacity building outcomes of the project, which for ten years has supported the minerals industry via the acquisition and synthesis of exploration data, and supported West African institutions in the training of geoscientists and the management of exploration-focused geoscience data. This project has resulted in positive outcomes for all partners, and the lessons learned in this project help provide an improved model for collaborative research in developing countries.

RESEARCH ACTIVITIES

The WAXI research program was designed after a process of consultation with industry in a pilot phase, during which a detailed data and information audit and gaps analysis was carried out. Its main focus is on the collection and synthesis of geological, regolith, metallogenic, geochemical and geochronological datasets from across the WAC. The resulting research program comprises a set of integrated research modules which are grouped into three themes: architecture and timing; mineralising systems; and surface processes.

The results of the research program have been progressively published over the last ten years (see http://www.tectonique.net/waxi3 for a complete list of papers and access to the thesis collection), but in particular as four special issues that were compiled following the end of confidentiality for stage two of the project (Jessell and Liegeois, 2015; Jessell et al., 2016a; Hein, 2016; and Goldfarb & André-Mayer, 2017).

Integrated Geophysical Analysis

The WAXI research program has taken a multi-scale approach to understanding the craton. At the largest scale, we have examined existing and newly compiled geophysical representations of the WAC in terms of its large-scale tectonic architecture, which provides a framework for specific regional studies (Figure 2, Jessell et al., 2016b). The different geophysical methods suggest a partitioning of the WAC into two tectonic domains at the largest scale, based on seismic tomographic data, lithosphere–asthenosphere boundary models and long wavelength gravity signals. A single 450 km magnetotelluric and gravity profile was acquired across south-west Burkina Faso and north-west Ghana, which showed that many of the structures mapped at the surface extend deep into the crust and even into the upper mantle. (Le Pape et al., 2014).

At the belt scale a number of studies have integrated geological mapping with the interpretation of regional geophysical datasets (magnetics, gravity, radiometrics and in some cases electromagnetic data). These studies share a common geodatabase so that we can produce seamless maps across country boundaries and between belts (Fig 3, Tshibududze et al., 2009 and 2015; Metelka et al., 2011; Baratoux et al., 2011; Perrouty et al., 2012; McFarlane, 2016; and Block et al., 2016). Combined with petrophysical acquisition campaigns, these maps provide important constraint for belt-scale 3D models (Metelka et al., 2015, Perrouty et al., 2014 and Diene et al., 2015). In South West Ghana this analysis led to the proposition of a model for the main regional-scale controls on gold mineralization to the southeast of the main Ashanti Belt by highlighting the lithological distribution and geometry of geological structures in 3D. The South West Ghana 3D model has also been used as a test case for more theoretical studies in geophysical inversion and the analysis of 3D lithological uncertainty (Lindsay et al., 2013a, b; Martin et al., 2013).

As in other cratons, the availability of airborne magnetic data allowed us to build up a comprehensive map of mafic dykes, and we are currently in the processes of systematically dating each swarm thanks to a collaboration with the Supercontinent consortium (Figure 4; Jessell et al., 2015; Baratoux et al., 2016), http://www.supercontinent.org/). This work has shown that more than two dozen dyke swarms intrude the WAC, with 8 newly dated swarms having ages ranging from 2700 Ma to 200 Ma. These Large Igneous Provinces form important constraints for our understanding of the relative position of West Africa during successive supercontinent cycles. There are also variations in spatial density of dyke swarms that may reflect underlying variations in the lower crust or mantle.

We have also undertaken a research program that characterised West Africa's regolith and landform evolution using airborne geophysical data and ground surveys, which has produced the first paleo-topographic map in the region (Grimaud et al., 2014 and 2015), has identified a previously unrecorded 230 km long paleochannel in the Volta Basin (Jessell et al., 2015b) and produced the first spectral library of rocks and regolith for West Africa (Figure 5, Metelka et al., 2015), which demonstrated that although weathering alters the spectral signature of the fresh rock, indicative absorption features located in the short wave infrared region remain detectable.
Integrated Geospatial Analysis

An extensive geochronological sampling program, together with isotopic studies, has allowed us to define large scale spatial variations in magmatic evolution of the southern WAC, which shows a systematic diachronous cessation of magmatic activity from east to west, which implies an intriguing rate of migration of tectonic activity of 3.5 cm per annum (Fig. 6, Parra-Avila et al., 2016). Spatial mapping of LuHf model ages and detrital zircons is helping us to define lithospheric-scale domains in the southern WAC (Parra-Avila, 2015).
Stratigraphic Synthesis

Starting with the stratigraphic synthesis of Baratoux et al., 2011, the project has systematically reanalysed existing and new data to produce 30 harmonised stratigraphic columns across the southern WAC. Although this has shown many similarities in stratigraphic succession across the craton, there are also second-order variations that are helping us to define sub-domains within the Birimian belts. When combined with the lithospheric-scale geophysical data, and the geochronological record we can see coincident signals suggesting a major lithospheric break running through Côte d'Ivoire.
Deposit Analysis
At the deposit scale the research program has characterised 25 deposits across the craton, principally gold deposits, which reflects the economic focus of much of the industry in the region over the last ten years. This includes grain scale studies to characterise structural, mineralisation, metamorphic and fluid evolution histories within and outside of ore deposits (Figure 7, Block et al., 2015; Fougerouse et al., 2016; Masurel et al., 2017; Le Brun et al., 2017; Le Mignot et al., 2017; and Salvi et al., 2016), and these studies show the remarkable diversity of host-rocks, structural controls and mineral associations found in what are still generally classed as orogenic gold systems. The dispersion of elemental and isotopic anomalies around these deposits has shown that 206/207Pb ratios in barren soils and ferruginous crusts is much higher compared with gossan and related altered rocks (Kríbek et al., 2016).
Exploration Database

This research represents one form of support of economic development in the region, as it provides key datasets (in GIS-ready formats) that help to reduce geological risk in the minerals exploration decision-making process. The development of an integrated exploration GIS has proved to be a very efficient approach for transferring information to partners, all of whom have access to an exploration GIS which has now expanded into a more than 650 Gigabyte, 180-layer online and static GIS database of metadata and data related to West African exploration. More that 80 of these layers consist of new data or compilations developed by project partners. In particular we have developed new georeferenced syntheses of harmonized geological maps covering 650,000 km2; a geochronology database with over 1000 zircon ages; a database of more than 8000 whole rock geochemical and isotope analyses for rocks and regolith; a new map of mafic dyke swarms; regolith maps; outcrop databases; petrophysical databases including a spectral library of fresh and weathered rocks; a new mineral deposit database for the region; a database of metamorphic observations; as well as compilations of several global geophysical datasets, such as receiver function data.

In order to provide immediate access to new datasets, we developed a WMS Web Client to provide on line access to the latest data sets (Figure 8). This same Web Client has also been supplied to the International Mining for Development consortium in support of their OpenData Initiative (http://opendata.im4dc.org/).

CAPACITY BUILDING ACTIVITIES

Based on UNESCO/Geological Society of Africa data, there are currently 38 public higher education institutions that provide geoscience training in West Africa (including Schools of Mines), of which 29 are in Nigeria. In the last ten years, the African Union via the African Mining Vision (AMV) and its associated action plan (African Union Commission, 2011), the World Bank and the African Development Bank have recognised the need for renewed investment in higher education to support the growing African population, which is predicted to have the world's largest labour force by the year 2040 (Africa Development Bank, 2014). These groups recognise the need for a broader spectrum of higher education models to meet the demand for a skilled workforce that does not necessarily have to involve degree-based courses. The African Development Bank, UNESCO's Earth Science Initiative in Africa, the AMV and African Network of Earth Sciences Institutions (ANESI) share many proposals in terms of enhanced regional collaboration, better integration of the private sector and the minerals industry, in particular via Public-Private Partnerships, and the use of ICT-based training programs as supports for Africa's education needs. Many of these same themes are also found in the UN's Sustainable Development Goals, and map directly to WAXI activities (Table 1).
The capacity building program is jointly led by the Luxembourg-based NGO Le Soleil dans la Main and the professional training centre Teng Tuuma Geoservices (I-TTG) based in Ouagadougou, Burkina Faso. Direct capacity building activities are supported in the form of student scholarships, financial support for student research, and in continuing education for industry, university and geological survey staff.

Graduate Scholarships and Research Support.

The different stages of the project, together with associated one-on-one industry projects and university-funded scholarships, have allowed us to support a total of 40 PhD projects, 44 masters and honours projects, and six postdoctoral fellowships, with more than 60% of these being African. Nevertheless the demand for scholarships, and in particular projects which provide support for research costs, far outstrip the capacity of the WAXI project's resources, and partnering with other training schemes provides a partial solution to meeting this demand, as many outside scholarships do not provide research funds.

Most if not all of the 70 Honours, Masters and PhD projects integrated combinations of geological, geophysical and geochemical datasets to arrive at their conclusions, so that the next generation of West African geoscientists are being taught the value of integrating multiple datasets.
Professional Training

Up until the end of 2017, the project has supported 23 three to five-day field and classroom training courses to over 350 industry, university and geological survey personnel. The courses have been held in Ghana, Burkina Faso, Côte d'Ivoire and Senegal. The vast majority of the attendees of these courses were African geoscientists. Many of these courses focus on integration of datasets for robust interpretation including integrating geology and geophysics in 2 & 3 dimensions; geochemical interpretation of the regolith; structural controls of ore deposits; and a minerals systems approach to prospectivity analysis. In addition to these technical courses, we organised a five-day course on research management aimed at West African university and geological survey personnel. (Figure 9, Table 2). Finally two international conferences (in Ougadougou, Burkina Faso in 2007, and Dakar, Senegal, in 2015) were held to stimulate new research ideas in the region and present project outcomes.

CONCLUSION

The success of the WAXI program comes from the commitment of the individuals and organisations that have been involved over the last ten years, but equally from the recognition that these different organisations have different drivers: industry benefits in the short term by the acquisition of new datasets and their interpretation, and in the long term through the availability of better trained existing and incoming staff; geological surveys benefit from better collaboration across the region, better trained staff, and the opportunity to explore common goals with industry; and the higher education sector benefits from access to student scholarships and research funds, which result in a supply of young well-networked researchers to take on the challenge of training the next generation of geoscientists, with a particular focus on data integration skills. The WAXI program has also partnered with a number of other research and capacity building initiatives working in West Africa which have complementary goals (including IGCP638, the GEOLOOC online training platform, the AEGOS data infrastructure program, the Côte d'Ivoire-focused T2GEM project, a proposed Burkina-Faso Geoscope project focusing on the Boromo Belt, together with several one-on-one projects between partner research organisations and industry.

The WAXI project forms part of a broad range of development geoscience initiatives in Africa that have overlapping aims that partially fulfil the aims of the African Mining Vision and the Sustainable Development Goals. This initiative demonstrates the significant achievements that become possible when the different stakeholders in the minerals sector (industry, academia, government and non-government organisations) partner together to combine datasets and knowledge across national borders in order to achieve their diverse goals.

ACKNOWLEDGEMENTS

We wish to gratefully acknowledge AMIRA International and the 34 industry sponsors, as well as AusAid and the ARC Linkage Project LP110100667, for their support of the different stages of the WAXI P934 series of projects. We are also appreciative of the contribution of the 12 geological surveys/departments of mines in West Africa who joined as sponsors in kind, as without their ongoing logistical support and provision of a range of country-level datasets, this project would not have been possible. Finally, we wish to recognize our research colleagues from 20 Institutions from around the world.

[#]The following people have contributed to the success of the WAXI project: Abdoulaye Ouedraogo, Abraham Traore, Adama Sangare, Adama Yameogo, Adele Symon, Adja Ndoye, Alain Kouamelan, Alan Jones, Alex Woolfe, Amara Fofana, Anathase Nare, Andile Mkentane, Anicet Beauvais, Anne-Sylvie André, Arnaud Fontaine, Asinne Tshibubudze, Augustin Yao Koffi, Aurélien Eglinger, Bohdan Kríbek, Bosh, B.R. Kouassi, T. Campbell McCuaig, Caswell Lehong, Catherine Zimmermann, Charlotte Magnette, Clare Desplats, Colin Hogg, Corinne Debat, Dan Apau, Daniel Asiedu, Daniel Stacík, David Baratoux, Denis Fougerouse, Didier Béziat, Dominique Chardon, Doria Aitadjedou, Edmond Dioh, Edmond Dioh, Elodie Le Mignot, Emmanuel Arhin, Emmanuel Baah-Danso, Eric Gloaguen, Erwann Lebrun, Eva Geršlová, Fabrice Traore, Ferdinand Majiba Misakabu, Florian Le Pape, Fortune Tulombe, Francois Ndiaye, František Laufek, František Veselovský, Frederic Sea, Germain Velasquez, Gloria Senyah, Goran Boren, Graham Begg, Guillaume De Boyer, Helen Mcfarlane, Ibrahima Labou, Ilja Knésl, Irvin Matsheka, Irvin Matsheka, Jacques Kone, James Davis, Jan Duda, Jan Jehlicka, Jan Malec, Jaroslav Hak, Jean Fossou, Jean Haba, Jean-Louis Grimaud, Jelena Markov, Jérôme Ganne, Jirí Zacharias, Joe Cucuzza, John Miller, Julie Carcone, Kim Hein, Kinane, Kwame Boamah, Laurent Aillères, Laurie Reisberg, Lenka Baratoux, Luc Siebenaller, Luis Gallardo, Luis Parra Avila, Luke Peters, Mahamadene Diene, Mahamadou Diallo, Makhoudia Fall, Mamadou Yossi, Marie Lefebvre, Mariette Minigou, Marieke van Lichtervelde, Mark Jessell, Martin Lompo, Martin Mihaljevic, Mathieu Benoit, Matt Hill, Mikael Grenholm, Mokobo Mohale, Monié, Morou Francois Ouedrago, Nicolas Kagambèga, Nicolas Meriaud, Nicolas Thebaud, Noziwe Simoko, Nuru Saïd, Olivier Bruguier, Oumar Sangare, Ousman Wane, Ousmane Bamba, Pascal Ouiya, Patrick Hayman, Patrick Ledru, Peter Ndibewu, Philippe Calcagno, Prince Amponsah, Pulane Sehloho, Quentin Masurel, Radislav Skoda, Ramabulana Tshifularo, Raymond Sagna, Renaud Caby, Saga Sawadogo, Seta Naba, Stanislav Ulrich, Stanislav Vrána, Stefano Salvi, Stéphane Perrouty, Sylvain Block, Thomas Fullgraf, Todani Funyufunyu, Vaclav Metelka, Vanessa Markwitz, Vera Jelíková, Vera Zoulková, Villa Ramos, Vincent Bouchot, Vladimir Majer, Xiaojun Feng, Yann Itard, Yolande Traore and Yu Chen.

Gold mineralisation in the Paleoproterozoic greenstone belt of Suriname: geochemical constraints on precursor rocks of the strongly silicified Overman deposit

Nicole Kioe-A-Sen

Anton de Kom University
Leysweg 86, Paramaribo, Suriname

nicole.kioe-a-sen@uvs.edu

Manfred van Bergen*

Utrecht University
Budapestlaan 4, Utrecht, Netherlands

m.j.vanbergen@uu.nl

SUMMARY

Gold deposits in the Proterozoic Marowijne Greenstone Belt of Suriname are generally classified as orogenic but their individual geological settings show significant variability. The Overman prospect, located to the north of the Rosebel gold mines, strongly differs from other deposits in this region, as gold accumulation is not associated with quartz veins but with a massif body of pervasively silicified host rocks. Disseminated gold tends to be concentrated in the most silicified rocks, where it occurs in close relationships with sulfides. Geochemical signatures identify a predominantly sedimentary nature of the rock unit prior to silicification, a vital element in identifying the original geological setting, the gold source and conditions of mineralisation.

Key words: orogenic gold, Guiana Shield, Marowijne Greenstone Belt, silicification

INTRODUCTION

Most of the gold deposits in Suriname occur in a NW-SE trending Paleoproterozoic granitoid-greenstone belt, formed during the Trans- Amazonian Orogeny (2,260-2,080 Ma) (Figure 1a). The deposits of primary gold are generally classified as orogenic, formed in different geological settings and have genetic links with gold mineralisations of similar Proterozoic age in West Africa (e.g., Kioe-A- Sen *et al.*, 2016). Modern studies into the geological settings and gold metallogeny of Suriname are restricted to the Rosebel mining area (Voicu *et al.*, 2001; Daoust *et al.*, 2011). Field evidence is consistent with ore formation late in the orogenic history, but in- depth studies into possible accumulation of gold earlier in the long sequence of Precambrian geological events have not been conducted so far. The Overman prospect, located 16 km north of the currently operating Rosebel gold mines (Figure 1b) is marked by the occurrence of gold within a rigid silica body, in a setting that differs from the mined deposits in the south where gold is associated with quartz veins. Mineral assemblages at Overman point to greenschist-facies conditions of metamorphism. The complex tectonic structure is not fully understood. Locally, intense brecciation and pervasive intense silicification obscure most of the primary lithological properties and preclude identification of the original precursor rock(s) from macroscopic inspection. Preliminary mapping suggests that the host rock mainly consists of a mudstone-siltstone sequence with a complex tectonic history, involving at least two phases of deformation. A significant graphitic-mudstone unit is present in sharp contact with the silica-body (Figure 2), and a late felsic intrusive cuts through the sedimentary sequence. A lithogeochemical investigation, in combination with petrographic and mineralogical observations, has been undertaken to explore the nature of the original parent rock. This contribution discusses the results, considered as a first step towards unravelling the mineralization environment, depositional conditions and origin of the gold.

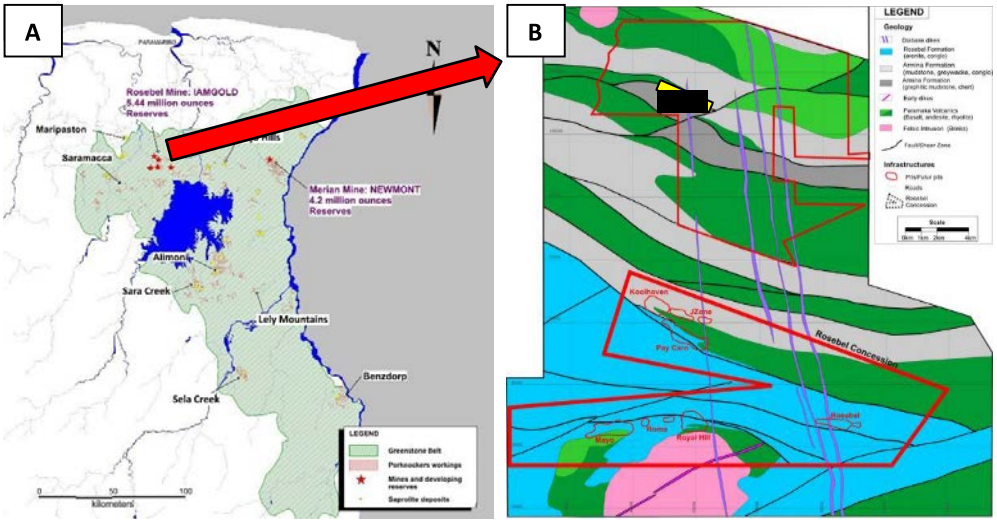

Figure 1: (A) Map of the Marowijne Greenstone Belt with the main gold occurrences; (B) Geological map of the Rosebel area with the gold mines and the Overman prospect illustrated with the yellow box (Daoust, 2016).

Figure 2: Sharp contact between the silica body and graphitic mudstone.

METHODS AND RESULTS

Twenty-four drill core samples from the main lithological units in the Overman area were analysed for major (XRF, ICP-AES) and trace element (ICP-MS) contents by ALS-Peru. The geochemical results were compared with data from a variety of non-silicified metasedimentary and metavolcanic rocks exposed elsewhere in the Rosebel area (Daoust, 2016). The bulk-rock geochemistry was complemented with macroscopic observations of core samples and optical microscopy on thin sections. Mineral assemblages and rock textures were investigated using electron backscatter imaging, and mineral compositions were determined by electron microprobe via (semi)quantitative spot analysis using Energy-Dispersive X-Ray Spectroscopy (EDS) at Utrecht University.

Geochemical diversity and lithological links

Based on the analytical results, five different groups could be distinguished (Figure 3): a high-silica group (SiO_2 mostly > 90 wt.%) representing almost completely silicified rocks, a low-silica group (56-62 wt.% SiO_2), two intermediate groups of graphitic mudstone and siltstone with different Al_2O_3 contents and trace-element signatures, and a separate group of samples from the felsic intrusive. Because the latter crosscuts the structure and was apparently emplaced much later than the main geological events it is further ignored here.

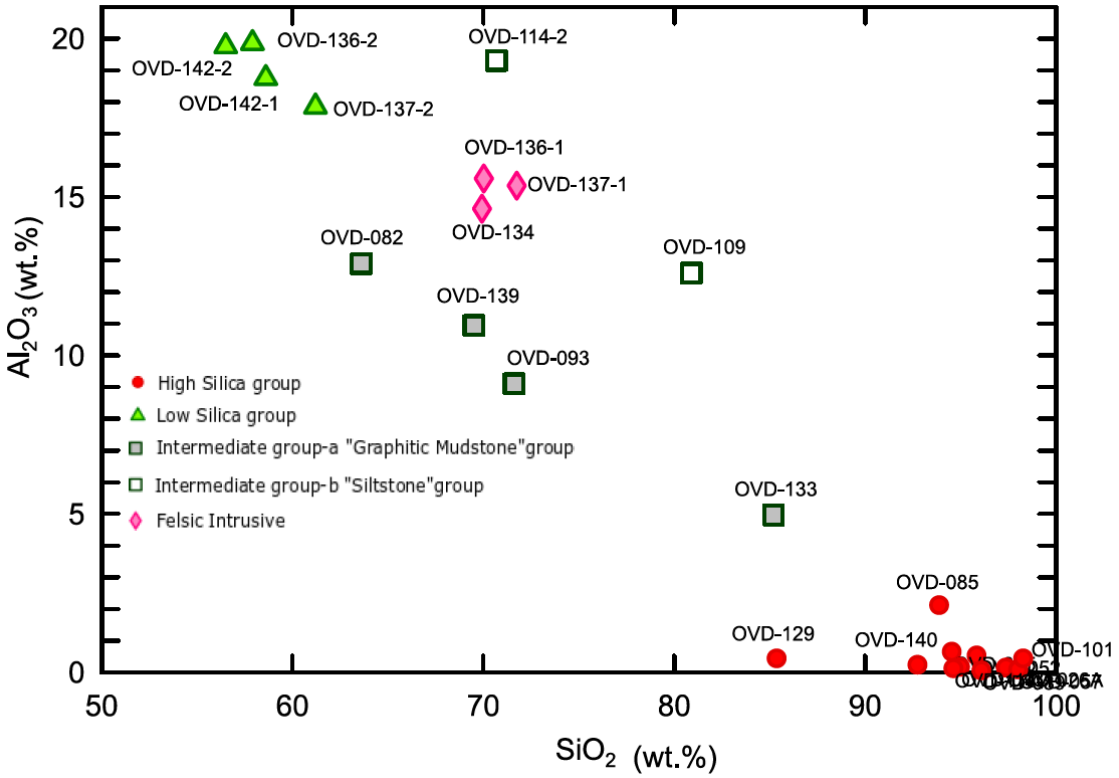

Figure 3: SiO2 - Al2O3 (wt.%) diagram showing a distinct grouping in rock samples from the Overman deposit

Silicification resulted in an overall increase in SiO_2 and a decrease in the concentrations of all other rock constituents, as illustrated in Figure 4 a-b. Because the distinct rock groups do not define a single trend, silicification must have affected heterogeneous precursor rocks rather than a single lithology. This suggests that the high-silica, chert-like rocks that dominate the Overman deposit are silicification products from different parent rocks. Textural evidence is consistent with this inferred lithological diversity.

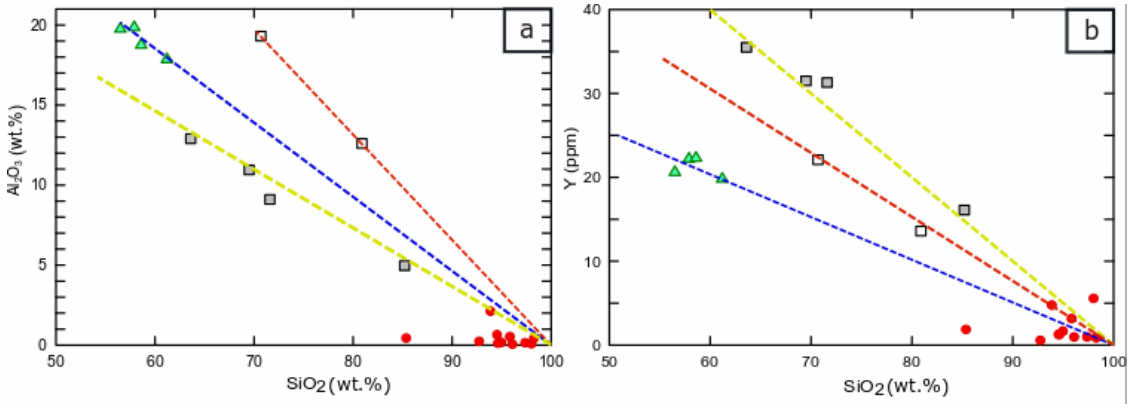

Figure 4 a-b: Diagrams of Al2O3 and Y against SiO2 illustrating near-linear decreases of element concentrations with increasing SiO2. The three separate trends point to original lithological heterogeneity of the Overman rocks, independent from any silicification effect.

In order to identify the nature of the precursor rock(s) through geochemical analogies with metavolcanic and metasedimentary rocks in neighbouring areas, measured concentrations of trace elements were normalised to average concentrations in major rock units, calculated from data on the Rosebel area reported by Daoust (2016). Resulting multi-element diagrams (Figure 5) show an excellent correspondence between the low-silica group and greywackes from the JZone (see Figure 1), as demonstrated by the horizontal trend (Figure 5a). There is also a reasonable fit with Pay Caro arenites and Koolhoven mudstones, whereas there is poor agreement with any of the volcanics found in the area (e.g. Fig. 5f). Although the trends for the intermediate groups of graphitic mudstone and siltstone are less smooth, the correspondence with sedimentary precursors is better than for volcanics, particularly when only considering the least mobile elements (HFSE and REE).

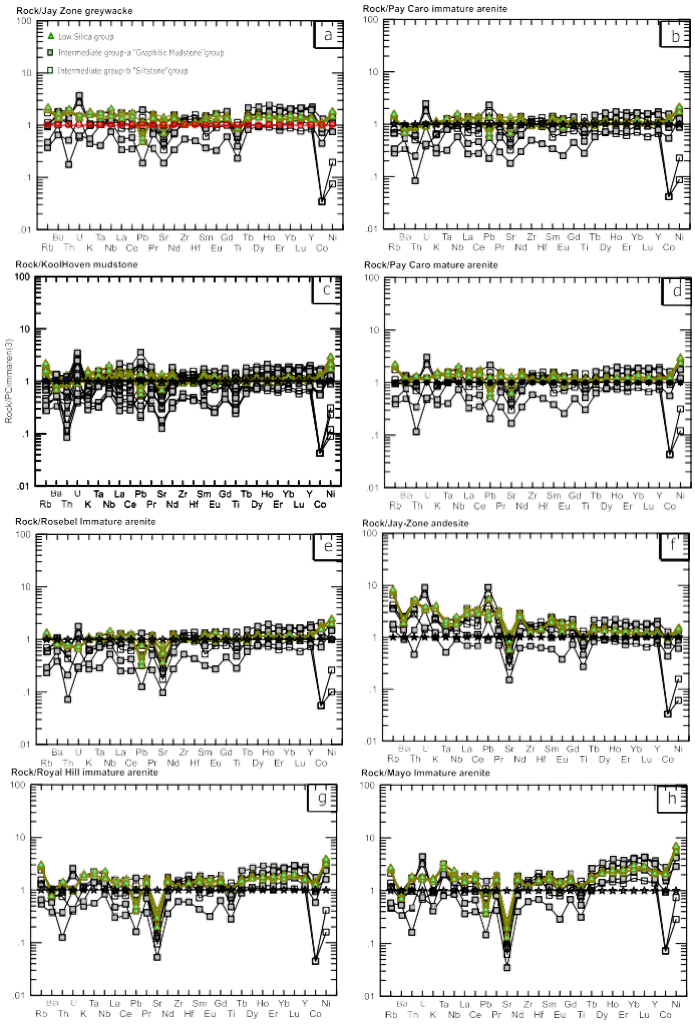

Figure 5: Multi-element diagrams for the low- and intermediate-silica rock groups of Overman, showing measured concentrations normalized to average concentrations in (a) JZone greywacke, (b) Pay Caro immature arenite, (c) Koolhoven mudstone, (d) Pay Caro mature arenite, (e) Rosebel immature arenite, (f) JZone andesite, (g) Royal Hill immature arenite, and
Mayo immature arenite according to data from Daoust (2016). Note the correspondence of the low-silica group with the Pay Caro greywacke (panel a) and other sediments from the northern Rosebel mines (Pay Caro, Koolhoven, JZone), and the poor agreement with the JZone andesites (panel f).

Link with gold

Microscopic observations show the presence of free gold, mainly associated with disseminated sulfides, in particular pyrite and arsenopyrite (Figure 6), which occur in different generations. Available data from bulk-rock analysis suggest that elevated gold concentrations are generally restricted to the high-silica rocks and hint at a positive relationship between gold and various chalcophile elements hosted in sulphides (Figure 7).

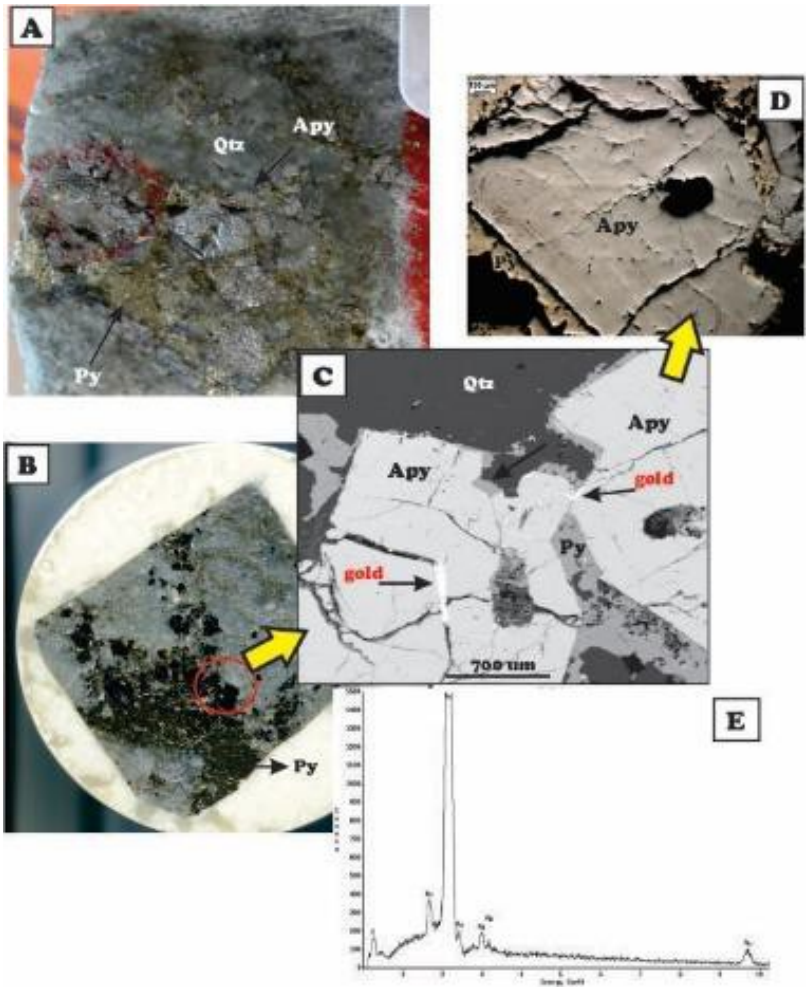

Figure 6: (A) Silica-rich core sample with pyrite (Py) and arsenopyrite (Apy), (B) polished block of (A), (C) BSE image of encircled area in (B), showing free gold in cracks of arsenopyrite, (D) Microphotograph of (C) in reflected light, and (E) EDS spectrum of gold in (C).

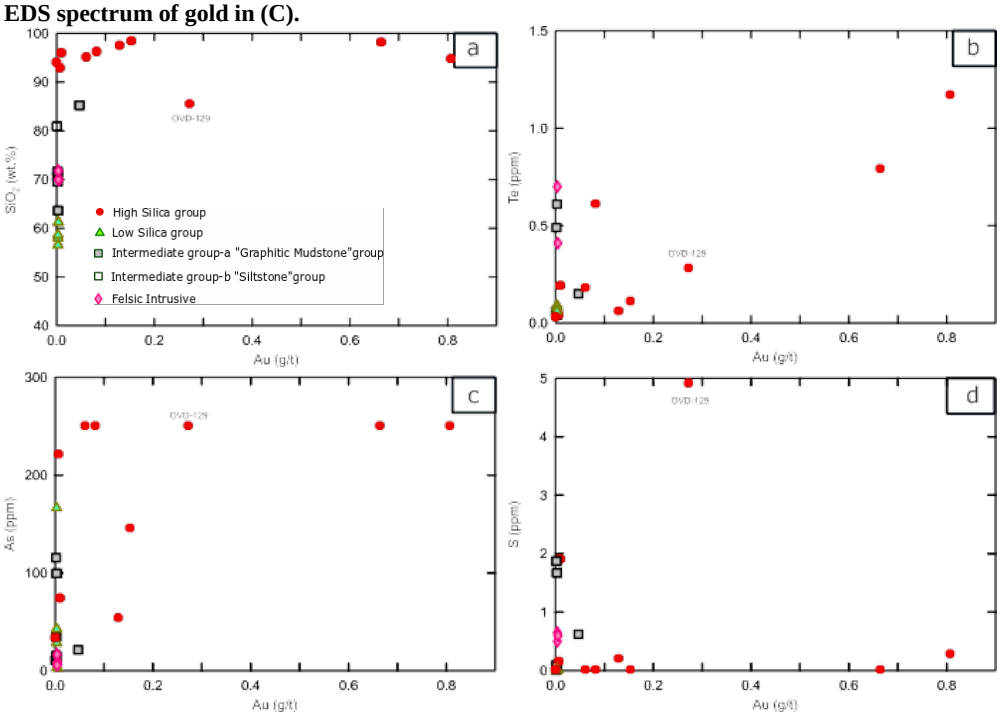

Figure 7 a-d: Plot of Au concentrations against SiO2 (a), Te (b), As (c) and S (d). illustrating that gold enrichment tends to coincide with elevated concentrations of chalcophile elements in the high-silica group.

CONCLUSIONS

- Major and trace element signatures of bulk samples from the Overman gold deposit indicate that the original parent rocks, prior to pervasive silicification, were heterogeneous and probably mainly of (meta-)sedimentary origin
- A group of least silicified rocks shows geochemical resemblance to meta-sediments present in the northern Rosebel deposits, especially JZone greywackes, Pay Caro arenites and Koolhoven mudstones.
- Gold and associated chalcophile elements tend to be enriched in the most siliceous rocks but an unequivocal relationship between gold mineralisation and silicification remains to be assessed.
- Further geochemical and mineralogical work is needed to constrain the mechanism and conditions of ore formation and to explore the potential role of graphite-bearing sediments as source of the gold.

ACKNOWLEDGMENT

This work forms part of a PhD research project (NK), sponsored by Rosebel Gold Mines N.V.

REFERENCES

Daoust, C., Voicu, G., Brisson, H. and Gauthier, M. (2011), Geological setting of the Paleoproterozoic Rosebel gold district, Guiana Shield, Suriname. Journal of South American Earth Sciences 32, 222-245.

Daoust, C. (2016), Caractérisation stratigraphique, structurale et géochimique du District minéralisé de Rosebel (Suriname) dans le Cadre de l'évolution géodynamique du Bouclier Guyanais, PhD thesis, Université du Québec á Montréal (Montréal): 330 pp.

Kioe-A-Sen, N. van Bergen, M.J., Wong, Th. and Kroonenberg, S.B. (2016), Gold deposits of Suriname: geological context, production and economic significance. Netherlands Journal of Geosciences-Geologie en Mijnbouw, 95-4, 429- 445.

Voicu, G., Bardoux, M. and Stevenson, R. (2001), Lithostratigraphy, geochronology and gold metallogeny in the northern Guiana Shield, South America: a review. Ore Geology Reviews 18, 211-236.

Metallogenic evolution of the Guiana Shield in Brazil

Evandro L. Klein

CPRM – Geological Survey of Brazil Brasília-DF, Brazil

evandro.klein@cprm.gov.br

SUMMARY

A review of present knowledge of the metallogenic evolution of the Guiana Shield in Brazil is presented here, and shows that about a dozen metallogenic epochs can be envisaged from Archean to recent times. Different mineral systems, operating in all tectonic domains, and related to metamorphism, felsic, mafic-ultramafic, and alkaline magmatism, in addition to sedimentary processes produced ferrous, non-ferrous, precious and special metals, along with diamonds and gemstones.

Key words: Guyana, Amazonian Craton, Metallogenesis, Mineral Resources, Mineral Systems

INTRODUCTION: GEOLOGICAL AND TECTONIC BACKGROUND

The geological evolution of the Brazilian portion of the Guiana Shield (northern sector of the Amazonian Craton) spans in time from the Paleoarchean Era to the Calymmian period (Rosa-Costa et al., 2009; Almeida et al., 2013; Fraga et al., 2017). Based on rock associations and on the age of the geological events, different domains can be considered for this sector (Figure 1). (1) The eastern Guiana Shield comprises an Archean medium- to high-grade metamorphic basement, which was reworked during Rhyacian (2.3-2.05 Ga) accretionary and collisional events (Transamazonian cycle). These events produced granite-greenstone sequences formed in variable tectonic settings, and were eventually intruded by anorogenic granites (1.75 Ga). (2) In the central portion of the shield, the Early-Orosirian orogen consists of arc-related granites and associated sedimentary basin that underwent medium- to high-grade metamorphism, and post-collisional igneous belts containing I- and A-type granites, which intruded the supracrustal sequence. (3) The widespread extension-related felsic magmatism of 1.90 to 1.86 Ga, which formed the Uatumã SLIP - Silicic Large Igneous Province, occur in the central-south portion of the shield. (4) Thick cratonic sedimentary sequence. (5) To the west, Late-Orosirian (1.81-1.70 Ga), arc-related plutonic and sedimentary sequences and A-type granites, and Calymmian (1.54-1.51 Ga) collision-type granites predominate. Younger Mesoproterozoic, Neoproterozoic, and Phanerozoic alkaline intrusions occur in different domains throughout the shield.

MINERAL RESOURCES AND MINERAL SYSTEMS

Eastern Guiana Shield (Archean-Rhyacian domain)

The eastern portion of the Guiana Shield in Brazil is the most endowed mineral province in the shield, even though still underexplored. Although Archean rocks made significant part of this sector, mineral systems of this age are only vestigial, and include possible sedimentary iron mineralization (<200 Mt) associated with relics of high-grade metasedimentary sequences (magnetite-bearing quartzite and itabirite) occurring within gneiss-granulite complexes, along with gold and diamond present in metaconglomerates (paleoplacer?) of Rhyacian greenstone belts. These greenstone belts are the main metallotect and host sedimentary iron (>400 Mt) and manganese (c. 42 Mt) ores deposited in the early phase of greenstone formation (2.26-2.15 Ga), which underwent subsequent metamorphism under greenschist to amphibolite facies conditions (2.11-2.08 Ga), and supergene enrichment during the Phanerozoic. The hematite sedimentary iron deposits (e.g., Vila Nova) consist of BIF, itabirite, and Fe-quartzite, whereas the genesis of manganese protores (e.g., Serra do Navio) involved modification of Mn-rich carbonate rocks associated with C-bearing pelites (Rodrigues et al., 1986; Spier and Ferreira Filho, 1999). Possible VMS systems are also associated with the early phase of greenstone development and account for semi-massive copper (±Zn) mineralization hosted in hydrothermally altered oceanic basalts (Faraco et al., 2006). Orogenic gold (>6 Moz) formed at about 2.11-1.94 Ga (two stages?), coeval with the metamorphism and deformation of the greenstone sequences (Galarza et al., 2006; Klein et al., 2009). Fluid inclusion and isotopic studies (Melo et al., 2003; Klein et al., 2009; Klein and Fuzikawa, 2010) indicate low-salinity metamorphic (partly granulitic) and magmatic (partly charnockitic) fluid sources, which deposited gold from 270 to >420°C (e.g., Tucano, Carará). Chromite deposits (Bacuri, 91 kt) occur at the base of the ultramafic layer of mafic- ultramafic layered complex (Spier

and Ferreira Filho, 2001) that intruded basement gneisses and the greenstone belts (Scarpelli and Horikawa, 2018). The layered complex and the ore bodies underwent folding and metamorphism under amphibolite condition (Spier and Ferreira Filho, 2001). Iron ore (magnetite-rich mafic rock) is also associated to the layered complex (Scarpelli and Horikawa, 2018). Greisen and pegmatite Sn and Nb-Ta deposits are probably related to anorogenic, A-type granites of 1.75 Ga (Klein et al., 2014).

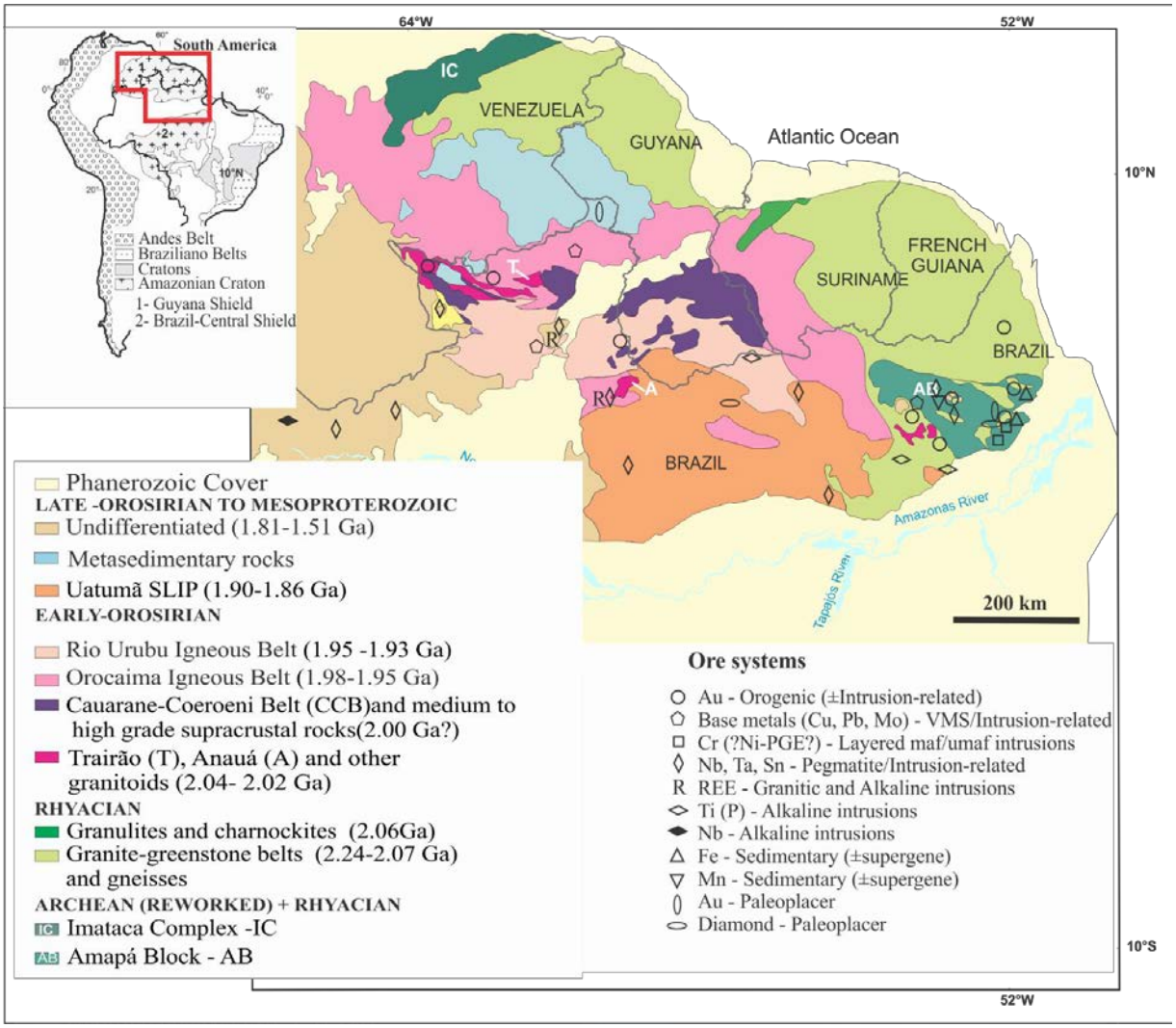

Figure 1: Simplified map depicting the main tectonic domains and associations of the Guiana Shield (modified from Fraga et al., 2017), with location of the main mineral systems.

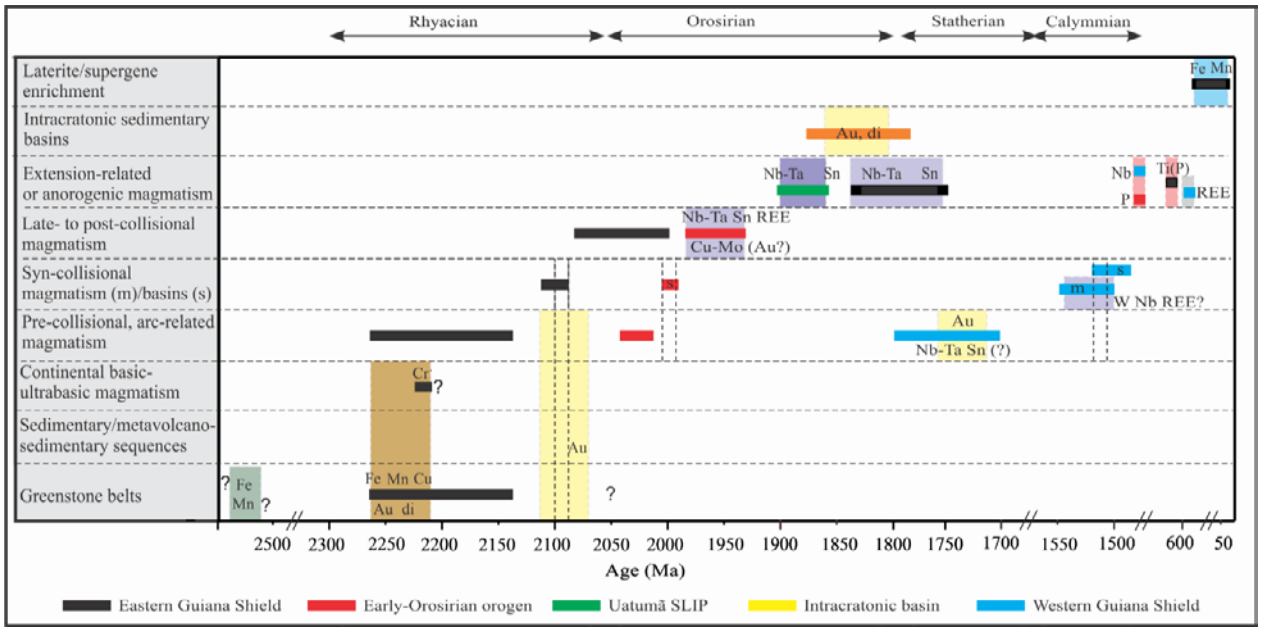

Figure 2: Main stages of the geological evolution of the Guiana Shield in Brazil and relationships with the formation of ore deposits. Vertical dashed lines indicate the estimated metamorphic age for each sector of the Guiana Shield.

Early-Orosirian Orogeny

Mineral systems of the Early-Orosirian to Statherian sector are likely magmatic (pegmatite) and magmatic-hydrothermal (intrusion-related) in origin, including Sn-Nb-Ta (±REE), base metals (Cu-Mo) and gold occurrences dispersed throughout the domain. These are associated with the igneous belts.

Uatumã SLIP (Late-Orosirian)

The Guiana Shield portion of the Uatumã SLIP is one of the least known domains in the Amazonian Craton regarding both geology and metallogeny. A few occurrences of Sn-Nb-Ta in veins/pegmatites and of gemstones (amethyst, amazonite) are spatially- and/or genetically-related to the widespread 1.88 Ga-old felsic magmatism, which is also potential for base metals (Klein and Carvalho, 2008). The most expressive mineral system in the Uatumã SLIP comprises the world-class Pitinga province (164 Mt, Sn ± F, Nb, Ta, Al, Th, U, Y, Zr, REE). Both magmatic (disseminated in albite granite) and hydrothermal (greisen and Na-episyenite) ores are hosted in 1.82-1.80 Ga rocks (Borges et al., 2014). However, given that these ages post-date the accepted age for the Uatumã magmatism (1.89-1.86 Ga, Klein et al., 2012), the relationship of Pitinga with Uatumã is still uncertain. The Pitinga magmatism and ore genesis relate more likely to a magmatic event occurring to the west of the Guiana Shield.

Cratonic sedimentary cover (Statherian)

In the Brazil-Venezuela-Guiana triple border, paleoplacer Au (±diamond) occurs at the basal formation of the intracontinental Roraima basin.

Western Guiana Shield (Statherian-Calymmian)

The western portion of the Guiana Shield in Brazil, with rock associations of Statherian to Calymmian age, is also little known in terms of metallogeny. Gold mineralization of unknown origin (orogenic?) is hosted in magmatic arc-related metasedimentary sequence with maximum sedimentation age at 1.74 Ga (Almeida et al., 2014), which is contiguous with similar sequences in Colombia (Machado belt) where orogenic and conglomerate-hosted gold deposits and occurrences are under exploration. Evidence of mineralization was reported by Almeida et al. (2014), including Sn-Nb-Ta associated to A-type granites (1.75 Ga), and W-Nb-REE associated to S-type granites (1.54 Ga).

Younger, extension-related (intracratonic) ore deposits

A series of intracratonic ore deposits formed long time after the main orogenic evolution of different sectors of the Guiana Shield (Archean to Mesoproterozoic), and are related to extensional, mainly alkaline, and subordinately mafic-ultramafic magmatism. Possibly formed in the end of the Mesoproterozoic (1.3-1.0 Ga), magmatic phosphate is contained in alkaline syenite (Mutum), whereas Nb deposit (Seis Lagos, 81.4 Mt Nb2O5) formed by supergene processes over carbonatite intrusion (Biondi, 2003; Almeida et al., 2014). Primary and supergene titanium (± P, Nb, REE, Cu) ore is associated with intracontinental ultramafic alkaline without (Maraconaí) and with carbonatite (Maicuru, 200 Mt) complexes of 0.6 Ga emplaced during extensional stages in the Neoproterozoic Brasiliano cycle and that preceded the opening of the Phanerozoic intracratonic Amazon basin. The ore is contained in anatase (Fonseca and Rigon, 1984; Castro et al., 1991). The youngest known alkaline mineral system comprises 111-116 Ma-old nepheline-bearing syenites and phonolites (Figueiredo et al., 2018), which host REE ± P-Ti mineralization (Repartimento). Evidence of Cu-Co-Ni-Cr- PGE mineralization is associated with mafic-ultramafic intrusions (1.17 Ga) (Almeida et al., 2014).

CONCLUSIONS

Despite the lack of significant metallogenic studies, the spatial and temporal distribution of ore deposits and associated mineral systems allow to draw the following interpretation about the metallogenic evolution of the Guiana Shield in Brazil, occurring in a dozen epochs (Figure 2). (1) Archean mineral systems (sedimentary iron and hydrothermal gold) are only vestigial; (2) the most endowed terranes are those from the Rhyacian Eastern Guiana Shield, with ferrous, base and precious metals contained in greenstone belts; (3) Sn, Nb- Ta, and Cu-Mo are associated with granitic magmatism, both orogenic and anorogenic, mostly from the Orosirian and subordinately from the Statherian; (4) Mesoproterozoic and Phanerozoic alkaline intrusions produced Ti, Nb, REE, and P mineralization; (5) Supergene processes favoured the enrichment of Rhyacian (±Archean?) iron and manganese ores.

ACKNOWLEDGMENTS

I thank Mark Jessell for the invitation to do this presentation, CNPq for a research grant (306798/2016-6), and Leda Fraga for discussions.

REFERENCES

Almeida, M.E., Macambira, M.J.B., Santos, J.O.S., Nascimento, R.S.C., and Paquette, J.L., 2013, Evolução crustal do noroeste do Cráton Amazônico (Amazonas, Brasil) baseada em dados de campo, geoquímicos e geocronológicos. XIII Simpósio de Geologia da Amazônia. Resumos expandidos, 201–204.

Almeida, M.E., Riker, S.R.L., and Oliveira, M.A., 2014, Metalogênese da Província Rio Negro. In: Silva, M.G., Rocha Neto, M.B., Jost, H., and Kuyumjian, R.M., (eds.), Metalogênese das Províncias Tectônicas Brasileiras. Belo Horizonte, CPRM, 285-291.

Biondi, J.C., 2003, Processos metalogenéticos e os depósitos minerais brasileiros. São Paulo, Oficina de Textos, 528 p.

Borges, R.M.K., Dreher, A.M., Almeida, M.E., Costi, H.T., Reis, N.J., and Andrade, J.B.F., 2014, Metalogênese da Província Tapajós- Parima: domínios Parima, Uiamiri e K'Mudku. In: Silva, M.G., Rocha Neto, M.B., Jost, H., and Kuyumjian, R.M., (eds.), Metalogênese das Províncias Tectônicas Brasileiras. Belo Horizonte, CPRM, 215-228.

Castro, C., Silva, G.R., and Costa, M.L., 1991, A viabilidade de termofosfatos a partir de matérias primas de Maicuru e sua imprtância para o desenvolvimento mineral e agronômico da Amazônia. 3 Simpósio de Geologia da Amazônia, Belém, Annals, 260-274.

Faraco, M.T.L, Fuzikawa, K., Ramboz, C., and McReath, I., 2006, A fluid inclusion study in the hydrothermal volcanogenic sulfide and orogenic gold mineralization at the Serra do Ipitinga, Amazon, Brazil. Revista Brasileira de Geociências, 36, 51-58.

Figueiredo, R.F., Santos, T.J.S., and Tonetto, E.M., 2018, Petrology, geochemistry and U-Pb zircon and baddeleyite ages of the alkaline rocks from the central-southern Guyana Shield, northern Amazonian Craton. Journal of South American Earth Sciences, 86, 461-474.

Fonseca, L.R., and Rigon, J.C., 1984, Ocorrências de titânio no complexo ultramáfico-alcalino de Maraconaí no Estado do Pará. 33 Congresso Brasileiro de Geologia, Annals, 3841-3852.

Fraga, L.M., Vasquez M.L., Almeida, M.E., Dreher, A.M., and Reis, N.J., 2017, A influência da orogenia Eo-Orosiriana na formação da SLIP Uatumã, parte central do Cráton Amazônico. 15 Simpósio de Geologia da Amazônia, Belém, Abstracts, 405-408.

Galarza, M.A., Lafon, J.M., and Macambira, M.J.B., 2006, Idades Pb-Pb das mineralizações auríferas dos depósitos Amapari (Amapá), Igarapé Bahia (Carajás) e Mamão (Rio Maria), Amazônia oriental. 9 Simpósio de Geologia da Amazônia, Resumos, on CD-ROM.

Klein, E.L., and Carvalho, J.M.A., 2008, Recursos Minerais. In: Vasquez, M.L., and Rosa-Costa, L.T., (eds), Geologia e recursos minerais do Estado do Pará. Escala 1:1,000,000. Belém, CPRM, 328 p.

Klein, E.L., and Fuzikawa, K., 2010 Origin of the CO2-only fluid inclusions in the Palaeoproterozoic Carará vein-quartz gold deposit, Ipitinga Auriferous District, SE-Guiana Shield, Brazil: implications for orogenic gold mineralization. Ore Geology Reviews, 37, 31- 40.

Klein, E.L., Lafon, J.M., Harris, C., Brito, R.S.C., and Vaconcelos, P., 2009, Fluid inclusion and isotopic constraints on the genesis of vein-quartz gold deposits of the Ipitinga Auriferous District, SE-Guiana Shield, Brazil. Contribuições à Geologia da Amazônia, 6, 15- 42.

Klein, E.L., Almeida, M.E., and Rosa-Costa, L.T., 2012, The 1.89-1.87 Ga Uatumã Silicic Large Igneous Province, northern South America. Large Igneous Provinces Commission. Available at: <http://www.largeigneousprovinces.org>.

Klein, E.L., Rosa-Costa, L.T., and Vasquez, M.L., 2014, Metalogênese da borda oriental do Cráton Amazônico. In: Silva, M.G., Rocha Neto, M.B., Jost, H., and Kuyumjian, R.M., (eds.), Metalogênese das Províncias Tectônicas Brasileiras. Belo Horizonte, CPRM, 171- 194.

Melo, L.V., Villas, R.N., and Faraco, M.T.L., and Soares, J.W., 2003, Geological setting and mineralizing fluids of the Amapari gold deposit, Amapá state, Brazil. Géologie de la France, 2-3-4, 243-255.

Rodrigues, O.B., Kosuki. R., and Coelho Filho, A., 1986, Distrito Manganesífero de Serra do Navio, Amapá. In: Schobbenhaus, C., Coelho, C.E.S., (eds.), Principais Depósitos Minerais do Brasil. V.II, Ferro e metais da indústria do aço. Brasília, DNPM/CVRD/CPRM, 167-175.

Rosa-Costa, L.T., Monie, P., Lafon, J.M., Arnaud, N., 2009, 40Ar-39Ar geochronology across Archean and Paleoproterozoic terranes from southeastern Guiana Shield (north of Amazonian Craton, Brazil): evidence for contrasting cooling histories. Journal of South American Earth Sciences, 27, 113-128.

Scarpelli, W., and Horikawa, E.H., 2018, Chromium, iron, gold and manganese in Amapá and northern Pará, Brazil. Brazilian Journal of Geology, 48, 415-433.

Spier, C.A., and Ferreira Filho, C.F., 1999, Geologia, estratigrafia e depósitos minerais do Projeto Vila Nova, Escudo das Guianas, Amapá, Brasil. Revista Brasileira de Geociências, 29, 173-178.

Spier, C.A., and Ferreira Filho, C.F., 2001 The chromite deposits of the Bacuri Mafic-Ultramafic Layered Complex, Guyana Shield, Amapá State, Brazil. Economic Geology, 96, 817-835.

Zircon U-Pb geochronology by LA-ICP-MS in the Marowijne Greenstone Belt, Suriname: methodology & preliminary results

Leo M. Kriegsman*
Institute of Earth Sciences
Utrecht University & Naturalis
Biodiversity Center Leiden
The Netherlands

leo.kriegsman@naturalis.nl

Paul R.D. Mason
Institute of Earth Sciences
Utrecht University
The Netherlands

p.mason@uu.nl

Salomon Kroonenberg
Anton de Kom University (AdeKUS),
Paramaribo, Suriname & Delft University
of Technology, The Netherlands

salomon.kroonenberg@uvs.edu

SUMMARY

The talk will discuss new zircon U-Pb ages on the Marowijne Greenstone Belt in Suriname, based on an LA-ICP-MS dating programme using museum specimens and new samples. So far, we have measured zircons from 27 samples from different lithologies, including metasediments, metavolcanics, and plutonic rocks (early TTG and younger granites). We are currently processing ~1000 spot analyses, incuding ~25% standard analyses. More than 95% of the zircons are magmatic. Our preliminary data confirm that the main events are due to the Trans-Amazonian Orogen between 2.26 and 1.98 Ga. The scarcity of older grains is consistent with an island arc setting, but this hypothesis requires more evidence. Some late Archaean to earliest Proterozoic zircons are present, suggesting the relative proximity of an older craton during part of the history. The youngest detrital grains dated in conglomerates so far give an age of 2.16 ± 0.01 Ma, providing a maximum deposition age. Nearby TTGs of the same age are likely source rocks.

Key words: Marowijne Greenstone Belt, geochronology.

INTRODUCTION

Zircon U-Pb geochronology is the main dating method in Precambrian terrains. The method with highest precision is isotope dilution, which involves separation and dissolution of entire grains or grain populations, with limited information on complex zoning patterns. SHRIMP spot analyses combines high spatial and temporal resolution, but is expensive and requires access to a small number of labs in the world. A more affordable method available from a growing number of labs, including Utrecht, is LA-ICP-MS linked with CL imaging. We believe this method is a key tool to develop a more detailed and comprehensive geochronological framework for Suriname that is currently lacking. In addition, involving BSc and MSc students adds an educational component to our dating programme.

METHOD AND RESULTS

Since late 2016 we have supervised 8 student projects to improve the U-Pb geochronological database for Suriname, focussing on the Palaeoproterozoic Marowijne Greenstone Belt, and several other student projects that deal with various petrological and geochemical aspects of this important mineralised belt. We have re-used a number of samples from past projects, mainly 1950s, now stored at Naturalis Biodiversity Center in Leiden, the main natural history museum and archive in The Netherlands. In addition, new field specimens and drill core samples from recent projects in Suriname were used, in collaboration with AdeKUS staff and students and co-sponsored by IAMGOLD.

So far, we have measured zircons from 27 samples from different lithologies, including metasediments, metavolcanics, and plutonic rocks (tonalites, trondhjemites and granites). We are now processing ~1000 spot analyses, incuding ~25% standard analyses, taking care to maximize the quality and information from each spot. In this talk, we will describe key steps in the process from samples to U-Pb ages, including data processing, and we will present a first overview of the U-Pb age pattern of the Marowijne Greenstone Belt based on data from Suriname. A comparison with data from French Guyana will also be included.

Our data confirm that the main events in the the Marowijne Greenstone Belt are due to the Trans-Amazonian Orogen that resulted from the convergence and ultimate collision of the Guiana Shield with the West-African Craton, roughly between 2.26 and 1.98 Ga. More than 95% of the zircons have magmatic morphology and Th/U ratios > 0.3. Some magmatic rocks contain at least two distinct age populations tens of Ma apart, indicating an older inherited, xenocrystic component that we interpret as evidence for deep crustal remelting. The scarcity of older grains are consistent with an island arc setting, but geochemical and additional isotopic analyses are required to test this hypthesis. The combined field data and U-Pb age patterns suggest various pulses of TTG magmatism within the period 2.17-2.10 Ga that can only be separated with difficulty in view of the >10 Ma uncertainties (1 sigma) in ages. A few late Archaean to early Proterozoic zircons have been observed in conglomerates, suggesting the relative proximity of an older craton. A detailed comparison with nearby Archaean blocks in the northern Guiana Shield (Imataca, Venezuela; Amapá, Brazil) is needed to establish whether these may represent the provenance regions.

CONCLUSIONS

The Marowijne Greenstone Belt in Suriname shows age patterns in line with those published on French Guyana. confirming that the main events are due to the Trans-Amazonian Orogen that resulted the convergence and ultimate collision of the Guiana Shield with the West-African Craton, roughly between 2.26 and 1.98 Ga. Magmatic zircons dominate and older inherited grains are scarce. We have tentatively defined various pulses of TTG magmatism. A few late Archaean zircons are present, suggesting the relative proximity of an older craton. A detailed comparison with nearby Archaean blocks in the northern Guiana Shield (Imataca, Venezuela; Amapá, Brazil) is needed to establish whether these may represent the provenance regions. At the Paramaribo meeting, we expect to show the full results of our dating programme.

2.12–2.08 Ga Late- to post-collisional peraluminous granitoid magmatism in the Marowijne Greenstone Belt of Suriname

Samantha C. Kromopawiro
Anton de Kom University of Suriname
Leysweg 86, Paramaribo, Suriname

Surinamesam.kromopawiro@gmail.com

Salomon Kroonenberg
Anton de Kom University of Suriname
Leysweg 86, Paramaribo,

salomonkroonenberg@gmail.com

Leo Kriegsman
Naturalis Biodiversity Center
Vondellaan 55 Leiden, NL

leo.kriegsman@naturalis.nl

Paul R.D.Mason
Utrecht University
Princetonlaan 8,

p.mason@uu.nl

SUMMARY

The Marowijne Greenstone Belt of Suriname is underexplored and has the potential to host other commodities other than gold alone. In order to explore for these additional resources, a good understanding of the geological events is required. This study aims at understanding the age and composition of various granitoids within the Marowijne Greenstone Belt, including the Akinto Soela granite, the Phedra granite and the Tibiti granite in relation to the Patamacca granite and the Brincks TTG pluton. Using petrography and geochemical analyses such as the XRF, LA-ICP-MS and zircon U-Pb age dating techniques, these granitic units are evaluated to establish their interrelationships. The geochemistry of the granites shows variations in their source rock derivation, depending on their tectonic emplacement setting. The Akinto Soela and Phedra granites show ages of around 2.08 ± 0.03 Ga, which corresponds to the D2a deformation stage by Delor et al. (2003a). The Tibiti granite has an age of 2119 ± 33 Ga, also corresponding to the D2a stage, but with more similarities to the Brincks TTG body.

Key words: Marowijne Greenstone Belt, Granitoid Magmatism, Suriname, geochemical classification.

INTRODUCTION

The Akinto Soela granite is a lung shaped unit on the geological map of Suriname (Bosma et al., 1977) and described by O'Herne (1958) as a medium-coarse, biotite-rich, porphyritic, microcline granite. So far, this biotite-granite is the only one of its kind found in northeastern Suriname; all other granitic units in the Greenstone Belt contain both biotite and muscovite in their mineralogical composition. Existing geochemical data from other granitoid intrusions were used to evaluate and compare compositional characteristics, including the Brincks TTG pluton, the Patamacca granite, the Phedra granite and the Tibiti granite. This study will identify whether the Akinto Soela Granite is associated to the nearby Phedra two-mica Granite or more related to the peraluminous S- type Patamacca granite or from a different magma pulse altogether. The position of each granitic unit within the evolution model of the Guiana Shield by Delor et al. (2003a) will also be investigated. Delor et al. (2003) classified the Trans-Amazonian Orogenic Cycle into several stages. After a first stage of basaltic ocean floor magmatism (2.26 – 2.20 Ga), TTG-plutonism occurred between 2.18 – 2.12 Ga, during ongoing convergence and finally collision of the Amazonian and West-African Cratons. In a later stage around 2.11
– 2.06 Ga, magmatism continued with the emplacement of syn-tectonic granites as a result of crustal stretching and dextral shearing. Characterizing the different granitic occurrences of the northeastern Greenstone Belt of Suriname, followed by understanding the position of these units within the crustal evolution, will guide exploration groups to look for additional and/or new resources in that specific part of the country.

METHOD AND RESULTS

Fieldwork was conducted during the months May and June of 2017 in the Phedra and Akinto Soela areas to gather first-hand field information and to establish the contact relationships of the granitic units. However, identifying the relationships with the surrounding units was unsuccessful due to extensive weathering conditions. In total, 12 field samples were collected from the Akinto Soela, Phedra and Tibiti granites for thin sections production, XRF, LA-ICP-MS and U-Pb age dating analyses. The thin section production as well as the analytical analyses were all done at the Utrecht University.

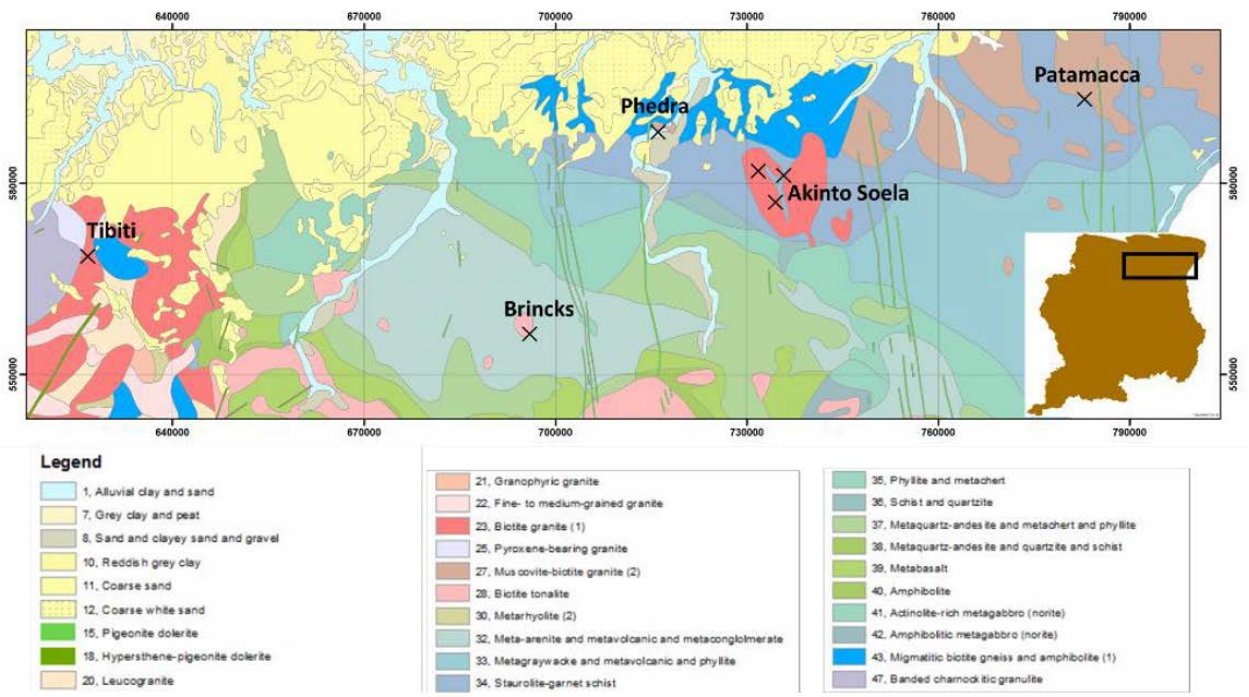

Figure 1: Simplified geology map of Suriname (Bosma et al., 1977), limited to the study area, including the location marks of granitic units under investigation Bricks and Patamacca granites were studied by other authors.

Figure 2: The left image shows the size of the boulders of the Akinto Soela Granite in an exploration pit. The image on the right illustrates drill core samples of the Akinto Soela granite, clearly showing the well-defined K-megacrysts in a coarse-grained texture.

PETROGRAPHY

Using a Leica 750P optical microscope at the Anton de Kom University of Suriname, petrographical observation were done on the thin sections (Figure 3). The granitic units are all holocrystalline varying from equigranular fine-grained (0.5 – 1 mm) to equigranular coarse-grained (1 – 5 mm). Textures to some minerals include the perthitic texture, where exsolved lamellae of plagioclase is hosted in a K-feldspar grain, and the graphic/granophyric texture, which is the intergrowth of quartz and K-feldspar. Alteration observed includes sericitization of plagioclase grains into epidote or sericite, partial chloritization of biotite, pleochroïc halos caused by radioactive decay of zircons are observed in biotite grains, and to a lesser extent carbonatization. The grains of the Akinto Soela granite in particular are marked by a porphyritic texture, characterized by K-feldspar megacrysts (microcline) set against a groundmass of smaller quartz and plagioclase grains. The various Akinto Soela thin sections show some differences in mineralogical composition as some contained biotite and hornblende as mafic minerals with no muscovite, and other samples contain small amounts of muscovite, and only biotite as the mafic constituent. No muscovite was observed in the thin section of the Tibiti granite, while the Phedra granite contains both muscovite and biotite along with the rock forming minerals quartz, K-feldspars and plagioclase. Significant accessory minerals to the rocks are apatite in the Phedra granite and tourmaline, allanite, apatite, epidote and titanite in the Akinto Soela granite.

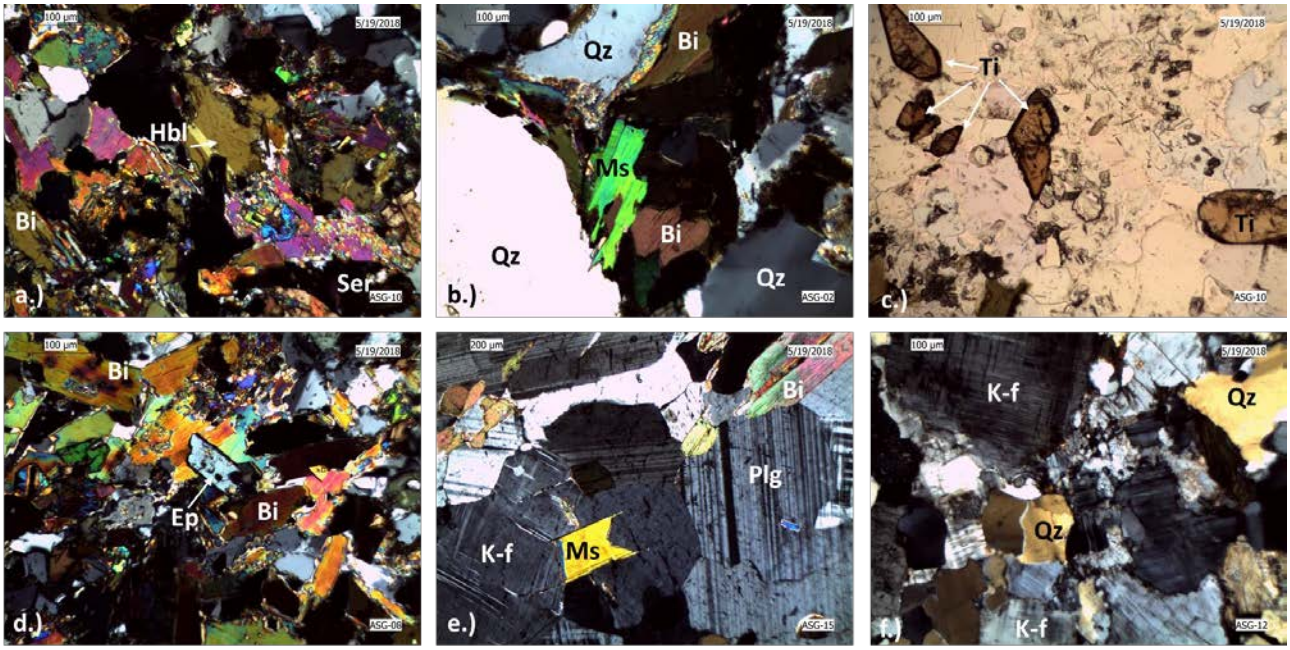

Figure 3: Microphotographs of the thin sections of the Akinto Soela (a, b, c, d), Phedra (e) and Tibiti (f) samples. a.) Hornblende in ASG-10, the only thin section with this mafic mineral. b.) Muscovite and biotite in the Akinto Soela thin section ASG-02. c.) Subhedral titanite grains in ASG-10. d.) Epidote crystal as part of the groundmass of the granite and biotite grains with pleochroïc halos (ASG-08). e.) Coarse grains of K-feldspar with biotite and muscovite plates in ASG-15. f.) Rock forming minerals of the Tibiti Granite, including quartz and K-feldspar.

GEOCHEMISTRY

Figures 4 to 6 are classification schemes used for the characterization of the different granitoids studied. The classification diagrams by Pearce et al. (1984) (Figure 5a) leaves uncertainty regarding the tectonic environments for the various granitic occurrences, therefore, the triangular plot by Harris et al. (1986) (Figure 5b) is introduced to elaborate on this. All samples show a strong enrichment in LREE when normalized to an average Cl chondrite (Figure 6a) and have the best pattern resemblance to an average continental crust with weak influences from the lower continental crust (Figure 6b). The Phedra granite is characterized as a syn-collisional, peraluminous granite, suggesting emplacement during collision and derived from a sedimentary protolith, with a negative Tb anomaly and a positive HREE slope. The Akinto Soela granite is classified as a late- to post collisional quartz-monzonite, with both meta- and peraluminous affinities. This suggests possible derivation from a mixture of mantle and crust derived magma and emplacement, either, during the last phase of deformation or right after collision had taken place. The Tibiti granite is classified as a within-plate, peraluminous granite, with a strong negative Eu anomaly and evidence for possible emplacement after deformation.

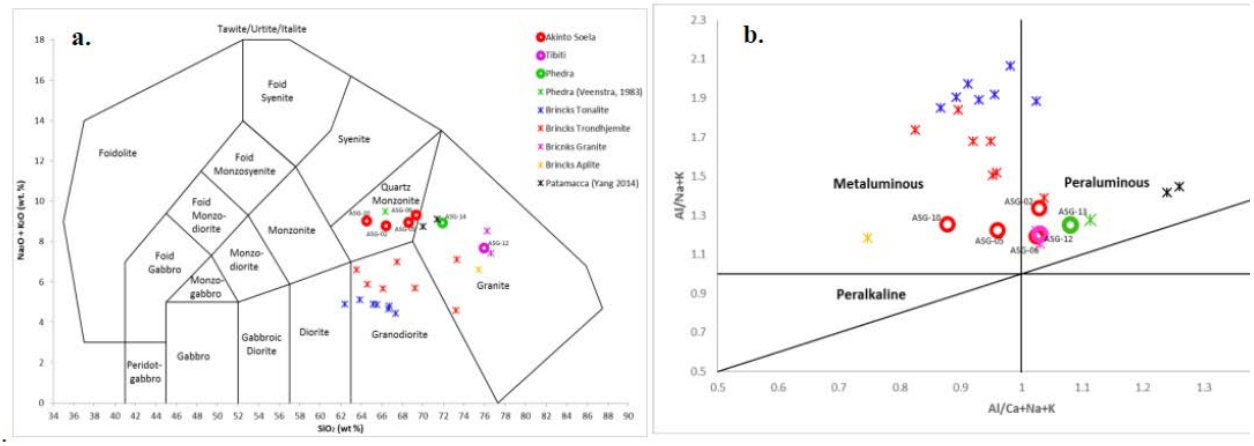

Figure 4: Classification diagrams using major element concentrations. Only samples analysed for this study are labelled. a.) TAS diagram after Middlemost et al. (1994), plotting the Phedra and Tibiti sample as granite and the Akinto Soela samples as quartz-monzonite. b.) ASI-classification of the granitoid rocks after Shand, (1947), with discrimination fields for the aluminium saturation of rocks after Maniar and Piccoli (1989). The Phedra and Tibiti samples plot as peraluminous and the Akinto Soela samples plot in both the meta- and peraluminous fields.

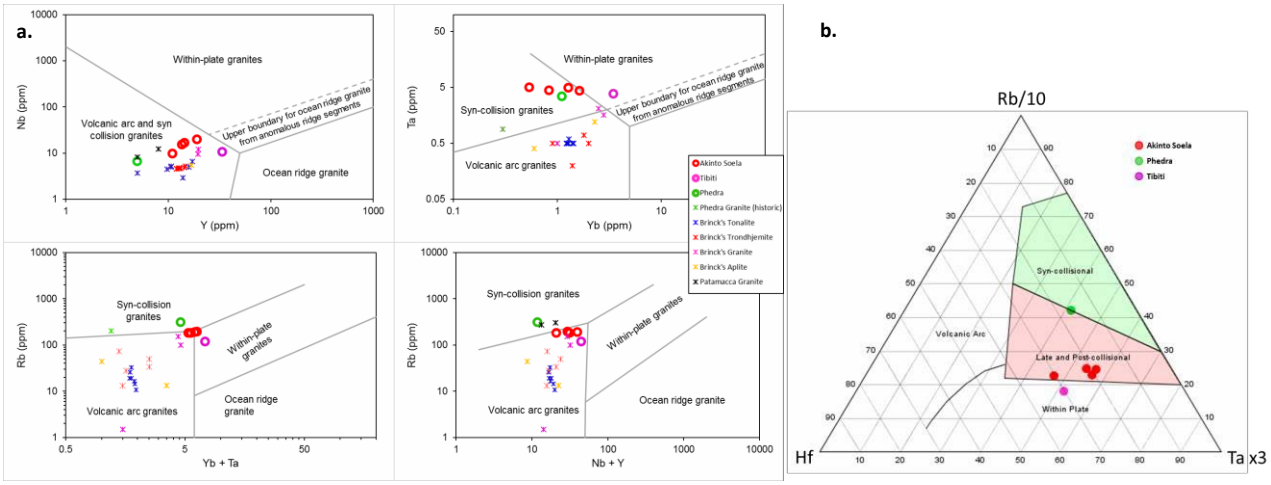

Figure 5: Tectonic classification diagrams using trace element concentrations. a.) Diagrams after Pearce et al. (1984) using Nb- Y, Ta-Yb, Rb-(Yb+Ta) and Rb-(Nb+Y) space. Inconsistent classifications, especially with the Akinto Soela samples, indicates possible mixture of mantle and crustal sources. b.) Ta-Hf-Rb triangular plot after Harris et al. (1986) suggest a syn-collisional environment for the Phedra granite, a within-plate tectonic setting for the Tibiti granite and a late- to post collisional emplacement environment for the Akinto Soela granite.

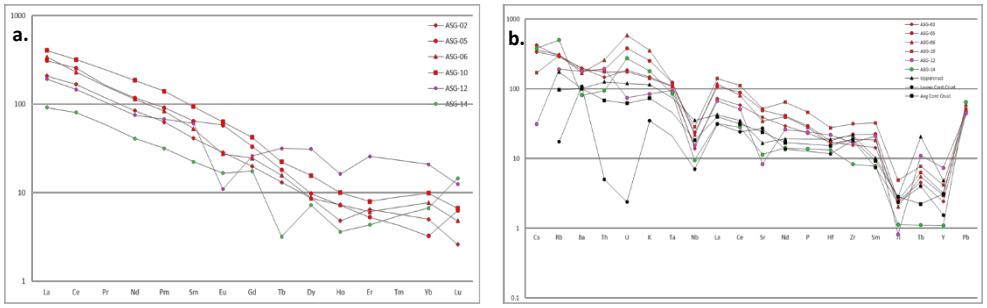

Figure 6: Normalization patterns. a.) REE patterns normalized to average C1 chondrite, after Evenson et al. (1978). b.) Spider diagram normalized to a primordial mantle after Sun and McDonough (1992), including patterns for the upper-, lower- and average continental crusts.

U-Pb ZIRCON AGE DATING

From U-Pb zircon age dating the approximate ages of the granitic samples were calculated, using the GLITTER software. It appears that the Tibiti granite dates 2119 ± 33 Ma, coinciding with the early D2a deformation stage (2.11 – 2.08 Ga), characterized as the

closure of the island-arc basins, due to sinistral sliding caused by continuing convergence (Delor et al., 2003a). Inherited ages of 2235
± 19 Ma (n=6) and 2361 ± 23 Ma (n=1) for this particular granite were obtained.

The Phedra granite dates 2093 ± 40 Ma and the Akinto Soela granite was calculated to have been emplaced around 2074 ± 29 Ma. These two occurrences are considered more or less coeval with a combined intrusion age of 2.08 ± 0.03 Ga, which coincides with the late D2a stage and possible early D2b tectonic stage of crustal stretching, leading to dextral shearing (Delor et al., 2003a). The Phedra granite has inherited ages between 2.4 and 2.8 Ga (n=3), indicating a possible late Archean to early Proterozoic source, while the Akinto Soela granite has two inheritance ages of 2202 ± 28 Ma (n=7) and between 2.3 (n=3) and 2.5 (n=3) Ga, approximately.

CONCLUSIONS

The granitic rocks studied show no significant age difference, and thus belong to the same range of intrusions. Based on their element concentrations and REE patterns, they show variance in tectonic setting and source rock derivation, and also slightly in mineralogical composition. The Tibiti granite with an age of 2119 ± 33 Ma, shows correlations to the Brincks granite (2109 ± 14 Ma) with its negative Eu anomaly and peraluminous nature (Ramlal, 2018). The Phedra granite does show similarities to the Patamacca granite in terms of REE patterns, its peraluminous nature and its mineralogy. The Akinto Soela and the Phedra intrusions relate to the Organabo (2069 ± 4 Ma) and the Petit Saut (2060 ± 4 Ma) monzogranites (Delor et al., 2003), respectively, in terms of age and composition.

ACKNOWLEDGMENTS

Helen de Waard from Utrecht University is thanked for her support with LA-ICPMS geochemical and U-Pb zircon analyses. The Anton de Kom University of Suriname is thanked for their support and the use of their facilities. Several institutes, such as Hazlo Geosolutions, Ponsor Mining and Kuldipsingh are thanked for their permission to generate a sample collection from the field.

REFERENCES

Bosma, W., et al., 1984, Explanation to the Geological map of Suriname 1:500,000: Mededelingen Geologische Mijnbouwkundige Dienst van Suriname.

Delor, C., et al., 2003, Transamazonian crustal growth and reworking as revealed by the 1:500,000-scale geological map of French Guiana (2nd edition): Géologia de la France, 2003, 2-3-4: 5-57

Evenson, N.M. et al., 1978. Rare-earth abundances in chondritic meteorites. Geochim. Cosmochim. Acta, 42 , pp. 1199-121

Harris. N.B.W., et al., 1986, Geochemical characteristics of collision-zone magmatism. Geological Society, London, Special Publications 19 (1): 67-81

Maniar, P.D., P.M. Piccoli, 1989 . Tectonic discrimination of granitoids: Geological Society of America Bulletin, 101: 635-643
Middlemost, E.A.K. 1994. Naming materials in the magma/igneous rock system. Earth-Science Reviews 37: 215-224

O' Herne, L., 1958, C7 Blad Berg en Dal: Geologische Mijnbouwkundige Dienst van Suriname

Pearce, J.A., et al., 1984, Trace element Discrimination Diagrams for the Tectonic Interpretation of Granitic Rocks: Journal of Petrology, 25: 956-983..

Ramlal, S.,, 2018. An investigation of the Brincks intrusion and its relationship to the surrounding gold deposits, Brokopondo, Suriname, South America. MSc thesis, Anton de Kom Universiteit van Suriname, 174 pp.

Shand, S.J. 1947 Eruptive Rocks. Eruptive rocks, their genesis, composition, classification, and their relation to ore deposits, with a chapter on meteorites. (3rd ed), Thomas Murphy, London. 488 pp.

Sun, SS & W.F McDonough 1989 Chemical and isotopic systematics of oceanic basalts: implications for mantle composition and processes Geological Society, London, Special Publications, 42, 313-345.

Geology and mineral deposits of the Guiana Shield

Salomon Kroonenberg
Anton de Kom University of Suriname
Leysweg 86, Paramaribo, Suriname

salomonkroonenberg@gmail.com

Paul R.D.Mason
Utrecht University
Princetonlaan 8,

p.mason@uu.nl

Leo Kriegsman
Naturalis Biodiversity Center
Vondellaan 55 Leiden, NL

leo.kriegsman@naturalis.nl

Emond W.F. de Roever
VU University
Amsterdam, the Netherlands

T.E. Wong
Anton de Kom University of Suriname
Leysweg 86, Paramaribo, Suriname

SUMMARY

The Guiana Shield records a long history that starts in the Archean, but culminates in the Trans-Amazonian Orogeny between 2.26-2.09 Ga as a result of an Amazonian-West-Africa collision. This event is responsible for the emplacement of a major part of its mineralisations, especially gold, iron and manganese. The diamondiferous Roraima Supergroup represents its molasse. Between 1.86 and 1.72 Ga the Rio Negro Block accreted in the west. The Grenvillian Orogeny caused shearing and mineral resetting between 1.3 and 1.1 Ga when Amazonia collided with Laurentia. Younger platform covers contain placer gold mineralisation. Several suits of dolerite dykes record short-lived periods of crustal extension. Bauxite plateaus cover various rock units.

INTRODUCTION

The Guiana Shield, the northern half of the Amazonian Craton, stretches over about 900,000 sq.km in northern South America, and is bounded in the north by the Atlantic Ocean and the south by the Amazon-Solimões basin. The dense rainforest cover, deep tropical weathering and difficult accessibility have hampered geological research, so it comes as no surprise that many different concepts exist about its general geological structure (Gibbs & Barron, 1993; Tassinari & Macambira, 1999; Santos, 2003; Delor et al., 2003; Fraga et al., 2009; Kroonenberg et al., 2016). Different mapping and classification approaches in the six countries involved, Brazil, Colombia, French Guiana, Guyana, Suriname and Venezuela also contributed to the present-day lack of consensus. Geochronology plays a key role in delimiting geological units in the shield and understanding its geological evolution. While past subdivisions were based essentially on Rb-Sr and K-Ar data, recent data obtained from zircon U-Pb chronology required a thorough revision of previous concepts. This paper attempts to summarise the major geological characteristics and evolution of the shield, and to place the numerous mineralisations in their geological context (Fig. 1). Mineral deposits in the Guiana Shield include gold, diamond, iron, manganese, chromium, nickel, copper, niobium, tantalum, tin, lithium, REE and bauxite, of which gold is by far the most important one at present.

MAJOR TECTONOSTRATIGRAPHIC UNITS AND THEIR MINERALISATIONS

Trans-Amazonian domains

Archean high-grade belts. There are two undisputed Archean terrains in the Guiana Shield, the Imataca Complex in its northwestern part in Venezuela, and the Amapá granulite belt in its easternmost extension in Amapá State of Brazil. The Imataca Complex (Kalliokoski, 1965, Gibbs & Barron, 1993; Tassinari et al., 2004) is an ENE-trending, fault-bounded block, consisting of amphibolite-facies quartzofeldspathic, locally garnetiferous paragneisses and granulite-facies hypersthene, cordierite and sillimanite-bearing gneisses, banded iron formation, amphibolites, amphibole-pyroxene granulites and some marbles. U-Pb SHRIMP dating of zircons gave a $^{207}Pb/^{206}Pb$ age of 3229 ± 39 Ma interpreted as indicating a mid-Archean age of at least some Imataca protoliths (Tassinari et al., 2004). Zircons from a second sample gave $^{207}Pb/^{206}Pb$ ages of 2629 (± 5) – 2739 (± 14) Ma, suggesting a period of high-grade metamorphism, extensive melting and migmatite injection in the Imataca Complex during the late Archean. Peak metamorphism and granitic plutonism took place during the Trans-Amazonian Orogeny around 2.05-1.98 Ga (Tassinari et al., 2004). Iron ore deposits formed by supergene enrichment in laterite plateaus over BIF of the Algoma type are being mined extensively. They are associated with minor manganese deposits (Sidder, 1995).

Archean rocks crop out in three tectonostratigraphic domains in Amapá and Pará States in Brazil, consisting of gneisses and charnockitic-enderbitic granulites showing Pb-Pb evaporation ages between 2.85 and 2.58 Ga and Sm-Nd model ages between 3.36 and 2.92 Ga. These are interpreted to represent at least two magmatic events in a Paleo-Meso-Archean phase of continental accretion (Rosa-Costa et al., 2003). Trans-Amazonian magmatism is evidenced by several plutons around 2.15-2.14 Ga (Rosa-Costa et al., 2003). A granulite-faces Trans-Amazonian metamorphic overprint between 2.10-2.08 Ga is contemporaneous to the development of a thrusting system associated to the collisional stage of the Transamazonian orogenesis (Rosa-Costa et al., 2008). Later post-collisional amphibolite-facies metamorphism and plutonism is recorded by monazite ages of 2056 ± 7 and
2038 ± 6 Ma. No known mineral deposits have been identified in the Archean domains in this area.

Paleoproterozoic (Rhyacian) greenstone belts (2.26-2.09 Ga). The northernmost portion of the Guiana Shield is occupied by a series of greenstone belts, roughly parallel to the Atlantic coast, stretching over 2000 km from Venezuela over the three Guianas into Amapá State in Brazil. They show the classical structure of steeply dipping, often cuspate synclinoria wrapped around ovoid TTG plutons. Also their stratigraphy shows the classical succession with tholeiïtic mid-ocean-ridge or back-arc basin basalts at the base, often with pillow structures, followed by sequences of more evolved island-arc-type andesites, dacites, rhyolites and intercalated chemical sediments. On top of this largely volcanic sequence, greywackes and shales were deposited as turbidites, finally overlain by a sequences of epicontinental fluvial deposits. They have been formed during the Trans-Amazonian Orogeny, mainly between 2.26 and 1.98 Ga, as a result of sea-floor spreading, southward subduction and finally continental collision between an ancestral Guiana Shield and the West-African Craton (Gibbs & Barron, 1993, Delor et al., 2003). Across the Atlantic they continue into the Birimian of West-Africa.

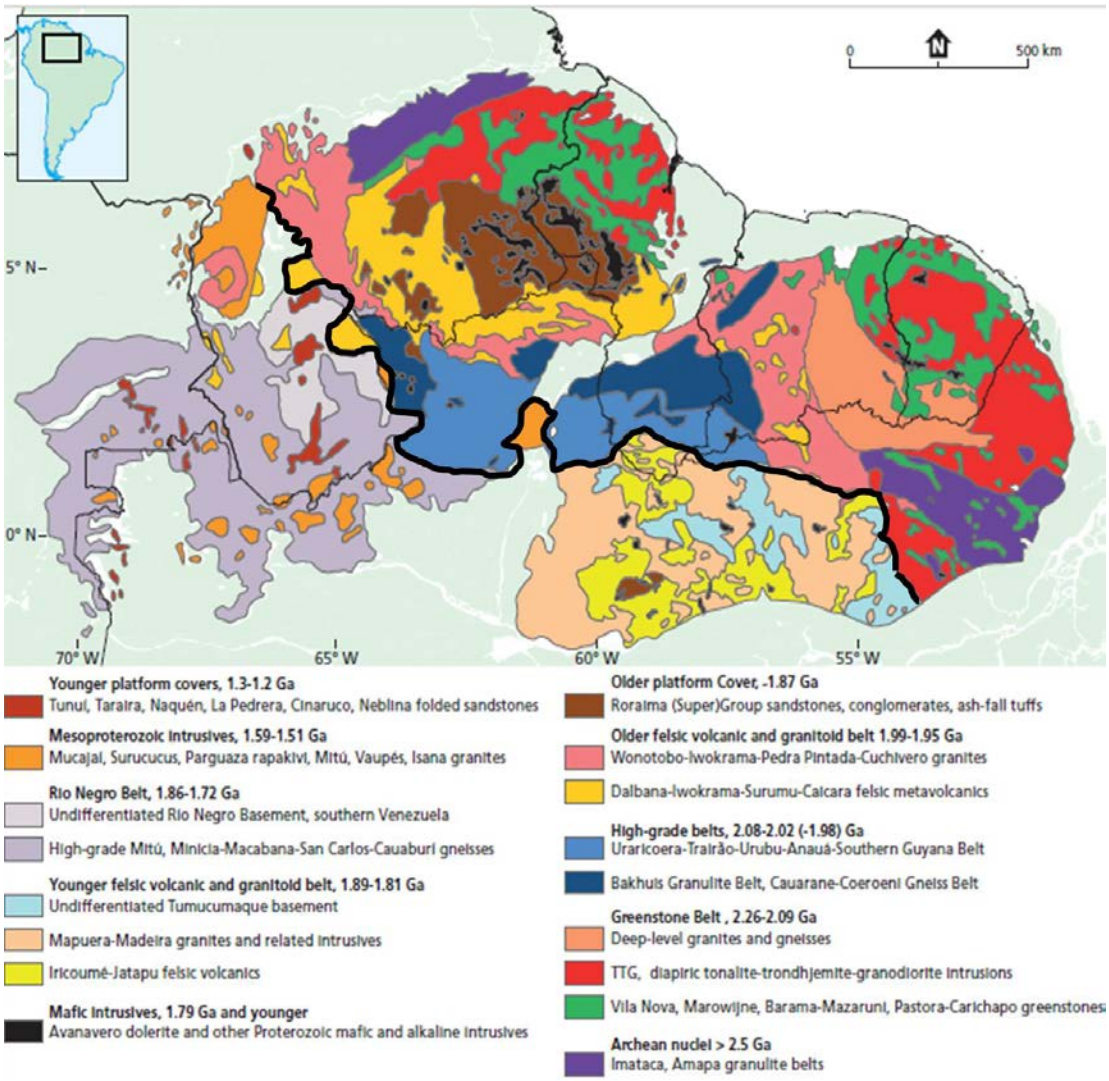

Geological sketch map of the Guiana Shield (after Kroonenberg et al., 2016). The heavy black line separates the Trans-Amazonian domains in the north from younger ones in the southern and western parts of the shield.

In Venezuela three more or less parallel greenstone belts have been distinguished (Pastora-Carichapo Group) which partly continue into northern Guyana (Barama-Mazaruni Group). In this western part of the greenstone belt the upper fluvial member is lacking. The eastern part of the greenstone belt in Suriname (Marowijne Greenstone Belt) and French Guiana (Maroni) has the complete sequence (Gibbs & Barron, 1993, Delor et al., 2003, Kroonenberg et al., 2016). In the easternmost greenstone belts of the Vila Nova Group in Amapá State in Brazil the uppermost fluvial deposits are lacking again. All rocks have been metamorphosed to greenschist facies conditions, reaching amphibolite facies around the diapiric TTG intrusions. The intrusions themselves are often multiphase and show ages between 2.18 and 2.11 Ga. The presence of Archean and even Hadean inherited zircons in them suggest the presence of an older basement reworked during the Trans-Amazonian Orogeny. Detrital zircons from the sedimentary sequences concentrate around 2.15 Ga, but so far no clear stratigraphic order can be derived from them (Daoust et al.,, 2011; Ramlal et al., 2018).

The greenstone belts are the main mineralised unit of the Guiana Shield. Gold is ubiquitous, mostly concentrated in late quartz veins, often with pyrite or arsenopyrite and in shear zones (Gibbs & Barron, 1993, Sidder, 1995; Voicu et al., 2001; Milési et al., 2003; Dardenne & Schobbenhaus, 2003; Kioe–A-Sen et al., 2016). The only probable VMS gold-copper deposit known is the Montagne d'Or in French Guiana (Guiraud et al., 2017). Artisanal small-scale miners concentrate on gold in placers and overburden, international mining companies also extract gold from the bedrock in open pits (Voicu et al., 2001; Daoust et al., 2011). Other

commodities are manganese, mostly from lateritic weathering profiles on top of gondites and manganese carbonates, which in the past have been mined in Guyana and Brazil (Scarpelli, 2017), and small itabiritic iron mineralisations. Ultramafic intercalations in the mafic volcanics and small mafic intrusions and enclaves show high Ni, Cr contents and locally chromitites but were considered uneconomic so far. In French Guiana small diamonds have been found in komatiitic volcaniclastic rocks (Capdevila et al., 1999), and the Nassau and Rosebel diamond occurrences in Suriname are possibly of the same type. Late peraluminous granitic intrusions (2.10-2.06 Ga) have Nb, Ta, Sn, Be and Li-bearing pegmatites, from which in the past Li and Be have been mined from the bedrock in small scale operations. Bauxite caps cover many outcrops of the metabasaltic rocks at the base of the greenstone sequences. Several plans exist to mine them, but none of them have been carried out so far.

Paleoproterozoic (Rhyacian) high-grade belts (2.08-2.05 Ga). A prominent sinuous E-W belt of high grade rocks runs over a distance of 1500 km from the Cauarane group in Roraima State in Brazil through the Kanuku Complex in southern Guyana into the Coeroeni Group of southwestern Suriname, the Central Guiana Granulite belt or Cauarane-Coeroeni belt (Fraga et al., 2009, 2017). It consists of amphibolite-facies to granulite facies migmatitic quartzofeldspathic and pelitic gneisses with minor amphibolites, calcsilicate rocks and quartzites, from which ages between 2.08-2.02 Ga have been obtained (Fraga et al., 2009; Kroonenberg et al., 2016). Also here Archean inherited zircons have been found (De Roever et al., 2015). The Uraricoera-Southern Guyana ranitoid-gneissic domain probably belongs to this same belt. The NE-SW trending Bakhuis Granulite Belt in Suriname shows UHT granulite-facies metamorphism along a an anti-clockwise cooling path, and shows similar ages (2.07-2.05 Ga) as the Cauarane-Coeroeni Belt (De Roever et al., 2003a; Klaver et al., 2015). There is no consensus between authors whether the Bakhuis Belt originally formed the third arm of a triple junction rift valley together with the Cauarane-Coeroeni belt or is an independent structure. Also opinions differ as to whether the high-grade belts record a second phase of the Trans-Amazonian Orogeny (Kroonenberg et al., 2016) or were formed by a continental collision with a continental block in the south in Roraima State of Brazil (Fraga et al., 2009, 2017). Mineralisation in the high-grade belts is restricted to an unusual copper-phosphate deposit in the Bakhuis Mountains (Dahlberg, 1982, 1987) and some bauxite caps on top of the granulites.

Paleoproterozoic (Early Orosirian), felsic volcanic and granitoid complexes (1.99-1.95 Ga). Another 2000 km long E-W belt, consisting of shallow-level I-type granitoid intrusions associated with ignimbritic felsic volcanics stretches from the Orinoco River in Venezuela (Cuchivero-Cairaca, respectively) through northern Roraima State (Pedra Pintada-Surumú), central Guyana (Iwokrama) to western and southern Suriname (Wonotobo-Dalbana). These rocks are associated with small gabbroic plutons, and within the Bakhuis Granulite Belt, with charnockitic and anorthositic intrusions, all showing ages around 1.98 Ga, rarely down to 1.95 Ga. (Gibbs & Barron, 1993). Also here there are different opinions about their geotectonic significance: are they a syn- or post-collision third phase of the Trans-Amazonian orogeny (Kroonenberg et al., 2016), or related to the postulated continental collision initiated from the south (Fraga et al., 2017). Nadeau et al., (2013) mention Hadean inherited zircons from the Iwokrama subvolcanic granites, also suggesting the presence of an older reworked basement. There no known mineralisations from this unit, apart from bauxite caps on top of the anorthositic intrusions in the Bakhuis Mountains.

Older platform cover: Roraima Supergroup (1.87 Ga). In the impressive Pakaraima Mountains area with their peak at 2810 metres where Brazil, Venezuela and Guyana meet, the Roraima Supergroup sandstone plateau covers an area of 73,000 sq.km (Beyer et al., 2015; Huber et al., 2018). At least 60 smaller outliers consist of the same rocks, some of them hundred kilometres removed from the main area, as in Suriname and far into Brazil. The total thickness amounts to at least 3000 m, in which up to 12 lithostratigraphic units have been discerned. Beyer et al (2015) discern two major lithostratigraphic associations: amalgamated channel and stacked deltaic-lacustrine lithofacies associations. Zircons in intercalated ash-fall tuffs show an age of 1873 Ma (Santos et al., 2003), Detrital zircons in the sandstones cluster around 2123 ± 14 Ma, suggesting that the Roraima Supergroup is essentially a molasse deposit of the Trans-Amazonian Orogeny. Diamonds are mined already since the 19th century from mature thin quartz pebble conglomerates in the lower part of the formation and from alluvial deposits of rivers draining the sandstone plateau (Santos et al., 2003). Exploration for uranium at the unconformable contact with the basement was unsuccessful (Beyer et al, 2015).

Post-Trans-Amazonian domains and events

Paleoproterozoic (Late-Orosirian) Iricoumé-Mapuera granitoid-volcanic domain (1.89-1.81 Ga). The southernmost part of the Guiana Shield east of the Rio Branco encompasses a younger domain, unrelated to the Trans-Amazonian nucleus of the Guiana Shield discussed so far. In Brazil it is characterised by 1.90 Ga I-type Água Branca plutonism, 1.89 Ga Iricoumé felsic to intermediate volcanics, the 1.87 Ga Mapuera granitoid intrusions and the 1.81 Ga A-type Madeira Intrusive Suite, including the unusual 1.81 Ga peralkaline albite granite from the Pitinga cryolite mine, bearing cryolite–zircon–cassiterite–pyroclore–columbite–xenotime mineralization (Barreto et al., 2014; Costi et al., 2010, Valério et al., 2009). This domain represents post-collisional anorogenic magnatism related to the accretion of the Rio Negro domain in the western Guiana Shield (Valério et al., 2009; see below). The Iricoumé volcanics correspond with the Kuyuwini Group in southern Guyana (Berrangé, 1977).

Paleoproterozoic (Late Orosirian-Statherian), Rio Negro high-grade belt (1.86-1.72 Ga). The Rio Negro high-grade belt in the westernmost part of the Guiana Shield straddles the borders between eastern Colombia, southern Venezuela and northeastern Brazil. It is composed mainly of amphibolite-facies migmatitic quartzofeldspathic and minor metapelitic gneisses and amphibolites, designated Mitú complex in Colombia, Minicia-Macabana-San Carlos gneisses in Venezuela and Cauaburí and Cumati gneisses in Brazil (Tassinari et al., 1996; Santos et al., 2003; Almeida et al., 2013; Kroonenberg, 2018). Their ages between 1.86-1.72 Ga and model ages reflect continental accretion of a largely juvenile block onto the older Trans-Amazonian core of the Guiana Shield during the Querarí orogeny (Tassinari et al., 1996; Almeida et al., 2013). They are intruded by the A-type Tiquié granites around 1.75 Ga and by Mesoproterozoic plutons (see below). No mineralisations are known from this unit.

Paleo-Mesoproterozoic mafic dykes. Two prominent suites of Proterozoic dolerite dykes traverse all previously mentioned rock units: the tholeiïtic Avanavero Dolerite (1783 Ma, Santos et al., 2003; Reis et al., 2013), with prominent NE-SW orientation, and the alkalibasaltic Käyser Dolerite with mainly NW orientation, mainly in Suriname (1501 Ma; de Roever et al, 2003b). The Avanavero Dolerite also intrudes conspicuously in the Roraima Supergroup in the Pakaraima Mountains and in the Tafelberg outlier in Suriname. They represent shortlived periods of extension in the shield. No mineral deposits are associated with those dykes.

Mesoproterozoic (Calymmian) granitoid intrusives (1.55-1.40 Ga) Well-defined plutons of rapakivi granites and biotite granites intrude into the Rio Negro belt, and a few also further east. The largest one, the Parguaza rapakivi granite straddles the border between Venezuela and Colombia across the Orinoco River, and covers over 30,000 sq. km. It intrudes in Trans-Amazonian granitoid and volcanic rocks and shows a range of ages between 1.55 and 1.40 Ga (Bonilla-Pérez et al (2013). Columbite-tantalite occurs in coarse crystals in 'quartz-pegmatites'. Heavy mineral concentrates from neighbouring creeks contain abundant cassiterite, Ta-rich rutile and columbite-tantalite (Pérez et al. 1985). The pluton is covered by the Pijiguaos bauxite deposit. Another 1.55 Ga rapakivi granite is the Mucajaí pluton in Roraima state (Reis et al., 2003). Unmineralised anorogenic megacryst biotite granite intrusions with ages around 1.55 Ga abound in the Rio Negro block.

Mesoproterozoic platform covers. In the Colombian-Brazilian border area several elongated plateaus of folded and slightly metamorphosed sandstone, conglomerate and minor mudstone protrude high above the surrounding lowlands, such as the Tunuí and Naquén ridges. Also the highest peak in the Guiana Shield Pico da Neblina belongs to this series. They rest unconformably, often with a tectonic contact, on top of <1.6 Ga basement rocks. The youngest detrital zircons are younger than 1.8 Ga, and metamorphic mica ages are around 1.3-1.2 Ga. Several of these plateaus are gold-bearing, mainly in placers in the conglomerates. Artisanal miners are active here. A younger, unmetamorphosed conglomeratic unit, probably of Neoproterozoic age is the Piraparaná Formation in eastern Colombia (Kroonenberg, 2018).

Nickerie-K'Mudku-Orinoquense Thermotectonic Episode (1.3-1.1 Ga) An important tectonic event affected the whole western part of the Guiana Shield up to central Suriname, testified by extensive mylonitization along shear zones and thermal resetting of Rb-Sr and K-Ar mineral ages. This event is attributed to the collision of Amazonia with Laurentia, as evidenced by a Grenvillian granulite belt in the Colombian Andes and the Subandean foredeep (Ibáñez-Mejía et al., 2011; Kroonenberg, 2018).

Meso-Neoproterozoic alkaline intrusives. As a possible corollary of the Grenvillian event, a number of alkaline to carbonatitic intrusions developed in the Guiana Shield (Cordani et al., 2010). They include Cerro Impacto in Venezuela, Seis Lagos carbonatite in Brazil, and Muri Mountains straddling the border between Brazil and Suriname. All show deep weathering mantles up to 200 m depth, which show specific mineralogy and geochemistry (high Nb, P, REE). Bossoni et al., (2017) established an U-Pb zircon maximum age of 1328 Ma for the Seis Lagos carbonatite, in the other occurrences bedrock was not attained during drilling. Nepheline syenite from the Muri Mountains (Sienito Mutum) gave an age of 1090 Ma (Nadeau, 2014). For the diamondiferous Guaniamo kimberlite in Venezuela an age of 710 Ma was obtained. This deposit is being mined extensively.

Phanerozoic Along the southeastern border of the shield Silurian , Devonian and Carboniferous sediments were deposited, as a part of the proto-Amazon basin. In Colombia the basement is overlain by the Ordovician Araracuara and Chiribiquete sandstone plateaus. A pervasive series of early Jurassic CAMP dolerite dykes, related to the opening of the Atlantic, traverses large areas of the shield. The 6000 m deep Jurassic-Tertiary Takutu graben in Guyana and Brazil divides the Guiana Shield almost in two parts, and represents a failed arm of an Atlantic triple junction.

CONCLUSIONS

The geological history of the Guiana Shield starts with an Archean event in the Imataca and Amapá blocks, followed by the pervasive Trans-Amazonian Orogeny between 2.26 and 1.98 Ga, which affected the whole northern and central part of the Shield and also overprinted the Archean rocks. This event records subduction and final collision of the Amazonian Craton with the West-African Craton, leading to the amalgamation of the Columbia supercontinent, according to paleomagnetic data. A younger event, the Querarí Orogeny (1.86-1.72 Ga) led to accretion of the Rio Negro block in the west, and also caused anorogenic magmatism along the southeastern part of the shield in the Iricoumé-Mapuera area. The Nickerie-K'Mudku tectonothermal event (1.3-1.1 Ga) records the collision of Amazonia and Laurentia. Gold mineralisation in concentrated in the Trans-Amazonian greenstone belts and in the Mesoproterozoic platform covers. Diamonds proceed from Trans-Amazonian volcaniclastic ultramafic rocks in French Guiana, from the Roraima Formation in Guyana and from the Guaniamo kimberlite in Venezuela. Iron and manganese deposits are largely formed by lateritic weathering of BIF and gondite and carbonate protores, respectively. Tin and coltan are largely bound to greenstone belt pegmatites, the Parguaza rapakivi granite and the Pitinga cryolite deposit. Bauxite caps are developed on several types of mafic and feldspathic rocks. No large sulfide deposits have been found so far.

SELECTED REFERENCES

Berrangé JP 1977 *The geology of southern Guyana, South America*. Inst. Geol. Sciences, London, Overseas Division, Mem. 4, 112p

Dardenne, MA, Schobbenhaus C, 2003. Metallogeny of the Guiana Shield. Géologie de la France 2003: 2-3-4, 291-319.

Delor, C, Lahondère D, Egal, E, Lafon, J-M, Cocherie A, Guerrot C, de Avelar V, 2003. Transamazonian crustal growth and reworking as revealed by the 1:500,000-scale geological map of French Guiana. Géologie de la France 2003, 2-3-4: 5-57.

Fraga, LM, Macambira MJB. Dall'Agnol R, Costa JBS, 2009. 1.94–1.93 Ga charnockitic magmatism from the central part of the Guyana Shield, Roraima, Brazil: Single-zircon evaporation data and tectonic implications. J. South American Earth Sciences 27: 247–257

Gibbs AK, Barron CN, 1993 *Geology of the Guiana shield*. Oxford University Press, New York., 246 pp

Kroonenberg, SB, 2018. The Proterozoic basement of the western Guiana Shield and the Northern Andes. *In*: F Cediel, RP Shaw (eds.) *Geology and Tectonics of Northwestern South America - The Pacific-Caribbean-Andean Junction*. Springer, 115-192.

Kroonenberg SB, de Roever EWF, Fraga LM, Reis NJ, Faraco MT, Lafon JM, Cordani UG, Wong TE, 2016. Paleoproterozoic evolution of the Guiana shield in Suriname: a revised model. Netherlands J Geosci – Geologie en Mijnbouw 95:491–522

Reis, NJ, Fraga LM, deFaria MSG, Almeida ME, 2003 Geologia do Estado de Roraima, Brasil. Géol. de la France 2-3-4: 121-134.

Santos JOS, 2003 Geotectônica dos Escudos das Guianas e Brasil-Central. *In*: LA Bizzi, C Schobbenhaus, RM Vidotti, JH Gonçalves (eds.) *Geologia, Tectônica e Recursos Minerais do Brasil.* CPRM, Brasília,169-226.

Sidder, GB, Garcia AE, Stoeser JW (eds.), 1995. *Geology and Mineral deposits of the Venezuelan Guayana Shield*, U.S. Geological Survey Bulletin 2124.

Tassinari, CCG, Macambira MJB, 1999. Geochronological provinces of the Amazonian Craton. Episodes, 1999: 174-182.

Voicu, G., Bardoux M, Stevenson R, 2001. Lithostratigraphy, geochronology and gold metallogeny in the northern Guiana Shield, South America: a review. Ore Geology Reviews 18: 211–236.

Magnetite geochemistry as a tool for exploration in Guyana

***Nikita L. La Cruz**
University of Michigan
Ann Arbor, MI, U.S.A.
nlacruz@umich.edu

Adam C. Simon
University of Michigan
Ann Arbor, MI, U.S.A.
simonac@umich.edu

Aaron S. Wolf
University of Michigan
Ann Arbor, MI, U.S.A.
aswolf@umich.edu

Marcus Harden
Alicanto Minerals Limited
West Perth, Western Australia
mharden@alicantominerals.com.au

SUMMARY

Magnetite is ubiquitous in mineralized systems, wherein the chemistry of magnetite reflects P-T-X conditions during mineralization and alteration. Here, we investigate the geochemistry of magnetite from 5 mining districts in Guyana, which remain under-explored owing to thick jungle cover and limited road access. Our goal is to use magnetite geochemistry to complement existing geochemical and geophysical data to identify locations for more targeted exploration. Detrital magnetite and magnetite from outcrops were sampled and analyzed using field emission scanning electron microscopy (FE-SEM) and electron-probe micro-analysis (EPMA). The analyses indicate variability in the chemistry of magnetite grains collected in individual streams.

Key words: magnetite geochemistry, exploration, indicator minerals

INTRODUCTION

There are still many questions regarding the geology and ore deposit potential of Guyana. Exploration in Guyana is challenging because the country is heavily forested and there is also a paucity of outcrops which results from high weathering rates due to the tropical climate in this region. Nonetheless, researchers have noted that the geology of Guyana, and particularly the early Proterozoic greenstone belts present in Guyana, and the Guiana Shield, is similar to many late Archean greenstone belts (Gibbs, 1987). Mining in Guyana has historically focused on gold; however, other commodities mined include bauxite, diamonds, and manganese. However, Gibbs (1987) noted that geologic evidence, e.g., synvolcanic hydrothermal activity, suggests that volcanogenic sulphide deposits may be present in Guyana. Sulphides are in important class of minerals present in many ore deposits. Therefore, sulphide saturation and the exsolution of a sulphide melt are integral processes in the formation of some ore deposits, e.g., nickel copper platinum group element deposits (Ni-Cu-PGEs). Additionally, Jenner et al. (2010) show that magnetite crystallization can result in sulphide saturation, and further that the trace element chemistry of the magnetite can be indicative of the occurrence of this process.

Magnetite is a ubiquitous mineral in many geologic and ore deposit environments. Grisby (1990) suggested that detrital magnetite can be used as a petrogenetic indicator. Since that publication, many researchers have shown that magnetite geochemistry is useful as a petrogenetic indicator and as a tool for exploration (Razjigaeva and Naumova, 1992; Beaudoin and Dupuis, 2007; Dupuis and Beaudoin, 2011; Dare et al., 2012; Nadoll et al., 2012, 2014; Boutroy et al., 2014; and references therein). Dupuis and Beaudoin (2011) and Nadoll et al. (2014) investigated the chemistry of magnetite from different ore environments and proposed specific minor and trace elements that may be used to discriminate magnetite from different ore environments. The goal of this project is to investigate the geochemistry of magnetite grains from catchments in Guyana to aid in regional exploration. In this orientation study, we use magnetite geochemistry and the plots proposed by Dupuis and Beaudoin (2011) and Nadoll et al. (2014) to determine the ore deposit potential of the catchments sampled in order to develop more targeted exploration programs.

METHODS

We analysed magnetite from rocks and detrital grains collected throughout Guyana. Rock samples were collected in the North West mining district, while detrital grains were collected from streams in mining districts in the North West, Cuyuni, Mazaruni, Potaro and Rupununi mining districts. The rocks samples were cut to produce thick (100µm) sections for analyses, and detrital magnetite grains were mounted in epoxy.

The magnetite grains were characterized using back-scattered electron (BSE) imaging and energy-dispersive X-ray spectrometry (EDS) point analyses by using the JEOL JSM – 7800FLV Field-Emission Scanning Electron Microscope (FE-SEM) at the University of Michigan Electron Microbeam Analysis Laboratory (EMAL) with an accelerating voltage of 15kV. Representative magnetite grains from each sample analysed via FE-SEM were analysed by using the EMAL Cameca SX100 electron probe micro-analyser (EPMA) in wavelength-dispersive X-ray spectrometry (WDS) mode. The concentrations of Fe, Ti, V, Mn, Ca, Ni, Cu, Cr, Zn, Al, Mg, and Si were measured by using an accelerating voltage of 20 keV, a beam current of 30 nA and a focused electron beam.

RESULTS AND INTEPRETATIONS

Energy-dispersive X-ray spectrometry (EDS) point analyses indicate the presence of magnetite of variable chemical compositions in most stream samples, and a few of the rock samples analysed. Further, in catchments where magnetite from both rock and stream samples were analysed, some detrital grains have chemical composition similar to that of magnetite grains from rock samples. The analyses also indicate presence of sulphide (pentlandite, pyrrhotite, pyrite, chalcopyrite, sphalerite, bornite, chalcocite), apatite, cobaltite, titanate, monazite, allanite, zircon, and gold grains associated with magnetite and other phases present in samples, e.g. ilmenite, rutile, quartz. The presence of sulfides and other inclusions in detrital magnetite grains likely indicate the presence of mineralization types and/or alteration halos in the catchment areas being sampled.

The geochemical data obtained for individual catchments were compared with the fields representing the composition of magnetite from a variety of ore deposits, including Ni-Cu-PGE, volcanogenic massive sulphide (VMS), Kiruna-type, Fe-Ti, V, iron oxide copper gold (IOCG), banded iron formation (BIF), Skarn, after Dupuis and Beaudoin (2011) and Nadoll et al. (2014). These comparisons indicate similarities in the chemistry of the magnetite grains analysed with that for magnetite from the aforementioned classes of deposits.

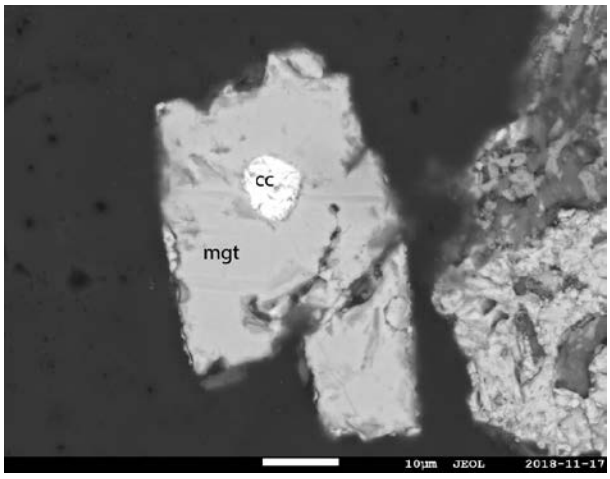

Figure 1. Detrital magnetite grain from north western Guyana with chalcocite inclusion.

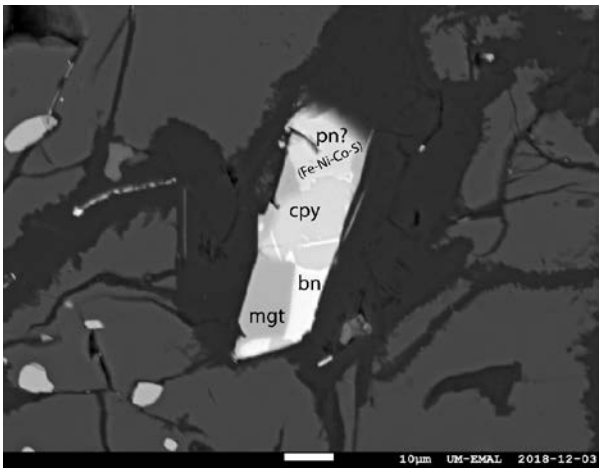

Figure 2. Multiphase assemblage (magnetite, bornite, chalcopyrite and cobalt enriched pentlandite) in rock sample from north western Guyana. The assemblage observed here can be explained by the cooling and crystallization of magma derived sulphide liquid (Barnes et. al., 2017).

This work is still on going, however, the interpretations of the data thus far indicate potential presence of a few classes of deposits, which have not been previously mined in Guyana (e.g., Ni-Cu-PGE, Fe-Ti, V and porphyry). The presence of sulphide minerals in magnetite and other phases in both detrital and rock samples, and the presence of assemblages similar to differentiated sulphide globules in rock samples, indicate equilibration of sulphide liquids with the magmas that constitute the rocks in the catchments sampled. This is an important ingredient for the formation of Ni-Cu-PGE deposits and other sulphide bearing ore deposits.

We will analyse the magnetite grains via laser ablation inductively coupled plasma mass spectrometry (LA-ICP-MS). The EPMA and LA-ICP-MS data will be compared to a global database containing magnetite geochemical data for ~240 ore deposits. We will conduct robust statistical analyses, including principle component analyses, to better determine the ore deposit potential of the catchments sampled.

ACKNOWLEDGMENTS

We thank Owen Neill for assistance with EPMA analyses.

REFERENCES

Barnes, S.J., Holwell, D.A., and Le Vaillant, M., 2017, Magmatic sulfide ore deposits: Elements, 13(2), 89-95.

Beaudoin, G., and Dupuis, C., 2007, Geochemical signature of iron oxides and application to mineral exploration-2nd component: DIVEX annual report (Subproject SC22), 2-13.

Boutroy, E., Dare, S.A., Beaudoin, G., Barnes, S.J., and Lightfoot, P.C., 2014, Magnetite composition in Ni-Cu-PGE deposits worldwide: application to mineral exploration: Journal of Geochemical Exploration, 145, 64-81.

Dare, S.A., Barnes, S.J., and Beaudoin, G., 2012, Variation in trace element content of magnetite crystallized from a fractionating sulfide liquid, Sudbury, Canada: Implications for provenance discrimination: Geochimica et Cosmochimica Acta, 88, 27-50.

Dupuis, C., and Beaudoin, G., 2011, Discriminant diagrams for iron oxide trace element fingerprinting of mineral deposit types: Mineralium Deposita, 46(4), 319-335.

Gibbs, A.K., 1987, Proterozoic volcanic rocks of the northern Guiana Shield, South America: Geological Society, London, Special Publications, 33(1), 275-288.

Grigsby, J.D., 1990, Detrital magnetite as a provenance indicator: Journal of Sedimentary Research, 60(6), 940-951.

Jenner, F.E., O'neill, H.S.C., Arculus, R.J., and Mavrogenes, J.A., 2010, The magnetite crisis in the evolution of arc-related magmas and the initial concentration of Au, Ag and Cu: Journal of Petrology, 51(12), 2445-2464.

Nadoll, P., Angerer, T., Mauk, J.L., French, D., and Walshe, J., 2014, The chemistry of hydrothermal magnetite: A review: Ore Geology Reviews, 61, 1-32.

Nadoll, P., Mauk, J.L., Hayes, T.S., Koenig, A.E., and Box, S.E., 2012, Geochemistry of magnetite from hydrothermal ore deposits and host rocks of the Mesoproterozoic Belt Supergroup, United States: Economic Geology, 107(6), 1275-1292.

Razjigaeva, N.G., and Naumova, V.V., 1992, Trace element composition of detrital magnetite from coastal sediments of northwestern Japan Sea for provenance study: Journal of Sedimentary Research, 62(5), 802-809.

Sr-Nd-Hf isotopic tracing of Archean continental crust in the Brazilian part of the Southeastern Guyana Shield: A review

Jean Michel Lafon*
Geoscience Institute – UFPA
66075 - Belém, Brazil.

lafonjm@ufpa.br

Lucia Travassos da Rosa-Costa
CPRM – Geological Survey of Brazil
66095-110 – Belém, Brazil

ltravassos@be.cprm.gov.br

João Marinho Milhomem Neto
Geoscience Institute – UFPA
66075 - Belém, Brazil

milhomem@ufpa.br

SUMMARY

The compilation of Sr-Nd-Hf isotopic signatures led to distinguish the main episodes of crustal generation and reworking in the Brazilian part of the Southeastern Guyana Shield. In the Archean Amapá block, at least two episodes of crust generation are evidenced in the Eoarchean (~ 4.0 Ga) and the Mesoarchean (3.0-3.1 Ga). In the Rhyacian Lourenço and Carecuru domains, magmatic rocks are derived from mixed Rhyacian juvenile sources with Archean crustal components. In the Orisirian Erepecuru-Trombetas domain, magmatic rocks are originated from melting of mantle-derived magmas with participation of Rhyacian sialic crust and the existence of an Archean basement is discarded.

Keywords: Southeastern Guiana Shield, Archean, Paleoproterozoic, crustal evolution, Sr-Hf-Nd isotopic signature

INTRODUCTION

The Amazonian Craton is composed by two shields, the Guyana Shield in the North and the Brazil Central Shield in the South separated by the Paleozoic Solimões-Amazonas basin. The occurrence of Archean terrains in the Amazonian Craton is restricted to its eastern part. The most prominent Archean area has been enclosed in the Central Amazonian Province that consists of the Carajás block in the Brazil Central Shield and the Xingu-Iricoumé block in the Guyana Shield (Tassinari and Macambira, 2004). On the edges of this Archean nucleus, Proterozoic mobile belts were agglutinated to form the Amazonian Craton. The unique preserved, not reworked Archean crust is restricted to the Carajás region and its extension to the whole Central Amazonian Province is still under debate (Macambira and Lafon, 2017; Leal et al., 2018). In the Guyana Shield the main records of Archean crust are located in the Imataca terrane (eastern Venezuela; 2.6-3.7 Ga; Tassinari et al., 2004) and Amapá Block (north of Brazil; 2.6-3.5 Ga; Rosa-Costa et al., 2006), both inserted in the Maroni-Itacaiúnas/Transamazonas geotectonic Province, according to the current models of geotectonic partitioning of the Amazonian Craton (Tassinari and Macambira, 2004; Santos et al. 2006). The Maroni-Itacaiúnas/Transamazonas Province is a widespread orogenic belt developed and accreted to the Central Amazonian Province during the Transamazonian orogenic cycle (2.26–1.95 Ga). In southeastern Guyana Shield (SGS) the Transamazonian evolution began with an Early stage of oceanic crust formation at 2.26-2.20 Ga. Greenstone belts and associated TTG suites reflect the consumption of this oceanic crust in a subduction context at 2.19-2.13 Ga. This stage may have continued up to 2.1 Ga in northern Brazil (Amapá state). Widespread granitic magmatism and migmatization prevailed at 2.10-2.08 Ga, with contemporaneous formation of pull apart basins in a tectonic context dominated by sinistral shearing. The formation of granulite complexes and associated charnockitic magmatism, including UHT assemblages in northwest Suriname, is the final product of continental shearing at 2.08-2.06 Ga, probably reflecting crustal stretching and mantle upwelling. Late granitic magmatism also marks the end of the Transamazonian event at 2.06-1.99 Ga (Vanderhaeghe et al. 1998; Delor et al. 2003). The Brazilian part of the SGS has been partitioned in domains within the geotectonic provinces. It encloses the Archean Amapá block surrounded respectively at north and south by two Rhyacian domains, namely the Lourenço and the Carecuru domains. Westward, the Carecuru Domain is limited by the Orosirian Erepecuru-Trombetas domain (Central Amazon Province), however, the border is not clearly established due to the lack of geological and geochronological information. Even considering the recent improvement of geological knowledge, the Erepecuru-Trombetas Domain remain poorly understood and may be considered as one of the least known of the Amazonian Craton.

The aim of this paper is to present an up-to-date compilation of the Sr-Nd-Hf isotopic records, with emphasis to recent Hf isotopic data in zircon, of Archean continental crust in the Brazilian part of the SGS and to estimate the extension of the influence of this Archean continental crust in the Paleoproterozoic domains. In addition, the geotectonic partitioning of the Brazilian part of the SGS is discussed at the light of the Sr-Nd-Hf isotopic signatures.

METHOD AND RESULTS

Previously published Sr-Nd-Hf isotopic results of Brazilian sectors of the SGS are compiled from scientific papers and reports of geological mapping projects conducted by the Geological Survey of Brazil (CPRM). In addition, unpublished results from Master and PhD theses focused on the Archean and Paleoproterozoic domains of the SGS are also reported. The Sr isotopic data are presented as Sr-T_{UR} model ages (UR = uniform reservoir – DePaolo and Wasserburg, 1977) and the Nd-T_{DM} model ages were calculated according to the model of DePaolo (1981) for depleted Mantle. The crystallization ages used for the calculation of the ε_{Nd} values were those obtained by U-Pb or Pb-Pb zircon dating or they have been inferred when not available. The zircon Hf-T_{DM}^{C} two-stage crustal model ages and corresponding ε_{Hf} were determined using decay constant of 1.867×10^{-11} $year^{-1}$, present-day $^{176}Lu/^{177}Hf$ of 0.0336 and $^{176}Hf/^{177}Hf$ of 0.282785 for the chondritic uniform reservoir - CHUR and $^{176}Lu/^{177}$ Hf of 0.0388 and $^{176}Hf/^{177}Hf$ of 0.28325 for the

depleted mantle - DM. For crustal model ages (T_{DM}^{C}) a $^{176}Lu/^{177}Hf$ ratio of 0.015 was assumed as a continental crust average value (Vervoot and Kemp, 2016 and reference herein).

- The Archean Amapá Block is a large continental landmass roughly oriented in a WNW-ESE direction, approximately 200 km wide and at least 400 km long. It consists mainly of Meso- to Neoarchean high-grade metamorphic complexes, strongly reworked during the Transamazonian orogeny. The tectono-stratigraphic associations include TTG-like orthogneisses, ortho and para derived granulite gneisses, charnockites, granitic orthogneisses and Neoarchean granites. Metavolcano-sedimentary sequences and granitoids form a Paleoproterozoic orogenic association. Three main magmatic episodes were defined by U-Pb and Pb-Pb zircon dating, two in the Mesoarchean (~3.19 Ga and ~2.85 Ga) and one in the Neoarchean (~2.69-2.65 Ga) (Avelar et al., 2003; Rosa-Costa et al., 2006, Milhomem Neto and Lafon, in press). Isolated U-Pb and Pb-Pb zircon ages around 3.32 and 3.49 Ga indicate the existence of some Paleoarchean crustal remnants (Rosa-Costa et al., 2017, Milhomem Neto and Lafon, in press). Nd-T_{DM} ages in the Mesoarchean and Neoarchean basements range, respectively, from 3.51 Ga to 2.94 Ga ($-3.97 < \varepsilon_{Nd} < +1.01$) and from 3.32 Ga to 2.83 Ga ($-11.23 < \varepsilon_{Nd} < -0.20$) and point to a main Mesoarchean episode of crustal growth while Neoarchean is dominated by crustal reworking. Nd-T_{DM} ages of the Rhyacian granitoids between 3.32 and 2.22 Ga ($-11.41 < \varepsilon_{Nd} < +1.96$) indicate mixing of Paleoproterozoic and Archean components in their source (Avelar, 2002; Avelar et al. 2003; Rosa-Costa et al. 2006; 2017; Milhomem Neto and Lafon, in press). Sr-T_{UR} model ages between 3.55 and 2.37 Ga for Archean and Paleoproterozoic units also account for the strong fingerprint of an Archean continental crust (Avelar 2002 and reference herein). The recent Lu-Hf isotopic data in zircon from magmatic rocks furnished predominant subchondritic ε_{Hf} values that indicate prevalent crustal reworking processes during their formation. The Hf-T_{DM}^{C} ages argue for at least two episodes of mantle extraction and continental crust generation in the Eoarchean (~ 4.0 Ga) and in the Mesoarchean (around 3.0-3.1 Ga). In addition, the Hf isotopic signatures suggest the existence of two Archean crustal segments geographically distinct, respectively in the southwest and northeast of the Amapá Block, which were aggregated at some time in the Archean to form the current Amapá Block configuration (Milhomem Neto and Lafon, in press).

- The Rhyacian Lourenço domain underwent a Transamazonian evolution roughly similar to that proposed by Vanderhaeghe et al, (1998) and Delor et al, (2003) for the French Guyana. However, the early oceanic stage around 2.26 Ga has not been recognized in the Lourenço domain. Greenstone belt sequences and widespread TTG-like magmatism developed in a magmatic arc environment since, at least, 2.19 Ga and may have persisted until 2.10 Ga. In the meantime, granitic magmatism and migmatization of earlier TTG-like granitoid-greenstone sequences occurred in response to tectonic accretion by collision of the newly formed continental arcs. A collisional - post-collisional stage, poorly constrained by the radiometric data, was registered around 2.08 and 2.02 Ga (Barreto et al. 2013, Rosa-Costa et al. 2017). This late stage coincides with the high-grade metamorphic event in western Suriname (de Roever et al., 2003; Klaver et al., 2015), which is also registered within the Lourenço domain (Oliveira et al., 2008). In its southern-central part, granites displaying positive ε_{Nd} values and Nd-T_{DM} ages younger than 2.50 Ga are limited to some early TTG-like granitoids while Archean Nd-T_{DM} ages ($-15.37 < \varepsilon_{Nd} < -1{,}51$) between 3.47 and 2.51 Ga are widespread and available Sr-T_{UR} ages are almost lower than 2.40 Ga (Nogueira et al. 2000; Avelar 2002; Barreto et al. 2013; Rosa-Costa et al. 2017). The Hf isotopic data in zircon of plutonic rocks furnished subchondritic ε_{Hf} values (-12.6 to -0.4) and Hf-T_{DM}^{C} ages from 2.67 Ga to 3.36 Ga revealing a strong influence of the Archean continental crust of the Amapá block. Such isotopic signatures together with the existence of inherited zircons as old as 3.05 Ga in some granitoids indicate mixing of Paleoproterozoic juvenile sources with Archean crustal components. In the northwestern part of the Lourenço domain at the frontier with French Guyana, positive ε_{Nd} values (+0.47 to + 4.28) and Nd-T_{DM} ages between 2.09 Ga and 2.35 Ga are prominent while granitoids with negative ε_{Nd} values and Archean Nd-T_{DM} ages are scarce (Avelar 2002, Lafon et al. 2003; Faraco and Théveniaut, 2011). The available Sr-T_{UR} ages are between 1.82 and 2.47 Ga (Avelar 2002 and reference herein). Positive to slightly negative ε_{Hf} values (-2.4 to +2.9) and younger Hf-T_{DM}^{C} model ages (from 2.52 to 2.82 Ga) also indicate a lower contribution of Archean components in the source of the Transamazonian magmatic rocks (Milhomem Neto and Lafon, in press). However, the Archean signature does not disappear totally according to Archean Pb-Pb ages of detrital zircon in a quartzite and negative ε_{Nd} values (-10.0 to -3.4) in metapelites from greenstone belts in the borderland of SE French Guyana with northern Brazil (Avelar et al., 2003; Delor et al., 2003).

- The Rhyacian Carecuru Domain represents a granitoid-greenstone terrane, developed in a magmatic arc setting that was accreted to the southwestern border of the Amapá Block during the Transamazonian event (Rosa-Costa et al., 2006). It consists mainly of calc-alkaline gneisses and granitoids formed between 2.19 and 2.14 Ga and supracrustal sequences constituted by mafic and intermediate metavolcanics. A large supracrustal belt, which marks the boundary between the Amapá Block and the Carecuru Domain, also comprises meta-sedimentary rocks (Ipitinga Group). Several granite plutons, one of them dated at about 2.10 Ga, cross-cut the calc-alkaline granitoids and supracrustal belts. The calc-alkaline rocks present Nd-T_{DM} ages between 2.28 and 2.50 Ga, with positive to slightly negative ε_{Nd} values (-0.84 to +1.63), revealing the participation of juvenile mantle-derived magmas and minor Archean components in their source (Rosa-Costa et al., 2006). On the other hand, the late Transamazonian syenogranite (2.10 Ga) exhibits a Nd-T_{DM} age of 2.83 Ga, within the range of model ages furnished by Archean rocks of the southern Amapá block. The strongly negative ε_{Nd} value of −6.61 indicates partial melting of Archean crust in the source of this granite. The Carecuru Domain contains an Archean inlier composed of granulitic orthogneisses derived from 2.60 Ga old igneous precursors and host 2.07 Ga charnockite plutons (Rosa-Costa et al., 2006, 2017). Most of the Nd-T_{DM} ages of the orthogneisses and charnockite plutons are between 2.61 and 2.83 Ga ($-5.89 < \varepsilon_{Nd} < -1.16$), beside one trondjhemitic gneiss which furnished a Nd-T_{DM} age of 2.32 Ga ($\varepsilon_{Nd} = +1.17$). A tonalitic orthogneiss furnished suprachondritic ε_{Hf} values up to +4.15 with Siderian to Neoarchean Hf-T_{DM}^{C} ages. On the other hand, a coeval diorite exhibited lower ε_{Hf} values (-1.0 to +0.3), Hf-T_{DM}^{C} ages (2.69 to 2.77 Ga) and Nd-T_{DM} (2.5 Ga) entirely Neoarchean. These Hf-Nd isotopic signatures indicate that the arc-related magmatism in the Carecuru domain resulted from mixing between Rhyacian juvenile magmas and Archean crustal components (Milhomem Neto and Lafon, in press).

- The Orosirian Erepecuru-Trombetas domain is limited at west by the Uatumã-Anauã Domain, which belongs to the Orosirian Tapajós-Parima/Ventuari-Tapajós Province (Reis et al., 2006) and at east by the Rhyacian Carecuru Domain. These limits are not clearly established due to the lack of geological and geochronological information. The Erepecuru-Trombetas Domain is constituted

by Archean (?) and/or Paleoproterozoic basement units, two distinct Orosirian magmatic associations, Paleoproterozoic and Paleozoic sedimentary rocks, mafic rocks, diabases and nepheline syenites. In the southwestern portion, the Orosirian magmatic associations are the most widespread rocks, whereas the basement units and the Paleozoic rocks are not found. The older association (2.0–1.97 Ga) is composed of granitic rocks of the Caxipacoré Suite and effusive/pyroclastic rocks of the Igarapé Paboca Formation. These rocks have a high-K to shoshonitic, calc-alkaline signature (Leal et al., 2018 and references herein). The Mapuera and Água Branca granitic suites and Iricoumé volcanics represent the younger association (1.90-1.87 Ga). The Mapuera and Iricoumé rocks share similar geochemical features with high-K and A-type affinity and the Água Branca granitoids consists of high-K and I-type calc-alkaline magmatism. The geochemical characteristics of the older Orosirian magmatism suggest that it formed in an orogenic tectonic setting, related to a subduction environment, while those of the younger Orosirian magmatism betray the evolution from a convergent context to an extensional intracontinental environment. Nd-T_{DM} (2.13–2.52 Ga) and Sr-T_{UR} (1.95–2.14 Ga) ages and ε_{Nd} values (-3.88 to +0.66) for the older Orosirian magmatism point to an origin from melting of mantle-derived magmas with participation of Rhyacian sialic crust. The younger Orosirian magmatic rock display Nd-T_{DM} (1.95–2.39 Ga) and Sr-T_{UR} (1.84–2.26 Ga) ages and ε_{Nd} (+2.92 to −3.73) that indicate parental magmas derived from melting of dominantly Rhyacian crustal sources with minor mantle contribution (Vianna et al. 2017; Leal et al. 2018 and reference herein). Excepting the Archean Nd-T_{DM} age of 2.94 Ga of one sample of the Iricoumé volcanics (Castro et al. 2014), Archean Nd-T_{DM} ages and Archean inherited zircon are lacking in the magmatic rocks of this part of the SGS.

IMPLICATIONS FOR THE EVOLUTION OF THE SOUTHEASTERN GUYANA SHIELD.

The Nd-Hf isotopic data led to a reappraisal of the early evolution of the continental crust in the SGS. the Hf-T_{DM}^{C} ages argue for at least two episodes of mantle extraction and continental crust generation during the Archean, an older one in the Eoarchean (~ 4.0 Ga) and a younger one in the Mesoarchean (3.0-3.1 Ga). The recognition of an Eoarchean episode (~4.0 Ga) of continental crust formation in the southeasternmost part of the Guyana Shield was not recorded by whole-rock Sm-Nd data, which were restricted to the Meso-Paleoarchean (2.83-3.51 Ga). Although younger than the Hf-T_{DM}^{C} ages in zircon, Nd-T_{DM} ages already gave a good indication that there were two distinct periods of continental crust formation in the SGS: A Mesoarchean episode, between 2.83 and 3.11 Ga, almost coincident with the Lu-Hf data, and a Paleoarchean or older episode revealed by the ages between 3.29 and 3.51 Ga much younger than those indicated by the Lu-Hf data. In the Guyana Shield, a Hadean zircon xenocryst with an U-Pb age of 4.22 Ga, along with zircon xenocrysts of Archean age (2.51-3.81 Ga) were identified in felsic volcanics and granitoids of the Paleoproterozoic Iwokrama Formation in southern Guyana (Nadeau et al., 2013). According to these authors, it demonstrates the existence of an underlying "Lost Hadean Crust". This Hadean-Eoarchean record implies that the geotectonic evolution of the Guyana Shield started at least 500 Ma earlier than previously proposed and suggests that this older crust may be more extensive in the Guyana Shield as more than 1000 km separate the two areas. However, such ancient crustal records are the only ones described for the entire Amazonian Craton, so far. In the Lourenço and Carecuru domains, The Lu-Hf data of magmatic rocks pointed to the predominance of crustal reworking processes (67% of $\varepsilon_{Hf} < 0$). The Hf-T_{DM}^{C} model ages were found to be mostly Archean (98.4%), even for zircon with positive ε_{Hf} values. In the south/southeast of the Lourenço Domain and in the Carecuru Domain, the Sr-Nd-Hf isotopic signatures and Hf-T_{DM}^{C} ages are in agreement with a continental magmatic arc environment, where assimilation of Archean crust of distinct ages and proportions is involved in the Rhyacian magmatism. In the northwestern part of the Lourenço domain, the Sr-Nd-Hf isotopic data are consistent with the Paleoproterozoic juvenile domain in French Guyana and Suriname mainly related to Mesorhyacian island arcs. In this latter domain, most of Nd-T_{DM} ages range from 2.40 Ga to 2.15 Ga with positive to slightly negative ε_{Nd} values (-0.37 to +3.41). Available Sr-T_{UR} ages of magmatic and metamorphic rocks are systematically lower than 2.26 Ga. An Archean fingerprint is displayed only locally by some negative ε_{Nd} values and Archean detrital zircons in metasedimentary rocks and by negative ε_{Nd} values and inherited Archean zircon in granitoids. However, the suprachondritic Hf-Nd isotopic signatures with Rhyacian to Neoarchean T_{DM} ages of magmatic rocks of the northwestern part of the Lourenço domain, at the border with French Guyana, indicate the participation of crustal material from the Amapá Block probably by sediments incorporation in island arc environment, as it has also been recorded in the northwest of Suriname and in some Birimian terrains of West African Craton (Klaver et al, 2015; Petersson et al. 2018). In the Erepecuru-Trombetas domain, Rhyacian Nd-T_{DM} and Sr-T_{UR} ages and Sr-Nd isotopic signatures for granitic and volcanic rocks from both older Orosirian (2.0–1.97 Ga) and younger Orosirian (1.90–1.87 Ga) episodes, together with the geochemical characteristics, point to an orogenic context related to a subduction setting for the older episode, followed by an intracontinental magmatism related to extensional tectonics for the younger episode. For all magmatic rocks, the Sr-Nd isotopic data preclude the involvement of Archean sources. The geochemical, isotopic and temporal similarities with the adjacent Uatumã-Anauá Domain indicate that the western limit of the Erepecuru-Trombetas does not exist and both domains likely belong to the same geotectonic province. In addition, the Nd signature and the lack of Archean inherited zircon in the magmatic rocks do not favor the existence of an Archean basement in this part of the SGS. Therefore, this set of data suggests that the Archean Central Amazon Province should not be extended to the Guyana Shield.

REFERENCE

Avelar, V.G., 2002. Geocronologia Pb–Pb em zircão e Sm–Nd em rocha total da porção centro-norte do Estado do Amapá-Brasil: Implicações para a evolução geodinâmica do setor oriental do Escudo das Guianas. Ph.D. thesis, UFPA - Brazil. 213 p.

Avelar, V.G., Lafon, J.M., Delor, C., Guerrot, C., Lahondère, D. 2003. Archean crustal remnants in the easternmost part of the Guiana Shield: Pb–Pb and Sm–Nd geochronological evidence for Mesoarchean vs. Neoarchean signatures. Géologie de la France 2-3-4, 83-100.

Barreto, C.J.S., Lafon, J.M., Rosa-Costa, L.T., Dantas, E.L., 2013. Paleoproterozoic granitoids from the northern limit of the Archean Amapá block (Brazil), Southeastern Guyana Shield: Pb-Pb evaporation in zircons and Sm-Nd geochronology. Journal of South American Earth Sciences 45, 97-116.

Castro, J.M.R., Silva, R.C.S., Rosa-Costa, L.T., Barbosa, J.P.O., 2014. Mapa geológico da folha Rio Trombetas–SA.21-X-A. Belém, CPRM-Serviço Geológico do Brasil, Programa Geologia do Brasil. Escala 1 250.000.

DePaolo, D.J., 1981. Nd isotopic studies: some new perspectives on Earth structure and evolution. EOS 62, 137–145.

DePaolo, D.J., Wasserburg, G.J., 1977. The sources of island arcs as indicated by Nd and Sr isotopic studies. Geophysical Research Letters. 4 (10), 465–468.

De Roever, E.W.F., Lafon, J.-M., Delor, C., Rossi, P., Cocherie, A., Guerrot, C. & Potrel, A., 2003a. The Bakhuis ultra-high temperature granulite belt: I Petrological and geochronological evidence for a counterclockwise P-T path at 2.07–2.05 Ga. Géologie de la France 2003 2-3-4, 175–205.

Faraco, M.T.L., Théveniaut, H. 2011. Geologia da porção brasileira da Folha Oiapoque, NA.22-V-B, estado do Amapá, escala 1:250.000. Belém: CPRM – Serviço Geológico do Brasil. 112p.

Klaver, M., Roever, E.W.F., Nanne, J.A.M., Mason, P.R.D., Davies, G.R., 2015. Charnockites and UHT metamorphism in the Bakhuis Granulite Belt, western Suriname: Evidence for two separate UHT events. Precambrian Research 262, 1-19. Lafon, J.M.; Delor, C.; Theveniaut, H.; Krymsky, R., Tavares, R.P.S., Roig, J.Y. 2003. Isotopic deciphering of Rhyacian crustal evolution along the northern oyapok river: new constraints from Sm-Nd, U-Pb and Pb-Pb geochronology. In: 8th Simpósio de Geologia da Amazônia, Manaus. Abstract volume. CD-ROM.

Leal, R.E., Lafon, J.M., Rosa-Costa, L.T., Dantas, E.L. 2018. Orosirian magmatic episodes in the Erepecuru-Trombetas Domain (Southeastern Guyana Shield): implications for the crustal evolution of the Amazonian Craton. Journal of South American Earth Sciences 85, 278-297

Macambira, M.J.B., Lafon, J.M., 2017. Avaliação da extensão da Província Amazônia Central com base em isótopos de Nd. In: 15th Simpósio de Geologia da Amazônia, Belém. Abstract volume. CD-ROM.

Milhomem Neto, J.M.; Lafon J.M. 2018. Zircon U-Pb and Lu-Hf isotope constraints on Archean crustal evolution in Southeastern Guyana Shield. Geoscience Frontiers. Accepted for publication.

Nadeau, S., Chen, W., Reece, J., Lachhman, D., Ault, R., Faraco, M.T.L., Fraga, L.M., Reis, N.J., Betiollo, L.M., 2013. Guyana: the Lost Hadean crust of South America? Brazilian Journal of Geology 43(4), 601-606.

Nogueira S.A.A., Bettencourt J.S., Tassinari C.C.G. 2000. Geochronology of the granitoid hosted Salamangone gold deposit Lourenço District Amapá, Brazil. Revista Brasileira de Geociências, 30(2), 261-264.

Oliveira, E.C., Lafon, J.M., Gioia, S.M.C.L., Pimentel, M.M., 2008. Datação Sm-Nd em rocha total e granada do metamorfismo granulítico da região de Tartarugal Grande, Amapá Central. Revista Brasileira de Geociências 38, 116–129.

Petersson, A., Scherstén, A., Kemp, A.I.S., Kristinsdóttira, B., Kalvigc, P., Anum, S., 2016. Zircon U–Pb–Hf evidence for subduction related crustal growth and reworking of Archaean crust within the Palaeoproterozoic Birimian terrane, West African Craton, SE Ghana. Precambrian Research 275, 286–309.

Reis, N.J., Almeida, M.E., Riker, S.R.L., Ferreira, A.L., 2006. Geologia e Recursos minerais do Estado do Amazonas. CPRM, Manaus (Convênio CPRM/CIAMA). Escala 1:1.000.000. 125p.

Rosa-Costa, L.T., Chaves, C.L., Silva, C.M.G., Campos L.D., Abrantes, B.K.C., Tavares, F.M., Lago, A.L. 2017. Áreas de Relevante Interesse: Mineral Reserva Nacional do Cobre e Associados. Informe de recursos minerais - Série Províncias Minerais do Brasil, n° 12. CPRM - Serviço Geológico do Brasil, Belém.182p.

Rosa-Costa, L.T., Chaves, C.L., Klein, E.L., 2014. Geologia e recursos minerais da Folha Rio Araguari – NA.22-Y-B, Estado do Amapá, Escala 1:250.000. Belém: CPRM. 159p

Rosa-Costa, L.T., Lafon, J.M., Delor, C., 2006. Zircon geochronology and Sm-Nd isotopic study: further constraints for the geodynamical evolution during Archean and Paleoproterozoic in the Southeast of Guiana Shield, north of Brazil. Gondwana Research 10, 277-300.

Santos, J.O.S., Hartmann, L.A., Faria, M.S., Riker, S.R., Souza, M.M., Almeida, M.E., McNaugthon, N.J., 2006. A compartimentação do cráton amazonas em províncias: avanços ocorridos no período 2000–2006. In: 9th Simpósio de Geologia da Amazônia, Belém. Abstract volume.

Tassinari, C.C.G., Macambira, M.J.B., 2004. A evolução tectônica do Cráton Amazônico. In: Mantesso, Neto V., Bartorelli, A., Dal Ré Carneiro, C., Neves, B.B.B. (Eds.), Geologia do continente Sul-Americano: evolução da obra de Fernando Flávio Marques de Almeida. São Paulo, Beca, pp. 471–485.

Tassinari, C.C.G., Munhá, J.M.U., Teixeira, W., Palacios, T., Nutman, A., Sosa, S.C., Santos, A.P., Calado, B.O., 2004. The Imataca Complex, NW Amazonian Craton, Venezuela: crustal evolution and integration of geochronological and petrological cooling histories. Episodes 27, 3–12.

Vanderhaeghe, O., Ledru, P., Thiéblemont, D., Egal, E., Cocherie, A., Tegyey, M., Milési, J., 1998. Contrasting mechanism of crustal growth Geodynamic evolution of the Paleoproterozoic granite–greenstone belts of French Guiana. Precambrian Research 92, 165-193.

Vervoort, J.D., Kemp, A.I.S., 2016. Clarifying the zircon Hf isotope record of crust–mantle evolution. Chemical Geology 425, 65–75.

Vianna, S.Q., Magalhães, L.B., Lafon, J.M., Rosa-Costa, L.T. 2017. Geocronologia U-Pb e Pb-Pb e geoquímica isotópica Sr-Nd da porção oeste do domínio Erepecuru - Trombetas, Província Amazônia Central, noroeste do Pará. In: 15th Simpósio de Geologia da Amazônia, Belém. Abstract volume. CD-ROM.

From Small scale miners to Discovery: the Nassau Project and the Discovery of the Merian Mine

Dennis. J. LaPoint
Appalachian Resources LLC
P.O. Box 3810 Chapel Hill, NC USA 27515

dennis.lapoint@gmail.com

SUMMARY

Súralco, the Suriname subsidiary of Alcoa, discovered the Merian 2 deposit and initiated the regional exploration that eventually led to other district discoveries and development by Newmont of the Merian mine. In 1999, the author travelled to the region to determine the gold potential for Alcoa. Alcoa had a bauxite resource on the Nassau Plateau and thought a gold mine would assist in development. The Nassau Project was located in the mapped greenstone belt and there was extensive small-scale mining of alluvial gravels in creeks by small scale miners. Exploration started in 2000 after reconnaissance rights were granted. An area of 140,000 hectares was initially evaluated using remote sensing, soil geochemistry, geophysics and mapping of small-scale mining operations in saprolite. Trenching, hollow-stem auger core drilling, and core drilling followed. The initial discovery was in an area of intense saprolite mining in the area referred to as Gowtu Bergi (Money Mountain). Drilling started at Gowtu Bergi on August 31, 2002 with a program of 12 holes and 1,500 meters. All holes were classified as "ore holes" and the team was on the way to the development of a new mine. Suralco encouraged the training and developing an effective team of local geologists. That discovery in 2002 is now part of the Merian Mine with total production of 1 million ounces in only two years of mining.

Key words: Merian Mine, Suriname, gold, Alcoa, Newmont

INTRODUCTION

Many mines have had a long history of mining and exploration, such as the Rosebel Mine in Suriname. Usually, information is gathered from each round of exploration by different groups, which leads to developing a resource and a mine. The Nassau Project is more unusual in that there was no prior mining or exploration and only minimal work by the Geological Survey of Suriname. By the time Suralco initiated an exploration program in the Nassau region, small scale miners had been actively mining the larger drainages. This is a true grassroots discovery that is based on using the information from the prospectors (the small scale miners) and early stage exploration methods. Suralco applied for reconnaissance rights for 140,000 hectares in 1999 and exploration started in 2000. The author started and managed the program from the inception until late 2003. A Suriname team of geologists and technicians was hired and developed rather than rely on international geologists. The intent of Alcoa was to find a gold mine to pay for the infrastructure needed to develop the bauxite resource on the Nassau Plateau. A new gold discovery was made, but not on the Nassau Plateau and the Nassau bauxite remains undeveloped. To make a new discovery in a previously unrecognized gold district in Suriname is a credit to Suriname and the support from Suralco.

HISTORY

At the start of the program in 2000, there was minimal geologic and geochemical data available, except for the areas of small-scale mining activity. Small scale miners were active in drainages that made up an area of more than 30,000 hectares. How to focus exploration? First, use the small scale miners, since they represent thousands of prospectors and their presence shows the existence of gold and their mining and roads exposed saprolite and created access. Because of the deep weathering, rock exposures are very limited and the primary exploration tools are geochemical sampling and geophysics. The files of the Geological Survey of Suriname were examined, but the results were misplaced or the samples were never assayed. Understanding the physical and chemical characteristics of weathering profile and recognizing transported or in situ material is essential in testing anomalous geochemical results.

Exploration started from the existing two roads, Langa Tabiki and the Suralco road to the Nassau Plateau, and progressed toward the west into less-accessible areas of small-scale mining. The small scale miners generated the access by their ATV trails. A program of Ridgecrest soil lines and rock sampling was developed based on pilot studies in the Jorka Creek area. This exploration tool best utilized the skills of the local crew and the available maps to locate samples in the field and maximized manpower. In addition, this strategy allowed us to explore the large region of alluvial mining and to minimize false anomalies due to gold transport by chemical and mechanical means, both common issues for deposits in this type of weathering environment (LaPoint, 2004). The historic topographic maps were georeferenced to WSG 84, but they were inaccurate and distorted and thus marking sample stations on the ground was critical.

The site of the Merian mine was remote with poor ATV trails and was not recognized until the ridgecrest sampling could reach that area. The ridgecrest soil and rock samples eventually defined a large area of anomalous gold in the Merian I and Merian II areas of

the concessions. Ridgecrest samples from other drainage basins had weaker or less-continuous gold values. Suralco's decision to continue exploration in the first year, in spite of the less-than-positive results, was critical to the success of the project. Because of the mechanical and chemical mobility of gold in the soil, laterite, and colluvium, gold anomalies in weathered bedrock (saprolite) are more representative of targeting diamond core drilling (LaPoint, 2004 and 2012). Establishing soil grids was not utilized extensively until the Merian target was being drilled. Suralco likes to drill and their auger rig was used to drill shallow hollow-stem core near Jorka Creek starting in 2001.

In May 2002, reports were received of intensive mining in a remote portion of the Merian Concession, referred to as Gowtu Bergi (Money Mountain). On June 6, 2002 this area was visited by the author with members of the Geological Survey of Suriname, military and police during a fact-finding mission. The mining activity in the saprolite was large scale and intense. On July 22, 2002, the miners left the area at the request of the police and military and the Nassau team, started sampling the large pit at Gowtu Bergi. A new access road and camp were constructed and the first phase of core drilling of 1500 meters started on August 31, 2002. Results were encouraging and justified a second phase of drilling, which started on November 11th, 2002. The third phase of drilling using two core rigs began on March 24th, 2003. This phase ended on September 14th, 2003. Gowtu Bergi is now part of Newmont's Merian Mine.

At Merian, to test for anomalous gold in saprolite, hand auger samples of saprolite were collected every 25 meters along a grid of lines spaced 200 meters apart. Samples were collected at a depth of one meter into saprolite. A mechanical auger core rig (Diedrich) was also used to sample up to depths of 34 meters in areas with anomalous auger results. The core was of good quality and was logged and sampled on site and incorporated into the database. In areas such as Gowtu Bergi, trenches and porkknocker pits that mined saprolite were also excavated, sampled and mapped. All of these methods were used to select targets for diamond core drilling. Diamond core holes were drilled to depths from 100 to 200 m in 50 to 55 degree angle holes to provide samples in both saprolite and unweathered rock. Suriname geologists were trained to initially log all saprolite and diamond core holes at the drill rig for recovery, rock quality data, and descriptive lithologies. This allowed the measurement of structures and veins that may be lost during sampling and transport. The geologist also provided quality control on site (LaPoint, 2006). The core was photographed, cut and sampled for assay. By 2003, the core drilling was extended over a two-kilometer strike interval and a width of up to one kilometer near the Gowtu Bergi Pit.

RESULTS

In the first half of 2003 there was an intense period of study focused on understanding the mineralization while drilling and modelling continued. The dominant controls of mineralization are structural, and lithology appears to play a subordinate, local role (Capps and others, 2004). Mineralization and alteration are consistent with the characteristics of mesothermal lode gold deposits in Proterozoic terrains. Mapping of the Gowtu Bergi pit and surrounding area suggests that a Tension Vein Array structural model (TVA), fits the structural data observed in the field. TVA's evolve with increasing shear strain through stages that can be recognized in the Merian trend. TVA-hosted gold deposits are localized at specific sites within the evolving shear zone and have shapes and orientations that change dramatically including a 90 degree change in the trend of the ore body and ore shoot geometry that is associated with a change from low shear strain to high shear strain. Some TVA's tend to host large, world-class ore deposits because of the high fluid-channeling capacity. Interpretation of drilling suggested that the Merian system is a long-lived, complex structural gold system that fits this model.

The extensive development of brittle fractures within a largely ductile deformation regime suggests that the mineralization may have formed at or near the brittle-ductile transition zone. Structural style and geometry are consistent with deformation in a transpressive orogenic setting, characterized by NE-SW compressional folding locally overprinted by zones of NW-SE dextral shearing. The complex geometry of the mineralized zones and deep supergene weathering are challenging to deposit definition and evaluation.

Tension vein arrays (TVAs) occur as zones 1 meter to over 20 meters in width, with lateral and vertical continuity probably measured in hundreds of meters. Individual quartz veins in tension-vein arrays dip 10° to 50° to the northeast or southwest, although the arrays dip moderately to steeply, generally to the northeast. TVA formation occurred at relatively low strain, probably during the initial phases of folding and development of the S_2 fabric.

Three phases of veining, alteration, and mineralization are recognized, all probably part of a continuum in the evolution of the hydrothermal system. An early generation of quartz veins with locally abundant accessory carbonate and sodic and possibly potassic feldspar are associated with largely ductile fabrics and are generally barren of gold. Vein sets two and three are dominantly quartz with local accessory sodic plagioclase, chlorite, minor pyrite or pyrrhotite, and local minor molybdenite and trace chalcopyrite. Gold is generally fine-grained native metal or possibly a trace component of sulfides, but is locally present as macroscopic grains up to several millimeters. Voids created by dissolution of carbonate are common in and adjacent to vein types two and three. TVAs are commonly vein type two, while vein swarms tend to be vein types two and three. Alteration associated with tension vein arrays is visually weak where only TVAs are present, but may be more intense where a through-going vertical vein array has formed.

Stratigraphic units in the Merian II area are largely sedimentary, are affected by low-grade metamorphism, and contain material derived from a volcanic source terrain. Much of the sequence is rheologically incompetent and deforms in a largely ductile manner, largely due to the development of abundant phyllosilicates. These include argillites, mudstones, silty mudstones, and siltstones. Perhaps 20 percent of the sequence is rheologically more-competent lithologies, including lithic arenite and arkosic arenite and tuffs that behave in a more brittle manner. White mica and chlorite form a phyllitic penetrative fabric in the originally clay-rich sedimentary rock protoliths and the phyllitic fabric is the most commonly observed texture. All lithologies are deformed by the transpressional trans-Amazonian orogeny and original thickness of the deformed sedimentary rocks is not known. The most common deformation is attenuation and thinning along the S_2 foliation planes.

Hydrothermal alteration associated with gold mineralization in the Merian II area is often visually subtle, and largely consists of pyrite as disseminated irregular grains and euhedral crystals and as a minor component of quartz veins and veinlets. Close examination of core is required to identify this alteration in unoxidized materials, but the former presence of pyrite produces often spectacular and readily identifiable color variations in oxidized saprolite. This color variation is characterized by an assemblage of sericite + quartz + gadolinite variably hued by ferric iron oxides, and is designated SQK. SQK (sericite + quartz + gadolinite) is an alteration designation applicable only to oxidized saprolite at the surface, in trenches, and in drill holes. It is formed by entirely supergene processes. SQK (or QSK) results from acid leaching of Fe, Mg, and Mn and the formation of supergene gadolinite due to hydrous oxidation of pyrite and the formation of sulfuric acid. SQK alteration is the oxidized equivalent of pyrite alteration in unoxidized saprolite, saprock, and fresh rock. Oxidation of relatively unaltered lithologies generally forms a saprolite characterized by dark gray-purple hues and deep dusky reds and red-browns and the pastel to pale hues of SQK are in stark contrast to these dark colors.

In 2003, the drill results were encouraging for a mineralized system that could lead to mine development, but exploration was too early to tell the size and economic potential to be mined. In an exercise with Western Mining geologists, a potential for 2.7 million ounces was the outcome! Merian has exceeded that by far. Early drill results from the Merian II area (Gowtu Bergi), contained mineralized intervals with an average 1.72 g/t gold (median 1.39 g/t) and an average apparent thickness of 12.7 meters (median 9.5 m) per mineralized interval, with a cut off of 0.5 g/t and internal waste of < 5m. Multiple mineralized zones are present in each drill hole. By 2003, of the 72 holes drilled, over 90 percent encountered reportable mineralization, although some of the holes only contained mineralized laterite. Mineralized intervals average 1.63 g/t (median 1.29 g/mt) with an average apparent thickness of 13.0 m (median 10.2 m). Individual mineralized intervals rapidly pinch and swell. The Merian II target is but one target within the Merian trend, a trend that extends northwest-southeast for over 12 kilometers, based on Ridgecrest soil sampling.

In 2003 it was noted that multiple drill targets are expected along this trend with further deep auger sampling, mapping and porkknocker sampling. The most advanced target is Merian I where saprolite core drilling, trenching and porkknocker activity define a target with similar size as Merian II, but grades were lower and less continuous. Based on the magnetic data that defines magnetic lows that may represent alteration zones and magnetic destruction, limited ridgecrest soil sampling along with new porkknocker activity will produce more drill targets on the Merian trend, especially to the northwest where drilling had not yet been conducted.

CONCLUSIONS

Suriname and the Guiana Shield are under-evaluated gold provinces with two large mines in Suriname, Rosebel and Merian. There are many additional opportunities but discovery is limited by the cyclic nature of the investment markets for gold, the difficulty in acquiring land from existing concession holders, logistics and access, and learning to do business in the region. Suriname is in an evolving gold rush. When the Nassau project was first started, small scale alluvial mining focused on the larger drainages. As mining by small scale miners continued, attention focused on the smaller drainages, colluvium, and quartz veins in saprolite, as well as reprocessing older tailings. Small scale mining and processing are now evolving into underground mining and the early stages of chemical extraction. Also small scale miners are prospecting more remote regions with higher logistic cost in southern Suriname. Mining is becoming more costly than most small miners can afford (LaPoint, 2003 and 2014).

Most concession holders in Suriname do not conduct exploration. Exploration companies must initially examine the scope and style of small-scale mining operations to assess the concession potential. Concessions do not follow geologic or mineralization boundaries, so multiple concessions may need to be acquired. However adjacent concession holders may have very different ideas on the value of their concession and “big eyes” are a common issue to address. In Suriname, at each renewal, 25 percent of the concession must be returned to the government. These pieces are small and may limit the overall exploration potential as they are often granted to people with no knowledge of the exploration business. Changes in the current mining laws are long overdue and are needed to protect the environment, insure exploration is conducted, create transparency in how to conduct business, and permit new investors access to concessions. The Mineral Agreement with Newmont allows Newmont first rights to any open concessions within a large area and this hinders new investors.

Governmental support in generating a new topographic maps based on Lidar and a recognized coordinate system, a country wide geophysical survey, new research and detailed geologic mapping and structural and stratigraphic analysis (Watson and LaPoint, 2006), and reforming the mining law with more transparency will increase the economic benefit to Suriname. More environmental controls should be encouraged. Competition in the mining sector is good and Suriname should encourage new local and international companies to invest (LaPoint, 2014).

ACKNOWLEDGMENTS

To make a new discovery in a previously unrecognized gold district in Suriname is a credit to Suriname and the support from Suralco, in particular Anton Brandon and Herman Alendy and Charlie Soh at Alcoa.

In 2003 there was an intense period of evaluation on the understanding of mineralization while drilling and modelling was on-going. Geologists Dr. Criss Capps, Robert J. Moye, Dave Christensen, Mary Stollenwerk, and Tom Watson from the United States were retained to assist the Suriname geologic team of Aroena Ramlal, Manuella Fung, Deepak Narsing, Ryan Kambel, and Linus Diko. Approximately five man-months of intense mapping, sampling and relogging of core drilling were completed through the end of June 2003. Such a level of understanding in a short period of time is a credit to the entire team. The geologists all state this was one of the most intense, productive phases of their career (Capps and others, 2004).

REFERENCES

LaPoint, Dennis J., 2003, Effects of Small-Scale Alluvial Gold Mining on the Environment and Society of the Eastern Interior of Suriname: invited paper presented at a workshop on social and cultural aspects of mining frontiers at the new Max Planck Institute for Social Anthropology in Halle/Saale, Germany, June 2003.

Capps, Richard C, Moye, Robert J., LaPoint, Dennis J., Watson, Thomas C., Christensen, Dave, Stollenwerk, Mary and Cherrywell, Christopher, The Evidence for Syntectonic Gold Mineralization at Gowtu Bergi, Eastern Suriname, South America: Geological Soc. Am Abst w/Programs, v. 36, no. 2.

LaPoint, Dennis J. 2004, A Comparison of Gold Exploration Techniques and New Gold Discoveries in Deeply Weathered Environments of the Southeastern United States and Suriname: Geological Soc. Am Abst w/Programs, v. 36, no. 2.

LaPoint, Dennis J., 2006, Developing new exploration geologists in Suriname, South America: Geological Society of America Abstracts with Programs, Vol. 38, No. 7, p. 219

LaPoint, Dennis J., 2012, Gold Exploration Methods in Deeply Weathered Environments: A Comparison of Southeastern US and Suriname, Geological Society of America, Abstracts with Programs, Vol.44.

LaPoint, Dennis, J., 2014, Exploring and Developing New Mines for the Republic of Suriname, SURIMEP 2014, Invited Presentation, 1st Suriname International Mining, Energy and Petroleum Conference and Exhibition, Paramaribo, June 17th, 2014.

LaPoint, Dennis J. and Watson, Thomas C., 2006, The Rosebel gold mine, Suriname, South America: A new window to understand orogenic evolution of a sedimentary basin and Earth's early history: Geological Society of America Abstracts with Programs, Vol. 38, No. 7, p. 344

Gold Systems in Brazil: brief review

Lydia Maria Lobato*
Universidade Federal do Minas Gerais
Campus Pampulha-IGC
Belo Horizonte-MG-Brazil-31270.910

llobato.ufmg@gmail.com

Marco Aurélio da Costa
Senior Consultant
Belo Horizonte, -MG-Brazil

mac13@uol.com.br

Steffen Hagemann
Centre for Exploration Targeting
University of Western Australia
35 Stirling Highway, Perth, Australia, 6009

steffen.hagemann@uwa.edu.au

Rosaline Cristina Figueiredo e Silva
Universidade Federal do Minas Gerais
Campus Pampulha-IGC
Belo Horizonte-MG-Brazil-31270.910

rosalinecris@yahoo.com.br

Gabriel V. Berni
Universidade Federal do Ceará
Campus do Pici, Bloco 912
Fortaleza-CE-Brazil, 60440-554

gvberni@ufc.br

SUMMARY

Brazil started gold production early after its discovery in 1500. Production by mining companies started chiefly in the late 1980's.

Archean or Paleoproterozoic granite-greenstone belts host most of Brazil's gold. Nevertheless, the giant Morro do Ouro orogenic gold deposit is hosted in a Neoproterozoic metasedimentary belt.

Orogenic gold systems are the most important. Gold is also associated with intrusion-related Cu-Au, metamorphosed Au-Cu porphyry deposits, and Au-rich IOCG, with Salobo in Carajás presently representing Brazil's largest gold resources. Small deposits or districts (<250,000 oz Au), *garimpos* and placer workings are being mined mainly in the Roraima, Amapá, Madeira, Tapajós, Alta Floresta and Borborema regions.

Key words: Gold deposits, Brazil

INTRODUCTION

After the discovery of Brazil in 1500, gold was subsequently found by the Portuguese in 1561 and afterwards by *bandeirantes* (Brazilian explorers), at the end of the 17th century. During the 18th and early 19th centuries Brazil led the world in gold production. Only small gold production, between 5-8 t Au (179,200-286,720 oz) per annum, was produced during the late 19th to the late 20th century. At least eight mines opened between 1983 and 1990, considered Brazil's first modern gold boom (Thorman et al. 2001). According to the DNPM (2017), company gold production in 2017 reached 77.8 t (~2.79 Moz). According to www.statista.com Brazil stood at 10th place in 2017 with an output of ~2.72 Moz Au.

For the period between 1982 and 1999, Brazil had 10 major (>20 t - >716,800 oz - Au produced) and seven minor (3-8 t Au produced; 107,520 - 286,720 oz) gold mines (Thorman et al., 2001). Sixty-six % of gold produced during this period was hosted in Archean rocks, 19% and 15% were hosted in Paleoproterozoic and Neoproterozoic rocks, respectively (Thorman et al. 2001; Lobato et al., 2016).

From the beginning to mid-2000, the second gold boom commenced with increased gold production in part due to new deposits opening up, as for example Chapada, Lamego, Turmalina and São Bento. Since then several new and significant gold deposits commenced production, for example, in 2010 Jaguar Mining's Caeté deposit; in 2011 Trek Gold's Aurizona deposit and Beadell Resources' Tucano deposit and in 2013 Leagold Pilar mine. A review on the state of gold geology and production in the country was recently put together by Lobato et al. (2016). Figure 1 displays the location of all gold districts and deposits mentioned in this contribution.

In recent years ongoing efforts by both AngloGold Ashanti Ltd. (AGA) and Yamana Gold Inc. (YG) have led to the reopening of older mines. In the Quadrilátero Ferrífero (QF) province these include the underground Lamego and São Bento projects (both owned by AGA), which became integrated into the Cuiabá and Córrego do Sítio mine complexes, respectively. Yamana Gold increased production at Jacobina and Chapada, as well as at Pilar, Riacho dos Machados and Fazenda Brasileiro, now Leagold, previously BrioGold, all these mines are presently operational.

TECTONIC SETTING AND RELATED GOLD DEPOSITS

Brazil contains three major cratons including Amazonas, São Francisco and Rio de la Plata. The latter is largely exposed in Uruguay and only smaller fragments outcrop in southern Brazil. These cratons are surrounded in the eastern part of Brazil by Neoproterozoic (900-550 Ma) Brasiliano Cycle belts (e.g., Brito Neves et al., 2014). Late Mesoproterozoic belts (~1020 Ma) occur in the western and northwestern Amazon Craton (e.g., Hasui, 2012).

Gold systems in Brazil are located in many rock types of various ages, but most systems have formed in the Neoarchean and Paleoproterozoic, a few forming in the Neoproterozoic although Brazil's largest gold deposit (with the lowest average gold grade), the Morro do Ouro deposit (8.82 Moz contained Au at 0.4 g/t), hosted in phyllites of the Neoproterozoic Brasiliano belt. Hartman and Delgado (2001) provide an excellent overview of the tectonic setting of Brazilian gold systems. Selected pertinent points are summarized below, as well as some more recent information:

1- Archean and Paleoproterozoic granite-greenstone belts contain numerous Au-only orogenic gold systems, e.g., in the QF region. There are also Au-rich IOCG and Cu-Au intrusion-related systems, e.g., in the Carajás gold province.

2- Paleoproterozoic sedimentary cover rocks, which overlie greenstone belts, contain a few examples of gold systems, e.g. Serra de Jacobina. This is hosted by quartz pebble conglomerates, at the base of fluvial and beach sequences (Teixeira et al., 2001). The Serra Pelada Au-Pd-Pt deposit in the Carajás province is another important Paleoproterozoic system, where the host is a sequence of carbonaceous metapelites, (e.g., Berni et al., 2014).

3- Paleoproterozoic intrusion-related gold systems formed during juvenile crust accretion and can form in syn-orogenic, post-orogenic and anorogenic (~2100 – 1800 Ma) calc-alkaline to subalkaline plutono-volcanic rocks. These comprise Au-Cu systems, as well as Au-Ag epizonal systems, e.g., in the Tapajós and Juruena gold provinces.

4- Mesoproterozoic rifts, reactivated in the Neoproterozoic Brasiliano Cycle, contain very small gold systems to date.

5- Mesoproterozoic to Neoproterozoic fold and thrust belts contain large, low grade (<1 g/t Au) Au-only, phyllite-hosted orogenic gold systems, e.g., in the Brasília fold belt between the towns of Paracatu and Brasília.

6- Neoproterozoic calc-alkaline plutonic and volcanic-sedimentary rocks contain metamorphosed Au-Zn-rich VHMS and Au-Cu rich porphyry systems that, locally, can be overprinted by Au-only orogenic gold systems. Examples are located in the Mara Rosa-Crixás gold province.

7- Late Neoproterozoic to Paleozoic foreland basins contain small stratabound to vein-style Cu-Au systems hosted by detrital sedimentary rocks or continental, acid alkaline volcanic and subvolcanic rocks.

8- Cenozoic cover rocks contain supergene, lateritic enrichments of hypogene gold systems and Recent sediments contain large placer gold systems, particularly in the Amazon.

MAJOR GOLD DEPOSITS, GOLD PROVINCES AND REGIONS IN BRAZIL

Figure 1 displays gold deposits or camps ranging in size from 0.3 to 18.1 Moz contained gold. Many of these deposits are located in several major gold provinces in a variety of states, and these are summarized below.

1- QF gold province (Minas Gerais), which contains the orogenic (Au-only) Morro Velho (closed), Cuiabá (the largest underground mine in Brazil), Lamego, Raposos (closed), Pilar, and Córrego do Sítio / São Bento mines.

2- Carajás gold province (Pará), which contains the IOCG (Cu-Au) related Salobo, Sossego, Igarapé Bahia and Alemão mines, the intrusion-related Au-Cu Breves deposit and the Serra Pelada Au-PGE deposit.

3- Mara Rosa-Crixás gold province (Goiás), which contains the metamorphosed porphyry (Au-Cu) Chapada and Posse deposits, and the orogenic (Au-only) Crixás (including Mina Nova and Mina III) and Pilar deposits.

4- Gurupi gold province (Maranhão and Pará), which contains the orogenic (Au-only) Cachoeira and Aurizona deposits (to be reopened in 2019).

Several deposits are located in gold provinces, but are the only significant (> 1 Moz Au) deposits in this province:

1- Tucano in the Amapá gold province (Amapá), which is a BIF-hosted orogenic (Au-only) deposit, and Lourenço hosted in Paleoproterozoic supracrustal sequences (Nogueira et al., 2000).

2- Tocantinzinho in the Tapajós gold province (Pará), which is an intrusion-related (Au-only) deposit.

3- Fazenda Brasileiro and C1-Santa Luz in the Itapicuru gold province (Bahia), which are orogenic gold deposits.

There are also individual gold deposits located within greenstone belts (unknown age) or Proterozoic mobile belts:

1- Morro de Ouro in the Neoproterozoic Brasília fold belt near Paracatu (Minas Gerais), which is a graphitic and pyritic phyllite-hosted orogenic (Au-only) deposit.

2- Volta Grande in the Três Palmeiras Paleoproterozoic greenstone belt (Pará), which is a mostly diorite-hosted orogenic (Au-only) deposit.

3- Jacobina in the Serra de Jacobina region (Bahia), which is either a Paleoproterozoic/Archean paleoplacer and/or orogenic (Au-only) deposit.

4- Pitangui region (Minas Gerais) with orogenic (Au-only) deposits in the Archean Pitangui greenstone belt.

Presently, the great majority of significant gold deposits in Brazil are defined as orogenic (Au-only) gold systems located in mid-crustal, mesozonal levels such as Morro Velho (closed in 2003; Lobato et al., 2001) and various others in the QF (see papers in a special issue on gold deposits in the QF published in Ore Geology Reviews, 2007), Fazenda Brasileiro

(Silva et al., 2001), Morro do Ouro (Freitas-Silva et al., 1991; Freitas-Silva, 1996), and Mina Nova & Mina III (Crixás) (Jost et al., 2001).

Figure 1 – Location of major gold deposits (> 0.3 Moz contained Au) in Brazil.

Several significant gold-rich IOCG (e.g., Salobo, Alemão, Igarapé Bahia) and intrusion-related Cu-Au deposits (Breves) are all located in the giant Carajás metallotect (Xavier et al., 2012), with Salobo presently representing Brazil's largest gold resources (Lobato et al., 2016). The Chapada gold deposit represents one of the rare metamorphosed Au-Cu porphyry systems (Richardson et al., 1986; Oliveira et al., 2016). The Jacobina deposit was, in the past, discussed as an Archean paleoplacer gold deposit, although Teixeira et al. (2001) and Milesi et al. (2002) propose an epigenetic origin similar to orogenic gold systems. Many Archean, Paleoproterozoic and Neoproterozoic terrains in Brazil contain small deposits (<300,000 oz Au), shallow-level gold workings (*garimpos*) and/or alluvial placer workings e.g., in the Roraima, Amapá, Madeira, Tapajós, Alta Floresta and Borborema regions. Given the past extensive exploration in these gold provinces and exploitation of small gold deposits (50,000 to <250,000 oz Au), it is likely that new and large gold deposits (>1 Moz Au) may be discovered in the future.

CONCLUSIONS

Brazil has been a gold producer since shortly after it was discovered in 1500. Many of the currently producing gold deposits started production in the 1980's, but in the past 15 years several new gold deposits were discovered and came into production (e.g., Lamego, Caeté, Turmalina, Pilar). One of the largest gold deposits, Morro Velho, was discovered in 1834 and only closed in 2003.

Most gold deposits are hosted in Archean or Paleoproterozoic granite-greenstone belts, but some are also hosted in the Neoproterozoic Brasiliano belt (e.g., Morro do Ouro). Although Brazil shows a variety of gold systems, including orogenic Au, intrusion-related Cu-Au, Au-rich IOCG or metamorphosed Au-Cu porphyry deposits, the orogenic gold system is by far the most important with respect to number of deposits and contained gold. Many small gold deposits

(<250,000 oz Au), *garimpos* and placer workings in various parts of Brazil, that have been or are currently explored, suggest that there are significant gold deposits to be discovered in the future.

REFERENCES

Berni, G.V., Heinrich, C.A., Lobato, L.M., Wall, V.J., Rosière, C.A., Freitas, M.A., 2014, The Serra Pelada Au-Pd-Pt deposit, Carajás, Brazil: geochemistry, mineralogy and zoning of hydrothermal alteration: Economic Geology, 109, 1883-1899.

DNPM: www.dnpm.gov.br/

DNPM, 2017, Anuário Mineral Brasileiro, Principais Substâncias Metálicas. http://www.anm.gov.br/dnpm/publicacoes/serie-estatisticas-e-economia-mineral/anuario-mineral/anuario-mineral-brasileiro/amb_metalicos2017.

Freitas-Silva, F.H., 1996, Metalogênese do depósito do Morro do Ouro, Paracatu, MG: PhD thesis, University of Brasília.

Freitas-Silva, F.H., Dardenne, M.A., and Jost, H., 1991, Lithostructural control of the Morro do Ouro gold deposit, Paracatu, Minas Gerais. In Ladeira, E.A., (ed), Brazil Gold '91, Balkema, 681-683.

Hartman, L.A., and Delgado, I. de M., 2001, Cratons and orogenic belts of the Brazilian shield and their contained gold deposits: Mineralium Deposita, 36 (3-4), 207-217.

Jost, H., de Tarso Ferro de Oliveira Fortes, P., 2007, Gold deposits and occurrences of the Crixás goldfields, central Brazil: Mineralium Deposita, 36, 3-4, 358-376.

Lobato, L.M., Costa, M.A., Hagemann, S.G., Rodrigo, R., 2016, Ouro no Brasil: Principais depósitos, produção e perspectivas. In: Campos, DA, Scheuenstuhl MCB (Organizers), Recursos Minerais do Brasil: Análises Estratégicas: Academia Brasileira de Ciências, Rio de Janeiro, Chapter 3, 46-59.

Milesi, J.P., Ledru, P., Marcoux, E., Mougeot, R., Johan, V., Lerouge, C., Sabate, P., Bailly, L., Respaut, J.P., and Skipwith, P., 2002, The Jacobina Paleoproterozoic gold-bearing conglomerates, Bahia, Brazil: a ''hydrothermal shear-reservoir'' model: Ore Geology Reviews, 19, 95-136.

Nogueira, S.A.A., Bettencourt, J.S. and Tassinari, C.C.G., 2000, Geochronology of the granitoid-hosted Salamangone gold deposit, Lourenço district, Amapá, Brazil: Revista Brasileira de Geociências, 30(2), 261-264.

Oliveira, C. G., Oliveira, F. B., Giustina, M.E.S.D., Marques, G.C., Dantas, E.L., Pimentel, M.M., Buhn, B.M., 2016, The Chapada Cu-Au deposit, Mara Rosa magmatic arc, Central Brazil: Constraints on the metallogenesis of a Neoproterozoic large porphyry-type deposit: Ore Geology Reviews, 72, 1-21.

Ore Geology Reviews, 2007, Special issue on gold deposits of Quadrilátero Ferrífero, Minas Gerais, Brazil (eds, Diógenes, S.V., Groves, D.I., Cook, N.J., and Lobato, L.M.), 32, issues 3-4, 469-688.

Richardson, S.V., Kesler, S.E., Essene, E.J., and Jones, L.M., 1986, Origin and geochemistry of the Chapada Cu-Au deposit, Goias, Brazil: a metamorphosed wall-rock porphyry copper deposit: Economic Geology, 81, 1884-1898.

Silva, M.G., Coelho, C.E.S., Teixeira, J.B.G., Silva, F.C.A., Silva R.A., Souza, J.A.B., 2001, The Rio Itapicuru greenstone belt, Bahia, Brazil: geologic evolution and review of gold mineralization: Mineralium Deposita, 36, 345-357.

Teixeira, J.B.G., de Souza, J.A.B., da Silva, M. da G., Leite, C.M.M., Barbosa, J.S.F., Coelho, C.E.S., Abram, M.B., Filho, V.M.C., and Iyer, S.S.S., 2001, Gold mineralization in the Serra de Jacobina region, Bahia Brazil: tectonic framework and metallogenesis: Mineralium Deposita, 36 (3-4), 332-344.

Thorman, C.H., DeWitt E., Marcos, A.C., Maron, E., and Ladeira, A., 2001, Major Brazilian gold deposits – 1982 to 1999: Mineralium Deposita, 36 (3-4), 218-227.

Xavier, R.P., Monteiro, L.V.S., Moreto, C.P.N., Pestilho, A.L.S., Melo, G.H.C., Silva, M.A.D., Aires, B., Ribeiro, C., Freitas e Silva, F.H. 2012, The iron oxide copper-gold systems of the Carajás Mineral Province, Brazil: Geology and Genesis of major copper deposits and districts of the world: a tribute to Richard Sillitoe. J.W. Hedenquist, M. Harris, and F. Camus, Editors, Special Publication of the Society of Economic Geologists. 16, 433 - 453.

Greenstone Belt Geochemistry: A window into early Earth processes and resources

Paul Mason*
Department of Earth Sciences
Princetonlaan 8A, 3584 CB Utrecht
The Netherlands

p.mason@uu.nl

SUMMARY

Greenstone-granite terrains are fragments of ancient crust that provide key data about the nature of the early Earth, frequently rich in mineral resources. Petrological and structural data record the transition into modern-style plate tectonics. Sediment geochemistry provides extensive information about the nature of the Earth's earliest surface environments, including the composition of the atmosphere and oceans and the evolution of early microbial life. Extensive work has been carried out over decades in Archean greenstones, whilst less attention has been given to those in the Paleoproterozoic, especially in the Guiana Shield. Here I review key areas that remain to be tackled in the greenstone-granite geology of Suriname.

Key words: Greenstone-granite terrains; geochemistry; Marowijne Greenstone Belt; Suriname

INTRODUCTION

The Paleoproterozoic (ca. 2.18-2.09 Ga) Marowijne greenstone belt on the Guiana Shield in north-eastern Suriname shows a typical structure with greenstone keels diapirically intruded by tonalite-trondhjemite-granodiorite (TTG) plutons (reviewed in Kroonenberg et al., 2016). It was emplaced during the time of the Lomagundi-Jatuli carbon isotope excursion (Karhu & Holland, 1996; Maheshwari et al., 2010), a period of elevated atmospheric oxygen concentrations immediately following Great Oxygenation Event (GOE) at 2.32 Ga (Bekker & Holland, 2012). This is an anomalous period of geological time against a background of fully anoxic (near)surface conditions in the Archean and subsequent low oxygen environments throughout the Proterozoic. The Marowijne greenstone belt is the host to world-class ore deposits (Kio-A-Sen et al., 2016) but their geological and geochemical context remains poorly studied. In this contribution, I review the wealth of background knowledge and methodology that can be taken from the study of greenstone-granite terrains elsewhere and could be further developed in Suriname. I suggest some avenues for future study that will link a deeper understanding of geological and geochemical processes to ore formation.

GLOBAL CONTEXT OF MAROWIJNE GREENSTONE BELT

The time period across which the Marowijne greenstone belt was formed is geochemically anomalous, sitting within the Lomagundi carbon isotope excursion. The Lomagundi event represents a period of high burial rates of organic carbon that was coupled with a large flux of oxygen into the atmosphere. Free oxygen was readily consumed, predominantly by reduced iron and sulfur minerals during crustal weathering. As a consequence, the Lomagundi period is characterized by an increased abundance in sulfate evaporites, red beds (paleosols) and high concentrations of redox sensitive metals such as Mo, Re, U in organic-rich shales. The early part of the Lomagundi (ca. 2.3-2.2 Ga) was closely linked to the Huronian glacial events. As oxygen concentrations fell at the end of the event, manganese-rich sediments and iron formations became locally abundant. The Marowijne Greenstone belt spans the middle to end of this largest and longest-lived excursion in oxygen concentrations in geological history. Evidence for the Lomagundi event has been provided from rocks elsewhere within South America and within the Birimian of West Africa, but not yet clearly identified in the geology of Suriname.

The Paramaka, Armina and Rosebel formations make up the stratigraphy of the Marowijne greenstone belt and record a transition in sedimentary environments from a deep-water back-arc extensional basin to younger shallow marine and fluvial settings (Kroonenberg et al., 2016). The oldest ca. 2.6 to 2.4 Ga Paramaka Formation consists of tholeiitic basalts intercalated with more felsic volcaniclastics and some chemical sediments. The rocks are variably metamorphosed from greenschist up to amphibolite facies. Within the more strongly metamorphosed parts, gondites and itabirites indicate original sedimentary enrichments in manganese and iron respectively. These occurrences are significant as iron formations and Mn oxides are rare during the Lomagundi event and have been shown to be limited to periods of deposition immediately subsequent to global glacial events or at the very end of the event (Bekker & Holland, 2012). These may be equivalent to Mn carbonates and gondites found in the Birimian (Nyame & Beukes, 2006). Additional puzzling aspects of the greenstone belt include the relative scarcity of chemical sediments including carbonate and sulfates. This may be a function of preservation but requires detailed scrutiny against comparative sections of the Birimian.

FUTURE OUTLOOK

Current research in the Marowijne Greenstone Belt is focussed on developing a more detailed geochronological framework to enable more accurate tectonic reconstructions and stratigraphic correlations (Kriegsman et al., this volume). The geochemistry of igneous and metamorphic rocks provides key data for testing tectonic models for this critical time period in plate tectonic evolution in the early Paleoproterozoic.

The geochemistry of chemical and clastic sedimentary rocks has yet to be investigated in detail across the Marowijne Greenstone Belt and will provide key information about the nature of crustal sources and marine redox conditions, as well as providing critical background information for assessing resource potential. An array of geochemical tools are available for the study of greenstone belt sediments and igneous rocks that I will review here. I will discuss some key areas that should be addressed in the coming years in the greenstone belt geology of Suriname.

REFERENCES

Bekker, A., and Holland, H.D., 2012, Oxygen overshoot and recovery during the early Paleoproterozoic: Earth and Planetary Science Letters, 317-318, 295-304.

Karhu, J.A. and Holland, H.D., 1996, Carbon isotopes and the rise of atmospheric oxygen: Geology, 24, 867-870.

Kioe-A-Sen, N.M.E., Van Bergen, M.J., Wong, T.E., and Kroonenberg, S.B., 2016, Gold deposits of Suriname: Geological context, production and economic significance: Geologie en Mijnbouw/Netherlands Journal of Geosciences, 95, 429-445.

Kroonenberg, S.B., De Roever, E.W.F., Fraga, L.M., Reis, N.J., Faraco, T., Lafon, J.-M., Cordani, U., and Wong, T.E., 2016, Paleoproterozoic evolution of the Guiana Shield in Suriname: A revised model: Geologie en Mijnbouw/Netherlands Journal of Geosciences, 95, 491-522.

Maheshwari, A., Sial, A.N., Gaucher, C., Bossi, J., Bekker, A., Ferreira, V.P. and Romano, A.W., 2010, Global nature of the Paleoproterozoic Lomagundi carbon isotope excursion: A review of occurrences in Brazil, India, and Uruguay: Precambrian Research, 182, 274-299.

Nyame, F.K. and Beukes, N.J., 2006, The genetic significance of carbon and oxygen isotopic variations in Mn-bearing carbonates from the Palaeo-Proterozoic (~2.2 GA) Nsuta deposit in the Birimian of Ghana: Carbonates and Evaporites, 21, 21-32.

Bauxite formation on Proterozoic basement and Tertiary sediments in Suriname

Dewany Monsels*
Anton de Kom University of Suriname
Leysweg 86

dewany.monsels@uvs.edu

SUMMARY

The lateritic bauxite deposits of Suriname developed on Cenozoic sediments in the coastal lowlands and metamorphic rocks of the Precambrian Guiana Shield. Weathering profiles were analyzed for geochemical and mineralogical properties aimed at exploring compositional diversity, underlying controls of bauxite-formation and the nature of precursor. Samples were analysed with polarized light microscope, microprobe, XRD, XRF and LA ICPMS. The complex petrologic characteristics and compositional heterogeneity of the deposits can essentially be explained by element fractionation in combination with relative and absolute enrichment processes, erosion and reworking during two-stage, polycyclic bauxitization of heterogeneous precursors during Late Cretaceous – Early Tertiary times.

Key words: bauxite, trace elements, LA ICPMS, Suriname

INTRODUCTION

The lateritic bauxite deposits in South America are developed on a variety of parent rocks (precursors) ranging from Phanerozoic siliciclastic sediments to Precambrian igneous and metamorphic lithologies (Bárdossy and Aleva, 1990; Carvalho *et al.*, 1997; Bogatyrev *et al.*, 2009). The most significant deposits are distributed within and along the Precambrian Guiana Shield in Suriname, northern Brazil, Venezuela, Guyana, and French Guiana (Fig. 1). These deposits are related to the Paleocene-Eocene "Main Bauxite Level" or "Sul-Americano" planation level and were mainly formed during Late Cretaceous to Quaternary times when long-lasting tropical and highly humid conditions favored intense chemical weathering (King *et al.*, 1964; Bárdossy and Aleva, 1990; Théveniaut and Freyssinet, 2002).

The lateritic bauxite deposits were once one of the economically vital natural resources of Suriname. The deposits are located in two major geographic areas (Fig. 2) with different precursors, properties and exploitation histories (Bárdossy and Aleva, 1990; Aleva and Wong, 1998; Monsels, 2016). The first group, referred to as "coastal-plain bauxites", formed on sedimentary parent material in the coastal lowlands and was mined since the early 20th century until 2015, while the second group of "plateau bauxites" developed on various metamorphosed Proterozoic rocks in interior parts of the country (Monsels, 2016; Monsels and Van Bergen, 2017), and has not been exploited to date.

The coastal bauxites are often buried by Miocene and younger sediments as a result of marine transgressions (Van der Hammen and Wijmstra, 1964; Bárdossy and Aleva, 1990; Théveniaut and Freyssinet, 2002; Wong et al., 2009). A so-called "Bauxite belt" runs subparallel to the Old Coastal Plain of Suriname and continues into Guyana (Valeton, 1983; Aleva and Wong, 1998). Similar to the world-class Brazilian deposits such as Paragominas and Rondon do Pará that developed in the Lower Amazon Basin (Oliveira *et al*., 2016), Suriname's lowland hosted some of the highest Al_2O_3-grade (frequently >50%) bauxites ores worldwide. The Surinamese bauxites are mentioned in several international classification schemes as "Suriname type"or "Trihydrate type", which generally stands for a gibbsite-rich bauxite with less than 3% boehmite (Patterson et al., 1986).

There is ongoing debate on the timing of bauxitization, the number of bauxitization cycles in Suriname and the nature of the precursor material of the coastal bauxites, for which arkosic sandstone interlayed with clayey sediments (Aleva, 1979; Krook, 1969; Wong *et al*., 1998, 2009 and references therein) and kaolinitic clays (Bakker *et al.*, 1953; Van Kersen, 1955; Moses and Michell, 1963) have been proposed. In addition to field relationships, trace-element signatures, in combination with petrographic and mineralogical constraints, can be helpful to solve these question, and are instrumental in exploring processes and controls of chemical weathering that accompanied bauxite formation, as well as in tracing the nature and provenance of precursor materials of the deposits (Oliveira *et al.*, 2016; Ling *et al*., 2018). This study of lateritic bauxites in Suriname concentrates on these issues, documents their geochemical characteristics in the context of local geological settings, and discusses implications for their genesis and origin. This study revealed that the complex petrologic characteristics and compositional heterogeneity of the bauxite deposits can basicly be explained by element fractionation in combination with relative and absolute enrichment processes, erosion and reworking during two-stage, polycyclic bauxitization of heterogeneous precursors during Late Cretaceous – Early Tertiary times.

METHOD AND RESULTS

Sample locations, methods and materials

The studied sites on which I report here are the Successor deposits (Klaverblad (KLB), Caramacca (CRM) and Kaaimangrasie (KMG)), Lelydorp-1, Para (Noord) and Kankantrie (Noord) in the Paranam-Onverdacht-Lelydorp (POL) bauxite district , and Coermotibo and the East Group of Hills (Adjoema, Madoekas and Lobato Hills) in the Moengo-Ricanau-Jones bauxite district (Fig.2). Samples from Bakhuis Base Camp, Snesie and Macousi in Area 10-1 from the Bakhuis bauxite district, and the Brownsberg and the Nassau deposit from the Nassau bauxite district are also studied (Fig.1). Sampling of the Successor and Lelydorp-1 deposits was performed when the mines were still in operation. Samples and chemical data of the remaining study areas are provided by the Bauxite Institute Suriname and the Suralco LLC. Samples from the lateritic weathering profiles of the Successor Mines are collected down to a maximum depth of 7.0, m, at variable vertical intervals depending on lithofacies changes. Supplementary samples of the Successor Mines, Lelydorp-1 and Bakhuis Base Camp are collected for comparison and reference purposes. In the Successor Mines, "chip and grab samples" are taken from fresh mine faces with a hammer or scoop, depending on the consistency of the material. The weathering profiles of Coermotibo are based on drill core samples (Monsels, 2004). Externally provided compositional data for Lelydorp-1, Kankantrie (Noord), Para (Noord), Coermotibo, Bakhuis (Snesie and Macousi) and Nassau (Plateau C) are all based on drill cuttings. It should be noted that not all of the POL and MRJ profiles reached the underlying kaolinitic clays, as the mining companies stopped drilling and excavating after reaching this level. Soil color descriptions are based on the Munsell color charts.

Analysis methods

Microscopic and geochemical analyses of samples from the Successor deposits, Snesie, Macousi, Bakhuis Base Camp and Nassau were performed at Utrecht University and VU University Amsterdam. Mineralogy and microtextures are investigated on polished thin sections with an optical microscope and an electron microprobe (JEOL JXA-8600 Superprobe) using both energy dispersive (EDS) and wavelength-dispersive (WDS) analytical techniques. Back-scatter electron imaging (BSE) is used to identify mineral phases and to study textural relationships. Quantitative compositions of mineral phases are determined via EDS microprobe analysis. X-ray diffraction (XRD) patterns are collected from randomly oriented powder samples using a Bruker D2 Phaser X-ray diffractometer, operated in a step-scan mode, with Co-Kα radiation (1.78897 Å). The counting time is 66 sec/step, the step size 0.05^0 and the range $5\text{-}85^0$. Total acquisition time per sample is approximately 15 minutes. Major-element compositions of the samples are determined by X-ray fluorescence (XRF) on fused glass beads (lithium borate) with a Thermo ARL 9400 sequential XRF (Utrecht University) and a Panalytical MagiXPro XRF (VU University Amsterdam). Loss-on-ignition data are obtained either by measuring weight loss upon heating of a powdered sample in an oven at > 1000ºC or by thermogravimetric analysis (TGA) during which weight loss was continuously monitored over a temperature range between room temperature and 1000ºC. Major-element XRF data for Lelydorp-1, Coermotibo, Snesie and Macousi are provided by Suralco L.L.C., while those for Kankantrie (Noord) and Para (Noord), Brownsberg and Nassau by the Bauxite Institute Suriname.

Because analytical results from solution-based techniques could be negatively influenced by incomplete digestion of zircon and other resistant mineral hosts of HFSE and REE, a method was developed to analyze bauxite samples with laser ablation ICPMS on lithium borate glass beads, which avoids these problems. This first effort to apply this technique on bauxite materials yielded excellent results, as could be validated by measurements on a set of international standard reference materials for bauxite. Trace-element concentrations in the Successor, Snesie, Macousi and Bakhuis Base Camp samples are determined by this method where laser ablation-inductively coupled plasma-mass spectrometry (LA-ICP-MS) was applied on the fused glass beads prepared for XRF, using a ThermoFischer Scientific Element 2 magnetic sector instrument, integrated with a Lambda Physik excimer laser (193 nm) with GeoLas optics. Details of the procedure are outlined in Monsels *et al.* (2018). Main parameters for the ablation spot setup are: 5 mJ laser energy, 10Hz pulse repetition rate and 120µm spot diameter. The ICP-MS operating conditions are plasma power: 1300W; gas flow rates (L/min): cool 16.0 Ar, auxiliary 1.0 Ar, carrier: 0.685 He, 0.696 He; peak-jump scanning mode; time-resolved acquisition mode; 60 seconds total ablation time. Si is employed as internal standard. SRM-NIST 612 is used during the measurements to correct for background and drift with double-standard measurements bracketing each six samples. Reported compositions are averages of three measurements for each sample. Accuracy of the results is monitored by analyzing USGS standard BCR-2 after each six samples. The percentage of deviation from recommended values, determined in multiple sessions, was generally ≤ 10% for all reported trace elements (Monsels *et al.*, 2018).

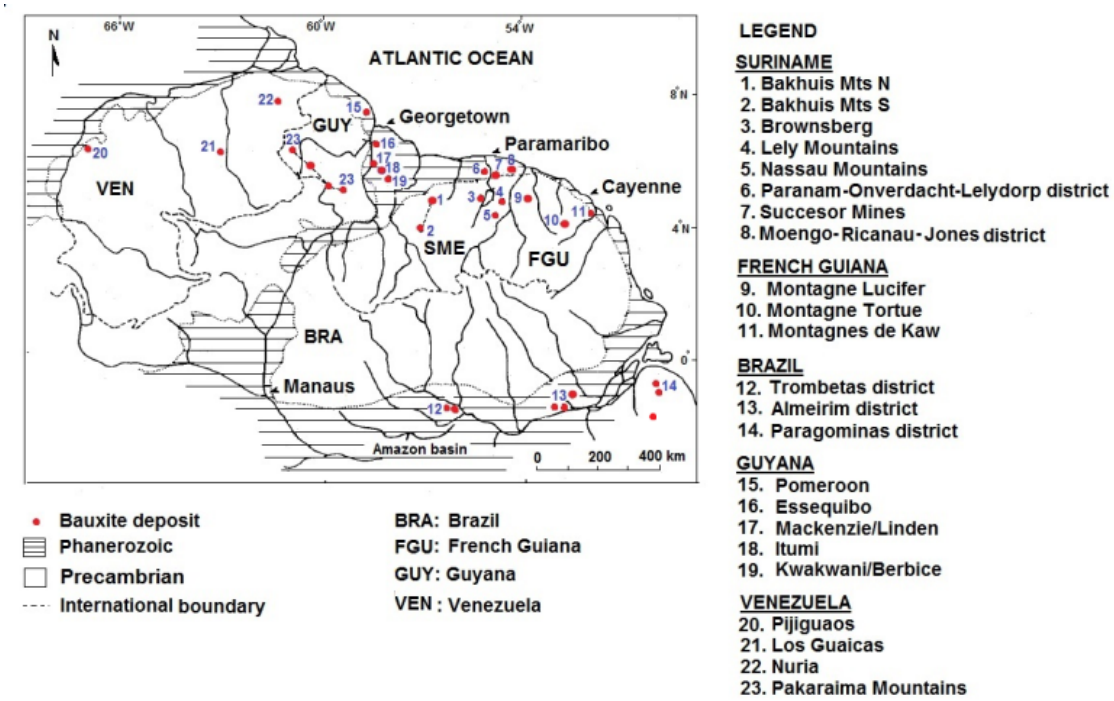

Figure 1. Bauxite districts of the Guiana Shield and Guiana Basin (modified after Bardossy and Aleva, 1990)

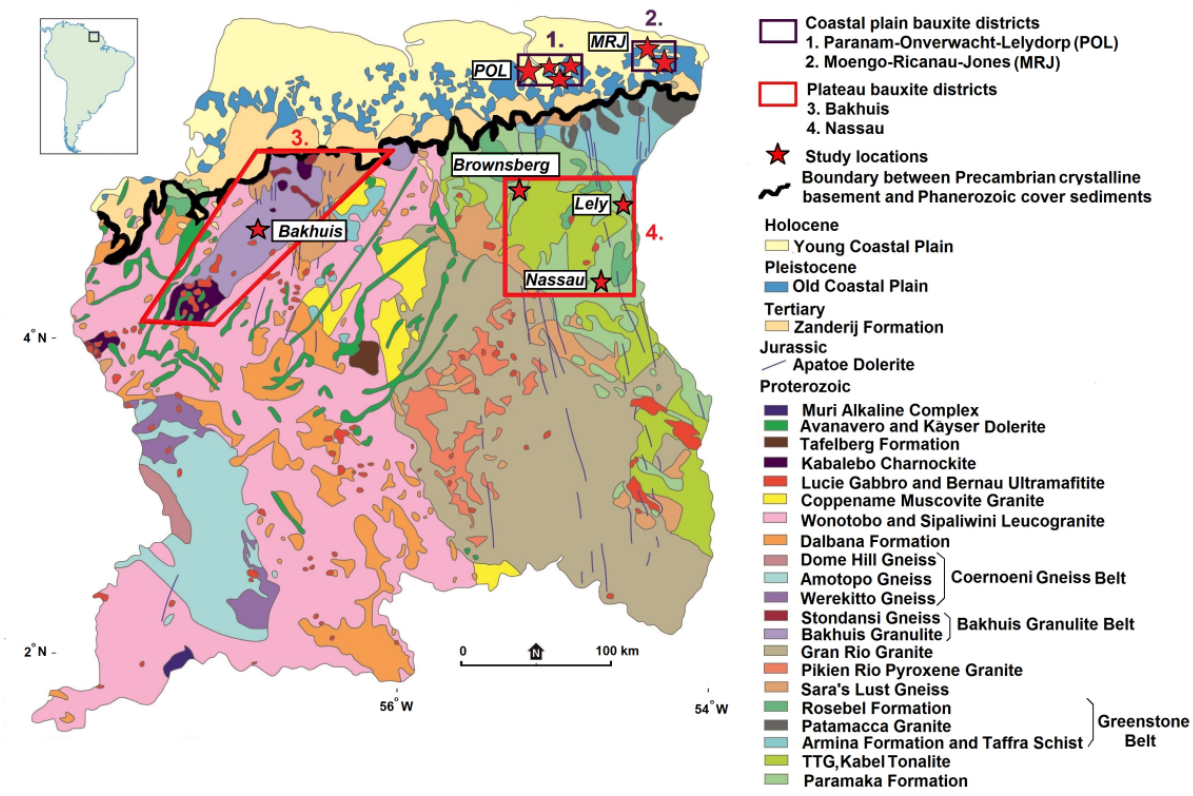

Figure 2. Geological map of Suriname with the bauxite districts and studied locations (modified after Kroonenberg *et al.*, 2016).

RESULTS

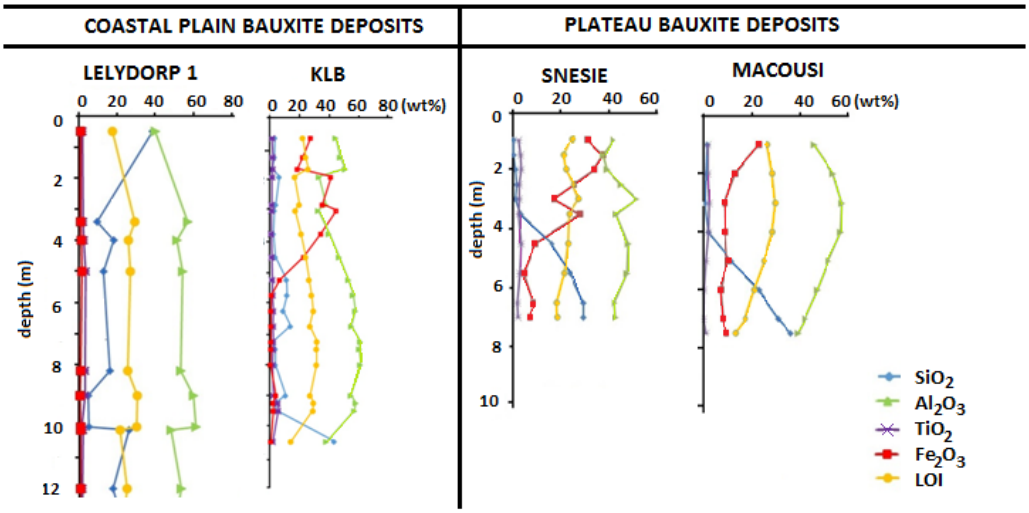

Figure 3. Variations in major-element contents in vertical profiles through selected Coastal-plain and Plateau bauxite deposits. Trends in the Plateau bauxites are largely due to in-situ weathering of Precambrian precursor rocks, whereas those in the Coastal plain bauxites are also influenced by stratigraphic heterogeneity within the original Tertiary precursor sediments and infiltrations from the sedimentary overburden (e.g SiO_2 of Lelydorp-1).

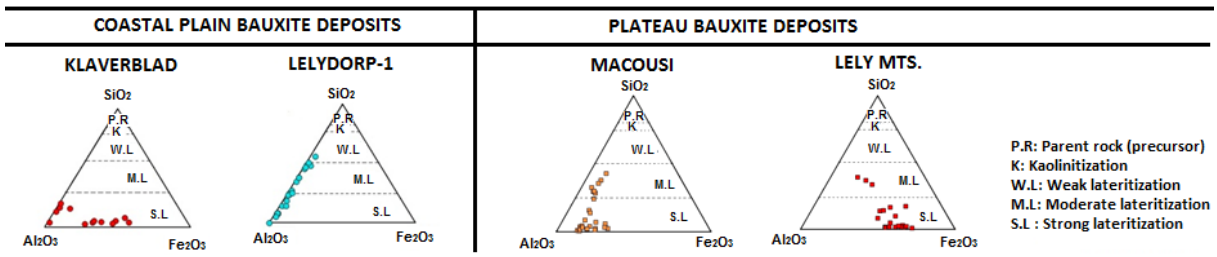

Figure 4. Triangular plots depicting the differences in chemical composition (especially iron) and degree of lateritization in the Coastal plain and Plateau bauxite deposits.

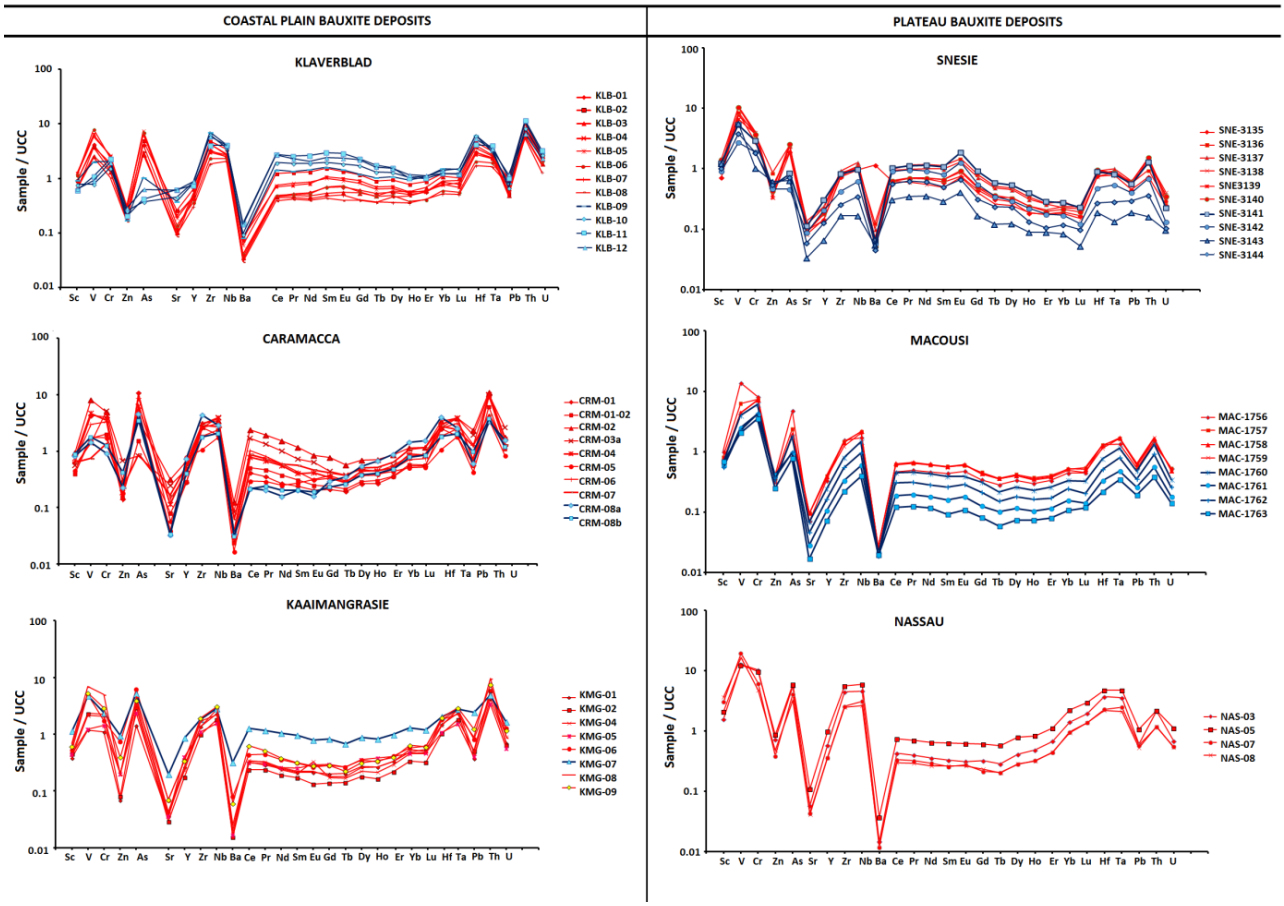

Figure 5. Upper-continental-crust (UCC) normalized contents of trace elements in selected weathering profiles of Plateau and Coastal plain bauxites. Samples indicated in red have < 5 wt% SiO_2, while those in blue contain >5 wt% SiO_2. Except for the group of easily leached elements (e.g., Zn, Sr, Ba), the trends largely reflect the precursor rock on which the bauxite developed. Note the existence of differences between the Plateau and Coastal-plain bauxites, as well as within these groups. Deviations from parallelism within a deposit are attributable to internal stratigraphic heterogeneity or mobility and weathering-induced redistribution.

CONCLUSIONS

The petrological and geochemical analysis of the studied samples revealed the following similarities between the Coastal-plain and Plateau bauxites:

- All of the deposits belong to the group of lateritic bauxites. In general, the investigated deposits display the classical sequence of a lateritic weathering profile: an iron-rich duricrust cap on top of a bauxite layer that covers a clay-rich saprolite interval, which in turn grades into weathered or fresh (often unexposed) bedrock. This sequence is more consistently developed in the Plateau bauxites than in the Coastal-plain deposits, where irregularities are common.
- Major-element contents reflect the distribution of principal mineral phases in the studied lateritic profiles. Highest SiO_2 contents (kaolinite) are usually observed in bottom parts (i.e., in the saprolite), maximum Al_2O_3 contents (gibbsite) in the bauxite zone, and maximum Fe_2O_3 contents (hematite and goethite) in duricrusts at the top (examples in Fig. 3).
- Overall chemical effects of immobile-versus-mobile behavior of major and trace elements during formation of the Plateau and Coastal-plain bauxites are similar: strong depletion of Si, K, Na, Mg and Ca as well as Rb, Ba, Sr, Zn and strong, largely residual relative enrichment of Al, Ti, Zr, Nb, Hf, Ta, Th and U (Fig. 5).

The two bauxite groups are distinct in the following aspects:

- On average, the investigated Plateau bauxites are chemically distinct from the sedimentary Coastal-plain bauxites. A conspicuous difference is the more ferruginous character of the former group, an obvious expression of the higher iron contents in the crystalline Precambrian precursor rocks, which range from (ultra)high-temperature metamorphic gneissic and amphibolitic rocks in the Bakhuis Mountains (granulite belt in west Suriname) to greenschist-facies metabasalts and other meta-igneous rocks in the Greenstone Belt in east Suriname (Nassau Mountains, Lely Mountains and Brownsberg) (Figures 3, 4, 5and 6).
- Chemical variation is also seen within each of the bauxite groups. Apart from the lithological diversity in Proterozoic rocks of Suriname's interior, the geochemical signatures, grade and volumes of the Plateau bauxites are influenced by physical rock properties, landscape morphology, local hydrological conditions and drainage efficiency. These factors are also responsible for the origin of textural differences within and between the Plateau deposits. Variations in major-element signatures within the various Coastal-plain bauxite deposits are modest, while differences in trace-element signatures are substantial. The investigated

bauxites of the Successor deposits contain more iron than those of the nearby POL district, which can be explained by differences in genesis (reworking) and the precursor sediments, possibly controlled by their provenance.

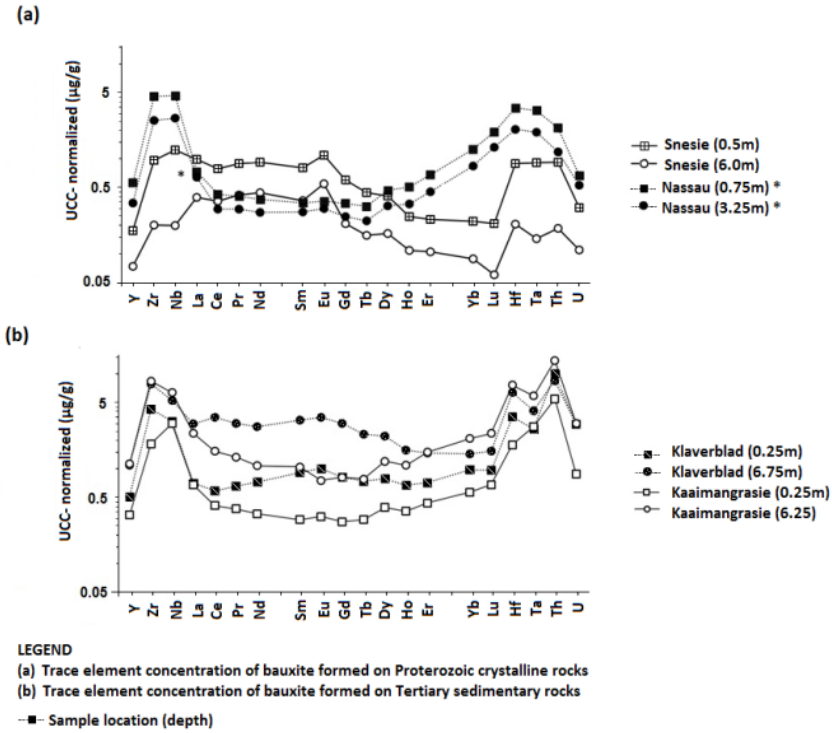

Figure 6. Trace element abundances of HFSE and REE, normalized to upper continental crust (UCC, McLennan 2001) in selected samples from four study areas (Figure 2), which reveals differences in trace-element signatures between bauxite groups and bauxite districts and deposits. (a) Samples from the top (squares) and bottom parts (circles) of Plateau bauxite on Proterozoic crystalline parent rocks; (b) Samples from the top (squares) and bottom parts (circles) of Coastal bauxite profiles on Tertiary sediments.* Note that La concentrations in the Nassau samples are overestimated due to impurity of the borate flux.

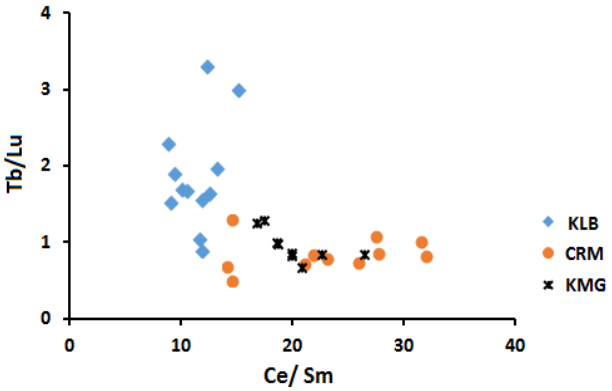

Figure 7. Ce/Sm vs. Tb/Lu ratios of the Successor bauxites, illustrating a chemically distinct trace-element signature of the Klaverblad (KLB) deposit which is chemically distinct from that of the two other Successor deposits. As this difference is difficult to explain by weathering effects, the KLB bauxite must have formed on a different sediment. In view of its separate location (next to the Suriname River), it was probably derived from another source than the sediments of the more remote Kaaimangrasie and Caramacca deposits (closer to the Commewijne River), which may have had a separate, common source.

- Accessory minerals of the Plateau bauxites are exclusively derived from the underlying crystalline parent rock, while the heavy mineral fraction of the Coastal-plain bauxites originated from multiple sources, including terrigenous sedimentary material eroded from Precambrian lithologies in the hinterland or, in some specific cases, the underlying Precambrian basement. Regional as well as local variations in the heavy mineral fraction of the Coastal-plain bauxites can be attributed to heterogeneity in the provenance area of precursor sediments and changing river systems (Figure 7).
- The enrichment of high field-strength elements (HFSE) and heavy rare earth elements (HREE) can be directly linked to the resistance of zircon and other mineral hosts against weathering. This effect is particularly significant in the Coastal-plain bauxites where placer-like accumulations of zircon and other heavy minerals in the terrigenous precursor sediments are locally responsible for stronger enrichments than bauxitization of eroded materials from average rock types would predict (Figure 5-6).

- Boehmite is of subordinate importance as secondary aluminium phase. Small amounts are locally present in the Plateau bauxites, whereas it is exceedingly scarce in the coastal plain, where its presence has only been documented for Coermotibo and Lelydorp-1 (Van der Laan, 1998). This difference might hint at changes in climatic and/or drainage conditions.
- The common presence of an up to 40 m thick sedimentary cover on top of the Coastal-plain bauxites stands out as a major contrast with the Plateau deposits. Infiltration from this overburden has locally resulted in pronounced resilication of the top section of the buried deposits (figure 3). Overlying swamps locally produced additional chemical effects. The most conspicuous example is the Coermotibo deposit in the Moengo area, where the reducing acidic marshy environment modified it into a sulphurous marcasite-rich bauxite. Sulphides are also present in the Lelydorp-I, II and III deposits.

The results of this work demonstrate that parent sediments are much more heterogeneous than previously thought. Also, genetic relationships between bauxite and kaolinite-rich or sandy layers are seemingly diverse but can also be non-existent. Such variability seems in line with presumed age differences among underlying sediments (Eocene for the Moengo deposits, Paleocene-Eocene for the Onverdacht deposits, Paleocene for the Successor deposits).
Overall it can be concluded that the intricate petrologic characteristics and compositional heterogeneity of the bauxite deposits can essentially be explained by element fractionation in combination with relative and absolute enrichment processes, erosion and reworking during two-stage, polycyclic bauxitization of heterogeneous precursors during Late Cretaceous – Early Tertiary times.

ACKNOWLEDGMENTS

I would like to thank my (co-)promotors prof. R. Wortel, Prof. Th. Wong and dr. M. van Bergen. I also want to thank T. Bouten, H.de Waard and A.van Leeuwen-Tolboom for help with analytical work at Utrecht University. I am also grateful to P.Vroon for generously providing access to the laboratory facilities at the VU University, Amsterdam. The Bauxite Institute of Suriname and Suralco L.L.C kindly provided major-element data and samples from exploration drilling campaigns. This research was funded by a grant from the Suriname Environmental and Mining Foundation (SEMIF).

REFERENCES

Aleva, G., 1979, Bauxites and other duricrusts in Suriname: A review. Geologie en Mijnbouw 58, 321-336.
Aleva, G. and Wong, Th., 1998,The history of bauxite exploration and mining in Suriname In: The history of earth sciences in Suriname- Royal Netherlands Academy of Arts and Sciences & Netherlands Institute of Applied Geoscience. TNO, 275-310.
Bárdossy, G. and Aleva, G., 1990, Lateritic bauxites. Developments in Economic Geology. Elsevier Science Publishing 27, 569 pp.
Bakker, J., Kiel, H. and Müller, H.,1953. Bauxite and sedimentation phases in the northern art o Surinam (Netherlands Guiana). Geologie en Mijnbouw 15, 215-226.
Bogatyrev, B. and Zhukov.V and Teskovky, Y., 2009, Formation conditions and regularities of the distribution of large and superlarge bauxite deposits. Lithology and mineral resources 44 (2), 135-151.
Carvalho, A., Boulangé, B., Melfi, A and Lucas, Y., 1997, Brazilian bauxites. Orstom, São Paolo-Paris, 331 pp.
King, L.C., Hobday, D.K. and Mellody, M., 1964, Cyclic denudation in Surinam. Internal report Geologische Mijnbouwkundige Dienst Suriname, Paramaribo, 1-12.
Krook, L., 1969. The origin of bauxite in the coastal plain of Surinam and Guyana. Mededelingen Geologisch Mijnbouwkundige Dienst, 20, 173-180.
Kroonenberg, S., De Roever, E., Fraga, L., Reis, N., Faraco, M., Lafon, J., Cordani, U. and Wong, Th., 2016, Paleoproterozoic evolution of the Guiana Shield in Suriname: A revised model. Netherlands Journal of Geoscience, Geologie en Mijnbouw, 95 (4), 491-522.
Ling K.., Zhu, X., Tang, H., Du, S., Ga, J., 2018, Geology and geochemistry of the Xiaoshanba bauxite deposit, Central Guizhou Province, SW China: Implications for the behavior of trace and rare earth elements. Journal of Geochemical Exploration, 190, 170–186.
McLennan, S., 2001, Relationships between trace element composition of sedimentary rocks and upper continental crust. Geochemistry, Geophysics, Geosystems (2), 4.
Monsels, D., 2016, Bauxite deposits in Suriname: Geological context and resource development. Netherlands Journal of Geosciences 95, 405-418.
Monsels, D. and Van Bergen, M., 2017, Bauxite formation on Proterozoic bedrock of Suriname. Journal of Geochemical Exploration, 180, 71-90.
Monsels, D. and Van Bergen, M., *with editor*, Bauxite formation on Tertiary sedimentary parent rocks in Suriname. Journal of South American Earth Sciences
Monsels, D., Van Bergen M. and Mason, P., 2018, Trace element analysis of bauxite using laser ablation inductively coupled plasma mass spectrometry on lithium borate glass beads. Geostandards and Geoanalytical Research, 42 (2), 239-251.
Moses, J. and Mitchell, W., 1963, Bauxite deposits of British Guiana and Surinam in relation to underlying unconsolidated sediments suggesting two-step origin. Economic Geology 58 (2), 250-262.
Oliveira, S., Costa, M. and Prazeres Filho, H., 2016, The lateritic bauxite deposit of Rondon do Pará: A new giant deposit in the Amazon region, Northern Brazil. Economic Geology, 111, 1277–1290
Patterson, S., Kurtz, H., Olson, J., Neeley, C.,1986, World Bauxite Resources; Geology and resources of Aluminum. U.S. Geological Survey professional paper, 1076-B. United States Government Printing Office, Washinghton, 158 pp.
Théveniaut, H. and Freyssinet, Ph., 2002. Timing of lateritization on the Guiana Shield: synthesis of paleomagnetic results from French Guiana and Suriname. Palaeography, Palaeoclimatology, Palaeoecology, Elsevier, 178, 91-117.
Valeton, I., 1983, Palaeoenvironment of lateritic bauxites with vertical and lateral differentiation. Geological Society, London, Special Publications 11, 77-90.

Van der Hammen, T. and Wijmstra, T., 1964, A palynological study on the Tertiary and the Upper Cretaceous of British Guiana. Leidse Geologische Mededelingen, 30, 183-241.

Van der Laan, S., 1998, Mineralogy and textures of Suriname bauxites: Report prepared for Billiton. Hoogovens Research and Development, IJmuiden, 1-15

Van Kersen, J., 1956, Bauxite deposits in Suriname and Demerara (British Guiana), Thesis Leiden; also published in Leidse Geologische Mededelingen 21, 247-375.

Wong, Th., de Kramer, R., de Boer, P, Langereis, C. and Sew-A-Tjon, J., 2009, The influence of sea-level changes on tropical coastal lowlands; the Pleistocene Coropina formation, Suriname. Sedimentary Geology 216, 125-137

Ultramafic rocks of the Paleoproterozoic greenstone belt in the Guiana Shield of Suriname, and their mineral potential

Renoesha Naipal
Department of Geosciences, Anton de Kom University of Suriname
Leysweg 86, Paramaribo, Suriname

renoesha.n@gmail.com

Salomon Kroonenberg
Department of Geosciences, Anton de Kom University of Suriname
Leysweg 86, Paramaribo, Suriname
and Delft University of Technology

salomonkroonenberg@gmail.com

Paul R.D. Mason
Faculty of Geosciences, Utrecht University

Vening Meinesz building A, Princetonlaan 8a, 3584 CB Utrecht, Netherlands

p.mason@uu.nl

SUMMARY

The ultramafic rocks of the Marowijne Greenstone Belt in Suriname and elsewhere in the Guiana Shield comprise both intrusive dunite-gabbroic bodies and ultramafic lavas and volcaniclastic rocks. They were emplaced in the early stages of the Trans-Amazonian Orogeny (2.26-2.09 Ga), but their petrogenesis and geotectonic significance have still to be elaborated. They present several economically interesting mineralisations, including chromium, nickel, platinum, gold and diamonds. In Suriname diamonds are found since the 19th century; possible source rocks show similarities with the diamondiferous komatiitic volcaniclastic rocks in Dachine, French Guiana and in Akwatia in the Birimian Greenstone Belt of Ghana. This might point to a regionally extensive diamond belt in the Guiana Shield and its predrift counterpart in the West-African Craton.

Key words: Ultramafic rocks, volcaniclastics, cumulates, greenstone belt, diamonds, nickel, chromium

INTRODUCTION

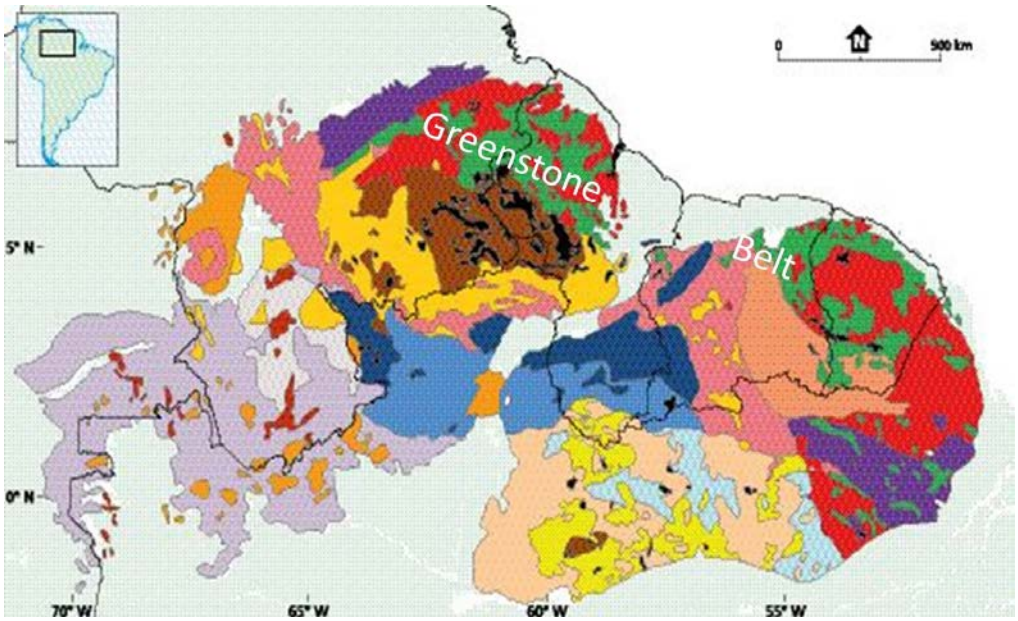

Figure 1: The Trans-Amazonian Greenstone Belt of the northern Guiana Shield, (Kroonenberg et al., 2016).

Ultramafic rocks are one of the least investigated but economically most promising rocks in the Paleoproterozoic greenstone belt of Suriname, stretching over a distance of 1500 km along the whole northern coast of the Guiana Shield from Venezuela to the Amapá state in Brazil (Figure 1). Ultramafic rocks are the host rocks of nickel, chromium, platinum, gold and diamond mineralisations in the Guiana Shield. On the Geological Map of Suriname, 1977 (Bosma et al., 1984) all ultramafic and mafic intrusions in the country were classified together as De Goeje Gabbro (Bosma et al., 1983; Bosma et al., 1984), and were considered to belong to a single magmatic event around 1870 Ma (Priem et al., 1971). However, recent zircon datings from French Guiana (± 2147 Ma; Tampok gabbro, Pb–zircon evaporation; Delor et al., 2003a), showed that the ultramafics in the greenstone belt are at least 100 million years older than those found in western and central Suriname (dated at 1985 Ma, Kroonenberg et al., 2016). The ultramafic bodies in the Surinamese part, the Marowijne Greenstone Belt, have therefore been renamed as the Bemau Ultramafitite, and those in western and central

Suriname Lucie Gabbro (Kroonenberg et al., 2016). These rocks are not only believed to differ in age but also have other rock associations. Rocks like talc schists, chlorite schists, tremolite rocks and serpentinites are common accompanying rock types in the greenstone belt, but absent in the Lucie Gabbro of western Suriname. The purpose of this study is to investigate the petrogenesis, emplacement and tectonic setting of ultramafic rocks in the greenstone belt, and evaluate their importance for mineralisation.

MAJOR OCCURRENCES OF ULTRAMAFIC ROCKS IN THE MAROWIJNE GREENSTONE BELT

The ultramafic rocks in the Marowijne Greenstone Belt as illustrated in figure 2 can be grouped into three (3) main occurrences as described below.

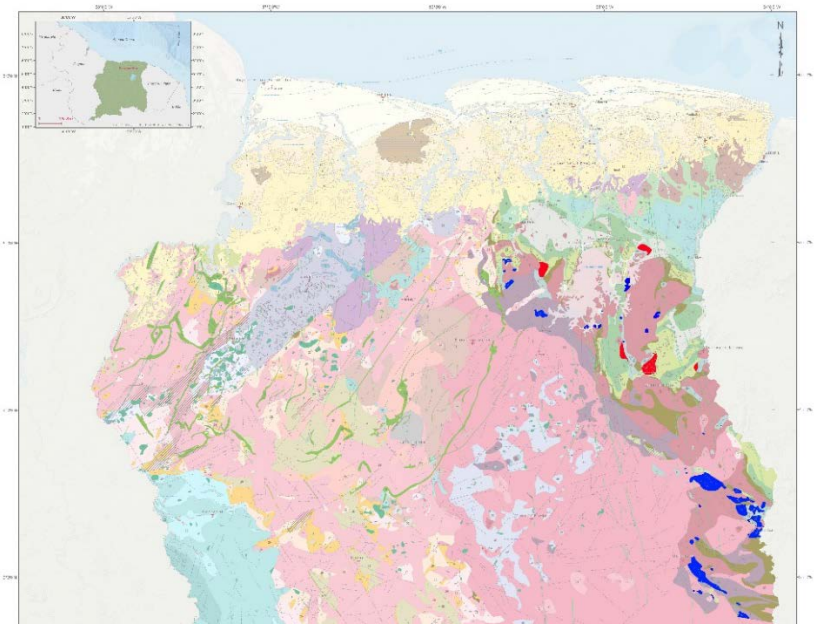

Figure 2: Occurrences of ultramafic rocks (red) and metagabbros (blue) (modified from geological map of Suriname, the national geological survey GMD).

(1) The **Bemau ultramafic complex** in the Saramacca area (Figure 3) consists of cumulate dunite-wehrlite-clinopyroxenites and gabbroic plutonic rocks, interpreted as Alaskan-type intrusives (Veenstra, 1983; Teuling, 2018) as well as ultramafic talc-chlorite schists, which might represent ultramafic lavas and volcaniclastic rocks on the basis of vesicular and sedimentary structures (Figure 4). An unusual corundum-chrome spinel rock is thought to represent a metasomatically desilicified cumulate (Teuling, 2018). The primary rocks in drill cores contain up to 0,5% Ni and 1,3% Cr, the overburden up to 0,25% Ni. The corundum-chrome spinel rocks contain up to 0,7% Ni and 6,5% Cr (Bosma et al., 1973; Veenstra, 1983).

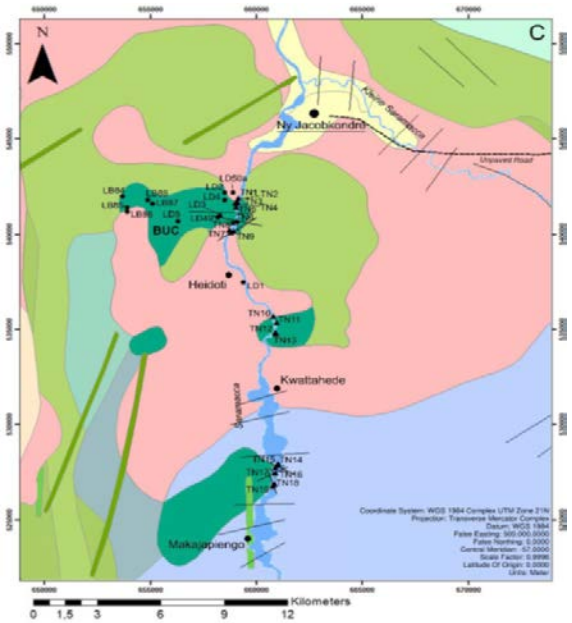

Figure 3: Geological map of the Bemau ultramafic complex and surroundings based on the geological map of Suriname from the national geological survey GMD.

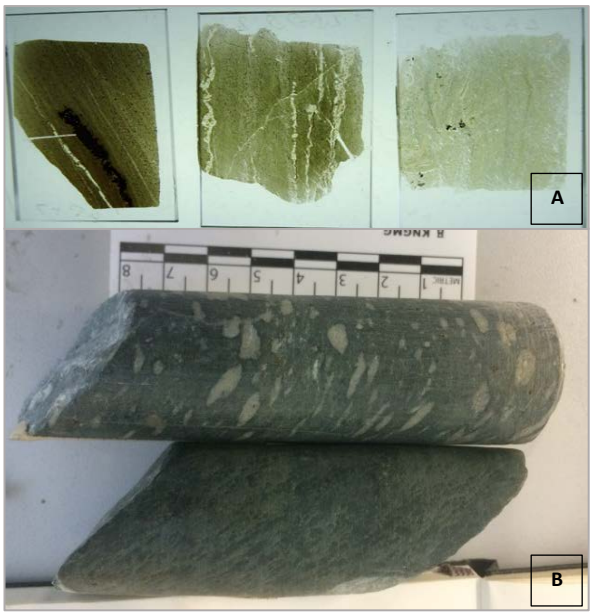

Figure 4: (a) Ultramafic volcaniclastic chlorite schists with sedimentary structures in thin sections of RGM cores and (b) vesicular textures in GMD chromite-bearing -chlorite-talc schists.

(2) Residual chromite deposits associated with peridotites and talc schists were found in a tributary of the Saramacca River, Upper **Toekoemoetoe Creek**. These deposits are found in a weathering zone on top of a ± 2 km long ultramafic body, intercalated between biotite-hornblende gneisses (Bisschops, 1969). Similar small chromite bodies were found in an area west of the **Upper Saramacca River** (Den Hengst, 1975). Cr-bearing ultramafic intrusive rocks with up to 1,0% Cr have been recovered from the **Piqué Hill**, east of the storage lake as well (Bosma et al., 1973).

(3) The **De Goeje Mountains ultramafics** (Figure 5) consist of intrusive metagabbronorite and meta-ultramafitite, ranging from pyroxene-bearing granite-granodiorite to peridotite-dunite. Further serpentines and talc rocks are found in smaller amounts. They usually contain both orthopyroxene and clinopyroxene, and furthermore brownish-green, hornblende and reddish-brown biotite or phlogopite. The plagioclase is dusty labradorite-bytownite. Opaque minerals found are apatite and spinel, the latter especially in olivine bearing rocks (Bosma et al., 1983; Bosma et al., 1984; Kroonenberg et al., 2016). Apart from placer gold, alluvial platinum has been recovered from this area as small rounded grains up to 0,5 g/t, but so far it has not been encountered in the primary rock (Bosma & Groeneweg, 1973). In French Guiana across the Marowijne River, alluvial platinum has been recovered as well in a similar setting (BRGM, 1980).

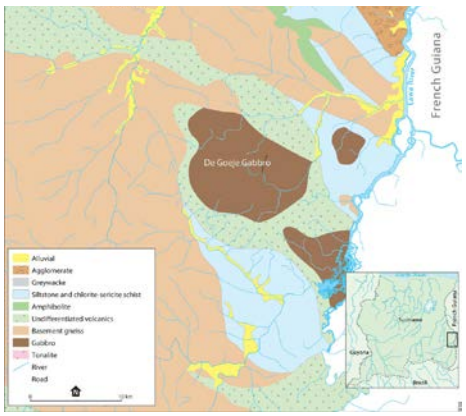

Figure 5: De Goeje Mountains, (Ultra-) mafic intrusive in dark brown (Kioe-A-Sen et al., 2016).

DIAMOND-BEARING ULTRAMAFIC ROCKS

In Suriname findings of diamonds have been reported since 1880, mainly from the the Rosebel - Sabanapasi area, which is now part of the Rosebel Gold Mines concession. According to van Kooten, (1954) diamonds in this area were found in the alluvium derived from the Rosebel conglomerates, but he could not find outcrops with primary diamonds. However, Schönberger (1975) washed many samples of Rosebel conglomerates with a negative result, and he concluded on the basis of the distribution of the diamonds and accompanying minerals that they could not come from the Rosebel Formation, but should have a source in ultramafic rocks (Schönberger & de Roever, 1974), but it is still a question which rock type is the source rock. An intensive search by AdeKUS staff in the archives of the Geological and Mining Service resulted in the discovery of ultramafic volcaniclastic rocks in a core (Figure 4a, as yet unpublished), that was drilled in the 1950ies in Schönbergers target area in the Rosebel area, for the purpose of copper exploration. Also recent IAMGOLD drill cores in the Rosebel Gold Mines concession, notably in the Koemboe area, showed the presence of volcaniclastic ultramafic rocks (chlorite-carbonate and phlogopite-talc –carbonate schists; (Ramlal, 2018). The latter rocks are characterised by high contents of chromium and nickel (>1000 ppm Cr and >600 ppm Ni, respectively). A perusal of the Rosebel Gold Mines chemical database shows that rocks with such high Cr and Ni content are widespread in the whole area, suggesting that ultramafic volcaniclastic rocks have a larger distribution than just the Rosebel area. Other areas where the findings of diamonds are reported are the northeastern part of the Nassau Mountains area, near the Conglomerate Creek and the Paramacca Creek (Headley, 1913). During fieldwork held in September 2018, metavolcaniclastic rocks are sampled of the Nassau Mountains area and several black aphanitic schistose rocks. These volcaniclastic rocks are agglomerates with more basaltic fragments, a few black aphanitic fragments enclosed in a darker groundmass. Large basalt boulders, which were insitu at some locations were encountered in the same fieldwork area, one of them intruded by mineralized (gold and pyrite) black veins.

Diamond occurrence in the neighbouring countries- In order to understand the diamond occurrences, it necessary to get an overview on the occurrences in the adjacent countries. According to Janse & Sheahan (1995) the main sources of gem-grade diamonds are ultrapotassic kimberlites or lamproites, which are mostly found in areas underlain by Archean cratons. In Venezuela, kimberlites have so far only been found in the Guaniamo region, here they occur as high diamond grade 710 Ma old sheets in massive to steeply foliated Paleoproterozoic granitoid rocks (Kaminsky et al., 2004). Apart from the Guaniamo deposit, other important diamond occurrences in Venezuela are alluvial deposits, mainly associated with Roraima Formation. Similar diamond deposits are found in Guyana, Roraima, which suggest that sources are found within sedimentary sequences of it. All rivers and streams that flow along or across Roraima group contain diamonds (Swiecki, 2011). However, in French Guiana recent research revealed an unusual diamond deposit in the Paleoproterozoic Inini Greenstone Belt at Dachine (Figure 6). The diamonds are hosted in a ultramafic volcaniclastic body consisting of chlorite-carbonate-talc schists and phlogopite-talc schist with komatiitic geochemical affinities (Capdevila, et al., 1999). A similar type of diamond deposit is found in the Akwatia diamond field, Ghana, within the Early Proterozoic Birimian Belt. The Akwatia diamonds are associated with syn-eruptive volcaniclastic metaturbidites, with a composition resembling komatiites (Canales, 2005), where the diamonds are hosted in actinolite-tremolite schist rocks.

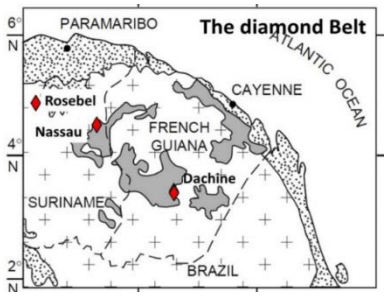

Figure 6: Possible regional diamond belt, modified from Capdivela et al., 1999.

A regional diamond belt? The ultramafic rocks of in the Marowijne Greenstone Belt show similarities with the diamond bearing rocks found in our neighbouring country Dachine (Figure 6) and Akwatia. Although the ultimate source rocks of the diamonds in the Rosebel and Nassau area have not yet been found with certainty, we might speculate that the ultramafic rocks represent a regional event of diamondiferous komatiitic volcanism in

the eastern Guiana Shield (Figure 6). This has important implications on the nature of the mantle processes below the Guiana shield. Further research is ongoing to test this hypothesis.

CONCLUSIONS

Ultramafic rocks in Suriname form an integral part of the Trans-Amazonian Orogeny, but their role in the magmatic history of this event still has to be elucidated. The age and stratigraphic relations between the ultramafic rocks and the other rock units in Marowijne Greenstone Belt should be investigated. Age dating is required to elucidate the position of these rocks in the magmatic deformational and metamorphic events in the greenstone belt. Also the processes that gave rise to the nickel, chromium, platinum and gold mineralisations have to be sorted out. It is as yet unclear whether the volcaniclastic ultramafic talc schists are co-magmatic with the ultramafic–gabbroic cumulate intrusions or represent a separate, possibly komatiitic event. It is also still unclear whether the source rock of the Suriname diamonds is comparable to the diamond bearing rock units occurring in Dachine and Akwatia as so far no insitu diamonds are found in Suriname.

REFERENCES

Bisschops, J.H., 1969. The Roraima Formation in Surinam. 7th Guiana Geological Conference. Verhandelingen Nederlands Geologisch Mijnbouwkundig Genootschap 27, 109–118.

Bosma, W., Ho Len Fat, A.G. & Welter, C.C., 1973. Minerals and mining in Suriname. Mededelingen Geologisch Mijnbouwkundige Dienst van Suriname 22: 71-101.

Bosma, W. & Groeneweg, W., 1973. Review of the stratigraphy of Suriname. Mededelingen Geologisch Mijnbouwkundige Dienst Suriname 22: 17–41.

Bosma, W., Kroonenberg, S. B., Maas, K. & De Roever, E. W. F., 1983. Igneous and metamorphic complexes of the Guiana shield in Suriname. Geologie en Mijnbouw 62 241–254. .

Bosma, W., Kroonenberg, S.B., van Lissa, R., Maas, K. & de Roever, E.W.F., 1984. Explanation to the Geological map of Suriname 1:500,000. Mededelingen Geologisch Mijnbouwkundige Dienst van Suriname 27, 31–82.

BRGM., 1980. Inventaire minier du Département de la Guyane. Bilan et perspectives au 31.12.1979. BRGM Direction Cayenne, 127 pp.

Caen-Vachette, M., 1988. The West African craton and the Guiana Shield: a single craton from the Lower Proterozoic Paleomagnetism. Journal of African Earth Sciences 7: 479-488.

Canales, D.G., 2005. The Akwatia diamond field, Ghana, West Africa: source rock. MSc thesis Department of earth and Environmental Science, New Mexico Institute of Mining and Technology, 145 pp.

Capdevila, R., Arndt, N., Letendre, J. & Sauvage, J. F., 1999. Diamonds in volcaniclastic komatiite from French Guiana. Nature London 399, 456-458.

Delor, C., Lahondere, D., Egal, E., Lafon, J.M., Cocherie, A., Guerrot, C. & de Avelar, V., 2003a. Transamazonian crustal growth and reworking as revealed by the1:500,000-scale geological map of French Guiana. Géologie de la France. 2-3-4, 5–57.

Den Hengst, P., 1975. The Upper Saramacca chromite. Mededelingen Geologisch Mijnbouwkundige Dienst Suriname 23, 244–249.

Gruau, G., Martin, H., Leveque, B., Capdevila, R. & Marot, A., 1985. Rb-Sr and Sm-Nd geochronology of lower Proterozoic granite-greenstone terrains in French Guiana. South America: Precambrian Research 30, 63-80.

Headley, D.E., 1913. Diamonds in Dutch Guiana. The Engineering and Mining Journal 94 no. 18, p. 888.

Janse, A.J.A., & Sheahan, A.P., 1995. Catalogue of world wide diamond and kimberlite occurences: a selective and annotative approach. Journal of Geochemical Exploration 53, 73-111.

Kaminsky, F.V., Sablukov, S.M., Sablu, L.I. & DeR. Channer, D.M., 2004. Neoproterozoic 'anomalous' kimberlites of Guaniamo, Venezuela: Mica kimberlites of 'isotopic transitional' type. Lithos 761 565-590.

Kioe-A-Sen, N.M., Van Bergen, M.J., Wong, T.E. & Kroonenberg, S.B., 2016. Gold deposits of Suriname: geological context, production and economic significance. Netherlands Journal of Geoscience; Geologie en Mijnbouw 95 4: 1-17.

Kroonenberg, S.B., de Roever, E.W.F., Fraga, L.M., Reis, N.J., Faraco, T., Lafon, J.M., Cordani, U. & Wong, T.H., 2016. Paleoproterozoic evolution of the Guiana Shield in Suriname: A revised model. Netherlands Journal of Geoscience 95, 491-522.

Priem, H.N.A., Boelrijk, N.A.I.M., Hebeda, E.H., Verdurmen, E.A.T. & Verschure, R.H., 1971. Isotopic ages of the Trans-Amazonian felsic magmatism and the Nickerie Episode in the Precambrian basement of Surinam, South America. Geological Society of America Bulletin 82, 1667–1680.

Ramlal, S., 2018. An investigation of the Brincks intrusion and its relationship to the surrounding gold deposits, Brokopondo, Suriname, South America. MSc thesis Anton de Kom University of Suriname, 142 pp

Schönberger, H. & de Roever, E.W.F., 1974. Possible origin of the diamonds in the Guiana Shield. Geology, 1974, 2 (10) 474-475

Swiecki, R., 2011. *http://www.minelinks.com*. March. Accessed October 23, 2018. http://www.minelinks.com/alluvial/diamondGeology42.html.

Teuling, F.S.R., 2018. Petrogenesis of the Bemau Ultramafic Complex, Guiana Shield, Surinam. MSc thesis Department of Earth Sciences, Utrecht University, 144 pp.

van Kooten, C., 1954. Eerste onderzoek op diamant: Rosebel-Sabanpassie. Geologisch Mijnbouwkundige Dienst van Suriname Mededeling 11, 63 pp..

Veenstra, E., 1983. Petrology and Geochemistry of Sheet Ston Broeke, Sheet 30, Suriname. Geologisch Mijnbouwkundige Dienst Suriname, Mededeling 26, 138 pp.

Lessons from the West African Craton, Archean and Paleoproterozoic tectonic evolution, derived from in-situ zircon data: applications to northern South American tectonic evolution?

Luis A. Parra-Avila*
School of Earth Sciences
University of Western Australia
Western Australia

Luis.parraavila@uwa.edu.au

Helen McFarlane
Centre for Exploration Targeting
School of Earth Sciences
University of Western Australia

Helen.mcfarlane@uwa.edu.au

Marco L. Fiorentini
Centre for Exploration Targeting
School of Earth Sciences
University of Western Australia

Marco.fiorentini@uwa.edu.au

Mike Tedeschi
Centre for Exploration Targeting
School of Earth Sciences
University of Western Australia

michael.tedeschi@research.uwa.edu.au

SUMMARY

The tectonic evolution of the Paleoproterozoic Baoule-Mossi domain is subject to much debate. In order to provide further constraint and shed some insights into the process that shaped the domain we utilised a combination of whole-rock geochemical characterisation of felsic intrusions along with in-situ zircon measurements of the U-Pb, O and Lu-Hf isotopic systems. The geochemical data display a signature that show intrusions sourced at different depths and that evolve from an arc-type environment to a collision-type one, while the zircon data show the emplacement ages between ca. 2260 and 2000 Ma, with the O and Lu-Hf data indicating a greater crustal contamination than previously identified.

Key words: Zircon, U-Pb, O and Lu-Hf isotopes, West African Craton.

INTRODUCTION

For over fifty years, the tectonic setting of the West African Craton has been the subject of much debate. Multiple tectonic models covering different time periods between 2200 and 1900 Ma have been proposed. Some of the models that describe the tectonic evolution of the West African Craton advocate for plume-related/oceanic plateau (e.g. Abouchami, et al. 1990), oceanic plumes and diapirs (e.g. Lompo 2009, Vidal, et al. 2009), convection-controlled crustal thickening (e.g. Cooper and Miller 2014), and subduction associated to arc systems (e.g. Ama Salah, et al. 1996, Baratoux, et al. 2011). In-situ zircon analyses are considered an invaluable tool that can provide further constraints and a deeper understanding of the tectonic setting for the formation of the craton. Zircon grains are capable of locking-in information regarding the U-Pb, O and Lu-Hf isotope systems during crystallization. More critically, due to their resilience and refractory characteristics, they can survive partial melting and high-grade metamorphism without resetting the mentioned isotopic systematics (Scherer, et al. 2007). These systems provide key information regarding the crystallisation of the studied rocks (U-Pb), the presence of crustal contamination (O) and the source of such crustal contaminant (Lu-Hf), which, when integrated, it provide a detail crustal growth and evolution picture (Hawkesworth, et al. 2010, Hawkesworth and Kemp 2006, Kemp, et al. 2009, Kemp and Hawkesworth 2014, Kemp, et al. 2006, Scherer, et al. 2007).

METHODS

In order to generate the in-situ U-Pb, O and Lu-Hf datasets required to study the crustal evolution of the Paleoproterozoic West African Craton, one hundred samples were collected from across the Baoule-Mossi domain (Figure 1). The samples are representative of felsic igneous complexes either exposed at surface level or obtained from drill core holes. All the samples were selected to maximise spatial distribution without compromising sample density in order to provide a comprehensive overview of the characteristics of the plutons exposed across the domain. Each sample (1-4 kg in weight) was described from hand specimens to document general appearance and characteristics. Thin sections were used to identify mineral phases and textures and provide an accurate identification of the rock type. Zircons were extracted from each sample using the methods described in Claoué-Long, et al. (1995) using heavy liquids and magnetic separation. The zircon crystals were hand-picked and mounted in epoxy discs (150-100 crystals/sample and four samples/mount) following the procedures described in Claoué-Long, et al. (1995). Each mount was imaged using transmitted and reflected light microscopy, as well as BSE and CL imaging techniques to characterise the internal crystal structure.

U-Pb dating (75 samples) was carried out using Sensitivity High Resolution Ion Micro Probe (SHRIMP), applying the methodology described by Claoué-Long, et al. (1995), De Laeter and Kennedy (1998), Kennedy and De Laeter (1994), and Williams (1998). O isotopes measurements = were collected for 20 of the dated samples using a CAMECA 1280 following the procedures described in Martin, et al. (2006) and (2008), followed by the acquisition of Lu-Hf analyses for 45 of the samples using LA-MC-ICPMS as described

in Griffin, et al. (2000), and Jackson, et al. (2004). Whole-rock geochemical characterisation was done in a private laboratory on samples from of veining and weathered material. The samples were washed, dried, crushed, and pulverized in vibrating low Chrome Steel Bowls, which utilise a single low Chrome steel puck to pulverize the sample. Major elements were analysed by XRF when possible or by X-Ray Fluorescence Spectrometry and the loss on ignition was determined between 105 and 1000 degrees Celsius. All the results are reported on a dry sample basis, and the LOI1000 was determined gravimetrically. Trace element concentrations were determined using acid digestion methods.

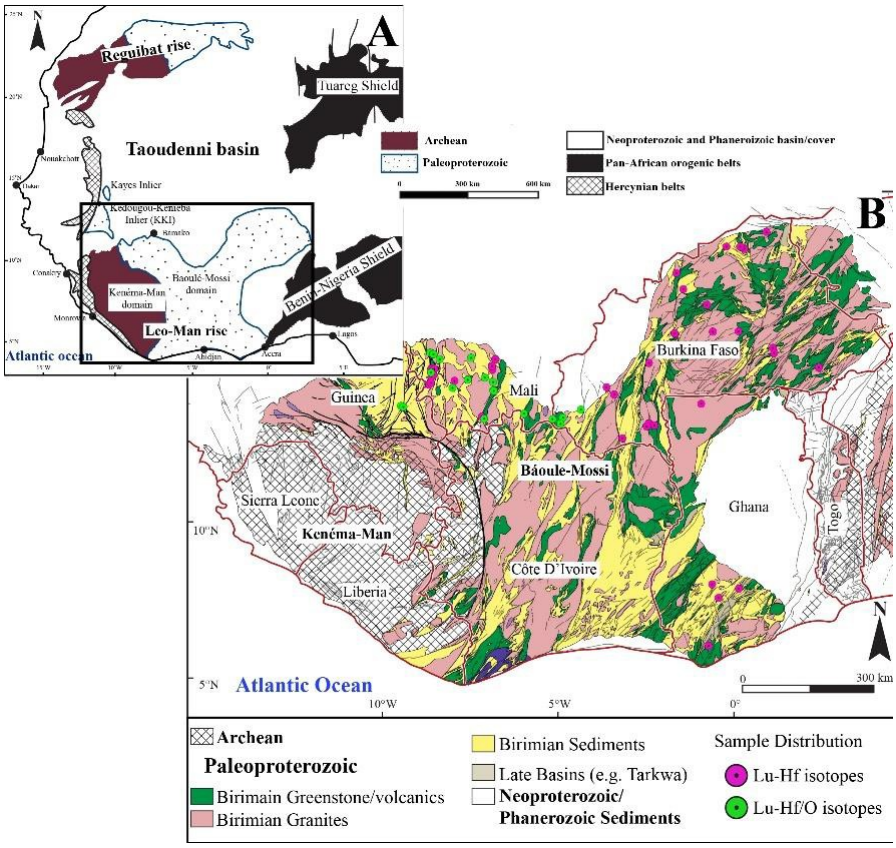

Figure 1. Simplified geological map of the West African Craton (Parra-Avila, et al. 2018 and references therein) showing the location of the samples collected during the present study.

RESULTS AND INTERPRETATIONS

Mineralogical observations indicate the presence of two dominant types of intrusions briefly summarised as: a) biotite-bearing intrusions characterised by plagioclase, alkali feldspar and quartz ± hornblende, and variable amounts of titanite, apatite, sulfides and oxide phases; b) biotite/muscovite plagioclase-rich intrusions dominated by alkali feldspar and quartz, with variable zircon and sulphide content, which is also reflected in existing literature.

The geochronological data obtained from the U-Pb isotope system revealed felsic intrusion ages spanning from ca. 2250 and 2000 Ma, expanding the age range of magmatism for the domain. It shows a diachronous evolution characterised by the westward migration of a magmatic front and the abrupt cessation of magmatism after ca. 2050 Ma. The presence of a number of Archean inherited grains were documented, ranging in age from 3600 to 2600 Ma, which was previously unrecognised. These observations were facilitated by the large amount of new U-Pb data generated during the study, complemented by available historical data.

O isotopes were collected from a subset of samples between southern Burkina Faso and southern Mali. The O values ranged from 6 and 11 ‰. When plotted as a function of the U-Pb ages, O data revealed a progressive increase in the O ‰ from older samples in the west to younger samples in the east. The increase in O concentration indicates that the samples become increasingly contaminated with crustal material that have being exposed to near surface processes. The collected Lu-Hf data provides information about the nature of the crustal contaminant. The Lu-Hf isotope measurements, expressed as $\varepsilon Hf_{(T)}$, range between 0 and +9, indicative of a predominately mantle derived source. The relatively large spread of $\varepsilon Hf_{(T)}$ for each sample, however, implies a more significant addition of a reworked or older crustal component which suggests magma contamination. The findings from the Lu-Hf data corroborate the contamination identified from the O data set and suggests that the region is recycling predominately juvenile material.

The combination of the U-Pb and Lu-Hf data plotted as a contour map show the presence of different crustal domains across theWest African Craton (Figure 2). Each domain show different levels of crustal contamination and can potentially be used to define isotopic boundaries between amalgamated crustal blocks that form the Baoule-Mossi Domain.

The whole rock geochemical signature of the studied rocks are analogous to modern arc-type environments (e.g. REE pattern and Pb, Ta, anomalies) for the period between ca. 2250 and 2100 Ma. After 2100 Ma the whole rock geochemical indicators are dominated by collision-related magmatism, demonstrated by a decrease in the Na_2O/K_2O ratio.

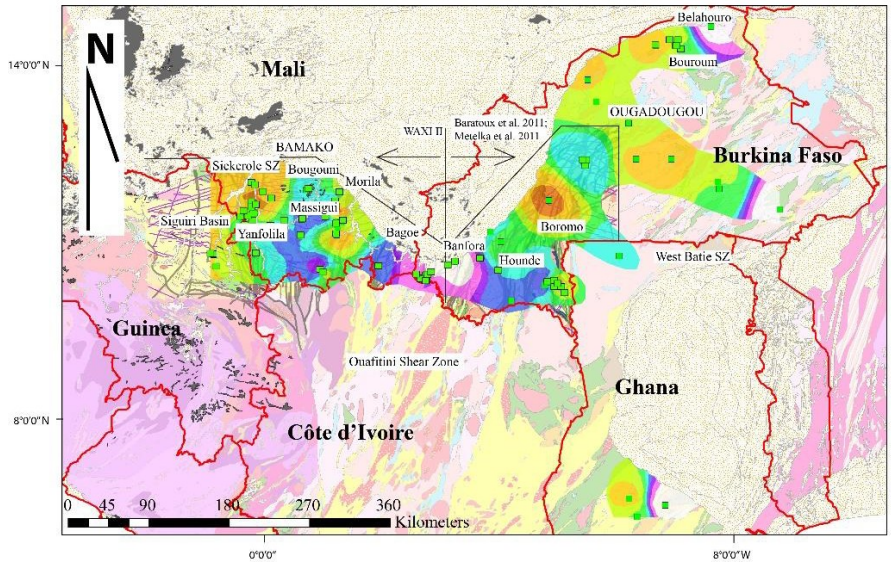

Figure 2. Lu-Hf isotopes map (Parra-Avila, et al. 2018). Map modelling after Champion and Huston (2016). Warm colours regions with a predominately juvenile component. Cold colours represent areas with higher crustal contamination. Notice the purple/dark blue region between Banfora and Bagoe separating 2 regions dominated by warm colours.

CONCLUSIONS

This study demonstrates that integration of in-situ analyses on zircon crystals using multiple isotopic systems, such as U-Pb, O and Lu-Hf, is an effective method to evaluate the tectonic evolution of Archean and Paleoproterozoic regions. In the case of the West African Craton, the combination of different methods revealed trends and tectonic characteristics that were previously unidentified in the region. Interrogation of the dataset indicate the diachronous nature and migration of the magmatic activity from east to west, the presence of more extensive crustal contamination represented by the presence of inherited zircons as old as ca. 3600 Ma, the increase of O ‰ values for younger samples and the large ranges in $\varepsilon Hf_{(T)}$ values that provide further proof of crustal contamination in a domain previously regarded as the product of entirely juvenile magmatic activity particularly in the western portion of the craton. The results of this study are used to examine and refine tectonic models proposed for crustal growth. The isotopic data suggests we have heterogeneous sources, including reworking of, or contamination by, an older crustal component. The geochemical signature tells us about the tectonic setting – ie. Subduction related arc -. So the reworking of the older crustal component is the product of the interaction of the older component with an active subduction zone. Subduction processes are also responsible for the growth and assembly of these blocks.

The methodology described in this study can be applied in other Archean-Paleoproterozoic terranes, in which exposures are limited. The north-eastern portion of the South America continent comprises multiple cratonic terranes, including the Guiana and Brazilian Shield and the São Francisco Craton, representing an ideal region to test this methodology. Many of the questions regarding the assembly of the cratonic domains and the growth of juvenile domains apply for this region of South America (e.g. the nature of the felsic volcanic province to the SW of the Trans-Amazonian province, onset a new subduction zone, or accretion of a different terranes or an anorogenic process). Both regions are dominated by Archean/Paleoproterozoic geology that is poorly understood and thought to be the result of a range of different competing tectonic models. In addition to the importance of understanding the tectonic setting evolution of the region, isotopic studies provide further insights into a period of time though to be a transition between Archean-type vs. modern-type tectonics As demonstrated by this study, the integration of geochemical and isotopic datasets can help narrow the number of competing models. The resulting geochemical and isotopic domains can be tested using complementary fields of geology, such as structural geology or geophysics, providing further constraints on the tectonic evolution of these ancient terranes. s. Overall a better understanding of the cratonic history is a valuable tool that can be used to refine metallogenic models and increase the success rate of ore deposits discovery.

The findings from this study of the West African Craton, in particular the Paleoproterozoic Baoule-Mossi Domain are of great importance for many of the cratonic regions of South America. In the Sao Luis Craton, for example, existing research suggests an accretionary phase between ca. 2240 Ma and 2150 Ma, evolving into a collisional phase at ca. 2080 Ma, similar to the processes identified across the West African Craton. More importantly, paleomagmatic reconstructions, geochronological and isotope data indicate that the Sao Luis Craton was contiguous with the West African Craton during the Paleoproterozoic (Klein and Moura 2008).

ACKNOWLEDGMENTS

We acknowledge AusAid, the ARC Linkage Project LP110100667, AMIRA International, industry and the various Geological Surveys and Departments of Mines in West Africa for their support of the WAXI II project (P934A). LA Parra-Avila acknowledges receipt of UWA Scholarships for International Research Fees (SIRF), University International Stipend (UIS) and Ad Hoc Safety-Net Top-Up Scholarship.

REFERENCES

Abouchami, W., Boher, M., Michard, A., and Albarede, F., 1990, A Major 2.1 Ga Event of Mafic Magmatism in West Africa: An Early Stage of Crustal Accretion. *Journal of Geophysical Research: Solid Earth* **95**, 17605-29.

Ama Salah, I., Liegeois, J.-P., and Pouclet, A., 1996, Evolution D'un Arc Insulaire Océanique Birimien Précoce Au Liptako Nigérien (Sirba): Géologie, Géochronologie Et Géochimie. *Journal of African Earth Sciences* **22**, 235-54.

Baratoux, L., Metelka, V., Naba, S., Jessell, M.W., Grégoire, M., and Ganne, J., 2011, Juvenile Paleoproterozoic Crust Evolution During the Eburnean Orogeny (~2.2–2.0 Ga), Western Burkina Faso. *Precambrian Research* **191**, 18-45.

Champion, D.C. and Huston, D.L., 2016, Radiogenic Isotopes, Ore Deposits and Metallogenic Terranes: Novel Approaches Based on Regional Isotopic Maps and the Mineral Systems Concept. *Ore Geology Reviews* **76**, 229-56.

Claoué-Long, J.C., Compston, W., Roberts, J., and Fanning, C.M., 1995, Two Carboniferous Ages: A Comparison of Shrimp Zircon Dating with Conventional Zircon Ages and 40ar/39ar Analysis, in Time Scales and Global Stratigraphic Correlation Edited by Wa Berggren, Dv Kent, M-P Aubrey, and J Hardenbol. *ociety for Sedimentary Geology, Special Publication* **54**, 3-21.

Cooper, C.M. and Miller, M.S., 2014, Craton Formation: Internal Structure Inherited from Closing of the Early Oceans. *Lithosphere* **6**, 35-42.

De Laeter, J.R. and Kennedy, A.K., 1998, A Double Focusing Mass Spectrometer for Geochronology. *International Journal of Mass Spectrometry* **178**, 43-50.

Griffin, W.L., Pearson, N.J., Belousova, E., Jackson, S.E., van Achterbergh, E., O'Reilly, S.Y., and Shee, S.R., 2000, The Hf Isotope Composition of Cratonic Mantle: Lam-Mc-Icpms Analysis of Zircon Megacrysts in Kimberlites. *Geochimica et Cosmochimica Acta* **64**, 133-47.

Hawkesworth, C.J., Dhuime, B., Pietranik, A.B., Cawood, P.A., Kemp, A.I.S., and Storey, C.D., 2010, The Generation and Evolution of the Continental Crust. *Journal of the Geological Society* **167**, 229-48.

Hawkesworth, C.J. and Kemp, A.I.S., 2006, The Differentiation and Rates of Generation of the Continental Crust. *Chemical Geology* **226**, 134-43.

Jackson, S.E., Pearson, N.J., Griffin, W.L., and Belousova, E.A., 2004, The Application of Laser Ablation-Inductively Coupled Plasma-Mass Spectrometry to in Situ U–Pb Zircon Geochronology. *Chemical Geology* **211**, 47-69.

Kemp, A.I.S., Foster, G.L., Scherstén, A., Whitehouse, M.J., Darling, J., and Storey, C., 2009, Concurrent Pb–Hf Isotope Analysis of Zircon by Laser Ablation Multi-Collector Icp-Ms, with Implications for the Crustal Evolution of Greenland and the Himalayas. *Chemical Geology* **261**, 244-60.

Kemp, A.I.S. and Hawkesworth, C.J., 2014, 4.11 - Growth and Differentiation of the Continental Crust from Isotope Studies of Accessory Minerals. in Heinrich D. HollandKarl K. Turekian (ed.) *Treatise on Geochemistry (Second Edition)*, Elsevier, 379-421.

Kemp, A.I.S., Hawkesworth, C.J., Paterson, B.A., and Kinny, P.D., 2006, Episodic Growth of the Gondwana Supercontinent from Hafnium and Oxygen Isotopes in Zircon. *Nature* **439**, 580-83.

Kennedy, A. and De Laeter, J., 1994, The Performance Characteristics of the Wa Shrimp Ii Ion Microprobe. *US Geological survey circular* **1107**, 16.

Klein, E.L. and Moura, C.A.V.J.G.S., London, Special Publications, 2008, São Luís Craton and Gurupi Belt (Brazil): Possible Links with the West African Craton and Surrounding Pan-African Belts. **294**, 137-51.

Lompo, M., 2009, Geodynamic Evolution of the 2.25-2.0 Ga Palaeoproterozoic Magmatic Rocks in the Man-Leo Shield of the West African Craton. A Model of Subsidence of an Oceanic Plateau. *Geological Society, London, Special Publications* **323**, 231- 54.

Martin, L., Duchêne, S., Deloule, E., and Vanderhaeghe, O., 2006, The Isotopic Composition of Zircon and Garnet: A Record of the Metamorphic History of Naxos, Greece. *Lithos* **87**, 174-92.

Martin, L., Duchêne, S., Deloule, E., and Vanderhaeghe, O., 2008, Mobility of Trace Elements and Oxygen in Zircon During Metamorphism: Consequences for Geochemical Tracing. *Earth and Planetary Science Letters* **267**, 161-74.

Parra-Avila, L.A., Belousova, E., Fiorentini, M.L., Eglinger, A., Block, S., and Miller, J., 2018, Zircon Hf and O-Isotope Constraints on the Evolution of the Paleoproterozoic Baoulé-Mossi Domain of the Southern West African Craton. *Precambrian Research* **306**, 174-88.

Scherer, E.E., Whitehouse, M.J., and Münker, C., 2007, Zircon as a Monitor of Crustal Growth. *Elements* **3**, 19-24.

Vidal, M., Gumiaux, C., Cagnard, F., Pouclet, A., Ouattara, G., and Pichon, M., 2009, Evolution of a Paleoproterozoic "Weak Type" Orogeny in the West African Craton (Ivory Coast). *Tectonophysics* **477**, 145-59.

Williams, I.S., 1998, U-Th-Pb Geochronology by Ion Microprobe. *Reviews in Economic Geology* **7**, 1-35.

The K3 Copper Deposit in the Bakhuis Granulite Belt, W Suriname

***Raysree S. Patadien**
Graduate student, Adekus
Leysweg # 86 Paramaribo, Suriname
raysree.patadien@gmail.com

Dennis J. LaPoint
Appalachian Resources LLC
P.O. Box 3810 Chapel Hill, NC 27515 USA
dennis.lapoint@gmail.com

Emond de Roever
Dept. of Earth Sciences, VU Amsterdams
De Boelelaan 1085, 1081 HV, Netherland
ederoever@ziggo.nl

SUMMARY

A Master's Thesis at the Anton de Kom University of Suriname (Adekus) was initiated to re-study the historic data collected from the copper-phosphate deposit discovered and drilled in the southwestern portion of the Bakhuis Mountains in west Suriname, in the late 1970's by the Geological and Mining Services (GMD). Strong magnetic and electromagnetic anomalies were detected during airborne surveys carried out by the GMD in the early sixties and then followed up by exploration (Dalhberg, 1981). The main objective of this thesis is to recompile and review the copper-phosphate reports and preserved diamond drill core, thin sections and pulps to re-evaluate the origin of this mineralization in light of more recent understanding of copper models.
Copper occurs as chalcopyrite and bornite hosted in pinkish colored bands in migmatitic granulites and in green Ca-silicate granulites. Apatite is predominantly associated with Ca-silicate granulite. There is no direct geochemical or petrographic link between the copper and phosphate mineralization. This study is a first step to use the available samples before they may be lost. The mineralization must be related to the metamorphic and structural history, protoliths, alteration assemblage, and effects of weathering on mineralization. No definite conclusions on copper model types are reached, but this project is a start to preserve and initiate further studies.

Key Words: Suriname, Copper, Bakhuis, Phosphate

INTRODUCTION

The K3 deposit lies in the SW part of the Bakhuis Granulite Belt (**Figure**), a metamorphic terrain located in the Bakhuis Mountains, W Surinam, in the center of the Paleoproterozoic Guiana Shield. Strong magnetic and electromagnetic anomalies were detected here during an airborne geophysical survey carried out for the Geological and Mining Service of Suriname (GMD) in the early sixties. In the 70's the GMD carried out exploration at the site to determine the economic potential of the copper and phosphate occurrences. Diamond drilling was part of the program and 66 shallow holes were completed, with a maximum depth of 100m. Dahlberg (1987) summarized this research and concluded that the copper and phosphate mineralized syenitic and monzonitic rocks and lenses of clinopyroxene-apatite rocks represent metamorphosed cupriferous felsic to intermediate volcanics and phosphatic siliceous carbonate sediments of the supracrustal succession.

The current research compiled and georeferenced this historic data and re-examined core and thin sections plus new ICP-MS analysis of pulps that are still retained. The intent of this research is to update and attempt to re-study the core and thin section, using new technology and mineralization models since the investigation of Dalhberg and other geologists in the seventies and eighties of the previous century on this mineralization.

The Bakhuis Granulite Belt (BGB) consists mainly of intermediate and mafic granulites, with metapelitic intercalations. Younger mafic and felsic intrusions are numerous in the SW part of the belt. The precursor rocks of the granulites are Paleoproterozoic sediments (including Ca-rich rocks, impure limestone?) and mafic and intermediate volcanics (de Roever et al., 2019). These rocks were subjected to ultrahigh-temperature (UHT) metamorphism at 2.07 to 2.05 Ga (de Roever et al, 2003), accompanied by migmatization and intense folding. Charnockites dominate the SW corner of the belt, near Kabalebo, they intruded at 1.99- 1.98 Ga (Klaver et al, 2015), further south west of the Cu deposit. Gabbroic and ultramafic bodies also intruded the SW part of the belt at 1.98 Ga (Klaver et al, 2015), including the Cu deposit area. The next major event effecting the BGB and the Cu area was doming up and steepening of the granulites, accompanied by retrograde metamorphism (de Roever et al, 2003). This research intends to give further information on how these events influenced the copper and phosphate mineralization.

HISTORIC RESEARCH

In the 70's Dahlberg carried out an extensive program of exploration on the K3 Cu-phosphate anomaly in the SW part of the BGB, including a combined magnetic-induced polarization-resistivity survey, soil sampling, geological mapping and diamond drilling. The drill core with the strongest copper mineralization averaged 0.33% (Dahlberg, 1987). The drill-core did not go deeper than ~ 100 m. The sulfidic copper mineralization consists mainly of chalcopyrite and bornite.

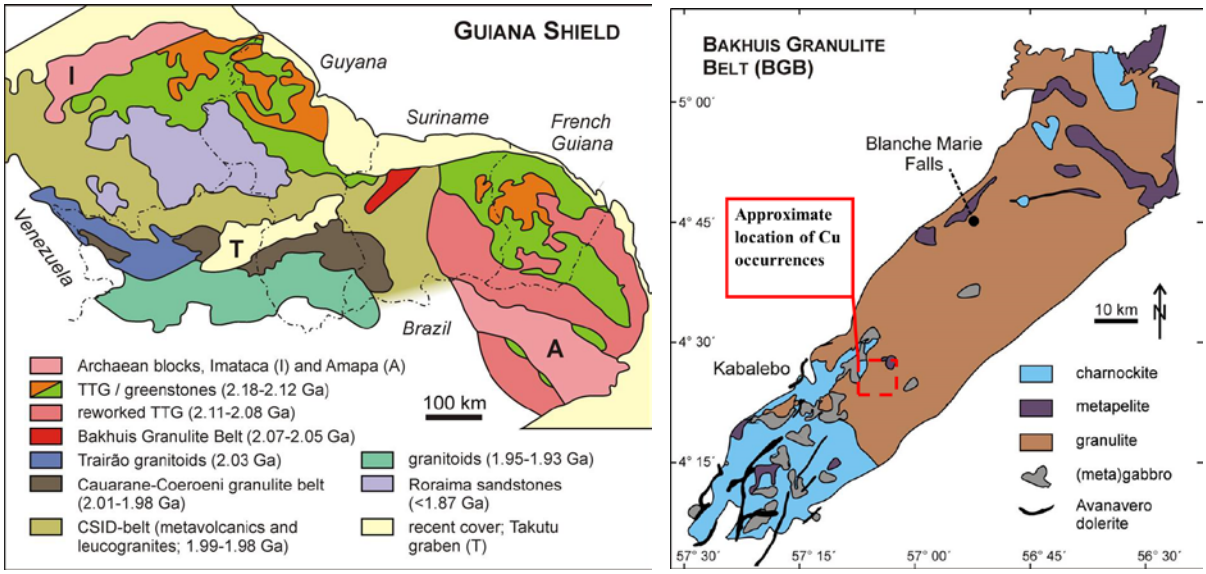

Figure 1 a: simplified geology of the northern part of the Guiana Shield (Klaver et al., 2015); 1b : geology of the BGB.

Phosphate mineralization in the form of apatite-rich lenses is associated to the Cu mineralization, but does not coincide exactly, the highest phosphate values were found outside the main copper mineralized zone (Dahlberg, 1987). Anomalous P, Ce, Th, Zr and Sr soils in an approximate north trending zone were thought to correspond to buried apatite-rich lenses. This zone is part of a larger northeast-trending Ce-Th anomaly found by stream sediment sampling (Dahlberg, 1987).

CURRENT RESEARCH

This research included core logging at the core storage of the Geological and Mining Service of Suriname (GMD). Core of 22 drill holes was described, thin sections were studied using an optical microscope and 220 pulp and sludge samples were analysed using ICP-OES. Part of the drill core is found in bad condition and sometimes the intervals are not readable and tags indicating the depth are not placed at the right location. The core is stored in the core storage of the GMD, which is in bad condition, e.g., the roof is leaking. This results in decomposing of wooden core boxes and contamination and mixed cores, unreadable intervals and notes. The thin sections are stored in an organised manner at the head office of the GMD. Sections from a total of 17 holes were studied using an optical microscope. 222 pulp and sludge samples of drill holes from two cross sections were analysed using ICP-MS at Filab based in Suriname. These pulps are stored in jars at the core storage of the GMD. The interpretation of the geochemistry data is in progress and final conclusions are yet to be drawn.

Historic data including yearly and quaternary GMD reports, maps and publications were reviewed and the maps are georeferenced in order to use GIS software. The field visit to study outcrops and locate drill holes could not be proceeded due to difficult accessibility, at very high costs.

RESULTS

Four main rock types were distinguished in the drill cores investigated: migmatitic granulite, Ca-silicate granulite, metagabbro and ultramafics. In the SW and NE of the area also metapelitic granulites have been found. New names, different from the names used by Dahlberg, have been assigned to the metamorphic rocks, based on their mineralogy and texture. The granulites show a conspicuous banding and foliation. These have a vertical to subvertical orientation. Drilling was vertical, so core may be parallel to the banding or show only a few subvertical bands.

Migmatitic granulites consist of dark melanosome bands and pink to greyish leucosome bands, as a result of ultrahigh-temperature (UHT) metamorphism with partial melting. The minerals in the melanosomes are mainly biotite, orthopyroxene and clinopyroxene, whereas the leucosomes consist of feldspar and local mm-cm-sized orthopyroxene crystals. The feldspar consists of perthite and plagioclase, in part in the form of a single feldspar, mesoperthite. Quartz is lacking.

Ca-silicate granulite consists of abundant, cm-mm-sized, green clinopyroxene crystals appearing as individual crystals or aligned in layers, in a light matrix of feldspar.

Copper mineralization seems to be distributed over various rock types, but higher values occur mainly in the migmatitic granulites but also in Ca-silicate granulites. The copper mineralization is mostly concentrated in the pink to crème bands in the migmatitic granulites, in the form of bornite, chalcopyrite and secondary minerals (Figure). In the Ca-silicate granulites the copper mineralization is macroscopically characterized by the presence of disseminated fine-grained chalcopyrite. Phosphate as apatite occurs in the migmatitic granulites, but higher concentrations have been observed in the Ca-silicate granulites.

In the cores the highest copper assay results are dominantly concentrated at shallow depths (5-50m range), and the copper values seem to decrease in depth. This suggests a supergene enrichment. Macroscopic determination showed that the highest grades of copper bearing rocks are characterized by bornite, chalcopyrite. The bornite is frequently present in fractures, accompanied with the secondary minerals. The bornite may represent a supergene enrichment based on presence in fractures. These fractures are irregular in length and crosscutting the foliation/lineation of the rock. Magnetite filling is another feature related to these fractures, although its presence is not in abundance, but frequently observed. Chalcopyrite appears as fine grain and disseminated usually found in the mafic layering and streaks, and sometimes filled in minor fractures.

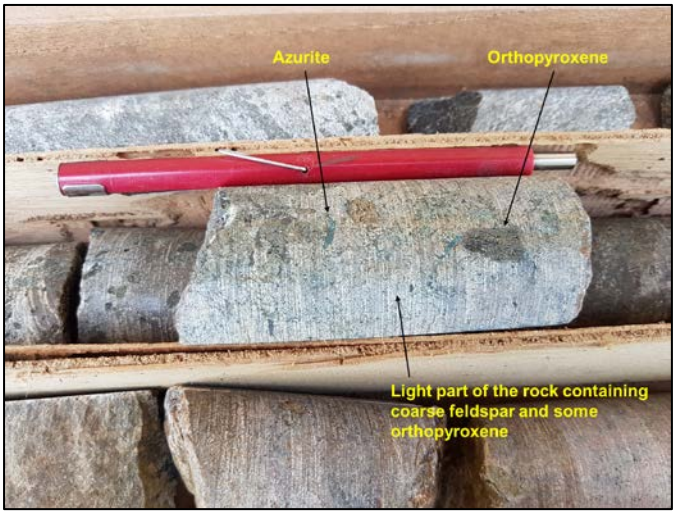

Figure 2. Drill core of crème to pinkish colored migmatitic granulite from drill holes LG 4 (average Cu 2425 ppm) with indications of copper mineralization

DISCUSSIONS AND CONCLUSIONS

Some preliminary conclusions can be drawn from the drill-core and thin section study. The copper mineralization is macroscopically indicated by the presence of chalcopyrite, bornite and secondary minerals that formed during weathering or during the storage of the core. The typical copper-bearing rock is a light, pinkish-cream colored band rich in feldspar, intercalated between dark bands. Sulphides are macroscopically visible in these light bands. In the historic studies, the pink rocks were initially described as syenite and monzonite, suggesting intrusive bodies, but in later articles migmatization was mentioned and the pink rocks were called monzonitic metavolcanics (Dahlberg, 1987). Another possibility for the origin of the pink colored rock is potassic alteration, which is then overprinted by UHT metamorphism, resulting in migmatization of the rock reflected by the bandings of leuco- and melanosome.

The copper mineralization in the migmatitic granulites and Ca-silicate granulites is not associated with hydrothermal alteration or other alteration of later age. The fresh appearance of the Cu mineralization in the cores and the lack of younger associated alteration suggest that the Cu enrichment occurred during UHT metamorphism or, more probably, before, during the precursor stage of the granulites. Copper models are being reviewed on evidence for the copper and phosphate mineralization, but this study will likely not present one model due to the effects of weathering, metamorphism, alteration and understanding the protoliths.

Correlation matrix of ICP-MS data shows that copper is strongly correlated with sulphur, which indicates the presence of copper-sulfide minerals. Silver, sodium, boron, beryllium, lithium, lead, antimony, selenium, and tin show weaker correlations with copper. A similar weak correlation is found with phosphate. The highest copper values are predominantly found in shallow depth and the copper values decrease in depth in these shallow holes. Supergene enrichment maybe a factor.

ACKNOWLEDGMENTS

We would like to acknowledge Professor Theo Wong, who is the faculty supervisor of the Mineral Geoscience course; all the personnel of the GMD who supported us to have access to the data.

REFERENCES

Dahlberg, E. H. (1977). The Upper Nickerie Copper mineralization Bakhuis mountains western Suriname (II).

Dahlberg, E. H. (1981). Geochemical investigation of magnetic and electromagnetic anomalies in the Upper Nickerie copper-rare earth mineralization area, Suriname.

Dahlberg, E. H. (1987). Copper and phosphate mineralization in the lower Proterozoic mobile belt of Bakhuis mountains, Upper Nickerie, Western Suriname, Guiana shield.

Dahlberg, E. H. (1989). Proterozoic phosphorite in the Bakhuis Mountains, Suriname.

de Roever, E., Lafon, J., & Cocherie, A. (2003). The Bakhuis ultrahigh- temperature granulite belt (Suriname): I. petrological

de Vletter, D.R. (1985). Contributions to the geology of Suriname 8, Mededeling 27.

Klaver M., de Roever E.W.F., Thijssen A.C.D., Bleeker W., Soderlund U., Chamberlain K., Ernst R., Berndt J., Zeh A. (2015). Mafic magmatism in the Bakhuis Granulite Belt (western Suriname): relationship with charnockite magmatism and UHT metamorphism.

Kroonenberg, S. B., de Roever, E. W., Fraga, L. M., Reis, N. J., Faraco, T., Lafon, J. M., . . . Wong, T. E. (2016). Paleoproterozoic evolution of the Guiana Shield in Suriname:A revised model.

Sheldon, R. (1982). Analysis of preliminary studies of the Bakhuis Mountains apatite deposit, Suriname.

Innovations for gold exploration in Precambrian greenstone belts: highlights from the Footprints and Metal Earth programs and potential applications to the Guiana Shield

Stéphane Perrouty*, the NSERC-CMIC Footprint Team and the CFREF Metal Earth Team
MERC, HSES, GSM, Laurentian University
935 Ramsey Lake Road, Sudbury, ON, P3E 2C6

sperrouty@laurentian.ca

SUMMARY

Precambrian greenstone belts are variably endowed with base and precious metal resources despite similarities in rock types and tectono-magmatic evolutions. What are the geological processes contributing to metal endowment and how to identify them are fundamental questions for mineral exploration that are being investigated, at two different scales, by the CFREF Metal Earth and the NSERC-CMIC Footprints research programs. This communication presents on-going crustal-scale investigation in the Superior Province and a district-sale synthesis of the multi-parameter footprint that have been identified for the Canadian Malartic deposit, Canada, with potential applications for exploration in the Guiana Shield.

Key words: Abitibi Subprovince, Canadian Malartic, Footprints

INTRODUCTION

The Superior Province is composed of several variably endowed Archean greenstone belts that host diverse base and precious metal deposits. Main gold deposits include volcanogenic massive sulfide deposits (e.g., Mercier-Langevin et al., 2007), intrusion-related deposits (e.g., Robert, 2001), and fault-hosted gold-bearing quartz – carbonate vein "orogenic" deposits (e.g., Dubé and Gosselin, 2007). The gold resources seem to be heterogeneously distributed between greenstones belts: e.g. the Abitibi Subprovince hosts more than 150 Moz Au whereas the Western Wabigoon Subprovince hosts less than 10 Moz Au (Frieman and Perrouty, in press). Identifying the factors that variably influence mineralization across the Canadian Shield will benefit gold exploration by providing new criteria for prospectivity analysis in greenfield environment and new vectoring tools for mineralized systems at depth. At the scale of the crust, the Metal Earth research program (https://merc.laurentian.ca/research/metal-earth), funded by the Canada First – Research Excellence Fund (CFREF), aims to understand whole mineral systems, from the deep crustal fluid sources to the deposit sites, and to characterize the major structural pathways for mineralization. At the scale of a mining camp, the multidisciplinary Mineral Exploration Footprints research program (https://cmic-footprints.laurentian.ca), funded by the Natural Sciences and Engineering Research Council (NSERC) and the Canadian Mining Innovation Council (CMIC), aims to characterize and expand the size of the distal signature of major ore systems, to identify new exploration criteria, and to develop exploration methodologies by integrating geological, structural, lithogeochemical, mineralogical, petrophysical and geophysical datasets (Lesher et al., 2017).

METHOD AND RESULTS

Crustal-scale investigations

Crustal-scale investigations require a good knowledge of the surface geology and extensive geophysical datasets. To that end, a series of eleven 100-km long seismic reflection, MT and gravity traverses were conducted across major greenstone belts in the Superior Province. Four of these transects are in the Abitibi greenstone belt, one in the Swayze greenstone belt, two in the Eastern Wabigoon greenstone belt, and four in the Western Wabigoon greenstone belt (Figure 1A). Each of these transects is being mapped by crews of post-doctoral research associate and graduate students to document the stratigraphic relationship, the nature of the lithological contacts (e.g., unconformities), the tectonic setting and the structural control on various type of base and precious metal mineralization. Objectives are to characterize and model the 3D geometry of the main geological features (e.g., crustal-scale deformation zones, terrane boundaries) that could be potential pathways for hydrothermal fluids. These new datasets will help to determine the key characteristics of gold-mineralized and barren geological setting, and ultimately provide new guidelines for greenfield exploration in Precambrian greenstone belts. Preliminary observations suggest that the relative timing between the hydrothermal activity, the metamorphism and the kinematic along crustal-scale deformation zones could be critical to control orogenic gold endowment in the Superior Province.

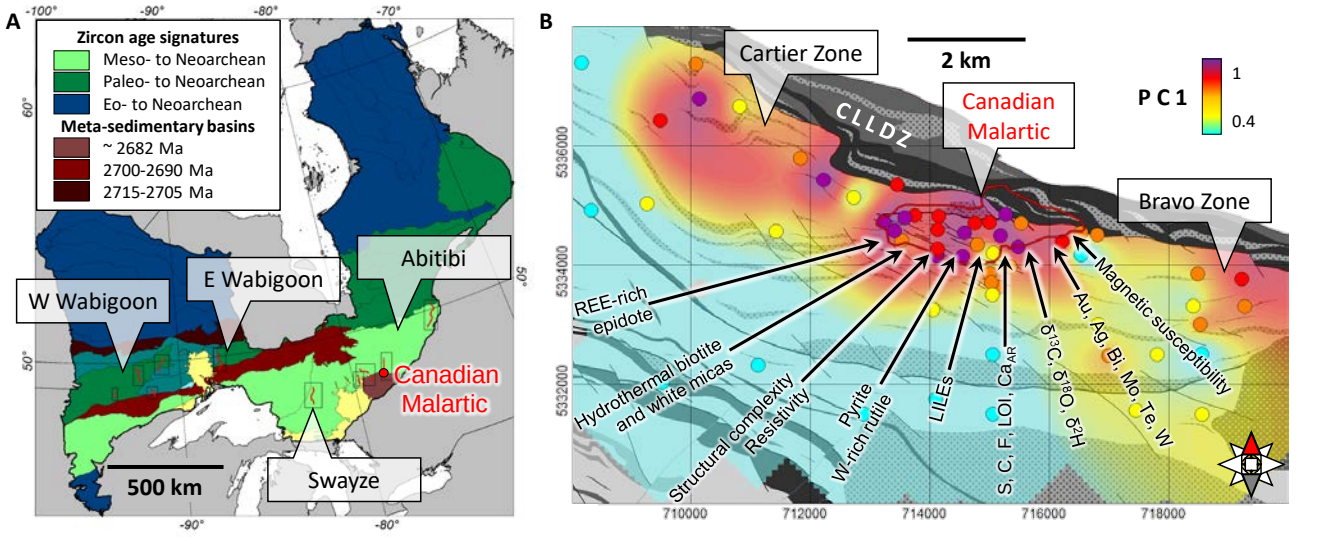

Figure 1: A) Geological sub-provinces of the Superior Province and location of the CFREF Metal Earth transects (red lines) across four Archean greenstone belts (modified after Frieman et al., 2017 and Montsion et al., 2018). The Canadian Malartic deposit is located south of the contact between the Abitibi (light green) and Pontiac (brown) subprovinces. B) Schematic footprint of the Canadian Malartic deposit (modified after Perrouty et al., in press). The color grid represents a metasomatic halo based on principal component analysis of lithogeochemical, mineralogical and petrophysical variables in mafic dykes. Several alteration centers can be seen (Cartier, Canadian Malartic and Bravo). The red line represents the open-pit mine (as designed in 2013). The coordinate system is NAD83-UTM17N.

District-scale investigations

The district-scale studies aim to identify key vectors toward mineralization. Over the last five years, the multi-parameter metasomatic footprint of the Canadian Malartic gold deposit has been extensively using and integrating multiple geological and geophysical datasets. Over one hundred structural, lithogeochemical, mineralogical, petrophysical and geophysical variables were identified, and they outline the spatial distribution of the alteration zones at the periphery of the deposit. The geometries of these metasomatic haloes are both structurally and lithologically controlled along progressive metasomatic fronts from the core to the periphery of the mineralized system.

Geological setting of the Canadian Malartic district

The world-class Canadian Malartic deposit (>18.6 Moz Au, Gervais et al., 2014) is hosted by metamorphosed (upper greenschist to lower amphibolite facies, Piette-Lauzière et al., submitted; protolith name are being used for simplicity) Archean sedimentary rocks and quartz-monzodiorite intrusions of the Pontiac Subprovince, south of the Cadillac Larder Lake Deformation Zone (CLLDZ, Figure 1B), and volcanic rocks of the Abitibi Subprovince. These lithologies were intruded by mafic dykes prior to the mineralization event(s). Volumetrically these mafic dykes are not significant, but they provide key information to characterize the distal alteration. Three major deformation events have been recognized in the area (Derry, 1939; Perrouty et al., 2017) and include: 1) a pre-mineralization and pre-intrusion D_1 deformation event that produced isoclinal F_1 folds and a pressure-solution bedding parallel S_1 cleavage, 2) a syn-mineralization D_2 deformation event that produced open to tight steeply dipping F_2 folds, an east-plunging L_2 stretching lineation and a NW-SE-trending penetrative biotite/amphibole foliation, and 3) a post-mineralization minor D_3 deformation event that produced open F_3 folds, a subtle NE-SW-trending crenulation S_3 cleavage and kinks. Low grade, large-tonnage, gold mineralization is early to syn-metamorphic peak, and is structurally controlled by the CLLDZ, by faulted contacts between intermediate-felsic intrusive and sedimentary host rocks, and by NW-SE high-strain structural corridors within fold hinges. Ore zones are spatially associated with quartz monzodiorites intrusions (Helt et al., 2014, De Souza et al., 2015). The proximal alteration mineralogy consists mainly of biotite, white mica, microcline, albite, quartz, calcite, ferroan-dolomite, rutile and pyrite in the sedimentary rocks (Gaillard et al., 2018) and biotite, albite, quartz, calcite, rutile, and pyrite in the mafic dykes (Perrouty et al., in press).

Integrated multi-parameter footprint

1) Structurally complex zones are systematically associated with gold occurrences in the Canadian Malartic district. They can be detected by field mapping, statistical processing of structural orientation data (e.g., variance of the bedding, Perrouty et al., 2017) and geophysics (Mir et al., in press). This latter technique can be applied at regional-scale and in area with poor outcrop exposure like in the Guiana Shield.

2) Lithogeochemical variations throughout the footprint of the deposit are controlled by protolith compositions, hydrothermal alteration and analytical methods (i.e., partial versus total digestion). Mass gains and losses were calculated and mapped for sedimentary rocks and mafic dykes. Gold and associated elements (e.g., Ag, Te, W, S, C) are enriched in and at the periphery of the deposit in both rock

types (Gaillard et al., 2018). Large-ion lithophile elements (e.g., K, Cs) outline a distal metasomatic halo, up to 6 km from the deposit using mafic dykes (Perrouty et al., in press). Stable isotopes (e.g., H, O) can also be used to detect the presence of hydrothermal alteration (Raskevicius et al., submitted).

3) Mineralogical changes are linked with major element lithogeochemical changes. In mafic dykes, the mineralogy evolves from a distal amphibole-rich composition to a proximal biotite–albite-calcite-quartz–rutile-pyrite mineral association and can be seen using hand lens or quantify through XRD analysis (Perrouty et al., in press). In sedimentary rocks, the relative abundances of alteration minerals such as microcline, calcite, rutile and pyrite increase toward the deposit and can be detected using felspar or carbonate staining (Gaillard et al., 2018). Mineral chemistry changes in biotite and white mica have been documented (Gaillard et al., 2018) and can be mapped efficiently using hyperspectral (Short-Wave InfraRed, SWIR) imagery techniques (Lypaczewski and Rivard, 2018; Lypaczewski et al., submitted). This technique was also applied to document the surficial dispersion of the footprint in the overlaying quaternary sediments (i.e., glacial till, Taylor et al, 2018).

4) Petrophysical properties and geophysical responses are controlled by multiple parameters including mineralogy, porosity and structures. The strong mineral abundance variations in mafic dykes results in a density decrease toward the mineralization. In the Canadian Malartic district, mafic dykes are not volumetrically significant and cannot produce a detectable gravity anomaly. However, a similar hydrothermal alteration in areas dominated by mafic volcanic rock may result in a negative gravity response. Historical Induced-Polarization surveys in the Canadian Malartic district were not successful to detect hydrothermal alteration and gold mineralization. Petrographic investigations of the ore textures highlighted that the increase of pyrite abundance toward the deposit is associated with encapsulation of the pyrite grains in microcline and albite, diminishing the surface of contact between the sulfide minerals and the porosity, and resulting in a negative chargeability anomaly (Bérubé et al., in press). This result suggests that a good understanding of the mineralization assemblage is critical to correctly interpret the geophysical signal. High resolution (meter-scale) time-domain and spectral induced polarization ground surveys were conducted and succeed to detect mineralized sedimentary rocks.

CONCLUSIONS

These innovative and multidisciplinary approaches to investigate mineralized systems revealed over one hundred field- and laboratory-based factors for gold exploration in Precambrian greenstone belt of the Superior Province. Combining these parameters using principal component analysis (Perrouty et al., in press), support vector machine (Bérubé et al., 2018) or other data integration solutions enhance their capacity to vector toward a deposit and decrease the possibility of false positive results. On-going 3D modeling, data integration work and prospectivity analysis at the scale of a greenstone belt (Montsion et al., in press) will contribute explaining the difference in gold endowment between greenstone belts and will provide a new perspective for greenfield exploration. Several vectors that were used to define the footprint Canadian Malartic are also applicable in other geological settings and could be developed further to enhance exploration success in challenging sub-tropical environment, with rare and highly weathered rock exposures, like in the Guiana Shield.

ACKNOWLEDGMENTS

Thanks to all my research colleague of the Metal Earth and Footprints programs for their contribution and thanks to the Canadian Malartic Mine, exploration and production departments for their logistical support during field work. Funding for Metal Earth and Footprints research programs was provided by Canada First – Research Excellence Fund, the Natural Sciences and Engineering Research Council of Canada and the Canada Mining Innovation Council through the NSERC Collaborative Research and Development Program. NSERC-CMIC Mineral Exploration Footprints Project Contribution 200. CFREF Metal Earth Project Contribution MERC-ME-2018-079.

REFERENCES

Bérubé, C.L., Olivo, G.R., Chouteau, M., Perrouty, S., Shamsipour, P., Enkin, R.J., Morris, W.A., Feltrin, L., Thiémonge, R., 2018, Predicting rock type and detecting hydrothermal alteration using machine learning and petrophysical properties of the Canadian Malartic ore and host rocks, Pontiac Subprovince, Quebec, Canada. Ore Geology Reviews, 96, 130–145.

Bérubé, C.L., Olivo, G.R., Chouteau, M., Perrouty, S. Mineralogical and textural controls on spectral induced polarization signatures of the Canadian Malartic gold deposit: applications to mineral exploration. Geophysics, in press.

Derry, D.R., 1939. The geology of the Canadian Malartic gold mine, N. Quebec. Economic Geology, 34, 495–523.

De Souza, S., Dubé, B., McNicoll, V.J., Dupuis, C., Mercier-Langevin, P., Creaser, R.A., Kjarsgaard, I.M., 2015. Geology, hydrothermal alteration, and genesis of the world-class Canadian Malartic stockwork-disseminated Archean gold deposit, Abitibi, Quebec. In: Dubé, B., Mercier-Langevin, P., (Eds), Targeted Geoscience Initiative 4: Contributions to the Understanding of Precambrian Lode Gold Deposits and Implications for Exploration. Geological Survey of Canada, Open File 7852, 113–126.

Dubé, B., Gosselin, P., 2007. Greenstone-hosted quartz-carbonate vein deposits. In: Goodfellow, W.D. (Ed.), Mineral Deposits of Canada: A Synthesis of Major Deposit Types, District Metallogeny, the Evolution of Geological Provinces, and Exploration Methods. Geological Association of Canada, Mineral Deposits Division, pp. 49–73. Special Publication 5.

Frieman, B.M., Kuiper, Y.D., Kelly, N.M., Monecke, T., Kylander-Clark, A., 2017. Constraints on the geodynamic evolution of the southern Superior Province: U-Pb LAICP-MS analysis of detrital zircon in successor basins of the Archean Abitibi and Pontiac subprovinces of Ontario and Quebec, Canada. Precambrian Research, 292, 398–416.

Frieman, B.M., Perrouty, S., 2018. Preliminary structural and stratigraphic investigations along the Metal Earth Dryden-Stormy Lake transect. Open-File Report, Ontario Geological Survey, in press.

Gaillard, N., Williams-Jones, A.E., Clark, J.R., Lypaczewski, P., Salvi, S., Perrouty, S., Piette-Lauzière, N., Guilmette, C., Linnen, R.L., 2018. Mica composition as a vector to gold mineralization: deciphering hydrothermal and metamorphic effects in the Malartic district, Quebec. Ore Geology Reviews, 95, 789–820.

Gervais, D., Roy, C., Thibault, A., Pednault, C., Doucet, D., 2014. Technical Report on the Mineral Resource and Mineral Reserve Estimates for the Canadian Malartic Property. Mine Canadian Malartic, 460 p.

Helt, K.M., Williams-Jones, A.E., Clark, J.R., Wing, B.A., Wares, R.P., 2014. Constraints on the Genesis of the Archean Oxidized, Intrusion-Related Canadian Malartic Gold Deposit, Quebec, Canada. Economic Geology, 109, 713–735.

Lesher, C.M, Hannington, M.D., Galley, A.G., and the Mineral Exploration Research Network , 2017. Integrated multi-parameter exploration footprints of the Canadian Malartic disseminated Au, McArthur River-Millennium unconformity U, and Highland Valley porphyry Cu Deposits: preliminary results from the NSERC-CMIC Mineral Exploration Footprints Research Network, Exploration '17, Toronto, ON, 23 p.

Lypaczewski, P., Rivard, B., 2018. Shortwave infrared reflectance spectroscopy of white mica, biotite and chlorite with variable mineral chemistries. International Journal for Earth Observation and Geoinformation, 68, 116–126.

Lypaczewski, P., Rivard, B., Gaillard, N., Perrouty, S., Piette-Lauzière, N., Bérubé, C.L., Linnen, R.L. Hyperspectral imaging as a tool for vectoring towards mineralization; study of the Canadian Malartic gold deposit, Quebec, Canada. Ore Geology Reviews, submitted.

Mercier-Langevin, P., Dubé, B., Lafrance, B., Hannington, M., Galley, A., Moorhead, J., Gosselin, P., 2007. Metallogeny of the Doyon-Bousquet-LaRonde mining camp, Abitibi Greenstone Belt, Quebec. In: Goodfellow, W.D. (Ed.), Mineral Deposits of Canada: A Synthesis of Major Deposit-Types, District Metallogeny, the Evolution of Geological Provinces, and Exploration Methods. Geological Association of Canada, Mineral Deposits Division, pp. 673–701. Special Publication 5.

Mir, R., Perrouty, S., Astic, T., Bérubé, C.L., Smith, R.S. Identification of structurally complex gold-mineralized zones using airborne EM and ground IP in the Canadian Malartic district, Quebec, Canada. Geophysics, in press.

Montsion, R.M., Thurston, P., Ayer, J., 2018. 1:2,000,000 scale geological compilation of the Superior Craton, Metal Earth, Mineral Exploration Research Center, Laurentian University. 1 p.

Montsion, R.M., Perrouty, S., Frieman, B.M. Preliminary regional interpretation and sampling program for modeling and prospectivity analysis of the Western Wabigoon subprovince. Open-File Report, Ontario Geological Survey, in press.

Perrouty, S., Gaillard, N., Piette-Lauzière, N., Mir, R., Bardoux, M., Olivo, G.R., Linnen, R.L., Bérubé, C.L., Lypaczewski, P., Guilmette, C., Feltrin, L., Morris, W.A., 2017. Structural setting for Canadian Malartic style of gold mineralization in the Pontiac Subprovince, south of the Cadillac Larder Lake Deformation Zone, Québec, Canada. Ore Geol Reviews, 84, 185–201.

Perrouty, S., Linnen, R.L., Lesher, C.M., Olivo, G.R., Piercey, S.J., Gaillard, N., Clark, J.R., Enkin, R.J. Expanding the size of multi-parameter metasomatic footprints in gold exploration: utilization of mafic dykes in the Canadian Malartic district, Quebec, Canada, Mineralium Deposita, in press.

Piette-Lauziere, N., Guilmette, C., Bouvier, A., Perrouty, S., Pilote, P., Gaillard, N., Lypaczewski, P., Linnen, R.L., Olivo, G.R. The timing and extent of prograde metamorphism in the Pontiac subprovince, Superior Craton: implications for Archean geodynamics and gold mineralization. Precambrian Research, submitted.

Raskevicius, T., Beaudoin, G., Kyser, T.K., Perrouty, S., Gaillard, N. Whole-rock $d^{18}O$ and $d^{2}H$ footprint of the Canadian Malartic Gold deposit, Pontiac subprovince, Quebec, Canada. Mineralium Deposita, submitted.

Robert, F., 2001. Syenite-associated disseminated gold deposits in the Abitibi greenstone belt, Canada. Mineralium Deposita 36, 503–516.

Taylor, C.E., Ross, M., Perrouty, S., Lypaczewski, P., Rivard, B., Clark, J.R., Linnen, R.L., Taves, R., 2017. Detecting increasingly larger exploration footprints of a world-class stockwork-disseminated Au deposit: integration of hyperspectral imaging and petrography of glacial clasts in surficial sediments. Abstract, CIM-GAC-MAC, Vancouver, BC, 1 p.

Multiphase TTG intrusions in the Paleoproterozoic greenstone belt of Suriname and their role in gold mineralization in the Rosebel gold district

Shardanand Ramlal

IAMGOLD Rosebel Gold Mines Suriname

Leysweg 86, Paramaribo, Suriname

renoesha.n@gmail.com

Salomon Kroonenberg

Department of Geosciences, Anton de Kom University of Suriname
Leysweg 86, Paramaribo, Suriname
and Delft University of Technology

salomonkroonenberg@gmail.com

Paul R.D. Mason

Faculty of Geosciences, Utrecht University

Vening Meinesz building A, Princetonlaan 8a, 3584 CB Utrecht, Netherlands

p.mason@uu.nl

L. M. Kriegsman

Naturalis Biodiversity Center, Leiden, the Netherlands

Institute of Earth Sciences, Utrecht University, the Netherlands

leo.kriegsman@naturalis.nl

P. O'Sullivan

Department of Geosciences, Anton de Kom University of Suriname Ma'aden Gold & Base Metals Riyadh
Leysweg 86, Paramaribo, Suriname
and Delft University of Technology

OSullivanP@maaden.com.sa

SUMMARY

Four new U-Pb ages of a TTG pluton intruding the gold-bearing greenstone belt of Suriname indicate two phases of TTG magmatism around 2.19 - 2.16 Ga and around 2.12 - 2.11 Ga. The two phases of TTG magmatism are separated by an erosional event. Both phases predate the main phase of gold mineralisation.

INTRODUCTION

The Rosebel gold district in the Paleoproterozoic greenstone belt of the Guiana Shield (Fig. 1) is a major orogenic gold district, formed during the Trans-Amazonian Orogeny between 2.26 and 1.95 Ga (Kroonenberg et al., 2016).

A large granitic pluton known as the Brincks intrusion is present at the southern boundary of the Rosebel Mining Concession. Several gold deposits, and further prospects, are located around and proximal to the Brincks intrusion, although the emplacement and its relationship with the neighboring gold deposits is not fully understood

This body of research investigates the role of the Brinck intrusion in the petrogeny of the Rosebel basin, whether it may have intruded as a single pulse (phase) or during multiple pulses (polyphase), and the genetic relationship between the intrusion and the neighboring gold deposits.

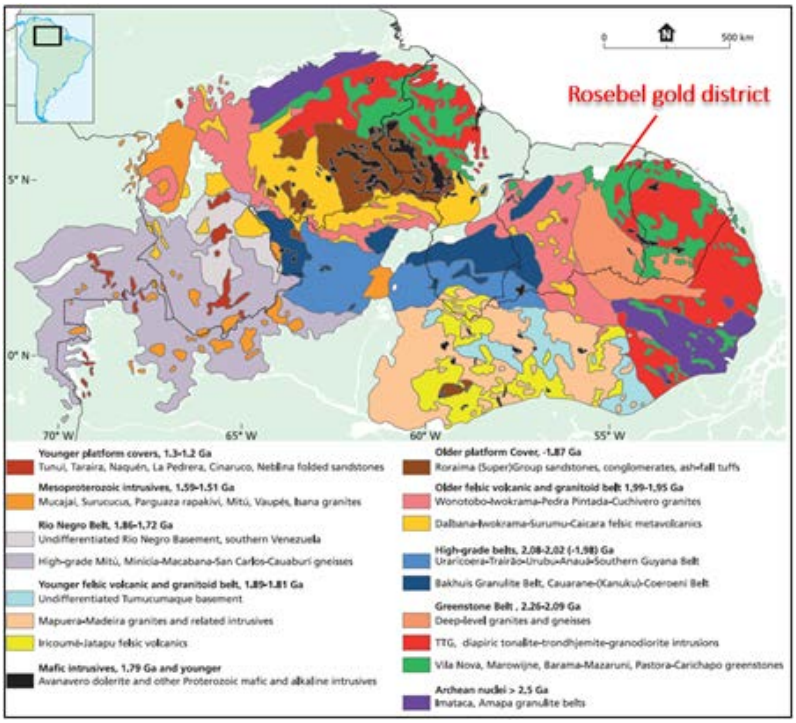

Fig. 1: Simplified geological map of the Guiana Shield (Kroonenberg et al., 2016).

METHODS

Accurate data on the absolute timing of crystallization of rock types defined in the Rosebel area were crucial in order to reconstruct the stratigraphic and deformational relationships and to elucidate the evolutionary history of mineralization around the granites.
Zircon U-Pb ages of the rocks were obtained using the LA-ICP-MS technique. Detailed internal textures of zircons have been analysed using Cathodoluminesence (CL) imaging methods (Fig. 2).

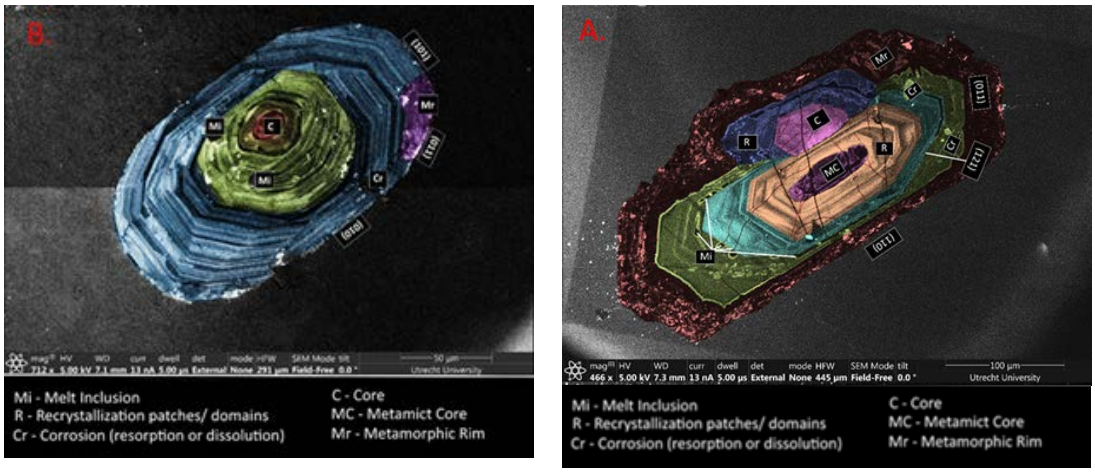

Figure 2. Cathodoluminescence images of isolated zircon crystals showing detailed zircon patterns and different domains. (A) Zircon from the Atjoni Road granite with a pronounced outer-rim due to changing T-P conditions. (B) Zircon from the Royal Hill rhyolite with well-developed oscillatory zoning and in which metamorphic remnants are minor features (Hoogendoorn, 2017).

RESULTS

Granite Atjoni Road The calculated 207Pb/206Pb ages tend to cluster around 2,186 Ma (Fig. 3). The rock contain inherited older Hadean-Archean zircon ages, which demonstrates the existence of an underlying crustal block representing the oldest crustal component of the Guiana Shield. An age of 4.25 Ma records the signature of Early Earth.

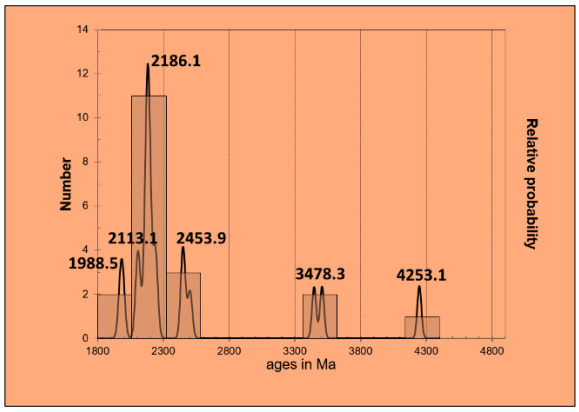

Figure 3 Probability frequency diagram of measured zircons of the granite sample from the Atjoni Road (Hoogendoorn, 2017)

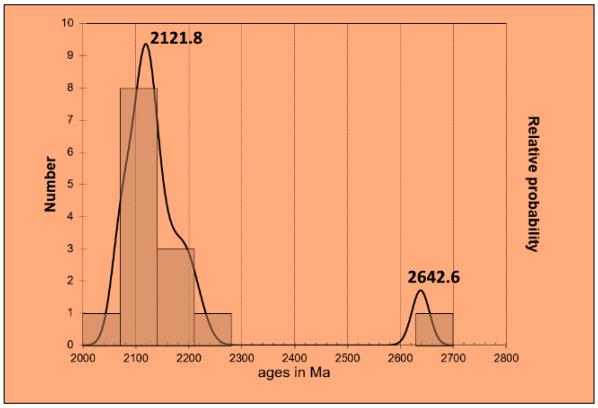

Figure 4 Probability frequency diagram of measured zircons of the rhyolite sample (Hoogendoorn, 2017).

Rhyolite (north of Royal Hill pit). The 207Pb/206Pb values tend to cluster around 2,121 Ma (Fig. 4). One of the zircons shows a significantly older age of 2,642 Ma which could be a recycled zircon from an Archean nucleus that has been reworked and mixed with a Paleoproterozoic source.

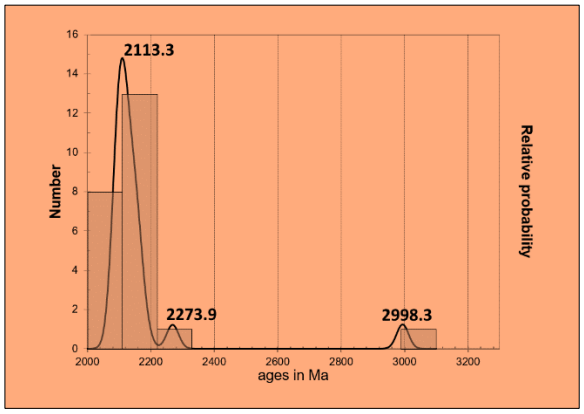

Figure 5 Probability frequency diagram of measured zircons zircons of of the trondhjemite sample (Hoogendoorn, 2017).

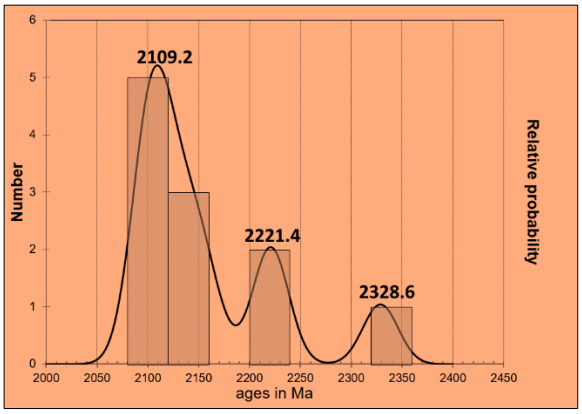

Figure 6 Probability frequency diagram of measured the granite sample from the Koemboe area (Hoogendoorn, 2017).

Trondhjemite (north of Brinck intrusion) The calculated 207Pb/206Pb ages tend to cluster around 2,113 Ma (Fig. 5). One of the zircons shows a significantly older age of 2,998 Ma which could be a recycled zircon from an older source rock.

Granite (Koemboe area The 207Pb/206Pb values tend to cluster around 2,109 Ma (Fig. 6). Some older cores exist which cluster around 2,221 Ma and in a specific case around 2,328 Ma.

CONCLUSIONS

Based on the age dating results two phases of TTG magmatism at ca. 2.19 - 2.16 Ga and 2.12 - 2.11 Ga with a lack of geochronological values in the 2.16 - 2.12 Ga range can be distinguished (Fig. 7, 8). The two phases of TTG magmatism are separated by an erosional event as evidenced by a basal conglomerate containing granite clasts, which also contains the 2.12 Ga rhyolite layer from Royal Hill higher in the sequence.

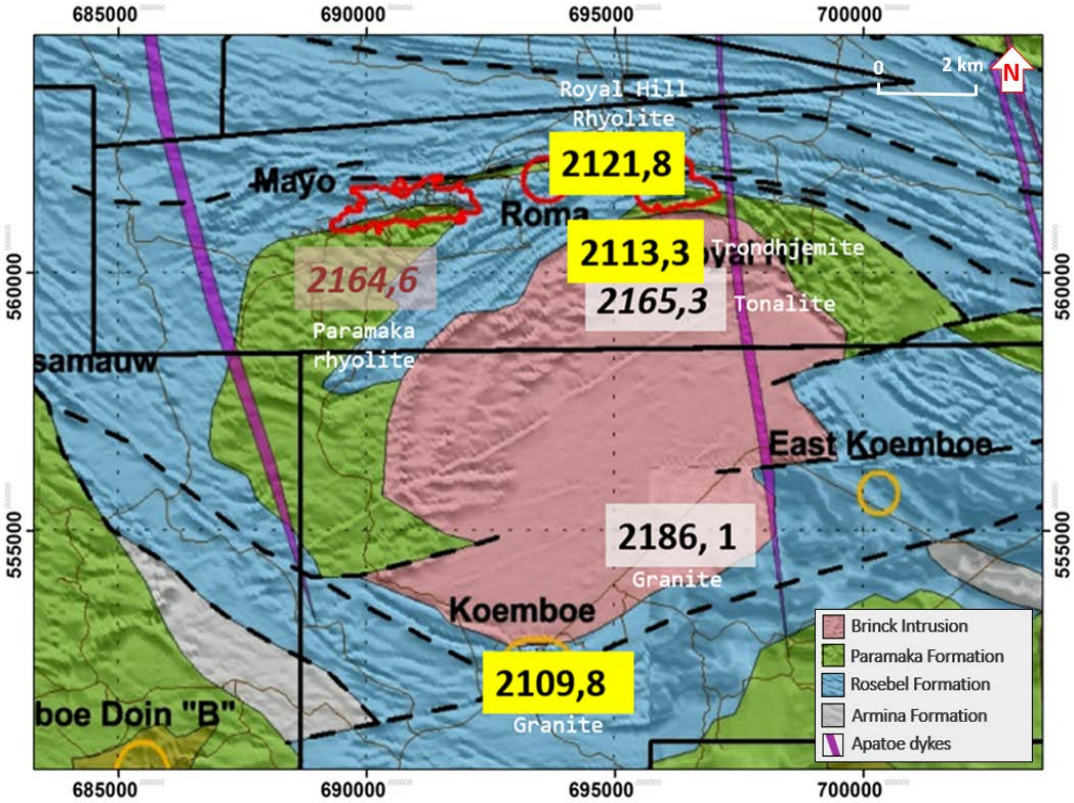

Figure 7: Age dating results of TTG intrusives in the Rosebel area. In grey dates which correlates with the first phase of TTG magmatism between 2.19 – 2.16 Ga and in yellow dates which correlates with the second stage of TTG magmatism between 2.12 – 2.11 Ga. In italic an age obtained by Daoust (2016) which correlates with the first phase of TTG magmatism.

Limited published geochronology for the Guiana Shield orogenic gold deposits indicates mineralization during two distinct episodes between 2.08 - 2.02 Ga and 2.0 - 1.95 Ga which is broadly coëval with post-peak metamorphism at shallow levels and post-peak metamorphism at deeper crustal levels (Fig. 8). The two phases of TTG magmatism predate the two episodes of gold mineralization and a direct bearing on the gold mineralization is unlikely.

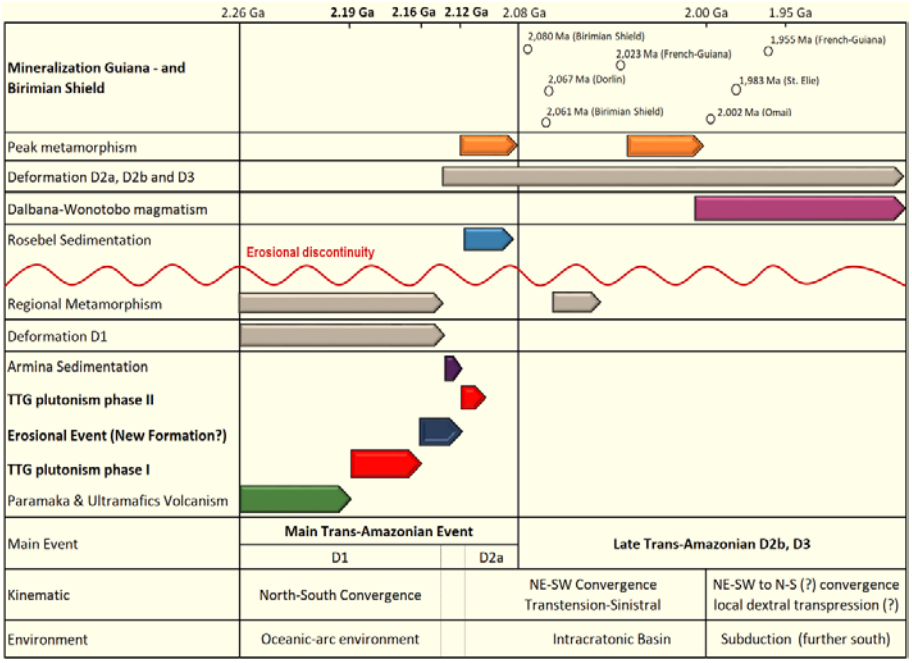

Figure 8: New dates for TTG magmatism at Rosebel with respect to the timing of major geotectonic events and gold mineralization in the Guiana Shield. Modified after Daoust (2016).

RECOMMENDATIONS

Further dating:

- To better assess whether the two-step TTG accretion is valid or whether we are dealing with a relatively continuous TTG process from 2.19 – 2.08 Ga.
- To better assess the implications of Archean material both on the source of gold and the development of the Guiana Shield in general.

Dating of the gold mineralization:

- further dating of the gold mineralization throughout the Guiana Shield including the Rosebel Gold district is recommended to constrain the two likely phases of gold deposition through time in relation to magmatic and deformation processes.

REFERENCES

Daoust C., 2016. Caractérisation stratigraphique, structural et géochimique du District Minéralisé De Rosebel (Suriname) dans le cadre de l'évolution géodynamique du bouclier Guyanais, Thése présentée comme exigence partielle du Doctorat en Sciences De La Terre et de l'atmosphère, Université de Québec à Montréal, pp. 1-353.

Hoogendoorn S. B., 2017. U-Pb Age determination of zircon crystals by LA-ICP-MS from rhyolites and granites in the Rosebel gold district, Marowijne Greenstone Belt, Suriname, Bachelor thesis, Department of Earth Sciences, University of Utrecht, Netherlands, pp. 1-52.

Kroonenberg S.B., de Roever E.W.F., Fraga L.M., Reis N.J., Faraco T., Lafon J.-M., Cordani U. and Wong T.E., 2016. Paleoproterozoic evolution of the Guiana Shield in Suriname: A revised model, Netherlands Journal of Geosciences, pp. 1 - 32.

Ramlal S. 2018. An investigation of the Brincks intrusion and its relationship to the surrounding gold deposits, Brokopondo, Suriname, South America, Master thesis, Anton De Kom University of Suriname, pp. 1 - 142.

Quaternary geochronology of detrital gold: an optical dating approach

***Joel Q.G. Spencer**

Kansas State University
Dept. Geology, Manhattan, KS 66506, USA

joelspen@ksu.edu

Brice J. Lacroix

Kansas State University
Dept. Geology, Manhattan, KS 66506, USA

blacroix@ksu.edu

SUMMARY

We propose a novel application of optically stimulated luminescence (OSL) dating to constrain absolute age of detrital gold deposition from alluvial clastic sediment sequences in actively-mined drainage basins in the Guianas. Alluvial gold operations, visible from aerial view, generally are a good guide for further primary gold source exploration. However, discovery of large primary gold deposits is rare, leading to a hypothesis that alluvial gold deposits are concentrated by rates of weathering and geomorphological processes. We anticipate this study will help refine models of alluvial gold deposition in Amazonian forest conditions, and better predict primary gold potential in specific watersheds.

Key words: geochronology of detrital gold, alluvial deposits, Guianas, late Quaternary

INTRODUCTION

With an area of more than 1.5 million km^2, the Guiana Shield spreads across Brazil, Venezuela, Colombia, and the "three Guianas" (Guyana, Suriname and French Guiana). Although official estimation of alluvial gold production is biased due to illegal gold operations, the Guiana Shield has produced more alluvial gold than any other region on the planet (Bardoux et al., 2018). Guyana has produced more than 9 Moz during the last 25 years, including 700 Koz in the last 3 years only, with more than half from alluvial operations (Bardoux et al., 2018). In French Guiana, official alluvial production has exceeded 1.9 Moz since 1990. Gold mining activity almost exclusively focuses on alluvial and eluvial deposits, with primary deposits representing only 2% of the inventoried gold sites (Cassard et al., 2008). Artisanal alluvial operations are generally a good exploration guide to track primary gold source within the watershed. In French Guiana, the most important primary gold source is the volcano-sedimentary Paramaca Series, which hosts quartz-tourmaline veins, Au-bearing conglomerate, and syngenetic hydrothermal Au-mineralization (Milesi et al., 2003). Despite large efforts made by companies to track primary sources, only a few large primary Au-deposits have been found.

With typical tropical weather, the Amazonian forest regions are characterized by an extremely important weathering rate of bedrock. Therefore, an important and unanswered question is how long an alluvial deposit takes to form? Are the important weathering and erosion rates, typical in these regions, sufficient enough to accumulate large alluvial resources, without any "significant" primary source in the watershed?

In this research, we propose to adopt the OSL method to date alluvial deposits within the Guianas. The results from this research will allow a better understanding of the weathering, transport and deposition processes related to alluvial gold deposition. In addition, it will allow estimation of the weathering rate of a watershed, and better constraint of the primary gold estimation and potential within properties.

We are looking for industrial partners to get access to samples and facilities to pursue this novel research. We invite those interested in this project to please contact the authors.

METHODOLOGY AND ANTICIPATED RESULTS

Luminescence dating is a chronological method that enables an understanding of Earth-surface or near-surface processes via establishing the age of crystalline minerals within sedimentary deposits or whole-rock specimens. This age-dating technique utilizes a physical phenomenon whereby the minerals emit a weak but measurable light signal when heated or exposed to another form of light. This "luminescence" signal records the time since sediment last saw daylight and was then deposited, by sedimentary agents such as glaciers, rivers, lakes or wind, enabling the nature of such processes that shape Earth's surface to be better understood. The luminescence dating method has a large dynamic age range applicable to sedimentary deposits as young as 5 years to those as old as several hundred thousand years. In favourable circumstances dates can be obtained for sediments up to a million years in age. The range of luminescence dating far surpasses carbon-14 dating, and even within the carbon-14 range is a useful alternative dating method when organic materials are rare or absent, where the uncertainties in calibrated carbon-14 ages are unacceptably high or where reservoir

effects cause overestimated carbon-14 ages. The main crystalline minerals utilized in luminescence dating are quartz and feldspar, which are found in most sedimentary deposits and many whole-rock specimens, allowing this dating method applicability in most Earth-surface environments and near-surface locations.

OSL age measurements on coarse-grained quartz or feldspar minerals will follow single-aliquot regenerative-dose (SAR) protocols (Murray and Wintle, 2000; 2003; Wintle and Murray, 2006). Where feasible, minerals 180 μm or greater in size will be prepared as such grains from fluvially-derived deposits have been shown to be give the most accurate results (Olley et al., 1998; Truelsen and Wallinga, 2003). Reliability in luminescence data will be monitored with intrinsic characterization tests (Wintle and Murray, 2006). Small aliquots of prepared minerals, ideally 1 mm-in-diameter, will be mounted on stainless steel discs for measurement using silicon oil and spray templates. Multiple single-aliquots will be measured from each sample and the distribution in data analysed using statistical approaches (Galbraith et al., 1999; Spencer et al., 2003).

At each sampling site, multiple time-equivalent samples will be recovered and, where possible, sequences of samples in stratigraphic superposition will also be taken. OSL measurements will be made at the dating facility at Kansas State University. Required environmental radioactivity measurements will be conducted at off-campus ICP-MS/-OES or high-resolution gamma-spectrometry facilities.

CONCLUSIONS

We infer that the OSL technique is perfectly suitable to study the chronology of alluvial gold deposition within the tropical forest regions of the Guianas. The technique involves field collection and laboratory measurement of detrital particles from alluvial terraces or fans. The data generated by such a study will allow a better understanding of the dynamics of Au-accumulation through the drainage system, as well as better predicting the primary gold potential within properties.
We are looking for industrial partners to develop and test such methodology.

REFERENCES

Bardoux, M., Moroney, M., Robert, F., 2018, Gold mineralization in the Guiana Shield, Guiana and Suriname, South America: a field trip to the 14th biennial Society for Geology Applied to Mineral Deposits (SGA) meeting: Geological Survey of Canada, Open File 8351, 28 p.

Cassard, D., Billa, M., Lambert, A., Picot, J.-C., Husson, Y., Lasserre, J.-L., Delor, C., 2008, Gold predictivity mapping in French Guiana using an expert-guided data-driven approach based on a regional-scale GIS: Ore Geology Reviews, 34(3), 471-500.

Galbraith, R. F., Roberts, R. G., Laslett, G. M., Yoshida, H., Olley, J.M., 1999, Optical dating of single and multiple grains of quartz from Jinmium rock shelter, Northern Australia. Part 1: experimental design and statistical models: Archaeometry, 41, 339–364.

Milesi, J.-P., Lerouge, C., Delor, C., Ledru, P., Billa, M., Egal, E., Fouillac, A.-M., Lahondère, D., Lasserre, J.-L., Marot, A., Martel-Jantin, B., Rossi, P., Tegyey, M., Théveniault, H., Thiéblemont, D., Vanderhaeghe, O., 2003, Gold deposits (gold-bearing tourmalinites, gold-bearing conglomerates, and mesothermal lodes), markers of the geological evolution of French Guiana: geology, metallogeny, and stable-isotope constraints: Geology of France and surrounding areas, 2-3-4, 257-296.

Murray, A.S., Olley, J.M., 2002, Precision and accuracy in the optically stimulated luminescence dating of sedimentary quartz: a status review: Geochronometrica, 21, 1-16.

Murray, A.S., Wintle, A.G., 2000, Luminescence dating of quartz using an improved single-aliquot regenerative-dose protocol: Radiation Measurements, 32, 57-73.

Murray, A. S., Wintle, A. G., 2003, The single regenerative dose protocol: potential for improvements in reliability: Radiation Measurements, 37, 377-381.

Olley, J.M., Caitcheon, G.G., Murray, A.S., 1998, The distribution of apparent dose as determined by optically stimulated luminescence in small aliquots of fluvial quartz: implications for dating young sediments: Quaternary Science Reviews, 17, 1033-1040.

Spencer, J. Q., Sanderson, D. C. W., Deckers, K., Sommerville, A. A., 2003, Assessing mixed dose distributions in young sediments using small aliquots and a simple two-step SAR procedure: the F-statistic as a diagnostic tool: Radiation Measurements, 37, 425–431.

Truelsen, J. L., Wallinga, J., 2003, Zeroing of the OSL signal as a function of grain size: investigating bleaching and thermal transfer for a young fluvial sample: Geochronometria, 22, 1-8.

Wintle, A.G., Murray, A. S., 2006, A review of quartz optically stimulated luminescence characteristics and their relevance in single-aliquot regeneration dating protocols: Radiation Measurements, 41, 369-391.

Geochemical and isotopic characterization of hydrothermal alteration and gold mineralization at the Karouni orogenic gold deposit: Guyana, South America

***Michael Tedeschi**
Centre for Exploration Targeting
University of Western Australia
35 Stirling Hwy, Crawley, WA,
Australia 6009

michael.tedeschi@research.uwa.edu.au

Steffen Hagemann
Centre for Exploration Targeting
University of Western Australia
35 Stirling Hwy, Crawley, WA
Australia 6009

steffen.hagemann@uwa.edu.au

James Davis
Troy Resources Guyana
82 Premniranjan Place
Prashad Nagar
Georgetown, Guyana

SUMMARY

The recently discovered Karouni gold deposit is located in the 2.2-2.1 Ga Trans-Amazonian Province of northern Guyana and contains approximately 1 Moz of Au. Gold mineralization is controlled by the Smarts Hicks shear zone and is hosted by sequence of greenschist facies mafic to ultramafic volcanic rocks and felsic intrusions. Gold-bearing quartz-carbonate veins formed during the end of the Trans-Amazonian Orogeny. Geochemical, petrographical and isotopic investigation into the Au mineralized veins and associated alteration has revealed a K-poor, sodic-dominated hydrothermal system with. W-Bi-Ag-Te-Mo-Pb elemental association. This is anomalous compared to other orogenic gold systems and has important implications into the potential fluid source of orogenic gold deposits.

Key words: Karouni, gold, orogenic, Trans-Amazonian Orogeny, Guyana, Guiana Shield

INTRODUCTION

The recently discovered Karouni gold deposit is located in north-central Guyana, approximately 170 km SW of the capital of Georgetown and 35 km NW of the 5 Moz Au Omai Mine (Fig. 1A, B). They represent one of the few active gold mines in the Rhyacian (2.2-2.05 Ga) Trans-Amazonian greenstone belts of the northern Guiana Shield. Gold mineralization is interpreted to have occurred at the end of protracted compressional to oblique slip deformation during the Trans-Amazonian Orogeny (Delor et al., 2001). Karouni consists of two deposits, Smarts and Hicks, located 2 km apart along the NW striking Smarts-Hicks Shear Zone. They contain approximately 1 Moz of gold in total endowment at grade of 2.2 g/t Au (Troy Resources, 2017). Both deposits are hosted within a sequence of greenschist facies mafic to ultramafic volcanic rocks and felsic intrusions. Features of the Karouni deposits include sulfide and base metal poor, structurally controlled quartz-carbonate veins hosted within greenschist facies volcano-sedimentary rocks, often characteristic of orogenic gold deposits (Groves et al., 1998; McCuaig and Kerrich, 1998; Hagemann and Cassidy, 2000; Goldfarb et al., 2005; Groves and Goldfarb 2015).

This study provides a unique opportunity to investigate an exposed and accessible gold deposit in the Guiana Shield. Karouni is one of the few active gold mines in the Guiana Shield and one of two active mines in Guyana. More than 200 years of placer mining has taken place in the region (Gibbs and Barron 1993), however, relatively few modern 'hard rock' mines have been discovered or developed. Exploration in the region has been challenged by dense tropical forest, Quaternary sedimentary cover, lack of infrastructure and overall poor understanding of geological controls for Au mineralization. Similarities between the Trans-Amazonian greenstone belts and the better endowed equivalent rocks of the Birimian greenstone belts of West Africa (Milési et al., 1992; Davis et al., 1994) point to the potential of the region for major gold discoveries.

METHODS

Geological mapping was undertaken on all accessible pit faces and limited outcrop exposures in the surrounding region. Detailed core logging was carried out on 15 diamond drill holes covering the major lithological, structural and mineralized settings at Smarts, Hicks, Larken and Whitehall. This allowed for the collection of structurally constrained, hydrothermally altered rock and vein samples representing the major alteration zones around gold mineralization in each major host rock. Polished thin sections were made for 115 samples and microscale textural and mineralogical relationships were defined using transmitted and reflected optical petrography, supported by the Tescan Vega 3 scanning electron microscope (SEM) at the Centre for Microscopy, Characterisation and Analysis (CMCA) at UWA. Whole rock geochemical data was collected on 65 samples from across the deposit allowed for mass balance modelling and elemental correlations. Detailed mineral chemical data were collected by electron probe micro- analysis (EPMA) using the JEOL JXA-8530F Hyperprobe fitted with five wavelength-dispersive spectrometers (WDS) also at the CMCA. LA-ICP-MS analyses on pyrite were carried out using a Resonetics RESOlution M-50A-LR incorporating a Compex 102 excimer laser, coupled to an Agilent 7700s quadrupole ICP-MS at the GeoHistory Facility, John de Laeter Centre, Curtin University, Western Australia. Multiple isotope sulfur analyses (SIMS) were conducted using a Cameca 1280 SIMS at the CMCA, UWA.

RESULTS

The Karouni mine consists of two deposits, Smarts and Hicks, located 3 km from each other along the NW-SE trending Smarts-Hicks shear zone (SHSZ) (Fig.1). In both deposits, Au is hosted within two sets of quartz-carbonate veins (V_{2a} and V_{2b} veins) associated with releasing jogs in the SHSZ during $D_{2(kar)}$ deformation. The NW-trending V_{2a} veins are shear zone hosted and are generally associated with ductily deformed high MgO basalts, whereas N-S trending V_{2b} extensional veins are hosted in brittley deformed rocks (dolerite, granodiorite, rhyolite porphyry) within and adjacent to the shear zones (Fig. 1). Gold occurs as free grains disseminated within the pyrite and also as coarse, free Au grains and fracture fills within the quartz-carbonate veins. The style of hydrothermal alteration at Karouni is lithology-dependent and is characterized by show narrow selvages (4 to <1 m in width) which display a progression from chlorite-calcite-rutile- to albite-dominated mineralogy in dolerite (Fig. 2), whereas a chlorite-talc-chlorite-calcite assemblage dominates in high MgO basalt. It is anomalous among orogenic gold deposits for its distinct lack of potassic alteration. Gold is located within inclusions in coarse, disseminated pyrite associated with the proximal alteration zones and as coarse native gold within the quartz-carbonate veins. Minor gold is also located within Au-bearing telluride minerals. The high TiO_2 dolerites formed a favorable chemical trap due to their high magnetite content suggesting sulfidation via redox reaction as a possible mechanism of gold deposition. Mass balance modelling of the hydrothermal alteration indicates a wallrock-dominated system with limited addition or subtraction of major elements with the exception of C, S and Na. Modelling of the proximal alteration has also shown strong trace element enrichment of W-Bi-Ag-Te-Mo-Pb all of which are correlative with gold. In-situ laser ablation inductively coupled plasma mass spectrometry (LA-ICP-MS) trace element geochemistry and secondary ion mass spectrometry (SIMS) S isotope analyses of pyrite from of the gold bearing hydrothermal system within the deposit indicate a geochemically and isotopically homogeneous system with minor trace element variation due to differences in host rock. U-Pb dating of hydrothermal titanite associated with proximal alteration indicates a mineralization age of 2084±14 Ma.

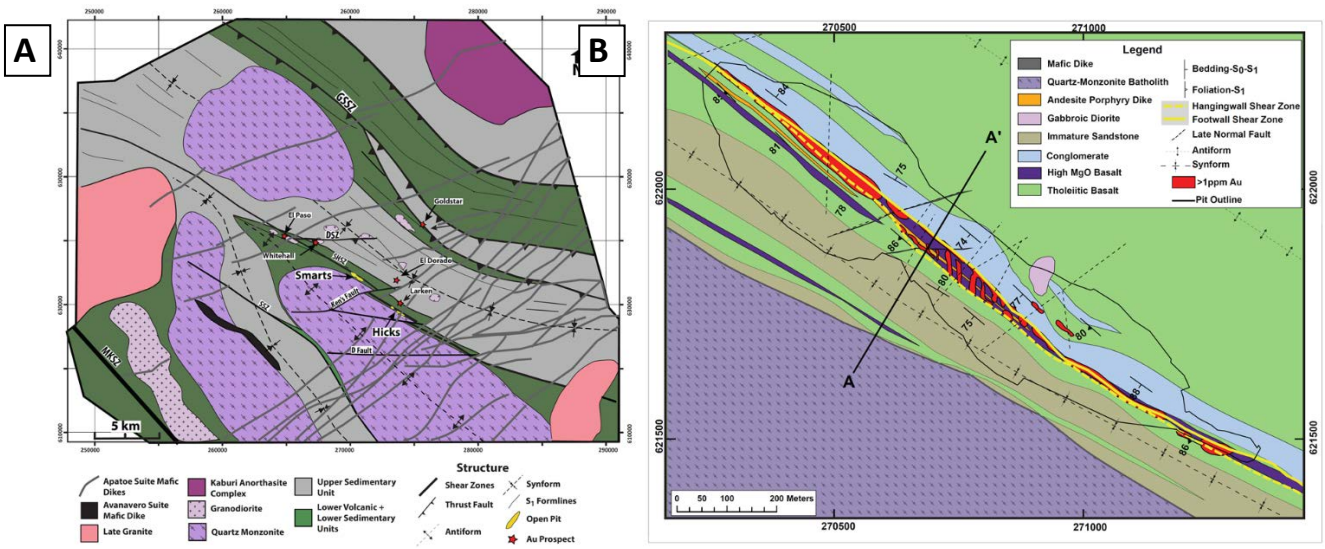

Figure 1 A) Geological Map of the Karouni camp. B) Plan view geological map of the Smarts Deposit.

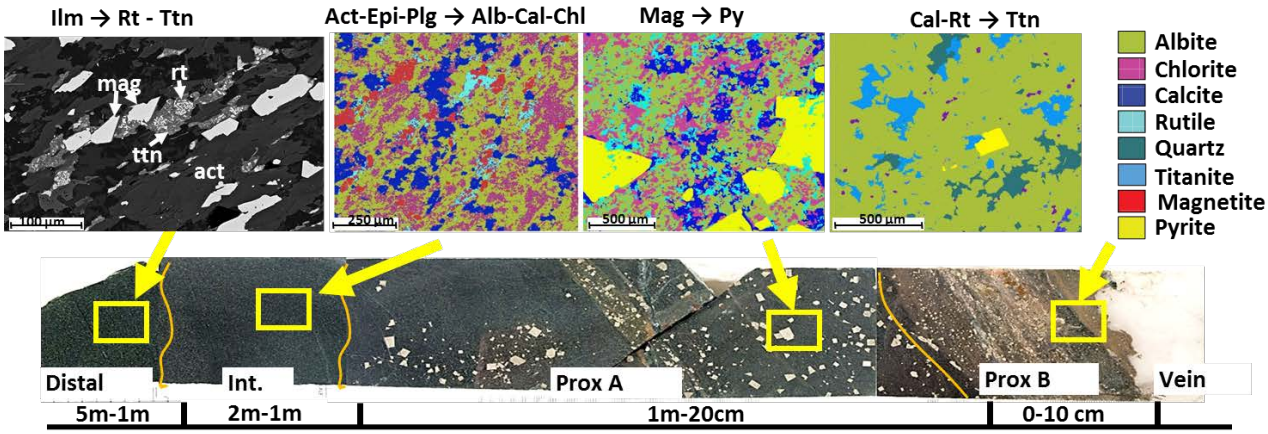

Figure 2. Composite photo showing the alteration zonation around a V2B vein hosted in high TiO_2 dolerite

CONCLUSIONS

Karouni has many features commonly associated with orogenic gold deposits including a gold-only metal suite, strong structural controls, and a similar geochemical signature (W-Bi-Ag-Te-Pb-Mo) to many other orogenic deposits. However, the lack of potassic and proximal ankerite/dolomite alteration is atypical for orogenic gold deposits and suggests there may be something unique about its fluid source. The high TiO_2 dolerites formed a favorable chemical trap due to their high magnetite content. Magnetite is replaced by gold inclusion-bearing pyrite in the proximal alteration zone suggesting sulfidation via redox reaction as a possible mechanism of gold deposition. Alteration is narrowly constrained around the veins but has a unique calcite and albite dominated alteration assemblage lacking in K-metasomatism. Evidence from LA-ICP-MS suggests insignificant structurally bound gold and overall geochemical homogeneity of the pyrite. LA-ICPMS dating from titanite indicates a mineralization age of 2084± 14 Ma, coeval with late Trans-Amazonian D_{2b} deformation.

ACKNOWLEDGMENTS

This paper forms part of a PhD project that began in October 2014 at the Centre for Exploration Targeting, University of Western Australia supervised by Prof. Steffen Hagemann and Dr. Anthony Kemp. The research is supported by an IRPS and APA scholarship granted to the first author by UWA. Further financial support for analytical work, travel and onsite accommodation was provided by Troy Resources Guyana. The authors would especially like to thank the Troy Resources Guyana exploration team, especially Peter Doyle, Neil Jones, Jens Langhoff and Boaz Wade, for their hospitality, support and invaluable discussions. The authors also acknowledge the Australian Microscopy & Microanalysis Research Facility at the Centre for Microscopy, Characterisation & Analysis (UWA) for assistance with the SEM.

REFERENCES

Davis, D.W., Hirdes, W., Schaltegger, U. and Nunoo, E.A., 1994, U/Pb age constraints on deposition and provenance of Birimian and gold-bearing Tarkwaian sediments in Ghana, West Africa: Precambrian Research, v. 67, p. 89-107.

Delor, C., de Roever, E.W.F., Lafon, J-M., Lahondère, D., Rossi, P., Cocherie, A., Guerrot, C., and Potrel, A., 2003b, The Bakhuis ultra-high-temperature granulite belt (Suriname): II. Implications for the late Transamazonian crustal stretching in a revised Guiana Shield framework: Geologie de la France 2-3-4, 207-230.

Gibbs, A.K., and Barron, C.N., 1993, Geology of the Guiana Shield: Oxford, Oxford University Press, p. 246

Goldfarb, R.J., Baker, T., Dubé, B., Groves, D.I., Hart, C.J.R., and Gosselin, P., 2005, Distribution, character, and genesis of gold deposits in metamorphic terranes: Economic Geology 100th Anniversary Volume, p. 407–450.

Goldfarb, R.J., and Groves, D.I., 2015, Orogenic gold: Common or evolving fluid and metal sources through time: Lithos v. 233, p. 2–26.

Groves, D.I., Goldfarb, R.J., Gebre-Mariam, M., Hagemann, S.G., and Robert, F., 1998, Orogenic gold deposits: A proposed classification in the context of their crustal distribution and relationship to other gold deposit types: Ore Geology Reviews, v. 13, p. 7–27.

Hagemann, S.G. and Cassidy, K.F., 2000, Archean orogenic lode gold deposits: Reviews in Economic Geology, v. 13, p.9-68.

McCuaig, T.C., and Kerrich, R., 1998, P–T–t–deformation-fluid characteristics of lode gold deposits: evidence from alteration systematics: Ore Geology Reviews v. 12, p. 381–454.

Milési, J.P., Ledru, P., Feybesse, J.L., Dommanget, A., and Marcoux, E., 1992, Early Proterozoic ore deposits and tectonics of the Birimian orogenic belt, West Africa: Precambrian Research. v. 58, p. 305–344.

Regional lithostratigraphic record as a proxy for mineral systems of the South West African Craton

Nicolas Thébaud*
School or Earth Sciences, CET, UWA, 35 Stirling Highway Crawley WA6009
nicolas.thebaud@uwa.edu.au

James Davis
School or Earth Sciences, CET, UWA, 35 Stirling Highway Crawley WA6009
jamesarchiedavis@googlemail.com

John Miller
School or Earth Sciences, CET, UWA, 35 Stirling Highway Crawley WA6009
jmclmiller@gmail.com

SUMMARY

Results from the WAXI project show how the tectonic evolution framing the metallogenic evolution of the craton, may be mapped out through detailed analysis of volcanic and sedimentary successions. Six major lithostratigraphic cycles have been identified and correlated across the Baoule-Mossi Domain: the Lower Birimian Cycle One (ca. 2300-2180 Ma), the Lower Birimian Cycle Two (ca. 2180-2150 Ma), the Upper Birimian Cycle One (ca. 2150-2130 Ma), the Upper Birimian Cycle Two (ca.2130-2115 Ma), the Tarkwaian Cycle (ca. 2115-2095 Ma) and the Bandamian Volcanics (ca. 2100-2070 Ma). These cycles can be linked to specific tectonic settings, allowing further the understanding of the Birimian/Paleoproterozoic Baoule-Mossi Domain formation and supporting future targeting strategies.

Key words: lithostratigraphic compilation, South West African Craton, mineral system, mineral exploration.

INTRODUCTION

Mineral deposits are a local manifestation of a range of earth processes that take place at different temporal and spatial scales (e.g. McCuaig et al., 2014). At the lithospheric scale geodynamic processes and associated lithospheric structures are commonly proposed to apply a strong control on metal endowment of mineralised provinces (Begg et al. 2014). Increasing high-resolution geochronological constraints on ore deposits further suggest that deposits form during a very narrow time interval over a prolonged geodynamic evolution suggesting a transient regional scale geodynamic setting (e.i. geodynamic transition from long compression period to a period of transcurrent tectonic (Goldfarb et al., 2005)). At the regional scale, inferred basement architecture is proposed to apply a multi-scale control on mineralised camp localisation (Lebrun et al., 2016). Similar to most Precambrian Terranes, the South West African Craton exhibits a protracted tectonic evolution of which only the latest structural increment is preserved. An insight into the early stages the South West African Craton formation may however be gathered through careful lithostratigraphic analysis and correlations of its supracrustal cover. Accordingly, the spatial and temporal mapping of fluid pathways (magmatic and hydrothermal) may be targeted indirectly through deciphering the lithostratigraphic record. In this paper we present the results from WAXI stage 2 and show how multidisciplinary data compilation may be used to advance the understanding of the South West African Craton and its metallogeny.

RESEARCH APPROACH

The South West African Craton SWAC refers to the southern portion of the West African Craton, consisting of the Archean Kenema-Man Domain juxtaposed against the Paleoproterozoic Baoule-Mossi Domain (Boher et al. 1992). The Archean Kenema-Man Domain spans the borders of Liberia, Guinea and Sierra Leone and is subdivided into three complexes; Pre-Liberian (ca. 3540-3050 Ma), Liberian (ca. 2900-2800 Ma) and the BIF Successions (ca. 2871-2615 Ma) (Egal et al. 2002). The Baoule-Mossi Domain which is the focus of this paper, consists of metavolcanic, metasedimentary and granitic rocks (Fig 1). Despite numerous studies, the South West African Craton lithostratigraphic sequence remains largely unconstrained. The lithostratigraphic compilation derived as part of the WAXI2 research project allows for craton wide lithostratigraphic compilation that may be used to assess the tectonic evolution of the South West African Craton (Davis et al., 2015). The following lithostratigraphic compilation was put together through the combination of lithostratigraphic from camps in Senegal, Guinea, Mali, Burkina Faso, Côte d'Ivoire and Ghana together with the acquisition of both lithogeochemical and geochronological data (Davis et al., 2015).

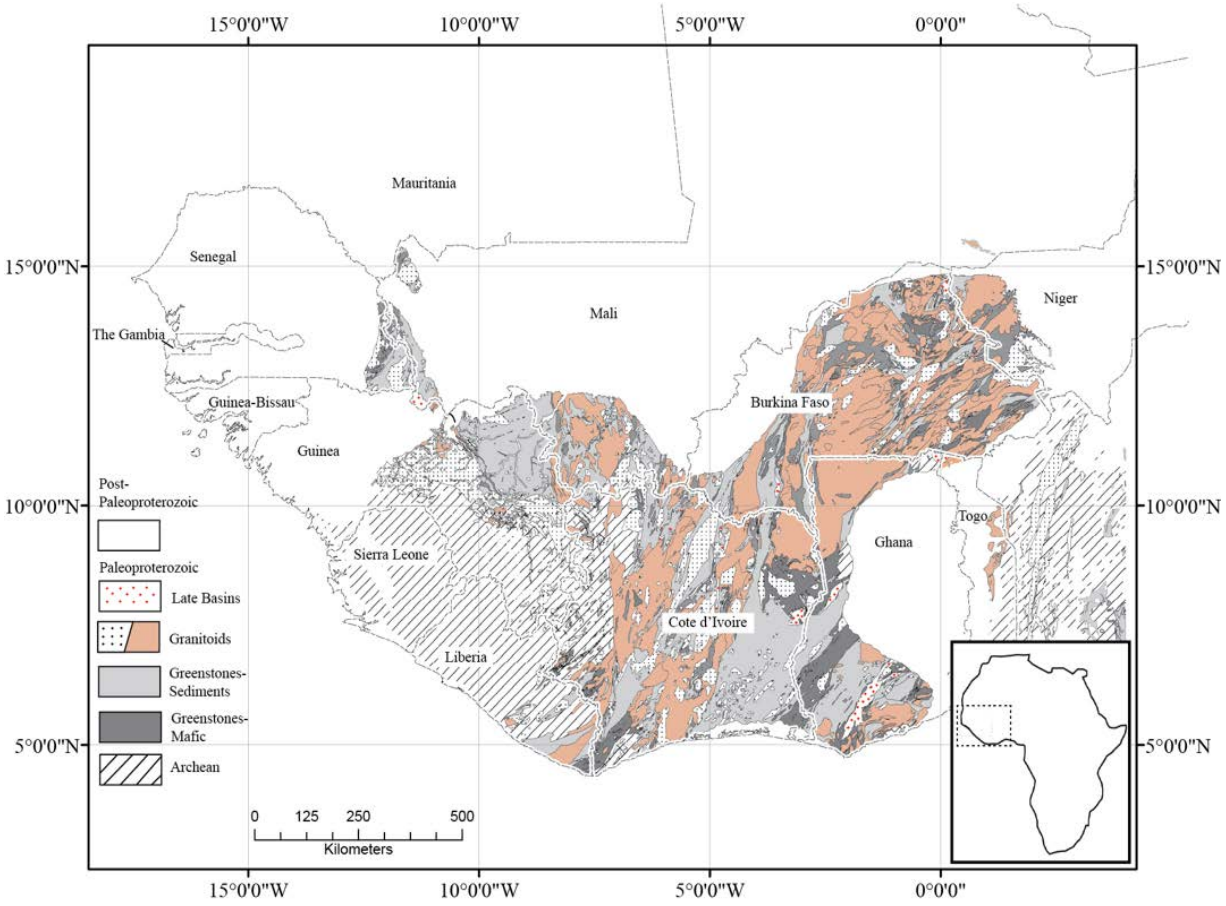

Figure 11: Simplified geological map of the South West African Craton showing the location of the Archean Kenema-Man Domain and the Birimian Baoule-Mossi Domain (Modified after the SIGAfrique map, BRGM).

TOWARDS A REGIONAL-SCALE LITHOSTRATIGRAPHIC COMPILATION

The results of this study suggest that the supracrustal rocks deposited between ca. 2300 and 2050 Ma can be correlated and mapped across the entire South West African Craton. Within this framework it is possible to identify distinct depositional cycles, which allow to further our understanding of the tectonic environment associated with the South West African Craton development. Within this time period, major breaks in the lithostratigraphy are observed to occur at ca. 2180, 2150, 2115 and 2100 Ma.

From 2300 to 2180 Ma, the Lower Birimian Cycle One forms the base of the stratigraphy and consists of thick sequences of spatially extensive basaltic lavas, gabbros and pyroxenites intercalated with bimodal intermediate andesitic – rhyolitic volcanics and rare granitoids. Mafic rocks appear to be consistently of tholeiitic composition, although discreet, and spatially restrictive mafic and ultramafic rocks of calc-alkaline composition have been recognised (e.g. Boromo Belt, Burkina Faso).

The period from ca. 2180 to 2150 Ma (Lower Birimian Cycle Two) represents the first major change, with the cessation of tholeiitic to calc-alkaline volcanism. Basalts are replaced, on a domain wide scale by intermediate-felsic extrusive lavas and pyroclastic deposits and is indicative of the beginnings of convergent tectonic setting.

From ca.2150 Ma, a second major event is recognised in the stratigraphic record and correspond to the caseation of volcanism and the onset of large scale/massive sedimentation (Upper Birimian Cycle One). This boundary is observed across the whole Baoule Mossi domain. Initially reworked volcanic material dominates before grading into thick sequences of greywacke at ca. 2130 Ma. This event represents the amalgamation of arc-like domains followed by their uplift and erosion leading to the formation of large sedimentary basins (Upper Birimian Cycle Two).

The third major event recognised across the craton is the deposition of late basins at ca. 2115 – 2097 Ma (e.g. Tarkwa). These sedimentary basins are spatially restricted, but regionally extensive and consist of polymitic conglomerates, coarse well bedded arentic sandstones and phyllite that unconformably overlie the Birimian volcanics (Tarkwaian Cycle). The deposition in narrow elongate late basins, and short depositional window is indicative of a change in the regional tectonic over the deposition of the greywacke basins that preceded it.

The restart and shift in volcanism to the western Baoule-Mossi domain at ca. 2100 – 2070 Ma represents a fourth major stratigraphic, and first major diachronous geological event in the Baoule-Mossi domain (Bandamian Volcanics). These volcanics consist of ultramafic intrusive and extrusive rocks, dacitic to andesitic lavas and hypovolcanic rocks (Bassot 1987) and intercalated with ryholitic flows and tuffs (Hirdes and Davis 2002) which on-lap the Birimian sediments of the Siguiri and Kofi Formations (Milési et al. 1989).

IMPLICATIONS FOR MINERAL EXPLORATION

The lithostratigraphic record not only provides a proxy for the tectonic evolution of the South West African Craton, it also provides a critical framework for the development of a metallogenic model critical to support mineral exploration strategies. The spatial analysis of the lithostratigraphic records as defined above shows that arc related magmatism is concentrated in a corridor extending from Cote d'Ivoire into Burkina Faso. Such corridor represent a favourable environment for the development of magmatic Cu-Au porphyry deposits (Gaoua) and or exhalative systems such as VMS or epithermal systems (Perkoa). In a more indirect manner, the lithostratigraphic record and its spatial distribution may help to narrow down the search space for Orogenic gold deposits. Early architecture as long been considered as crucial for mineral exploration and major stratigraphic interfaces are commonly targeted (Robert et al., 200). These interfaces often represent major structures within depot centres that control the deposition of the stratigraphic content at the time of deposition (Lebrun et al., 2016). The basin inversion that is taking place through the following orogenic cycle leads to the re-activation of these structures and often provide critical pathways, channelling deep seated fluids and/or magmas. Accordingly the recognition of these interfaces appears critical for exploration targeting. The well-known Tarkwa formation and associated late basins represent fault bounded, elongated basins that are parallel to volcanic belts that are commonly targeted as seen as prospective for gold.

CONCLUSIONS

The lithostratigraphic synthesis presented shows that the South West African Craton lithostratigraphic record deposited between ca. 2300 – 2100 Ma can be correlated across the entire Baoule-Mossi Domain. Such regional continuity implies that the tectonic process acting upon the Baoule-Mossi Domain between 2300 – 2100 Ma was uniform across the domain. Finding its foundation in the concept of mineral system approach, this study demonstrate how the development of a unified lithostratigraphic analysis provides a critical tool for the development of a metallogenic model of West Africa critical to support mineral exploration strategies. The extension of such lithostratigraphic compilation over the Guiana shield represents a logical extension of the work conducted over the South West African Craton.

ACKNOWLEDGMENTS

This work was supported through the West African Exploration Initiative (WAXI) and the results presented benefited from numerous discussions with colleagues including but not limited to: Cam McCuaig, Graham Begg, Mark Jessel, Kim Hein, Lenka Baratoux, Quentin Masurel and Erwann Lebrun. We acknowledge AMIRA International and industry sponsors, including AusAID and the ARC Linkage Project LP110100667, for their support of the WAXI project (P934A). We acknowledge the various Geological Surveys/ Department of Mines in West Africa as sponsors in kind of WAXI.

REFERENCES

Bassot JP (1987) Le complexe volcano-plutonique calco-alcalin de la rivi6re Dal ma (Est S n6gal): discussion de sa signification godynamique dans le cadre de l'orog6nie eburn6enne (Prot6rozoique inf6rieur) Journal of African Earth Sciences 6:505-519.

Begg, G.C., Griffin, W.L., Natapov, L.M., O'Reilly, S.Y., Grand, S., O'Neill, C.J., Hronsky, J.M.A., Poudjom Djomani, Y., Deen, T., and Bowden, P. 2009, The lithospheric architecture of Africa: Seismic tomography, mantle petrology and tectonic evolution: Geosphere, v. 5, p. 23–50

Boher M, Abouchami W, Michard A, Albarede F, Arndt NT (1992) Crustal growth in West Africa at 2.1 Ga. Journal of Geophysical Research 97:345.

Davis, J.,Miller,J.,Thébaud,N.,McCuaig,C.,Begg,G.,Jessel,M.,Hein,K.,Baratoux, L., 2015. Craton-scale lithostratigraphic correlation as an insight for the geodynamic evolution of the South West African Craton. In:Proceedings of the 50th SGA Conference

Goldfarb, R.J., Baker, T., Dubé, D., Groves, D.I., Hart, C.J.R., and Gosselin, P., 2005, distribution, character, and genesis of gold deposits in metamorphic terranes: Economic Geology 100th Anniversary Volume, p. 407–450.

McCuaig, T.C., Hronsky, J.M.A., 2014. The mineral system concept: the key to exploration targeting. Econ. Geol. Spec. Publ. 18,153–175.

Lebrun O, E, Thébaud N, Miller J, Ulrich S, Bourget J, Terblanche O (2016) Geochronology and lithostratigraphy of the Siguiri district: implications for gold mineralisation in the Siguiri Basin (Guinea, West Africa). Precambrian Research 274, 136–160.

McCuaig, T.C., Hronsky, J.M.A., 2014. The mineral system concept: the key to exploration targeting. Econ. Geol. Spec. Publ. 18,153–175.

Milési JP, Feybesse JL, Ledru P, Dommanget A, Ouedraogo MF, Marcoux E, Prost A, Vinchon C, Sylvain JP, Johan V, Tegyey M, Calvez JY, Lagny P (1989) Les mineralisations auriferes de l'Afrique de I'Quest. Chronique recherche miniere 497:3-98.

Robert, F.,Poulsen,K.H.,Cassidy,K.F.,Hodgson,C.J.,2005. Gold metallogeny of the Superior and Yilgarn cratons. Econ. Geol. 100,1001–1033

Geochemical Exploration in Regolith Dominated Terrains

Robert Thorne
CSIRO
26 Dick Perry Av.
Perth, Australia

Robert.thorne@csiro.au

Ravi Anand
CSIRO
26 Dick Perry Av
Perth, Australia

Ravi.anand@csiro.au

Walid Salama*
CSIRO
26 Dick Perry Av
Perth, Australia

Walid.Salama@csiro.au

Vaclan Metelka
CSIRO
26 Dick Perry Av
Perth, Australia

Vaclav.metelka@csiro.au

SUMMARY

Deeply weathered profiles are widespread in Australian and South American terrains. In these regions mineral deposits may be concealed by a thick continuous regolith horizon and significant geochemical dispersion patterns can form within the weathering horizon.

Careful appraisal of regolith and landforms at a district to regional scale is necessary for efficient mineral exploration in deeply weathered terrains. Sample media and sample preparation will depend on the nature and origin of the regolith and the climatic regime under which it has formed. Regolith-landform mapping is a prerequisite for sampling in areas of deeply weathered terrains and regolith-landform models can be derived for specific locations in order to inform geochemical sampling and sample data analysis.

Key words: Deep weathering, sampling, mapping.

REGOLITH DISTRIBUTION AND EXPLORATION SIGNIFICANCE

Regolith encompasses the range of materials found between unweathered bedrock and the earth's surface. Originally the term was defined as only unconsolidated material (Merril, 1897) but now indurated materials such as lateritic duricrusts and silcrete as well as materials formed by processes such as secondary enrichment and dehydration are now included in the definition. Regolith may be comprised of materials that have been weathered in-situ or it can be transported e.g. alluvium and colluvium. The regolith is therefore a product of processes such as erosion, transportation, and sedimentation as well as weathering.

Deeply weathered profiles, commonly ferruginous and/or bauxitic towards the surface, although in some places covered by overburden, are widespread in northern and South America, Africa, Australia and India. The thickness of these weathered profiles may be over 150 m depending on the age of the land surface, tectonic activity, climate history and the nature of the bedrock. In many areas, the weathered mantle may extend regionally resulting in no exposure of the underlying bedrock for thousands of square kilometres.

Regolith in parts of both Australia and South America have been forming continuously for over 100 my and has therefore evolved under a variety of climatic and tectonic environmental conditions. Regolith in these regions will be an expression of the cumulative effects of this extended weathering history. The resultant landforms in arid, savannah and rainforest are broadly similar. The common characteristic of all these areas is deep weathering, modified to varying degrees by leaching, erosion and any subsequent depositional processes. This has led to a thick and complex regolith which presents particular challenges to mineral exploration.

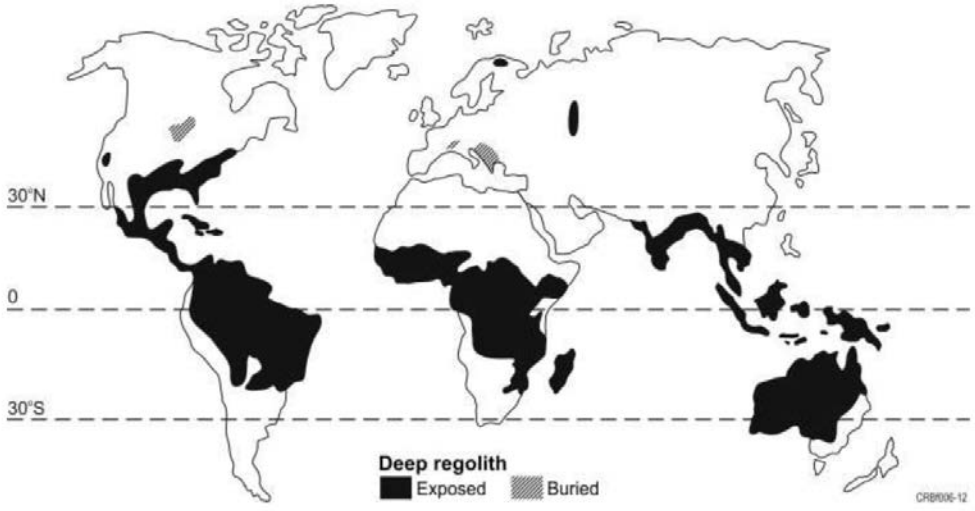

Figure 1. Distribution of deeply weathered profiles (After Bardossy and Aleva, 1990)

REGOLITH MATERIALS

Regolith can be divided into four different broad types of materials; in-situ, transported, lag and soils. In-situ regolith is the weathered basement that has not undergone transport. The typical in-situ weathering profile consists of the saprolith and the overlying pedolith. The saprolith retains evidence of original igneous textures and the base of this zone is the weathering front, below which is unweathered rock. The boundary between the saprolith and the pedolith is termed the pedoplasmation front; above this boundary the pedolith does not display any original textures and is subject to soil forming processes. The saprolith can be sub-divided into the saprock and saprolite. The saprock is a slightly weathered horizon where less than 20 % of the weatherable minerals are altered. The saprolite retains the original rock fabric expressed by the primary minerals of the protolith and has more than 20 % of the weatherable minerals altered as a product of isovolumetric weathering (Anand and Paine, 2002). The pedolith has been subjected to soil forming processes that result in the loss of the parent rock fabric and the development of a new fabric by collapse and the precipitation of introduced materials. The principal horizons in the pedoltih are the plasmic and arenose zones, the mottled zone, the lateritic residuum and/or ferricrete (Fig 2).

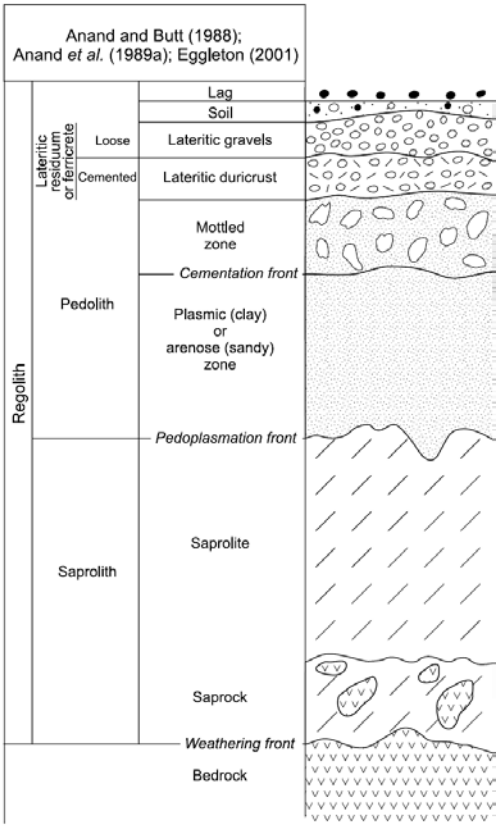

Figure 2. Regolith terminology used for a deeply weathered profile (After Anand and Paine 2002).

Transported regolith, or overburden, refers to exotic or redistributed material, dominantly of continental origin that blankets weathered and fresh rock. It may be partially cemented by Fe oxides, silica or carbonates. Lag represents the coarse residual accumulation of fragments left by physical and chemical dismantling of the upper regolith. Monomictic lag is generally derived from the underlying regolith, whereas polymicitic lag is an indicator of transportation. Soils form as an in-situ weathering product of the underlying parent material and may contain a component of transported generally wind-blown material.

MINERALOGY

Most primary minerals in the bedrock are broken down during weathering, many components released are leached whilst others are retained within secondary minerals. Carbonates and sulfides are the first minerals to weather followed by ferromagnesium minerals and aluminosilicates. The final assemblage is more stable at surface conditions than its precursors. Generally the same minerals are formed from different lithologies but in varying proportions. Kaolinite, halloysite and smectites are generally the most common in saprolite developed from mafic and felsic rocks. Iron oxides increase in abundance towards the surface and the upper horizons consist of kaolinite, goethite and hematite. Aluminium hydroxides and oxyhydroxides are particularly abundant in bauxitic duricrusts in humid regions. Quartz and goethite assemblages will be dominant in profiles developed over Al-poor ultramafic rocks. Resistate minerals within the bedrock can survive the weathering process and be preserved in the weathering profile. Quartz, zircon, rutile and chromite all can become residually concentrated in the lateritic residuum.

REGOLITH LANDFORM MAPPING

Regolith mapping provides for an assessment of regolith materials and their distribution and is crucial for successful exploration in regolith dominated terrains. Commonly there is a strong correlation between landform and regolith type and hence these can be mapped together (Pain et al 1991). A regolith landform unit is classified as an area on a map that has a specific association with regolith materials, landforms and possibly bedrock geology. Firstly a factual map with no genetic bias is produced and subsequently a derivative map based on genetic grouping of the regolith and associated geomorphological features can be drawn. The derivative map may display some aspects of weathering and erosional history, for example by grouping the regolith landforms into three major regimes i.e., relict erosional and depositional (Anand et al. 1989, 1993a). Despite conceptual limitations, this simplified scheme can assist in identifying probable dispersion models and the most appropriate exploration methods, including sample selection and procedures, sample interval analysis and interpretation. There are several types of ferruginous duricrusts in weathered terrains. These have formed in a variety of residual and transported materials at different times and cannot all be grouped together. Lateritic residuum (residual duricrust) is grouped under the relict regime, whereas ferricrete (Fe-cemented sediment) is included in the depositional regime. Models can apply across many deeply weathered terrains (Fig. 3) and can be used to assist in planning geochemical sampling programs.

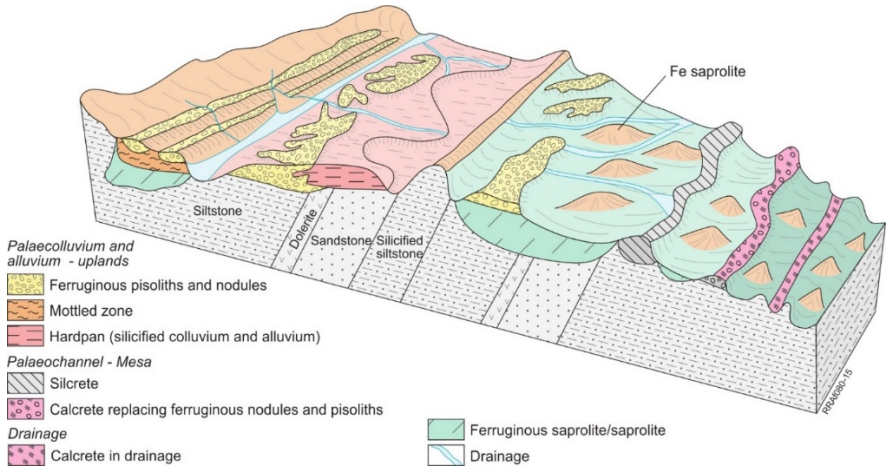

Figure 3. An example of a block model representing regolith types and locations in the Capricorn region of northern Western Australia (After Thorne et al. 2018).

SAMPLING GUIDELINES

There are a range of potential sampling media that can be used for geochemical sampling, but the challenge is to select the most appropriate which can depend on; the nature of the regolith, the type of deposit targeted, the thickness of transported cover, types of dispersion patterns in the specific regolith landform, sampling budget and the level anomaly definition required (Anand and Butt, 2010; Anand et al. 2014). In erosional regimes, soil and lag sampling are generally effective for detecting mineralisation. In relict regimes, lateritic residuum dominated by iron oxides can scavenge and concentrate ore-related elements and is therefore an effective geochemical sampling medium. Sampling of lateritic nodules and pisoliths has contributed to the discovery of Au and VMS deposits (Smith and Perdrix, 1983; Smith *et al*., 1989; Smith and Anand, 1992; Anand et al., 1993b; Smith *et al*, 2000; Anand, 2001; Anand et al., 2019). In depositional regimes, lateritic residuum may be buried beneath transported cover which can be sampled, however this may not be present in all environments. In these situations, interface sampling can be successfully employed. The boundary between the in-situ and transported cover is an interface (unconformity) along which physical dispersion may occur before the deposition of the cover and/or represents a boundary along which geochemical dispersion is possible. Interface sampling presents a method to sample the regolith in areas of deeper transported cover that does not require drilling down to fresh rock and has the potential to increase the anomaly size compared to fresh rock. When it is possible to locate the boundary to the nearest metre, the metre interval crossing the interface is the ideal choice, but closer spacing would be preferred. Geophysics, specifically airborne electromagnetics (AEM), can be used to help define cover thickness and plan exploration campaigns targeting interfaces for geochemical sampling (Gonzalez-Alvarez 2016). In depositional regimes, Au can be enriched in the carbonate horizon of a soil profile and may give rise to, or enhance, a near-surface expression of concealed primary or secondary mineralization (Lintern, 2015). Vegetation and termite mound sampling have also proven effective in defining anomalies over mineralisation (Anand et al. 2007; Hill et al 2008; Fabris at al 2008; Stewart and Anand, 2012; Anand et al., 2014)) and has been successful in regions were soil sampling is ineffective. There are however important variations in how different plants accumulate elements that need to be understood before sampling can take place.

CONCLUSIONS

Much of the methodology for geochemical sampling in regolith dominated terrains has been developed from a broad variety of locations within Australia. This methodology has proven to be applicable globally and has resulted in increasing the likelihood of success in deeply weathered regions.

ACKNOWLEDGMENTS

The authors gratefully acknowledge Nathan Reid for their review of this abstract.

REFERENCES

Anand, R.R., Smith, R.E., Innes, J. and Churchward, H.M., 1989, Exploration Geochemistry about the Mt Gibson Gold Deposits, W.A: CSIRO Division of Exploration Geoscience Restricted Report 20R, 93pp. Reissued as LEME Open File Report, 35, 1998, Perth.

Anand, R.R., Churchward, H.M., Smith, R.E., Smith, K., Gozzard, J.R., Craig, M.A. and Munday, T.J., 1993a, Classification and atlas of regolith-landform mapping units - exploration perspectives for the Yilgarn Craton: CSIRO Division of Exploration and Mining Report 440R (Unpaginated). Reissued as LEME Open File Report, 2, 1998, Perth.

Anand, R.R., Smith, R.E., Phang, C., Wildman, J.E., Robertson, I.D.M. and Munday, T.J., 1993b, Geochemical exploration in complex lateritic environments of the Yilgarn Craton, Western Australia. Final Report for the CSIRO/AMIRA Project P240A. CSIRO Division of Exploration and Mining Report 442R, 297pp. Reissued as LEME Open File Report, 58, 1998, Perth.

Anand, R.R., 2001, Evolution, classification and use of ferruginous regolith materials in gold exploration, Yilgarn Craton, Western Australia: Geochemistry: Exploration, Environment, Analysis 1: 221-236.

Anand, R.R. and Paine, M., 2002, Regolith geology of the Yilgarn Craton-implications for exploration: Australian Journal of Earth Sciences One paper issue 49:3-164.

Anand, R.R., Cornelius, M. and Phang, C., 2007, Use of vegetation and soil in mineral exploration in areas of transported overburden, Yilgarn Craton, Western Australia: Geochemistry, Exploration, Environment and Analysis 7: 267-288.

Anand, R.R. and Butt, C.R.M., 2010, A guide for mineral exploration through the regolith in the Yilgarn Craton: Australian Journal of Earth Sciences One paper issue 57: 1015-1114.

Anand, R., Lintern, M., Noble, R., Aspandiar, M., Macfarlane, C., Hough, R., Stewart, A., Wakelin, S., Townley, B., and Reid, N., 2014, Geochemical dispersion through transported cover in regolith-dominated terrains – towards an understanding of process: Society of Economic Geologist Special Publication, 18, 97-126.

Anand, R.R., Hough, R., Salama, W., Aspandiar, M., Butt, C.R.M., Gonzales-Alvarez, I., Metaelka, V., 2019, Gold and pthfinder elements in ferricrete gold deposits of the Yilgarn Craton of Western Australia: a reviw with new concepts: Ore Geology Reviews, 104, 294-355.

Bardossy, G. and Aleva, G.J.J., 1990. Lateritic Bauxite. Developments in Economic Geology, 27, Elsevier, Amsterda,, Oxford, 624pp.

Gonzalez-Alvarez, I., Ley, Y., Salama, W., 2016, A geological assessment of airborne electromagnetics for mineral exploration through deeply weathered profiles in the southeast Yilgarn Cratonic margin, Western Australia: Ore Geology Reviews. 73 522-539.

Hill, S.M., Greenfield, J.E., Gilmour, P.G., and Reid, W.J., 2008, Guide for mineral exploration through and within the regolith in the southwestern Thomson Orogen, New South Wales. CRC LEME, perth.

Merrill, G.P., 1897, A Treatise on Roacks, Rock weathering and Soils. Macmillan, New York.

Pain, C.F., Chan, R., Criag, M., Gibson, D., Kilgour, P., and Willford, J., 1991, RTMAP BMR Regolith Database Field Handbook, Bureau of Mineral Resources, Geology and Geophysics Record 1991/29, Canberra.

Stewart, A and Anand, R.R., 2012, Source of anomalous gold concentrations in termite nests, Moolart Well, Western Australia: implications for exploration: Geochemistry, Exploration, Environment and Analysis 12:327-337.

Smith, R.E., 1989, Using lateritic surfaces to advantage in mineral exploration. In: G.D. Garland (eds), Proceedings of Exploration'87. Third Deceenial International Conference on Geophysical and Geochemical Exploration for Minerals and Groundwater. Ontario. Ontario Geological Survey, Special Volume 3, pp. 312-322.

Smith, R.E., and Perdrix, R.L., 1983, Pisolitic laterite geochemistry in the Golden Grove massive sulphide district, Western Australia: Journal of Geochemical Exploration, 9, 1-22.

Smith R.E. and Anand, R.R., 1992, Mount Gibson gold deposit, W.A. In: Butt and Zeegers (eds) Regolith exploration geochemistry in tropical and subtropical terrains, Volume IV, Handbook of Exploration Geochemistry, pp. 313-317, Elsevier, Amsterdam.

Smith, R.E., Anand, R.R. and Alley, N.F., 2000, Use and implications of paleoweathering surfaces in mineral exploration in Australia. Ore Geology Reviews 16, 185-204.

Thorne, R., Spinks, S., Anand, R., Metelka, V., Davis, A., Ibrahimi, T., Reid, N., leGras, M., Brant, F., Munday, T., 2018, Regolith landform processes and geochemical exploration of the Capricorn Orogen, Western Australia. Perth, Western Australia: CSIRO; 2018. CSIRO:EP183025.

Pre-Atlantic connections between Africa and South America configurations – an argument for adding paleomagnetic investigations to the ongoing study of mafic dyke swarms

Eric Tohver *

Departamento de Geofísica
Instituto de Astronomia,
Geofísica e Ciências Atmosféricas
Rua do Matão, 1226 - Cidade
Universitária São Paulo-
SP - Brasil - 05508-090

eric.tohver@iag.usp.br

Paul Yves Antonio

Departamento de Geofísica
Instituto de Astronomia,
Geofísica e Ciências Atmosféricas
Rua do Matão, 1226 - Cidade
Universitária São Paulo-
SP - Brasil - 05508-090

Ricardo Trindade

Departamento de Geofísica
Instituto de Astronomia,
Geofísica e Ciências Atmosféricas
Rua do Matão, 1226 - Cidade
Universitária São Paulo-
SP - Brasil - 05508-090

Manoel D'Agrella Filho

Departamento de Geofísica
Instituto de Astronomia,
Geofísica e Ciências Atmosféricas
Rua do Matão, 1226 - Cidade
Universitária São Paulo-
SP - Brasil - 05508-090

The pre-Atlantic fit of South America and Africa has a special historical significance in the Earth Science revolution that culminated with the acceptance of plate tectonic theory. Based on matching coastlines between eastern South America and western Africa, Alfred Wegener proposed that "continental wandering" had separated these once-conjoined continents, with additional support provided by lithostratigraphic similarities and fossil occurrences. This daring speculation was later confirmed and improved upon by Edward Bullard, who made use of the shelf-slope break (ca. 1000 m water depth) to eliminate considerable underlap. Among the lines of evidence that are now routinely used for paleogeographic reconstructions, we can count paleontological recognition of related fauna and flora, the symmetric patterns of magnetic seafloor anomalies, the matching of geochronological and isotopic provinces, and the use of paleomagnetism for continental rocks such as mafic dykes.

For Pre-Cambrian paleogeographic reconstructions, some of these lines of evidence are simply not available. For example, diagnostic faunal assemblages were non-existent or highly cosmopolitan (e.g., stromatolites) and of limited use for correlation purposes. In addition, the destruction of pre-Jurassic oceanic crust by subduction means that reconstruction of West Africa and South America must rely on matching age and isotopic provinces and the use of paleomagnetism. Mafic dyke swarms are, in many ways, ideally suited to the task of paleogeographic reconstruction. For example, the radial pattern of large mafic dyke swarms provide possible "piercing points" for different continents. Too, the high-precision age dating afforded by the igneous mineral baddeleyite, means that both orientation and dyke age can be used. In this contribution, we will examine the potential of mafic dyke swarms as carriers of a primary, paleomagnetic record.

Paleomagnetism is the study of the natural remanent magnetization of rocks. Although there are different types of magnetization carried by different rock types, mafic dykes have a high potential for preserving local geomagnetic field acquired during crystallization and cooling. The two components of the recovered field geometry, declination and inclination, are specific to the latitude and orientation (relative to N) of the rock unit at the time of formation. The comparison of this paleomagnetic record between different geological units allows for quantitative paleogeographic reconstructions. Our presentation will focus on some successful applications of paleomagnetism for Precambrian units of South America and Africa. Over the past twenty years, the paleomagnetic record for the Precambrian of the Amazon and São Francisco cratons has increased by a factor of 10, in terms of published paleomagnetic studies. We propose that these efforts be extended to include piggyback studies of already-dated mafic dyke swarms in western Africa.

Tectono-metamorphic and hydrothermal evolution of the world-class Amaruq BIF-associated gold deposit, Churchill Province, Canada

Manon Valette
Université du Québec à Montréal
201, ave. Président-Kennedy,
Montréal, QC, Canada
H2X 3Y7
valette.manon@courrier.uqam.ca

***Stéphane De Souza**
Université du Québec à Montréal
201, ave. Président-Kennedy
Montréal, QC, Canada
H2X 3Y7
de_souza.stephane@uqam.ca

Patrick Mercier-Langevin
Geological Survey of Canada
490, de la Couronne,
G1K 9A9
Québec, QC, Canada
patrick.mercier-langevin@canada.ca

Alfredo Camacho
University of Manitoba
125, Dysart road
Winnipeg, Manitoba, Canada
R3T 2N2
Alfredo.camacho@umanitoba.ca

Olivier Côté-Mantha
Agnico Eagle Mines Ltd
765, chemin de la mine Goldex
Val d'Or, QC, Canada
J9P 4N9
olivier.cote-mantha@agnicoeagle.com

Marjorie Simard
Agnico Eagle Mines Ltd
10 200, route de Preissac
Rouyn-Noranda, QC, Canada
J0Y 1C0
marjorie.simard@agnicoeagle.com

Vicki McNicoll
Geological Survey of Canada
601, Booth Street
Ottawa, ON, Canada
K1A 0E8
Vicki.McNicholl@NRCan-RNCan.gc.ca

SUMMARY

The Amaruq gold project is part of an emerging gold province in the Canadian North. Two styles of ore are present with discordant to stratabound replacement-style mineralization and quartz±carbonate veins. The ore zones are hosted in deformed and metamorphosed Archean volcanosedimentary rocks. Evidence of Paleoproterozoic deformation and metamorphism highlight a complex tectonic and hydrothermal history. Fieldwork was combined with the U-Pb (zircon and titanite), Re-Os (arsenopyrite) and ^{40}Ar-^{39}Ar (muscovite and amphibole) geochronometers to determine the local- to regional-scale deposit history and exploration guides. Preliminary results indicate a probable Archean metamorphic and hydrothermal heritage and an incremental tectonothermal history possibly spanning up to 800 m.y.

Key words: Nunavut Territory, Arctic Canada, Amaruq, iron formation, gold

INTRODUCTION

The Amaruq gold project (5.2 Moz Au) is 100% owned by Agnico Eagle Mines Ltd. It is located to the NW of the Meadowbank mine (50 km) and Meliadine district (400 km), in the Nunavut Territory of Canada, ~ 150 km south of the Arctic Circle (Figure 1a). Together with Meadowbank and Meliadine, the Amaruq project defines a new emerging gold province containing ~20 million ounces of gold (cumulative production, reserves and resources), where exploration is largely focused on orogenic BIF-hosted or associated gold deposits (Figure 1a; Côté-Mantha et al., 2015; Mercier-Langevin et al., 2017a). The Amaruq project is located in the Rae domain, which is composed of a Mesoarchean (2.9 – 2.8 Ga) gneissic basement, and several Archean greenstone belts (ca. 2.73 – 2.63 Ga) that are locally covered by Paleoproterozoic sedimentary basins (ca. 2.2 – 1.9 Ga: Perhsson et al., 2013; Jefferson et al., 2015). The Amaruq gold deposit is hosted in the Woodburn Lake group, which has been complexly deformed and metamorphosed during the Archean and Proterozoic (Perhsson et al, 2013; Janvier et al., 2015; Janvier, 2016). Several studies on the Meliadine and Meadowbank districts (e.g., Lawley et al., 2015; Janvier, 2016; Mercier-Langevin et al., 2018) suggest that gold was introduced during the Paleoproterozoic Trans-Hudson orogen (ca. 1.91 – 1.81 Ga), but that older hydrothermal events may have played a key role in deposit formation. Nevertheless, in the Amaruq area, the stratigraphy and tectonic evolution of the Woodburn Lake group is poorly known and isotopic age constraints are lacking. Significant uncertainties remain about the evolution of the area (volcanism, sedimentation and magmatism), the structural controls on the ore zones, the effects of metamorphism and the relative timing of events, which are key to understand the distribution of gold at deposit to province scale. A major collaborative research activity was initiated at Amaruq between the Geological Survey of Canada through its 2015-2020 Targeted Geoscience Initiative and the Gold Project (Mercier-Langevin et al., 2017b), Agnico Eagle Mines ltd., and the Université du Québec à Montréal (UQAM) to get a better understanding of the geology at Amaruq and how the various magmatic and tectonometamorphic events influenced the concentration of gold. Among some of the thematic elements to consider are: Is there an early Archean gold event affected by, and possibly upgraded by later Proterozoic orogenesis, or was gold only introduced during the Paleoproterozoic? How is this reflected in the rock record and what is the age gap between the host stratigraphy, the main metamorphic events and hydrothermal gold mineralization? These questions are being addressed by a detailed study of stratigraphic and structural relationships, and a comprehensive sampling of host rocks and mineralized zones for whole-rock geochemistry and mineralogy, as well as U-Pb (zircon and titanite), Re-Os (arsenopyrite) and ^{40}Ar-^{39}Ar (muscovite and hornblende) geochronology.

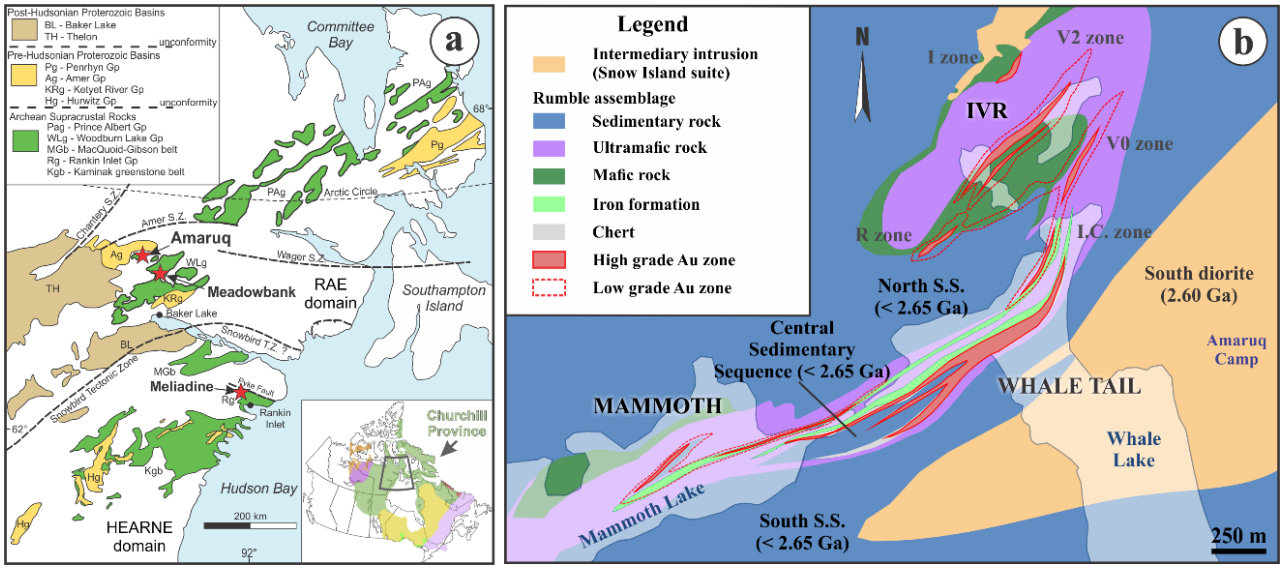

Figure 1. a) Simplified geological map of the Rae and Hearne domains of the western Churchill Province with the location of the Amaruq gold project in the Woodburn Lake greenstone belt (modified from Hrabi et al., 2003). b) Simplified geological map of the Amaruq area showing the location of the Whale tail and IVR zones (modified from Agnico Eagle Mines, 2016).

METHODS AND PRELIMINARY RESULTS

At Amaruq, the Woodburn Lake group is comprised of a 250 meters-thick volcanosedimentary sequence that consists of mafic-ultramafic volcanic rocks and greywacke interlayered with chert and silicate-facies iron-formation (Figures 1b; 2a). The greywacke was divided into south, central and north packages, which are separated by slivers of volcanic and fine-grained/chemical sedimentary rocks (Figure 1b). Mafic-ultramafic rocks are characterized by contrasting geochemical signatures, north and south of the central sedimentary package, and show tholeiitic to transitional signatures, respectively. The two packages of mafic-ultramafic rocks seem to be folded and to pinch-out toward the E-NE. Detailed mapping and analysis of drill sections highlight at least two phases of deformation controlling the geometry of the ore zones. The main phase of deformation, defined as D_2, is represented by a shallow to steeply SE-dipping schistosity, which is affected by a shallow dipping crenulation cleavage associated to D_3. Evidence of D_1 is locally preserved and observed in hinge zone of F_2 folds (Figure 2b). Mafic volcanic rocks and greywacke are represented by actinolite-epidote-chlorite-hornblende, and biotite-muscovite-chlorite metamorphic mineral assemblages, respectively, thus indicating metamorphic conditions transitional between the upper greenschist and amphibolite facies. Metamorphic garnet is only present in silicate-facies BIF in the deposit area. There is also evidence of retrograde and/or probably another metamorphic event at lower greenschist facies coeval with the formation of the crenulation cleavage, which is locally associated with the crystallisation of andalusite porphyroblasts in sedimentary rocks.

The Whale Tail and the IVR zones represent the two main mineralized zones, which comprise distinct styles of ore and structural domains (Figure 1) (Coté-Mantha et al., 2017; Valette et al., 2017, 2018). The Whale Tail zone is dominantly characterized by stratabound replacement-style ore zones, with “silica flooding” and veining developed along iron formation, chert and lithological contacts with mafic-ultramafic rocks in open fold hinge zones (Figure 2c). In the IVR area, gold is mainly associated with several sets of laminated and sulphide poor quartz±carbonate veins preferentially developed in the hinge of a shallow plunging fold affecting the volcanosedimentary sequence. The auriferous veins, with free native gold (figure 2d), are recrystallized, deformed and interpreted as early- to syn-D_2. Both the orebodies associated with BIF and the main auriferous quartz veins are characterized by metamorphosed calcic and potassic alteration halos, and shallowly east-plunging ore shoots. Gold is commonly present as inclusion in arsenopyrite or at the contact between arsenopyrite and löllingite (Figure 2e). The latter texture (cf. Tomkins and Mavrogenes, 2001) suggests that gold was introduced before, or during peak metamorphism and exsolved from löllingite during retrograde metamorphism (Mercier-Langevin et al., 2018).

Preliminary geochronology

SHRIMP U-Pb geochronology on detrital zircons from the north, south and central sedimentary packages indicate that the central, ore-hosting sedimentary rock package has a younger overall heritage, with detrital zircons varying in age between 2.65 and 2.73 Ga, whereas zircons in the north and south packages vary between 2.65 and 3.15 Ga. All three packages have a maximum depositional age of 2.65 Ga (Valette et al., 2018). The minimum age of the sedimentary and volcanic rocks is constrained at 2.6 Ga (U-Pb SHRIMP; zircon: Valette et al., 2018) by a crosscutting diorite intrusion, presumably of the Snow Island Suite (Pehrsson et al., 2013; Jefferson et al., 2015). Samples collected for U-Pb age determination of the volcanic rocks are still pending. Provisional Re-Os model ages were obtained from multiple arsenopyrite aliquots separated from four different samples. Model ages vary from Neoarchean to Rhyacian (2650 and 2250 Ma; Mercier-Langevin et al., 2018), and younger Paleoproterozoic ages, which prevail at Meadowbank (~1.9 Ga; Janvier, 2016) and Meliadine (2.3 to 1.8 Ga; Lawley et al., 2015), are lacking at Amaruq.

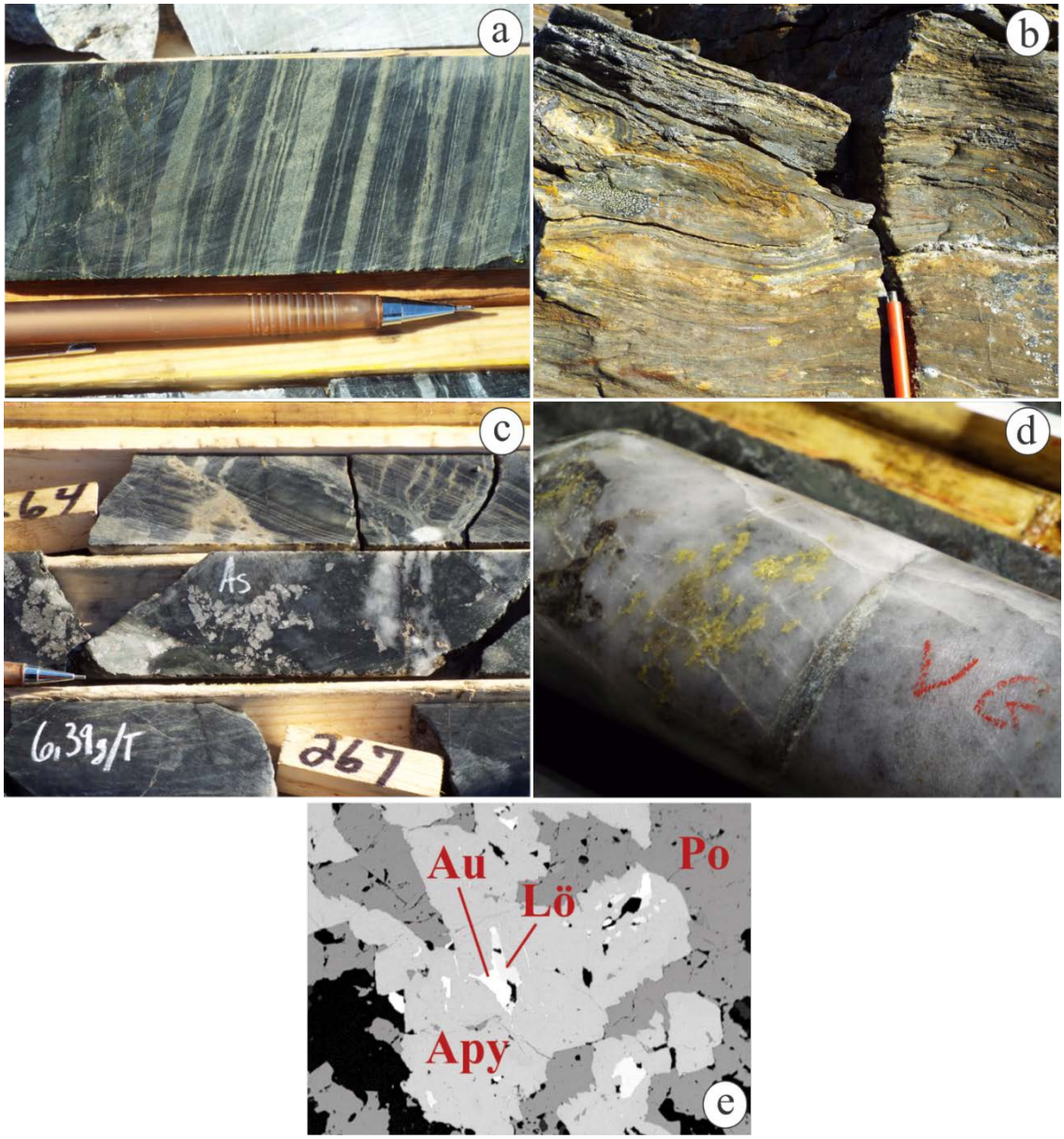

Figure 2: a) Grunerite layers (light green) in silicate-facies banded iron formation of the Woodburn Lake group; b) Isoclinal F_2 fold in zone of high strain; c) Coarse-grained arsenopyrite in replacement-style "silica flooding" zones at Whale Tail; d) Visible gold in a quartz±carbonate vein of the IVR zone; e) Löllingite-arsenopyrite-pyrrhotite-gold association in IVR zone.

A total of twenty muscovite and amphibole samples from the Whale Tail and IVR zone host rocks were collected for ^{40}Ar-^{39}Ar thermochrology. Initial step-heating ages were obtained for hornblende porphyroblasts separated from metavolcanic rocks, and for vein-hosted muscovite porphyroblastes from the IVR zone. The muscovite grains yielded Paleoproterozoic plateau ages of 1985 ± 11 Ma and 1858 ±10 Ma, whereas a weighted mean age of 2522 ± 21 Ma was calculated from two hornblende aliquots.

CONCLUSIONS

Available data to date and preliminary interpretations indicate that gold is associated with a specific pre-2.6 Ga volcanosedimentary rock package containing silicate-facies iron formation and volcanic rock slivers. Two styles of ore are present, with replacement-style ore at the Whale tail zone and quartz±carbonate veins at the IVR zone. The wide span of Re-Os model ages obtained for ore-related arsenopyrite highlights a complex history of sulphide crystallisation that predates the Trans-Hudson and Snowbird orogenies. The ~ 2522 Ma ^{40}Ar-^{39}Ar hornblende age is significantly younger than the maximum depositional age of the sedimentary rocks and the initial interpretation is that it represents an amphibole crystallisation age, thus suggesting the presence of Archean metamorphism. Vein-hosted muscovite porphyroblasts with plateau age differences of ~120 m.y. suggest that muscovite was not completely reset by a late thermal event. These muscovite ages can either be interpreted as representing the cooling of the muscovites at ca. 1985 Ma and subsequent muscovite crystallisation at ca. 1858 Ma, or as two separate muscovite crystallisation ages, possibly during the Snowbird (1.91-1.87) and Trans-Hudson orogenies (1.86-1.75 Ga), respectively. Further U-Pb, Re-Os and ^{40}Ar-^{39}Ar isotopic age results are

pending and will be necessary to establish a more precise tectonic and hydrothermal framework of the Amaruq deposit area. Nevertheless, the data indicate an incremental history of deformation and metamorphism with potentially distinct hydrothermal events, spanning up to ~ 800 m.y.

ACKNOWLEDGMENTS

This report is a contribution to NRCan's Targeted Geoscience Initiative Program (TGI). Support for this study was provided through the Gold Project's 'Activity G-2.4: Lithotectonic controls on Paleoproterozoic gold distribution in the Archean rocks of the Amaruq area, Nunavut'. Manon Valette is conducting a Ph.D. at Université du Québec à Montréal. Agnico Eagle Mines Ltd. is most gratefully acknowledged for the logistical and scientific support, and for access to the property, drill core and data.

REFERENCES

Côté-Mantha, O., Gosselin, G., Vaillancourt, D. and Blackburn, A., 2015, Amaruq: A new gold discovery in Nunavut, Canada, NewGenGold, 41–46.

Hrabi, R.B., Barclay, W.A., Fleming, D., and Alexander, R.B., 2003, Structural evolution of the Woodburn Lake group in the area of the Meadowbank gold deposit, Nunavut; Geological Survey of Canada, Current Research 2003-C27, p. 10.

Janvier, V., Castonguay, S., Mercier-Langevin, P., Dubé, B., Malo, M., McNicoll, V.J., Creaser, R.A., de Chavigny, B., and Pehrsson, S.J., 2015, Geology of the banded iron formation-hosted Meadowbank gold deposit, Churchill Province, Nunavut, In: Targeted Geoscience Initiative 4: Contributions to the Understanding of Precambrian Lode Gold Deposits and Implications for Exploration, (ed.) B. Dubé and P. Mercier-Langevin; Geological Survey of Canada, Open File 7852, 255-269.

Janvier, V., 2016, Géologie du gisement d'or Meadowbank encaissé dans des formations de fer rubanées, Nunavut, Canada : Ph.D. Thesis, Institut National de Recherche Scientifique – Centre Eau Terre Environnement (INRS-ETE), Quebec City.

Jefferson, C.W., White, J.C., Young, G.M., Patterson, J., Tschirhart, V.L., Pehrsson, S.J., Calhoun, L., Rainbird, R.H., Peterson, T.D., Davis, W.J., Tella, S., Chorlton, L.B., Scott, J.M.J., Percival, J.A., Morris, W.A., Keating, P., Anand, A., Shelat, Y. and MacIsaac, D., 2015, Outcrop and remote predictive geology of the Amer Belt and basement beside and beneath the northeast Thelon Basin, in parts of NTS 66-A, B, C, F, G and H, Kivalliq Region, Nunavut. Geological Survey of Canada, Open file 7242, 1 sheet.

Mercier-Langevin, P., Valette, M., De Souza, S., McNicoll, V., Grondin-LeBlanc, P., Creaser, R.A., Côté-Mantha, O., Simard, M. and Malo, M., 2017a, Lithologic and tectonic controls on Paleoproterozoic BIF-hosted/associated gold. *In* Targeted Geosciences Initiative – 2016 Report of Activities, (ed), N. Rogers; Geological Survey of Canada, Open File 8199, p. 39–42.

Mercier-Langevin, P., Rogers, N., Dubé, B., Bleeker, W., Castonguay, S., McNicoll, V.J., Chapman, J.B., Lawley, C.J.M., Bellefleur, G., Houlé, M.G., Pinet, N., Jackson, S., Davis, B., Bécu, V., Peter, J.M., Paradis, S., Potter, E.G., Bjerkelund, C., Villeneuve, M.E., and Evans, R., 2017b, Targeted Geoscience Initiative: 2016 Report of Activities – an overview: *in* Targeted Geoscience Initiative 2016 Report of Activities (ed.) N. Rogers; Geological Survey of Canada Open File 8199, p. 7-16.

Mercier-Langevin, P., Valette, M., De Souza, S., Creaser, R.A., McNicoll, V.J., Grondin-LeBlanc, P., St.Pierre, B., Lauzon, M.-C., Malo, M., Côté-Mantha, O., and Simard, M., 2018, Lithologic controls on Paleoproterozoic BIF-hosted/associated gold: Overview of Re-Os geochronology and Pb isotopes preliminary results; *in* Targeted Geoscience Initiative: 2017 report of activities, volume 1, (ed.) N. Rogers; Geological Survey of Canada, Open File 8358, 147–152.

Pehrsson, S.J., Berman, R.G., and Davis, W.J., 2013, Paleoproterozoic orogenesis during Nuna aggregation: A case study of reworking of the Rae craton, Woodburn Lake, Nunavut; Precambrian Research, 232, 167–188.

Tomkins, A.G. and Mavrogenes, J.A., 2001, Redistribution of Gold within Arsenopyrite and Löllingite during Pro- and Retrograde Metamorphism: Application to Timing of Mineralization. Economic Geology, Vol. 96, p. 525–534.

Valette, M., De Souza, S., Mercier-Langevin, P., Côté-Mantha, O., Simard, M., McNicoll, V.J, and Barbe, P., 2017, Geology of the 4.2 Moz Au Amaruq project, Nunavut; Proceedings of the 14th Biennial SGA meeting, 20-23 August 2017, Québec City, Canada, p. 199–202.

Valette, M., De Souza, S., Mercier-Langevin, P., McNicoll, V.J., Grondin-LeBlanc, P., Côté-Mantha, O., Simard, M., and Malo, M., 2018, Lithological, hydrothermal, structural and metamorphic controls on the style, geometry and distribution of the auriferous zones at Amaruq, Churchill Province, Nunavut; *in* Targeted Geoscience Initiative 2017 Report of Activities volume I, (ed.) N. Rogers; Geological Survey of Canada Open File 8358, p. 153-156.

Paleoproterozoic crustal growth and differentiation of the Transamazonian orogenic belt of French Guiana: A guide for the understanding of Au mineral system

***Olivier Vanderhaeghe**
GET, Université de Toulouse, CNRS, IRD, UPS, France
Olivier.vanderhaeghe@get.omp.eu

Patrick Ledru
Orano
patrick.ledru@orano.group

SUMMARY

The Paleoproterozoic granite-greenstone belts of French Guiana have recorded a major period of crustal growth and differentiation characterized by (1) 60 Myrs of magmatic accretion with tholeiitic mafic rocks dated from 2.26 to 2.20 Ga, (2) 120 Myrs of tectonic accretion marked by widespread polyphased deformation (D1-D2), HT/LP metamorphism and magmatism evolving from calc-alkaline, peraluminous to metaluminous. Gold deposits range from stratabound disseminated in metavolcanic rocks, paleoplacers in basins controlled by transcurrent shear zones also localizing mesothermal quartz veins. Accordingly, these granite-greenstone belts document a full orogenic cycle with mobilization-transfer-deposit of gold associated with magmatic, metamorphic-hydrothermal and sedimentary processes.

Key words: Paleoproterozoic, Transamazonian, French Guiana, granite-greenstone belts, Au mineral system.

INTRODUCTION

The goal of this paper is to discuss growth-differentiation and gold mineral system based on a synthesis of geological data available for the Paleoproterozoic granite-greenstone belts of French Guiana integrating gold deposits. A number of geological markers point to the Archaean-Proterozoic transition as a period of global change both at the surface as attested to by fundamental modification of the composition of the Earth's atmosphere and oceans, and at depth as indicated by a change in the style of crustal tectonics and a potential evolution of the continental growth/recycling balance (Hamilton, 2007; Reddy et Evans, 2009; Bradley, 2011).

The bulk continental crust, andesitic to first approximation (Taylor et McLennan, 1985; Rudnick, 1995) and enriched in incompatible elements, appears to be complementary to the depleted upper mantle (Allègre et Rousseau, 1984) suggesting a two stage extraction by (1) partial melting of the primitive mantle generating a mafic crust and leaving a depleted mantle followed by (2) differentiation through fractional crystallization and/or partial melting of this mafic crust leading to the generation of the continental crust (Hoffmann, 1988; Arndt et Goldstein, 1989; Martin, 1993; Luais et Hawkesworth, 1994; Albarède, 1998).

Structural, petrologic and geochronological data indicate that the current day continents are composite, consisting of old Archaean nuclei (4.0 to 2.5 Ga) surrounded by younger, Precambrian and Phanerozoic, orogenic belts suggesting progressive growth of the continents (Hoffman, 1978; Condie, 2000). The generation of a felsic continental crust in the very early stage of the Earth's evolution has been corroborated by the discovery of 4.4 Ga zircon grains in the 3.3 Ga Jack Hills metaconglomerate, Western Australia (Wilde, 2001; Blichert-Toft and Albarède, 2008). Progressive crustal growth since the Archaean has been advocated on the basis of depletion in Nd relative to Sm in mantle-derived magmas (McCulloch and Bennett, 1993), Nd model ages of detrital sediments (McCulloch et Wasserburg, 1978; Allègre et Rousseau, 1984) and Sr isotopic signatures of marine sediments (Shields et Veizer, 2002).

The oldest cratons are characterized by granitic domes separated by greenstone belts pointing at the importance of the development of crustal-scale gravitational instabilities (Collins et al., 1998; Van Kranendonk et al., 2007). Domes are cored by grey gneisses characterized by the so-called trondhjemite-tonalite-granodiorite (TTG) suite and greenstone belts are dominated by mafic/ultramafic magmatic complexes associated with minor sedimentary deposits (Moyen et Martin, 2012). These geological characteristics are significantly different from present-day orogenic crust and whether they record a primitive form of plate tectonics or a totally different dynamic regime dominated by the development of gravitational instabilities is still passionately disputed (Van Kranendonk et al., 2007; Stern, 2008, Bédard et al., 2012). Some authors consider that Archaean crustal growth might have been dominated by the differentiation of mafic magmatic complexes emplaced above mantle plumes in a hotter and more dynamic Earth (Kröner et Layer, 1992; (Bédard, 2006) whereas others favor an actualistic view with continental accretion by magmatic and tectonic accretion of magmatic arcs along convergent plate boundaries (Martin, 1993; Wyman, 2012). Compared to those of the Archaean, Proterozoic orogenic belts show a much wider range of lithologies, with magmatic complexes characterized by signatures ranging from alkaline to calc-alkaline and from metaluminous to peraluminous, and with sedimentary sequences dominated by silicic-clastic deposits associated with carbonates. The organization around cratonic nuclei of linear belts comprising magmatic complexes and detrital and carbonate sedimentary sequences suggests a succession of magmatic and tectonic accretion at convergent plate boundaries (Barbey et Raith, 1990; Vanderhaeghe et al., 1998; Cagnard et al., 2011). Nevertheless, these belts are also structured in domes and basins but with a tendency to develop a preferred elongation suggesting the contribution of horizontal shortening (Duclaux et al., 2007).

Growth and evolution of continents and metallogenesis are classically treated separately. However, the need to understand mineral systems within a broader geodynamic architectural and temporal framework has been demonstrated over the past decade (Goldfarb et al., 2001; Weihed et al., 2005; Bierlein et al., 2009). Gold, owing to its siderophile character, mobility in a fluid phase only in restricted physical-chemical conditions, and density, is a particularly efficient tracer of (i) juvenile accretion, (ii) intermediate metamorphism associated with hydrothermal fluid circulation, and (iii) sedimentary processes.

METHOD AND RESULTS

This paper is based on a synthesis and critical analysis of data presented in (Vanderhaeghe et al., 1998; Delor, et al., 2003; Milési et al., 2003) building on previous pioneer work by Choubert (1974) and Gruau et al., (1985). These data show that the Paleoproterozoic granite–greenstone belts of French Guiana are part of the Transamazonian orogenic belt (Figure 1), which has recorded a period of major crustal growth at the scale of the Earth from 2.26 to 2.05 Ga (Abouchami et al., 1990). Greenstone belts are separated by a composite batholith of plutonic rocks designated as the Central Guiana Complex. The greenstone belts comprise a Lower Volcanic and Sedimentary Unit composed of migmatitic grey gneisses exposed in the Ile de Cayenne and along the border with Brazil, of mafic to intermediate metavolcanic rocks of the Paramaca formation, and of metaturbidites of the Armina-Orapu formation. These rocks are characterized by a pervasive steep diping S0/1 foliation associated with greenschist facies metamorphism depicting deformation under a HT/LP gradient reaching locally partial melting as attested by the migmatitic TTG grey gneisses. Metagabbros and amphibolites found as enclaves or large panels in migmatitic TTG grey gneisses in the northern and the southern greenstone belts display a tholeitic signature and yield U-Pb ages ranging between 2.26 and 2.20 Ga. An Upper Sedimentary Unit is composed of metasandstones and metaconglomerates that were deposited in en-echelon pull-apart basins formed along a sinistral strike-slip shear zone affecting the northern greenstone belt and transposing the S0/1 foliation into an S2 schistosity. These rocks are also affected by HT/LP metamorphism with a counterclockwise path depicted by andalousite transformation into kyanite. The plutonic rocks display petrological and geochemical features pointing to calc-alkaline, peraluminous and metaluminous magmatic series dated respectively at about 2.18-2.13 Ga, 2.11-2.08 Ga, and 2.07-2.06 Ga. Greenstone belts and plutonic rocks almost all display positive ε(Nd)t values indicating a dominant juvenile character. The contribution of an Archean crustal component is only attested by the negative ε(Nd)t values on some metapelites, by detrital zircons grains in a quartzite and by inherited zircon cores in some granitoids from northern and southeastern French Guiana.

This geologic record rocks allows to identify three successive magmatic-tectonic stages for the evolution of the Transamazonian belt in French Guiana, namely a 60 Myrs stage of magmatic accretion of a juvenile mafic crust from 2.26 to 2.20 Ga followed by 120 Myrs of tectonic accretion coeval with differentiation of the crust associated with progressive implication of more evolved sedimentary rocks and the potential input from mantle magmas marked by the successive emplacement of calc-alkaline plutons during D1, of peraluminous plutons during D2 and metaluminous plutons after deformation. Each of these stages is marked by mobilization, transfer and deposition of gold under specific conditions. Stratiform-stratabound deposits in the Paramaca volcaniclastic sequences are marked by disseminated gold with sulphides and tourmaline and are attributed to an early pre-D1 stock. This stock has been remobilized first during deformation and metamorphism as attested by gold-bearing quartz veins discordant to transposed into the foliation of the greenstone belts. The Upper Sedimentary Unit comprises gold-oxide paleoplacer, disseminated sulphide deposits and mesothermal quartz stockworks attesting for erosion of the former gold deposits from the greenstone belts, deposition in pull-apart basins and remobilization during progressive D2 deformation and associated hydrothermal activity.

CONCLUSIONS

The geological record of the Transamazonian belt in French Guiana has been tentatively related to subduction followed by collision (Vanderhaeghe et al., 1998; Delor et al., 2003). However, the single trend of differentiation, the absence of an age gradient in the distribution of these different magmatic rocks and the widespread HT/LP metamorphism suggests that the differentiation of the Transamazonian orogenic crust was controlled by the persistence of a regional scale (at least 300 km) thermal anomaly that could be related to the upwelling of a mantle plume followed by its thermal relaxation coeval with tectonic accretion of the juvenile crust in between cratonic blocks. In this context, gold mineral systems is characterized by extraction from the mantle through magmatic processes followed by remobilization-transfer-deposition during deformation, metamorphism and hydrothermalism but also through erosion and sedimentation.

Conflicting views regarding the tectonic-geodynamic evolution of the Transamazonian belt of French Guiana can be resolved by providing a more homogeneous coverage of data in order to document (i) the PTtD record of metamorphic rocks combining structural geology, metamorphic petrology and precise in situ geochronology and (ii) the nature, source and conditions of emplacement of magmatic rocks based on petrology, whole rock and mineral geochemistry and isotopic tracing. The relatively good understanding of the Au mineral system in this context could be used as a basis to quantify mass transfer associated with each of the stages identified in French Guiana by documenting the pre-concentration of gold in volcanic protoliths and in turn determine the concentration factors associated with metamorphism-hydrothermalism and alteration and sedimentary processes. Such an approach could be further extended to other metals and elements of economic interest such as Cu, U or REE.

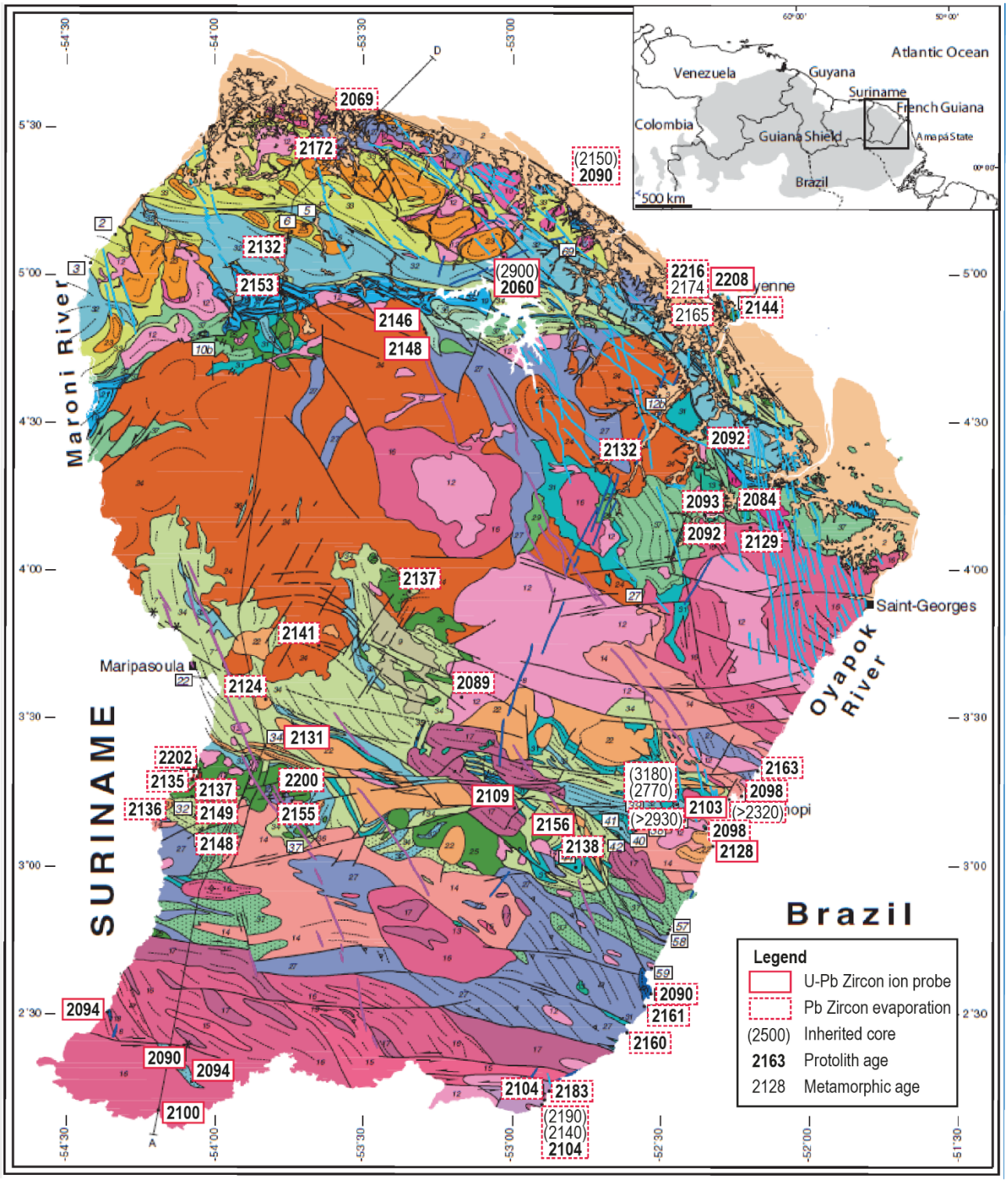

Figure 12: Geochronological data on magmatic and metamorphic rocks of the Paleoproterozoic granite-greenstone belts of French Guiana (compiled and modified after Vanderhaeghe et al., 1998; Delor et al., 2003).

ACKNOWLEDGMENTS

This work benefited from the support of the BRGM and from a number of collaborations including the most significant input of Jean-Pierre Milési.

REFERENCES

Abouchami, W., Boher, M., Michard, A., Albarede, F., 1990. A major 2.1 Ga old event of mafic magmatism in West Africa: An early stage of crustal accretion. J. Geophys. Res. 95, 17605–17629.

Allègre, C.J., & Rousseau, D., 1984, The growth of the continent through geological time studied by Nd isotope analysis of shales: Earth and Planetary Science Letters, v. 67, p. 19-34.

Bédard, J.H., 2006. A catalytic delamination-driven model for coupled genesis of Archaean crust and sub-continental lithospheric mantle. Geochimica et Cosmochimica Acta 70, 1188-1214.

Bierlein, F.P., Groves D., Cawood P. (2009). Metallogeny of accretionary orogens — The connection between lithospheric processes and metal endowment. Ore Geology Reviews 36 (2009) 282–292

Bradley, D.C., 2011, Secular trends in the geologic record and the supercontinent cycle: Earth-Sci. Rev., v. 108, no. 1-2, p. 16-33.

Cagnard, F., Barbey, P., & Gapais, D., 2011, Transition between « Archaean-type » and « modern-type » tectonics: Insights from the Finnish Lapland Granulite Belt: Precambrian Research, v. 187, no. 1-2, p. 127-142.

Choubert B. (1974) - Le Précambrien des Guyanes. Mém. BRGM, Orléans, 81, 213 p.

Collins, W.J., Van Kranendonk, M.J., & Teyssier, C., 1998, Partial convective overturn of Archean crust in the east Pilbara Craton, western Australia: Driving mechanisms and tectonic implications: Journal of Structural Geology, v. 20, p. 1405-1424.

Condie, K.C., 1982, Plate tectonics and crustal evolution: Pergamon Press.

Delor, C., Lahondère, D., Egal, E., Lafon, J.M., Cocherie, A., Guerrot, C. & de Avelar, V., 2003. Transamazonian crustal growth and reworking as revealed by the 1:500,000-scale geological map of French Guiana. Géologie de la France 2003 2-3-4: 5–57.

Duclaux, G., Rey, P., Guillot, S., & Ménot, R.P., 2007, Orogen-parallel flow during continental convergence: Numerical experiments and archean field examples: Geology, v. 35, p. 715-718.

Goldfarb, R.J., Groves, D.I., & Gardoll, S., 2001, Orogenic gold and geologic time: A global synthesis: Ore Geol. Rev., v. 18, p. 1-75.

Gruau G., Martin H., Leveque B., Capdevila R., Marot A. (1985) - Rb-Sr and Sm-Nd geochronology of Lower Proterozoic granite-greenstones belts terrains in French Guiana, South America. Precambrian Res., 30, 63-80.

Hamilton, W.B., 2007, Earth's first two billion years—The era of internally mobile crust, in Geological Society of America Memoirs, Geological Society of America, p. 233-296.

Hoffman, P.F., 1978, United plates of America, the birth of a craton: early Proterozoic assembly and growth of Laurentia: Ann. Rev. Earth Planet. Sci., v. 16, p. 543-603.

Hoffmann, A.W., 1988, Chemical differentiation of the Earth. The relationship between mantle, continental crust, and oceanic crust: Earth and Planetary Science Letters, v. 90, p. 297-314.

Kröner, A., & Layer, P.W., 1992, Crust formation and plate motion in the Early Archean: Science, v. 256, p. 1405-1411.

Martin, H., 1993, The mechanisms of petrogenesis of Archean continental crust-comparison with modern processes: Lithos, v. 30, p. 373-388.

McCulloch, M. & Bennett, V. (1994). Progressive growth of the Earth's continental crust and depleted mantle: geochemical constraints. Geochim. Cosmochim. Acta 58, 4717-4738.

McCulloch, M. & Wasserburg G. (1978). Sm-Nd and Rb-Sr chronology of continental crust formation. Science, 200(4345):1003-11.

Milesi J.P., Lerouge C., Delor C., Ledru P., Billa M., Cocherie A., Egal E., Fouillac A.M., Lahondere D., Lasserre J.L., Marot A., Martel-Jantin B., Rossi P., Tegyey M., Théveniaut H., Thiéblemont D., Vanderhaeghe O., (2003). Gold deposits (gold-bearing tourmalinites, gold-bearing conglomerates, and mesothermal lodes), markers of geological evolution of French Guiana. Geology, metallogeny and stable-isotope constraints. Géologie de la France, 2, 257-290.

Moyen, J.-F., & Martin, H., 2012, Forty years of TTG research: Lithos, v. 148, p. 312-336, doi: 10.1016/j.lithos.2012.06.010

Reddy, S.M., & Evans, D.A.D., 2009, Palaeoproterozoic supercontinents and global evolution: correlations from core to atmosphere: Geological Society, London, Special Publications, v. 323, no. 1, p. 1-26, doi: 10.1144/SP323.1.

Rudnick, R.L., 1995, Making continental crust: Nature, v. 378, p. 571-578.

Stern, R.J., 2008, Modern-style plate tectonics began in Neoproterozoic time: An alternative interpretation of Earth's tectonic history, in Special Paper 440: When Did Plate Tectonics Begin on Planet Earth? Geological Society of America, p. 265-280.

Taylor, S.R., & McLennan, S.M., 1985, The continental crust: Its composition and evolution: Blackwell, Oxford.

Vanderhaeghe, O., Ledru, P., Thiéblemont, D., Egal, E., Cocherie, A., Tegyey, M., & Milési, J.-P., 1998, Contrasting mechanism of crustal growth. Geodynamic evolution of the Paleoproterozoic granite-greenstone belts of French Guiana: Precambrian Research, v. 92, p. 165-193.

Van Kranendonk, M.J., Smithies, R.H., Hickman, A.H., & Champion, D.C., 2007, Review: secular tectonic evolution of Archean continental crust: interplay between horizontal and vertical processes in the formation of the Pilbara craton, Australia: Terra Nova, v. 19, p. 1-38. Weihed et al., 2005

Wilde, S. (2001), Evidence from detrital zircons for the existence of continental crust and oceans on the Earth 4.4 Gyr ago: Nature (London), v. 409, p. 175-178.

Wyman, D.A., 2012, A critical assessment of Neoarchean « plume only » geodynamics: Evidence from the Superior Province: Precambrian Research, doi: 10.1016/j.precamres.2012.01.010.

Implication of the geological characterization on gold endowment at the El Callao District, Guayana Craton, Venezuela: from the exploration to mining planning optimization

German Velásquez
Advanced Mining Technology Center (AMTC), FCFM, Universidad de Chile
Av. Tupper, 2007; 8320000, Santiago, Chile
german.velasquez@amtc.cl

Stefano Salvi
Géosciences Environnement Toulouse, Université de Toulouse, CNRS, IRD, OMP
14 Av. Edouard Belin, 31400 Toulouse, France
stefano.salvi@get.omp.eu

Didier Béziat
Géosciences Environnement Toulouse, Université de Toulouse, CNRS, IRD, OMP
14 Av. Edouard Belin, 31400 Toulouse, France
didier.beziat@get.omp.eu

Daniel Carrizo
Advanced Mining Technology Center (AMTC), FCFM, Universidad de Chile
Av. Tupper, 2007; 8320000, Santiago, Chile
daniel.carrizo@amtc.cl

SUMMARY

The El Callao mining district, with a total endowment of more than 2,000 t Au, is the most important gold-producing region in the Guyana Craton, Venezuela. It is a giant orogenic deposit hosted by the El Callao Shear Zone, which is parallel to the Guri Fault and located south of it. Here we show that the gold endowment at El Callao is associated to the shear-zone development and exhumation, and fluid-rock interactions with the metabasaltic host rock. Gold is found in pyrite and the crystallization of native-refined gold grains is associated to multiple deformation episodes under brittle cortical conditions.

Key words: Guayana Craton, orogenic gold, El Callao District, giant deposit, Venezuela.

INTRODUCTION

This contribution summarizes several years of research on one of the most prolific orogenic gold deposit in the Guayana Craton, Venezuela (Figure 1a), known as the El Callao District (>2000 t gold; Figure 1b) (Velásquez *et al.*, 2011, 2012, 2014, 2018a, 2018b), which along to the Las Cristinas Deposit (Sidder and Mendoza, 1995) represent the two giant orogenic gold deposits located in the Guiana Shield (Sidder and Mendoza, 1995) (Figure 1a). Our research has been developed mainly on the Colombia Mine (Figure 1b) which is the largest underground producing mine in the El Callao district. The research here presented can be used as a "study-case" for characterize other mineralized shear zones in the Guiana Shield and analogous orogenic systems worldwide, such as we showed for the Pampe mine, an orogenic gold deposit that is genetically related to the Ashanti shear zone, in the West African Craton (Salvi *et al.*, 2016). Additionally, a comprehensive characterization can be used to improve the mining planning, focusing on the transition form open pit to underground mine operation.

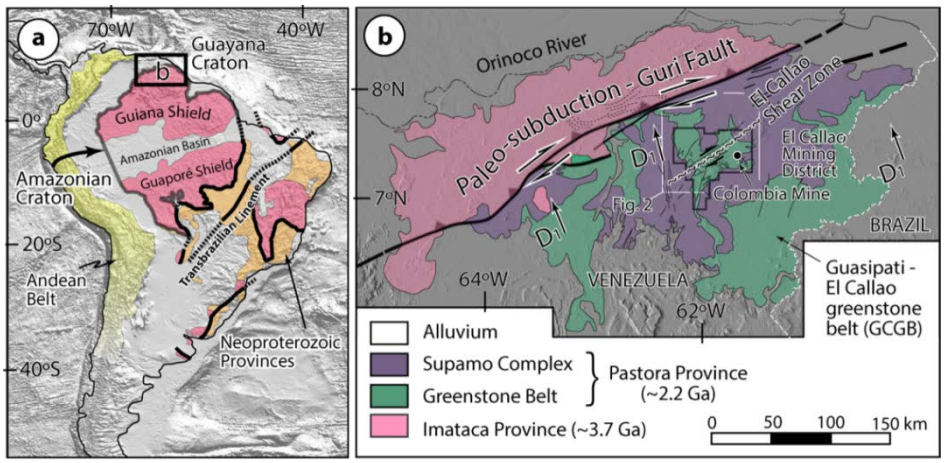

Figure 1: (a) Simplified geological setting of the geotectonic provinces of South America, showing the Amazonian Craton (Guiana and Guaporé Shields). b) A sketch map illustrating the regional geology of the orogenic deposits in the Guayana Craton (Venezuela), including the location of the Guri Fault, the El Callao Shear Zone, and the El Callao Mining District (from Velásquez et al., 2018). Dashed inset in (b) outlines the position of the study area shown in Figure 2.

Regional geology and tectonic framework

The El Callao District is mined on a vein system associated to the El Callao Shear Zone (Figure 1b), a mineralized deformation zone parallel to the Guri Fault (Figure 1b). The NE–SW trending Guri fault is the main megatectonic feature for the entire Guiana Shield, because it juxtaposes Paleoproterozoic greenstone belts against continental crust rocks of the Archean Imataca Province, located at Venezuela (Figure 1b). The Guri Fault is interpreted as a tectonic plate contact, in which the Pastora oceanic plate subducted under the Imataca continental plate at the climax of the Trans-Amazonian Orogenesis (Sidder and Mendoza, 1995). Later, this plate contact was transformed from a subduction to a plate collision, in which the Pastora oceanic plate accommodated mainly trench-orthogonal deformation (Velásquez *et al*., 2018a), evidenced by metamorphic cleavage fabrics and kilometric-scale folds (Figure 1b),

corresponding to D1 deformation event, which affected mainly the basaltic host rocks (Velásquez *et al*., 2011). This change on the tectonic framework, defined as the D2 deformation event, transformed the subduction plate contact on the lithospheric-scale Guri fault (Velásquez *et al*., 2011, 2018a) (Figure 1b), and generated several N45–65° shear zones which are mainly located in the oceanic Pastora plate and parallel to the Guri Fault (Velásquez *et al*., 2011, 2018a). Finally, N140–180° brittle fracturing (D3 deformation event) affected the entire El Callao shear zone. These D1-D2-D3 events are associated to the shear zone formation and exhumation; however the long-term kinematics of the Guri Fault seems to be consistent with several re-activation processes, which are considered to postdate mineralization (Velásquez *et al*., 2018a).

Mining and metallurgical framework

El Callao gold district (Figures 1b and 2a) is exploited in two neighbour mining operations (Figure 2b) namely: the Lo Increible Mine, which is developed as an open pit operation (with a gold grade mean value of 5 g/t) and several underground operations, including the Colombia, Sosa-Mendez, Union, Peru, and Chile mines (with a gold grade mean value of 9 g/t) (Figure 2a,b). Of these, the Colombia (Figure 2a,b) is the most developed and still producing mine and it is constituted by seven exploitation levels: the more superficial (L1) is located at 133 m depth, while the deepest (L7) at 433 m (Velásquez *et al*., 2014, 2018a). Considering the initial geological characterization, obtained from the superficial description, i.e., a gold deposit associated to quartz veins, a metallurgical planning was started up by the installation of a mineral processing plant consisting of an agitated leaching plus a carbon-in-pulp (CIP) process (Velásquez *et al*., 2018b). This plant was designed to process up to 10,000 tons by day of mined material with gold grades of up to 20 g/t and a particle size larger than 75 µm. The very simplified metallurgical process is developed as follow: initially the mined material is crushed and then it is mixed with cyanide, in several tanks, to leach gold forming a cyanide complex. Gold is then extracted from the pulp by adsorption onto activated carbon. During the CIP stage, the gold-loaded carbon is separates from the "barren" pulp which is stored in the tailing zones.

METHOD AND RESULTS

Our research on the mineralization at El Callao District has been focused on the host rock petrogenetic study (Velásquez *et al*., 2011) and gold metallogenic characterization (Velásquez *et al*., 2014, 2018a), taking as the study case the underground Colombia Mine (Figure 2a,b). Rock samples were collected at different levels of the Mine (Figure 2b). Sample characterization was carried out at the Géosciences Environnement Toulouse (GET) laboratory in Toulouse, France, on some one-hundred representative samples. Petrographic studies were performed on thin and 200-µm thick sections using, among other techniques: (1) a polarizing microscope Nikon Eclipse LV100POL, (2) a JEOL 6360LV scanning electron microscopy (SEM), equipped to acquire images in backscattered electron (BSE) mode, (3) a CAMECA SX50 electron microprobe, and (4) a Geolas Excimer housing a 193-nm nanosecond laser coupled with a high-resolution ThermoFinnigan ICP-MS. For a complete revision of the analytical techniques see Velásquez *et al*., 2012, 2014, 2018a.

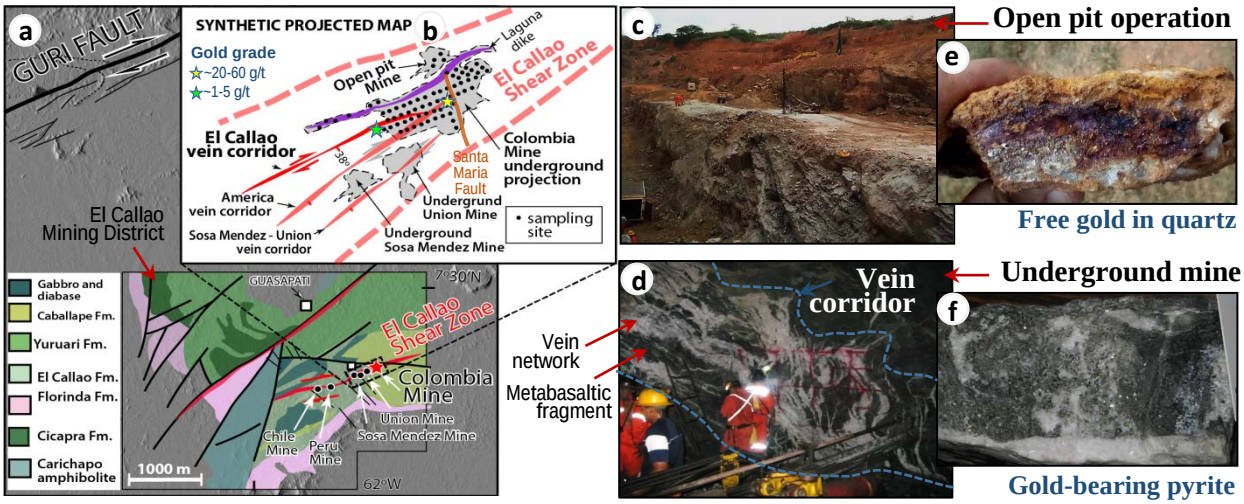

Figure 2: (a) Simplified geology of the El Callao mining district (modified after Velásquez *et al.* 2018) showing the localization of the El Callao District, the Colombia Mine (study area). (b) a sketch map showing a superficial projection of the underground observations at the Colombia mine, locating the vein corridor, the Santa Maria Fault and sampling sites; location of the open pit operation is also shown. Photograph from open pit operation (c) and from underground galleries (d) developed at the Colombia Mine. Photograph of two hand samples (10 cm across) showing a close-up view of a quartz vein containing free gold grains (e) and a metabasaltic fragment hosting gold-bearing pyrite crystals (f).

Main geological results

In the El Callao District gold was initially recognized hosted by quartz veins. According to this geological information, which was obtained from the superficial characterization, i.e., open pit mine, a metallurgical design was implemented and developed (Velásquez *et al.*, 2018b). However, when we performed an in-depth characterization of the mineralization at the underground mine we realized that gold was not associated to the quartz veins and, in turn, the mineralized system showed a different configuration, i.e., it consist of a vein network of interconnected quartz plus albite–ankerite veins enveloping a large number of metabasaltic fragments rich in pyrites and these crystals host most of the gold mineralization, while the veins are almost barren. Both vein network and enclosed fragments

form a large, discrete body contained between metabasaltic hanging- and foot-walls into the El Callao host rock, named as the El Callao vein corridor, which is genetically associated to the El Callao Shear Zone (Velásquez *et al.*, 2014, 2018a). Mean gold grade for the vein corridor is 9 g/t, however we identified and characterized a gold grade variation from ~60 g/t in the intersection with the Santa Maria Fault to 1-5 g/t in the most southwest part of the mine (Figure 2b).

Main mineralogical and geochemical results

Considering that gold was found in the metabasaltic fragments (Figure 3a), these fragments were found to be suitable for in-depth investigation of ore characterization. From the characterization we can highlight important results (Velásquez *et al.*, 2014, 2018a), such as: (1) gold is systematically associated to pyrite crystals in the metabasaltic fragments and it does not occur on the (quartz-ankerite-albite) veins (Figure 3b,c); (2) native (visible) gold occurs as both mineral inclusions (generally smaller than 30 µm, Figure 3e) and grains filling the fractures crosscutting the pyrites (Figure 3d), where the latter form represents most of the economic mineralization; (3) "invisible" gold (Au) and arsenic (As) concentrations were detected in pyrite with values of up to 30 ppm and of up to 8 wt%, respectively (Figure 3f); (4) Average gold grain fineness, calculated from the relationship 1,000Au/(Au + Ag) was determined in ~920; (5) ore paragenesis is constituted by pyrite (host mineral) plus quartz, ankerite, albite, chlorite, muscovite and rutile; (6) two habits for pyrite crystals were described: large euhedral crystals isolated in the groundmass of the metabasaltic fragments (Figure 3b) and small subhedral pyrite crystals grouped in large clusters (Figure 3c), which are associated with the highest gold grades. Interestingly, the last type is commonly found close to late-stage faults, particularly at the intersection between the Colombia corridor and the Santa Maria fault (Figure 2b).

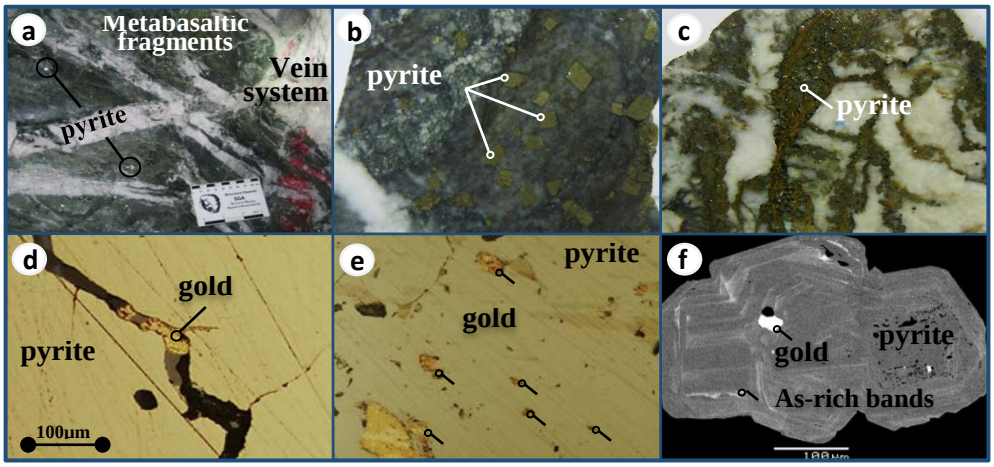

Figure 3: (a) photograph of the underground Colombia Mine showing the interconnected veins, enclosing pyrite-rich metabasaltic fragments. Photographs of two hand samples (10 cm across) showing a close-up view of metabasaltic fragments hosting large isolated (b) and small grouped-in-clusters (c) pyrite crystals. Photomicrographs of pyrite crystals, under reflected light, showing native gold grains filling fractures (d) as well as mineral inclusions (e). (f) SEM backscattered electron images illustrating features in pyrite at El Callao.

Simplified metallogenic model: Control of deformation on gold mineralization

Based on geological, mineralogical and crystallochemical data we developed a metallogenic model for the El Callao gold mineralization and the main results can be summarized as follow (Velásquez *et al.*, 2014, 2018a). Gold exploited in the underground operations is secondary in origin, and was generated from remobilization of primary-invisible gold in pyrite, generating precipitation of native-refined (fineness of ~920) gold grains and the formation of the economic deposit. The endowment at the El Callao mining district (more than 2000 t Au) is associated to the formation and exhumation of the El Callao Shear Zone, throughout the ductile-brittle transition (DBT) cortical domains, and the fluid-rock interaction with the metabasaltic host rock, which were found fertile with respect to gold (Velásquez *et al.*, 2011). Thus, during the earliest stages of shear zone formation and exhumation crystallized the pyrite and precipitated invisible gold, under ductile and ductile-brittle transition strain conditions, associated to D1 and D2 deformation events (Figure 1b), in which precipitated most of the gold mineralization, but not the economic one. At late stages, primary gold trapped in the pyrite was remobilized via coupled dissolution-precipitation reactions, associated to multiple deformation episodes under brittle conditions, during late D3 deformation event (Figure 1b), triggering precipitation of native-refined (fineness > 900) gold grains within the same pyrite crystal, as inclusions and mainly in fractures that crosscut the crystals. Our model explains why gold in fractures of pyrite represents most of the economic mineralization (Figure 4) and can be related to the mine galleries observations where small pyrite crystals, grouped in large clusters (e.g., Figure 3c) are associated to higher gold grades zones (Figure 4c) in relation to large isolated crystals (Figures 3b and 4a,b). In fact, small crystals are the result of fracturing large isolated ones (e.g., Figure 4b) and for this reason there is more possibility to find native gold grains. At the district scale, the highest gold concentrations (up to 60 g/t) are found in the intersection between the shear zones and the late brittle faults, e.g., the El Callao vein system and Santa Maria fault for the underground Colombia Mine (Figure 4d).

CONCLUSIONS

The metallogenic model developed for the formation of the El Callao deposit and gold enrichment can be used as a vector to characterize and explore similar shear zones in other mining districts in the Guiana Shield, and there are some implications on brown-field exploration and mining planning that can be considered.

Considerations on mining planning optimization

We want to highlight the importance of a comprehensive geological-mineralogical characterization in the mining planning, in particular when a change in the operation from open pit to underground is considered. For the El Callao District the lack of a geological in-depth characterization triggered the following metallurgical issues (Velásquez *et al.*, 2018b): i) the crushing system was designed to process mined material formed by mainly quartz and gold; however the plant is now fuelled by different minerals including phyllosilicates such as chlorite and muscovite, which affect the performance of the system; ii) the plant was design to process particles with a size higher than 75 µm and gold grains occurring as inclusions are smaller than 30 µm in size, generating that these particles are not recovered and are stored in tailings. With this in mind, we analysed the material stored in tailings and we found gold grades of up to 3 g/t, which implies the discovery of a new mine in the mine.

Considerations on gold exploration

When we visited the District for the first time the geologists of the mine let us know that they recognized two types of pyrite, i.e., a fine pyrite and a coarse one and, for them, gold was associated mainly with the fine pyrite. Following our results, we showed them that gold grades are not related to the crystal size, but rather to the fracturing of the crystal, i.e., a highly fractured crystal can look like fine crystals grouped in large clusters, which was implemented as a vector to track the highest gold grades in the mine. Considering that gold enrichment processes occur in the intersection zones between the vein corridor with late shear fractures, for a brown-field exploration is suitable to look for these shear fractures, which are associated to D3 deformation events and differentiate them from faults generated during the final superficial exposure of the shear zone, which postdate mineralization (Velásquez *et al.*, 2018a). To achieve this goal the structural model of the District must be systematically updated and improved and we have proposed some recommendations on this subject (Carrizo *et al.*, 2018).

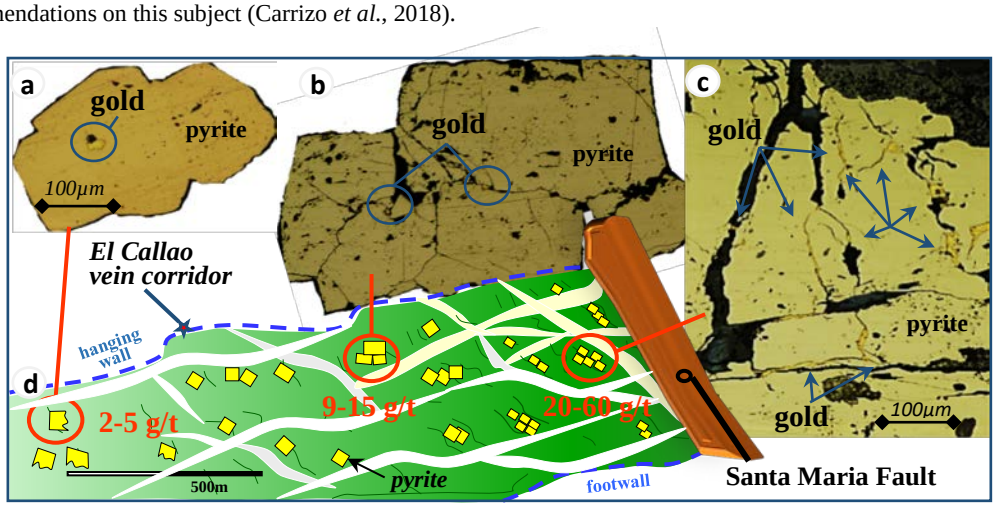

Figure 4: Photomicrographs under reflected light of gold-bearing pyrite crystals, in which native gold grains occurs as mineral inclusions (a,b) and filling the fractures (c). (d) Schematic illustration of the El Callao vein corridor, depicting the gold grade variation in relation to the intersection with the Santa Maria Fault.

REFERENCES

Carrizo, D., Barros, C., and Velásquez G., 2018, The Arsenic Fault-Pathfinder: A Complementary Tool to Improve Structural Models in Mining. Minerals 8, 364, pp. 12.

Salvi, S., Velásquez, G., Miller, J.M., Béziat, D., Siebenaller, L., and Bourassa, Y., 2016, The Pampe gold deposit (Ghana): Constraints on sulfide evolution during gold mineralization. Ore Geology Reviews, 78, 673–686.

Sidder, G.B., and Mendoza, V., 1995, Geology of the Venezuela Guayana Shield and its relation to the entire Guayana Shield. In Geology and Mineral Deposits of the Venezuelan Guayana Shield; Sidder, G.B., Garcia, A.E., Stoeser, J.W., Eds.; U.S. Government Publishing Office: Washington, DC, USA; B1–B41.

Velásquez, G., Béziat, D., Salvi, S., Tosiani, T., and Debat, P., 2011, First occurrence of Paleoproterozoic oceanic plateau in the Guiana Shield: The gold-bearing El Callao Formation, Venezuela. Precambrian Reserach, 186, 181–192.

Velásquez, G., Borisova, A.Y., Salvi, S., and Béziat, D., 2012, In situ determination of Au and Cu in natural pyrite by near-infrared femtosecond laser ablation-inductively coupled plasma-quadrupole mass spectrometry: No evidence for matrix effects. Geostandards and Geoanalytical Research, 36, 315–324.

Velásquez, G., Béziat, D., Salvi, S., Siebenaller, L., Borisova, A.Y., Pokrovski, G.S., and de Parseval, P., 2014, Formation and deformation of pyrite and implications for gold mineralization in the El Callao District, Venezuela. Economic Geology, 109, 457–486.

Velásquez, G., Salvi, S., Siebenaller, L., Béziat, D., and Carrizo, D., 2018a, Control of Shear-Zone-Induced Pressure Fluctuations on Gold Endowment: the Giant El Callao District, Guiana Shield, Venezuela. Minerals, 8, 430, pp. 21.

Velásquez, G., Carrizo, D., Salvi, S., Béziat, D., Aguilar, G., and Estay, H., 2018b, Rol de la caracterización geológica en la optimización del negocio minero: Distrito aurífero El Callao, Venezuela. Proceedings del II Congreso Iberoamericano en Minería Subterránea y a Cielo Abierto – Umining2018, Santiago, Chile.

Arc volcanism and sedimentation in a synkinematic Paleoproterozoic basin: Rosebel Gold Mine, northeastern Suriname

***Thomas Watson**

Department of Geological Sciences
University of North Carolina at Chapel Hill
NC 27599 USA

****Dennis J. LaPoint**

Appalachian Resources LLC
Chapel Hill P.O. Box 3810
NC USA 27515

dennis.lapoint@gmail.com

Kevin Stewart

Department of Geological Sciences
University of North Carolina at Chapel Hill
NC 27599 USA

Kevin_Stewart@unc.edu

** deceased*
*** presenting author, corresponding author*

SUMMARY

The Rosebel Gold Mine (RGM) of northeast Suriname preserves the remnants of a Paleoproterozoic island arc system. Field mapping, geochemical analyses, and petrographic observation obtained during this study have allowed us to produce a model for the evolution of the rocks at RGM during the Transamazonian orogeny. Geochemical and petrographic analyses of igneous rocks from the RGM indicate that they likely formed in an island-arc setting. Analyses of sedimentary rocks reveal the presence of four depositional environments with different sediment provenances, although most of the sediments provenances are consistent with erosion of an undissected arc province. Structural analyses of the rocks at RGM have led to the recognition of three phases of deformation (D_1-D_3), resulting in thrusting and nappe style folding, steepening of these folds and development of pervasive axial planar foliation, and later, sinistral strike-slip faulting.

Key words: Rosebel, Transamazonian orogeny, Suriname, tectonics

INTRODUCTION

The Rosebel Gold Mine (RGM) is located within a regional Paleoproterozoic greenstone belt of the Guiana Shield (Figure 1). This study focused on pit exposures, road cuts, and drill core from within the RGM concession. Mapping and data collection were completed in 2006-2007 and were concentrated in the Mayo, Royal Hill, and Pay Caro pits (Figure 2). The rocks in this study are Paleoproterozoic volcanic and sedimentary rocks that compose part of the Marowijne Supergroup. The Marowijne Supergroup locally consists of a basal-volcanic sequence interlayered with thin-sedimentary units (Paramaka Group), overlain by the mainly sedimentary Armina and Rosebel Formations (Voicu et al., 2001). The rocks of the Marowijne supergroup are metamorphosed to low-to-mid greenschist facies, and are locally cut by gold bearing quartz veins, that comprise the main source of ore for RGM.

The nature of the volcanic and sedimentary rocks that comprise the Paramaka group, the Armina and Rosebel Formations, and the nature of the contacts between these units have been subject to considerable debate (e.g. Bosma and Groeneweg, 1969, Gibbs and Barron, 1993). However, geological studies that might elucidate some of these uncertainties in Suriname have historically been hindered by political instability, tropical vegetation, and a thick tropical weathering profile. Mining and exploration of the RGM area have generated a significant amount of geological data, which is used in this paper to shed light on various aspects of the rock formations mentioned above. Field mapping, diamond drilling, aerial and ground magnetic surveys, and other mining-related activities have created a large database for potential use in assembling an understanding of the local geology.

This study incorporates some of the available data from RGM, supplemented with additional studies and analyses by the authors, in an attempt to elucidate some aspects of Paleoproterozoic volcanism, sedimentation, and tectonism in this part of the Guiana shield. Provenance studies of sedimentary rocks are used to determine the likely tectonic settings and environments of deposition (e.g. Dickinson et al., 1983). Whole-rock and trace-element-geochemical analyses of volcanic rocks are used to determine their likely tectonic provenances (e.g. Woodhead et al., 1992) and oceanic vs. continental affinities (e.g. Barrett and MacLean, 1993). These studies, combined with detailed field and stratigraphic mapping, are used to generate a regional model of volcanism and sedimentation at RGM, associated with the Transamazonian orogeny.

METHOD AND RESULTS

The rocks at RGM represent different types of volcanism and sedimentation attributable to changing volcanism, and the development of different depositional environments during the Paleoproterozoic. Igneous rocks range from mafic to felsic, and show tholeiitic to calk alkaline affinities. The tholeiitic rocks show REE patterns similar to those of other Paleoproterozoic volcanic arcs (e.g. Wang et al., 2004), and the intermediate to felsic rocks have REE distributions consistent with island arcs as well. Figure 3 shows a geochemical discrimination diagram for the rocks from the North Trend (Figure 2) indicating that these rocks likely formed in an arc setting.

Sedimentary rocks from pelagic environments, shallow marine environments, and fluvial environments are found in different locations throughout the concession, and have been tectonically juxtaposed. These rocks range in provenance from undissected arc to transitional arc, to recycled orogenic. In general, sedimentary units that are stratigraphically lower consist of conglomerates and wackes, and grade

upwards into finer grained units. These are correlative sequences (Figure 4), and represent primary erosion in a fold and thrust belt that probably formed early on in the Transamazonian orogeny. The provenance of the lower rocks range from undissected arc, to recycled orogenic. This is probably reflective of contemporaneous erosion of different source material.

The structure of the RGM property resembles a synclinorium, about 30 kilometers wide, and trending 110°. The northern limb of the synclinorium is delineated by the hill- forming rocks of the north trend, and the southern limb is thought to be delineated by the hill-forming rocks of Brownsberg, approximately 18 kilometers southwest of the RGM property. The geometry of the rocks at RGM is indicative of at least three episodes of deformation, reflecting a changing stress regime during the Transamazonian Orogeny, resulting in folds, refolded folds, faulted folds, and folded faults. Most commonly, the rocks are isoclinally folded, with axial surfaces of folds striking parallel to the regional foliation (110°).

There are also three different orientations of quartz veins found at RGM that reflect the multi-deformational history of the rocks. Early veins are deformed and sometimes cut by later vein sets. Gold deposition at RGM is directly related to the quartz veins. The quartz veins range in thickness from less than one centimeter to two meters, and are most prevalent in areas of rheological contrast, especially near the contacts between sedimentary and volcanic rocks. Gold occurs as individual crystals within veins, and as inclusions in pyrite crystals in vein selvages. Metasomatic alteration associated with the quartz veins varies from the north to the south of the RGM concession. In the north, the veins are more often associated with a potassic alteration, whereas in the south they are more often associated with tourmaline and carbonate alteration. The tourmaline alteration may be related to the intrusion of the granite. All of the rocks at RGM, with the exception of the mafic dikes, have been metamorphosed to low-to-mid-greenschist facies. Minerals such as chlorite, sericite, epidote, carbonate, tourmaline, chloritoid, and in some cases andalusite, are secondary minerals in the RGM rocks.

A unique and not obviously correlative rock sequence is present in the turbidites of the north-trend, and this probably represents an earlier phase of deposition in a pelagic environment, that was later juxtaposed with the younger rocks to the south, through thrusting. In general, the sequence of rocks at RGM consists of mafic to felsic igneous rocks, comprising the base of the stratigraphy, and this is overlain by turbiditic rocks, and partly by basal conglomerates and wackes. The sequence most likely represents: (1) The formation of an island arc system, related to the convergence of the West African and South American cratons; (2) deposition of volcanogenic turbidites in either fore arc or back-arc basin positions; (3) continued convergence of the cratons, and the formation of thrust sheets and horizontal folds along the northern margin of the South American craton; (4) erosion of these thrust sheets and primary deposition of the basal conglomerates and wackes; (5) sinistral shearing and felsic plutonism. Later, weathering of the orogenic rocks probably gave rise to the Rosebel Group. This sequence is analogous to the proposed development of Paleoproterozoic rocks elsewhere in the Guiana shield, and also in other Paleoproterozoic circum-South Atlantic provinces in Brazil and in West Africa.

CONCLUSIONS

The sedimentary rocks at RGM show four different lithofacies associations. (1) A deep-water, turbiditic series of wackes, conglomerates, and mudstones comprise the north-trend rocks. These rocks consist of distal to proximal facies and deposit mafic and felsic clastic material in a submarine slope environment. (2) Steep, syn-deformational sub-aerial to shallow-water alluvial processes disperse mafic and felsic sediment of the Royal Hill deposit. These deposits probably originated in an alluvial fan - braided stream environment. (3) Alluvial deposits in the Mayo area show bimodal volcanic association and are related to late-phase volcanism. (4) A shallow marine deposit in which volcanic and terrigenous material comprise proximal facies, and mainly terrigenous material comprises distal facies is evident in the rocks of Pay Caro. This sequence is unconformably overlain by a younger, mainly terrigenous conglomeratic sandstone, locally, the Rosebel Group.

Volcanic rocks of RGM reflect a changing island arc-system during the Paleoproterozoic. Royal Hill mafic volcanic rocks represent the earliest phase of volcanism, and are relatively un-enriched in incompatible REE's, although they are still 10 to 20 times more enriched in REE's than chondrites, and are therefore probably arc- basalts. Pay Caro rocks represent intermediate phase of volcanism, and have a greater enrichment in incompatible REE's. Finally, Mayo rocks the most enriched in incompatible REE's, and probably represent the most advanced phase of volcanism in the life of the island arc system. Brinck's granite is similarly enriched in incompatible REE's as are the Mayo igneous rocks, and is therefore also associated with a later phase of magmatism than the other igneous rocks at RGM.

Structural evolution of the RGM rocks is polyphase, and probably represents three deformational events: (1) Early thrusting and nappe-folding related to the initial stages of the Transamazonian orogeny; (2) Refolding of early nappe-style folds, and development of a penetrative axial planar foliation; (3) Sinistral strike slip deformation related to the final stages of the Transamazonian orogeny.

The rocks at RGM have direct analogues throughout the Proterozoic in the rocks elsewhere in the Guiana shield. The Paramaka, Armina, and Rosebel Groups in French Guiana should not be discarded as relevant analogues. Although volcanism, and sedimentations vary through space and time so these rocks will have different characteristics in different locations, they should not be disregarded as useful references.

The rocks at RGM are analogous to a great number of Archaean and Proterozoic greenstone-belts described throughout the world. Examples from the Rio das Velhas greenstone belt in Brazil, the Birimian greenstone belts in west Africa, arc-related rocks in the Canadian shield, greenstone belts in India, and many other places are relevant analogues to the rocks at RGM.

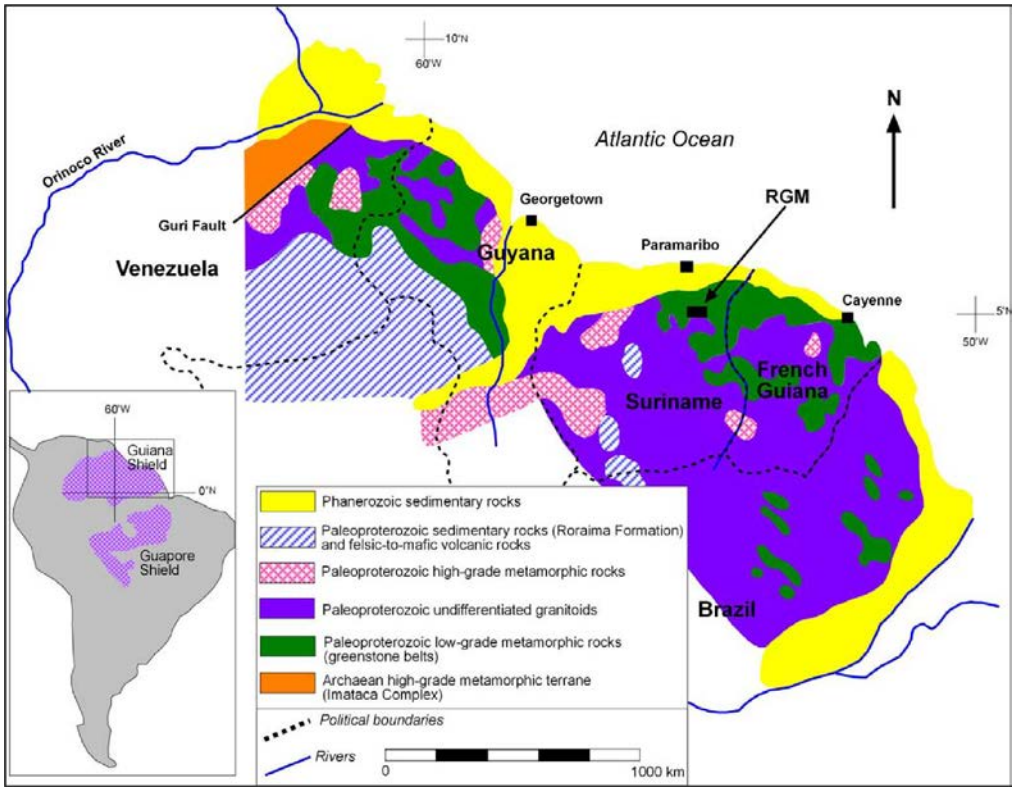

Figure 1: Location map and general geology of the Guiana Shield from Venezuela to Brazil. Modified from Voicu et al., (2001).

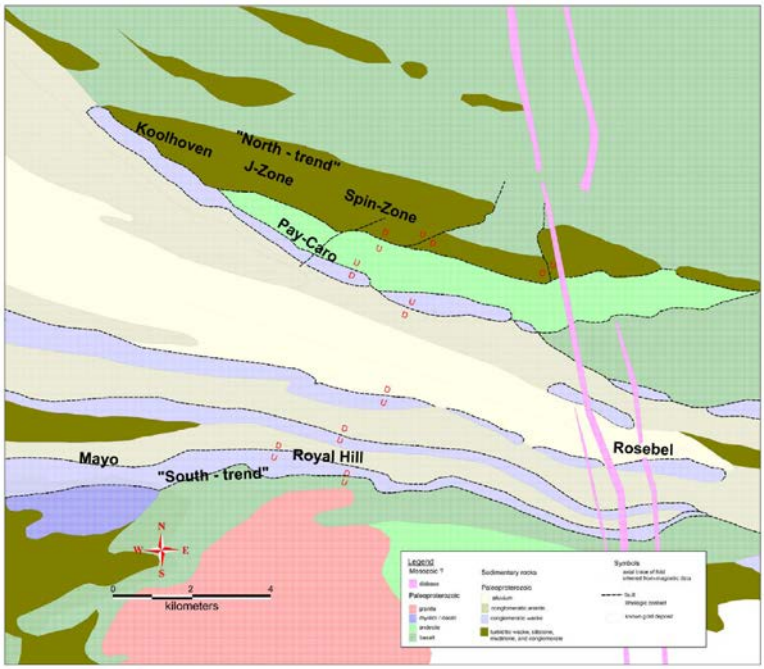

Figure 2. General geologic map of the Rosebel gold mine concession.

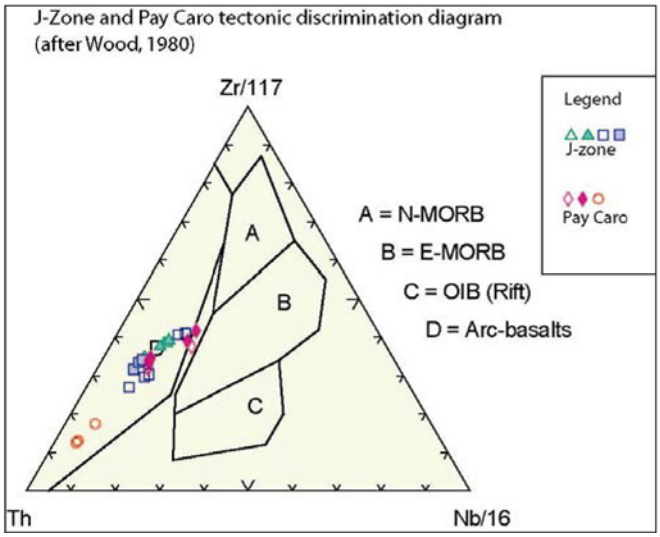

Figure 3. Tectonomagmatic discrimination diagram based on HFSE of J-Zone and Pay Caro rocks.

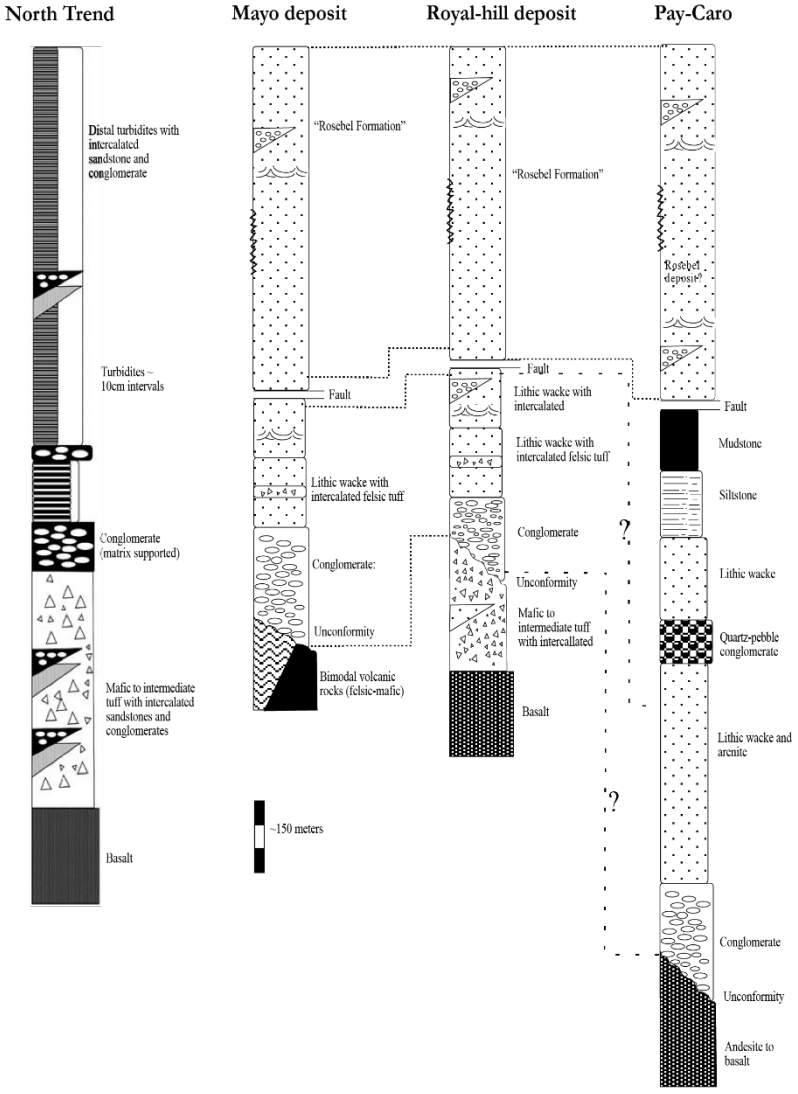

Figure 4. Generalized stratigraphic columns of RGM deposits illustrating major sequences of rock. Stratigraphic correlations are denoted by dashed lines. Thicknesses are approximate and are based on drill-hole and field data.

ACKNOWLEDGEMENTS

This paper is dedicated to the memory of Tom Watson, who died way too young. His spirit lives on in the memories of many geologists and the other friends he made in Suriname at the Rosebel Mine, earlier during the initial exploration and discovery of the Merian Mine, and later at other exploration programs in Suriname and Guyana. We are all enriched by knowing and working with Tom.

REFERENCES

Barrett, T.J., and Maclean, W.H., 1993, Lithogeochemical techniques using immobile elements: Journal of Geochemical Exploration, 48, p. 109 - 133.

Bosma, W., and Groeneweg, W., (1969), Review of the stratigraphy of Suriname: Geologie en Mijnbouw Dienst, 4. 31 p.

Gibbs, A. K., and Barron, C. N., 1993. The Geology of the Guiana Shield: Oxford Monographs on Geology and Geophysics, 213 p.

Voicu, G., Bardoux, M., Stevenson, R., 2001, Lithostratigraphy, geochronology, gold metallogeny in the northern Guiana Shield, South America: A review: Ore Geology Reviews, 18, 211-236.

Wang, Z., Wilde, S. A., Wang, K., and Yu, L, 2004, A MORB-arc basalt-adakite association of the 2.5 Ga Wutai greenstone belt: late Archaean magmatism and crustal growth in the North China Craton: Precambrian Research, 131, p. 323 - 343.

Woodhead, J., Eggins, S., Gamble, J., 1993, High field strength and transition element systematics in island and back-arc basin basalts: evidence for multi-phase melt extraction and a depleted mantle wedge. Earth and Planetary Science Letters, 114, p. 491 - 504.

Petrography, geochemistry and age of the Armina Formation metaturbidites of the Coppename River, Suriname

Genevieve W. Wijngaarde*
Anton de Kom University of Suriname
Leysweg 86, Paramaribo, Suriname
genevieve.wijngaarde1992@gmail.com

Salomon B. Kroonenberg
Anton de Kom Universiteit van Suriname
Leysweg 86, Paramaribo, Suriname
salomon.kroonenberg@uvs.edu

Paul R.D. Mason
Utrecht University
Fac.Geosciences
p.mason@uu.nl

Leo M. Kriegsman
Utrecht University
and Naturalis, Leiden
leo.kriegsman@naturalis.nl

SUMMARY

The Armina Formation along the Coppename River is a part of the 2.26-2.10 Ga Paleoproterozoic Marowijne Greenstone Belt of Suriname. It is in faulted contact with the 2.08-2.05 Ga Bakhuis Granulite Belt. This paper studies the relation between these units based on field observations, petrographic, geochemical and age data. The metaturbidites show a volcanic arc-type setting in the north, and a continental arc setting in the south. No traces of any Bakhuis provenance could be demonstrated in the metaturbidites. Detrital zircons from the Armina metaturbidites show ages around 2162 ± 30 Ma, which is similar to the age of Armina Formation detrital zircons elsewhere in northern Suriname. As Bakhuis sillimanite gneisses also show inherited zircons between 2120 and 2150 Ma, the Bakhuis granulites and Armina metaturbidites protoliths might be coeval and share a common provenance area. Younger granites intruding the Armina metaturbidites show ages of 2005 (Voltzberg), 2004 (Raleigh Falls) and 1990 Ma (Vankaaikisula), slightly higher than most Wonotobo granites in western Suriname.

Key words: Armina Formation; Marowijne Greenstone Belt; Bakhuis Granulite Belt; detrital zircons; metaturbidites.

INTRODUCTION

The sedimentological, petrographic, geochemical and age characteristics of the Armina Formation along the Coppename River are described in detail based on field observations and laboratory analyses. The Armina Formation is the middle unit in the Paleoproterozoic Marowijne Greenstone belt (MGB), which consists essentially of mafic volcanics at the base (Paramaka Formation), followed by the turbiditic Armina Formation and topped by the mature fluvial sandstones of the Rosebel Formation. The greenstone belt is diapirically intruded by numerous TTG (tonalite-trondhjemite-granodiorite) bodies and the Armina Formation in turn by bi-mica and biotite granite bodies (Bosma et al., 1983; De Vletter 1984; Delor et al. 2003a). The meta-sediments (greywackes) of the Armina Formation in the Rosebel Gold Mine area and along the Marowijne River are derived predominantly from erosion of the associated Paramaka Formation volcanics, based on REE signatures correlation with calc-alkaline volcanic rocks (Daoust, et al. 2011) and show widespread graded bedding indicative of deposition by turbidity currents probably in an arc-trench environment (Bosma et al. 1983; Maas in Bosma et al. 1984); Naipal & Kroonenberg, 2016). According to Kroonenberg et al. (2016) and Daoust et al. (2011), the detrital zircons in the Armina Formation of eastern Suriname indicate a maximum age of about 2127 ± 7 Ma for the metaturbidite sequence.

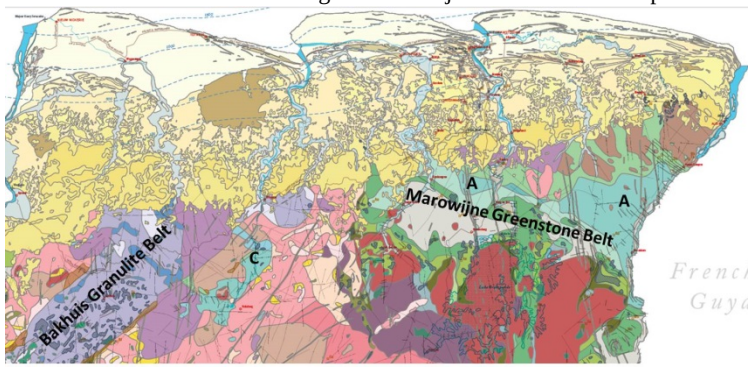

Figure 1. Geological map of northern Suriname. C=Coppename area, A=main outcrops Armina Formation within the greenstone belt.

The Armina Formation in the Coppename area is situated outside the main trend of the Greenstone Belt, but is in (faulted) contact with the Bakhuis high-grade Granulite belt (BGB). The Coppename area, the place where east and west meet, is a key area to understand the relation between the older eastern and the younger western Suriname, but previous mapping efforts suffered from the lack of exposure and lack of sedimentological, structural and age data. The presence of high-grade metamorphic rocks of the BGB has been known since 1902, but the nature and extent of the rocks was established in the seventies (De Roever, 1975). Formerly the Bakhuis Granulite Belt was considered to be older (of Archean age) than the Marowijne Greenstone belt (Bosma, et al. 1983), whereas recent research showed that it is just the reverse. Recent research (De Roever et al., 2003; Klaver et al. 2015; Kroonenberg et al. 2016) showed a more precise age of 2.08-2.05 Ga for the BGB, whereas the age of the MGB is said to be between 2.26 and 2.09 Ga. On the other hand aeromagnetic surveys show that in northernmost Suriname, an area covered with Cenozoic sediments, the greenstone belt cuts the Bakhuis belt, thus reopening the question of age relations. The position of the Armina Formation outcrop in contact with the Bakhuis belt offers an opportunity to confirm or reject the present ideas. The question now is whether the Coppename metaturbidites are deposited in an outlier and/or tectonically displaced basin of the same greenstone belt, or whether it could be a part of the same trans-

tensional basin in which the Bakhuis protoliths have been deposited, and only escaped from being incorporated in the part of the basin that suffered granulite-facies metamorphism.

METHODS AND RESULTS

Methods. Fieldwork was carried out along the Coppename River, which is the key area to understand the relation between the older eastern and the younger western rocks of Suriname. Several outcrops over a distance of 35 km from Grantabiki in the north (formerly called Makambo Island) to Koddji creek, a tributary of the Tanjimamma creek which in turn is a right tributary of the Coppename River, in the south are described and sampled. The most extensive outcrops are at Grantabiki and along the Tanjimamma creek. The major sedimentary structures of the relevant outcrops were described and photographed, and of the sequences the length, width and bedding orientations were measured. 25 samples were studied for petrography and geochemistry, and 6 for geochronology. Major elements were analysed using XRF, trace elements with LA –ICPMS on fragments of the XRF beads, and U-Pb zircon dating was performed using LA -ICPMS as well, all at Utrecht University, the Netherlands.

Figure 2. Outcrop of Armina Formation metaturbidites at Grantabiki, Coppename River.

Field characteristics. The Armina Formation rocks along the Coppename River were deposited in 1-5 m thick fining-upwards turbiditic sequences characterised by constant layer thickness, graded stratification in the coarser parts, small ripple-, wavy-, and convolute lamination and cross stratification in the finer parts. The Armina Formation metagreywackes are intruded by a younger granite evidenced by pegmatite veins, contact metamorphism in the metagreywackes, and metagreywacke xenoliths in the granite (Figure 3).

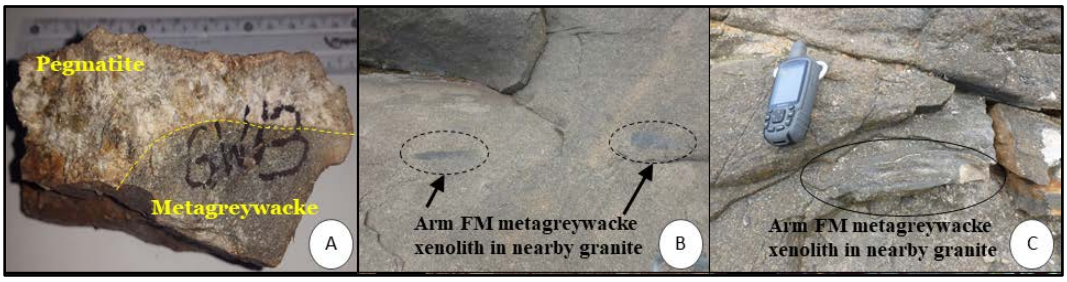

Figure 3. Vankaaiki sula (a) Contact of pegmatite vein and metagreywacke, (b & c) Armina Formation meta-greywacke xenoliths in the nearby granite. Abbreviations: Arm FM = Armina Formation.

Petrography. The meta-greywackes range from north to south from texturally and mineralogical immature to sub-mature, and consist of quartz, plagioclase, K-feldspar (including microcline), biotite, muscovite, chlorite, epidote, allanite, rutile, zircon, tourmaline, titanite, magnetite/ilmenite, pyrite/other sulfide mineral, and magmatic (both plutonic and volcanic; Fig 4 a, b & c), metamorphic and sedimentary lithic fragments. From modal analysis of seven meta-greywackes samples there can be concluded that in the north lithic wackes occur, while southwards they are more feldspathic. The plutonic fragments in the meta-greywacke are probably derived from TTG (Tonalite-Trondhjemite-Granodiorite) plutons due to the abundance of plagioclase relative to alkali feldspar. Volcanic fragments decrease from north (Grantabiki) to south (Koddji creek), indicating a volcanic source in the north. QFL & QmFLt provenance diagrams indicate that greywackes with a volcanic provenance in the north at Grantabiki were deposited in an active island-arc, whereas from Adenagado sula southwards the rocks become more arkosic with a more granitic provenance deposited in an active continental margin. The mineral assemblages of the meta-greywackes indicate regional metamorphism from greenschist facies (chlorite and biotite zone) to lower amphibolite facies (garnet zone), whereas in the vicinity of granitoid rocks contact metamorphism occurred (Figure 4 d,e and f).

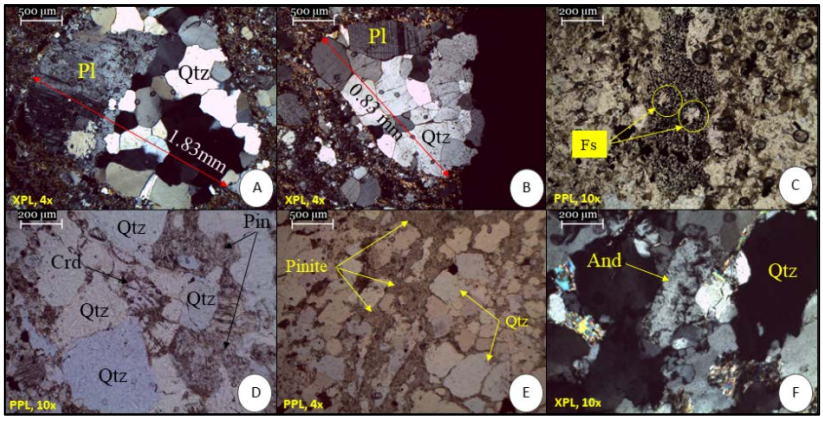

Figure 4. (a & b) Tonalitic/granitic fragments, consisting of sericitized plagioclase and polycrystalline quartz in sample GW 3 and GW 25, (c) Fine-grained mafic volcanic fragment with lots of small opaque minerals and feldspars in sample GW 3 (d) Contact metamorphic variants of the meta-greywacke with the typical metamorphic mineral Cordierite (Cor) in sample GW 15, (e) Pinite, alteration of cordierite to micas, and (f) Andalusite within a contact metamorphic variant of the meta-greywacke in sample GW 36 and GW 15 respectively. Abbreviations: Pl= Plagioclase; Qtz= Quartz; Crd = Cordierite; Pin = Pinite; And = Andalusite

Geochemistry. Geochemical analysis (bivariate and trivariate plots) and higher Ni concentrations in the northern samples point to a partly mafic igneous provenance (volcanic), while higher Th and U concentrations in the southern samples suggest a more felsic igneous provenance (granitic). The geochemical data confirm the volcanic arc depositional environment for the northernmost samples and a continental margin type setting for the southernmost ones (Figure 5).

Age. Detrital zircons in the Armina Formation along the Coppename River indicate an age of about 2162 ± 30 Ma for the major sediment source of the metaturbidite sequence, which is similar to that of the eastern Marowijne Armina Formation. The intrusive character of the second pulse of the granites is confirmed by their determined ages. The granite of Vankaaiki sula with an age of about 1990 ± 19 Ma shows affinity to the western Wonotobo Biotite Granite (1980.2 ± 5.8 Ma), whereas the Raleigh Falls and Voltzberg granite with ages of respectively 2004 ± 43 Ma and 2005 ± 29 Ma, are slightly higher. According to observed tectonic structures the following order of events can be observed: after deposition of the Armina Formation extension occurred resulting in the formation of quartz veins, followed by compression resulting in folding of the Armina Formation and the quartz-veins and subsequent uplift and exposure resulting in the formation of joints.

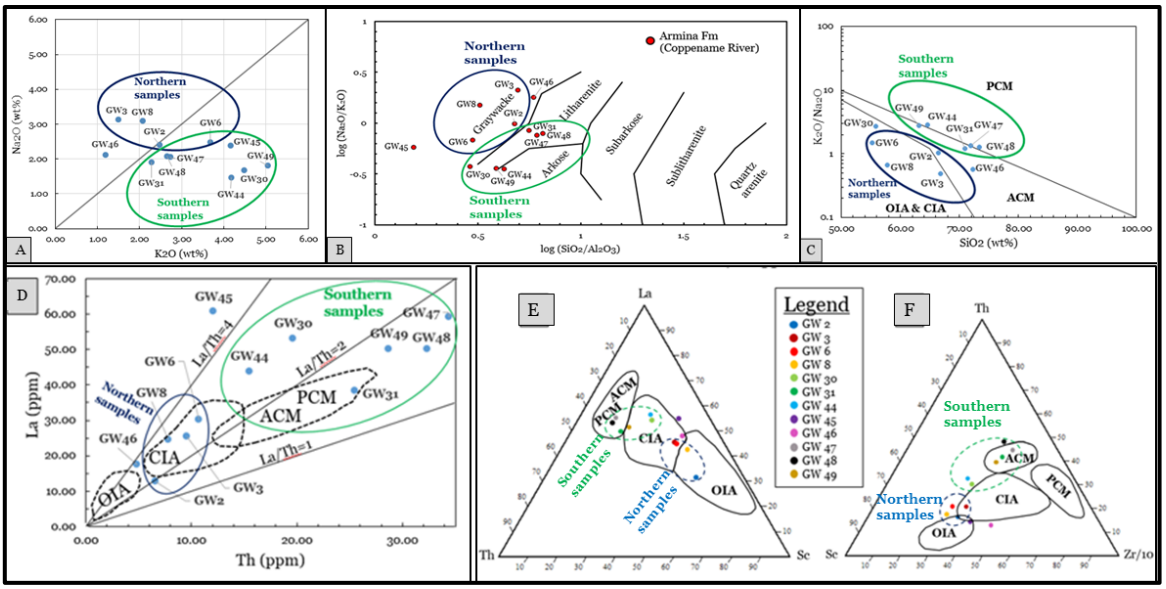

Figure 5. (a) Correlation plot of K_2O vs Na_2O after Pettijohn et al. (1972), (b) Classification of analyzed Armina Formation meta-sedimentary rock samples from the Coppename River according to their logarithmic ratios of SiO_2/Al_2O_3 and Na_2O/K_2O after Pettijohn et al (1972), with limits redefined by Herron (1988), (c) Tectonic discrimination diagram based on K_2O/Na_2O versus SiO_2 after Roser & Korsch (1986), (d) La versus Th bivariate discrimination diagram for the meta-greywackes of the Coppename Armina Formation after Bhatia & Crook (1986), (e) La-Th-Sc and (f) Th-Sc-Zr/10 trivariate discrimination diagrams for the meta-greywackes of Coppename Armina Formation after Bhatia & Crook (1986). Abbreviations: OIA=Oceanic Island-Arc; CIA=Continental Island-Arc; ACM=Active Continental Margin; PCM=Passive Continental Margin.

CONCLUSIONS

Although the Armina Formation of the Marowijne Greenstone Belt along the Coppename River is in faulted contact with the Bakhuis Granulite belt, the turbidite deposits of this formation show no affinity to the Bakhuis rocks according to determined ages of about 2162 ± 30 Ma for the metaturbidites based on detrital zircon dating. No zircons in the Bakhuis age range of 2.08-2.05 Ga have been found in the Armina metagreywackes of the Coppename area, and no granulite clasts have been found either. However, the presence of inherited zircons with ages between 2120 and 2150 Ma in the sillimanite gneisses of the Bakhuis Belt (Klaver et al., 2015) might indicate that the Bakhuis granulites could represent the high-grade equivalents of the Armina metaturbidites, and hence share the same provenance area. The Armina Formation along the Coppename River represents a part of the same greenstone belt of northeastern Suriname, and is deposited on the fore-arc side in an arc trench environment probably as follows. After the formation of an oceanic basin due to major mantle extraction processes and separation of the West-African Craton and the Amazonian Craton ~2.26 Ga ago, the two cratons converged again, resulting in subduction of the denser oceanic crust under the continental plate leading to the formation of an active continental margin and island arc systems (volcanic arcs). Partial melting of the subducting plate provided the material for the construction of the volcanic arc on the leading edge of the continental plate. During early stages of arc development, the fore-arc descended rapidly, directly into the oceanic trench formed over the site of initial subduction. The trench filled with turbidite deposits which are gradually dragged downward by subduction resulting in folding, shearing, and combining scraped up slivers of oceanic crust from the descending plate into mélange (varied mixture), and thrust upward onto the leading edge of the arc as an accretionary wedge. As the wedge grew, a trough formed between it and the volcanic arc called the fore-arc basin which accumulated submarine fan turbidites during later stages of arc development. The sediments in this basin are probably derived from previous generations of sedimentary strata and subordinate volcanic rocks (recycled orogen), pre-existing TTG and granitoid basement and sediments of continental interior deposited along continental margins (continental block), which are exposed and eroded due to orogenic uplift in the fore arc. The deposited turbidite sequences are the result of turbidity currents, which in turn occur due to slope failure. In the north at Grantabiki greywackes with a volcanic provenance are deposited within an active island-arc and from Adenagado sula southwards the rocks become more arkosic with a more granitic provenance deposited in an active continental margin. This is probably related to development of the arc over time which resulted in the bottom of the sequence being more volcanic while still an island arc, whereas higher in the sequence more granitic when it has already become an active continental margin due to the development of the subduction zone. Another explanation could be that the turbidites in the north and south were fed by different river systems and the two sequences lay on each other on the same level.

ACKNOWLEDGEMENTS

This paper represents part of the first author's MSc research project, which was supported by a research fund of the Stichting Dr. Schürmann Foundation. We acknowledge the Geological and Mining Service of Suriname and the Anton de Kom University of Suriname and its staff, respectively for their support during fieldwork and logistic support.

REFERENCES

Bhatia, M.R., and Crook, K.A., 1986. Trace Element Characteristics of Greywackes and Tectonic Discrimination of Sedimentary Basins. Contribution to Mineralgy and Petrology, volume 92: 181-193.

Bosma, W., Kroonenberg, S.B., Maas, K. and De Roever, E.W.F., 1983.Igneous and metamorphic complexes of the Guiana shield in Suriname. Geologie en Mijnbouw 62: 241-254.

Bosma, W., Kroonenberg, S.B., van Lissa, R., Maas, K. and De Roever, E.W.F., 1984. Explanation to the Geological map of Suriname 1:500,000. Mededelingen Geologisch Mijnbouwkundige Dienst van Suriname 27: 31-82.

Daoust, C., Voicu, G., Brisson, H. and Gauthier, M., 2011. Geological setting of the Paleoproterozoic Rosebel gold district, Guiana Shield, Suriname. Journal of South American Earth Sciences, volume 32: 222-245.

De Roever, E.W.F., 1975. Geology of the Central part of the Bakhuis Mountains (W Suriname). Mededelingen Geologisch Mijnbouwkundige Dienst Suriname 23: 65–101.

De Roever, E.W.F., Lafon, J.-M., Delor, C., Rossi, P., Cocherie, A., Guerrot, C. & Potrel, A., 2003a. The Bakhuis ultra-high temperature granulite belt: I Petrological and geochronological evidence for a counterclockwise P-T path at 2.07–2.05 Ga. Géologie de la France 2003 2-3-4: 175–205.

De Vletter, D.R., 1984. Synthesis of the Precambrian of Suriname and review of some outstanding problems. In De Vletter, D. R. (ed.): Geologische Mijnbouwkundige Dienst Suriname, Mededelingen 27: 11-30.

Delor, C., Lahondére, D., Egal, E., Lafon, J-M., Cocherie, A., Guerrot, C., Rossi, Ph., et al., 2003a. Transamazonian crustal growth and reworking as revealed by the 1:500,000-scale geological map of French Guiana (2nd edition). Géologie de la France, issue 2-3-4: 5-57.

Herron, M.M., 1988. Geochemical classification of terrigenous sands and shales for core or log data. Journal of sedimentary petrology, volume 58: 820-829.

Klaver, M., De Roever, E.W.F., Nanne, J.A.M., Mason, P.R.D. and Davies, G.R., 2015. Charnockites and UHT metamorphism in the Bakhuis Granulite Belt, western Suriname: Evidence for two separate UHT events. Precambrian Research 262: 1-19.

Kroonenberg, S.B., De Roever, E.W.F., Fraga, L.M., Reis, N.J., Faraco, T., Lafon, J-M., Cordani, U. and Wong, Th.E., 2016. Paleoproterozoic evolution of the Guiana Shield in Suriname: A revised model. Netherlands Journal of Geosciences — Geologie en Mijnbouw 95-4: 491-522.

Naipal, R., and Kroonenberg, S. B., 2016. Provenance signals in metaturbidites of the Paleoproterozoic greenstone belt of the Guiana Shield in Suriname. Netherlands Journal of Geosciences — Geologie en Mijnbouw: 1-23.

Pettijohn, F.J., Potter, P.E., and Siever, R., 1972. Sand and sandstones. New York: Springer Verlag.
Roser, B.P. and Korsch, R.J., 1986. Determination of tectonic setting of sandstone-mudstone suites using SiO2 content and K2O/Na2O ratio. Geology, volume 94: 635-650.